

09-545199

## WEST Search History

Hide Items Restore Clear Cancel

DATE: Wednesday, May 11, 2005

*updated search notes 5/10/05*

Hide?	Set Name	Query	Hit Count
	DB=USPT; PLUR=YES; OP=AND		
<input type="checkbox"/>	L1	atpg or atp-g or uncG or papc or pap-c or unc-g	512
<input type="checkbox"/>	L2	pasteurellaceae	42
<input type="checkbox"/>	L3	L2 same members	11
<input type="checkbox"/>	L4	l2 and l1	1
<input type="checkbox"/>	L5	multocida or actinobacil\$ or pasteurel\$ or pleuropneumon\$ or pleuro-pneumon\$ or haemophilus or hemophilus! or somnus or haemolytica or hemolytica	5674
<input type="checkbox"/>	L6	(l1 or (atpase or atpases or atpsynthase or atpsynthetase or atp-synthase or atp-synthetase))	3907
<input type="checkbox"/>	L7	L6 and (l2 or l5)	194
<input type="checkbox"/>	L8	L6 same (l2 or l5)	34
<input type="checkbox"/>	L9	l1.clm.	36
<input type="checkbox"/>	L10	L9 not l8	36
	DB=PGPB,USPT,USOC,EPAB,JPAB,DWPI,TDBD; PLUR=YES; OP=AND		
<input type="checkbox"/>	L11	atp-g or atpg or (atp near3 (synthase or synthetase or ase))	2332
<input type="checkbox"/>	L12	multocida or actinobacil\$ or pasteurel\$ or pleuropneumon\$ or pleuro-pneumon\$ or haemophilus or hemophilus! or somnus or haemolytica or hemolytica	12063
<input type="checkbox"/>	L13	L12 same l11 not l8 not l9	48

END OF SEARCH HISTORY

*P multocida*

6846651. 03 Jun 02; 25 Jan 05. Nucleotide sequence of the *Haemophilus influenzae* Rd genome, fragments thereof, and uses thereof. Fleischmann; Robert D., et al. 435/69.1; 435/252.3 435/320.1 536/23.7. C12N015/63 C12N001/21 C12N015/31.

---

☐ 2. 6833267. 27 Dec 99; 21 Dec 04. Tissue collection devices containing biosensors. Kayyem; Jon Faiz. 435/287.1; 422/68.1 435/6 435/7.1 435/91.1. C12M001/34 C12Q001/68 G01N033/53 G01N015/06 C12D019/34.

---

☐ 3. 6824783. 07 Jun 95; 30 Nov 04. Methods for inhibition of membrane fusion-associated events, including HIV transmission. Bolognesi; Dani Paul, et al. 424/188.1; 424/208.1 435/5 530/360. A61K039/21.


---

☐ 4. 6800744. 30 Jun 98; 05 Oct 04. Nucleic acid and amino acid sequences relating to *Streptococcus pneumoniae* for diagnostics and therapeutics. Doucette-Stamm; Lynn A., et al. 536/23.1; 435/320.1 435/325 435/419 435/6 536/23.4 536/24.1 536/24.32. C12Q001/68 C12N001/14 C12N015/00 C12N005/00 C12N005/04 C07H021/02 C07H021/04.

---

☐ 5. 6797466. 20 Oct 00; 28 Sep 04. Complete genome sequence of the methanogenic archaeon, *Methanococcus jannaschii*. Bult; Carol J., et al. 435/6; 435/252.3 435/320.1 435/325 536/23.7 536/24.32. C12Q001/68.

---

 ☐ 6. 6790950. 15 Mar 01; 14 Sep 04. Anti-bacterial vaccine compositions. Lowery; David E., et al. 536/23.7; 435/243 435/252.3 435/320.1 435/6 435/69.1 536/23.1. C07H021/00 C12N021/00 C12N001/21 C12N015/31.

---

☐ 7. 6747137. 12 Feb 99; 08 Jun 04. Nucleic acid sequences relating to *Candida albicans* for diagnostics and therapeutics. Weinstock; Keith G., et al. 536/23.1; 435/6 536/24.3 536/24.31 536/24.32 536/24.33. C07H021/00 C12Q001/68.

---

☐ 8. 6737248. 03 Jan 97; 18 May 04. *Staphylococcus aureus* polynucleotides and sequences. Kunsch; Charles A., et al. 435/69.1; 435/252.3 435/320.1 536/23.1 536/23.7. C12P021/02.

---

☐ 9. 6696561. 23 Jun 00; 24 Feb 04. *Corynebacterium glutamicum* genes encoding proteins involved in membrane synthesis and membrane transport. Pompejus; Markus, et al. 536/23.7; 530/350. C12N015/31 C07K014/195.

---

☐ 10. 6632636. 16 Jun 00; 14 Oct 03. Nucleic acids encoding 3-ketoacyl-ACP reductase from *Moraxella catarrhalis*. Lagace; Robert E., et al. 435/69.1; 435/189 435/252.3 435/254.11 435/320.1 435/325 435/440 435/70.1 435/71.1 536/23.2 536/24.32. C12P021/06 C12N015/00 C12N005/00 C12N001/20 C07H021/04.

---

☐ 11. 6617156. 13 Aug 98; 09 Sep 03. Nucleic acid and amino acid sequences relating to *Enterococcus faecalis* for diagnostics and therapeutics. Doucette-Stamm; Lynn A., et al. 435/320.1; 435/252.3 435/6 435/69.1 536/23.7 536/24.32. C12N015/31 C12N015/63 C12N001/13 C12Q001/68.

---

☐ 12. 6593114. 20 Oct 97; 15 Jul 03. *Staphylococcus aureus* polynucleotides and sequences. Kunsch; Charles A., et al. 435/91.41; 435/252.3 435/254.11 435/257.2 435/320.1 435/325 435/91.4 536/23.7. C12N015/64 C07H021/04.

---

☐ 13. 6583275. 30 Jun 98; 24 Jun 03. Nucleic acid sequences and expression system relating to *Enterococcus faecium* for diagnostics and therapeutics. Doucette-Stamm; Lynn A., et al. 536/23.1;

435/243 435/320.1 435/325 435/6 536/24.3 536/24.32. C07H021/00 C12Q001/68 C12N015/00  
C12N001/00 C12N005/00.

---

☐ 14. 6562958. 04 Jun 99; 13 May 03. Nucleic acid and amino acid sequences relating to *Acinetobacter baumannii* for diagnostics and therapeutics. Breton; Gary, et al. 536/23.7; 536/23.1. C07H021/02.

---

☐ 15. 6559294. 23 Nov 98; 06 May 03. *Chlamydia pneumoniae* polynucleotides and uses thereof. Griffais; Remy, et al. 536/23.1; 435/320.1 435/69.1 435/70.1 536/24.1. C07H021/02 C07H021/04 C12P021/06 C12P021/04 C12N015/00.

---

☐ 16. 6551795. 18 Feb 99; 22 Apr 03. Nucleic acid and amino acid sequences relating to *Pseudomonas aeruginosa* for diagnostics and therapeutics. Rubenfield; Marc J., et al. 435/69.1; 435/253.3 435/320.1 435/325 435/6 536/23.1 536/23.7. C12P021/06 C12N015/00 C07H021/04.

---

☐ 17. 6537773. 19 Oct 95; 25 Mar 03. Nucleotide sequence of the *Mycoplasma genitalium* genome, fragments thereof, and uses thereof. Fraser; Claire M., et al. 435/69.1; 435/252.3 435/320.1 536/23.7 536/24.32. C12Q001/68.

---

☐ 18. 6528289. 23 Aug 00; 04 Mar 03. Nucleotide sequence of the *Haemophilus influenzae* Rd genome, fragments thereof, and uses thereof. Fleischmann; Robert D., et al. 435/91.41; 435/252.3 435/320.1 435/6 536/23.1 536/23.7. C12N015/64.

---

☐ 19. 6518013. 07 Jun 95; 11 Feb 03. Methods for the inhibition of Epstein-Barr virus transmission employing anti-viral peptides capable of abrogating viral fusion and transmission. Barney; Shawn O'Lin, et al. 435/5; 424/230.1 530/300 530/324 530/325 530/326. C12Q001/70.

---

☐ 20. 6506581. 25 Apr 00; 14 Jan 03. Nucleotide sequence of the *Haemophilus influenzae* Rd genome, fragments thereof, and uses thereof. Fleischmann; Robert D., et al. 435/69.1; 435/252.3 435/320.1 435/69.3 435/91.41 536/23.7. C12N001/21 C12N015/31 C12N015/63.

---

☐ 21. 6503729. 22 Aug 97; 07 Jan 03. Selected polynucleotide and polypeptide sequences of the methanogenic archaeon, *Methanococcus jannashii*. Bult; Carol J., et al. 435/69.1; 435/252.3 435/320.1 435/325 536/23.1 536/23.5. C12P021/06.

---

☐ 22. 6479055. 06 Jun 95; 12 Nov 02. Methods for inhibition of membrane fusion-associated events, including respiratory syncytial virus transmission. Bolognesi; Dani Paul, et al. 424/211.1; 424/186.1 530/324. A61K039/145.

---

☐ 23. 6355450. 07 Jun 95; 12 Mar 02. Computer readable genomic sequence of *Haemophilus influenzae* Rd, fragments thereof, and uses thereof. Fleischmann; Robert D., et al. 435/69.1; 435/252.3 435/320.1 435/85.1 536/23.1 536/23.7 536/24.32 536/24.33. C12P021/06 C12N001/20 C12N015/00 C07H021/04.

---

☐ 24. 6348582. 23 Sep 97; 19 Feb 02. Prokaryotic polynucleotides polypeptides and their uses. Black; Michael Terence, et al. 536/23.1; 424/185.1 435/252.3 435/320.1 435/69.1 530/350 536/22.1. C07H021/00 C07H021/02 C12P021/06 A61K038/00.

---

☐ 25. 6348328. 14 May 97; 19 Feb 02. Compounds. Black; Michael Terence, et al. 435/69.1; 435/252.3 435/320.1 536/23.1 536/23.7. C12P021/02.

---

- ☐ 26. [6239264](#). 24 Dec 97; 29 May 01. Genomic DNA sequences of ashbya gossypii and uses thereof. Philippsen; Peter, et al. 536/23.1; 435/320.1 536/24.3 536/24.32. C07H021/04 C12N015/11 C12N015/63.
- 
- ☐ 27. [6228983](#). 07 Jun 95; 08 May 01. Human respiratory syncytial virus peptides with antifusogenic and antiviral activities. Barney; Shawn O'Lin, et al. 530/300; 424/186.1 424/211.1 530/324 530/325 530/326. A61K038/00.
- 
- ☐ 28. [6093794](#). 07 Jun 95; 25 Jul 00. Isolated peptides derived from the Epstein-Barr virus containing fusion inhibitory domains. Barney; Shawn O'Lin, et al. 530/300; 424/186.1 424/230.1 530/324 530/325 530/326 530/350. A61K038/00 A61K039/12 A61K039/245.
- 
- ☐ 29. [6068973](#). 07 Jun 95; 30 May 00. Methods for inhibition of membrane fusion-associated events, including influenza virus. Barney; Shawn O'Lin, et al. 435/5; 424/147.1 424/206.1 424/230.1 530/324 530/389.4. C12Q001/70 A61K038/00 A61K039/42 C07K016/00.
- 
- ☐ 30. [6060065](#). 07 Jun 95; 09 May 00. Compositions for inhibition of membrane fusion-associated events, including influenza virus transmission. Barney; Shawn O'Lin, et al. 424/209.1; 424/186.1 424/192.1 424/206.1 530/300 530/324 530/325 530/326 530/327 530/328 530/329 530/330. A61K039/145 A61K039/12 A61K039/00 A61K038/00.
- 
- ☐ 31. [6054265](#). 26 Sep 97; 25 Apr 00. Screening assays for compounds that inhibit membrane fusion-associated events. Barney; Shawn O'Lin, et al. 435/5; 435/7.2. C12Q001/70.
- 
- ☐ 32. [6017536](#). 20 Dec 94; 25 Jan 00. Simian immunodeficiency virus peptides with antifusogenic and antiviral activities. Barney; Shawn O'Lin, et al. 424/188.1; 424/208.1 530/300 530/324 530/325 530/326. A61K039/21.
- 
- ☐ 33. [6013263](#). 07 Jun 95; 11 Jan 00. Measles virus peptides with antifusogenic and antiviral activities. Barney; Shawn O'Lin, et al. 424/212.1; 424/184.1 424/186.1 530/300 530/324 530/325 530/326. A61K039/165.
- 
- ☐ 34. [5994066](#). 04 Nov 96; 30 Nov 99. Species-specific and universal DNA probes and amplification primers to rapidly detect and identify common bacterial pathogens and associated antibiotic resistance genes from clinical specimens for routine diagnosis in microbiology laboratories. Bergeron; Michel G., et al. 435/6; 435/91.2 536/22.1. C12Q001/68 C12P019/34 C07H021/02.
- 

[Generate Collection](#)[Print](#)

Terms	Documents
L6 same (L2 or L5)	34

[Prev Page](#)[Next Page](#)[Go to Doc#](#)



[First Hit](#) [Fwd Refs](#)[Previous Doc](#)[Next Doc](#)[Go to Doc#](#)

Generate Collection

[Print](#)

L10: Entry 18 of 36

File: USPT

Mar 5, 2002

DOCUMENT-IDENTIFIER: US 6352839 B1

**\*\* See image for Certificate of Correction \*\***

TITLE: Streptogramins for preparing same by mutasynthesis

## CLAIMS:

1. A process for preparing a streptogramin analog, comprising the steps of

selecting a streptogramin-producing microorganism strain which possesses at least one genetic modification which prevents the synthesis of an active enzyme encoded by at least one nucleic acid sequence consisting of a single gene comprising a sequence selected from SEQ ID NO. 14, SEQ ID NO. 16, SEQ ID No. 2, SEQ ID No. 4, SEQ ID No. 7, SEQ ID No. 9, and SEQ ID No. 12, genes isolated from *S. pristinaespiralis* which correspond to the papA, papM, papC, papB, pipA, snbF, and hpaA genes and encode a polypeptide with the enzymatic activity of the papA, papM, papC, papB, pipA, snbF, and hpaA polypeptides, and genes which code for polypeptides encoded by the papA, papM, papC, papB, pipA, snbF, and hpaA genes and differ from those genes on account of the degeneracy of the genetic code;

growing said streptogramin-producing microorganism on a culture medium which is appropriate for said microorganism and which is supplemented with at least one precursor analog; and

recovering said streptogramin analog from said culture medium.

2. The process according to claim 1, wherein at least one of the nucleic acid sequence selected from the papA (SEQ ID No. 14), papM (SEQ ID No. 16), papC, (SEQ ID NO: 2), papB (SEQ ID NO: 4), pipA (SEQ ID NO: 7), snbF (SEQ ID NO: 9) and hpaA (SEQ ID NO: 12) genes.

3. The process according to one of claims 1 or 2, wherein the genetic modification prevents the synthesis of an active enzyme encoded by at least one nucleic acid esquence selected from the papA (SEQ ID No.14), papM (SEQ ID No. 16), papC (SEQ ID No. 2), papB (SEQ ID No. 4), pipA (SEQ ID No. 7), snbF (SEQ ID No. 9), and hpaA (SEQ ID No. 12).

4. The process according to claim 3, wherein the genetic modification consists of a disruption of one gene selected from the papA (SEQ ID No. 14), papM (SEQ ID No. 16), papC (SEQ ID No. 2), papB (SEQ ID No. 4), pipA (SEQ ID No. 7), snbF (SEQ ID No. 9), and hpaA (SEQ ID No. 12).

9. An isolated nucleic acid sequence, consisting of a single gene or a portion of a single gene comprising a sequence selected from among:

(a) SEQ ID No. 2, SEQ ID No. 4, SEQ ID No. 7, SEQ ID No. 9, and SEQ ID No. 12,

(b) genes isolated from *S. pristinaespiralis* which correspond to papC , papB, pipA, snbF, and hpaA and encode polypeptides with the enzymatic activity of papC, papB, pipA, snbF, and hpaA polypeptides, and

(c) sequences which code for polypeptides encoded by the nucleic acid sequences of (a) and (b) and differ from (a) and (b) sequences on account of the degeneracy of the genetic code.

10. An isolated nucleic acid sequence according to claim 9, which is selected from the papC (SEQ ID No. 2), papB (SEQ ID No. 4), pipA (SEQ ID No. 7), snbF (SEQ ID No. 9) and hpaA (SEQ ID No. 12) genes.

11. Recombinant DNA consisting of a single gene comprising a nucleic acid sequence selected among papC (SEQ ID NO. 2), papB (SEQ ID NO. 4), pipA (SEQ ID NO. 7), snbF (SEQ ID No. 9), and hpaA (SEQ ID No. 12).

16. A mutant *S. pristinaespiralis* strain comprising at least one genetic modification in at least one of its papC (SEQ ID No. 2), papB (SEQ ID No. 4), pipA (SEQ ID No. 7), snbF (SEQ ID No. 9) and hpaA (SEQ ID No. 12) genes, wherein said genetic modification prevents synthesis of an active enzyme encoded by said genes.

[Previous Doc](#)

[Next Doc](#)

[Go to Doc#](#)

Arch Microbiol. 1987 Sep;148(3):187-92.

[Related Articles, Links](#)

**Evolutionary relationship between Enterobacteriaceae: comparison of the ATP synthases (F1F0) of *Escherichia coli* and *Klebsiella pneumoniae*.**

**Kauffer S, Schmid R, Steffens K, Deckers-Hebestreit G, Altendorf K.**

Arbeitsgruppe Mikrobiologie, Universitat Osnabruck, Federal Republic of Germany.

The ATP synthase complex of *Klebsiella pneumoniae* (KF1F0) has been purified and characterized. SDS-gel electrophoresis of the purified F1F0 complexes revealed an identical subunit pattern for *E. coli* (EF1F0) and *K. pneumoniae*. Antibodies raised against EF1 complex and purified EF0 subunits recognized the corresponding polypeptides of EF1F0 and KF1F0 in immunoblot analysis. Protease digestion of the individual subunits generated an identical cleavage pattern for subunits alpha, beta, gamma, epsilon, a, and c of both enzymes. Only for subunit delta different cleavage products were obtained. The isolated subunit c of both organisms showed only a slight deviation in the amino acid composition. These data suggest that extensive homologies exist in primary and secondary structure of both ATP synthase complexes reflecting a close phylogenetic relationship between the two enterobacteric tribes.

PMID: 2890332 [PubMed - indexed for MEDLINE]

J Bioenerg Biomembr. 1996 Feb;28(1):49-57.

[Related Articles, Links](#)

**A role for the disulfide bond spacer region of the *Chlamydomonas reinhardtii* coupling factor 1 gamma-subunit in redox regulation of ATP synthase.**

**Ross SA, Zhang MX, Selman BR.**

Department of Biochemistry, College of Agricultural and Life Sciences, University of Wisconsin-Madison 53706, USA.

The gamma-subunit of chloroplast coupling factor 1 contains a disulfide bond which is involved in the redox regulation of the enzyme. In all the sequence plant gamma-subunits this disulfide bond is separated by a five amino acid spacer region. To investigate the regulatory significance of this region genetic transformation experiments were performed with *Chlamydomonas reinhardtii*. *C. reinhardtii* strain atpC1 (nit1-305, cw 15, mt-), which does not accumulate the CF1 gamma-subunit polypeptide, was independently transformed with two constructs, each bearing mutations within the disulfide bond spacer region between Cys198 and Cys204 of the gamma-subunit. Successful complementation was confirmed by phenotypic selection, Northern blot analysis, and reverse transcription polymerase chain reaction. Whereas wild-type thylakoid membrane particles catalyze in vitro, PMS-dependent photophosphorylation that is stimulated 2-fold by the addition of DTT, similar particles from each of the mutant strains exhibit rates of ATP synthesis that are independent of DTT. Consistent with these results, wild-type CF1 ATPase activity is stimulated by DTT which is in contrast to the ATPase activities of both the mutant strains which are independent of DTT addition. These results suggest a role of the gamma-subunit disulfide bond spacer region in the redox regulation of chloroplast ATP synthase.

PMID: 8786238 [PubMed - indexed for MEDLINE]

[First Hit](#) [Fwd Refs](#)[Previous Doc](#)[Next Doc](#)[Go to Doc#](#)

Generate Collection

Print

L3: Entry 1 of 11

File: USPT

Sep 14, 2004

DOCUMENT-IDENTIFIER: US 6790950 B2

TITLE: Anti-bacterial vaccine compositions

Brief Summary Text (4):

The family Pasteurellaceae encompasses several significant pathogens that infect a wide variety of animals. In addition to *P. multocida*, prominent members of the family include *Pasteurella* (Mannheimia) *haemolytica*, *Actinobacillus pleuropneumoniae* and *Haemophilus somnus*. *P. multocida* is a gram-negative, nonmotile coccobacillus which is found in the normal flora of many wild and domestic animals and is known to cause disease in numerous animal species worldwide [Biberstein, In M. Kilian, W. Frederickson, and E. L. Biberstein (ed.), *Haemophilus, Pasteurella, and Actinobacillus*. Academic Press, London, p.61-73 (1981)]. The disease manifestations following infection include septicemias, bronchopneumonias, rhinitis, and wound infections [Reviewed in Shewen, et al., In C. L. Gyles and C. O. Thoen (ed.), *Pathogenesis of Bacterial Infections in Animals*. Iowa State University Press, Ames, p. 216-225 (1993), incorporated herein by reference].

Detailed Description Text (131):

Transport of scarce compounds necessary for growth and survival are critical in vivo. ExbB is a part of the TonB transport complex [Hantke, and Zimmerman, *Microbiology Letters*. 49:31-35 (1981)], interacting with TonB in at least two distinct ways [Karlsson, et al., *Mol Microbiol*. 8:389-96 (1993), Karlsson, et al., *Mol Microbiol*. 8:379-88 (1993)]. Iron acquisition is essential for pathogens. In this work, attenuated exbB mutants in both APP and *P. multocida* have been identified. Several TonB-dependent iron receptors have been identified in other bacteria [Biswas, et al., *Mol. Microbiol*. 24:169-179 (1997), Braun, *FEMS Microbiol Rev*. 16:295-307 (1995), Elkins, et al., *Infect Immun*. 66:151-160 (1998), Occhino, et al., *Mol Microbiol*. 29:1493-507 (1998), Stojiljkovic and Srinivasan, *J Bacteriol*. 179:805-12 (1997)]. *A. pleuropneumoniae* produces 2 transferrin-binding proteins, which likely depend on the ExbB/ExbD/TonB system, for acquisition of iron. PotD is a periplasmic binding protein that is required for spennidine (a polyamine) transport [Kashiwagi, et al., *J Biol Chem*. 268:19358-63 (1993)]. Another member of the Pasteurellaceae family, *Pasteurella haemolytica*, contains a homologue of potD (Lpp38) that is a major immunogen in convalescent or outer membrane protein vaccinated calves [Pandher and Murphy, *Vet Microbiol*. 51:331-41 (1996)]. In *P. haemolytica*, PotD appeared to be associated with both the inner and outer membranes. The role of PotD in virulence or in relationship to protective antibodies is unknown although previous work has shown porD mutants of *Streptococcus pneumoniae* to be attenuated [Polissi, et al., *Infect. Immun*. 66:5620-9 (1998)].

[Previous Doc](#)[Next Doc](#)[Go to Doc#](#)

[0609]

## The Stalk Region of the *Escherichia coli* ATP Synthase

TYROSINE 205 OF THE  $\gamma$  SUBUNIT IS IN THE INTERFACE BETWEEN THE  $F_1$  AND  $F_0$  PARTS AND CAN INTERACT WITH BOTH THE  $\epsilon$  AND  $c$  OLIGOMER\*

(Received for publication, May 25, 1996, and in revised form, August 6, 1996)

Spencer D. Watts, Chunlin Tang, and Roderick A. Capaldi†

From the Institute of Molecular Biology, University of Oregon, Eugene, Oregon 97403-1229

The soluble portion of the *Escherichia coli*  $F_1F_0$  ATP synthase ( $ECF_1$ ) and *E. coli*  $F_1F_0$  ATP synthase ( $ECF_1F_0$ ) have been isolated from a novel mutant  $\gamma Y205C$ .  $ECF_1$  isolated from this mutant had an ATPase activity 3.5-fold higher than that of wild-type enzyme and could be activated further by maleimide modification of the introduced cysteine. This effect was not seen in  $ECF_1F_0$ . The mutation partly disrupts the  $F_1$  to  $F_0$  interaction, as indicated by a reduced efficiency of proton pumping.  $ECF_1$  containing the mutation  $\gamma Y205C$  was bound to the membrane-bound portion of the *E. coli*  $F_1F_0$  ATP synthase ( $ECF_0$ ) isolated from mutants  $cA39C$ ,  $cQ42C$ ,  $cP43C$ , and  $cD44C$  to reconstitute hybrid enzymes.  $Cu^{2+}$  treatment or reaction with 5,5'-dithio-bis(2-nitro-benzoic acid) induced disulfide bond formation between the Cys at  $\gamma$  position 205 and a Cys residue at positions 42, 43, or 44 in the  $c$  subunit but not at position 39. Using  $Cu^{2+}$  treatment, this covalent cross-linking was obtained in yields as high as 95% in the hybrid  $ECF_1\gamma Y205C/cQ42C$  and in  $ECF_1F_0$  isolated from the double mutant of the same composition. The covalent linkage of the  $\gamma$  to a  $c$  subunit had little effect on ATPase activity. However, ATP hydrolysis-linked proton translocation was lost, by modification of both  $\gamma$  Cys-205 and  $c$  Cys-42 by bulky reagents such as 5,5'-dithio-bis(2-nitro-benzoic acid) or benzophenone-4-maleimide. In both  $ECF_1$  and  $ECF_1F_0$  containing a Cys at  $\gamma$  205 and a Cys in the  $\epsilon$  subunit (at position 38 or 43), cross-linking of the  $\gamma$  to the  $\epsilon$  subunit was induced in high yield by  $Cu^{2+}$ . No cross-linking was observed in hybrid enzymes in which the Cys was at position 10, 65, or 108 of the  $\epsilon$  subunit. Cross-linking of  $\gamma$  to  $\epsilon$  had only a minimal effect on ATP hydrolysis. The reactivity of the Cys at  $\gamma$  205 showed a nucleotide dependence of reactivity to maleimides in both  $ECF_1$  and  $ECF_1F_0$ , which was lost in  $ECF_1$  when the  $\epsilon$  subunit was removed. Our results show that there is close interaction of the  $\gamma$  and  $\epsilon$  subunits for the full-length of the stalk region in  $ECF_1F_0$ . We argue that this interaction controls the coupling between nucleotide binding sites and the proton channel in  $ECF_1F_0$ .

$F_1F_0$  type ATP synthases play a key role in oxidative phosphorylation and photophosphorylation. The  $F_1$ , which can be detached from the  $F_0$  and studied separately, is a complex of five different types of subunits called  $\alpha$ ,  $\beta$ ,  $\gamma$ ,  $\delta$ , and  $\epsilon$  that are present in the molar ratio 3:3:1:1:1. The  $F_0$  part in the *Esche-*

*richia coli* enzyme is composed of three different subunits:  $a$ ,  $b$ , and  $c$  in the molar ratio 1:2:10–12 (1–4). Electron microscopy first showed that the  $\alpha$  and  $\beta$  subunits are arranged hexagonally and alternate around a central cavity in which the  $\gamma$  subunit is located (5–7). Biochemical studies place the  $\epsilon$  subunit (nomenclature for the *E. coli* enzyme) at the bottom of the  $\alpha_3\beta_3$   $\gamma$  core complex (4, 8) in the stalk region, which is a 40–45-Å-long structure that links the  $F_1$  to the  $F_0$  part (9, 10).

The recently published high resolution structure of a major part of the beef heart  $F_1$  molecule confirms the above-described arrangement of the  $\alpha$ ,  $\beta$ , and  $\gamma$  subunits and adds important details (11). In particular, it shows the  $\gamma$  subunit arranged with a long C-terminal  $\alpha$ -helix extending from the top of the  $\alpha$  and  $\beta$  subunits into the stalk region. A shorter N-terminal  $\alpha$ -helix is also present, running from the catalytic site region into the stalk region. These two  $\alpha$  helices form a coiled coil. A third short  $\alpha$ -helix of the  $\gamma$  subunit (residues 83–99 in the *E. coli* sequence) is inclined at about 45° to the two larger helices at the bottom of the  $F_1$  as it becomes the stalk. Approximately half of the  $\gamma$  subunit is unresolved in the structure, presumably because it is disordered in the crystal form.

Recently, we observed cross-linking between a Cys introduced at position 44 of the polar loop of the  $c$  subunits and a site or sites on the  $\gamma$  subunit in the region between residues 202 and 230 (12). This result implies that the  $\gamma$  subunit extends the full length of the stalk to interact with the  $F_0$  part in the intact ATP synthase. Tentatively, we concluded that this cross-linking involved a Cys to Tyr covalent bond (12). There are four Tyr residues in the  $\gamma$  subunit between residues 202 and 230, i.e. Tyr-205, Tyr-207, Tyr-222, and Tyr-228.

The other subunit known to extend from the  $\alpha_3\beta_3$  domain to the  $F_0$  subunits is the  $\epsilon$  subunit. We have previously obtained a structure for the  $\epsilon$  subunit by NMR (13), which shows this stalk-forming subunit arranged as two domains, a 10-stranded  $\beta$ -sandwich structure formed by the N-terminal 85 residues and an  $\alpha$ -helix-loop- $\alpha$ -helix structure of the C-terminal approximately 50 residues. In  $ECF_1F_0$ , the C-terminal domain interacts with the  $\alpha$  and  $\beta$  subunits (8, 14–16). The N-terminal domain is positioned below this, attached to the first of the two  $\alpha$  helices of the C-terminal domain at its top (13) and to the  $c$  subunits of the  $F_0$  part via the bottom of the  $\beta$  sandwich in an interaction that involves residues Glu-31 (17, 18) and possibly His-38 (19). Our recent cross-linking and protease protection studies have established that one face of the  $\beta$ -sheet sandwich of the  $\epsilon$  subunit interacts with the  $\gamma$  subunit (16). In one set of experiments, cross-linking was obtained from Cys-10 of  $\epsilon$  to a region of the  $\gamma$  subunit around residue 228. There was also cross-linking from a Cys placed at either residue position 38 or 43 of  $\epsilon$  to a region of the  $\gamma$  subunit between residues 202 and approximately 230. This is the same region of  $\gamma$  that was identified in preliminary experiments as involved in binding to the  $c$  subunits (12).

\* This work was supported by National Institutes of Health Grant HL 24526. The costs of publication of this article were defrayed in part by the payment of page charges. This article must therefore be hereby marked "advertisement" in accordance with 18 U.S.C. Section 1734 solely to indicate this fact.

† To whom correspondence should be addressed. Tel.: 541-346-5881; Fax: 541-346-4854.

To explore the interactions of the region of the  $\gamma$  subunit between residues 202 and 230 in more detail, we have now converted  $\gamma$  Tyr-202 to a Cys. This introduced Cys is shown to cross-link by disulfide bond formation with Cys residues in both the  $\epsilon$  subunit and in the polar loop of the  $c$  subunits. Functional consequences of such cross-links are described.

#### EXPERIMENTAL PROCEDURES

**Strains and Plasmid Construction**—The M13mp18 template used consisted of a 1.4-kilobase *uncG*-containing *SmaI*-*EcoRI* fragment as described by Aggeler and Capaldi (20). The oligonucleotide used for the mutagenesis was ATAAATCCTGGGATTGCCTCTACGAACCCGATC where the first underlined G changes a TAC codon (Tyr) to TGC (Cys), creating the  $\gamma$ Y205C mutation, and the CTC codon replaces CTG, retaining Leu at position  $\gamma$ 206. A *RsaI* site is eliminated at position 8393 of the *unc* operon (numbering according to Walker *et al.* (21)), which is diagnostic of the presence of the mutation. The mutant phage was identified by *RsaI* digestion and transferred into pRA100 (14). The final plasmid containing the mutation  $\gamma$ Y205C was called pCT100. Mutants cA39C, cQ42C, cP43C, and cD44C were obtained from Dr. Robert Fillingame and are described elsewhere (18). For construction of the double mutants  $\gamma$ Y205C/cA39C and  $\gamma$ Y205C/cQ42C, plasmids pYZ203 and pYZ217 were isolated from the strains expressing mutants cA39C and cQ42C, respectively. The 5.8-kilobase pair *XhoI*/*NsiI* fragment of plasmid pCT100 containing the *uncG* gene with the  $\gamma$ Y205C mutation was used to replace the corresponding region of plasmids pYZ203 and pYZ217. These new plasmids are called pSW101 and pSW102. Strain AN888 (*uncB*<sup>+</sup> *Mu*::416, *argH*, *entA*, *nalA*, *recA*) (14) was transformed with plasmids pCT100, pSW101, pSW102, and pYZ217 for expression of mutant enzyme.  $\epsilon$  subunit mutants were obtained, and the  $\epsilon$  subunit was isolated as described elsewhere (13, 14, 16).

**Labeling ECF<sub>1</sub> and ECF<sub>1</sub>F<sub>0</sub> ATPases with Maleimides**—ECF<sub>1</sub><sup>1</sup> and ECF<sub>1</sub>F<sub>0</sub> were isolated from various mutants and from AN1460 as a control for biochemical studies, as described in Wise *et al.* (22) and Aggeler *et al.* (23), respectively. For reaction of ECF<sub>1</sub> with maleimides, enzyme was passed through two consecutive centrifuge columns (Sephadex G-50, fine, 0.5 × 6 cm equilibrated with 50 mM MOPS, pH 7.0, 0.5 mM EDTA, 10% glycerol). ECF<sub>1</sub> was then labeled at a concentration of 1.0–2.0 mg/ml with 200  $\mu$ M CM (20 mM stock solution in dimethyl sulfoxide), 200  $\mu$ M TFPAM-3 (20 mM stock solution in dimethyl sulfoxide) or 25  $\mu$ M [<sup>14</sup>C]NEM (2.5 mM stock solution in dimethyl sulfoxide) at room temperature. In each experiment, one sample of enzyme was incubated in Mg<sup>2+</sup> (5.5 mM) + ATP (5 mM) for 30 min to convert the ATP to ADP + P<sub>i</sub>. Mg<sup>2+</sup> (5.5 mM) + AMP-PNP (5 mM) was added to a second sample. Aliquots were removed for analysis at the times indicated. Excess CM or TFPAM-3 was quenched with 20 mM cysteine. The reaction with [<sup>14</sup>C]NEM was stopped by addition of 10 mM nonradioactive NEM.

ECF<sub>1</sub>F<sub>0</sub> was reconstituted in vesicles of egg lecithin by mixing detergent-dissolved ECF<sub>1</sub>F<sub>0</sub> with egg lecithin solution in a ratio of 1:2 (w/w ECF<sub>1</sub>F<sub>0</sub>:lecithin) and passing the mixture through a 1.0 × 26-cm Sephadex G-50 (medium) column equilibrated with a buffer containing 50 mM MOPS, pH 7.5, 5 mM MgSO<sub>4</sub>, and 10% glycerol. The ECF<sub>1</sub>F<sub>0</sub> ATPase (0.5–0.7 mg/ml) was labeled with NEM, TFPAM-3, or CM as for ECF<sub>1</sub> (above) but using 10 mM DTT to quench excess maleimide. The time course of labeling of ECF<sub>1</sub>F<sub>0</sub> with CM was conducted by first incubating the enzyme with 2 mM ATP or 2 mM AMP-PNP in column buffer at room temperature for 30 min and subsequent addition of 25  $\mu$ M CM. At various time points, 10 mM DTT was added to the corresponding aliquots to stop the reaction.

**Hybrid and Double Mutant F<sub>1</sub>F<sub>0</sub> Preparation**—ECF<sub>1</sub>F<sub>0</sub> from wild-type and  $c$  subunit mutant strains was prepared by KSCN extraction of purified ECF<sub>1</sub>F<sub>0</sub> reconstituted into vesicles of egg lecithin as described previously (19). These ECF<sub>1</sub>F<sub>0</sub>-containing membranes were centrifuged at 150,000 × *g* for 30 min at 4 °C in a Beckman TLA100.2 rotor and resuspended at 1 mg/ml in Buffer A (50 mM MOPS, pH 7.0, 10%

glycerol, 2 mM MgCl<sub>2</sub>) with 1 mM DTT and 5 mM ATP. ECF<sub>1</sub> from the mutant  $\gamma$ Y205C (1 mg/ml) was added, and samples were incubated for 10 h at 22 °C. Excess unbound ECF<sub>1</sub> and reducing agent were removed by washing the membranes twice by centrifugation at 150,000 × *g* for 30 min at 4 °C. Samples were resuspended in Buffer A to a final concentration of 1 mg/ml with or without DTT depending on the experiment to be performed.

ECF<sub>1</sub>F<sub>0</sub> containing a Cys at  $\gamma$ 205 and one of the  $\epsilon$  subunit mutations reconstituted as above was pelleted and resuspended in a buffer containing 10 mM Hepes, pH 7.5, 100 mM KCl, 5 mM MgCl<sub>2</sub>, and 10% glycerol (Buffer B).

**CuSO<sub>4</sub>/1,10-Phenanthroline and DTNB-induced Cross-linking**—Hybrid enzyme complexes, along with ECF<sub>1</sub>F<sub>0</sub> isolated from double mutants, that contained the subunit  $c$  mutations were suspended at 1 mg/ml in Buffer A and then reacted with CuSO<sub>4</sub>/1,10-phenanthroline (30  $\mu$ M) for 1 h at 22 °C. Hybrid forms of ECF<sub>1</sub> were cross-linked by incubating ECF<sub>1</sub>\* (ECF<sub>1</sub> from which both the  $\delta$  and  $\epsilon$  have been removed) (16) from the mutant  $\gamma$ Y205C with a 10-fold excess of pure  $\epsilon$  subunit in 50 mM MOPS, pH 7.0, 5 mM MgCl<sub>2</sub>, 10% glycerol, before adding CuCl<sub>2</sub> to a final concentration of 200  $\mu$ M. Hybrid ECF<sub>1</sub>F<sub>0</sub> complexes containing  $\epsilon$  subunit mutations were suspended at 1 mg/ml in the Buffer B and reacted with 200  $\mu$ M CuCl<sub>2</sub>. The reaction was quenched in each case by the addition of 10 mM EDTA. The reaction mixtures were assayed immediately for ATPase activity or frozen at –20 °C for subsequent SDS-polyacrylamide gel electrophoresis (PAGE). DTNB cross-linking was carried out by incubating ECF<sub>1</sub>F<sub>0</sub> at 1 mg/ml in Buffer A with 200  $\mu$ M DTNB for 1 h at 22 °C. The DTNB-treated samples were divided into two aliquots, and 20 mM DTT was added to one, before incubating both for 30 min at 22 °C. Samples were then assayed for ATPase activity and ACMA fluorescence quenching and subjected to SDS-PAGE.

ECF<sub>1</sub>F<sub>0</sub> was reacted with 200  $\mu$ M BM following the same procedure used for DTNB. The reaction was stopped after 1 h by a 30-min incubation with 20 mM DTT at room temperature.

**ACMA Fluorescence Quenching**—Assays of ACMA fluorescence quenching were performed essentially as described in Aggeler *et al.* (19). ECF<sub>1</sub>F<sub>0</sub> was reconstituted into egg lecithin vesicles as described before (12), except that 0.75% sodium deoxycholate was used in the column buffer, and 2 mg/ml of egg lecithin was used in the reconstitution step. These vesicles were collected by centrifugation and resuspended to a protein concentration of 20  $\mu$ g/ml in 10 mM Hepes, pH 7.5, 100 mM KCl and 2 mM MgCl<sub>2</sub>, and then valinomycin (3.6  $\mu$ M), ACMA (31  $\mu$ M), ATP (1 mM), and nigericin (3.6  $\mu$ M) were added sequentially. ACMA fluorescence was measured at 480 nm with an excitation wavelength of 410 nm in an SLM8000 fluorometer.

**Other Methods**—Samples for SDS-PAGE were supplemented with 20 mM NEM and incubated for 30 min at 22 °C prior to addition of one-half volume of dissociation buffer (10% SDS, 100 mM Tris, pH 6.8, 30% glycerol, and 0.03% bromophenol blue) with or without reducing agent as indicated. Subunits were separated by electrophoresis on 10–22% polyacrylamide gradient gels (24). Protein bands on SDS-PAGE were visualized by staining with Coomassie Brilliant Blue R according to Downer *et al.* (25). Proteins were transferred from the gel to polyvinylidene difluoride (Millipore Corp.) as described previously (12). The mouse monoclonal antibody to  $\gamma$ , anti- $\gamma$ <sub>II</sub>, was characterized previously (26). The rabbit antiserum to subunit  $c$  was described by Girvin *et al.* (27). Immunodetection was by the alkaline phosphatase method. ATPase activities were performed according to Löttscher *et al.* (28). 500  $\mu$ M dicyclohexylcarbodiimide was used in inhibitor studies because of the large excess of phospholipid. Protein concentrations were determined by the BCA protein assay from Pierce. Quantitation of [<sup>14</sup>C]NEM incorporated into  $\gamma$  Cys-205 was carried out as described previously (e.g. Ref. 15).

#### RESULTS

**Characterization of ECF<sub>1</sub> and ECF<sub>1</sub>F<sub>0</sub> Isolated from the Mutant  $\gamma$ Y205C**—ECF<sub>1</sub> isolated from the mutant  $\gamma$ Y205C contained  $\alpha$ ,  $\beta$ ,  $\gamma$ ,  $\delta$ , and  $\epsilon$  subunits in the same relative amounts as wild-type strain, whereas ECF<sub>1</sub>F<sub>0</sub> isolated from the mutant had the same subunit composition as wild type based on SDS-polyacrylamide gel electrophoresis (see later).

The ATPase activity of ECF<sub>1</sub> isolated from the mutant  $\gamma$ Y205C was around 3.5-fold higher than for wild-type enzyme (Table I). This is due to an altered binding of the inhibitory  $\epsilon$  subunit, as demonstrated by the concentration dependence of the inhibition of ECF<sub>1</sub>\* (16) by purified  $\epsilon$  subunit. ECF<sub>1</sub>\* from

<sup>1</sup> The abbreviations used are: ECF<sub>1</sub>, soluble portion of the *E. coli* F<sub>1</sub>F<sub>0</sub> ATP synthase; ECF<sub>1</sub>F<sub>0</sub>, membrane-bound portion of the *E. coli* F<sub>1</sub>F<sub>0</sub> ATP synthase; ECF<sub>1</sub>F<sub>0</sub>, *E. coli* F<sub>1</sub>F<sub>0</sub> ATP synthase; ACMA, 9-amino-6-chloro-2-methoxy acridine; DTNB, 5,5'-dithio-bis(2-nitro-benzoic acid); DTT, dithiothreitol; MOPS, 3-(N-morpholino) propanesulfonic acid; AMP-PNP, 5'-adenylyl- $\beta$ , $\gamma$ -imidodiphosphate; PAGE, polyacrylamide gel electrophoresis; NEM, *N*-ethylmaleimide; mAb, monoclonal antibody; BM, benzophenone maleimide; TFPAM-3 tetrafluorophenylazide maleimide-3.

TABLE I  
ATPase activity of  $ECF_1$  or  $ECF_1F_0$

Numbers are averages of duplicate measurements unless the number of measurements is shown in the parenthesis. DCCD, dicyclohexylcarbodiimide. ND, not determined.

$ECF_1$	$\gamma Y205C$	$\gamma Y205C + CM$	$\gamma Y205C + TFPAM-3$	$\gamma Y205C-\epsilon$	Wild-type
Activity	36 (5)	68	65	69 (6)	10 (5)
$ECF_1F_0$	$\gamma Y205C$	$\gamma Y205C + NEM$	$\gamma Y205C + TFPAM-3$	$\gamma Y205C + CM$	Wild-type
Activity	26	26	25	25	22
DCCD inhibition (%)	15 (2)	ND	ND	ND	73 (2)

the mutant  $\gamma Y205C$  showed half-maximal inhibition at a concentration of 16 nM of added pure  $\epsilon$  subunit, compared with only 9 nM for  $ECF_1^*$  from wild type (result not shown). ATPase activity was also measured in  $ECF_1F_0$  isolated from the mutant  $\gamma Y205C$ . In the intact ATP synthase, the rate of ATP hydrolysis was essentially the same as that of wild-type enzyme (Table I).

$ECF_1F_0$  isolated from the mutant  $\gamma Y205C$  showed ATP hydrolysis linked to proton translocation, but this was somewhat less efficient than observed for wild-type enzyme under equivalent conditions (see below), implying that the mutation  $\gamma Y205C$  caused some disruption of the  $F_1$ - $F_0$  interface.  $ECF_1F_0$  from the mutant also showed a significantly lower sensitivity to dicyclohexylcarbodiimide than wild-type enzyme (Table I).

**Reaction of  $\gamma$  Cys-205 with Maleimides under Different Nucleotide Conditions**—The Cys introduced at residue 205 of the  $\gamma$  subunit was reactive to a variety of maleimides in both  $ECF_1$  and  $ECF_1F_0$  isolated from the mutant  $\gamma Y205C$ . As shown in Table I, reaction of  $\gamma$  Cys-205 in  $ECF_1$  with CM or TFPAM-3 (without photolysis) resulted in an increase in activity such that with these bulky maleimides, the modified enzyme had the same activity as  $\epsilon$ -free  $ECF_1$  (from either the mutant  $\gamma Y205C$  or wild-type enzyme). After reaction of  $ECF_1^*$  from the mutant  $\gamma Y205C$  with CM to modify the introduced Cys, there was essentially no inhibition of ATPase activity on addition of a large excess of purified  $\epsilon$  subunit. The Cys at residue 205 was also reactive to maleimides in  $ECF_1F_0$ , but in this case, the modification did not activate the enzyme significantly (Table I).

The rates of incorporation of [ $^{14}$ C]NEM and the fluorescent maleimide CM into  $\gamma$  Cys-205 were compared under different nucleotide conditions. In  $ECF_1$  and  $ECF_1F_0$ , the rate of modification of this Cys by both reagents was significantly faster when ATP (as AMP-PNP +  $Mg^{2+}$ ) was bound in catalytic sites than with ADP present (generated on the enzyme by adding ATP +  $Mg^{2+}$  and allowing turnover for 30 min). With [ $^{14}$ C]NEM, there was twice as much reagent incorporated into  $\gamma$  Cys-205 within 2 min in AMP-PNP +  $Mg^{2+}$  compared with in ADP +  $P_i$  +  $Mg^{2+}$  (result not shown). Fig. 1A shows the time course of reaction with CM in AMP-PNP +  $Mg^{2+}$  (left side) compared with ADP +  $P_i$  +  $Mg^{2+}$  (right side), whereas Fig. 1B summarizes the reactivity of  $\gamma$  Cys-205 in  $ECF_1$ ,  $ECF_1^*$  and  $ECF_1F_0$ . In  $ECF_1^*$ , there was no nucleotide dependence in the reactivity of  $\gamma$  Cys-205 to CM. With ADP +  $P_i$  +  $Mg^{2+}$  bound, the rate of modification was as fast as in AMP-PNP +  $Mg^{2+}$ .

**Studies with Reconstituted  $ECF_1F_0$  Establish the Proximity of  $\gamma$  Cys-205 to the Polar Loop Region of the  $c$  Subunits**— $F_1$  purified from the  $\gamma$  subunit mutant  $Y205C$  was reconstituted with membrane vesicles containing  $F_0$  isolated from the  $c$  subunit mutants cA39C, cQ42C, cP43C, and cD44C (see "Experimental Procedures"). Cross-linking within the reconstituted  $ECF_1F_0$  complexes was induced by the addition of  $Cu^{2+}$  (1,10-phenanthroline). Fig. 2 shows the results obtained using a hybrid enzyme  $ECF_1(\gamma Y205C)F_0(cQ42C)$ . The oxidizing reagent generated a cross-link between the  $\gamma$  subunit and  $c$  subunit of apparent  $M_r$  38,000 that was readily observed in Coomassie Blue-stained gels. Based on the disappearance of the  $\gamma$

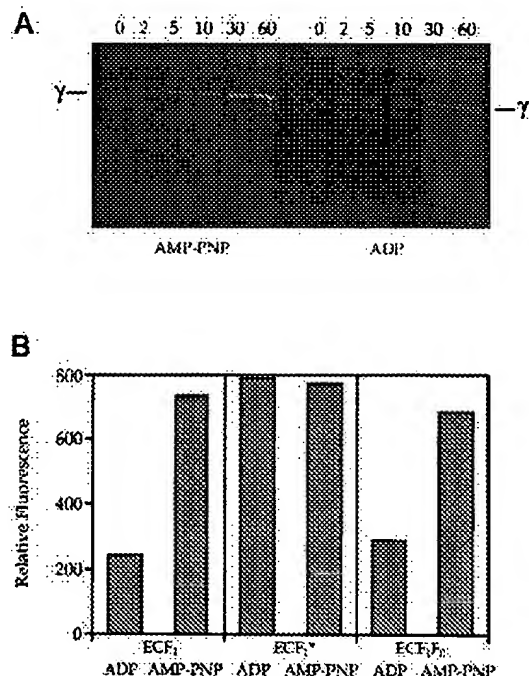


Fig. 1. Nucleotide-dependent labeling of residue  $\gamma Y205C$  in  $ECF_1F_0$ ,  $ECF_1$ , and  $ECF_1^*$ . A, a time course of CM labeling of  $\gamma Y205C$  residue in  $ECF_1F_0$ . At the times (min) indicated, addition of 10 mM DTT was made to quench the unreacted CM. First six lanes,  $Mg^{2+}$ /AMP-PNP; last six lanes,  $Mg^{2+}$ /ADP/ $P_i$ . B, the relative fluorescence intensity of the  $\gamma$  subunit after labeling with CM for 2 min under two nucleotide conditions ( $Mg^{2+}$ /ADP/ $P_i$  and  $Mg^{2+}$ /AMP-PNP) for different preparations. In  $ECF_1$  or  $ECF_1^*$ , a CM concentration of 5  $\mu$ M was used. To quantitate the fluorescence intensity of the bands in the gels, pictures were taken with a transilluminator (Spectroliner, Model 302) and then scanned with EPSON scanner. The images from scanning were quantitated with the NIH Image program. The ATPase preparation and the nucleotide condition for CM labeling are below the barograph.

subunit, the yield of cross-linked product was 95%. No cross-linked product involving  $\gamma$  and  $c$  was observed in  $ECF_1F_0$  from the single mutant  $\gamma Y205C$  or in  $ECF_1F_0$  from the single mutant cQ42C after  $Cu^{2+}$  treatment. The  $M_r$  38,000 product was lost and the  $\gamma$  subunit (monomer) reappeared in the gel profile when  $Cu^{2+}$ -treated samples were incubated with DTT prior to electrophoresis (result not shown), confirming that the cross-link is a disulfide bond between the introduced Cys in  $\gamma$  and that in the  $c$  subunit.

As shown by the Western blot in Fig. 2B, there was also  $Cu^{2+}$ -induced generation of the  $M_r$  38,000 cross-linked product of  $\gamma$  and  $c$  subunits in the hybrid mutants  $ECF_1(\gamma Y205C)F_0(cP43C)$  and  $ECF_1(\gamma Y205C)F_0(cD44C)$ . This product was lost on the addition of DTT with both mutants. No cross-linking between the  $\gamma$  and  $c$  subunits was obtained using the hybrid enzyme  $ECF_1(\gamma Y205C)F_0(cA39C)$  (result not shown). There were additional cross-linked products in small amounts con-



taining  $\gamma$  and  $c$ , particularly in the mutant  $ECF_1(\gamma Y205C)F_0$  (cD44C) (see Fig. 2B), some of which did not disappear with DTT treatment. These probably involve the Cys on the  $c$  subunit with remaining Tyr residues in the  $\gamma$  subunit region 205–228, particularly Tyr-207. One band migrating just above the main  $\gamma$ - $c$  product could be a cross-link between  $\gamma$  and two  $c$  subunits, one via a Cys-Cys linkage involving Cys-205, the second a Cys-Tyr linkage to Tyr-207.

The Western blotting data in Fig. 2B show that with all three hybrid mutants,  $Cu^{2+}$  also induced considerable subunit  $c$  dimer formation. Dimers of subunit  $c$  have been observed in the studies of Zhang and Fillingame (18), as well as in our previous studies using mutants with Cys residues in the polar loop region of the  $c$  subunit (12).

ATPase activities were measured before and after cross-linking. For the mutant  $ECF_1(\gamma Y205C)F_0$ (cQ42C), a 95% cross-linking of  $\gamma$  to  $c$  caused at most a 30% inhibition of ATP hydrolysis. This inhibition is most likely partly due to subunit  $c$  dimer formation, because there was a similar loss of ATPase activity when  $ECF_1F_0$  from the single mutant cQ42C was reacted with  $Cu^{2+}$  (result not shown).

Cross-linking of the  $\gamma$  subunit to a  $c$  subunit could also be induced by adding DTNB instead of  $Cu^{2+}$ . Fig. 3 shows data obtained with the double mutant  $\gamma Y205C:cQ42C$ . In the experiment in Fig. 3A, the yield of  $\gamma$ - $c$  cross-linked product was 50% based on the disappearance of  $\gamma$  (lane 2), compared with a 95% cross-linking yield in the double mutant when  $Cu^{2+}$  was used (lane 3). Note that a small amount of cross-linking of  $\gamma$  to  $c$  occurs in the absence of DTNB, probably due to oxidation reactions during sample preparation and incubations. Western blotting results in Fig. 3B confirm the cross-linking and show the greater selectivity of DTNB in generating the  $\gamma$ - $c$  cross-linked product over the subunit  $c$  dimer even under conditions where the  $\gamma$ - $c$  product obtained with  $Cu^{2+}$  is in nearly the same yield as with DTNB. We assume that at the levels of DTNB used, Cys residues in the  $c$  subunit are modified more rapidly than the Cys at position 205 in the  $\gamma$  subunit. With most or all of the Cys of  $c$  modified, disulfide bond formation between these sites is prevented. One of the DTNB modified  $c$  subunit monomers then reacts with unmodified  $\gamma$  Cys-205 to generate the  $\gamma$ - $c$  cross-linked product.

Table II lists the ATPase activities of the mutant after reaction with DTNB. Reaction of the double mutant with DTNB to generate around a 50% yield of cross-linked product  $\gamma$ - $c$  caused an approximately 10–15% reduction in ATP hydrolysis. This compares with an approximately 40% inhibition of ATPase activity for  $ECF_1F_0$  from the single mutant cQ42C but no inhibition of  $ECF_1F_0$  from the mutant  $\gamma Y205C$  after the identical DTNB treatment. Apparently, in the double mutant, the modification of both  $\gamma$  Cys-205 and  $c$  Cys-42 in some enzyme molecules compensates for the inhibition due to DTNB reaction with  $c$  Cys-42 alone.

**A Cys at Position 205 of the  $\gamma$  Subunit Forms Disulfide Bonds with Cys Residues Introduced at Positions 38 or 43 of the  $\epsilon$  Subunit**—In the course of our recent studies, we have made several mutants containing a Cys in the  $\epsilon$  subunit (14, 16). These include  $\epsilon S10C$ ,  $\epsilon H38C$ ,  $\epsilon T43C$ ,  $\epsilon S65C$ , and  $\epsilon S108C$ .  $ECF_1^*$  (the  $\alpha_3\beta_3$   $\gamma$  complex) isolated from the mutant  $\gamma Y205C$  was combined with each of the above-listed  $\epsilon$  subunit mutants to examine the proximity of Tyr-205 to the  $\epsilon$  subunit. In each case, the mutant  $\epsilon$  subunit was added in a 10-fold molar excess to ensure full occupancy of the  $\epsilon$  binding site. Samples were treated with 200  $\mu M$   $Cu^{2+}$  to induce disulfide bond formation. This led to cross-linking of  $\epsilon$  to the  $\gamma$  subunit in the hybrids made with  $\epsilon H38C$  and  $\epsilon T43C$  but not with  $\epsilon S10C$ ,  $\epsilon S65C$ , or  $\epsilon S108C$  (result not shown). This cross-linking of  $\gamma$  to  $\epsilon$  had little

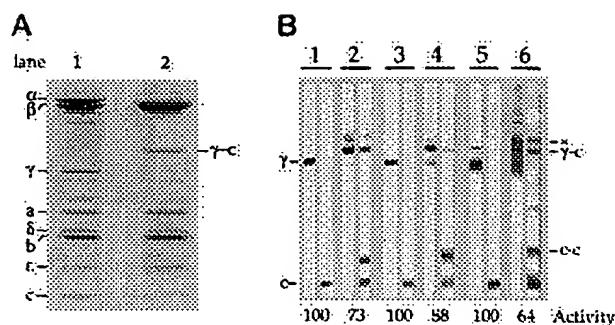


FIG. 2. Cross-linking between the  $\gamma$  subunit of  $ECF_1\gamma Y205C$  and the  $c$  subunit of  $ECF_0$  mutants cQ42C, cP43C and cD44C. A, Coomassie Brilliant Blue-stained gel of  $F_1\gamma Y205C/F_0cQ42C$  (lane 1), untreated control; (lane 2)  $CuSO_4/1,10$ -phenanthroline-treated enzyme. B, immunoblots of untreated and  $CuSO_4/1,10$ -phenanthroline-treated samples of hybrid  $ECF_1F_0$ s ( $F_1\gamma Y205C/F_0cQ42C$ , lanes 1 and 2;  $F_1\gamma Y205C/F_0cP43C$ , lanes 3 and 4; and  $F_1\gamma Y205C/F_0cD44C$ , lanes 5 and 6), probed with either monoclonal antibody  $\gamma_{III}$  (left-hand strip of each set) or antiserum to subunit  $c$  (right-hand strip of each set). The asterisk denotes the band corresponding to the  $\gamma$ - $c_2$  cross-linked product mentioned in the text. For each mutant, the two left-hand lanes are untreated, and the right-hand lanes are  $Cu^{2+}$ -treated samples.

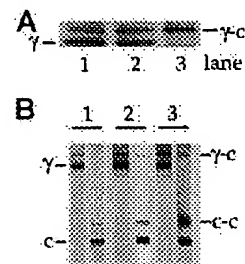


FIG. 3. Comparison of DTNB and  $CuSO_4/1,10$ -phenanthroline cross-link induction in purified  $ECF_1F_0\gamma Y205C/cQ42C$ . A, Coomassie-stained gel showing the  $\gamma$  and  $\gamma$ - $c$  bands for untreated (lane 1), DTNB-treated (lane 2), and  $CuSO_4/1,10$ -phenanthroline-treated (lane 3)  $ECF_1F_0$  from the mutant  $\gamma Y205C/cQ42C$  run under nonreducing conditions of SDS-PAGE. B, immunoblots of samples: untreated (lane 1), DTNB-treated (lane 2), and  $CuSO_4/1,10$ -phenanthroline-treated  $ECF_1F_0$  (lane 3). Strips were probed with either monoclonal antibody  $\gamma_{III}$  (left-hand strip of each pair) or antiserum to subunit  $c$  (right-hand strip of each pair).

effect on the rates of ATP hydrolysis.

Cross-linking studies were also conducted in  $ECF_1F_0$ . For these experiments,  $ECF_1F_0$  from wild type was stripped of  $F_1$  and these  $F_0$ -containing membranes were then reconstituted with the  $\alpha_3\beta_3$   $\gamma$  complex from the mutant  $\gamma Y205C$ , along with purified  $\delta$  subunit and one of the different  $\epsilon$  subunit mutants. After the reconstitution step, membranes were separated from excess  $\delta$  and  $\epsilon$  subunits prior to addition of  $Cu^{2+}$ . There was  $Cu^{2+}$ -induced cross-linking of the  $\gamma$  to the  $\epsilon$  subunit in hybrids containing the mutations  $\epsilon H38C$  (maximum yields 50%) and  $\epsilon T43C$  (yields as high as 90%) but not with the other  $\epsilon$  subunit mutants. As in  $ECF_1$ , the cross-linked product  $\gamma$ - $\epsilon$  ran very close to the  $\beta$  subunit in SDS-PAGE and was best observed in Western blotting experiments, such as in Fig. 4 (A and B). The monoclonal antibody anti- $\gamma_{III}$  was used for analysis (Fig. 4A). This mAb, like the others we have obtained to the  $\gamma$  subunit, reacted close to Tyr-205 (see Ref. 29), giving only a weak reaction with the  $\gamma$ - $\epsilon$  cross-linked product. As a result, high concentrations of the mAb had to be used and mAb  $\gamma_{III}$  then cross-reacted with the  $\alpha$  subunit. Nevertheless, Fig. 4 (A and B) shows clearly the disappearance of  $\gamma$  and  $\epsilon$  and appearance of the  $\gamma$ - $\epsilon$  cross-linked in  $ECF_1F_0$  containing  $\gamma$  Cys-205 and  $\epsilon$  Cys-38 (lanes 3) or  $\epsilon$  Cys-43 (lanes 4). The yield of cross-linking was estimated from Coomassie Brilliant Blue-stained gels. Fig.

TABLE II  
Effect of treatment with DTNB and BM on the ATPase activity of  $ECF_1F_0$  preparations from various mutants

Mutant	Treatment	ATPase activity <sup>a</sup>
		%
cQ42C	Untreated control	100
	+DTNB +DTT	98
	+DTNB	61
$\gamma$ Y205C	Untreated control	100
	+DTNB +DTT	100
	+DTNB	100
$\gamma$ Y205C/cQ42C	Untreated control	100
	+DTNB +DTT	104
	+DTNB	87
	+BM	100

<sup>a</sup> Values are expressed as a percentage of remaining activity compared with the untreated control. Values represent the average of results from two experiments.

4C shows data for  $Cu^{2+}$ -induced cross-linking of  $ECF_1F_0$  containing the  $\gamma$ Y205C and  $\epsilon$ T43C mutations. The yield of cross-linking in this experiment, calculated from the change in area of the  $\gamma$  subunit band using the  $\alpha$  subunit band as a control, was 55%. This was accompanied by a 20% loss of ATPase activity.

**Effect of Chemical Modification of  $\gamma$  Cys-205 and Cross-linking of  $\gamma$  to  $\epsilon$  or  $c$  Subunits on Proton Pumping**— $ECF_1F_0$  from the  $\gamma$ Y205C mutant or the mutant cQ42C showed a reduced proton pumping activity compared with wild-type enzyme, when measured by the ACMA fluorescence quenching assay (compare Fig. 5, traces A and B). Modification of the introduced Cys-205 with several maleimides (result not shown) or by DTNB reduced the levels of proton pumping by the mutant further. With DTNB reaction, proton pumping activity was partly recovered on adding DTT (Fig. 5A). Maleimide or DTNB modification of  $ECF_1F_0$  isolated from the mutant cQ42C also had a small effect on the proton pumping activity (Fig. 5B), whereas DTNB modification of the double mutant  $\gamma$ Y205C:cQ42C caused essentially full loss of ATP-driven proton pumping (Fig. 5C), which was also mostly recovered on DTT addition. This essentially full inhibition occurred with around a 50% yield of cross-linking of  $\gamma$  to  $c$ , suggesting that it was the chemical modification of both sites in the complex rather than the cross-linking that was responsible. As shown by Fig. 5 (trace D), reaction of the mutant  $\gamma$ Y205C:cQ42C with benzophenone maleimide likewise caused full loss of proton pumping activity. This reagent reacts with the introduced Cys residues but does not induce disulfide bond formation. The proton pumping activity of benzophenone maleimide-modified enzyme was not recovered upon the addition of DTT.

Attempts were made to measure the proton pumping activity after  $Cu^{2+}$  treatment of various double mutants including both the Cys at  $\gamma$  205 and mutations in the  $\epsilon$  or  $c$  subunits described above. The combination of mutations  $\gamma$ Y205C and  $\epsilon$ H38C was found to abolish ATP-driven proton pumping, whereas each mutation individually retained this activity.  $Cu^{2+}$  treatment to induce cross-linking greatly reduced the proton pumping activity of all mutants tested under conditions where ATPase activity was retained. However, this treatment inhibited proton pumping activity to 80% even in wild-type enzyme, an inhibition that was only partly regained by incubation with DTT. As a consequence, the effect of cross-linking on proton pumping was not pursued further.

#### DISCUSSION

The studies described here extend our original finding (12) that oxidizing conditions generate a covalent cross-link between a Cys introduced at position 44 of the  $c$  subunit of the  $F_0$  and the  $\gamma$  subunit of the  $F_1$  part of  $ECF_1F_0$ . Here Tyr-205, one

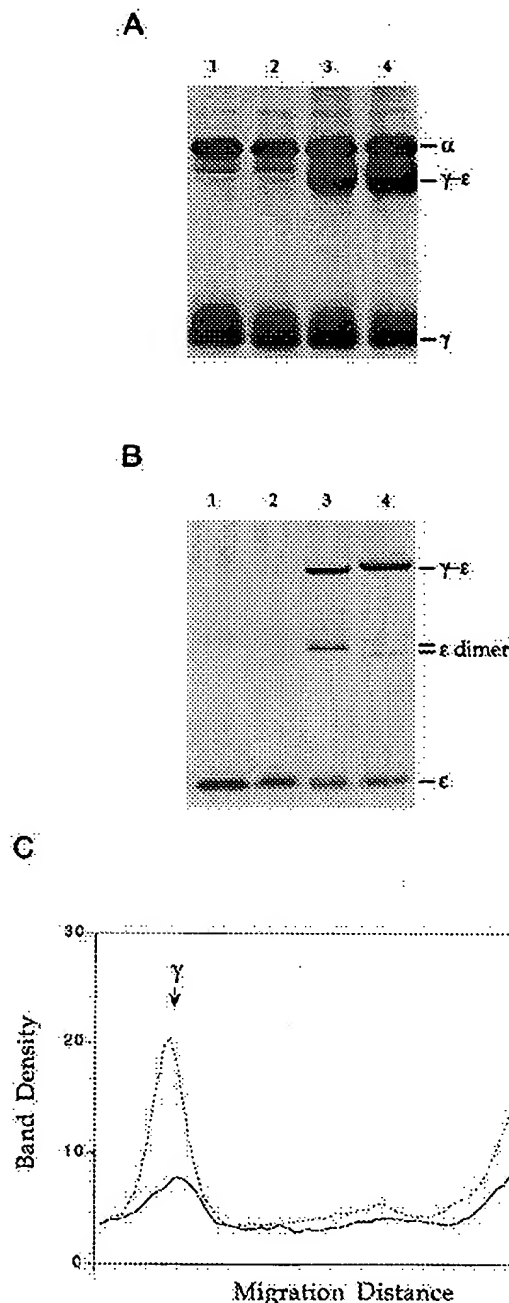


FIG. 4. Cross-linking between  $\gamma$ Y205C and sites on the  $\epsilon$  subunit in  $ECF_1F_0$ . A, Western blot analyzed with mAb anti- $\gamma_{III}$  using a 12% SDS-polyacrylamide mini gel to separate the  $\gamma$ - $\epsilon$  product from  $\alpha$  and  $\beta$  subunits. This mAb also had significant reaction with the  $\alpha$  subunit under the conditions used. The reactivity with the  $\gamma$  subunit is diminished in the cross-linked product, probably because of steric effects, and so the Western blot was heavily over-exposed. B, Western blot analyzed with the anti- $\epsilon$  antibody after identical  $Cu^{2+}$  treatments. Lane 1, wild-type enzyme; lane 2,  $\epsilon$ S10C; lane 3,  $\epsilon$ H38C; lane 4,  $\epsilon$ T43C. C, density scanning profile of  $ECF_1F_0$  reconstituted with the  $\gamma$ Y205C,  $\alpha_3\beta_3$   $\gamma$  complex, and  $\epsilon$ T43C. The dotted line shows untreated enzyme. The solid line is after treatment with  $Cu^{2+}$ . The region of the SDS-polyacrylamide gel (10–22%) between the  $\gamma$  and  $\alpha$  subunit is shown to demonstrate the disappearing gradient of the  $\gamma$  subunit by cross-linking to the  $\epsilon$  subunit.

of four Tyr residues in the short stretch of the  $\gamma$  subunit identified as involved in the cross-linking reaction with the  $c$  subunits, has been replaced by a Cys.  $ECF_1$  from the mutant,

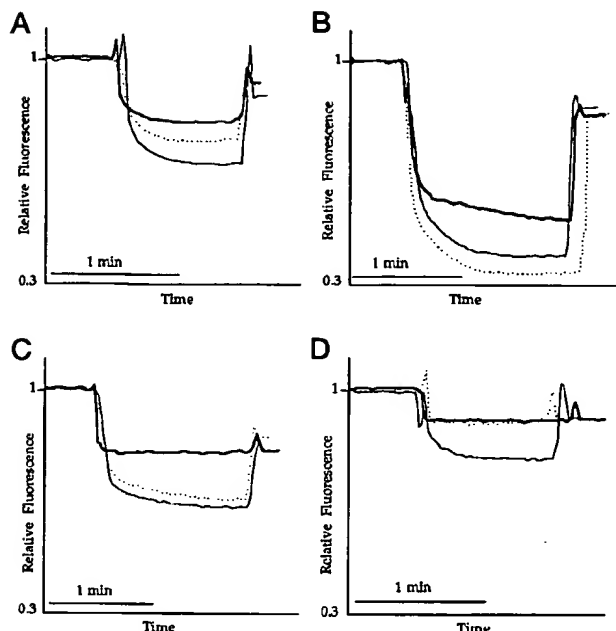


FIG. 5. Effect on ATP-coupled  $H^+$  translocation of DTNB and benzophenone maleimide modification of the enzyme.  $ECF_1F_0$   $\gamma Y205C$  (A),  $ECF_1F_0$  cQ42C (B), and  $ECF_1F_0$   $\gamma Y205C/cQ42C$  (C and D). A–C, untreated control (thin line), DTNB treated (thick line), and DTNB-treated followed by reduction with DTT (dotted line). In D, benzophenone maleimide was used as the modifying reagent. Traces represent the results from a single experiment, but in each case equivalent results were obtained in several experiments.

$\gamma Y205C$ , had an increased ATPase activity due to an altered affinity of the  $\alpha_3\beta_3$   $\gamma$  core complex for the inhibitory  $\epsilon$  subunit, but the ATPase activity of the intact  $ECF_1F_0$  was not altered compared with wild type by the mutation. The Tyr  $\rightarrow$  Cys change also caused a small reduction in efficiency of ATP-driven proton translocation when measured by the ACMA quenching assay, but the  $ECF_1F_0$  clearly retained this coupling function.

A key finding of the present study is that the Cys in  $\gamma$  at position 205 can be cross-linked to Cys residues introduced in the c subunits at positions 42, 43, or 44 in essentially full yield by  $Cu^{2+}$  treatment and in good yield by reaction with DTNB. This establishes that the  $\gamma$  subunit extends the full 40–45 Å of the stalk. The other subunit now known to extend the entire length of the stalk is the  $\epsilon$  subunit (13). In addition to covalent linkage to the c subunits,  $\gamma$  Cys-205 could also be cross-linked to the  $\epsilon$  subunit via Cys residues in this subunit at positions 38 and 43 (but not at positions 65 or 108). Residues 38 and 43 are at one end of the 10-stranded  $\beta$  sandwich structure constituted by the N-terminal domain of the  $\epsilon$  subunit (13). This end has been shown to interact with the c subunit oligomer by a combination of genetic and cross-linking experiments (17, 18).

The fact that  $\gamma$  Cys-205 can interact with Cys introduced into either the c subunits or the  $\epsilon$  subunit not only indicates the proximity of these sites but also emphasizes the dynamic character of the complex. The ATP synthase presumably switches between several conformations during energy coupling. In this regard, the observed nucleotide dependence of the reactivity of  $\gamma$  Cys-205 to maleimides is interesting. This site reacted significantly faster with maleimides in both isolated  $ECF_1$  and in  $ECF_1F_0$  in the ATP state (with Mg AMP-PNP bound) than in the ADP ( $Mg^{2+}$ ) state. We have previously observed nucleotide-dependent conformational changes in the  $\gamma$  subunit near catalytic sites (by cross-linking and fluorescence changes of probes attached at Cys introduced at position 8 (30)) at Cys-87 (by

changes in reactivity to maleimides (31)) and at position 106 (from fluorescence changes of CM bound to a Cys at this site (30)). The results for  $\gamma$  Cys-205 now establish that the conformational change occurring with ATP hydrolysis is propagated by the  $\gamma$  subunit from the catalytic sites to the interface of the  $F_1$  with  $F_0$ .

As with the conformational changes detected at other parts of the  $\gamma$  subunit (30, 31), the nucleotide dependence of the reaction of Cys-205 was lost on removal of the  $\epsilon$  subunit.  $ECF_1$  from which the  $\epsilon$  subunit has been removed is a highly active ATPase, and therefore, as we have discussed before (30, 31), the conformational changes observed at residues 8, 87, 106, and now 205 cannot be necessary for ATP hydrolysis. Rather, they likely represent structural changes that are part of the energy coupling within the complex that are in addition to rotation of the  $\gamma$  and  $\epsilon$  subunits that occurs during the cooperative functioning of catalytic sites (32–34).

The covalent linkage of  $\gamma$  via Cys-205 to the c subunits at positions 42, 43, or 44 proved to have very little effect on ATPase activity. A pattern of effects of covalent cross-linking of subunits to one another on enzyme function is emerging. Cross-linking of  $\gamma$  or  $\epsilon$  to  $\alpha$  or  $\beta$  subunits in our studies has in all cases fully inhibited ATPase activity (14–16, 35) (also see Ref. 36). In contrast, cross-linking of  $\gamma$  to  $\epsilon$  (14, 16) and now of  $\gamma$  to c subunits did not greatly reduce ATP hydrolysis. The implication is that the rotations or translocations of subunits that are a part of the cooperativity of catalytic sites must involve the  $\alpha_3\beta_3$  domain moving relative to  $\gamma$  and  $\epsilon$  plus the c subunit oligomer. This could occur by the  $\alpha_3\beta_3$  domain rotating relative to a fixed unit of the rest of the ATP synthase or the  $\gamma$ ,  $\epsilon$ , and c subunit oligomers rotating within a scaffold of the  $\alpha_3\beta_3$  domain plus the  $\delta$ , a, and b subunits.

It is not clear at present whether covalent cross-linking of  $\gamma$  to the c subunit oligomer alters proton pumping. It was not possible to assess this issue when  $Cu^{2+}$  oxidation was used to generate cross-links. After DTNB-induced cross-linking, there was complete loss of proton pumping without concomitant loss of ATPase activity, implying an uncoupling of the two functions. However, it was the maleimide modification of both  $\gamma$  Cys-205 and the adjacent Cys in the c subunits that caused the effect, not the cross-linking reaction *per se*.

**Acknowledgments**—The excellent technical assistance of Kathy Chicas-Cruz and useful discussions with our colleagues S. Wilkens, R. Aggeler, and G. Grüber are gratefully acknowledged.

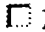
#### REFERENCES

- Senior, A. E. (1988) *Physiol. Rev.* 68, 177–231
- Senior, A. E. (1990) *Annu. Rev. Biophys. Biophys. Chem.* 19, 7–41
- Boyer, P. D. (1993) *Biochim. Biophys. Acta* 1140, 215–250
- Capaldi, R. A., Aggeler, R., Turina, P., and Wilkens, S. (1994) *Trends Biochem. Sci.* 19, 284–289
- Lunsdorf, H., Ehrig, K., Freidl, P., and Schairer, H. U. (1984) *J. Mol. Biol.* 173, 131–136
- Gogol, E. P., Lücken, U., Bork, T., and Capaldi, R. A. (1989) *Biochemistry* 28, 4709–4716
- Gogol, E. P., Aggeler, R., Sagermann, M., and Capaldi, R. A. (1989) *Biochemistry* 28, 4717–4724
- Dallmann, H. G., Flynn, T. G., and Dunn, S. D. (1992) *J. Biol. Chem.* 267, 18953–18960
- Gogol, E. P., Lücken, U., and Capaldi, R. A. (1987) *FEBS Lett.* 219, 274–278
- Lücken, U., Gogol, E. P., and Capaldi, R. A. (1990) *Biochemistry* 29, 5339–5343
- Abrahams, J. P., Leslie, A. G. W., Lutter, R., and Walker, J. E. (1994) *Nature* 370, 621–628
- Watts, S. D., Zhang, Y., Fillingame, R. H., and Capaldi, R. A. (1995) *FEBS Lett.* 368, 235–238
- Wilkens, S., Dahlquist, F. W., McIntosh, L. P., Donaldson, L. W., and Capaldi, R. A. (1995) *Nat. Struct. Biol.* 2, 961–967
- Aggeler, R., Chicas-Cruz, K., Cai, S.-X., Keana, J. F. W., and Capaldi, R. A. (1992) *Biochemistry* 31, 2956–2961
- Aggeler, R., Haughton, M. A., and Capaldi, R. A. (1995) *J. Biol. Chem.* 270, 9185–9191
- Tang, C., and Capaldi, R. A. (1996) *J. Biol. Chem.* 271, 3018–3024
- Zhang, Y., Oldenburg, M., and Fillingame, R. H. (1994) *J. Biol. Chem.* 269, 10221–10224
- Zhang, Y., and Fillingame, R. H. (1995) *J. Biol. Chem.* 270, 24609–24614

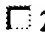
19. Aggeler, R., Weinreich, F., and Capaldi, R. A. (1995) *Biochim. Biophys. Acta* **1230**, 62–68
20. Aggeler, R., and Capaldi, R. A. (1992) *J. Biol. Chem.* **267**, 21355–21359
21. Walker, J. E., Gay, N. J., Saraste, M., and Eberle, A. N. (1984) *Biochem. J.* **244**, 799–815
22. Wise, J. G., Latchney, L. R., and Senior, A. E. (1981) *J. Biol. Chem.* **256**, 10383–10389
23. Aggeler, R., Zhang, Y.-Z., and Capaldi, R. A. (1987) *Biochemistry* **26**, 7107–7113
24. Laemmli, U. K. (1970) *Biochemistry* **9**, 4620–4626
25. Downer, N. W., Robinson, N. C., and Capaldi, R. A. (1976) *Biochemistry* **15**, 2930–2936
26. Aggeler, R., Mendel-Hartvig, J., and Capaldi, R. A. (1990) *Biochemistry* **29**, 10387–10393
27. Girvin, M. E., Hermolin, J., Pottorf, R., and Fillingame, R. H. (1989) *Biochemistry* **28**, 4340–4343
28. Lötscher, H.-R., deJong, C., and Capaldi, R. A. (1984) *Biochemistry* **23**, 4140–4143
29. Tang, C., Wilkens, S., and Capaldi, R. A. (1994) *J. Biol. Chem.* **269**, 4467–4472
30. Turina, P., and Capaldi, R. A. (1994) *J. Biol. Chem.* **269**, 13465–13471
31. Feng, Z., Aggeler, R., Haughton, M. A., and Capaldi, R. A. (1996) *J. Biol. Chem.* **271**, 17986–17989
32. Gogol, E. P., Johnston, E., Aggeler, R., and Capaldi, R. A. (1990) *Proc. Natl. Acad. Sci. U. S. A.* **87**, 9585–9589
33. Duncan, T. M., Bulygin, V. V., Zhou, H., Hutcheon, M. L., and Cross, R. L. (1995) *Proc. Natl. Acad. Sci. U. S. A.* **92**, 10964–10968
34. Aggeler, R., and Capaldi, R. A. (1996) *J. Biol. Chem.* **271**, 13888–13891
35. Aggeler, R., Cai, S. X., Keana, J. F. W., Koike, T., and Capaldi, R. A. (1993) *J. Biol. Chem.* **268**, 20831–20837
36. Musiers, K. M., and Hammes, G. G. (1987) *Biochemistry* **26**, 5982–5988

Items 1 - 20 of 470

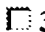
Page 1 of 24 Next

 1: [Watts SD, Tang C, Capaldi RA.](#)[Related Articles, Links](#)

The stalk region of the Escherichia coli ATP synthase. Tyrosine 205 of the gamma subunit is in the interface between the F1 and F0 parts and can interact with both the epsilon and c oligomer. J Biol Chem. 1996 Nov 8;271(45):28341-7. PMID: 8910457 [PubMed - indexed for MEDLINE]

 2: [Aggeler R, Weinreich F, Capaldi RA.](#)[Related Articles, Links](#)

Arrangement of the epsilon subunit in the Escherichia coli ATP synthase from the reactivity of cysteine residues introduced at different positions in this subunit. Biochim Biophys Acta. 1995 Jun 1;1230(1-2):62-8. PMID: 7612642 [PubMed - indexed for MEDLINE]

 3: [Zhang Y, Fillingame RH.](#)[Related Articles, Links](#)

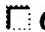
Subunits coupling H<sup>+</sup> transport and ATP synthesis in the Escherichia coli ATP synthase. Cys-Cys cross-linking of F1 subunit epsilon to the polar loop of F0 subunit c. J Biol Chem. 1995 Oct 13;270(41):24609-14. PMID: 7592682 [PubMed - indexed for MEDLINE]

 4: [Feng Z, Aggeler R, Haughton MA, Capaldi RA.](#)[Related Articles, Links](#)

Conformational changes in the Escherichia coli ATP synthase (ECF1F0) monitored by nucleotide-dependent differences in the reactivity of Cys-87 of the gamma subunit in the mutant betaGlu-381 --> Ala. J Biol Chem. 1996 Jul 26;271(30):17986-9. PMID: 8663500 [PubMed - indexed for MEDLINE]

 5: [Tang C, Capaldi RA.](#)[Related Articles, Links](#)

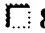
Characterization of the interface between gamma and epsilon subunits of Escherichia coli F1-ATPase. J Biol Chem. 1996 Feb 9;271(6):3018-24. PMID: 8621695 [PubMed - indexed for MEDLINE]

 6: [Ogilvie I, Aggeler R, Capaldi RA.](#)[Related Articles, Links](#)

Cross-linking of the delta subunit to one of the three alpha subunits has no effect on functioning, as expected if delta is a part of the stator that links the F1 and F0 parts of the Escherichia coli ATP synthase. J Biol Chem. 1997 Jun 27;272(26):16652-6. PMID: 9195980 [PubMed - indexed for MEDLINE]

 7: [Watts SD, Capaldi RA.](#)[Related Articles, Links](#)

Interactions between the F1 and F0 parts in the Escherichia coli ATP synthase. Associations involving the loop region of C subunits. J Biol Chem. 1997 Jun 13;272(24):15065-8. PMID: 9182524 [PubMed - indexed for MEDLINE]

 8: [Aggeler R, Haughton MA, Capaldi RA.](#)[Related Articles, Links](#)

Disulfide bond formation between the COOH-terminal domain of the beta subunits and the gamma and epsilon subunits of the Escherichia coli F1-ATPase. Structural implications and functional consequences. J Biol Chem. 1995 Apr 21;270(16):9185-91. PMID: 7721834 [PubMed - indexed for MEDLINE]

[Gruber G, Capaldi RA.](#)[Related Articles, Links](#)

9:



The trapping of different conformations of the Escherichia coli F1 ATPase by disulfide bond formation. Effect on nucleotide binding affinities of the catalytic sites.

J Biol Chem. 1996 Dec 20;271(51):32623-8.

PMID: 8955091 [PubMed - indexed for MEDLINE]

10: [Aggeler R, Mendel-Hartvig J, Capaldi RA.](#)[Related Articles, Links](#)

Monoclonal antibody modification of the ATPase activity of Escherichia coli F1 ATPase.

Biochemistry. 1990 Nov 13;29(45):10387-93.

PMID: 2148117 [PubMed - indexed for MEDLINE]

11: [Aggeler R, Capaldi RA.](#)[Related Articles, Links](#)

ATP hydrolysis-linked structural changes in the N-terminal part of the gamma subunit of Escherichia coli F1-ATPase examined by cross-linking studies.

J Biol Chem. 1993 Jul 15;268(20):14576-8.

PMID: 8392054 [PubMed - indexed for MEDLINE]

12: [Aggeler R, Capaldi RA.](#)[Related Articles, Links](#)

Nucleotide-dependent movement of the epsilon subunit between alpha and beta subunits in the Escherichia coli F1F0-type ATPase.

J Biol Chem. 1996 Jun 7;271(23):13888-91.

PMID: 8662953 [PubMed - indexed for MEDLINE]

13: [Aggeler R, Capaldi RA.](#)[Related Articles, Links](#)

Cross-linking of the gamma subunit of the Escherichia coli ATPase (ECF1) via cysteines introduced by site-directed mutagenesis.

J Biol Chem. 1992 Oct 25;267(30):21355-9.

PMID: 1400447 [PubMed - indexed for MEDLINE]

14: [Rodgers AJ, Capaldi RA.](#)[Related Articles, Links](#)

The second stalk composed of the b- and delta-subunits connects F0 to F1 via an alpha-subunit in the Escherichia coli ATP synthase.

J Biol Chem. 1998 Nov 6;273(45):29406-10.

PMID: 9792643 [PubMed - indexed for MEDLINE]

15: [Garcia JJ, Capaldi RA.](#)[Related Articles, Links](#)

Unisite catalysis without rotation of the gamma-epsilon domain in Escherichia coli F1-ATPase.

J Biol Chem. 1998 Jun 26;273(26):15940-5.

PMID: 9632641 [PubMed - indexed for MEDLINE]

16: [Schulenberg B, Aggeler R, Murray J, Capaldi RA.](#)[Related Articles, Links](#)

The gammaepsilon-c subunit interface in the ATP synthase of Escherichia coli. cross-linking of the epsilon subunit to the c subunit ring does not impair enzyme function, that of gamma to c subunits leads to uncoupling.

J Biol Chem. 1999 Nov 26;274(48):34233-7.

PMID: 10567396 [PubMed - indexed for MEDLINE]

17: [Aggeler R, Chicas-Cruz K, Cai SX, Keana JF, Capaldi RA.](#)[Related Articles, Links](#)

Introduction of reactive cysteine residues in the epsilon subunit of Escherichia coli F1 ATPase, modification of these sites with tetrafluorophenyl azide-maleimides, and examination of changes in the binding of the epsilon subunit when different nucleotides are in catalytic sites.

Biochemistry. 1992 Mar 24;31(11):2956-61.

PMID: 1532326 [PubMed - indexed for MEDLINE]

## The Na<sup>+</sup>-F<sub>1</sub>F<sub>0</sub>-ATPase Operon from *Acetobacterium woodii*

OPERON STRUCTURE AND PRESENCE OF MULTIPLE COPIES OF *atpE* WHICH ENCODE PROTEOLIPIDS OF 8- AND 18-kDa\*

(Received for publication, August 12, 1999, and in revised form, September 13, 1999)

Stefan Rahlfs†, Sascha Aufurth§, and Volker Müller§¶

From the ‡Institut für Mikrobiologie und Genetik der Georg-August-Universität, Grisebachstrasse 8, 37077 Göttingen, Germany and the §Lehrstuhl für Mikrobiologie der Ludwig-Maximilians-Universität, Maria-Ward-Strasse 1a, 80638 München, Germany

Eight genes (*atpI*, *atpB*, *atpE*<sub>1</sub>, *atpE*<sub>2</sub>, *atpE*<sub>3</sub>, *atpF*, *atpH*, and *atpA*) upstream of and contiguous with the previously described genes *atpG*, *atpD*, and *atpC* were cloned from chromosomal DNA of *Acetobacterium woodii*. Northern blot analysis revealed that the eleven *atp* genes are transcribed as a polycistronic message. The *atp* operon encodes the Na<sup>+</sup>-F<sub>1</sub>F<sub>0</sub>-ATPase of *A. woodii*, as evident from a comparison of the biochemically derived N termini of the subunits with the amino acid sequences deduced from the DNA sequences. The molecular analysis revealed that all of the F<sub>1</sub>F<sub>0</sub>-encoding genes from *Escherichia coli* have homologs in the Na<sup>+</sup>-F<sub>1</sub>F<sub>0</sub>-ATPase operon from *A. woodii*, despite the fact that only six subunits were found in previous preparations of the enzyme from *A. woodii*. These results unequivocally prove that the Na<sup>+</sup>-ATPase from *A. woodii* is an enzyme of the F<sub>1</sub>F<sub>0</sub> class. Most interestingly, the gene encoding the proteolipid underwent quadruplication. Two gene copies (*atpE*<sub>2</sub> and *atpE*<sub>3</sub>) encode identical 8-kDa proteolipids. Two additional gene copies were fused to form the *atpE*<sub>1</sub> gene. Heterologous expression experiments as well as immunolabeling studies with native membranes revealed that *atpE*<sub>1</sub> encodes a duplicated 18-kDa proteolipid. This is the first demonstration of multiplication and fusion of proteolipid-encoding genes in F<sub>1</sub>F<sub>0</sub>-ATPase operons. Furthermore, *atpE*<sub>1</sub> is the first duplicated proteolipid ever found to be encoded by an F<sub>1</sub>F<sub>0</sub>-ATPase operon.

*Acetobacterium woodii* is a strictly anaerobic, homoacetogenic bacterium which relies on a sodium ion potential across its membrane for energy-dependent reactions (1). The sodium ion potential is established by a yet not identified primary pump, connected to the acetyl-CoA pathway (2, 3). The Δμ<sub>Na<sup>+</sup></sub> established is used as driving force for flagellar rotation as well as ATP synthesis (3–6). The enzyme responsible for Δμ<sub>Na<sup>+</sup></sub>-driven ATP synthesis was purified and characterized as a Na<sup>+</sup>-translocating enzyme (7). It was characterized by immu-

nological methods, inhibitor studies, and by the molecular analysis of the genes encoding subunits γ, β, and ε as a Na<sup>+</sup>-F<sub>1</sub>F<sub>0</sub>-ATPase (8–10). A gene encoding subunit c was cloned, and the sequence analysis together with biochemical studies revealed residues potentially involved in Na<sup>+</sup> liganding in the proteolipid (11). To date, there are only two thoroughly studied examples in this class of Na<sup>+</sup>-F<sub>1</sub>F<sub>0</sub>-ATPases, the enzymes from *Propionigenium modestum* (12) and *A. woodii*.

Interestingly, the purified Na<sup>+</sup>-F<sub>1</sub>F<sub>0</sub>-ATPase of *A. woodii* contained only six polypeptides (7). Five were identified as subunits α, β, γ, ε, and c, respectively. Because all bacterial ATPases known to date contain eight non-identical subunits, two subunits (including at least one of the membrane-bound subunits a and b) were apparently missing in the purified enzyme. Nevertheless, the purified enzyme was capable of coupling ATP hydrolysis to Na<sup>+</sup> transport. A simpler architecture was also postulated for some F<sub>1</sub>F<sub>0</sub>-ATPases from phylogenetically related clostridia (13–15).

To determine whether the ATPase from *A. woodii* does indeed contain less subunits than the enzyme from *Escherichia coli*, an alternative way was chosen. To delineate the subunit composition of the enzyme, we chose a molecular approach taking advantage of the fact that (most) bacterial F<sub>1</sub>F<sub>0</sub>-ATPase encoding genes are organized in operons (16). Here we describe the cloning and characterization of a DNA region containing eight genes (*atpI*, *atpB*, *atpE*<sub>1</sub>, *atpE*<sub>2</sub>, *atpE*<sub>3</sub>, *atpF*, *atpH*, and *atpA*) upstream of and contiguous with the previously described genes *atpG*, *atpD*, and *atpC*.

### EXPERIMENTAL PROCEDURES

**Materials**—All chemicals used were reagent grade and purchased from Merck AG, Darmstadt, Germany. [<sup>35</sup>S]Methionine was from Hartmann Analytik, Braunschweig, Germany. Antibodies were prepared by Bioscience, Göttingen, Germany.

**Organisms and Plasmids**—*A. woodii* (DSMZ 1030) was obtained from the "Deutsche Sammlung für Mikroorganismen und Zellkulturen" (DSMZ), Braunschweig, Germany, and grown under strictly anaerobic conditions on carbonate-buffered medium supplemented with 0.4% glycine (17). *E. coli* DH5α (*supE*44 Δ*lac*U169 (Φ80*lacZ*Δ*M*15) *hsdR*17 *recA*1 *endA*1 *gyrA*96 *thi*1 *relA*1 (18)) was grown on Luria broth at 37 °C. *E. coli* DK6 (F<sup>–</sup>, Str<sup>r</sup>, *hsdR*, *minA*, *minB*, *purE*, *pdxC*, *his*, *ilv*, *met* Δ(*uncB-uncC*) (19)) at 30 °C on Luria broth plus 1% glucose. Plasmids used were pBluescript SK and KS (Stratagene), pACYC184 (20), pHSG398 and pHSG399 (21), and pMalc2X (New England Biolabs).

**Molecular Procedures**—Chromosomal DNA of *A. woodii* was isolated by a modified Marmur preparation as described before (11, 22), restricted, size-fractionated by gradient centrifugation, and cloned into pBluescript SK or pACYC184. All procedures used were standard techniques (23). Oligonucleotides were from Life Technologies, Inc. GmbH, Eggenstein, Germany. DNA sequence was determined by the chain termination method of Sanger (24) and analyzed on a VAX computer using the Wisconsin Genetics Computer Group sequence analysis software package, Version 8.1 (University of Wisconsin Biotechnology Cen-

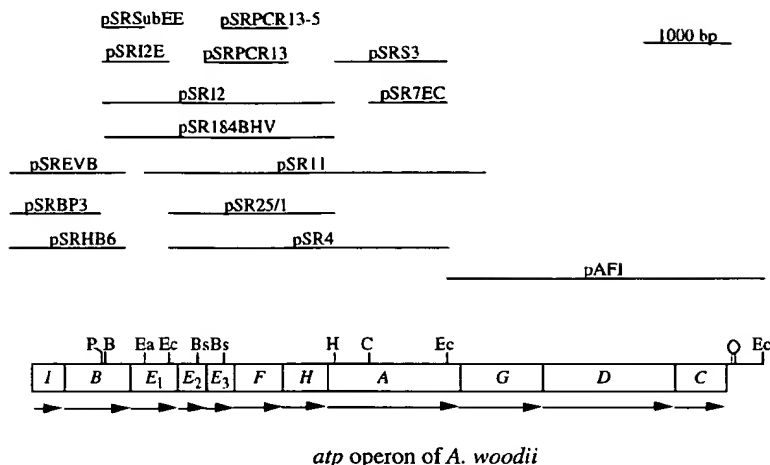
\* This work was supported by grants from the Deutsche Forschungsgemeinschaft (Graduiertenkolleg "Chemische Aktivitäten von Mikroorganismen" and Mu801/7–2/3). The costs of publication of this article were defrayed in part by the payment of page charges. This article must therefore be hereby marked "advertisement" in accordance with 18 U.S.C. Section 1734 solely to indicate this fact.

The nucleotide sequence(s) reported in this paper has been submitted to the GenBank™/EBI Data Bank with accession number(s) U10505.

¶ To whom correspondence should be addressed: Tel.: 49-89-21806126; Fax: 49-89-21806127; E-mail: v.mueller@lrz.uni-muenchen.de.

† The abbreviations used are: Δμ<sub>Na<sup>+</sup></sub>, electrochemical sodium ion potential; PAGE, polyacrylamide gel electrophoresis; kbp, kilobase pair(s); bp, base pair(s); PCR, polymerase chain reaction; IPTG, isopropyl-1-thio-β-D-galactopyranoside; PAGE, polyacrylamide gel electrophoresis.

FIG. 1. Physical maps of the *atp* operon and plasmids used in this study. B, BglII; Bs, BstXI; C, ClaI; Ea, EagI; Ec, EcoRI; H, HindIII; P, PstI. A transcriptional terminator is indicated.



ter, Madison, WI). Cloning of pAF1 and pSR4 was described before (8, 11). A 2.7-kbp *Bgl*III/*Hind*III fragment from pSR4 that hybridized with a 1.9-kbp *Eco*RI/*Hind*III fragment was cloned into *Bam*HI/*Hind*III restricted pACYC184 (pSR184BHV). The cloning of the 5'-terminal region of the *atp* operon was not possible by conventional methods. However, from Southern blots the presence of a *Sma*I site ~1600 bp upstream of *atpE*<sub>1</sub> was evident. A degenerated primer carrying the *Sma*I restriction site (OSmaV, 5'-TT(GT)(GT)(GT)(GT)(GT)CCCGGG-3') and a homologous primer (OAwar, 5'-TCCATCGCCCCAGAAATAAA-3') derived from the 3'-terminal end of the *atpB* gene were used to amplify by PCR the 5'-terminal region of the *atp* operon. The resulting 1.6-kbp fragment was cloned into *Eco*RV restricted pACYC184 and designated pSREVB. After DNA sequencing, PCR was used to verify that this fragment is present as such on the chromosome (data not shown).

**Northern Blotting**—For RNA isolation, cells were harvested in the logarithmic growth phase and immediately used or frozen at -70 °C. RNA isolation was done with the "RNeasy™ Total RNA Kit," Qiagen, Hilden, Germany, as described by the manufacturer.

**Heterologous Expression**—pSR184BHV was restricted with *Eco*RV, and *atpE*<sub>1</sub>, *atpE*<sub>2</sub>, and *atpE*<sub>3</sub> were cloned into *Eco*RV restricted pHSG399 (pSR7v). *atpE*<sub>1</sub> derived by PCR was cloned into pHSG398 (pSRc1v). A 10-bp *Xho*I linker (CCCTCGAGGG) was inserted into the unique *Eco*47III site within *atpE*<sub>1</sub> of pSRc1v, resulting in pSRc1vX. Plasmids were transformed into *E. coli* DK6, and minicells were isolated essentially as described (25). Gene expression was induced by IPTG. Two identical minicell preparations were pooled, pelleted, and resuspended in buffer (pH 8.0) containing 50 mM Tris-HCl, 50 mM EDTA, 15% sucrose, and 0.3 mg of lysozyme/ml. After incubation on ice for 30 min, cells were centrifuged and resuspended in ice-cold H<sub>2</sub>O. The membranes were pelleted by centrifugation, the supernatant containing cytoplasm and periplasm was removed, and the membranes were washed twice. SDS-PAGE, fluorography, and autoradiography was as described (26, 27).

**Construction of Plasmid pMal-*atpE*<sub>1</sub>\* and Overexpression of *AtpE*<sub>1</sub>\***—Base pairs 154 to 212 of *atpE*<sub>1</sub> (named *atpE*<sub>1</sub>\*) were amplified from chromosomal DNA of *A. woodii* by PCR using two oligonucleotides which introduced *Eco*RI and *Pst*I sites, respectively (PatpE<sub>1</sub>-3, 5'-ATCGGACAGGAATTCGCGGCC-3'; PatpE<sub>1</sub>-4, 5'-TGCTCCTAGCTGCAGAAATCAT-3'). The PCR fragment was cloned in pMalc2X, and the resulting plasmid was transformed into *E. coli* DH5α. Cultures were grown in Luria broth at 37 °C, and expression was induced at an A<sub>600</sub> of 0.5 by adding IPTG to a final concentration of 0.3 mM. After 2 h of growth, cells were harvested, washed, and disrupted at high pressure in a French press. Further purification of the fusion protein was performed as recommended by the manufacturer. For immunization of a rabbit, the entire fusion protein was used.

**Immunoblotting**—Cytoplasm and washed membranes of *A. woodii* were prepared as described previously (7), subjected to SDS-PAGE (26), and transferred to nitrocellulose membranes (Schleicher & Schuell, Dassel, Germany). The membranes were blocked for 1 h, washed three times with PBST (140 mM NaCl, 10 mM KCl, 6.4 mM Na<sub>2</sub>HPO<sub>4</sub>, 2 mM KH<sub>2</sub>PO<sub>4</sub>, 0.05% Tween 20) for 10 min, and incubated with antisera (4 μg of protein/ml of PBST) for 12 h at room temperature. The membranes were washed again three times with PBST (30 min) and then incubated for 1 h with protein A-horseradish peroxidase conjugate. After three further washing steps (10 min), luminescence was detected

using the chemiluminescence blotting substrate from Roche Molecular Biochemicals (Germany).

## RESULTS

**Organization and transcriptional analysis of the genes coding for the Na<sup>+</sup>-F<sub>1</sub>F<sub>0</sub>-ATPase from *A. woodii***—Previously, an *Eco*RI fragment containing the 3' end of *atpA*, the complete *atpG*, *atpD*, and *atpC* genes, as well as the downstream intergenic region, and a following partial open reading frame encoding AlgD was cloned and sequenced (8). We have now cloned the DNA region upstream of this *Eco*RI fragment on a series of overlapping clones (see "Experimental Procedures"). DNA sequence analysis revealed the presence of eight genes which, based on data base searches, primary sequence alignments, secondary structure predictions, and by comparisons with the experimentally derived N termini of the subunits of the purified protein, encode the previously purified and characterized Na<sup>+</sup>-F<sub>1</sub>F<sub>0</sub>-ATPase (7). These genes are organized in the order *atpI*, *atpB*, *atpE*<sub>1</sub>, *atpE*<sub>2</sub>, *atpE*<sub>3</sub>, *atpF*, *atpH*, and *atpA* (Fig. 1). A strong transcriptional terminator downstream of *atpC* has been described before (8). To determine whether these genes are organized in an operon, RNA was isolated from fructose-grown cells and probed with a 1.9-kb fragment covering *atpE*<sub>1</sub>-*atpA*. As can be seen in Fig. 2, the probe hybridized to a fragment of ~10 kb. Because the deduced size of the *atpI*-*atpC* transcript is 8.035 kb, this experiment gives evidence that *atpI* through *atpC* are transcribed, together with non-coding regions upstream and downstream, as one message.

The genes *atpI*, *atpB*, *atpE*<sub>1</sub>, *atpE*<sub>2</sub>, *atpE*<sub>3</sub>, *atpF*, and *atpH* are predicted to start with an ATG codon, but *atpA* starts with the rare codon TTG. Every start codon is preceded by well conserved Shine-Dalgarno sequences. Characteristic translational features are shown in Table I. The codon usage of the genes is similar to other organisms, and the GC content of the genes correspond to the GC content of chromosomal DNA of *A. woodii*.

**Properties of the Gene Products**—The properties of the gene products are summarized in Table II. Generally, *atpI* through *atpF* code for hydrophobic polypeptides, whereas *atpH* through *atpC* code for hydrophilic ones.

***AtpI***—*atpI* codes for a polypeptide with a deduced molecular mass of 14.86 kDa. It is very hydrophobic with two predicted transmembrane spans. 26, 36, and 20% of its residues are identical in *AtpI* from *P. modestum* (28), *E. coli* (29), and *Moorella thermoacetica* (13), respectively. *AtpI* was not detected in the purified enzyme (7).

***AtpB***—The deduced molecular mass of *atpB* is 24.48 kDa. It is similar to subunit *a* from other F<sub>1</sub>F<sub>0</sub>-ATPases; 45, 41, and



37% of its residues are identical in subunit  $\alpha$  of *P. modestum* (30, 31), *E. coli* (32), and *M. thermoacetica* (13), respectively. Subunit  $\alpha$  is essential for Na<sup>+</sup> transport across the membrane, and its structure and function in Na<sup>+</sup> transport is described elsewhere (33). AtpB was not detected in the purified enzyme (7).

**AtpE**—Interestingly, we found three genes downstream of *atpB*, each encoding a proteolipid-like protein. To exclude any cloning artifacts, different primers were derived from the DNA sequence obtained and used to amplify this region from chromosomal DNA. All controls revealed that there are indeed three copies of *atpE* present on the chromosome (data not shown). Because this finding is very unusual it is analyzed in more detail below.

**AtpF**—*atpF* codes for a polypeptide with a molecular mass of 20.8 kDa. It has a hydrophobic N terminus. The hydrophilic domain is largely  $\alpha$  helical, as revealed by secondary structure predictions. 24, 22, and 28% of its residues are identical in subunit  $b$  of *P. modestum* (30, 31), *E. coli* (29), and *M. thermoacetica* (13), respectively, indicating that AtpF is the homolog of subunit  $b$ . The similarities are 37, 36, and 42%, respectively. AtpF was not detected in the purified enzyme (7).

**AtpH**—The deduced N-terminal sequence of AtpH is identical to the biochemically derived N-terminal sequence (XLVASKYA) of the 19-kDa subunit of the purified enzyme (7). The deduced molecular mass of 20.68 kDa fits well to the experimentally derived value. 29, 22, and 23% of its residues

are identical in subunit  $\delta$  of *P. modestum* (28, 34), *E. coli* (29), and *M. thermoacetica* (13), respectively, indicating that the 19-kDa subunit is the homolog of subunit  $\delta$ .

**AtpA**—The deduced N-terminal sequence of AtpA is identical to the biochemically derived N-terminal sequence (XNL-PEEI) of the 57-kDa subunit of the purified enzyme, which was shown by immunological methods to be the homolog of subunit  $\alpha$  (7). This is supported by the molecular data: 53, 60, and 61% of its residues are identical in subunit  $\alpha$  of *E. coli* (29), *P. modestum* (28, 34), and *M. thermoacetica* (13), respectively. The deduced molecular mass of AtpA (54.82 kDa) corresponds well to the experimentally derived value.

**Three Genes Coding for Subunit c**—The most unusual property which is without precedence in any bacterial species was the finding of three proteolipid-encoding genes (*atpE*<sub>1</sub>, *atpE*<sub>2</sub>, *atpE*<sub>3</sub>) in the F<sub>1</sub>F<sub>0</sub>-ATPase operon. The DNA sequences of *atpE*<sub>2</sub> and *atpE*<sub>3</sub> are nearly identical. Both have 246 base pairs, and only 18 substitutions occurred on the DNA level. The amino acid sequence of the deduced polypeptides is 100% identical, the deduced molecular mass is 8.18 kDa. 69, 42, and 40% of the residues are identical in subunit  $c$  of *P. modestum*, *E. coli*, and *M. thermoacetica*, respectively (Fig. 3). The deduced N-terminal sequence matches exactly the biochemically derived sequence (XE(I)LDF(I)K) of the proteolipid detected in the purified enzyme (7). The structure and function of AtpE<sub>2</sub>/AtpE<sub>3</sub> and the role of Pro-25, Gln-29, Glu-62, and Thr-63 in Na<sup>+</sup> transport have been discussed elsewhere (11). However, it should be noted that the previously published sequence was erroneous which led to a protein extended C-terminally by seven residues.

Most interestingly, *atpE*<sub>1</sub> has 546 base pairs, and repeated sequencing did not reveal a stop codon within the sequence of *atpE*<sub>1</sub>. It is more than double the size of *atpE*<sub>2</sub>/*atpE*<sub>3</sub>. The first and second halves are 66% identical on the DNA level, indicating a duplication and subsequent fusion of a precursor gene.

The deduced molecular mass of AtpE<sub>1</sub> is 18.37 kDa with four predicted transmembrane helices arranged in two hairpins. Only 60% of the residues of hairpins 1 and 2 are identical. 70 and 72% of the residues of hairpins 1 and 2, respectively, are identical in AtpE<sub>2</sub>/AtpE<sub>3</sub>. However, the membrane-buried Na<sup>+</sup>-translocating residue (Glu-62 in AtpE<sub>2</sub>/AtpE<sub>3</sub>), which is also conserved in H<sup>+</sup>-F<sub>1</sub>F<sub>0</sub>-ATPases (35, 36), is substituted by a glutamine residue in hairpin 2 (Fig. 3). Apart from Glu-62, the residues Pro-25, Gln-29, and Thr-63 have been proposed to be involved in Na<sup>+</sup> binding in AtpE<sub>2</sub>/AtpE<sub>3</sub> (11); these three residues are conserved in both hairpins. Interestingly, from the multiple alignment it is evident that AtpE<sub>1</sub> contains an enlarged N terminus of 17 residues which is not present in AtpE<sub>2</sub>/AtpE<sub>3</sub> (Fig. 3).

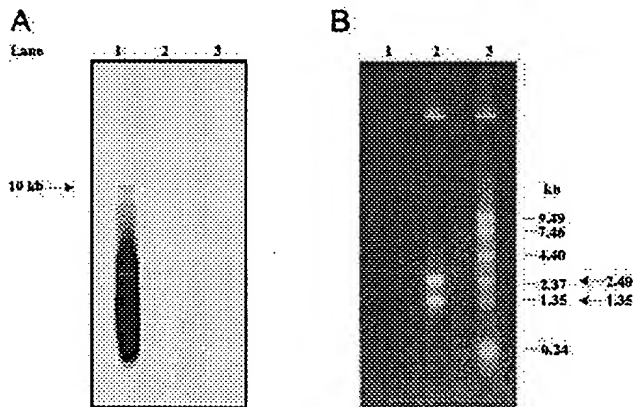


FIG. 2. Northern blot of *A. woodii* mRNA probed with *atpE*<sub>1</sub>-*atpA*. RNA was isolated as described and separated by agarose gel electrophoresis. The gel was blotted and hybridized with a fragment covering *atpE*<sub>1</sub>-*atpA* (A). RNA was visualized by UV light after ethidium bromide staining (B). Ethidium bromide was added to only one aliquot of the RNA preparation (lane 2) and the RNA standard (lane 3), but not to the sample in lane 1.

TABLE I  
Ribosomal binding sites, stop, and start codons of the *atp* genes

Shine-Dalgarno sequences are underlined, start codons are shown in bold, and stop codons are shown in italics. There are small intergenic regions between *atpI* and *atpB* (65 bp from stop to start), *atpE*<sub>1</sub> and *atpE*<sub>2</sub> (42 bp), *atpE*<sub>2</sub> and *atpE*<sub>3</sub> (56 bp), and *atpG* and *atpD* (84 bp). The sequence of *atpG*, *atpD*, and *atpC* were published previously (8) but are included here for the sake of completeness.

Gene	Sequence	GC content
Consensus	... TAAGGAGGT ...	
<i>atpI</i>	... GTAAAAAAGGAAGATAACGAACGTG ATG.	33.84
<i>atpB</i>	... ACAATGAGGTGAAAAACA ATG...	40.91
<i>atpE</i> <sub>1</sub>	.. TAATGAGAAAGAAAGGAGGGAACAGT ATG.....	43.77
<i>atpE</i> <sub>2</sub>	..... TTAGGAGGAAAACATAATT ATG..	46.75
<i>atpE</i> <sub>3</sub>	..... CAAGGAGGAACATATACAC ATG..	45.94
<i>atpF</i>	.... TTAAATTGAGGTGATTCACAA ATG...	35.51
<i>atpH</i>	.... GATAAGGGAGGGATGCGCA ATGA...	34.81
<i>atpA</i>	.... ATTAAGGAGGTGAGTAAAG TTG...	43.25
<i>atpG</i>	TAGATTGTGAGCGAGGTGATTTTCGA GTG...	41.10
<i>atpD</i>	..... CAAGGAGGTAGTGGGA ATG....	41.13
<i>atpC</i>	..... TAGTTGAGGTGAGTTTAA ATG....	41.80

From the data presented here and elsewhere (8), it is evident that the Na<sup>+</sup>-F<sub>1</sub>F<sub>0</sub>-ATPase operon of *A. woodii* contains eleven genes. All the genes found in other bacterial species (37) have

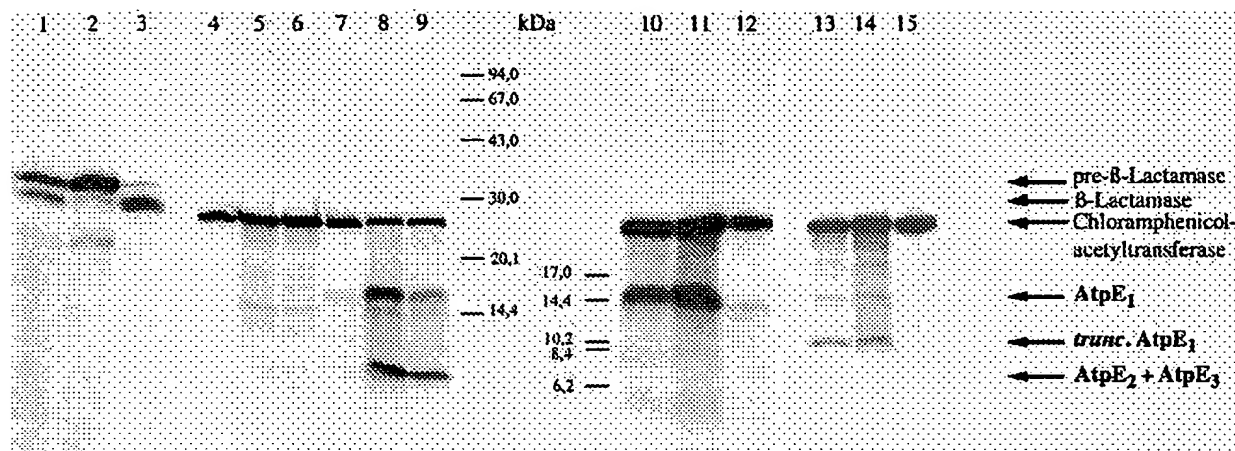


FIG. 4. Heterologous expression of proteolipids from *A. woodii* in *E. coli*. Plasmids were transformed in *E. coli* DK6, proteins were expressed in the presence of [<sup>35</sup>S]methionine, and membranes and cytoplasm were separated and subjected to SDS-PAGE and autoradiography. Lane 1, pBluescript SK, cell free extract; lane 2, pBluescript SK, membranes; lane 3, pBluescript SK, cytoplasm; lane 4, pHSG399, cytoplasm; lane 5, pHSG399, membranes; lane 6, pHSG399, cell free extract; lane 7, pSR7v (*atpE*<sub>1</sub> + *atpE*<sub>2</sub> + *atpE*<sub>3</sub>), cytoplasm; lane 8, pSR7v, membranes; lane 9, pSR7v, cell free extract; lane 10, pSRc1v (*atpE*<sub>1</sub>), cell free extract; lane 11, pSRc1v, membranes; lane 12, pSRc1v, cytoplasm; lane 13, pSRc1vX (*atpE*<sub>1</sub> + linker), cell free extract; lane 14, pSRc1vX, membranes; lane 15, pSRc1vX, cytoplasm.

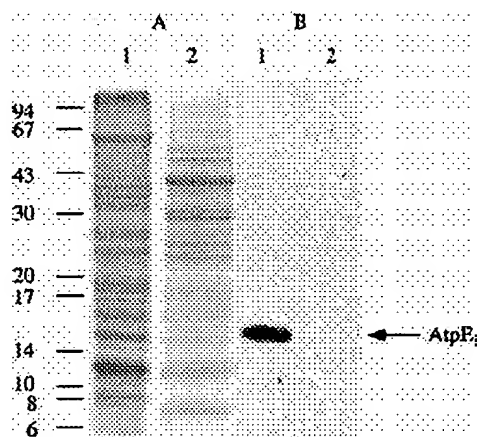


FIG. 5. Immunological detection of the duplicated proteolipid, AtpE<sub>1</sub>, in *A. woodii*. Cells were grown to late exponential growth phase and harvested by centrifugation. Cytoplasm and membranes were separated by centrifugation, and proteins were separated by SDS-PAGE, transferred to nitrocellulose, and probed with the anti-AtpE1\* antibody. The silver-stained gel is shown in panel A and the immunoblot in panel B. Lane 1, membranes; lane 2, cytoplasm. Molecular masses are indicated.

homologs in *A. woodii*, and the overall genetic organization in the operons is the same. However, only six polypeptides were previously found in the purified enzyme (7). From the biochemically derived N-terminal sequences of the polypeptides and the deduced sequences, it is now possible to clearly establish the gene-polypeptide correspondence of the purified Na<sup>+</sup>-ATPase from *A. woodii* (Table III). From this comparison, it is obvious that previous enzyme preparations lacked the duplicated proteolipid (AtpE<sub>1</sub>) as well as subunit *a* (AtpB) and subunit *b* (AtpF). The same was observed in *M. thermoacetica* and *Moorella thermoautotrophica*. Although the encoding genes were present in the *atp* operon from *M. thermoacetica*, subunit *a* and subunit *b* were not found in purified enzymes (13, 14). Furthermore, antisera against synthetic polypeptides derived from the sequences of subunit *a* and *b* of *M. thermoacetica* did not cross-react with cell free extract of the same organism (13). Since *atpB* and *atpF* were transcribed, it was concluded that the messages are not translated in *M. thermoacetica*. Whether this is also true for *A. woodii* or whether the subunits *a* and *b*

TABLE III  
Gene-polypeptide correspondence of the Na<sup>+</sup>-F<sub>1</sub>F<sub>0</sub>-ATPase of *A. woodii*

Gene products and ATPase subunits <sup>a</sup>	N-terminal sequences <sup>b</sup>								
AtpA (subunit <i>α</i> )	M	N	L	R	P	E	E	I	
57-kDa subunit	?	N	L	-	P	E	E	I	
AtpD (subunit <i>β</i> )	M	A	Q	N	I	G	K	V	V
52-kDa subunit	?	Q	N	I	?	K	V	V	
AtpG (subunit <i>γ</i> )	M	A	E	N	V	Q	D	I	K
35-kDa subunit	(A)	E	N	V	Q	D	(I)	(K)	
AtpH (subunit <i>δ</i> )	M	S	L	V	A	S	K	Y	A
19-kDa subunit	?	L	V	A	S	K	Y	A	
AtpC (subunit <i>ε</i> )	M	A	E	T	F	R	L	K	I
16-kDa subunit	?	(E)	(T)	-	R	L	K	I	
AtpE <sub>2</sub> /AtpE <sub>3</sub> (subunit <i>c</i> <sub>2</sub> / <i>c</i> <sub>3</sub> )	M	E	G	L	D	F	I	K	
8-kDa subunit <sup>c</sup>	?	E	(I)	L	D	F	(I)	K	

<sup>a</sup> The sequences deduced from the DNA sequences are shown above the experimentally derived N-termini of the polypeptides found in the purified enzyme. The subunits *a*, *b*, and *c*<sub>1</sub> as well as AtpI were not detected in the purified enzyme.

<sup>b</sup> ?, no unequivocal signal was obtained; ( ), other amino acids were detected in minor amounts; -, no amino acid was detected.

<sup>c</sup> The molecular mass of AtpE<sub>2/3</sub> was previously determined by SDS-PAGE to be 4.8 kDa (7) but was probably underestimated in the gel system used.

were simply lost during the purification procedure remains to be determined. The subunit composition of the enzyme from *A. woodii* is currently under reinvestigation.

One of the most striking and unique features of the *atp* operon of *A. woodii* is the presence of multiple copies of proteolipid-encoding genes. Multiplication of proteolipid-encoding genes have been found before only in V<sub>1</sub>V<sub>0</sub>-ATPases from *Eucarya* (38–40) and A<sub>1</sub>A<sub>0</sub>-ATPases from archaea (41). What could be the selective pressure for multiplication of proteolipid-encoding genes? One has to keep in mind that the subunits of the ATPase are present in different amounts (a<sub>1</sub>b<sub>2</sub>c<sub>12</sub>δ<sub>3</sub>γβ<sub>3</sub>ε), and the proteolipid (subunit *c*) has by far the highest copy number in the complex. Most of our knowledge concerning the regulation of the synthesis of the proteolipid is derived from the paradigm *E. coli*. There, the proteolipid-encoding gene is part of a polycistronic message, and enhanced synthesis of the polypeptide is achieved by enhancement of translation. In addition, but to a lesser extent, regulation of the mRNA stability contributes to differential gene expression (42, 43). However, an enhancer could not be identified in any of the *atpE* genes of

*A. woodii*. What other mechanisms could lead to the high copy number of the proteolipid? First, the proteolipid-encoding gene could be part of the polycistronic message but is transcribed, in addition, also separately from its own promoter. This is apparently encountered in the archaeon *Methanosarcina mazei* (44). Such a mechanism appears to be unlikely in *A. woodii*, judged from the Northern blots presented here. Second, multiplication of the gene and embedding the copies into the operon would be another way to increase the proteolipid message. This strategy is apparently realized by *A. woodii*.

Another striking and unique feature is the finding in a F<sub>1</sub>F<sub>0</sub>-ATPase operon of a gene encoding a duplicated proteolipid. This is without precedence in bacteria. Duplicated proteolipids were, for a long time, seen as an exclusive feature of eucaryal V<sub>1</sub>V<sub>0</sub>-ATPases (45). In archaea, duplication and triplication of proteolipid-encoding genes with subsequent fusion of the genes was described very recently (41, 46). With the experiments described here we add another argument, now derived from a bacterial species, that multiplied and fused proteolipid-encoding genes are not exclusively present in *Eucarya*, but also in the other domains of life. This does not necessarily argue against the commonly favored view of evolution of ATPases but could result from horizontal gene transfer which is very often underestimated in natural systems.

It remains to be established whether the duplicated proteolipid is assembled into the enzyme. This question is very crucial in view of the substitution of the membrane-buried carboxylate in hairpin 1 by a glutamine residue. However, it should be noted that the glutamine is capable to ligand Na<sup>+</sup>, the physiological coupling ion in *A. woodii*. The assembly and oligomeric structure of the proteolipid oligomer of *A. woodii* is currently under investigation.

**Acknowledgment**—We are indebted to Dr. G. Gottschalk, Göttingen, Germany, for generous support.

#### REFERENCES

- Müller, V., and Gottschalk, G. (1994) in *Acetogenesis* (Drake, H. L., ed), pp. 127–156, Chapman & Hall, New York.
- Heise, R., Müller, V., and Gottschalk, G. (1989) *J. Bacteriol.* **171**, 5473–5478.
- Heise, R., Müller, V., and Gottschalk, G. (1993) *FEMS Microbiol. Lett.* **112**, 261–268.
- Heise, R., Reidlinger, J., Müller, V., and Gottschalk, G. (1991) *FEBS Lett.* **295**, 119–122.
- Heise, R., Müller, V., and Gottschalk, G. (1992) *Eur. J. Biochem.* **206**, 553–557.
- Müller, V., and Bowien, S. (1995) *Arch. Microbiol.* **164**, 363–369.
- Reidlinger, J., and Müller, V. (1994) *Eur. J. Biochem.* **223**, 275–283.
- Forster, A., Daniel, R., and Müller, V. (1995) *Biochim. Biophys. Acta* **1229**, 393–397.
- Reidlinger, J., Mayer, F., and Müller, V. (1994) *FEBS Lett.* **356**, 17–20.
- Spruth, M., Reidlinger, J., and Müller, V. (1995) *Biochim. Biophys. Acta* **1229**, 96–102.
- Rahlfs, S., and Müller, V. (1997) *FEBS Lett.* **404**, 269–271.
- Dimroth, P. (1997) *Biochim. Biophys. Acta* **1318**, 11–51.
- Das, A., and Ljungdahl, L. G. (1997) *J. Bacteriol.* **179**, 3746–3755.
- Das, A., Ivey, D. M., and Ljungdahl, L. G. (1997) *J. Bacteriol.* **179**, 1714–1720.
- Clarke, D. J., Fuller, F. M., and Morris, J. G. (1979) *Eur. J. Biochem.* **98**, 597–612.
- Futai, M., Park, M. Y., Iwamoto, A., Omote, H., and Maeda, M. (1994) *Biochim. Biophys. Acta* **1187**, 165–170.
- Tschech, A., and Pfennig, N. (1984) *Arch. Microbiol.* **137**, 163–167.
- Hanahan, D. (1983) *J. Mol. Biol.* **166**, 557–580.
- Klionsky, D. J., William, S. A., Brusilow, A., and Simoni, R. D. (1984) *J. Bacteriol.* **160**, 1055–1060.
- Chang, A. C., and Cohen, S. N. (1978) *J. Bacteriol.* **134**, 1141–1156.
- Takeshita, S., Sato, M., Toba, M., Masahashi, W., and Hashimoto-Gotoh, T. (1987) *Gene (Amst.)* **61**, 63–74.
- Marmur, J. (1961) *J. Mol. Biol.* **3**, 208–218.
- Sambrook, J., Fritsch, E. F., and Maniatis, T. (1989) *Molecular Cloning: A Laboratory Manual*, Cold Spring Harbor Laboratory Press, Cold Spring Harbor, NY.
- Sanger, F. S., Nickelen, F., and Coulson, A. R. (1977) *Proc. Natl. Acad. Sci. U. S. A.* **74**, 5463–5467.
- Homma, M., Kutsukake, K., and Iino, T. (1985) *J. Bacteriol.* **163**, 464–471.
- Schägger, H., and von Jagow, G. (1987) *Anal. Biochem.* **166**, 369–379.
- Chamberlain, J. P. (1979) *Anal. Biochem.* **98**, 132–135.
- Krumholz, L. R., Esser, U., and Simoni, R. D. (1992) *FEMS Microbiol. Lett.* **91**, 37–41.
- Walker, J. E., Saraste, M., and Gay, N. J. (1984) *Biochim. Biophys. Acta* **768**, 164–200.
- Esser, U., Krumholz, L. R., and Simoni, R. D. (1990) *Nucleic Acids Res.* **18**, 5887.
- Kaim, G., Ludwig, W., Dimroth, P., and Schleifer, K. H. (1990) *Nucleic Acids Res.* **18**, 6697.
- Cain, B. D., and Simoni, R. D. (1986) *J. Biol. Chem.* **261**, 10043–10050.
- Rahlfs, S., and Müller, V. (1999) *FEBS Lett.* **453**, 35–40.
- Kaim, G., Ludwig, W., Dimroth, P., and Schleifer, K. H. (1992) *Eur. J. Biochem.* **207**, 463–470.
- Fillingame, R. H., Jones, P. C., Jiang, W., Valiyaveetil, F. I., and Dmitriev, O. Y. (1998) *Biochim. Biophys. Acta* **1365**, 135–142.
- Deckers-Hebestreit, G., and Altendorf, K. (1996) *Annu. Rev. Microbiol.* **50**, 791–824.
- Futai, M., Noumi, T., and Maeda, M. (1989) *Annu. Rev. Biochem.* **58**, 111–136.
- Hirata, R., Graham, L. A., Takatsuki, A., Stevens, T. H., and Anraku, Y. (1997) *J. Biol. Chem.* **272**, 4795–4803.
- Oka, T., Yamamoto, R., and Futai, M. (1997) *J. Biol. Chem.* **272**, 24387–24392.
- Oka, T., Yamamoto, R., and Futai, M. (1998) *J. Biol. Chem.* **273**, 22570–22576.
- Müller, V., Ruppert, C., and Lemker, T. (1999) *J. Bioenerg. Biomembr.* **31**, 15–27.
- McCarthy, J. E., Schairer, H. U., and Sebald, W. (1985) *EMBO J.* **4**, 519–526.
- McCarthy, J. E. (1990) *Mol. Microbiol.* **4**, 1233–1240.
- Ruppert, C., Wimmers, S., Lemker, T., and Müller, V. (1998) *J. Bacteriol.* **180**, 3448–3452.
- Nelson, N., and Taiz, L. (1989) *Trends Biochem. Sci.* **14**, 113–116.
- Ruppert, C., Kavermann, H., Wimmers, S., Schmid, R., Kellermann, J., Lottspeich, F., Huber, H., Stetter, K. O., and Müller, V. (1999) *J. Biol. Chem.* **274**, 25281–25284.
- Ludwig, W., Kaim, G., Laubinger, W., Dimroth, P., Hoppe, J., and Schleifer, K. H. (1990) *Eur. J. Biochem.* **193**, 395–399.
- Kakinuma, Y., Kakinuma, S., Takase, K., Konishi, K., Igarashi, K., and Yamato, I. (1993) *Biochem. Biophys. Res. Commun.* **195**, 1063–1069.
- Krumholz, L. R., Esser, U., and Simoni, R. D. (1989) *Nucleic Acids Res.* **17**, 7993–7994.
- Ohta, S., Yohda, M., Ishizuka, M., Hirata, H., Hamamoto, T., Otawara-Hamamoto, Y., Matsuda, K., and Kagawa, Y. (1988) *Biochim. Biophys. Acta* **933**, 141–155.
- Brusilow, W. S., Scarpetta, M. A., Hawthorne, C. A., and Clark, W. P. (1989) *J. Biol. Chem.* **264**, 1528–1533.
- Lill, H., and Nelson, N. (1991) *Plant Mol. Biol.* **17**, 641–652.

## Phylogenetic transfer of organelle genes to the nucleus can lead to new mechanisms of protein integration into membranes

Doris Michl, Ivan Karnauchov, Jürgen Berghöfer,  
Reinhold G. Herrmann and Ralf Bernd Klösgen\*  
Botanisches Institut der Ludwig-Maximilians-Universität,  
Menzinger Straße 67, D-80638 München, Germany

### Summary

Subunits Cfo-I and Cfo-II of ATP synthase in chloroplast thylakoid membranes are two structurally and functionally closely related proteins of bitopic membrane topology which evolved from a common ancestral gene. In higher plants, Cfo-I still originates in plastid chromosomes (gene: *atpF*), while the gene for Cfo-II (*atpG*) was phylogenetically transferred to the nucleus. This gene transfer was accompanied by the reorganization of the topogenic signals and the mechanism of membrane insertion. Cfo-I is capable of integrating correctly as the mature protein into the thylakoid membrane, whereas membrane insertion of Cfo-II strictly depends on a hydrophobic targeting signal in the transit peptide. This requirement is caused by three negatively charged residues at the N-terminus of mature Cfo-II which are lacking from Cfo-I and which have apparently been added to the protein only after gene transfer has occurred. Accordingly, the Cfo-II transit peptide is structurally and functionally equivalent to typical bipartite transit peptides, capable of also translocating hydrophilic luminal proteins across the thylakoid membrane. In this case, transport takes place by the Sec-dependent pathway, despite the fact that membrane integration of Cfo-II is a Sec-independent, and presumably spontaneous, process.

### Introduction

Eukaryotic cells are the result of endocytobioses. They originated in conglomerates of cells, two in animals and up to five in plants, which arose through the incorporation of bacterial or, in the case of plastids, also of unicellular eukaryotic cells into a host organism (Kowallik, 1997; Martin and Müller, 1998). The integration of the endosymbionts with their respiratory or photosynthetic potential was accompanied by a massive restructuring of the genetic

information within that cell, including loss, gain and transfer of genes which led to an integrated compartmentalized genetic system represented by nucleus/cytosol, mitochondria and, in plants, plastids. Recent data suggest that these genome rearrangements were substantially more complex than generally assumed (Martin and Schnarrenberger, 1997). It becomes more and more evident that the biogenesis and evolution of the eukaryotic cell and its organelles cannot be understood without knowledge of the history of that cell (summarized in Herrmann, 1997). Gene translocation which took place preferentially, although not exclusively, from the endocytobiont to the nucleus caused the chimeric genetic origin of central organelle structures and required the establishment of novel, intercompartmental regulatory circuitries. An intracellular transfer of genes was inherently accompanied by the acquisition of new regulatory sequences for expression and information for product targeting. While the regulation of promoter activity of such nuclear genes or the mechanism of (re)import of proteins into the respective target organelles have been extensively studied, the consequences of intracellular gene rearrangement on the later processes in the biogenesis of organelle structure, such as the assembly of the supramolecular protein complexes of the respiratory and photosynthetic membranes, have barely been examined thus far.

The comparison of phylogenetically closely related proteins that are functional within the same structure but are encoded by different cellular subgenomes provides an appropriate strategy to study this fundamental question in cell biology. The plastid-encoded subunit I or b (gene: *atpF*) and the nuclear encoded subunit II or b' (*atpG*) of the Cfo-assembly of chloroplast ATP synthase, which are derived from the duplication of a common progenitor gene (Hennig and Herrmann, 1986; Herrmann *et al.*, 1993), represent a unique example. To date, they are the only pair known of the various gene duplications from plastids whose members reside in different cellular subgenomes, at least in the chlorophyll *a/b*-lineage of plants. In red algae, *glaucozystophytae* and secondary plastids, both genes still reside in the plastid chromosomes of these organisms (Kowallik, 1997). The gene duplication has already occurred at the level of photosynthetic prokaryotes because all ATP synthases involved in photosynthetic processes contain these b-subunit homologs in a b/b'-stoichiometry, in contrast to the 2b-stoichiometry found in the corresponding respiratory enzymes (e.g. Cozens and Walker, 1987; Herrmann *et al.*, 1993; Walker *et al.*, 1984).

Received 19 August 1998; revised 27 October 1998; accepted 29 October 1998.

\*For correspondence: Institut für Pflanzen- und Zellphysiologie, Martin-Luther-Universität Halle-Wittenberg, Am Kirchtor 1, 06108 Halle (Saale), Germany (fax +49 345 5527 095; e-mail klosgen@pflanzenphys.uni-halle.de).

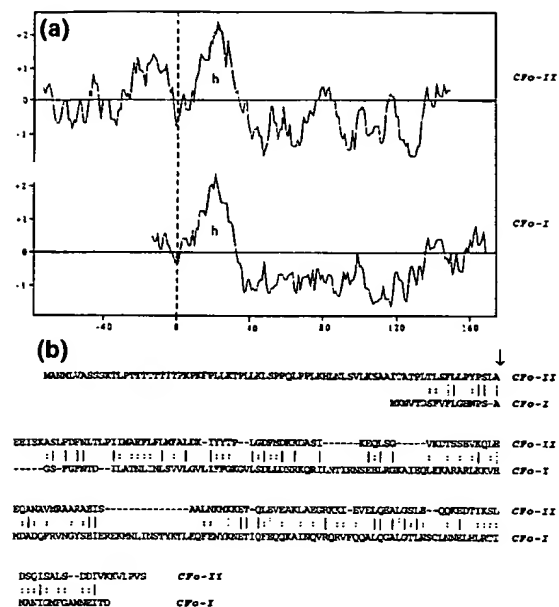


Figure 1. (a) Hydropathy analysis of Cfo-I and Cfo-II from spinach according to Kyte and Doolittle (1982) using an average moving interval of 19 residues. The dotted line indicates the beginning of the mature polypeptides. The transmembrane segments found close to the N-termini of the mature proteins are designated (h).

(b) Alignment of the amino acid sequences, given in the one letter code, of Cfo-I and Cfo-II according to the algorithm described by Lipman and Pearson (1985). Identical amino acids are marked by a dash, conservative replacements by a colon. The arrow indicates the terminal processing sites in both polypeptide sequences.

In spinach, Cfo-I and Cfo-II are bitopic proteins of 167 and 147 residues, respectively, which span the lipid bilayer once with a single hydrophobic segment close to the N-terminus. This results in a topology with a short luminal N-terminal and a long C-terminal segment that protrudes into the stroma. The two proteins are assumed to cooperate in proton conduction across the membrane and in anchoring the CF1 assembly (Berzborn *et al.*, 1990). Cfo-I and Cfo-II display only moderate homology (approximately 25% amino acid identity, Figure 1), as do b- and b'-subunits in general (Cozens and Walker, 1987; Herrmann *et al.*, 1993). In spinach, both polypeptides are synthesized with N-terminal extensions which are not found in the native proteins. The 75 N-terminal residues of the Cfo-II precursor provide the transit peptide for import of the cytosolically synthesized polypeptide into the chloroplast (Herrmann *et al.*, 1993), whereas the function of the only 17 transitory amino acid residues of Cfo-I (Bird *et al.*, 1985) is unclear.

Cfo-II was shown to integrate independently of any known targeting machinery as a precursor molecule into the thylakoid membrane, i.e. it does not depend on stromal factors, nucleoside triphosphates or a transthylakoidal  $\Delta$ pH for insertion. It is processed in a single step by a thylakoidal

processing activity (Michl *et al.*, 1994) that is located with its catalytic domain on the luminal face of the thylakoid membrane (Kirwin *et al.*, 1988). Cfo-II can even insert into mildly protease-treated thylakoid membranes which strictly abolishes the other protein transport routes at the thylakoid membrane (see below), suggesting that a proteinaceous receptor or translocase is not required for integration of this protein (Robinson *et al.*, 1996). This presumably spontaneous membrane integration appears to be the principal mechanism for bitopic thylakoid proteins, at least for the nuclear encoded ones, because it was recently demonstrated also for PsbW and PsbX, two subunits of photosystem II which possess a membrane topology resembling that of Cfo-II (Kim *et al.*, 1996, 1998; Lorkovic *et al.*, 1995). In contrast, integration of LHCP, the polytopic apoprotein of the light-harvesting apparatus associated with photosystem II, requires GTP, a stromal homolog to the 54 kDa subunit of the signal recognition particle, and protease-sensitive component(s) in or at the thylakoid membrane (Li *et al.*, 1995; Robinson *et al.*, 1996).

In addition to these two membrane integration mechanisms, two further protein transport pathways have been characterized which are predominantly involved in the translocation of hydrophilic proteins across the thylakoid membrane. Each of them is specific for a distinct subset of thylakoid proteins and operates with a different mechanism (summarized in Klösgen, 1997). The Sec-dependent pathway requires the presence of ATP and SecA protein in the stroma and is thus homologous to the major pathway for protein secretion into the periplasmic space of *E. coli* (Pugsley, 1993). In contrast, the  $\Delta$ pH-dependent pathway is independent from stromal components but depends on the transthylakoidal proton gradient. Both pathways are generally engaged by cleavable thylakoid transfer domains of similar, signal peptide-like structure (von Heijne *et al.*, 1989). Pathway specificity is mediated by a twin-arginine motif upstream and a Sec-avoidance signal downstream of the hydrophobic core segment in the  $\Delta$ pH-specific transport signals (Bogsch *et al.*, 1997; Chaddock *et al.*, 1995).

In contrast to a wealth of detailed studies on thylakoid transport of nuclear encoded proteins, thylakoid targeting of plastid-encoded polypeptides has barely been examined. Cytochrome *f* from the thylakoidal cytochrome-complex was shown to be probably targeted by the Sec-dependent pathway (Mould *et al.*, 1997; Zak *et al.*, 1997) and there are also indications for Sec-dependent thylakoid transport of cytochrome *b<sub>6</sub>* and subunit IV from this complex (Zak *et al.*, 1997). The sorting mechanism of the other thylakoid proteins has remained elusive. The well-characterized integration pathway of Cfo-II, its close phylogenetic relationship to plastid-encoded Cfo-I, and their favorably simple topologies has prompted us to compare the targeting, integration and assembly characteristics of this interes-

ting pair of twin proteins in order to obtain insight into the consequences of intracellular gene transfer on the late stages of the biogenesis of membrane proteins.

## Results

### *Subunits Cfo-I and Cfo-II of ATP synthase are correctly targeted by the transit peptide of Cfo-II*

A prerequisite for the comparative analysis of integration and assembly of nuclear and plastid-encoded proteins are appropriate assays which are suitable for both protein classes. *In organello* assays in which radiolabelled precursor proteins synthesized *in vitro* are incubated with isolated intact chloroplasts were chosen as strategy because this approach has successfully been applied not only to nuclear encoded proteins but recently also to plastid-encoded polypeptides, and even to a cyanobacterial protein, CtpA (Karnauchov *et al.*, 1997; Mould *et al.*, 1997; Zak *et al.*, 1997).

In order to examine the suitability of the *in organello* approach for the analysis of Cfo-I, a chimeric precursor protein consisting of mature Cfo-I and the transit peptide of Cfo-II was generated. When incubated with isolated chloroplasts, the resulting polypeptide, designated Cfo-II/Cfo-I, is imported into the organelle with an efficiency similar to that of the authentic Cfo-II precursor (Cfo-II/Cfo-II; Figure 2). Intraorganellar routing is correct in both instances because the two proteins integrate into the thylakoid membrane in a way that is indistinguishable from the respective authentic ATP synthase subunits (Westhoff *et al.*, 1985). Their apparent molecular masses, 19 kDa for Cfo-I and 17 kDa for Cfo-II, as judged from electrophoretic mobilities in various gel systems, indicate that the transit peptide is correctly removed in both instances. Protease treatment of thylakoids that were isolated from chloroplasts after import shows that both Cfo-I and Cfo-II are sensitive to proteolysis yielding specific degradation products of 3.0 kDa and 3.5 kDa, respectively (Figure 2). These sizes coincide with those expected for the N-terminal, lumenal parts plus the respective transmembrane segments (Figure 1) and are thus consistent with the topology predicted for the two proteins. Generally, some residual mature protein is still found after the protease reaction (Figure 2 and data not shown) which indicates that proteolytic degradation takes place with delayed kinetics. Presumably, some initially still attached CF1 shields the Cfo-subunits. This assumption is further supported by the observation that the imported proteins co-migrate with the native ATP synthase complex on non-denaturing protein gels (data not shown). Collectively, these findings strongly suggest that the Cfo-I and Cfo-II proteins are correctly assembled after import into isolated organelles.

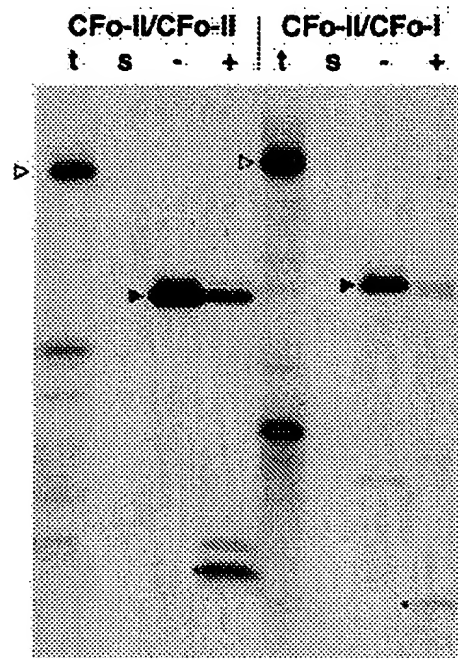


Figure 2. *In organello* import of the authentic Cfo-II precursor (Cfo-II/Cfo-II) and the chimeric Cfo-II/Cfo-I polypeptide.

*In vitro* translation products were incubated with intact chloroplasts isolated from spinach. The chloroplasts were then treated with protease, re-isolated and fractionated into stroma (lanes s) and thylakoids which were subsequently either treated with thermolysin (lanes +) or mock-treated (lanes -). Stoichiometric amounts of each chloroplast fraction, corresponding to 25 µg chlorophyll, were loaded onto a 10–19% SDS-polyacrylamide gradient gel and visualized by fluorography. In lanes t, 0.5 µl of the *in vitro* translation assay was loaded. The positions of the precursor and mature polypeptides are indicated by open and closed arrowheads, respectively. The asterisks mark specific degradation products obtained after protease treatment of the thylakoid membranes.

### *Cfo-II depends on bipartite transit peptides for its integration into the thylakoid membrane*

The contribution of the mature part of a thylakoid protein to the targeting process within the chloroplast can be assessed from its behaviour in combination with mere chloroplast import signals, i.e. transit peptides lacking thylakoid-targeting properties. Representative examples of such stroma-targeting transport signals are the transit peptides from the small subunit of ribulose-1,5-bisphosphate carboxylase/oxygenase (SSU) and ferredoxin-NADP<sup>+</sup>-oxidoreductase (FNR) (Bartling *et al.*, 1990; Clausmeyer *et al.*, 1993; Van den Broeck *et al.*, 1985). When fused to mature Cfo-II, neither of the two transit peptides turned out to be sufficient for correct targeting of the protein. They either misroute the protein into the stroma (FNR/Cfo-II) or are even import-incompetent (SSU/Cfo-II; Figure 3a). Furthermore, FNR/Cfo-II is apparently not, or not correctly, processed by the stromal processing peptidase (see also Clausmeyer *et al.*, 1993). The predominant product accu-



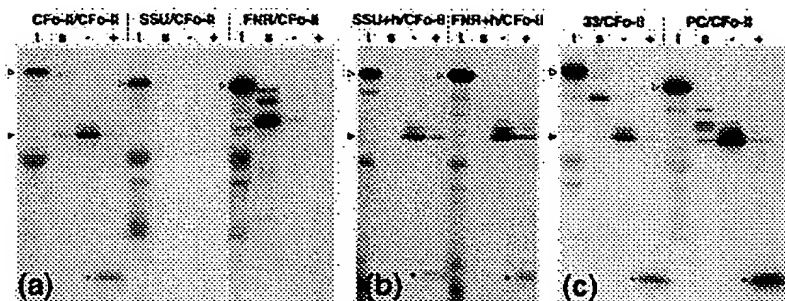


Figure 3. *In organello* import of chimeric precursors composed of mature CfO-II fused to (a) stroma-targeting transit peptides, (b) stroma-targeting transit peptides carrying additionally the 22 C-terminal residues of the CfO-II transit peptide, or (c) bipartite, thylakoid-targeting transit peptides.

*In organello* import of the authentic CfO-II precursor is shown for comparison (a). For further details see the legend to Figure 2.

mulating in the stroma after import is slightly larger than mature CfO-II, and two further cleavage products observed migrate with an even lower electrophoretic mobility on denaturing protein gels (Figure 3a). None of these polypeptides is associated with the thylakoid membrane indicating that, in spite of the hydrophobic segment at its N-terminus (Figure 1), mature CfO-II *per se* is not capable of interacting with the membrane.

Such interaction depends on the presence of an additional, hydrophobic targeting signal which, for example, can be provided by the C-terminal part of the CfO-II transit peptide. If residues 54–75 of this transit peptide are inserted between either of the two stroma-targeting transit peptides and mature CfO-II, the resulting chimeras (designated SSU+h/CfO-II and FNR+h/CfO-II) are not only imported into chloroplasts but are also properly integrated into the thylakoid membrane and processed to mature CfO-II (Figure 3b). This result strongly suggests that the C-terminal segment of the CfO-II transit peptide, which structurally resembles thylakoid transfer domains from bipartite transit peptides (Figure 1; von Heijne *et al.*, 1989), contains targeting information that is both indispensable and sufficient for membrane insertion of the protein. This signal is not restricted to the CfO-II transit peptide but can likewise be provided by the corresponding epitopes of bipartite transit peptides from hydrophilic lumen proteins such as plastocyanin or the 33 kDa subunit of the oxygen-evolving system (Figure 3c).

#### *Thylakoid integration of CfO-I does not depend on a cleavable transport signal*

Membrane integration of CfO-I operates with a different mechanism. When fused to stroma-targeting transit peptides, CfO-I is not only imported into isolated chloroplasts, it also accumulates quantitatively in the thylakoid fraction (Figure 4a). The appearance of the diagnostic 3.0 kDa degradation product after protease treatment of the thylakoids strongly suggests that the protein was properly assembled into the ATP synthase complex. This indicates that, in contrast to its nuclear encoded sister protein, CfO-I is capable of integrating as the mature polypeptide

into the thylakoid membrane, independent of any transient targeting signal.

On the other hand, the presence of an additional thylakoid-targeting signal does not impair thylakoid integration of CfO-I. A chimeric protein in which mature CfO-I was combined with the bipartite plastocyanin transit peptide is correctly targeted to and inserted into the thylakoid membrane (Figure 4b). Although PC/CfO-I accumulates predominantly as a processing intermediate (Figure 4b), indicating that terminal processing is delayed or even abolished in this case, assembly of the protein into ATP synthase is apparently not affected by the residual part of the transit peptide. The CfO-I degradation product observed after protease treatment of the thylakoids exceeds 3 kDa in this instance (Figure 4b), probably due to the residual amino acids from the plastocyanin transit peptide at the N-terminus of the protein.

Likewise, CfO-I can also correctly integrate into the thylakoid membrane if the N-terminal 17 residues of the primary CfO-I translation product which had been omitted from the constructs described above are present. In combination with both stroma-targeting and bipartite transit peptides the protein was targeted to the thylakoids where it integrated correctly into the membrane (data not shown). This indicates that the 17 transitory residues of the CfO-I translation product (Bird *et al.*, 1985) are both dispensable for and compatible with targeting and integration of CfO-I, at least if these processes are performed in a post-translational manner.

#### *Negative charges at the N-terminus of mature CfO-II cause the requirement for a hydrophobic transport signal*

In order to determine the basis for the different integration mechanisms of CfO-I and CfO-II, hybrid forms of the two mature proteins were analyzed. In hybrid H1CfO-II, the N-terminal 41 residues of CfO-I comprising the membrane anchor and the lumenal part of the protein were combined with the stroma-exposed C-terminal part of CfO-II (residues 46–147; Figure 1). Hybrid H2CfO-I represents the reciprocal combination (residues 1–44 from CfO-II combined with residues 43–167 from CfO-I).



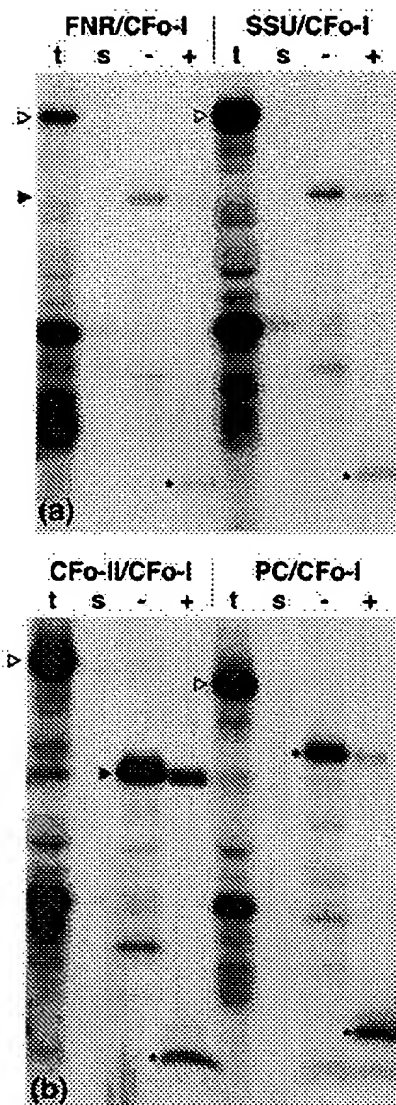


Figure 4. *In organello* import of chimeric precursors consisting of (a) stroma-targeting or (b) bipartite, thylakoid-targeting transit peptides that were fused to mature Cfo-I.

The position of the polypeptide of intermediate size found after import of PC/CFo-I is indicated by  $\blacklozenge$ . All further details are explained in the legend to Figure 2.

When fused to the stroma-targeting transit peptide of FNR, both polypeptides (designated FNR/H1Cfo-II and FNR/H2Cfo-I, respectively) are imported with comparable efficiency into isolated chloroplasts. However, they accumulate in different regions of the organelle. While FNR/H1Cfo-II is integrated into the thylakoid membrane, FNR/H2Cfo-I remains soluble in the stroma (Figure 5). Obviously, the intraorganellar routing of each hybrid corresponds to that Cfo subunit from which the N-terminal segment was derived. This indicates that the luminal

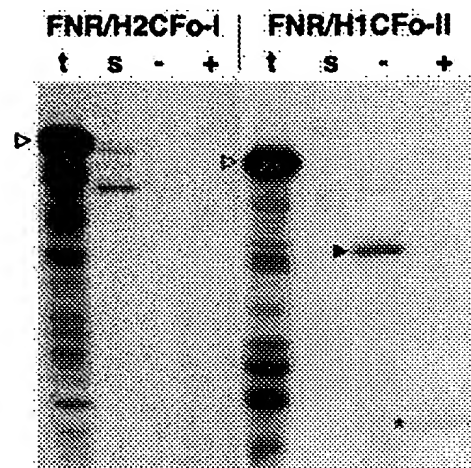


Figure 5. *In organello* import of the chimeric precursor polypeptides FNR/H2Cfo-I and FNR/H1Cfo-II.

For details, see the legend of Figure 2.

residues and/or the membrane anchors dictate the mechanism of membrane integration for these polypeptides, while their C-terminal, stroma-exposed parts exert no, or no significant, impact on this process.

Comparison of the respective N-terminal segments reveals a relatively high degree of sequence conservation (Figure 1). However, the very N-termini of Cfo-I and Cfo-II are strikingly different. Cfo-II possesses five additional residues of which four are charged (Glu at positions 1, 2 and 4, and Lys at position 5) resulting in a negatively charged N-terminus for Cfo-II. In Cfo-I, the N-terminal residues are neutral (Figure 1). In order to examine a possible influence of these charges on the mode of integration, the N-terminus of mature Cfo-II was modified in two ways. In mutant DEL, residues 1–5 were deleted from mature Cfo-II yielding an N-terminally truncated polypeptide, while in mutant SUB the three glutamic acid residues were replaced by either asparagine (pos. 1) or glutamine (pos. 2 and 4). Thus, in the latter polypeptide the N-terminal negative charges were removed without altering the number of residues translocated across the membrane.

The mutant polypeptides were combined with the transit peptides from SSU, FNR and Cfo-II and analyzed in *in organello* experiments. It turned out that all chimeras are imported into the chloroplast (Figure 6). In other words, both mutations cure the import incompetence observed for SSU/Cfo-II (Figure 3a). However, the polypeptides accumulate only at relatively low rates within the organelle (even those carrying the authentic Cfo-II transit peptide) indicating a reduced import efficiency and/or increased degradation rate of the mutant polypeptides. Furthermore, the mutations appear to affect the cleavage of the precursor polypeptides by the chloroplastic processing enzymes, since in some instances the precursor protein (CfoII/DEL,

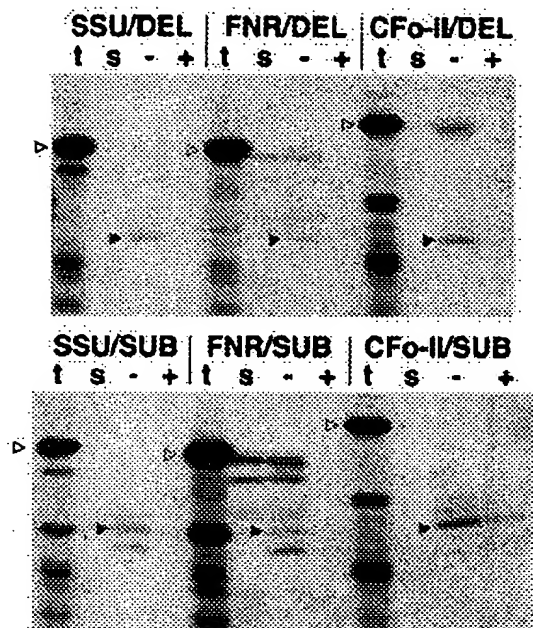


Figure 6. *In organello* import of the Cfo-II derivatives DEL and SUB in combination with different transit peptides.

The positions of the correct cleavage products are indicated by closed arrowheads. All further details are explained in the legend to Figure 2.

FNR/SUB) and/or aberrant cleavage products (FNR/DEL, FNR/SUB, SSU/SUB) were found in addition to the proper processing products (Figure 6).

The most striking result of this experiment is, however, that both mutant Cfo-II derivatives are capable of integrating into the thylakoid membrane independent of a hydrophobic targeting signal in the transit peptide (Figure 6). In each instance, the imported protein is predominantly found in the thylakoid fraction, irrespective of whether the transit peptide present carries a thylakoid-targeting signal (Cfo-II) or not (SSU, FNR). This result strongly suggests that the negative charges at the N-terminus of Cfo-II which are lacking in both mutants prevent the interaction of the protein with the thylakoid membrane and, consequently, its integration. The membrane-repelling effect of this cluster of charges can apparently only be revoked by two flanking hydrophobic domains, in line with the model proposed for the mechanism of Cfo-II integration (Michl *et al.*, 1994).

*The transit peptide of the Cfo-II precursor protein is capable of operating as a Sec-type thylakoid translocation signal*

The requirements delineated for the correct intraorganellar routing of Cfo-II indicate that its transit peptide possesses features reminiscent of bipartite thylakoid-targeting transit peptides. Indeed, *in organello* import of the chimera Cfo-II/PC, which consists of the Cfo-II transit peptide fused

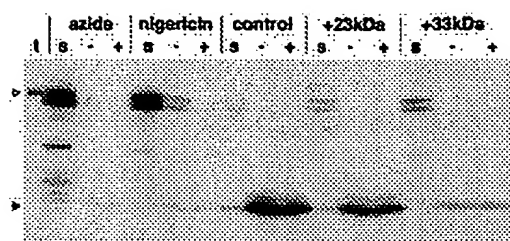


Figure 7. *In organello* import of Cfo-II/PC, a chimeric precursor consisting of the transit peptide of Cfo-II and the mature part of plastocyanin, into chloroplasts isolated from pea.

As indicated above the lanes, the import reactions were performed either under standard conditions (control), in the presence of translocation inhibitors (10 mM sodium azide or 2  $\mu$ M nigericin), or in the presence of 3  $\mu$ M competitor protein (the precursor proteins of the 23 kDa or the 33 kDa subunit of the oxygen-evolving system, respectively). For further details see the legend to Figure 2.

to mature plastocyanin, shows that this transit peptide is capable of mediating transport of a hydrophilic protein into the thylakoid lumen (Figure 7). Since plastocyanin strictly depends on thylakoid-targeting domains of transit peptides for its correct intraorganellar routing (Clausmeyer *et al.*, 1993; Smeekens *et al.*, 1986), this result proves that the Cfo-II transit peptide is functionally equivalent to the bipartite transit peptides of hydrophilic thylakoid proteins.

Thylakoid transport of Cfo-II/PC apparently takes place by the Sec-dependent pathway, in spite of the fact that the authentic Cfo-II precursor integrates in a Sec-independent manner into the membrane (Michl *et al.*, 1994). Translocation of the chimera into the thylakoid lumen is substantially affected by saturating amounts of the precursor of the 33 kDa subunit from the oxygen-evolving system (Figure 7) which is a specific substrate for the Sec-machinery in chloroplasts (Hulford *et al.*, 1994; Yuan *et al.*, 1994). Unfortunately, this effect is covered to some extent by the strong inhibitory effect of the competitor protein on import of Cfo-II/PC into the organelle which leads to overall reduced signal strengths. However, it is obvious that the ratio of precursor protein accumulating in the stroma and mature polypeptide in the thylakoid lumen is largely increased in the presence of the Sec-specific competitor, indicating transport of Cfo-II/PC by the Sec-dependent pathway. In contrast, saturation of the  $\Delta$ pH-dependent route by excess amounts of the precursor of the 23 kDa protein from the oxygen-evolving system reduces the rate of organelle import for Cfo-II/PC as well, but does not affect the subsequent thylakoid translocation step to a significant degree.

In line with that, the transport process is sensitive to sodium azide, a potent inhibitor of SecA function in bacteria (Oliver *et al.*, 1990) that was recently shown to also inhibit Sec-dependent protein transport in chloroplasts (Knott and Robinson, 1994; Yuan *et al.*, 1994). Furthermore, membrane transport of Cfo-II/PC depends on the transthylakoidal proton gradient since it is strongly inhibited in the presence

of the ionophore nigericin (Figure 7). Although remarkably pronounced here, the requirement for  $\Delta pH$  is not unusual for protein transport along the Sec-pathway since it has also been described for other Sec-dependent substrates, such as, for example, the 33 kDa subunit of the oxygen-evolving system (Mant *et al.*, 1995; Yuan and Cline, 1994).

### Discussion

The primary goal of the outlined work was to study the consequences of phylogenetic gene transfer between cellular subgenomes on late stages of the biogenesis of the corresponding proteins. For this purpose, the two phylogenetically and structurally closely related subunits Cfo-I and Cfo-II of thylakoidal ATP synthase which are encoded in the plastid and the nucleus of higher plant cells, respectively, were compared with respect to the mechanism of their thylakoid transport and assembly.

#### *Cfo-I and Cfo-II integrate with different mechanisms into the thylakoid membrane*

The most striking finding of this study is that Cfo-I and Cfo-II integrate with fundamentally different mechanisms into thylakoids, despite the fact that after assembly both proteins reside with similar topology in the membrane. In Cfo-I, the membrane integration signals reside in the mature protein (Figure 4a), notably in the N-terminal segment carrying the membrane anchor that consequently houses two signals, for targeting and anchoring (Figure 5). In contrast, mature Cfo-II is not capable of integrating into the thylakoid membrane on its own; it is completely dependent on the presence of an additional hydrophobic transport signal in the transit peptide (Figure 3). Thus, in Cfo-II the membrane transport signals extend into both parts of the precursor molecule, the transit peptide and the mature protein, which probably act in a co-operative manner during the integration process (Michl *et al.*, 1994). This implies that the phylogenetic transfer of *atpG* into the nucleus has caused a change both in thylakoid-targeting signals and integration mechanism.

*A priori*, such a change is not an obligatory consequence of the gene transfer because plastid-encoded Cfo-I can still properly integrate and assemble if it is artificially imported into the chloroplast by transit peptides lacking thylakoid-targeting properties (Figure 4a). It should be considered, however, that the experiments presented here were performed with isolated organelles which excludes any interaction of the protein with non-target cellular membranes. In an intact plant cell, however, such mistargeting of the Cfo-I chimeras might well occur which would reduce the rate of correctly targeted protein even if the actual thylakoid-integration process was not hampered. It is conceivable, therefore, that the change in the mechanism

of Cfo-II integration was primarily necessary to minimize the rate of non-specific membrane interactions rather than to improve the efficiency of membrane insertion.

The cause for the dependance of Cfo-II integration on a hydrophobic transport signal in the transit peptide is the presence of three negatively charged residues in the N-terminal region of the mature protein (Figure 6). The function of these residues is unknown, but it is interesting to note that they are lacking in subunit Fo-b' of *Synechocystis* PCC 6803, the cyanobacterial homolog to Cfo-II (Lill and Nelson, 1991). Accordingly, the cyanobacterial protein is not synthesized with a signal peptide which indicates that the N-terminal charges and the cleavable, hydrophobic transport signal have probably been introduced into the protein in a co-ordinated manner. The integration mode of the cyanobacterial protein is not yet known, but the similarity of b and b' subunits and the lack of a signal peptide suggest a mechanism similar to that of Cfo-I.

A remarkable similarity to the membrane integration mechanism of Cfo-II is found in the insertion mode described for the procoat of bacteriophage M13. Integration of this protein into the bacterial membrane is a Sec-independent process which involves membrane transfer of a short, negatively charged segment located at the N-terminus of the mature polypeptide (Kuhn *et al.*, 1987). Membrane transport of this segment strictly depends on the presence of two flanking hydrophobic domains which are provided by the signal peptide and the transmembrane helix, respectively (Cao *et al.*, 1994; Kuhn *et al.*, 1986). In analogy to Cfo-II, substitution of these charges allows procoat to integrate independently of a hydrophobic signal peptide (Rohrer and Kuhn, 1990). However, integration of M13 procoat differs from that of Cfo-II in an additional requirement for an electrochemical transmembrane gradient (Cao *et al.*, 1995; Date *et al.*, 1980), demonstrating that the mechanism for the membrane transfer of small, highly negatively charged peptide domains is basically conserved but not completely identical in the two cases.

#### *Phylogenetic origin of the Cfo-II transit peptide*

At the prokaryotic level proteins such as plastocyanin or the 33 kDa subunit of the photosynthetic oxygen-evolving system which are found in the thylakoid lumen of both cyanobacteria and chloroplasts, are synthesized as precursor molecules carrying transitory signal peptides for the transport across the thylakoid membrane. In the corresponding nuclear encoded proteins of higher plants, the signal peptides are conserved in the C-terminal parts of the respective transit peptides where they still operate as thylakoid-translocation signals. It is therefore widely accepted that the thylakoid-targeting signals in these bipartite transit peptides are of prokaryotic origin. Con-

sequently, after phylogenetic gene transfer only an organelle import signal was added and required to preserve correct biogenesis of these proteins.

The transit peptide of CFo-II must have a different phylogenetic origin. As mentioned above, its homolog from *Synechocystis* 6803 is synthesized in the prokaryotic cytosol as the mature protein lacking any additional residue (Lill and Nelson, 1991). On the other hand, CFo-I is synthesized in the chloroplast with an N-terminal extension of 17 amino acids which appears to be conserved in the transit peptide of CFo-II (Figure 1b). However, this extension does not show any similarity to signal peptides and our data demonstrate that it is indeed dispensable for membrane integration (Figure 4a). Thus, although the C-terminal part of the CFo-II transit peptide might be of organellar, prokaryotic origin, its structure was obviously modified after phylogenetic transfer of *atpG* to provide new functions for thylakoid targeting. These modifications include the acquisition of apolar amino acids to increase the hydrophobic moment of the signal and by this means compensate for the negative charges that have apparently been added to the N-terminus of the mature protein. Furthermore, a single residue, leucine, was inserted at position -2 of the terminal processing site (Figure 1b) which generated a recognition sequence for the thylakoidal processing activity (Michl et al., 1994). This unusual descent of its thylakoid-targeting signal might also explain why the CFo-II transit peptide lacks an intermediary processing site (Michl et al., 1994).

#### *The CFo-II transit peptide is a cryptic Sec-type transport signal*

Despite the fact that CFo-II integrates into the thylakoid membrane spontaneously (Michl et al., 1994; Robinson et al., 1996), its transit peptide is capable of interacting with the thylakoidal protein transport machinery and operating as a Sec-dependent translocation signal (Figure 7). However, it is restrictive with regard to its passenger. Of four polypeptides tested, notably the 16 kDa, 23 kDa and 33 kDa subunits of the oxygen-evolving system and plastocyanin, only the latter is correctly targeted by the CFo-II transit peptide, while the other proteins are mistargeted to the chloroplast stroma in *in organello* experiments (Figure 7 and data not shown). Similar limitations have also been observed for other Sec-type transit peptides (see for example Clausmeyer et al., 1993) which points to a rather restricted passenger compatibility of this pathway.

A comparable switch from Sec-independent to Sec-dependent protein transport has been described for M13 procoat and leader peptidase from *E. coli* (Andersson and von Heijne, 1993; Kuhn, 1988). This suggests that targeting signals involved in spontaneous membrane transport have an inherent property to interact with the Sec-type mem-

brane transport machinery. Sec-dependence apparently increases with the length of the translocated segment (Andersson and von Heijne, 1993; Kuhn, 1988) which implies that spontaneous membrane transport is restricted to short oligopeptides.

## Experimental procedures

### *Chloroplast isolation and protein transport experiments*

Chloroplasts were isolated from young spinach leaves by Percoll gradient centrifugation and used for *in organello* import experiments as described by Cai et al. (1993) and Clausmeyer et al. (1993). Authentic and chimeric precursor proteins were synthesized by *in vitro* transcription of cDNA clones followed by *in vitro* translation in cell-free wheat germ or rabbit reticulocyte lysates in the presence of [<sup>35</sup>S]-methionine. Competition experiments with saturating amounts of the 23 kDa and 33 kDa precursor proteins followed the protocol of Michl et al. (1994).

### *Generation of chimeric and hybrid polypeptides*

According to the protocols outlined earlier (Bartling et al., 1990; Cai et al., 1993; Clausmeyer et al., 1993), gene cassettes for transit peptides and mature proteins were obtained from the respective cDNA by *in vitro* mutagenesis introducing unique restriction sites at the position of the terminal processing site in the precursor protein. For the CFo-II transit peptide cassette, a *NaeI* restriction site was introduced. To generate the *HincII*-site for the cassette of mature CFo-II, a nucleotide exchange in the first codon (GAA to GAC) leading to a conservative amino acid replacement in this position (Glu → Asp) was required. The cassette for mature CFo-I was obtained from plasmid pAN573 carrying the uninterrupted coding sequence for this protein (Hudson et al., 1987; Schmidt et al., 1990) by introducing an *NdeI*-site leading to an amino acid exchange from Gly to Met.

The gene cassette H1CFo-II was generated by fusing the 134 bp *XhoI*/*SalI*/*EcoRI*-fragment from the cassette of mature CFo-I with the 457 bp *AhaI*/*Klenow*/*BamHI*-fragment from the cassette of mature CFo-II. The cassette H2CFo-I was generated by fusing the 132 bp *AhaI*/*SalI*/*SalI*-fragment from the CFo-II cassette with the 398 bp *XhoI*/*Klenow*/*BamHI*-fragment from the CFo-I cassette. The gene cassette +h/CFo-II was generated by introducing a *DraI* restriction site in front of codon 54 of the coding sequence for the CFo-II precursor. The gene cassette of mutant DEL carries an *FspI*-site in front of codon 6 of the mature CFo-II coding sequence. In mutant SUB, the three Glu codons at position 1, 2 and 4 of the mature CFo-II coding sequence were replaced by codons for Asn (pos. 1) and Gln (pos. 2 and 4) and, in addition, an *HincII*-site was introduced at the position of the terminal processing site in the precursor polypeptide. The construction of the cassettes for the transit peptides of SSU, FNR, plastocyanin, and the 33 kDa protein of the oxygen-evolving system as well as for the mature part of plastocyanin have been described previously (Cai et al., 1993; Clausmeyer et al., 1993).

The restriction sites introduced were subsequently utilized for the assembly of coding sequences for chimeric precursor proteins by in-frame combination of the respective coding cassettes. The resulting recombinant DNA fragments were cloned into pBSC M13<sup>+</sup> (Stratagene, La Jolla, USA), and the correctness of the mutageneses and fusions was verified by sequence analysis (Sanger et al., 1977).

## Miscellaneous

Gel electrophoresis under denaturing conditions was carried out according to Laemmli (1970) or Schagger and von Jagow (1987). The gels were processed by fluorography using 16% sodium salicylate (Chamberlain, 1979). All other methods followed the protocols collected in Sambrook *et al.* (1989).

## Acknowledgements

We thank Dr Günther Schmidt for providing plasmid pAN573. This work was supported by the Deutsche Forschungsgemeinschaft (SFB 184) and the Fonds der Chemischen Industrie.

## References

- Andersson, H. and von Heijne, G. (1993) Sec dependent and sec independent assembly of *E. coli* inner membrane proteins: the topological rules depend on chain length. *EMBO J.* **12**, 683–691.
- Bartling, D., Clausmeyer, S., Oelmüller, R. and Herrmann, R.G. (1990) Towards epitope models for chloroplast transit sequences. *Bot. Mag. Tokyo*, (Special Issue) **2**, 119–144.
- Berzborn, R.J., Klein-Hitpaß, L., Otto, J., Schünemann, S. and Owarah-Nkruma, R. (1990) The 'additional subunit' CF<sub>0</sub> of the photosynthetic ATP-synthase and the thylakoid polypeptide, binding ferredoxin NADP reductase: are they different? *Zeitschr. Naturforsch.* **45c**, 772–784.
- Bird, C.R., Koller, B., Auffret, A.D., Huttly, A.K., Howe, C.J., Dyer, T.A. and Gray, J.C. (1985) The wheat chloroplast gene for Cfo subunit I of ATP synthase contains a large intron. *EMBO J.* **4**, 1381–1388.
- Bogsch, E., Brink, S. and Robinson, C. (1997) Pathway-specificity for a delta pH-dependent precursor thylakoid lumen protein is governed by a 'Sec-avoidance' motif in the transfer peptide and a 'Sec-incompatible' mature protein. *EMBO J.* **16**, 3851–3859.
- Cai, D., Herrmann, R.G. and Klösgen, R.B. (1993) The 20 kD apoprotein of the CP24 complex of photosystem II: an alternative model to study import and intraorganellar routing of nuclear-encoded thylakoid proteins. *Plant J.* **3**, 383–392.
- Cao, G., Cheng, S., Whitley, P., von Heijne, G., Kuhn, A. and Dalbey, R.E. (1994) Synergistic insertion of two hydrophobic regions drives Sec-independent membrane protein assembly. *J. Biol. Chem.* **269**, 26898–26903.
- Cao, G., Kuhn, A. and Dalbey, R.E. (1995) The translocation of negatively charged residues across the membrane is driven by the electrochemical potential: evidence for an electrophoresis-like membrane transfer mechanism. *EMBO J.* **14**, 866–875.
- Chaddock, A.M., Mant, A., Kamauchov, I., Brink, S., Herrmann, R.G., Klösgen, R.B. and Robinson, C. (1995) A new type of signal peptide: central role of a twin-arginine motif in transfer signals for the  $\Delta$ pH-dependent thylakoidal protein translocase. *EMBO J.* **14**, 2715–2722.
- Chamberlain, J.P. (1979) Fluorographic detection of radioactivity in polyacrylamide gels with the water-soluble fluor sodium salicylate. *Anal. Biochem.* **98**, 132–135.
- Clausmeyer, S., Klösgen, R.B. and Herrmann, R.G. (1993) Protein import into chloroplasts: the hydrophilic luminal proteins exhibit unexpected import and sorting specificities in spite of structurally conserved transit peptides. *J. Biol. Chem.* **268**, 13869–13876.
- Cozens, A.L. and Walker, J.E. (1987) The organization and sequence of the genes for ATP synthase subunits in the cyanobacterium *Synechococcus* 6301. *J. Mol. Biol.* **194**, 359–383.
- Date, T., Goodman, J.M. and Wickner, W.T. (1980) Procoat, the precursor of M13 coat protein, requires an electrochemical potential for membrane insertion. *Proc. Natl Acad. Sci. USA*, **77**, 4669–4673.
- von Heijne, G., Steppuhn, J. and Herrmann, R.G. (1989) Domain structure of mitochondrial and chloroplast targeting peptides. *Eur. J. Biochem.* **180**, 535–545.
- Hennig, J. and Herrmann, R.G. (1986) Chloroplast ATP synthase of spinach contains nine nonidentical subunit species, six of which are encoded by plastid chromosomes in two operons in a phylogenetically conserved arrangement. *Mol. Gen. Genet.* **203**, 117–128.
- Herrmann, R.G. (1997) Eukaryotism, towards a new interpretation. In *Eukaryotism and Symbiosis* (Schenk, H.E.A., Herrmann, R.G., Jeon, K.W., Müller, N.E. and Schwemmler, W., eds). Berlin: Springer-Verlag, pp. 73–118.
- Herrmann, R.G., Steppuhn, J., Herrmann, G.S. and Nelson, N. (1993) The nuclear-encoded polypeptide Cfo-II from spinach is a real, ninth subunit of chloroplast ATP synthase. *FEBS Lett.* **326**, 192–198.
- Hudson, G.S., Mason, J.G., Holten, T.A., Koller, B., Cox, G.B., Whitefield, P.R. and Bottomley, W. (1987) A gene cluster in the spinach and pea chloroplast genomes encoding one CF<sub>1</sub> and three Cfo subunits of the H<sup>+</sup>-ATP synthase complex and the ribosomal protein S2. *J. Mol. Biol.* **196**, 283–298.
- Hulford, A., Hazell, L., Mould, R.M. and Robinson, C. (1994) Two distinct mechanisms for the translocation of proteins across the thylakoid membrane, one requiring the presence of a stromal protein factor and nucleotide triphosphates. *J. Biol. Chem.* **269**, 3251–3256.
- Karnauchov, I., Herrmann, R.G., Pakrasi, H. and Klösgen, R.B. (1997) Transport of CtpA protein from the cyanobacterium *Synechocystis* 6803 across the thylakoid membrane in chloroplasts. *Eur. J. Biochem.* **249**, 497–504.
- Kim, S.J., Robinson, C. and Mant, A. (1998) Sec/SRP-independent insertion of two thylakoid membrane proteins bearing cleavable signal peptides. *FEBS Lett.* **424**, 105–108.
- Kim, S.J., Robinson, D. and Robinson, C. (1996) An Arabidopsis thaliana cDNA encoding PSII-X, a 4.1 kDa component of photosystem II: a bipartite presequence mediates SecA/ $\Delta$ pH-independent targeting into thylakoids. *FEBS Lett.* **390**, 175–178.
- Kirwin, P.M., Elderfield, P.D., Williams, R.S. and Robinson, C. (1988) Transport of proteins into chloroplasts: organization, orientation and lateral distribution of the plastocyanin processing peptidase in the thylakoid network. *J. Biol. Chem.* **263**, 18128–18132.
- Klösgen, R.B. (1997) Protein transport into and across the thylakoid membrane. *J. Photochem. Photobiol. B: Biology*, **38**, 1–9.
- Knott, T. and Robinson, C. (1994) The SecA inhibitor, azide, reversibly blocks the translocation of a subset of proteins across the chloroplast thylakoid membrane. *J. Biol. Chem.* **269**, 7843–7846.
- Kowallik, K.V. (1997) Origin and evolution of chloroplasts: current status and future perspectives. In *Eukaryotism and Symbiosis* (Schenk, H.E.A., Herrmann, R.G., Jeon, K.W., Müller, N.E. and Schwemmler, W., eds). Berlin: Springer-Verlag, pp. 3–23.
- Kuhn, A. (1988) Alterations in the extracellular matrix domain of M13 procoat protein makes its membrane insertion dependent on secA and secY. *Eur. J. Biochem.* **177**, 267–271.
- Kuhn, A., Kreil, G. and Wickner, W. (1987) Recombinant forms of M13 procoat with an OmpA leader sequence or a large carboxy-terminal extension retain their independence of secY function. *EMBO J.* **6**, 501–505.
- Kuhn, A., Wickner, W. and Kreil, G. (1986) The cytoplasmic carboxy terminus of M13 procoat is required for the membrane insertion of its central domain. *Nature*, **322**, 335–339.

- Kyte, J. and Doolittle, R.F. (1982) A simple method for displaying the hydropathic character of a protein. *J. Mol. Biol.* **157**, 105–132.
- Laemmli, U.K. (1970) Cleavage of structural proteins during the assembly of the head of bacteriophage T4. *Nature*, **227**, 680–685.
- Li, X., Henry, R., Yuan, J., Cline, K. and Hoffman, N.E. (1995) A chloroplast homologue of the signal recognition particle subunit SRP54 is involved in the posttranslational integration of a protein into thylakoid membranes. *Proc. Natl Acad. Sci. USA*, **92**, 3789–3793.
- Lill, H. and Nelson, N. (1991) The *atp1* and *atp2* operons of the cyanobacterium *Synechocystis* sp. PCC 6803. *Plant Mol. Biol.* **17**, 641–652.
- Lipman, D.J. and Pearson, W.R. (1985) Rapid and sensitive protein similarity searches. *Science*, **227**, 1435–1441.
- Lorkovic, Z.J., Schröder, W.P., Pakrasi, H.B., Irrgang, K.D., Herrmann, R.G. and Oelmlüller, R. (1995) Molecular characterization of PsbW, a nuclear-encoded component of the photosystem II reaction center complex in spinach. *Proceedings Natl Acad. Sci. USA*, **92**, 8930–8934.
- Mant, A., Schmidt, I., Herrmann, R.G., Robinson, C. and Klösigen, R.B. (1995) Sec-dependent thylakoid protein translocation:  $\Delta$ pH requirement is dictated by passenger protein and ATP concentration. *J. Biol. Chem.* **270**, 23275–23281.
- Martin, W. and Müller, M. (1998) The hydrogen hypothesis for the first eukaryote. *Nature*, **392**, 37–41.
- Martin, W. and Schnarrenberger, C. (1997) The evolution of the Calvin cycle from prokaryotic to eukaryotic chromosomes: a case study of functional redundancy in ancient pathways through endosymbiosis. *Curr. Genet.* **32**, 1–18.
- Michl, D., Robinson, C., Shackleton, J.B., Herrmann, R.G. and Klösigen, R.B. (1994) Targeting of proteins to the thylakoids by bipartite presequences: C<sub>fol</sub> is imported by a novel, third pathway. *EMBO J.* **13**, 1310–1317.
- Mould, R.M., Knight, J.S., Bogsch, E. and Gray, J.C. (1997) Azide-sensitive thylakoid membrane insertion of chimeric cytochrome *f* polypeptides imported into isolated pea chloroplasts. *Plant J.* **11**, 1051–1058.
- Oliver, D.B., Cabelli, R.J., Dolan, K.M. and Jarosik, G.P. (1990) Azide-resistant mutants of *Escherichia coli* alter the SecA protein, an azide-sensitive component of the protein export machinery. *Proc. Natl Acad. Sci. USA*, **87**, 8227–8231.
- Pugsley, A.P. (1993) The complete general secretory pathway in gram-negative bacteria. *Microbiol. Rev.* **57**, 50–108.
- Robinson, D., Karnauchov, I., Herrmann, R.G., Klösigen, R.B. and Robinson, C. (1996) Protease-sensitive thylakoidal import machinery for the Sec-,  $\Delta$ pH- and signal recognition particle-dependent protein targeting pathways, but not for C<sub>Fo</sub>-II integration. *Plant J.* **10**, 149–155.
- Rohrer, J. and Kuhn, A. (1990) The function of a leader peptide in translocating charged amino acyl residues across a membrane. *Science*, **250**, 1418–1421.
- Sambrook, J., Fritsch, E.F. and Maniatis, T. (1989) *Molecular Cloning. A Laboratory Manual*. Cold Spring Harbor: Cold Spring Harbor Laboratory Press.
- Sanger, F., Nicklen, S. and Coulson, A.R. (1977) DNA sequencing with chain-terminating inhibitors. *Proc. Natl Acad. Sci. USA*, **74**, 5463–5467.
- Schägger, H. and von Jagow, G. (1987) Tricine-sodium dodecylsulfate-polyacrylamide gel electrophoresis for the separation of proteins in the range from 1 to 100 kDa. *Anal. Biochem.* **166**, 368–379.
- Schmidt, G., Rodgers, A.J.W., Howitt, S.M., Munn, A.L., Hudson, G.S., Holten, T.A., Whitfield, P.R., Bottomley, W., Gibson, F. and Cox, G.B. (1990) The chloroplast C<sub>Fol</sub> subunit can replace the *b*-subunit of the F<sub>o</sub>F<sub>1</sub>-ATPase in a mutant strain of *Escherichia coli* K12. *Biochim. Biophys. Acta*, **1015**, 195–199.
- Smeekens, S., Bauerle, C., Hageman, J., Keegstra, K. and Weisbeek, P. (1986) The role of the transit peptide in the routing of precursors toward different chloroplast compartments. *Cell*, **46**, 365–375.
- Van den Broeck, G., Timko, M.P., Kausch, A.P., Cashmore, A.R., van Montagu, M. and Herrera-Estrella, L. (1985) Targeting of a foreign protein to chloroplasts by fusion to the transit peptide from the small subunit of ribulose-1,5-bisphosphate carboxylase. *Nature*, **313**, 358–363.
- Walker, J.E., Saraste, M. and Gay, N.J. (1984) The *unc* operon: nucleotide sequence, regulation and structure of ATP-synthase. *Biochim. Biophys. Acta*, **768**, 164–200.
- Westhoff, P., Alt, J., Nelson, N. and Herrmann, R.G. (1985) Genes and transcripts for the ATP synthase C<sub>Fo</sub> subunits I and II from spinach thylakoid membranes. *Mol. Gen. Genet.* **199**, 290–299.
- Yuan, J. and Cline, K. (1994) Plastocyanin and the 33-kDa subunit of the oxygen-evolving complex are transported into thylakoids with similar requirements as predicted from pathway specificity. *J. Biol. Chem.* **269**, 18463–18467.
- Yuan, J., Henry, R., McCaffery, M. and Cline, K. (1994) SecA homolog in protein transport within chloroplasts: evidence for endosymbiont-derived sorting. *Science*, **266**, 796–798.
- Zak, E., Sokolenko, A., Unterholzner, G., Altschmied, L. and Herrmann, R.G. (1997) On the mode of integration of plastid-encoded components of the cytochrome *b<sub>f</sub>* complex into thylakoid membranes. *Planta*, **201**, 334–341.

## Isolation and Purification of an Active $\gamma$ -Subunit of the $F_0 \cdot F_1$ -ATP Synthase from Chromatophore Membranes of *Rhodospirillum rubrum*

THE ROLE OF  $\gamma$  IN ATP SYNTHESIS AND HYDROLYSIS AS COMPARED TO PROTON TRANSLOCATION\*

(Received for publication, April 2, 1982)

Daniel Khananshvili and Zippora Gromet-Elhanan

From the Department of Biochemistry, The Weizmann Institute of Science, Rehovot 76100, Israel

We have earlier shown that extraction of *Rhodospirillum rubrum* chromatophores with LiCl removed completely the  $\beta$ -subunit of their coupling factor ATPase complex leaving the other four subunits attached to the membrane (Philosoph, S., Binder, A., and Gromet-Elhanan, Z. (1977) *J. Biol. Chem.* 252, 8747-8752). Further treatment of these  $\beta$ -less chromatophores with LiBr, under the described optimal conditions, resulted in specific removal of one additional subunit, the  $\gamma$ -subunit, and both subunits were purified to homogeneity.

The  $\beta, \gamma$ -less chromatophores as well as the  $\beta$ -less ones lost their ATP-linked activities, but retained their light-induced proton uptake, resulting in the formation of an electrochemical gradient of protons composed of both a pH gradient and a membrane potential. These results indicate that the removed  $\beta$  and  $\gamma$  subunits cannot be an integral part of an  $H^+$  gate in the *R. rubrum* chromatophore membrane.

Each of the removed subunits could bind to the  $\beta, \gamma$ -less chromatophores, but such separate reconstitution of either  $\beta$  or  $\gamma$  alone did not lead to restoration of any ATP-linked activity. ATP synthesis and hydrolysis could be restored to the same extent to these chromatophores by their reconstitution with both  $\beta$  and  $\gamma$ . It is thus concluded that the presence of both subunits is required for ATP synthesis as well as hydrolysis by the *R. rubrum*  $F_0 \cdot F_1$  complex. The identical degree of elimination and restoration of ATP synthesis and hydrolysis upon removal and reconstitution of  $\beta$  and  $\gamma$  indicates that in *R. rubrum* at least, there seems to be no reason for suggesting the operation of different catalytic sites for the two activities.

complex structure. Thus, the  $RrF_0 \cdot F_1$  complex purified from chromatophores of the photosynthetic bacterium *Rhodospirillum rubrum* contained eight nonidentical polypeptide subunits (5, 6). Five of these subunits,  $\alpha$ ,  $\beta$ ,  $\gamma$ ,  $\delta$ , and  $\epsilon$ , correspond to those composing the  $RrF_1$ -ATPase purified from the same bacterium (7), and the remaining three subunits form the  $F_0$  component of this  $RrF_0 \cdot F_1$  (6). A similar number of subunits has been reported for  $F_0 \cdot F_1$  complexes purified from the thermophilic bacterium PS3 (8), the mesophilic heterotrophic bacterium *Escherichia coli* (9), and from green plant chloroplasts (4, 10), whereas the best  $F_0 \cdot F_1$  preparations obtained from animal or yeast mitochondria contain a larger number of subunits (1, 11-13).

According to the chemiosmotic theory (14), these  $F_0 \cdot F_1$ -ATPase complexes are reversible proton translocators that can synthesize ATP at the expense of the electrochemical proton gradient formed across the membranes during electron transport. The capacity to couple the translocation of protons across the membrane to the synthesis of ATP has been clearly demonstrated with some of the most purified  $F_0 \cdot F_1$  complexes (10, 15-17). However, the detailed mechanism of ATP synthesis by these  $F_0 \cdot F_1$ -ATP synthases is as yet unknown. For the complete elucidation of the mechanism of action of these enzyme complexes, a precise determination of the function of each of their individual subunits is required. Some information on the function of different subunits of  $F_1$  has been obtained by following reconstitution of active ATPase complexes from isolated purified subunits of two species of bacteria (2, 18). These studies have indicated that mixtures containing the  $\alpha$ ,  $\beta$ , and  $\gamma$  subunits are required for regaining an ATP hydrolyzing activity (18, 19). In studies of another type Yoshida *et al.* (20) have reported that incorporation of an  $F_0$  preparation from a thermophilic bacterium into phospholipid vesicles increased their  $H^+$  permeability, and further addition of the  $\gamma$ -subunit together with  $\delta$  and  $\epsilon$ , but not  $\delta$  and  $\epsilon$  alone, caused a marked decrease of this  $H^+$  permeability. So they tentatively concluded that  $\gamma$  is the gate of proton flow through the  $F_0$  sector.

A different approach, which can provide information on the role of specific subunits of the  $F_0 \cdot F_1$  complex in all its known activities, namely  $H^+$  translocation, as well as ATP synthesis and hydrolysis, has been developed by us in *R. rubrum* chromatophore membranes (21-24). It involves a stepwise removal and reconstitution of individual subunits of this complex at its membrane-bound state. Up to now two subunits,  $\beta$  and  $\gamma$ , were removed by two consecutive extractions, starting with LiCl followed by LiBr (21-23). The removed subunits retained their native active state, since upon their reconstitution into the depleted membranes, which lost both their ATP synthesis and hydrolysis activities but not their proton translocating one, about 60% of the lost activities were restored (21, 24).

All energy-transducing membranes that synthesize ATP contain an enzyme complex which is composed of two distinct structures (1-4),  $F_1$  and  $F_0$ . The  $F_1$  sector is an active ATPase and the  $F_0$  sector is involved in the flux of protons across the membrane. The whole  $F_0 \cdot F_1$  complex has been isolated by detergent extraction from a large number of respiratory and photosynthetic membranes and found to have an extremely

\* This investigation was partially supported by a grant from the United States-Israel Binational Science Foundation (BSF), Jerusalem, Israel. The costs of publication of this article were defrayed in part by the payment of page charges. This article must therefore be hereby marked "advertisement" in accordance with 18 U.S.C. Section 1734 solely to indicate this fact.

<sup>1</sup> The abbreviations and trivial names used are  $F_1$ , the water-soluble catalytic sector of the complex;  $F_0 \cdot F_1$ , the proton translocating-ATP synthase-ATPase complex;  $F_0$ , the intrinsic membrane sector of the complex;  $RrF_0 \cdot F_1$  and  $RrF_1$ , the  $F_0 \cdot F_1$  and  $F_1$  of *R. rubrum*; Tricine, N-[2-hydroxy-1,1-bis(hydroxymethyl)ethyl]glycine.



The LiCl extraction was shown to release completely the  $\beta$ -subunit leaving all the other  $RrF_0F_1$  subunits attached to the  $\beta$ -less chromatophore membranes (21, 25).

In this paper we establish the conditions required for maximal release of the  $\gamma$ -subunit by LiBr extraction, for an improved purification of both  $\beta$  and  $\gamma$ , and for their correct rebinding that ensures almost full restoration of both ATP synthesis and hydrolysis activities.

#### MATERIALS AND METHODS

**Buffers**—TMSA buffer: 50 mM Tricine-NaOH (pH 8.0), 0.25 M sucrose, 4 mM  $MgCl_2$ , 4 mM ATP. Buffer A: 100 mM Tricine-NaOH (pH 8.0), 4 mM ATP, 4 mM  $MgCl_2$ , 10% glycerol. Buffer B: 5 mM Tricine-NaOH (pH 8.0), 4 mM ATP, 4 mM  $MgCl_2$ , 5% glycerol. Buffer C: 50 mM Tricine-NaOH (pH 8.0), 1.0 M KCl, 2 mM  $MgCl_2$ , 10% glycerol. Buffer D: 50 mM Tricine-NaOH (pH 8.0), 1.0 M KCl, 1.0 M urea, 10% glycerol. Buffer E: 10 mM 4-morpholineethanesulfonic acid-NaOH (pH 6.2), 150 mM NaCl, 2 mM  $MgCl_2$ , 5% glycerol.

**Preparation of Coupled and Depleted Chromatophores**—*R. rubrum* cells (strain S1) were grown as previously described (21). Coupled chromatophores were prepared according to published procedures (26, 27), except that after cell rupture in the Yeda Press deoxyribonuclease and ribonuclease were added, each to a final concentration of 10  $\mu$ g/ml and  $MgCl_2$  to a final concentration of 10 mM. The suspension was incubated for 20 min at room temperature and then centrifuged, washed, and resuspended as outlined previously (27). This treatment increased the yield of coupled chromatophores by at least 50%. It also decreased the ratio of protein/bacteriochlorophyll from 25:1 (see Ref. 28) to about 12:1 without decreasing the rate of photophosphorylation, which ranged between 800–1100  $\mu$ mol/h/mg of bacteriochlorophyll. For preparation of  $\beta$ -less chromatophores, the washed, coupled chromatophores, were finally resuspended in TMSA buffer, and after 2 h at 4 °C they were extracted with LiCl, washed, and resuspended as previously described (29). For preparation of  $\beta,\gamma$ -less chromatophores, the washed  $\beta$ -less preparation was resuspended in TMSA buffer, extracted with LiBr by stirring for 1 h at 4 °C, then washed and resuspended as outlined above. The final concentrations of LiBr and of the chromatophores during the extraction were 2 M and 0.2–0.3 mg of bacteriochlorophyll/ml, respectively, unless otherwise stated.

**Purification of the  $\beta$  and  $\gamma$  subunits**—The  $\beta$  subunit was purified by an improved method that gave a better yield of a clean homogeneous  $\beta$  than the earlier described procedure (21), as follows. The LiCl crude extract (about 350 mg of protein obtained from chromatophores containing 400 mg of bacteriochlorophyll) was brought to 60% ammonium sulfate saturation and allowed to stand overnight at 4 °C. The precipitate was dissolved in buffer A at a concentration of 1 mg of protein/ml. This step is essential for complete removal of LiCl. The protein solution was fractionated by ammonium sulfate, and the fraction precipitating between 15–50% saturation was collected, dissolved in about 35 ml of buffer A at 5 mg of protein/ml, dialyzed for 4 h against 100 volumes of buffer A, and applied on a column (2.9  $\times$  25 cm) of DEAE-Sephadex A-50. The column was washed with 200 ml of buffer A containing 80 mM sodium chloride, and a linear gradient of 80–400 mM sodium chloride in 400 ml of buffer A was applied. Two main protein peaks were eluted (not shown). Only the second peak contained  $\beta$  subunit activity that was measured by its ability to restore photophosphorylation when reconstituted into  $\beta$ -less chromatophores (see below). Fractions containing  $\beta$ -activity were pooled. The protein in the pooled fractions was precipitated at 60% ammonium sulfate saturation, dissolved in buffer A at 10 mg of protein/ml, and all insoluble materials were removed by 1 h of centrifugation at 350,000  $\times g$ . Traces of bacteriochlorophyll, which are sometimes still present at this stage, were removed by applying the supernatant (about 8 ml) on a column (2.0  $\times$  80 cm) of Bio-Gel A-0.5 m agarose and eluting with buffer A. Fractions containing  $\beta$  subunit activity were pooled and applied to a column (1.2  $\times$  25 cm) of DEAE-cellulose (DE23). The column was washed with 40 ml of buffer A containing 0.1 M sodium chloride, and a linear gradient of 0.1–0.4 M sodium chloride in 200 ml of buffer A was applied (Fig. 3A). The flow rate was 30 ml/h, and fractions of 5.2 ml were collected. These containing pure active  $\beta$  were pooled, concentrated by ultrafiltration to 3 mg of protein/ml, and dialyzed exhaustively against buffer B. The  $\beta$  subunit (yield 7 mg) was stored in buffer B in liquid nitrogen without loss of activity for at least 6 months.  $\beta$  activity at each step of purification was also stable in liquid nitrogen and could withstand

at least four cycles of freezing and thawing during the whole purification procedure.

The  $\gamma$  subunit was purified from the LiBr crude extract as follows. LiBr was removed by precipitation at 60% ammonium sulfate saturation as described above for the  $\beta$ -subunit. The precipitate was dissolved in 60 ml of buffer C at a concentration of 1 mg of protein/ml and then reprecipitated at 45% ammonium sulfate saturation. The precipitate was dissolved in buffer C and dialyzed for 2 h against 100 volumes of buffer C. The dialyzed protein solution was diluted with an equal volume of buffer C to about 0.5 mg of protein/ml, and all insoluble materials were removed by 2 h of centrifugation at 270,000  $\times g$ . The supernatant (32 mg in 65 ml) was applied on a column (1.7  $\times$  15 cm) of hydroxyapatite. The column was washed with 70 ml of buffer C, and a linear gradient of 0–0.4 M sodium phosphate in 300 ml of buffer D was applied (Fig. 3B). The flow rate was 120 ml/h (with a peristaltic pump), and fractions of 5.0 ml were collected. All fractions were dialyzed exhaustively against buffer E. In order to obtain any  $\gamma$  subunit activity, the chromatography and dialysis should be done as rapidly as possible, since in the presence of the high concentrations of salt and urea of buffer D,  $\gamma$  activity is not stable. Fractions containing  $\gamma$  subunit activity, measured as described below, were pooled and concentrated by vacuum dialysis against buffer E to no more than 0.4 mg of protein/ml. Glycerol was then added to a final concentration of 10%, and the pure  $\gamma$  subunit (yield 6 mg) was stored in liquid nitrogen without loss of activity for at least 4 months.  $\gamma$ , as  $\beta$ , could withstand at least three cycles of freezing and thawing during the purification procedure.

**Reconstitution of  $\beta$ -Less and  $\beta,\gamma$ -Less Chromatophores**—The depleted chromatophores were reconstituted with the missing subunits as follows (unless otherwise stated).  $\beta$ -Less or  $\beta,\gamma$ -less chromatophores (10  $\mu$ g of bacteriochlorophyll) were incubated for 30 min at 35 °C with 100  $\mu$ g of purified  $\beta$  and/or 30  $\mu$ g of purified  $\gamma$  in a reaction mixture containing, in a final volume of up to 0.7 ml, 10 mM 4-morpholineethanesulfonic acid-NaOH (pH 6.2), 25 mM  $MgCl_2$ , 4 mM ATP, and 15 mM glucose. The reconstituted chromatophores were either assayed immediately or, where indicated, centrifuged for 30 min at 4 °C in the microfuge (Eppendorf 5414) to remove any remaining free subunits, then dissolved in the reconstitution buffer and assayed for restored ATP-linked activities. For optimal reconstitution of the  $\gamma$  subunit, a pH of 6.2 was required (24), whereas the rates of photophosphorylation and ATP hydrolysis were higher, around pH 8.0. Therefore, concentrated Tricine-NaOH (pH 8.0) was added to a final concentration of 80 mM to all reconstituted chromatophores, and the suspension was equilibrated for 15 min at 4 °C before being assayed.

**Analytical Methods and Assays**—Photophosphorylation was carried out as previously described (26), but illumination was for 3 min at 35 °C. The reaction mixture contained, in 3 ml, 80 mM Tricine-NaOH (pH 8.0), 6 mM  $MgCl_2$ , 2 mM ATP, 5 mM sodium phosphate containing about  $10^6$  cpm of  $^{32}P$ , 15 mM glucose, 150  $\mu$ g of hexokinase, 66  $\mu$ M *N*-methylphenazonium methosulfate, and chromatophores containing 10  $\mu$ g of bacteriochlorophyll. The reaction was stopped by 0.2 ml of 50% perchloric acid, and ATP formation was measured according to Avron (30).

ATPase activity was assayed for 10 min at 35 °C as previously described (28), either via the radiochemical method using [ $\gamma$ - $^{32}P$ ]ATP or by measuring the released  $P_i$  colorimetrically (31).

$\Delta pH$  and  $\Delta\psi$  were determined in the presence of the fluorescent probes 9-aminoacridine and anilinoanthracene sulfonic acid, respectively, as outlined before (32).

Electrophoresis in 7.5% polyacrylamide gels containing sodium dodecyl sulfate was performed according to Weber and Osborn (33). The samples were prepared as previously described (21). Gels were stained and destained as outlined by Lanzillo *et al.* (34).

Protein was determined by the method of Lowry *et al.* (35), and bacteriochlorophyll was measured using the *in vivo* extinction coefficient given by Clayton (36).

#### RESULTS

**Optimal Conditions for Release of the  $\gamma$  Subunit From  $\beta$ -Less *R. rubrum* Chromatophores**—The concentrations of LiBr and chromatophores and the pH of the suspension during extraction were found to be crucial factors for achieving a maximal release of the  $\gamma$  subunit. As is illustrated in Fig. 1, extraction with less than 1.0 M LiBr did not release the  $\gamma$  subunit, since reconstitution with  $\beta$  alone restored over 90%



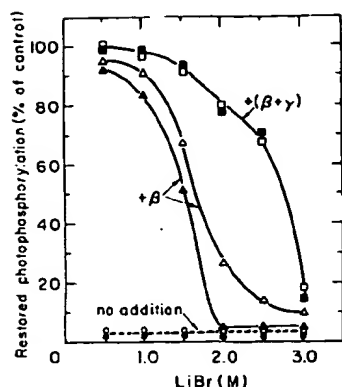


FIG. 1. Dependence of the efficiency of the release and reconstitution of the  $\gamma$  subunit on the concentration of LiBr during extraction of  $\beta$ -less chromatophores. The extraction with LiBr was carried out as described under "Materials and Methods," except that the LiBr concentration was varied as indicated, and in one set of experiments the extraction was carried out at pH 6.2 using 50 mM 4-morpholineethanesulfonic acid-NaOH instead of at pH 8.0 with Tricine-NaOH. All the  $\beta$ -less LiBr-extracted chromatophores were washed, resuspended, reconstituted with either  $\beta$  or  $\beta + \gamma$  as indicated, and the restored photophosphorylation was assayed as described under "Materials and Methods." The control photophosphorylation restored in  $\beta$ -less chromatophores after their reconstitution with  $\beta$  alone was 750  $\mu\text{mol/h/mg}$  of bacteriochlorophyll.  $\bullet$ ,  $\Delta$ ,  $\blacksquare$ , extracted at pH 8.0;  $\circ$ ,  $\triangle$ ,  $\square$ , extracted at pH 6.2.

of the control photophosphorylation in preparations that had not been extracted with LiBr. Extraction with increasing concentrations of LiBr caused a release of  $\gamma$ , and with 2.0 M LiBr most of the  $\gamma$  was released when the extraction was carried out at pH 8.0, since reconstitution with  $\beta$  alone did not restore any photophosphorylation activity, whereas reconstitution with  $\beta$  and  $\gamma$  together restored about 80% of the control photophosphorylation. When the extraction was carried out at pH 6.2, there was always some residual restored photophosphorylation after reconstitution with  $\beta$  alone, indicating that at this pH not all the  $\gamma$  is released, even after extraction with up to 3.0 M LiBr. Moreover, after extraction with more than 2.0 M LiBr there is a drastic decrease in the degree of restoration of photophosphorylation even after reconstitution with  $\beta$  and  $\gamma$  together. It is, therefore, concluded that for optimal release of the  $\gamma$  subunit 2.0 M LiBr at pH 8.0 is required.

The importance of the concentration of chromatophores is shown in Fig. 2. With 2 M LiBr at pH 8.0, all the  $\gamma$  was released as long as the chromatophore concentration was kept below 0.3 mg of bacteriochlorophyll/ml, whereas at a higher concentration there was some restoration of activity even after reconstitution with  $\beta$  alone, indicating that not all the  $\gamma$  was released.

**Purification of the  $\beta$  and  $\gamma$  subunits**—The  $\beta$  and  $\gamma$  subunits released by LiCl and LiBr extraction of *R. rubrum* chromatophores were purified as described under "Materials and Methods." The protein elution profiles from columns used in the final stage of purification of each subunit are shown in Fig. 3. The purity of these subunit preparations was assessed by sodium dodecyl sulfate-polyacrylamide gel electrophoresis (Fig. 4). Both  $\beta$  (lane B) and  $\gamma$  (lane C) were obtained in essentially homogeneous form. These purified subunits were used in all the experiments reported in this work.

Preliminary characterization of the  $\beta$  and  $\gamma$  subunits showed a large difference in their solubility. Solutions of up to 3.0 mg of  $\beta$ /ml of buffer B could be prepared, whereas  $\gamma$  was soluble to only 0.4 mg/ml of buffer E and tended to form aggregates above this concentration. The subunits were stored in these

different buffers because, as we have previously reported, the  $\beta$  subunit required the presence of at least 2 mM ATP to keep it active during storage and reconstitution (21, 29), whereas  $\gamma$  showed no need for ATP, but required a low pH of around 6.0

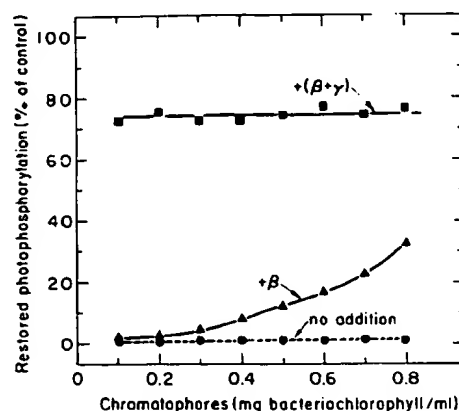


FIG. 2. Efficiency of the release of the  $\gamma$  subunit as a function of the concentration of  $\beta$ -less chromatophores during LiBr extraction. The extraction was carried out as described under "Materials and Methods," except that the chromatophore concentration was varied as indicated. Conditions of reconstitution, assay, and the control activity were as in Fig. 1.

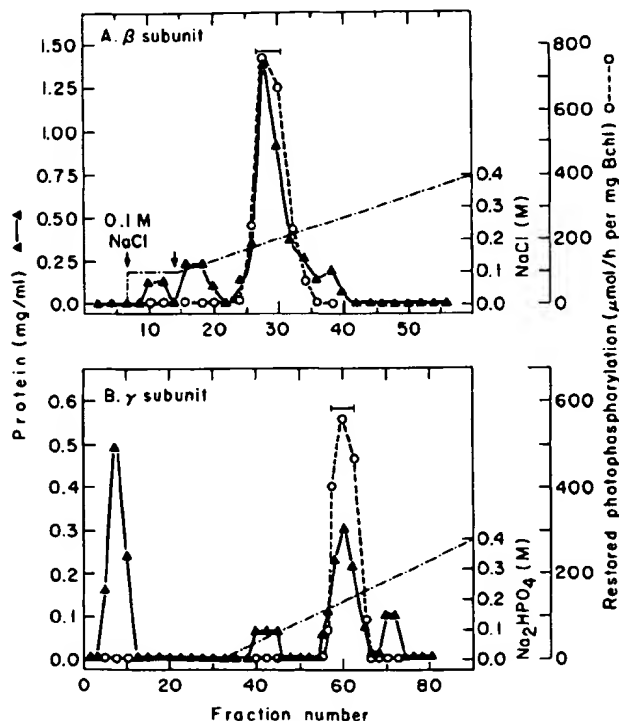


FIG. 3. Purification of the  $\beta$  and  $\gamma$  subunits released from *R. rubrum* chromatophores. The purification is described in detail under "Materials and Methods." A, column chromatography of the  $\beta$ -subunit on DEAE-cellulose. B, column chromatography of the  $\gamma$ -subunit on hydroxyapatite. The bars indicate fractions of pure  $\beta$  (A) or pure  $\gamma$  (B) that were pooled. For testing  $\beta$  activity,  $\beta$ -less chromatophores were reconstituted with 100  $\mu\text{g}$  of protein from each fraction in A as described under "Materials and Methods," except that 10 mM Tricine-NaOH (pH 8.0) were used. For testing  $\gamma$  activity,  $\beta$ ,  $\gamma$ -less chromatophores were reconstituted with 100  $\mu\text{g}$  of pure  $\beta$  and 50  $\mu\text{g}$  of protein from each fraction in B. The reconstituted chromatophores were assayed immediately for restored photophosphorylation activity as described under "Materials and Methods." BChl = bacteriochlorophyll.

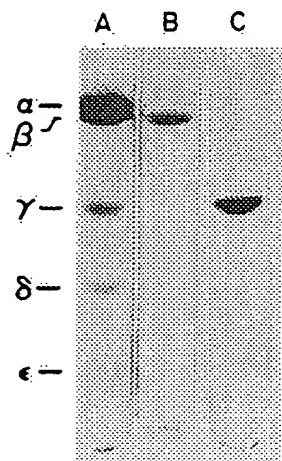


Fig. 4. Sodium dodecyl sulfate-polyacrylamide gel electrophoresis of subunits  $\beta$  and  $\gamma$  of  $RrF_1$ . A,  $RrF_1$  purified according to (25). B, purified  $\beta$  from the pooled fractions of Fig. 3A that were concentrated and dialyzed as described under "Materials and Methods." C, purified  $\gamma$  from the pooled fractions of Fig. 3B that were concentrated and dialyzed as described above.

to keep it active (23, 24). Neither  $\beta$  nor  $\gamma$  needed reducing conditions, since inclusion of 0.1 mM dithiothreitol during their purification did not increase the activity of the final purified preparations. These properties of  $\beta$  and  $\gamma$  isolated from *R. rubrum* are quite similar to those previously reported for  $\beta$  and  $\gamma$  isolated from *E. coli* (37).

**Optimal Conditions for Reconstitution of the  $\gamma$  Subunit—**Reconstitution of the  $\gamma$  subunit into  $\beta, \gamma$ -less chromatophores in an active manner resulting in restoration of both photophosphorylation and ATPase activities requires the presence of three components: the  $\beta, \gamma$ -less chromatophores and each of the missing subunits (24). The concentrations of all three components are crucial for obtaining maximal restoration of the ATP-linked activities. Thus, at a fixed concentration of chromatophores, the reconstitution of  $\beta$ -less chromatophores with increasing amounts of the  $\beta$  subunit followed a simple saturation curve, whereas the reconstitution of  $\beta, \gamma$ -less chromatophores with  $\beta$  and  $\gamma$  together exhibited a completely different pattern (Fig. 5). Increasing amounts of  $\gamma$  with a fixed, saturating concentration of  $\beta$  led first to a linear increase in the extent of restoration of photophosphorylation up to a plateau value which was seen with the amount of  $\gamma$  ranging between 30 to 100  $\mu$ g. A further increase in the amount of  $\gamma$  caused, however, a rather severe decrease in the extent of the restored activity (Fig. 5). So in the presence of a fixed level of  $\beta$  the restored photophosphorylation is dependent on addition of an optimal concentration of  $\gamma$ .

A number of additional factors were found to be important for obtaining maximal restoration of activity. Fig. 6 illustrates the effect of the duration of reconstitution. Here, the extent of restored  $Mg^{2+}$ -ATPase activity increased with time, reaching a maximal extent when the reconstitution was carried out for about 40 min. The pattern was similar in both  $\beta$ -less chromatophores reconstituted with a saturating amount of  $\beta$  (100  $\mu$ g) and  $\beta, \gamma$ -less chromatophores reconstituted with the saturating amount of  $\beta$  and an optimal amount of  $\gamma$  (30  $\mu$ g). Furthermore, in both systems the extent of restored activity remained constant even when the reconstitution was continued for 2 h (Fig. 6). A similar pattern was obtained when the restoration of photophosphorylation or  $Ca^{2+}$ -ATPase activities were assayed (not shown).

We have previously reported (24) that the concentration of  $MgCl_2$  and the pH during reconstitution are also important

for achieving a maximal restoration of activity in  $\beta, \gamma$ -less chromatophores reconstituted with  $\beta$  and  $\gamma$  together. All these factors have been incorporated into the optimal reconstitution system that is described under "Materials and Methods."

**Role of the  $\gamma$  Subunit in Various Chromatophore Activities—**It has been earlier reported that  $\beta, \gamma$ -less chromatophores as well as the  $\beta$ -less ones lost over 98% of their photophosphorylation and  $Mg^{2+}$ - or  $Ca^{2+}$ -ATPase activities, while retaining over 70% of their ability to take up protons during light-induced electron transport (21, 23, 24, 29). As is illustrated in Table I, this proton uptake leads to the formation of an electrochemical proton gradient composed of a  $\Delta pH$  and a  $\Delta \psi$  in both types of depleted chromatophores. Moreover, the calculated values of  $\Delta pH$  and  $\Delta \psi$  attained in the depleted chromatophores were not very different from those attained in the coupled chromatophores (Table I, see also Ref. 32). In the  $\beta$ -less chromatophores they were lower by less than 10%.

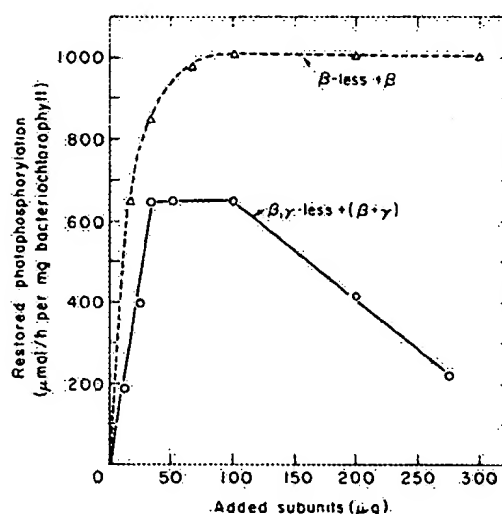


Fig. 5. Effect of the amount of subunits added during reconstitution on the degree of restoration of photophosphorylation in depleted chromatophores.  $\beta$ -less and  $\beta, \gamma$ -less chromatophores were reconstituted and immediately assayed as described under "Materials and Methods," except that the  $\beta$ -less chromatophores were reconstituted with varying concentrations of  $\beta$ , and the  $\beta, \gamma$ -less chromatophores were reconstituted with 100  $\mu$ g of  $\beta$  together with varying concentrations of  $\gamma$ , as indicated.

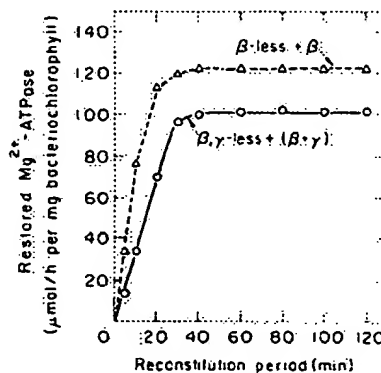


Fig. 6. Effect of the duration of reconstitution on the degree of restoration of the  $Mg^{2+}$ -ATPase activity of depleted chromatophores. The reconstitution and assay were carried out as described under "Materials and Methods" except that the depleted chromatophores were incubated with the missing subunits for the indicated time intervals before performing the ATPase assay.

TABLE I  
Determination of  $\Delta pH$  and  $\Delta\psi$  generated during illumination of coupled and depleted chromatophores

Chromatophore preparation <sup>a</sup>	Electrochemical proton gradient			
	-Valinomycin -KCl		+Valinomycin +KCl <sup>b</sup>	
	$\Delta pH^c$	$\Delta\psi^c$ mV	$\Delta pH^c$	$\Delta\psi^c$ mV
Coupled	2.4	95	3.3	0
$\beta$ -Less	2.3	85	3.1	ND <sup>d</sup>
$\beta,\gamma$ -Less	2.0	70	3.0	ND

<sup>a</sup> Coupled and depleted chromatophores were prepared as described under "Materials and Methods."

<sup>b</sup> Valinomycin was added at a concentration of 2  $\mu M$  and KCl at 120 mM.

<sup>c</sup>  $\Delta pH$  and  $\Delta\psi$  were measured by following changes in the fluorescence of 9-aminoacridine and anilinonaphthalene sulfonic acid, respectively, and the calculations were done as outlined in (32).

<sup>d</sup> Not determined.

and in the  $\beta,\gamma$ -less ones by about 20%. It should be emphasized that these  $\beta,\gamma$ -less chromatophores were prepared by extraction with LiBr under conditions that were shown to result in a maximal release of the  $\gamma$  subunit (Figs. 1 and 2), and they lost practically all their ATP-linked activities. These results indicate, therefore, that removal of the  $\gamma$  subunit does not increase the  $H^+$  permeability of the *R. rubrum* chromatophores. It also did not change their response to the addition of valinomycin and KCl, which leads to an elimination of the  $\Delta\psi$ , since in all types of chromatophores this was compensated to a large extent by an increase in the  $\Delta pH$  (Table I).

In all the experiments presented above, the reconstitution of  $\beta,\gamma$ -less chromatophores was carried out by adding the  $\beta$  and  $\gamma$  subunits together. Table II summarizes a series of experiments attempting to answer the following questions. (a) Can either  $\beta$  or  $\gamma$  rebind separately to the  $\beta,\gamma$ -less chromatophores? (b) If yes, does a separate rebinding of either one of them restore any activity? (c) Is a separate but consecutive rebinding of both subunits as effective in restoring activity as their binding when present together? Answers to these questions were sought by introducing two separate periods of reconstitution, enabling a stepwise addition of either  $\beta$  or  $\gamma$  first, followed by the other subunit in the second period, and by running a double series of assays on every two-period reconstitution experiment. In the second series each period of reconstitution was followed by a centrifugation step, which removed any unbound soluble subunit.

The above described setup experiments 2 and 3 in Table II clearly demonstrate that reconstitution of either  $\beta$  or  $\gamma$  alone to  $\beta,\gamma$ -less chromatophores does not restore any activity, although these can rebind separately to the  $\beta,\gamma$ -less chromatophores, as is indicated from the results of experiments 4 and 5 in Table II. In these experiments photophosphorylation was restored, and to a very similar extent, in assays carried out in chromatophores reconstituted either with or without centrifugation after each period of reconstitution. These results suggest that the separate rebinding of each subunit is strong enough not to be removed by centrifugation, thus enabling restoration of photophosphorylation activity after the consecutive rebinding of the missing subunit in the second period of reconstitution. It is thus clear that the presence of both  $\beta$  and  $\gamma$  is required for restoration of photophosphorylation to  $\beta,\gamma$ -less chromatophores.

The order of rebinding of  $\beta$  and  $\gamma$  is not important at all, because a similar extent of restored phosphorylation was obtained when either  $\beta$  (experiment 4) or  $\gamma$  (experiment 5) were added first, followed by the other subunit in the second period of reconstitution. However, reconstitution of  $\beta$  and  $\gamma$

together (experiment 6) resulted always in a 30 to 50% increase in the extent of restoration as compared to a separate consecutive reconstitution (compare experiments 4, 5, and 6 in Table II and 3, 4, and 5 in Table III).

We have previously reported (21) that removal of the  $\beta$  subunit resulted in loss of both ATP synthesis and hydrolysis, and its reconstitution restored both activities to a similar extent, thus indicating that the  $\beta$  subunit is absolutely necessary for both catalytic activities. The role of the  $\gamma$  subunit in these activities is summarized in Table III. Rebinding of  $\beta$  alone to  $\beta,\gamma$ -less chromatophores did not restore any activity, suggesting that in *R. rubrum* chromatophores even ATP hydrolysis requires the presence of  $\gamma$ . Moreover, the separate, but consecutive rebinding of  $\beta$  and  $\gamma$  restored ATP hydrolysis as well as synthesis and to a similar extent. Also, the reconstitution of  $\beta$  and  $\gamma$  together increased by about 50% the extent of the restored activities in all three assays as compared to a separate consecutive reconstitution. The similar decrease and increase in both ATP synthesis and hydrolysis activities of *R. rubrum* chromatophores subjected to different types of treat-

TABLE II  
Effect of the separate binding of the  $\beta$  and  $\gamma$  subunits to the  $\beta,\gamma$ -less chromatophores on the degree of restoration of their photophosphorylation activity

Experiment No.	Type of depleted chromatophores	Subunits added during the periods of reconstitution <sup>a</sup>		Restored photophosphorylation assayed in chromatophores reconstituted	
		First	Second	Without centrifugation	With centrifugation <sup>b</sup>
				$\mu mol/h/mg$ Bchl <sup>c</sup>	
1	$\beta$ -Less	$\beta$	None	753	761
2	$\beta,\gamma$ -Less	$\beta$	None	16	13
3	$\beta,\gamma$ -Less	$\gamma$	None	9	8
4	$\beta,\gamma$ -Less	$\beta$	$\gamma$	400	417
5	$\beta,\gamma$ -Less	$\gamma$	$\beta$	396	410
6	$\beta,\gamma$ -Less	$\beta + \gamma$	None	590	589

<sup>a</sup> Reconstitution was as described under "Materials and Methods," except that where indicated each subunit was separately reconstituted for a period of 30 min at the indicated order. In other cases the reconstitution was continued for an overall period of 60 min.

<sup>b</sup> In chromatophores reconstituted with centrifugation, each period of reconstitution was followed by centrifugation as described under "Materials and Methods."

<sup>c</sup> Bchl = bacteriochlorophyll.

TABLE III  
Comparison of the extent of restoration of ATP synthesis and  $Mg^{2+}$ - or  $Ca^{2+}$ -catalyzed ATP hydrolysis after reconstitution of  $\beta,\gamma$ -less chromatophores

Experiment No.	Type of depleted chromatophores	Subunits added during the periods of reconstitution <sup>a</sup>		Type of restored activity assayed		
		First	Second	ATP synthesis	ATP hydrolysis with	
					$Mg^{2+}$	$Ca^{2+}$
					% control <sup>b</sup>	
1	$\beta$ -Less	$\beta$	None	100	100	100
2	$\beta,\gamma$ -Less	$\beta$	None	3	3	6
3	$\beta,\gamma$ -Less	$\beta$	$\gamma$	55	65	71
4	$\beta,\gamma$ -Less	$\gamma$	$\beta$	54	66	74
5	$\beta,\gamma$ -Less	$\beta + \gamma$	None	78	91	99

<sup>a</sup> Reconstitution conditions were as described in Table II, for chromatophores reconstituted with centrifugation.

<sup>b</sup> The control rates of the restored activities in  $\beta$ -less chromatophores reconstituted with  $\beta$  were in micromoles per h per mg of bacteriochlorophyll, as follows: 761 for ATP synthesis, 123 for  $Mg^{2+}$ -ATPase, and 89 for  $Ca^{2+}$ -ATPase.

ments used for release or rebinding of  $\beta$  and  $\gamma$  is consistent with the operation of one catalytic site for both activities in these chromatophores.

#### DISCUSSION

Extraction of *R. rubrum*  $\beta$ -less chromatophores by LiBr was previously reported to remove the  $\gamma$ -subunit from their membrane-bound  $RrF_1$  (23, 24). Here we show that no other subunit besides  $\gamma$  is removed by this treatment, since reconstitution of the resulting washed  $\beta,\gamma$ -less chromatophores with  $\beta$  and  $\gamma$ , that have been purified to homogeneity (Figs. 3 and 4), restores 80 to 90% of their lost ATP-linked activities (Table III). We have also defined conditions for obtaining a maximal removal of the  $\gamma$  subunit. These involve extraction of  $\beta$ -less chromatophores containing 0.2–0.3 mg of bacteriochlorophyll/ml with 2 M LiBr at a pH of 8.0 (Figs. 1 and 2). With lower LiBr concentrations, a lower pH, or higher chromatophore concentrations, not all the  $\gamma$  is released, because under such conditions there is always some restoration of activity after reconstituting  $\beta,\gamma$ -less chromatophores with  $\beta$  alone. Higher LiBr concentrations have a generally deleterious effect on the chromatophore membranes resulting in a drastic decrease in their capacity to synthesize ATP after reconstitution of the missing subunits. More dilute chromatophore suspensions should also be avoided, since it has been earlier reported (27) that dilution of *R. rubrum* chromatophores to less than 0.1 mg of bacteriochlorophyll/ml leads to the release of endogenous electron transport carriers.

Under the above stated conditions, all the  $\gamma$  subunit seems to be released, because there is no restoration of activity in the resulting  $\beta,\gamma$ -less chromatophores upon their reconstitution with  $\beta$  alone, but there is excellent restoration of activity by reconstitution of  $\beta$  and  $\gamma$  together (Tables II and III). In all these experiments, ATP synthesis as well as hydrolysis activities have been lost and restored to a very similar extent. These data, therefore, indicate that the presence of both  $\beta$  and  $\gamma$  is required for the operation of these activities, but they do not seem to support the suggestion that different catalytic sites are involved in ATP synthesis and hydrolysis.

The  $\beta,\gamma$ -less chromatophores, that have been obtained under the conditions developed above for maximal release of  $\gamma$ , have retained their capacity for generating an electrochemical proton gradient during light-induced electron transport (Table I). These results suggest that in *R. rubrum* chromatophores the  $\gamma$  subunit does not function as the gate for proton flow through the  $F_0$  sector. Such a function for  $\gamma$  has been suggested by Yoshida *et al.* (20), but their experimental system is very different from ours. They have added various mixtures of soluble subunits to phospholipid vesicles containing an  $F_0$  sector and found that the mixture of  $\gamma$ ,  $\delta$ , and  $\epsilon$  decreased the  $H^+$  permeability of the  $F_0$  vesicles (20). We have used native chromatophore membranes containing an assembled complex of  $\alpha$ ,  $\delta$ , and  $\epsilon$  that were not more leaky to protons than the coupled or  $\beta$ -less chromatophores (Table I). So in our case, when  $\gamma$  is absent,  $\alpha$  in the presence of  $\delta$  and  $\epsilon$  could function as the proton gate. This possibility has not been tested by Yoshida *et al.* (20) as they have not tried to add a mixture of  $\alpha$ ,  $\delta$ , and  $\epsilon$ . Moreover, even if such a mixture would fail to function as a proton gate in their setup, the failure could be due to difficulties in the correct assembly of the added soluble subunits into an active complex which, in our system, is already assembled. Weiss and McCarty (38) have reported that in spinach chloroplast thylakoids cross-linking of two groups in the  $\gamma$  subunit by a bifunctional maleimide caused an inhibition of photophosphorylation and an increased  $H^+$  permeability. These and further studies (39) led McCarty (40) to suggest that  $\gamma$  might function in the transmission of protons

to the active site of ATP synthesis. But it is also possible that the cross-linking in  $\gamma$  could cause conformational changes in  $\alpha$  or other subunits.

The above results demonstrate that in *R. rubrum* chromatophores the  $\gamma$  subunit does not play a role in proton translocation but is required together with  $\beta$  for the operation of ATP synthesis and hydrolysis. However, whereas  $\beta$  has been shown to be absolutely necessary for the catalysis itself (21), it cannot be decided as yet whether  $\gamma$  is needed for the catalysis or for the correct rebinding of  $\beta$ . Clearly, rebinding of  $\beta$  alone to  $\beta,\gamma$ -less chromatophores does not restore even ATP hydrolysis (Table III, experiment 2), although these " $\gamma$ -less" chromatophores contain both  $\alpha$  and  $\beta$ , and a soluble  $\alpha\beta$  complex has been reported to have ATPase activity (41). This inactivity might, however, be due to an incorrect binding of  $\beta$ , in the absence of  $\gamma$ , to the  $\beta,\gamma$ -less chromatophores. If so, such incorrect binding may be corrected upon addition of  $\gamma$ , since after a separate consecutive reconstitution of  $\beta$  followed by  $\gamma$  both ATP synthesis and hydrolysis were restored (Table III, experiment 3). In this system the activities were, however, restored to a lower extent than upon reconstitution of  $\beta$  and  $\gamma$  together (Table III, experiment 5), thus suggesting that the correction needs time. It is also possible that when both subunits are present in solution, a complex of  $\beta\gamma$  is formed (see Ref. 19), and this complex rebinds more efficiently or in a more effective conformation or configuration to the  $\beta,\gamma$ -less chromatophores. These possibilities merit further investigations.

#### REFERENCES

1. Pedersen, P. L., Amzel, L. M., Soper, J. W., Cintron, N., and Hulihan, J. (1978) in *Energy Conservation in Biological Membranes* (Schafer, G., and Klingenberg, M., eds) pp. 159–194, Springer-Verlag, Heidelberg.
2. Kagawa, Y., Sone, N., Hirata, H., and Yoshida, M. (1979) *J. Bioenerg. Biomembr.* 11, 31–78.
3. Fillingame, R. H. (1981) *Curr. Top. Bioenerg.* 11, 35–106.
4. Nelson, N. (1981) *Curr. Top. Bioenerg.* 11, 1–33.
5. Bengis-Garber, C., and Gromet-Elhanan, Z. (1979) *Biochemistry* 18, 3577–3581.
6. Gromet-Elhanan, Z. (1981) in *Photosynthesis II. Electron Transport and Photophosphorylation* (Akoyunoglou, G., ed) pp. 731–740, Balaban International Science Services, Philadelphia.
7. Johansson, B. C., and Baltscheffsky, M. (1975) *FEBS Lett.* 53, 221–224.
8. Sone, N., Yoshida, M., Hirata, H., and Kagawa, Y. (1975) *J. Biol. Chem.* 250, 7917–7923.
9. Foster, D. L., and Fillingame, R. H. (1979) *J. Biol. Chem.* 254, 8230–8236.
10. Pick, U., and Racker, E. (1979) *J. Biol. Chem.* 254, 2793–2799.
11. Serrano, R., Kanner, B. I., and Racker, E. (1976) *J. Biol. Chem.* 251, 2453–2461.
12. Galante, Y. M., Wong, S. Y., and Hatefi, Y. (1979) *J. Biol. Chem.* 254, 12372–12378.
13. Ryrie, I. J., and Gallagher, A. (1979) *Biochim. Biophys. Acta* 545, 1–14.
14. Mitchell, P. (1966) *Chemiosmotic Coupling in Oxidative and Photosynthetic Phosphorylation*, Glynn Research Bodmin, Cornwall, England.
15. Yoshida, M., Sone, N., Hirata, H., Kagawa, Y., Takeuchi, Y., and Ohno, K. (1975) *Biochem. Biophys. Res. Commun.* 67, 1295–1300.
16. Ryrie, I. J., Critchley, C., and Tillberg, J. C. (1979) *Arch. Biochem. Biophys.* 198, 182–194.
17. Oren, R., Weiss, S., Garty, H., Caplan, S. R., and Gromet-Elhanan, Z. (1980) *Arch. Biochem. Biophys.* 205, 503–509.
18. Futai, M., and Kanazawa, H. (1980) *Curr. Top. Bioenerg.* 10, 181–215.
19. Kagawa, Y., and Nukiwa, N. (1981) *Biochem. Biophys. Res. Commun.* 100, 1370–1376.
20. Yoshida, M., Okamoto, H., Sone, N., Hirata, H., and Kagawa, Y. (1977) *Proc. Natl. Acad. Sci. U. S. A.* 74, 936–940.

21. Philosoph, S., Binder, A., and Gromet-Elhanan, Z. (1977) *J. Biol. Chem.* **252**, 8747-8752
22. Philosoph, S., and Gromet-Elhanan, Z. (1981) in *Photosynthesis II. Electron Transport Photophosphorylation* (Akoyunoglou, G., ed) pp. 741-751, Balaban International Science Services, Philadelphia
23. Philosoph, S., Khananshvil, D., and Gromet-Elhanan, Z. (1981) *Biochem. Biophys. Res. Commun.* **101**, 384-389
24. Gromet-Elhanan, Z., Philosoph, S., and Khananshvil, D. (1981) in *Energy Coupling in Photosynthesis* (Selman, B. R., and Selman-Reimer, S., eds) pp. 323-331, Elsevier/North-Holland
25. Philosoph, S., and Gromet-Elhanan, Z. (1981) *Eur. J. Biochem.* **119**, 107-113
26. Gromet-Elhanan, Z. (1970) *Biochim. Biophys. Acta* **223**, 174-182
27. Gromet-Elhanan, Z. (1974) *J. Biol. Chem.* **249**, 2522-2527
28. Oren, R., and Gromet-Elhanan, Z. (1979) *Biochim. Biophys. Acta* **548**, 106-118
29. Binder, A., and Gromet-Elhanan, Z. (1974) in *Proceedings of the 3rd International Congress on Photosynthesis* (Avron, M., ed) Vol. 2, pp. 1163-1170, Elsevier, Amsterdam
30. Avron, M. (1960) *Biochim. Biophys. Acta* **40**, 257-272
31. Ames, B. N. (1966) *Methods Enzymol.* **8**, 115-118
32. Leiser, M., and Gromet-Elhanan, Z. (1977) *Arch. Biochem. Biophys.* **178**, 79-88
33. Weber, K., and Osborn, U. (1969) *J. Biol. Chem.* **244**, 4406-4412
34. Lanzillo, J. J., Sterens, J., and Fanbury, B. L. (1980) *Electrophoresis* **1**, 180-186
35. Lowry, O. H., Rosebrough, N. J., Farr, A. L., and Randall, R. J. (1951) *J. Biol. Chem.* **193**, 265-275
36. Clayton, R. K. (1963) in *Bacterial Photosynthesis* (Gest, H., San Pietro, A., and Vernon, L. P., eds) pp. 495-500, Antioch Press, Yellow Springs
37. Dunn, S. D., and Futai, M. (1980) *J. Biol. Chem.* **255**, 113-118
38. Weiss, M. A., and McCarty, R. E. (1977) *J. Biol. Chem.* **252**, 8007-8012
39. Moroney, J. W., and McCarty, R. E. (1979) *J. Biol. Chem.* **254**, 8951-8955
40. McCarty, R. E. (1979) *Annu. Rev. Plant Physiol.* **30**, 79-104
41. Deters, D. W., Racker, E., Nelson, N., and Nelson, H. (1975) *J. Biol. Chem.* **250**, 1041-1047

## Unisite Catalysis without Rotation of the $\gamma$ - $\epsilon$ Domain in *Escherichia coli* $F_1F_0$ -ATPase\*

(Received for publication, December 22, 1997, and in revised form, April 9, 1998)

José J. García and Roderick A. Capaldi†

From the Institute of Molecular Biology, University of Oregon, Eugene, Oregon 97403-1229

Unisite [ $\gamma$ - $^{32}$ P]ATP hydrolysis was studied in  $ECF_1$  from the mutant  $\beta E381C$  after generating a single disulfide bond between  $\beta$  and  $\gamma$  subunits to prevent the rotation of the  $\gamma/\epsilon$  domain. The single  $\beta$ - $\gamma$  cross-link was obtained by removal of the  $\delta$  subunit from  $F_1$  and then treating with  $CuCl_2$  as described previously (Aggeler, R., Haughton, M. A., and Capaldi, R. A. (1996) *J. Biol. Chem.* 270, 9185–9191). The mutant enzyme,  $\beta E381C$ , had an increased overall rate of unisite hydrolysis of [ $\gamma$ - $^{32}$ P]ATP compared with the wild type  $ECF_1$  due to increases in the rate of ATP binding ( $k_{+1}$ ),  $P_i$  release ( $k_{+3}$ ), and ADP release ( $k_{+4}$ ). Release of bound substrate ([ $\gamma$ - $^{32}$ P]ATP) was also increased in the  $\beta E381C$  mutant. Cross-linking between Cys-381 and the intrinsic Cys-87 of  $\gamma$  caused a further increase in the rate of unisite catalysis, mainly by additional effects on nucleotide binding in the high affinity catalytic site ( $k_{+1}$  and  $k_{+4}$ ). In  $\delta$ -subunit-free  $ECF_1$  from wild type or  $\beta E381C$   $F_1$ , addition of an excess of ATP accelerated unisite catalysis. After cross-linking, unisite catalysis of  $\beta E381C$  was not enhanced by the cold chase. The covalent linkage of  $\gamma$  to  $\beta$  increased the rate of unisite catalysis to that obtained by cold chase of ATP of the noncross-linked enzyme. It is concluded that the conversion of Glu-381 of  $\beta$  to Cys induces an activated conformation of the high affinity catalytic site with low affinity for substrate and products. This state is stabilized by cross-linking the Cys at  $\beta 381$  to Cys-87 of  $\gamma$ . We infer from the data that rotation of the  $\gamma/\epsilon$  rotor in  $ECF_1$  is not linked to unisite hydrolysis of ATP at the high affinity catalytic site but to ATP binding to a second or third catalytic site on the enzyme.

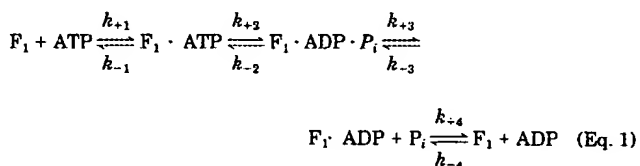
$F_1F_0$ -type ATPases are membranous protein complexes responsible for oxidative and photosynthetic ATP synthesis in eubacteria, mitochondria, and chloroplasts. The simplest form of this enzyme, as found in *Escherichia coli* ( $ECF_1F_0$ ),<sup>1</sup> contains eight different subunits. Five of these subunits ( $\alpha_3$ ,  $\beta_3$ ,  $\gamma$ ,  $\delta$ ,  $\epsilon$ ) are located outside the membrane in the catalytic  $F_1$  portion. The other three subunits ( $a_1$ ,  $b_2$ ,  $c_{9-12}$ ) form a channel that transports protons through the membrane (for recent reviews, see Refs. 1 and 2). Each enzyme complex contains three catalytic sites located predominantly on  $\beta$  subunits (3), which work

cooperatively during ATP hydrolysis or synthesis (reviewed in Refs. 1 and 2). How catalytic site events are coupled to proton translocation is only now beginning to be understood.

It had been shown several years ago that the  $\gamma$  and  $\epsilon$  subunits undergo conformational changes in  $F_1F_0$  upon membrane energization (4–6) and that they shift their positions between the  $\alpha$  and  $\beta$  subunits of soluble  $F_1$  in response to nucleotide binding (7–9). Recently, it has been established conclusively that these movements represent rotation of a domain formed by the  $\gamma$  and  $\epsilon$  subunits (10, 11). Such rotation has been visualized directly during ATP hydrolysis in the soluble  $F_1$  (12, 13) and is inferred by cross-linking studies of the hydrolytic and synthetic reaction when catalyzed by the whole  $F_1F_0$  complex (11, 14).

As yet, no correlation has been established between the rate of rotation of the  $\gamma$ - $\epsilon$  domain and the kinetics of individual steps in the ATP hydrolysis or synthesis reactions. However, the hydrolytic activity of the enzyme is almost fully inhibited by cross-linking either  $\gamma$  or  $\epsilon$ , or both subunits, to  $\alpha$  or  $\beta$  subunits through engineered disulfide bonds (8–10), thereby confirming the direct linkage between catalytic site events and rotation. The driving force for this rotation in the direction of ATP hydrolysis could be the binding energy of ATP and/or the free energy change associated with the ATP splitting reaction. However, complicating any analysis, ATP can bind in three catalytic sites that are characterized by high, medium, and low affinities for nucleotides (1–2, 15–16), *a priori*, binding in any of these sites could drive the rotation.

To some extent, the functioning in these sites can be differentiated because ATP hydrolysis in the high affinity catalytic site can be monitored by so-called “unisite” catalysis measurements (17). It is distinguished from nucleotide binding into low affinity sites which accelerates product release from the first site, as in cold chase experiments (18). Unisite catalysis is measured with substoichiometric amounts of [ $\gamma$ - $^{32}$ P]ATP in relation to  $F_1$  and is characterized by a highly exergonic ATP binding step ( $K_1$ ), a reversible ATP hydrolysis/synthesis equilibrium that occurs with a negligible change in free energy ( $K_2$ ), and a very slow product release step which is rate-limiting ( $k_{+3}$  and  $k_{+4}$ ) (see Equation 1 and review in Ref. 19). Therefore, if subunit rotation is coupled to unisite catalysis, ATP binding in the high affinity site would be the most probable driving force (20). The kinetic steps of the unisite catalytic cycle are as follows.



Here, we measure unisite catalysis in  $ECF_1$  in which the  $\gamma$  subunit has been cross-linked to a  $\beta$  subunit to prevent rota-

\* This work was supported by National Institutes of Health Grant HL24526. The costs of publication of this article were defrayed in part by the payment of page charges. This article must therefore be hereby marked “advertisement” in accordance with 18 U.S.C. Section 1734 solely to indicate this fact.

† To whom correspondence should be addressed. Tel.: 541-346-5881; Fax: 541-346-4854.

<sup>1</sup> The abbreviations used are:  $ECF_1$ , soluble portion of the *Escherichia coli*  $F_1F_0$ -ATP synthase; BSA, bovine serum albumin; EACA,  $\epsilon$ -amino- $n$ -caproic acid; MOPS, 3-( $N$ -morpholino)propanesulfonic acid; DTT, dithiothreitol; LDAO,  $N,N$ -dimethyldodecylamine- $N$ -oxide.

tion. Our results are interpreted to indicate that ATP binding at a catalytic site other than the high affinity site, drives the rotation of the  $\gamma$  and  $\epsilon$  domain.

#### EXPERIMENTAL PROCEDURES

**Materials**—[ $\gamma$ - $^{32}$ P]ATP (PB 218) was purchased from Amersham Pharmacia Biotech, and [ $\alpha$ - $^{32}$ P]ATP was a gift from the laboratory of Dr. Peter von Hippel of this Institute of Molecular Biology. ATP was from Sigma. The mutant  $\beta$ E381C is described elsewhere (21). Wild type and mutant  $F_1$ -ATPases were purified as described before (22). ECF<sub>1</sub> was depleted of  $\delta$  subunit by gel filtration chromatography through Sephacryl S-300 in the presence of 0.5% LDAO. Enzyme (8–10 mg) was dissolved in 1 ml of a buffer containing 50 mM Tris, 20% glycerol, 2 mM EDTA, 1 mM ATP, 1 mM DTT, and 40 mM EACA, pH 7.4 (4 °C), along with 0.5% LDAO (buffer A). Samples were loaded onto a Sephacryl column (1.2 m  $\times$  1.0 cm), and protein was eluted with the same buffer. Samples lacking the  $\delta$  subunit based on SDS-polyacrylamide electrophoresis were collected and concentrated to 2–3 mg/ml in Amicon tubes and stored in liquid nitrogen.

**CuCl<sub>2</sub>-induced Cross-linking of  $F_1$  Preparations**—Cross-linking was induced by CuCl<sub>2</sub> as described previously (21). Before starting the cross-linking reactions, enzyme dissolved in buffer A under liquid nitrogen was defrosted at room temperature and precipitated with 70% saturated ammonium sulfate at 4 °C for 1–2 h. These suspensions were centrifuged at 16000  $\times$  g for 6 min at 4 °C, resuspended in 60–100  $\mu$ l of 50 mM MOPS, 10% glycerol, and 0.1 mM EDTA, pH 7.0, and gel filtered through two consecutive Sephadex G-50 columns in the same buffer to remove nucleotides and ammonium sulfate. ECF<sub>1</sub> from the mutant  $\beta$ E381C was reacted with 200  $\mu$ M CuCl<sub>2</sub> for 2–4 h to maximize the cross-linking yield. The control enzyme was reacted under the same conditions but with 5 mM DTT present. Multisite hydrolytic activity was measured after cross-linking and before starting the unisite catalysis measurements. For the mutant  $\beta$ E381C, it was 15–20  $\mu$ mol/min/mg for the control (reduced with 5 mM DTT) and 0.3–0.4  $\mu$ mol/min/mg after cross-linking, i.e. multisite activity was inhibited 97–98%. The steady-state ATPase activity at 37 °C of the wild type ECF<sub>1</sub> was 30  $\mu$ mol/min/mg. These activities were not altered significantly by the removal of the  $\delta$  subunit.

**Time Courses of Unisite Hydrolytic Activities**—Fully cross-linked and control ECF<sub>1</sub> from the  $\beta$ E381C mutant were diluted approximately 10-fold (to 1  $\mu$ M) for measurement of unisite ATPase activity in 50 mM Tris-SO<sub>4</sub>, 5 mM MgSO<sub>4</sub>, and 2 mM K<sub>2</sub>HPO<sub>4</sub>, pH 7.5. DTT (5 mM) was present in the samples of control enzyme.

Unisite reactions were started by adding 50  $\mu$ l of [ $\gamma$ - $^{32}$ P]ATP to 50  $\mu$ l of  $F_1$  during rapid mixing in a 13  $\times$  100 mm glass test tube. The [ $\gamma$ - $^{32}$ P]ATP/ $F_1$  ratio used was 0.1 or 0.2 without significant differences on the results obtained in both conditions. The final concentration of  $F_1$  was 0.5  $\mu$ M and that of [ $\gamma$ - $^{32}$ P]ATP was 0.1 or 0.05  $\mu$ M. Reactions were stopped during mixing at different reaction times with 0.4 ml of trichloroacetic acid (6% final concentration). In the case of cold chase experiments, 100  $\mu$ l of 10 mM MgATP was added to the  $F_1$  + [ $\gamma$ - $^{32}$ P]ATP mixture at the times shown, and the reactions were stopped 2 s later with acid. In the control samples, 5 mM DTT was present in all reaction mixtures, except for the trichloroacetic acid solution, to avoid any cross-linking. To quantify the amount of [ $\gamma$ - $^{32}$ P]ATP remaining, [ $^{32}$ P]P<sub>i</sub> was extracted from these aqueous samples as [ $^{32}$ P]P<sub>i</sub>-phosphomolybdate as described before (23). Reduction of this complex by DTT was avoided by two different methods, which gave exactly the same results. In one, the reaction was quenched directly with 0.5 ml of activated charcoal in 1 N HCl, and the adsorbed [ $\gamma$ - $^{32}$ P]ATP was washed twice with 1 N HCl containing 20 mM P<sub>i</sub>. The bound [ $\gamma$ - $^{32}$ P]ATP was eluted with ethanol/ammonium hydroxide (24), and radioactivity was counted directly by liquid scintillation or Cerenkov counting. In the second method, control samples were treated with trichloroacetic acid as before, but then DTT was reacted with a 10-fold excess of *N*-ethylmaleimide for 5 min before the formation of the [ $^{32}$ P]P<sub>i</sub>-phosphomolybdate complex. Reaction with *N*-ethylmaleimide was preceded by the neutralization of each sample with NaOH or Tris to a pH of 7–7.5. Samples without DTT were processed in the same way.

**Rate Constants for Unisite Catalysis**—The rate of [ $\gamma$ - $^{32}$ P]ATP binding was measured by a hexokinase trap (25). This was used instead of the cold chase method to avoid any inhibition of the cold chase response due to cross-linking and because of possible release of the bound [ $\gamma$ - $^{32}$ P]ATP induced by the cold chase (26). In the hexokinase trap, the unisite reactions were started as described before, but at the times shown, 100 units of hexokinase were added in the presence of 10 mM glucose. The hexokinase reaction was allowed to proceed for

10 s, and the reactions were stopped with 1.3 N HCl. The remaining [ $\gamma$ - $^{32}$ P]ATP was hydrolyzed by boiling for 12 min, and the [ $^{32}$ P]P<sub>i</sub> produced was extracted as described above. The radioactivity of the aqueous phase was taken as the amount of [ $^{32}$ P]glucose-6-phosphate formed, i.e. [ $\gamma$ - $^{32}$ P]ATP that was not bound to  $F_1$ . Controls showed that 98–99% of the [ $\gamma$ - $^{32}$ P]ATP was heat hydrolyzed, that 99–100% of the [ $^{32}$ P]glucose-6-phosphate was heat-resistant, and that the efficiency of the hexokinase trap mixed with  $F_1$  was 97–99%. The decay on the hexokinase accessible [ $\gamma$ - $^{32}$ P]ATP against time was used to calculate the rate constant of [ $\gamma$ - $^{32}$ P]ATP binding, supposing a second order association process according to Penefsky (27). The further measurement of the rate of [ $\gamma$ - $^{32}$ P]ATP release ( $k_{-1}$ ) showed that the amount of [ $\gamma$ - $^{32}$ P]ATP released in the first 10 s of reaction was negligible, allowing for a good estimation of  $k_{-1}$ . On the other hand,  $k_{-1}$  was measured by a similar hexokinase trap according to the method of Penefsky (27), in which the [ $\gamma$ - $^{32}$ P]ATP/ $F_1$  mixture was aged for 30 s and the free  $^{32}$ P was removed by gel filtration through Sephadex columns equilibrated with the standard unisite buffer containing 1 mg/ml bovine albumin (BSA). After saving aliquots for determination of [ $\gamma$ - $^{32}$ P]ATP and [ $^{32}$ P]P<sub>i</sub> coeluted with  $F_1$ , the effluent was diluted 10-fold in the same buffer containing 1 mg/ml BSA, 1 mg/ml hexokinase, and 20 mM glucose. At different times, aliquots were removed and the hexokinase reactions were stopped with 1.3 N HCl. The amount of [ $^{32}$ P]glucose-6-phosphate formation, measured as described before, was used to calculate  $k_{-1}$  according to Penefsky (27), i.e. multiplying by the respective values of  $(1 + K_2)$  and correcting for rate of [ $^{32}$ P]P<sub>i</sub> release measured as described below.

To calculate the catalytic equilibrium constant ( $K_2$ ), the [ $\gamma$ - $^{32}$ P]ATP/ $F_1$  mixture made at ratios of 0.2 or 0.1, was filtered at different times through Sephadex columns equilibrated with buffer and BSA. The eluted protein was collected directly in 6% trichloroacetic acid, and the coeluted [ $\gamma$ - $^{32}$ P]ATP and [ $^{32}$ P]P<sub>i</sub> were measured as described before (23). The rate of decay of the total bound  $^{32}$ P was used to calculate the rate of [ $^{32}$ P]P<sub>i</sub> release.  $k_{+3}$  was obtained by multiplying the P<sub>i</sub> off rate by the respective values of  $(1 + 1/K_2)$ , according to Penefsky (27) and Al-Shawi and Nakamoto (40).

Using the values obtained for  $k_{-1}$ ,  $k_{-2}$ ,  $K_2$ , and  $k_{+3}$ , the respective forward ( $k_{+2}$ ) and reverse ( $k_{-2}$ ) rate constants were obtained through a computer-assisted numerical integration of the unisite catalytic cycle (Equation 1). The software used was KINSIM (28) as described previously (29). Fitting of the  $k_{+3}$  and  $k_{-3}$  rate constants to the experimental data was made with the FITSIM program (30). The values of  $k_{+3}$  and  $k_{-4}$  were not obtained. Therefore, the calculation of  $k_{+2}$  and  $k_{-2}$  was made using only the values of  $k_{-1}$ ,  $k_{-2}$ ,  $K_2$ , and  $k_{+3}$ . The validity of this procedure as has been used before (27) is based on the irreversibility of the  $^{32}$ P<sub>i</sub> release step (with 2 mM P<sub>i</sub> present) and on the negligible amounts of ADP that are released in the first seconds of the reactions (values for  $k_{+4}$  are in the range of  $10^{-3}$ , see Table I).

The rate of [ $\alpha$ - $^{32}$ P]ADP release was measured by the dilution/gel filtration method of Cunningham and Cross (31) as modified by Al-Shawi and Senior (32). Unisite catalysis was started by mixing 2.5  $\mu$ l of 2 mM  $F_1$  with 2.5  $\mu$ l of 0.4  $\mu$ M [ $\alpha$ - $^{32}$ P]ATP at 0 time. After 30 s, the samples were diluted 100-fold, and 120- $\mu$ l aliquots were filtered through Sephadex columns at different times. The 0 time points were filtered 30 s after the dilution step. The Sephadex columns were equilibrated with buffers containing 1 mg/ml of BSA to minimize the loss of  $F_1$  during gel filtration. The decay in the radioactivity eluted with  $F_1$  from the columns was used to calculate the rate of ADP release according to a first order exponential decay of the bound  $^{32}$ P. This rate was multiplied by  $(1 + 1/K_2)$  to correct for the equilibrium distribution of ATP and ADP as it was made for the calculation of  $k_{-3}$ .

To test the accuracy of mixing, gel filtration, and curve fitting methods employed, some rate constants ( $k_{+1}$ ,  $k_{+3}$ ,  $K_2$ ,  $k_{+2}$ , and  $k_{-2}$ ) were measured in parallel using the wild type enzyme ( $\pm$   $\delta$  subunit) treated in the same conditions used for the  $\beta$ E381C ECF<sub>1</sub>. The values of the rate constants obtained were in the range reported for the wild type ECF<sub>1</sub> (see Table I).

**Other Methods**—Multisite ATPase activities were measured spectrophotometrically with the ATP regenerating system of Löttscher *et al.* (33) at 37 °C. Gel electrophoresis was performed according to Laemmli (34) using SDS-polyacrylamide gradient gels of 10–18%. Protein concentrations were measured using the BCA method.

#### RESULTS

ECF<sub>1</sub> from the mutant  $\beta$ E381C was used in the present study. The properties of this mutant have been described in detail elsewhere (21). Cross-linking in essentially full yield can



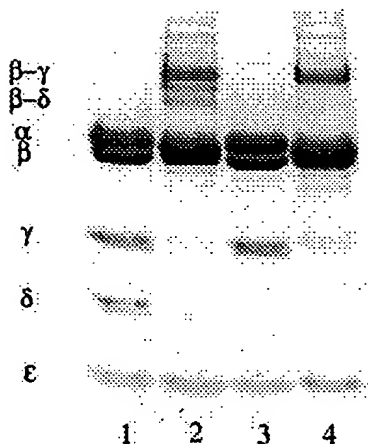


FIG. 1. SDS gel electrophoresis of the  $\beta$ E381C mutant before and after cross-linking induced by  $\text{CuCl}_2$ . The  $\beta$ E381C mutant, with (lanes 1 and 2) or without  $\delta$  subunit (lanes 3 and 4), was cross-linked with  $200 \mu\text{M}$   $\text{CuCl}_2$  as described under "Experimental Procedures." The control enzymes (lanes 1 and 3) were incubated and loaded into the gel in the presence of  $5 \text{ mM}$  DTT. The multisite hydrolytic activity of these enzymes was diminished from  $15 \mu\text{mol}/\text{min}/\text{mg}$  to  $0.3$ – $0.4 \mu\text{mol}/\text{min}/\text{mg}$  after cross-linking.  $15 \mu\text{g}$  of each protein were loaded per lane.

be obtained between Cys-381 of  $\beta$  and the intrinsic Cys-87 of the  $\gamma$  subunit. The effect of this cross-linking is to inhibit multisite ATPase activity as reported before (21), and confirmed here. In the present study, the effects of the cross-linking on unisite catalysis have been examined. The kinetics of ATP hydrolysis in a single high affinity catalytic site was measured using  $[\gamma\text{-}^{32}\text{P}]\text{ATP}$ , and the effect of a large excess of ATP as a "cold chase" on this kinetics was studied. This so-called cold chase examines the effect of ATP binding at a second and/or third catalytic site on the kinetics of  $[\gamma\text{-}^{32}\text{P}]\text{ATP}$  hydrolysis in the first, highest affinity site.

In  $\text{ECF}_1$ , the promotion of unisite ATP hydrolysis by excess ATP is maximized in enzyme from which the  $\delta$  subunit has been removed (35). This may have to do with non-physiological binding of the  $\delta$  subunit in isolated  $\text{ECF}_1$  (21). Recent studies have shown that the  $\delta$  subunit is a two domain protein (41, 42). In  $\text{ECF}_{10}$ , the N- and C-terminal domains interact with each other (43, 44), whereas in isolated  $\text{ECF}_1$ , the C-terminal domain can swing away to interact with the DELSEED region of a  $\beta$  subunit (21). This is evident from the observed cross-linking from  $\beta$ E381C to the intrinsic Cys-140 of  $\gamma$  shown previously and confirmed here (Fig. 1).

A selective removal of the  $\delta$  subunit was accomplished by gel filtration of  $\text{ECF}_1$  in the presence of LDAO as described fully under "Experimental Procedures." Fig. 1 shows the separation of the subunits of intact  $\text{ECF}_1$  and  $\delta$ -free enzyme from  $\beta$ E381C by SDS-polyacrylamide gel electrophoresis. Removal of  $\delta$  was obtained without a significant loss of the  $\epsilon$  subunit, *c.f.* lanes 3 and 1. Fig. 1 also shows cross-linking of  $\text{ECF}_1$  from the mutant  $\beta$ E381C induced by incubation with  $200 \mu\text{M}$   $\text{CuCl}_2$  (lanes 2 and 4). Removal of the  $\delta$  subunit not only prevents non-physiological reactions of this subunit, but facilitates interpretation of experiments because the only cross-linked product observed in significant amounts is now between  $\beta$ - $\gamma$ . Therefore, the fixing of these two subunits can be correlated directly with the observed effects.

In the presence or absence of the  $\delta$  subunit, multisite or cooperative ATPase activity was inhibited by 97–98% in different experiments, in comparison with control samples treated with the equivalent levels of  $\text{CuCl}_2$ , but with  $5 \text{ mM}$  DTT present. This inhibition was at roughly the same level as the yield of cross-linking.

The removal of the  $\delta$  subunit had very little effect in the rate of acid quench-measured unisite hydrolysis of  $[\gamma\text{-}^{32}\text{P}]\text{ATP}$  in either wild type or mutant ( $\beta$ E381C)  $\text{ECF}_1$ , as reported previously (35) and see Table I. Fig. 2 compares the rates of unisite catalysis of wild type  $\text{ECF}_1$  and  $\beta$ E381C, both before and after cross-linking. The rates of unisite catalysis by wild type  $\text{ECF}_1$  are comparable with those obtained by others under similar experimental conditions (35, 40); see Table I for rate constants of catalysis. As evident in Fig. 1, the substitution of Cys for Glu-381 in the mutant  $\beta$ E381C significantly increased the rate of unisite ATP hydrolysis of  $\text{ECF}_1$ , and this rate is increased more dramatically after cross-linking of the Cys at position 381 of  $\beta$  with Cys-87 of the  $\gamma$  subunit.

Before making a detailed kinetic analysis of the unisite activity of the  $\beta$ E381C mutant, the possible contribution of multisite activity in the present experiments was examined by testing the effect of sodium azide ( $\text{NaN}_3$ ).  $\text{NaN}_3$  is an inhibitor which effectively blocks multisite ATPase activity of  $\text{F}_1$ -ATPases without significant effect on unisite catalysis, presumably by affecting catalytic site cooperativity (36, 37). Previous studies had suggested that cooperative or multisite catalysis could contribute even when ratios of  $[\gamma\text{-}^{32}\text{P}]\text{ATP}$  to  $\text{F}_1$  of  $0.3 \text{ mol}/\text{mol}$  were used (38). Although cross-linking itself inhibits the multisite catalysis, this control is still relevant because small amounts of noncross-linked enzyme are present and could be providing all of the  $[\gamma\text{-}^{32}\text{P}]\text{ATP}$  hydrolysis being observed. However, as shown in Fig. 2,  $\text{NaN}_3$  at concentrations that completely blocked multisite catalysis in noncross-linked enzyme (results not shown; Refs. 36 and 37) had no effect on the rates of unisite catalysis after cross-linking. Taken together, the above results confirm that the ATP hydrolysis being followed occurs in the so-called "high affinity" catalytic site in the cross-linked enzyme.

Table I lists the rate and equilibrium constants that were measured. In relation to wild type  $\text{ECF}_1$ , the rate of ATP binding ( $k_{+1}$ ) is faster for the  $\beta$ E381C mutant both before and after cross-linking. Also,  $[\gamma\text{-}^{32}\text{P}]\text{ATP}$  release was faster in the mutant by a factor of 25 before cross-linking and more than 100-fold after cross-linking. The result is a 10-fold decrease in the affinity for ATP. As indicated in Table I, the mutant showed a more than 20-fold increase in  $k_{+3}$ , the rate of  $\text{P}_i$  release, which was not enhanced greatly by cross-linking. The cross-linking also increased the rate of ADP release from the mutant  $\text{ECF}_1$ . Table I also lists  $K_2$  measured for the different preparations. This equilibrium constant was not greatly affected in the mutant with or without cross-linking.

The effect of a cold chase of excess ATP on unisite catalysis for the wild type and mutant is shown in Fig. 3. There was the expected burst of  $[\gamma\text{-}^{32}\text{P}]\text{ATP}$  hydrolysis after addition of cold ATP in the wild type  $\text{ECF}_1$  and in enzyme from the mutant without cross-linking. However, after cross-linking, the rate of unisite catalysis carried out by the  $\beta$ E381C mutant was by itself as fast as the accelerated unisite catalysis of the noncross-linked mutant. Unisite catalysis of the  $\beta$ E381C mutant was also much faster than the promoted and non-promoted unisite catalysis carried out by the wild type enzyme, which is limited by the rate of  $[\gamma\text{-}^{32}\text{P}]\text{ATP}$  binding (Fig. 3).

#### DISCUSSION

In the mutant  $\beta$ E381C, a cross-link can be obtained between  $\beta$  and  $\gamma$  subunits in essentially full yield. Previous studies made in  $\text{ECF}_1$  from the triple mutant  $\beta$ Y331W: $\beta$ E381C: $\epsilon$ S108C (39) have established that binding of ATP to this cross-linked  $\text{F}_1$  is similar to that of noncross-linked enzyme, *i.e.* there is one high affinity binding site ( $K_d = 90$ – $200 \text{ nM}$ ), a loose site ( $K_d = 2$ – $7 \mu\text{M}$ ), and a weak binding site ( $K_d = 40$ – $50 \mu\text{M}$ ). The results here show that enzyme cross-linked between  $\beta$  (at Cys-381) and



TABLE I  
Effect of the  $\beta$ E381C mutation and the  $\beta$ - $\gamma$  cross-link on the single site catalysis carried out by  $ECF_1$

Rate constants were measured according to those under "Experimental Procedures." Experiments were made with  $[\gamma\text{-}^{32}\text{P}]\text{ATP}/ECF_1$  ratios of 0.1 and 0.2. The wild type values were measured in duplicate experiments and those for the  $\beta$ E381C  $ECF_1$  in three or four different determinations. Standard deviations were omitted for simplicity, but these were no higher than 20%. Significant changes produced by the  $\beta$ E381C mutation are highlighted, and further increases induced by cross-linking are highlighted in italics.

	$k_{+1}$	$k_{-1}$	$K_1$	$K_2$	$k_{+3}$	$k_{+4}$
	$(M^{-1}s^{-1}) \times 10^5$	$(s^{-1}) \times 10^{-5}$	$(M^{-1}) \times 10^9$		$(s^{-1}) \times 10^{-4}$	$(s^{-1}) \times 10^{-3}$
wt $ECF_1$ (+ $\delta$ ) <sup>a</sup>	1.1	2.5	4.4	2.9	12.0	1.6
wt $ECF_1$ (- $\delta$ ) <sup>b</sup>	1.2	2.2	5.4	0.18	7.8	—
wt $ECF_1$ (+ $\delta$ , this work)	0.55	2.5	2.2	1.4	12.0	—
wt $ECF_1$ (- $\delta$ , this work)	0.77	2.2	3.5	2.1	10.0	—
$\beta$ E381C $ECF_1$ (- $\delta$ , DTT)	5.3	60.0	0.88	1.0	220.0	2.2
$\beta$ E381C $ECF_1$ (- $\delta$ , $\beta$ - $\gamma$ )	6.1	310.0	0.20	2.1	280.0	7.7

<sup>a</sup> Values taken from Ref. 40.

<sup>b</sup> Values taken from Ref. 35.

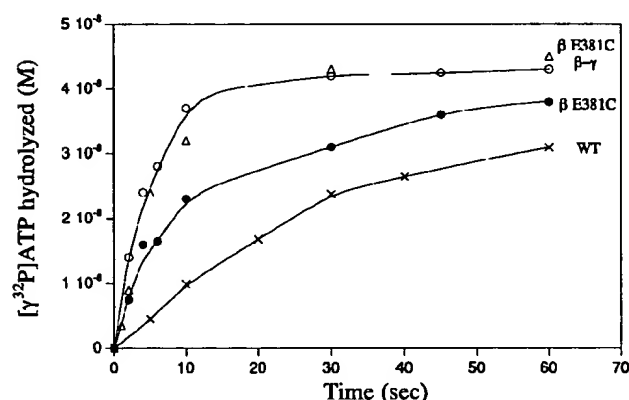


FIG. 2. Effect of  $\text{CuCl}_2$  induced cross-linking on the unisite catalysis of  $\beta$ E381C  $ECF_1$  after removal of the  $\delta$  subunit. Unisite hydrolysis of  $0.05 \mu\text{M}$   $[\gamma\text{-}^{32}\text{P}]\text{ATP}$  by  $0.5 \mu\text{M}$   $ECF_1$  was measured as explained under "Experimental Procedures." The circles show the amount of  $[\gamma\text{-}^{32}\text{P}]\text{ATP}$  hydrolyzed by the  $\beta$ E381C  $F_1$  in the presence (●—●) and in the absence (○—○) of 5 mM DTT. For comparison, the same experiment was made with the wild type  $ECF_1$  (×—×). For the reactions measured in the presence of  $\text{NaN}_3$  (△—△),  $ECF_1$  was preincubated with this inhibitor for 10 min before starting the experiment. The experimental points are the average of triplicate measurements. All reactions were stopped by an acid quench at the times shown by the experimental points.

$\gamma$  (at Cys-87) retains a high affinity catalytic site with a  $K_d$  for ATP in the nanomolar range (Table I). At the same time, cooperative multisite ATPase activity is essentially lost after cross-linking. Taken together, these results indicate that negative cooperativity of nucleotide binding and positive cooperativity of multisite ATPase activity need not be coupled to each other.

In novel labeling studies using laser-induced covalent incorporation of 2-azido-ATP, we have established a direct relationship between nucleotide binding affinity and the different interactions between  $\gamma$  and  $\epsilon$  subunits with the three  $\beta$  subunits (15). The site with highest affinity is in that  $\beta$  subunit which has neither of the smaller subunits cross-linked to it ( $\beta_{\text{free}}$ ), the loose binding site is in that  $\beta$  which cross-links with  $\epsilon$ , and the weak site is in the  $\beta$  which cross-links to  $\gamma$  (15). This relationship can only be retained during enzyme turnover if nucleotide binding in at least one  $\beta$  subunit, with the associated conformational changes that must occur, results in the movement of the  $\gamma$ - $\epsilon$  subunit domain from one  $\alpha/\beta$  pair to the next. *A priori*, the movements of  $\gamma$  and  $\epsilon$  could be due to binding in any of the three catalytic sites. The studies described here were directed toward asking whether nucleotide binding in the highest affinity catalytic site, bond cleavage in this site, or substrate binding in a

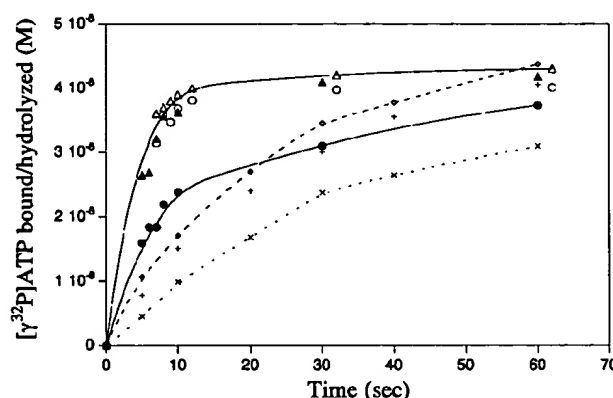


FIG. 3. Acceleration of unisite catalysis in  $\beta$ - $\gamma$  cross-linked  $\beta$ E381C  $ECF_1$  (- $\delta$ ). The unisite catalysis of the  $\beta$ E381C  $F_1$  (- $\delta$ ) was measured at a  $[\gamma\text{-}^{32}\text{P}]\text{ATP}/F_1$  ratio of 0.1. In the presence of 5 mM DTT, nonpromoted unisite catalysis (●—●) was stopped by the standard acid quench. Promoted unisite catalysis (○—○) was measured by adding a volume of 10 mM  $\text{MgATP}$  to  $ECF_1$  undergoing unisite catalysis and allowing the reaction to proceed 2 s further during rapid mixing before adding the acid. The open circles indicate the time at which the reactions were stopped. The same procedure was used to measure the promoted (△—△) and non-promoted (▲—▲) unisite catalysis of the  $\beta$ E381C  $F_1$  (- $\delta$ ) previously cross-linked between  $\beta$  and  $\gamma$  subunits. For comparison, the figure also shows the promoted (×—×) and non-promoted (×—×) unisite catalytic activity of wild type  $ECF_1$  (- $\delta$ ). For the wild type  $ECF_1$ , promoted experimental data are plotted at the time of addition of the cold chase, but the reactions were stopped 1 min later, the same results were obtained if the cold chase reactions of the wild type  $ECF_1$  were stopped after 2 or 5 s. Bound  $[\gamma\text{-}^{32}\text{P}]\text{ATP}$  (◇—◇) was also measured in parallel for the wild type enzyme by the hexokinase trap method.

second or third catalytic site, drives the rotation of  $\gamma/\epsilon$ .

It was found that the mutation of Glu-381 of the DELSEED region of  $\beta$  to a Cys (without any cross-linking) led to altered unisite catalysis by  $ECF_1$ . This mutation increased the overall rate of unisite catalysis significantly by affecting both substrate and product binding. The most dramatic effect was on ATP release rate which was 30-fold faster than that for wild type enzyme. ATP binding ( $k_{+1}$ ) was also increased, and there was a more than 20-fold increase in the rate of  $P_i$  release. Fig. 4 compares the unisite rate constants for  $\beta$ E381C and those for two mutations in the  $\gamma$  subunit. The  $\gamma$ T106C mutation also increased  $k_{-1}$  while both this mutation and the change of Met-23 of  $\gamma$  to a Lys affected  $k_{+3}$ . In fact, for the mutant  $\gamma$ M23K,  $k_{+3}$  was twice as fast again as for the DELSEED mutation. Structural studies show that Met-23 of  $\gamma$  interacts with the DELSEED region of one of the three  $\beta$  subunits. This is a different  $\beta$  subunit from that which forms the disulfide bond with Cys-87 of  $\gamma$  studied here. Clearly, the interaction of the DELSEED region of two different  $\beta$  subunits with  $\gamma$  has a

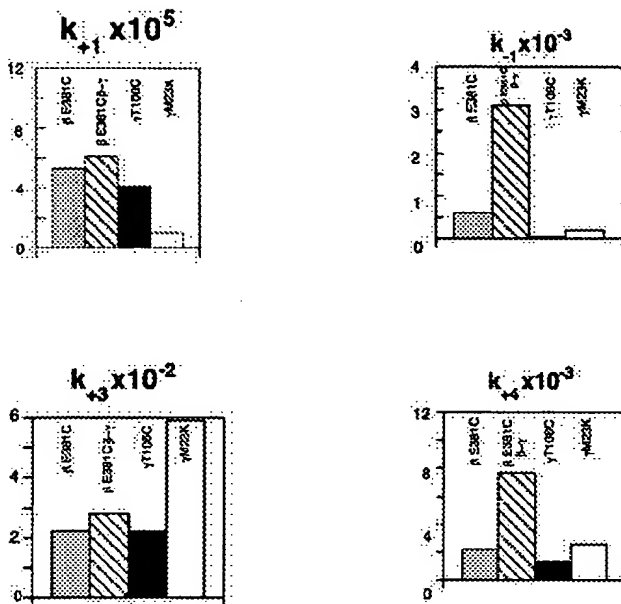


FIG. 4. Comparison of rate constants of unisite catalysis of  $\beta$ E381C,  $\gamma$ T106C, and  $\gamma$ M23K mutants. This figure compares the rate constants of unisite catalysis affected by the  $\beta$ E381C mutation and by cross-linking, with those previously reported for the  $\gamma$ T106C and  $\gamma$ M23K mutations. The data for these other two mutants were taken from Refs. 6 and 40, respectively.

similar and direct effect on catalysis in the highest affinity site, as would be expected if  $\gamma$  subunit binding is determined and/or is a determinant of nucleotide binding affinities.

Cross-linking between  $\beta$  and  $\gamma$  subunits of the mutant  $\beta$ E381C which inhibits multisite catalysis by 97%, was found to further increase the rate of unisite catalysis to the point that the reaction was essentially over within the first few seconds under the standard conditions used here. Curve fitting was used to analyze the kinetics of unisite catalysis as described under "Experimental Procedures." Good fits (S.E.  $\leq 20\%$  in the constants fitted) were obtained for wild type enzyme and for mutant, giving values of 0.71 and 0.33 (wt) and 0.84 and 0.84 ( $\beta$ E381C) respectively for  $k_{+2}$  and  $k_{-2}$ . These values are similar to those reported earlier for wild type enzymes (35, 40) but lower than those of the  $\gamma$ T106 mutation (6, 29), presumably due to the differences introduced by this mutation and/or its labeling with a fluorescent probe. The kinetics of unisite catalysis after cross-linking of  $\beta$ E381C was so fast that no satisfactory fit could be obtained (S.E.  $\geq 50\%$  in  $k_{+2}$  and  $k_{-2}$ ), therefore it remains unclear if cross-linking alters these two rate constants.

As shown in Fig. 3, the effect of covalently linking  $\beta$ Cys-381 to  $\gamma$ Cys-87 is to increase the rate of unisite catalysis to that of non-cross-linked enzyme obtained with a cold chase of ATP. After cross-linking, the ATP cold chase did not increase the observed rate of unisite catalysis. The implication is that ECF<sub>1</sub> from the mutant  $\beta$ E381C is in a conformation facilitating the rapid release of nucleotide and  $P_i$  that occurs on substrate binding in a second or third site. This conformation is then stabilized by cross-linking. A similar activation of the high affinity catalytic site can be obtained in *Rhodospirillum rubrum*  $F_1$ -ATPase in the presence of  $Ca^{2+}$ , but in this case, multisite ATPase activity is also enhanced (45). Further studies are needed to determine if these activated states are structurally similar.

The rapid rate of bond cleavage of ATP to ADP +  $P_i$  in enzyme in which the  $\gamma$  subunit is covalently linked to a  $\beta$

subunit indicates that rotation of the  $\gamma/\epsilon$  subunit domain is not driven by, and does not require, nucleotide binding, or bond cleavage, in the high affinity catalytic site. Additional testing requires that methods such as those employed by Sabbert *et al.* (12) or Noji *et al.* (13) for demonstrating rotation of the  $\gamma$  subunit are adapted to unisite conditions.

An absence of rotation of the  $\gamma/\epsilon$  subunits driven by ATP binding or bond cleavage in the high affinity catalytic site does not necessarily rule out that these reactions drive the coupling of ATP hydrolysis (or synthesis) to proton translocation. Conformational changes induced by ATP hydrolysis within the high affinity catalytic site could be transmitted to the c subunit ring and result in translocation of protons without rotation of the  $\gamma/\epsilon$  subunit ring domain (presently, the favored model of energy transduction within the ATP synthase (10, 44, 46)). Instead, rotation could realign the molecule after each catalytic site-driven proton translocation event for the next turnover to proceed. In this connection, it is interesting that conformational changes have been observed by fluorescent probes attached at positions 8 and 106 of the  $\gamma$  subunit which correlate with unisite catalysis (6, 29). Critical testing of the rotation of the c subunit ring as a function of catalytic site events remains an important prerequisite to getting a better understanding of the mechanism of the ATP synthase.

**Acknowledgments**—The excellent technical assistance in the purification of mutant  $F_1$ -ATPases provided by Kathy Chicas-Cruz is gratefully acknowledged. We thank Dr. Robert Aggeler for providing the mutants used in this study and for helpful discussions. We acknowledge the collaboration of Prof. Marietta Tuena de Gómez-Puyou and Armando Gómez-Puyou in the initial part of this project and for helpful discussions.

#### REFERENCES

- Boyer, P. D. (1997) *Annu. Rev. Biochem.* **66**, 717–749
- Weber, J., and Senior, A. E. (1997) *Biochim. Biophys. Acta* **1319**, 19–58
- Abrahams, J. P., Leslie, A. G., Lutter, R., and Walker, J. E. (1994) *Nature* **370**, 621–628
- Nalin, C. M., and McCarty, R. E. (1984) *J. Biol. Chem.* **259**, 7275–7280
- Richter, M. L., and McCarty, R. E. (1987) *J. Biol. Chem.* **262**, 15037–15040
- Turina, P., and Capaldi, R. A. (1994) *Biochemistry* **33**, 14275–14280
- Gogol, E. P., Johnston, E., Aggeler, R., and Capaldi, R. A. (1990) *Proc. Natl. Acad. Sci. U. S. A.* **87**, 9585–9589
- Aggeler, R., Chicas-Cruz, K., Cai, S.-X., Keana, J. F. W., and Capaldi, R. A. (1992) *Biochemistry* **31**, 2956–2961
- Aggeler, R., and Capaldi, R. A. (1996) *J. Biol. Chem.* **271**, 13888–13891
- Duncan, T. M., Bulygin, V. V., Zhou, Y., Hutcheon, M. L., and Cross, R. L. (1995) *Proc. Natl. Acad. Sci. U. S. A.* **92**, 10964–10968
- Aggeler, R., Ogilvie, I., and Capaldi, R. A. (1997) *J. Biol. Chem.* **272**, 19621–19624
- Sabbert, D., Engelbrecht, S., and Junge, W. (1996) *Nature* **381**, 623–625
- Noji, H., Yasuda, R., Yoshida, M., and Kinosita, K., Jr. (1997) *Nature* **386**, 299–302
- Zhou, Y., Duncan, T. M., and Cross, R. L. (1997) *Proc. Natl. Acad. Sci. U. S. A.* **94**, 10583–10587
- Grübler, G., and Capaldi, R. A. (1996) *Biochemistry* **35**, 3877–3879
- Weber, J., Wilke-Mounts, S., Grell, E., and Senior, A. E. (1994) *J. Biol. Chem.* **269**, 11261–11268
- Grubmeyer, C., Cross, R. L., and Penefsky, H. S. (1982) *J. Biol. Chem.* **257**, 12092–12100
- Cross, R. L., Grubmeyer, C., and Penefsky, H. S. (1982) *J. Biol. Chem.* **257**, 12101–12105
- Penefsky, H. S., and Cross, R. L. (1991) *Adv. Enzymol.* **64**, 173–214
- Al-Shawi, M. K., Parsonage, D., and Senior, A. (1990) *J. Biol. Chem.* **265**, 4402–4410
- Aggeler, R., Haughton, M. A., and Capaldi, R. A. (1996) *J. Biol. Chem.* **270**, 9185–9191
- Gogol, E. P., Aggeler, R., Sagermann, M., and Capaldi, R. A. (1989) *Biochemistry* **28**, 4717–4724
- García, J. J., Gómez-Puyou, A., and Tuena de Gómez-Puyou, M. (1997) *J. Bioenerg. Biomembr.* **29**, 61–70
- Tuena de Gómez-Puyou, M., Sandoval, F., and Gómez-Puyou, A. (1995) *J. Biol. Chem.* **270**, 16820–16825
- Penefsky, H. S. (1985) *Proc. Natl. Acad. Sci. U. S. A.* **82**, 1589–1593
- García, J. J., Gómez-Puyou, A., Maldonado, E., and Tuena de Gómez-Puyou, M. (1997) *Eur. J. Biochem.* **249**, 622–629
- Penefsky, H. S. (1986) *Methods Enzymol.* **126**, 608–618
- Barshop, B. A., Wrenn, R. F., and Frieden, C. (1983) *Anal. Biochem.* **130**, 134–145
- Turina, P., and Capaldi, R. A. (1994) *J. Biol. Chem.* **269**, 13465–13471
- Zimmerle, C. T., and Frieden, C. (1989) *Biochem. J.* **258**, 381–387
- Cunningham, D., and Cross, R. L. (1988) *J. Biol. Chem.* **263**, 18850–18856

32. Al-Shawi, M., and Senior, A. E. (1992) *Biochemistry* **31**, 878–885
33. Lötscher, H.-R., deJong, C., and Capaldi, R. A. (1984) *Biochemistry* **23**, 4134–4140
34. Laemmli, U. K. (1970) *Biochemistry* **227**, 680–685
35. Xiao, R., and Penefsky, H. S. (1994) *J. Biol. Chem.* **269**, 19232–19237
36. Noumi T., Maeda, M., and Futai, M. (1987) *FEBS Lett.* **213**, 381–384
37. Harris, D. A. (1989) *Biochim. Biophys. Acta* **974**, 156–162
38. Muneyuki, E., Yoshida, M., Bullough, D. A., and Allison, W. S. (1991) *Biochim. Biophys. Acta* **1058**, 304–311
39. Grüber, G., and Capaldi, R. A. (1996) *J. Biol. Chem.* **271**, 32623–32628
40. Al-Shawi, M. K., and Nakamoto, R. K. (1997) *Biochemistry* **36**, 12954–12960
41. Wilkens, S., Rodgers, A., Olgivie, I., and Capaldi, R. A. (1997) *Biophys. Chem.* **68**, 95–102
42. Wilkens, S., Dunn, S. D., Chandler, J., Dahlquist, F. W., and Capaldi, R. A. (1997) *Nat. Struct. Biol.* **4**, 198–201
43. Zeigler, M., Xiao, R., and Penefsky, H. S. (1994) *J. Biol. Chem.* **269**, 4233–4239
44. Olgivie, I., Aggeler, R., and Capaldi, R. (1997) *J. Biol. Chem.* **272**, 16652–16656
45. Maldonado, E., Dreyfus, G., García, J. J., Gómez-Puyou, A., and Tuena de Gómez-Puyou, M. T. (1998) *Biochim. Biophys. Acta* **1363**, 70–78
46. Elston, T., Hongyun, W., and Oster, G. (1998) *Nature* **391**, 510–513

## Conformational Changes in the *Escherichia coli* ATP Synthase (ECF<sub>1</sub>F<sub>0</sub>) Monitored by Nucleotide-dependent Differences in the Reactivity of Cys-87 of the $\gamma$ Subunit in the Mutant $\beta$ Glu-381 $\rightarrow$ Ala\*

(Received for publication, March 7, 1996, and in revised form, May 2, 1996)

Zhaoyang Feng, Robert Aggeler, Margaret A. Haughton, and Roderick A. Capaldi†

From the Institute of Molecular Biology, University of Oregon, Eugene, Oregon 97403-1229

Cys-87, one of two intrinsic cysteines of the  $\gamma$  subunit of the *Escherichia coli* ATP synthase (ECF<sub>1</sub>F<sub>0</sub>), is in a short segment of this subunit that binds to the bottom domain of a  $\beta$  subunit close to a glutamate (Glu-381). Cys-87 was unreactive to maleimides under all conditions in wild-type ECF<sub>1</sub> and ECF<sub>1</sub>F<sub>0</sub> but became reactive when Glu-381 of  $\beta$  was replaced by a cysteine or alanine. The reactivity of Cys-87 with maleimides was nucleotide-dependent, occurring with ATP or ADP + EDTA in catalytic sites, in the presence of AMP-PNP + Mg<sup>2+</sup> but not with ADP + Mg<sup>2+</sup> bound, whether P<sub>i</sub> was present or not, and not when nucleotide binding sites were empty. Binding of *N*-ethylmaleimide had no effect, whereas 7-diethyl-amino-3-(4'-maleimidylphenyl)-4-methylcoumarin increased the ATPase activity of ECF<sub>1</sub> more than 2-fold by reaction with Cys-87. In ECF<sub>1</sub>F<sub>0</sub>, these reagents inhibited activity. The nucleotide dependence of the reaction of Cys-87 of the  $\gamma$  subunit depended on the presence of the  $\epsilon$  subunit. In  $\epsilon$  subunit-free ECF<sub>1</sub>, maleimides reacted with Cys-87 under all nucleotide conditions, including when catalytic sites were empty. These results are discussed in terms of nucleotide-dependent movements of the  $\gamma$  subunit during functioning of the F<sub>1</sub>F<sub>0</sub>-type ATPase.

F<sub>1</sub>F<sub>0</sub>-type ATPases catalyze oxidative or photo-phosphorylation by using a transmembrane proton motive force to drive ATP synthesis (reviewed in Senior, 1988; Futai *et al.*, 1989; Hatefi, 1993). In the reverse direction, these enzymes use ATP hydrolysis to generate a proton gradient that can be used in ion transport processes. The simplest F<sub>1</sub>F<sub>0</sub>-type ATPases are found in bacteria. The hydrophilic F<sub>1</sub> part of the *Escherichia coli* enzyme (ECF<sub>1</sub>)<sup>1</sup> contains five different subunits in the stoichiometry  $\alpha$ 3,  $\beta$ 3,  $\gamma$ ,  $\delta$ , and  $\epsilon$ , whereas the membrane-integrated F<sub>0</sub> part (ECF<sub>0</sub>) contains three different subunits in the molar ratio  $\alpha$ 1,  $\beta$ 2,  $c$ 10–12.

As first demonstrated by electron microscopy studies (Tiedge *et al.*, 1985; Gogol *et al.*, 1989a, 1989b), the three  $\alpha$  and three  $\beta$  subunits alternate in a hexagonal arrangement surrounding a central cavity containing the  $\gamma$  subunit. The recent high reso-

lution structure of the beef heart F<sub>1</sub> (MF<sub>1</sub>) confirms this arrangement and shows that the part of the  $\gamma$  subunit within the  $\alpha$ <sub>3</sub> $\beta$ <sub>3</sub> domain is in the form of two large  $\alpha$  helices, one provided by residues 1–45 (ECF<sub>1</sub> numbering system) and the other by residues 223–286 (Abrahams *et al.* 1994). A third short  $\alpha$  helix of the  $\gamma$  subunit has been resolved in the x-ray analysis (Abrahams *et al.* 1994). This short segment of residues 82–99, including an intrinsic Cys residue (Cys-87), binds to the so-called DELSEED region (residues 380–386) of one of the  $\beta$  subunits.

Recent evidence indicates that the  $\gamma$  subunit runs from within the  $\alpha$ <sub>3</sub> $\beta$ <sub>3</sub> domain of the F<sub>1</sub> through the stalk region that connects the F<sub>1</sub> to F<sub>0</sub> (Gogol *et al.*, 1987; Lücken *et al.*, 1990) and binds to the *c* subunits of the F<sub>0</sub> that are a part of the proton channel (Watts *et al.*, 1995). It is now generally agreed that energy coupling within the F<sub>1</sub>F<sub>0</sub> complex is by conformational changes involving the stalk-forming subunits, including the  $\gamma$  subunit (reviewed in Boyer, 1993; Capaldi *et al.*, 1994). Previously, we have provided evidence of nucleotide-dependent conformational changes in the  $\gamma$  subunit around Cys residues site-directed into positions 8 and 106 of this subunit (Aggeler and Capaldi, 1992, 1993; Turina and Capaldi, 1994a, 1994b). Here, we describe studies in which one of the two intrinsic Cys residues of the  $\gamma$  subunit is reacted with various maleimides in both ECF<sub>1</sub> and ECF<sub>1</sub>F<sub>0</sub>. This residue, shown to be Cys-87, is shielded in wild-type enzyme but becomes available for reaction in ECF<sub>1</sub> (and ECF<sub>1</sub>F<sub>0</sub>) when Glu-381 of the  $\beta$  subunit is replaced by a smaller side chain, *e.g.* by a Cys or an Ala. The interaction of the short  $\alpha$  helix of  $\gamma$  with the DELSEED region is shown to be nucleotide-dependent and, as with ATP hydrolysis-driven structural changes already observed at residues 8 or 106, requires binding of the  $\epsilon$  subunit.

### EXPERIMENTAL PROCEDURES

**Materials**—CM and BM were obtained from Molecular Probes; Sephadex G-50 was purchased from Pharmacia Biotech Inc.; all other chemicals were of analytical grade and obtained from Sigma.

**Plasmids and Bacteria Strains**—Routine cloning was carried out in *XL1-Blue* and site-directed mutagenesis in *CJ236* according to Kunkel *et al.* (1987). Mutant ATPase and ATP synthase was isolated from *AN888* (*unc*), transformed with *unc* operon containing plasmids.

The Cys residue at position 87 of the  $\gamma$  subunit was replaced with Ser by using M13mp18 that contained the 1.4-kb *EcoRI/SmaI* fragment (Aggeler and Capaldi, 1992) and the oligonucleotide GACCGTGGTTT-GACCGTGGTTT. Successful mutagenesis was shown by testing for the newly created *BsrBI* restriction site. The mutation was incorporated in an *unc* operon-containing plasmid in two steps. (i) The 1.1-kb *SfiI/EcoRI* fragment from M13mp18 was inserted in the pBlue-script derivative pRA13 (Aggeler *et al.*, 1995). (ii) The 2.8-kb *SstI/XhoI* fragment of this plasmid was then introduced in pRA134 (Aggeler *et al.*, 1995), creating pRA149 with the mutation  $\beta$ E381C/ $\gamma$ C87S/ $\epsilon$ S108C.

The Glu in position 381 of the  $\beta$  subunit was replaced with an Ala by using M13mp18 that contained the 1.01-kb *NcoI* insert, described in Aggeler *et al.* (1992), and the oligonucleotide TTCTTCAGACAAT-CCATCCATACC (nucleotide A was introduced to obtain a new *NsiI* restriction site for analysis). The *NcoI* fragment was introduced in

\* This work was supported by National Institutes of Health Grant HL24526 (to R. A. C.). The costs of publication of this article were defrayed in part by the payment of page charges. This article must therefore be hereby marked "advertisement" in accordance with 18 U.S.C. Section 1734 solely to indicate this fact.

† To whom correspondence should be addressed. Tel.: 541-346-5881; Fax: 541-346-4854.

<sup>1</sup> The abbreviations used are: ECF<sub>1</sub>, soluble portion of the *E. coli* F<sub>1</sub>F<sub>0</sub>-ATP synthase; ECF<sub>1</sub>F<sub>0</sub>, *E. coli* F<sub>1</sub>F<sub>0</sub>-ATP synthase; MOPS 3-(*N*-morpholino)propanesulfonic acid; NEM, *N*-ethylmaleimide; AMP-PNP, 5'-adenyl- $\beta$ , $\gamma$ -imidodiphosphate; DTT, dithiothreitol; CM, 7-diethyl-amino-3-(4'-maleimidylphenyl)-4-methylcoumarin; BM, benzophenone-4-maleimide; kb, kilobase pair(s).

pRA13 and then the 5.8-kb *XhoI/NsiI* fragment in pRA100 (Aggeler *et al.*, 1992), creating pRA155 with the mutation  $\beta$ E381A.

The mutants  $\beta$ E381C and  $\beta$ E381C/ $\epsilon$ S108C have been described already (Aggeler *et al.*, 1995).

**Preparation of  $ECF_1$  and  $ECF_1F_0$ .**— $ECF_1$  was isolated by a modification of the method of Wise *et al.* (1981) described in Gogol *et al.* (1989b). The enzyme was precipitated for 1 h at 4 °C in 70%  $(NH_4)_2SO_4$ , pelleted by centrifugation at  $10,000 \times g$  for 15 min, and the protein then dissolved in 50 mM MOPS, pH 7.0, 0.5 mM EDTA, and 10% glycerol (v/v). Loosely bound nucleotides were removed by passing samples of enzyme through two consecutive centrifuge columns (Sephadex G-50, fine,  $0.5 \times 5.5$  cm) (Penefsky, 1977) equilibrated in the same buffer. The resulting  $ECF_1$  preparations retain 1.6–1.8 mol of ADP + ATP bound in noncatalytic sites (see also Haughton and Capaldi, 1995).  $ECF_1F_0$  was prepared according to Foster and Fillingame (1979) with modifications described in Aggeler *et al.* (1987). This ATP synthase was reconstituted into egg-lecithin vesicles by the method described in Aggeler *et al.* (1995).

**Maleimide Reaction of  $ECF_1$  and  $ECF_1F_0$ .**—For modification by maleimides, nucleotide-depleted  $ECF_1$  (2–3  $\mu$ M) was equilibrated at room temperature in 50 mM MOPS, pH 7.0, 0.5 mM EDTA, and 10% glycerol (v/v) buffer for 0.5–1 h. After addition of nucleotide, as stated, the enzyme was incubated for 5 min before the various maleimides were added. Samples were incubated in the dark at room temperature and at specific time intervals, aliquots withdrawn, and the reaction quenched by the addition of 20 mM DTT. The reaction of  $ECF_1F_0$  with maleimides was done similarly, except in 50 mM MOPS, pH 7.0, 5 mM  $MgCl_2$ , and 10% glycerol. Labeling of  $ECF_1$  from the mutant  $\beta$ E381C with [ $^{14}C$ ]NEM (DuPont NEN) was conducted in 50 mM MOPS, pH 7.0, 0.5 mM EDTA, 10% glycerol, in the presence of different nucleotides as indicated, using 20  $\mu$ M of the maleimide. Data were analyzed as described in Haughton and Capaldi (1995).

**Other Methods.**—ATPase activity was measured with a regenerating system described by Löttscher *et al.* (1984).  $\epsilon$ -Depleted  $ECF_1$  was prepared according to Dunn (1986) but using Sephacryl S300 (Pharmacia) followed by two passages through an  $\epsilon$ -4 monoclonal antibody affinity column. Protein concentrations were determined with the BCA protein assay (Pierce Chemical Co.). SDS-polyacrylamide gel electrophoresis was performed with a 10–18% SDS-containing gradient gel (Laemmli, 1970). Protein bands on gels were stained with Coomassie Brilliant Blue R (Downer *et al.*, 1976).

## RESULTS

**Cys-87 of the  $\gamma$  Subunit shows a Nucleotide-dependent Reactivity with Maleimides When Glu-381 of  $\beta$  Is Mutated to a Smaller Residue.**—In earlier studies, using the mutant  $\beta$ E381C, we had noted that an intrinsic Cys of the  $\gamma$  subunit was reactive to various maleimides. This preliminary observation was followed up as an approach to examining the conformation of the  $\gamma$  subunit under different nucleotide conditions. As shown in Fig. 1, there was incorporation of [ $^{14}C$ ]NEM into the  $\gamma$  subunit of  $ECF_1$  isolated from the mutant  $\beta$ E381C when the reaction was carried out in ATP + EDTA, but no significant labeling if the reaction was carried out in EDTA alone (no nucleotide in catalytic sites) or in ADP +  $Mg^{2+}$  +  $P_i$ . In these experiments, NEM was incorporated rapidly into the Cys at position 381 of  $\beta$ , as well as into the  $\delta$  subunit (not shown). The  $\delta$  subunit is reactive to maleimides in wild-type  $ECF_1$ , but its modification (at Cys-140) has no effect on activity (Mendel-Hartvig and Capaldi, 1991; Ziegler *et al.*, 1994). Activity measurements showed that NEM incorporation, into either the  $\gamma$  subunit, or into Cys-381 of  $\beta$ , or both, activated the enzyme more than 2-fold. In contrast, CM modification of one or both sites caused essentially full inhibition (Fig. 2B).

Recently, Duncan *et al.* (1995a, 1995b) used a mutant  $\beta$ D380C/ $\gamma$ C87S to distinguish which of the two Cys in the  $\gamma$  subunit (Cys-87 or Cys-112) was involved in disulfide bond cross-linking between  $\gamma$  and the  $\beta$  DELSEED region. Following the same approach, we constructed the mutant  $\beta$ E381C/ $\gamma$ C87S/ $\epsilon$ S108C to identify which of the intrinsic Cys in  $\gamma$  was being reacted by maleimides. There was reactivity of the  $\beta$  subunit in the Cys at 381 and modification of both  $\delta$  and  $\epsilon$  (via Cys-108) but no labeling of the  $\gamma$  subunit by CM in this mutant (Fig. 3, lanes 10 and 11). Therefore, Cys-87 must be the site of male-

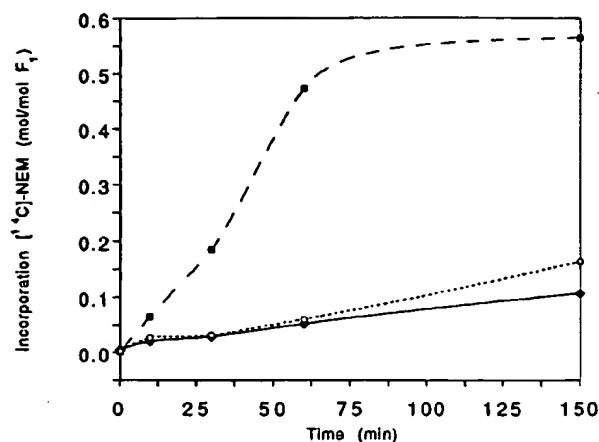


FIG. 1. Labeling of  $ECF_1$  from the mutant  $\beta$ E381C with [ $^{14}C$ ]NEM. Enzyme was reacted with 20  $\mu$ M [ $^{14}C$ ]NEM in the presence of 5 mM ATP + 0.5 mM EDTA (closed squares), 5 mM ATP + 5.5 mM  $MgCl_2$  (open circles), or with no nucleotide additions (closed diamonds), and the reaction was stopped at the times indicated by adding 20 mM DTT. The  $\gamma$  subunit was excised from a polyacrylamide gel and radioactivity counted.

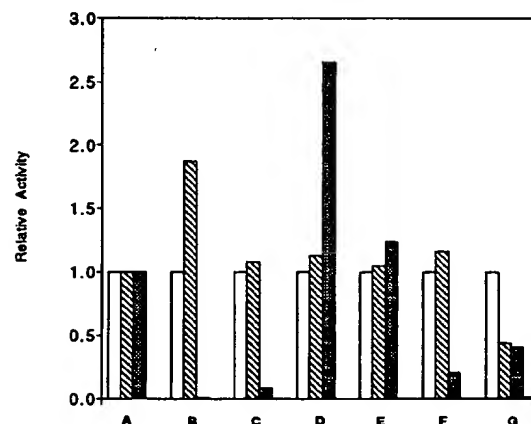


FIG. 2. Effect of maleimides on the ATPase activity of mutants.  $ECF_1$  preparations equilibrated in MOPS buffer, pH 7.0, containing 10% glycerol, 2.5 mM ATP, 0.5 mM EDTA were incubated with 100  $\mu$ M NEM (hatched), CM (cross-hatched), or BM. The ATPase activity determined after 3 h incubation with the different maleimides is presented relative to the basal unmodified enzyme (open). A,  $ECF_1$  from wild-type; B,  $ECF_1$  from  $\beta$ E381C; C,  $ECF_1$  from  $\beta$ E381C/ $\gamma$ C87S/ $\epsilon$ S108C; D,  $ECF_1$  from  $\beta$ E381A; E,  $\epsilon$ -free  $ECF_1$  from  $\beta$ E381A; F,  $\epsilon$ -free  $ECF_1$  from  $\beta$ E381C/ $\gamma$ C87S/ $\epsilon$ S108C; G,  $ECF_1F_0$  from  $\beta$ E381A.

imide incorporation into the  $\gamma$  subunit. CM modification of the mutant  $\beta$ E381C/ $\gamma$ C87S/ $\epsilon$ S108C reduced the ATPase activity by 90% (Fig. 2C). This inhibition is not due to modification of Cys-8140 as discussed above. Moreover, CM modification of the  $ECF_1$  isolated from mutant  $\epsilon$ S108C had no effect on activity (result not shown). Therefore, it must be modification of Cys-381 in the DELSEED region of the  $\beta$  subunit that caused the observed inhibition of activity in this mutant.

To explore the reactivity of Cys-87 more fully, the mutant  $\beta$ E381A was prepared. This change preserves the short side chain but avoids a maleimide-reactive cysteine in the  $\beta$  subunit. The reactivity of Cys-87 with CM under different nucleotide conditions is shown in Fig. 3 (lanes 1–8). There was rapid and strong incorporation of CM in EDTA + ATP, EDTA + ADP, or AMP-PNP +  $Mg^{2+}$ , a low incorporation of reagent in EDTA or  $Mg^{2+}$  alone, but essentially no modification of  $\gamma$  with  $Mg^{2+}$  + ADP-bound, either when added directly, or as generated on the protein by addition of ATP +  $Mg^{2+}$  followed by

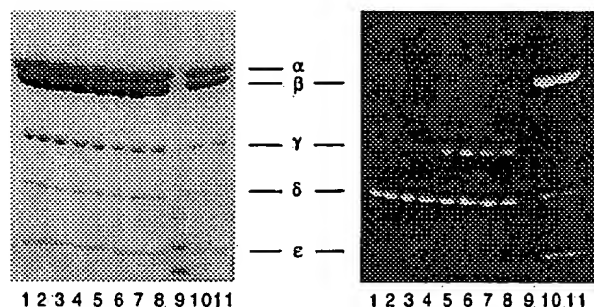


FIG. 3. CM reactivity of  $\beta$ E381A and  $\beta$ E381C/ $\gamma$ C87S/ $\epsilon$ S108C mutant  $ECF_1$  preparations under different nucleotide conditions.  $ECF_1$  from the mutant  $\beta$ E381A, treated to remove loosely bound nucleotides as described under "Experimental Procedures," was reacted with 100  $\mu$ M CM for 6 h in a buffer containing 50 mM MOPS, pH 7.0, 10% glycerol, and 0.5 mM EDTA with 2 mM  $Mg^{2+}$  + 2 mM ADP (lane 1), 2 mM  $Mg^{2+}$  + 2.5 mM ATP (lane 2), 2 mM  $Mg^{2+}$  (lane 3), without additions (lane 4), 2 mM ADP (lane 5), 2.5 mM ATP (lane 6), 2 mM AMP-PNP (lane 7), 2 mM  $Mg^{2+}$  + 2 mM AMP-PNP (lane 8).  $ECF_1$  from the mutant  $\beta$ E381C/ $\gamma$ C87S/ $\epsilon$ S108C was reacted with 100  $\mu$ M CM for 6 h in the presence of 2.5 mM ATP (lane 10) or 2 mM  $Mg^{2+}$  + 2.5 mM ATP (lane 11). The reaction was quenched by 20 mM DTT. Lanes 1–8 contain 75  $\mu$ g of protein. Lanes 10 and 11 contain 50  $\mu$ g of protein. Lane 9 contained molecular weight markers. The left side shows Coomassie Blue staining and the right side shows the fluorescence pattern.

enzyme turnover. Reaction of the  $\gamma$  subunit with NEM in enzyme from the mutant  $\beta$ E381A had no effect on activity. In contrast, CM modification caused almost 2.5-fold activation of the ATPase activity (Fig. 2D) compared with almost full inhibition when both Cys-87 and the Cys at residue 381 of  $\beta$  were modified.

**Nucleotide Dependence of the Reactivity of  $\gamma$  Cys-87 Is Lost in  $\epsilon$ -Free  $ECF_1$** —The reactivity of CM was monitored in  $ECF_1$  from the mutant  $\beta$ E381A that had been freed of  $\epsilon$  subunit by affinity chromatography with a monoclonal antibody against the  $\epsilon$  subunit (Dunn, 1986). Fig. 4 shows that Cys-87 is labeled by CM under all nucleotide conditions including ADP +  $Mg^{2+}$  or AMP-PNP +  $Mg^{2+}$ . This site was also labeled by CM in EDTA or  $Mg^{2+}$  alone (results not shown). The ATPase activity of the  $\epsilon$ -free  $ECF_1$  from mutant  $\beta$ E381A was high, i.e. 70  $\mu$ mol of ATP hydrolyzed per min per mg. There was no significant increase in the activity on reaction of CM (Fig. 2E), in contrast to the activation observed with enzyme that had not been freed of  $\epsilon$  subunit.

In another set of experiments, the effect of removing the  $\epsilon$  subunit on the inhibition of ATPase activity by CM was investigated in the mutant  $\beta$ E381C/ $\gamma$ C87S/ $\epsilon$ S108C. As shown in Fig. 2F, CM inhibited  $\epsilon$ -free  $ECF_1$  from this mutant. Therefore, it is the interaction between  $\beta$  and  $\gamma$ , rather than between  $\beta$  and  $\epsilon$ , which is perturbed when the Cys at residue 381 of  $\beta$  is reacted with CM.

**Cys-87 Is Reactive to Various Maleimides in  $ECF_1F_0$  from the Mutant  $\beta$ E381A**— $ECF_1F_0$  purified from the mutant  $\beta$ E381A had normal ATPase activity, i.e. around 20  $\mu$ mol of ATP hydrolyzed per min per mg protein, which was inhibited to 90% by 50  $\mu$ M dicyclohexylcarbodiimide, results similar to those obtained with wild-type enzyme. Reaction of this preparation with CM gave a similar pattern of labeling to that with  $ECF_1$  from this mutant, i.e. strong labeling of the  $\gamma$  subunit in AMP-PNP +  $Mg^{2+}$ , but little or none in  $Mg^{2+}$  alone, or in ADP +  $Mg^{2+}$  (result not shown). There was also some reaction of the reagent with the  $\delta$  subunit, but no significant reaction of the intrinsic Cys in the  $\beta$  subunit under the labeling conditions employed. Fig. 2G summarizes the effects on the ATPase activity of modification by three different maleimides. Modification by NEM, CM, and BM all led to an inhibition of activity that was not seen with wild-type  $ECF_1F_0$ , indicating that the

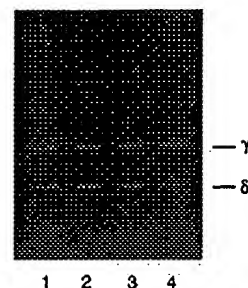


FIG. 4. CM labeling of  $\epsilon$ -free  $ECF_1$  from the mutant  $\beta$ E381A.  $ECF_1$  from the mutant  $\beta$ E381A depleted of nucleotides as described under "Experimental Procedures" was reacted with 100  $\mu$ M CM in the dark at room temperature for 6 h in 50 mM MOPS, pH 7.0, 0.5 mM EDTA, 10% glycerol, after addition of 2.5 mM ATP (lane 1), 2 mM  $Mg^{2+}$  + 2.5 mM ATP (lane 2), 2 mM  $Mg^{2+}$  + 2 mM ADP (lane 3), or 2 mM  $Mg^{2+}$  + 2 mM AMP-PNP (lane 4). The labeling was quenched by 20 mM DTT. 25  $\mu$ g of enzyme was applied per lane.

effect is due to reaction of Cys-87 and not Cys-140 of the  $\delta$  subunit. The highest amount of inhibition was with the BM (more than 90%).

## DISCUSSION

Cys-87 is at the end of a short  $\alpha$  helix of the  $\gamma$  subunit that interacts with the so-called DELSEED region of the  $\beta$  subunit (Abrahams *et al.* 1994). We have found that Cys-87 can be cross-linked in essentially 100% yield by disulfide bond formation to a Cys replacing Glu at 381 (Aggeler *et al.*, 1995), indicating the close proximity of the two residues, consistent with the  $\sim 4$ -Å spacing from side chain S to S, estimated from the x-ray structural data (Abrahams *et al.*, 1994). Cys-87 is buried in wild-type  $ECF_1$  and  $ECF_1F_0$ . However, when Glu-381 of the  $\beta$  subunit is exchanged for a smaller and uncharged side chain, such as Cys or Ala, this residue of  $\gamma$  becomes exposed for reaction with maleimides at least as large as CM. This exposure is nucleotide-dependent.

In enzyme from which catalytic site nucleotide has been removed, Cys-87 is essentially buried. Addition of nucleotide, either ADP or ATP in the presence of EDTA, exposes Cys-87 for reaction with various maleimides. In the absence of  $Mg^{2+}$ , the binding constants for nucleotide in each of the three catalytic sites, including that in the  $\beta$  which is linked to the short  $\alpha$  helix of  $\gamma$ , is around 100  $\mu$ M (Weber *et al.*, 1994; Grüber and Capaldi, 1996), similar to that of isolated  $\beta$  subunit, suggesting an open arrangement of the sites (as in  $\beta_E$  in the structure of MF<sub>1</sub>). In the presence of  $Mg^{2+}$ , Cys-87 is exposed when ATP is bound, as demonstrated by the data for AMP-PNP, but the residue is buried in ADP or ADP +  $P_i$ . It appears, therefore, that the short  $\alpha$  helix undergoes a release or reorganization that exposes Cys-87 when the catalytic sites are all open, or when ATP is bound, and that this is reversed on ATP hydrolysis.

A conformational change of the  $\gamma$  subunit related to ATP binding and hydrolysis has been seen previously by changes in cross-linking from a Cys introduced at position 8 of the  $\gamma$  subunit (in the long N-terminal  $\alpha$  helix) with the  $\beta$  subunit(s) (Aggeler and Capaldi, 1993). This process has also been followed by fluorescence changes of CM bound to either the Cys introduced at position 8 or another Cys introduced at residue 106 of the  $\gamma$  subunit (Turina and Capaldi, 1994a, 1994b). Fluorescence measurements under unisite catalysis conditions showed that the conformational change in the  $\gamma$  subunit occurs with bond cleavage of ATP to product ADP +  $P_i$ , rather than with  $P_i$  release (Turina and Capaldi, 1994a, 1994b).

Importantly, the conformational rearrangements observed here by changes in the reaction of Cys-87 were lost on removal of the  $\epsilon$  subunit. Without the  $\epsilon$  subunit bound, Cys-87 is ex-

posed for reaction under all nucleotide conditions, including when catalytic sites are empty. The conformational changes observed for Cys-8 by cross-linking and from both Cys-8 and Cys-106 by fluorescence measurements were also lost when the  $\epsilon$  subunit was removed (Aggeler and Capaldi, 1993; Turina and Capaldi, 1994a). The enzyme continues to show highly cooperative ATPase activity in the absence of the  $\epsilon$  subunit. The implication, therefore, is that the  $\epsilon$  subunit in some way controls or regulates structural changes in the  $\gamma$  subunit, and these changes are likely a part of the energy transduction mechanism.

The second interesting aspect of the reactivity of Cys-87 is the effect on activity of the enzyme. When Glu-381 is replaced by an Ala, reaction of Cys-87 with NEM has very little effect in isolated  $ECF_1$ , whereas incorporation of CM activates the enzyme around 2.5-fold. This activation is related to  $\epsilon$  subunit binding, as it is lost when the  $\epsilon$  subunit is removed. By contrast, the reaction of Cys-87 in  $ECF_1F_0$  with either NEM or CM leads to inhibition of ATPase activity by 50% or more, while modification by BM induces almost full inhibition. These results for  $ECF_1$  and  $ECF_1F_0$  can be compared with data for  $CF_1$  and  $CF_1F_0$ . In the chloroplast enzyme, the equivalent residue of Cys-87, numbered Cys-89, is reactive to NEM even with a Glu in the DELSEED region (McCarty and Fagan, 1973; Moroney *et al.*, 1984; Soteropoulos *et al.*, 1994). Reaction of NEM with Cys-89 occurs in thylakoid membranes when these are energized by light (*i.e.* when ATP is being made) and does not occur in the dark (with ADP bound) (McCarty and Fagan, 1973). However,  $CF_1$  isolated from thylakoids modified with NEM in the light is inhibited by the reagent, as is the ATPase activity of the membrane-bound enzyme (Soteropoulos *et al.*, 1994).

Recent results by Soteropoulos *et al.* (1994) have shown an altered affinity of catalytic sites for ADP in  $CF_1$  that has been modified with NEM, leading these authors to propose that inhibition is due to altered binding of nucleotides in one, or more, catalytic sites. This cannot explain the activity effects with  $ECF_1$ , as the modification of Cys-87 by CM activates the enzyme when the  $\epsilon$  subunit is present and gives the same activity as unmodified enzyme in  $\epsilon$ -free  $ECF_1$ . Rather, the effect of modification of Cys-87 seems to be a steric effect, based on the results with  $ECF_1F_0$  from the mutant  $\beta E381A$ , where inhibition occurs with any of the maleimides used. Studies with the mutant  $\beta E381C/\gamma C87S/\epsilon S108C$  also point to the importance of steric constraints for conformational changes involving the short  $\alpha$  helix of  $\gamma$  and DELSEED region of  $\beta$ . Modification of a Cys-at 381 in the  $\beta$  subunit with NEM activated, whereas reaction of this site with CM causes a dramatic inhibition of activity.

Taken together, the nucleotide dependence and activity effects suggest that there is a loosening and possibly a release of the  $\gamma$  subunit at its catch region with a  $\beta$  subunit on ATP binding, which is reversed on ADP formation. Such a release,

followed by rebinding, may be a part of coupling catalytic sites with the proton channel and would be a necessary step if the  $\gamma$  subunit moves relative to the  $\alpha_3\beta_3$  domain, as suggested by the structural features of the enzyme (Abrahams *et al.*, 1994) and as visualized by electron microscopy (Gogol *et al.*, 1990) and, more recently, by biochemical methods (Duncan *et al.*, 1995a, 1995b).

**Acknowledgment**—The excellent technical assistance of Kathy Chicas-Cruz is gratefully acknowledged.

## REFERENCES

- Abrahams, J. P., Leslie, A. G. W., Lutter, R., and Walker, J. E. (1994) *Nature* **370**, 621–628
- Aggeler, R., and Capaldi, R. A. (1992) *J. Biol. Chem.* **267**, 21355–21359
- Aggeler, R., and Capaldi, R. A. (1993) *J. Biol. Chem.* **268**, 14576–14578
- Aggeler, R., Zhang, Y.-Z., and Capaldi, R. A. (1987) *Biochemistry* **26**, 7107–7113
- Aggeler, R., Chicas-Cruz, K., Cai, S.-X., Keana, J. F. W., and Capaldi, R. A. (1992) *Biochemistry* **31**, 2956–2961
- Aggeler, R., Haughton, M. A., and Capaldi, R. A. (1995) *J. Biol. Chem.* **270**, 9185–9191
- Boyer, P. D. (1993) *Biochim. Biophys. Acta* **1140**, 215–250
- Capaldi, R. A., Aggeler, R., Turina, P., and Wilkens, S. (1994) *Trends Biochem. Sci.* **19**, 284–289
- Downer, N. W., Robinson, N. C., and Capaldi, R. A. (1976) *Biochemistry* **15**, 2930–2936
- Duncan, T. M., Zhou, Y., Bulygin, V. V., Hutcheon, M. L., and Cross, R. L. (1995a) *Trans. Biochem. Soc.* **23**, 736–740
- Duncan, T. M., Bulygin, V. V., Hutcheon, M. L., and Cross, R. L. (1995b) *Proc. Natl. Acad. Sci. U. S. A.* **92**, 10964–10968
- Dunn, S. D. (1986) *Anal. Biochem.* **159**, 35–42
- Foster, D. L., and Fillingame, R. H. (1979) *J. Biol. Chem.* **254**, 8230–8236
- Futai, M., Noumi, T., and Maeda, M. (1989) *Annu. Rev. Biochem.* **58**, 111–136
- Gogol, E. P., Lücken, U., and Capaldi, R. A. (1987) *FEBS Lett.* **219**, 274–278
- Gogol, E. P., Aggeler, R., Sagermann, M., and Capaldi, R. A. (1989a) *Biochemistry* **28**, 4717–4724
- Gogol, E. P., Lücken, U., Bork, T., and Capaldi, R. A. (1989b) *Biochemistry* **28**, 4709–4716
- Gogol, E. P., Johnston, E., Aggeler, R., and Capaldi, R. A. (1990) *Proc. Natl. Acad. Sci. U. S. A.* **87**, 9585–9589
- Grüber, C., and Capaldi, R. A. (1996) *Biochemistry* **35**, 3875–3879
- Hatefi, Y. (1993) *Eur. J. Biochem.* **218**, 759–767
- Haughton, M. A., and Capaldi, R. A. (1995) *J. Biol. Chem.* **270**, 20568–20574
- Kunkel, T. A., Roberts, J. D., and Zakour, M. A. (1987) *Methods Enzymol.* **154**, 367–382
- Laemmli, U. K. (1970) *Nature* **227**, 680–685
- Lötscher, H.-R., deJong, C., and Capaldi, R. A. (1984) *Biochemistry* **23**, 4140–4143
- Lücken, U., Gogol, E. P., and Capaldi, R. A. (1990) *Biochemistry* **29**, 5339–5343
- McCarty, R. E., and Fagan, J. (1973) *Biochemistry* **12**, 1503–1507
- Mendel-Hartvig, J., and Capaldi, R. A. (1991) *Biochim. Biophys. Acta* **1060**, 115–124
- Moroney, J. V., Fullmer, C. S., and McCarty, R. E. (1984) *J. Biol. Chem.* **259**, 7281–7285
- Penefsky, H. S. (1977) *J. Biol. Chem.* **252**, 2891–2899
- Senior, A. E. (1988) *Physiol. Rev.* **68**, 177–231
- Soteropoulos, P., Ong, A. M., and McCarty, R. E. (1994) *J. Biol. Chem.* **269**, 19810–19816
- Tiedge, H., Lunsdorf, H., Schafer, G., and Schairer, H. V. (1985) *Proc. Natl. Acad. Sci. U. S. A.* **82**, 7874–7878
- Turina, P., and Capaldi, R. A. (1994a) *J. Biol. Chem.* **269**, 13465–13471
- Turina, P., and Capaldi, R. A. (1994b) *Biochemistry* **33**, 14275–14280
- Watts, S. D., Zhang, Y., Fillingame, R. H., and Capaldi, R. A. (1995) *FEBS Lett.* **368**, 235–238
- Weber, J., Wilke-Mounts, S., and Senior, A. E. (1994) *J. Biol. Chem.* **269**, 20462–20467
- Wise, J. G., Latchney, R. L., and Senior, A. E. (1981) *J. Biol. Chem.* **256**, 10383–10389
- Ziegler, M., Xiao, R., and Penefsky, H. S. (1994) *J. Biol. Chem.* **269**, 4233–4239



# RESEARCH ARTICLES

7. A. L. Casselman and J. B. Nasrallah, unpublished data.
8. J. A. Conner, P. Conner, M. E. Nasrallah, J. B. Nasrallah, *Plant Cell* 10, 801 (1998).
9. cDNA libraries were constructed with the  $\lambda$ UNIZAP phagemid system (Stratagene). Hybridization conditions for RNA and DNA gel blots were as described [D. C. Boyes, C.-H. Chen, T. Tantikajana, J. J. Esch, J. B. Nasrallah, *Genetics* 127, 221 (1991)] except that washes (each 20 min at 65°C) were extended by using successively 2 $\times$  SET, 0.5% SDS and 1 $\times$  SET, 0.1% SDS and 0.2 $\times$  SET, and 0.1% SDS, unless indicated otherwise.
10. The  $S_2S_6$  F<sub>2</sub> population was derived from a cross between *B. oleracea*  $S_6S_6$  and  $S_2S_2$  homozygotes. The genotypes and SI phenotypes of 153 individual plants had been determined previously. Gel blot analysis of Hind III-digested genomic DNA revealed coinciding hybridization patterns for *SLG<sub>6</sub>*- and *SCR<sub>6</sub>*-specific probes. All 116 plants hybridizing to *SLG<sub>6</sub>* also hybridized to *SCR<sub>6</sub>*, whereas all 37 plants devoid of *SLG<sub>6</sub>* also lacked *SCR<sub>6</sub>*. Similarly, 80 plants of an F<sub>2</sub> population segregating for  $S_6$  and  $S_{13}$  were genotyped by hybridization of Hind III-digested genomic DNA with *SLG<sub>6</sub>*- and *SLG<sub>13</sub>*-specific probes. Hybridization with an *SCR<sub>13</sub>*-specific probe revealed that 34 *SLG<sub>13</sub>*-containing plants contained *SCR<sub>13</sub>*, in contrast to 46 plants lacking both *SLG<sub>13</sub>* and *SCR<sub>13</sub>*.
11. The *B. campestris*  $S_6$  haplotype also appears to contain an *SCR*-related sequence [G. Suzuki et al., *Genetics* 153, 391 (1999)].
12. Polyadenylated RNA was analyzed as in (2, 9). Microspores were staged by DAPI (4',6'-diamidino-2-phenylindole) staining [S. Detchepare, P. Heizmann, C. Dumas, *J. Plant Physiol.* 135, 129 (1989)] and purified as described [D. C. Boyes and J. B. Nasrallah, *Plant Cell* 7, 1283 (1995)].
13. J. B. Nasrallah et al., *Ann. Bot.*, in press.
14. As host for the transformation of the *SCR<sub>6</sub>* cDNA, we chose a *B. oleracea*  $S_2S_2$  homozygote. Besides ease of transformation and regeneration, this strain is expected to have an endogenous *SCR* allele with only low sequence similarity to the transgene, which reduces the risk of homology-dependent gene silencing (Fig. 2A). The transformation construct contained the *SCR<sub>6</sub>* cDNA preceded by the *SCR<sub>6</sub>* 1.3-kb upstream region and followed by the nos terminator. After introducing appropriate restriction sites by polymerase chain reaction followed by DNA sequence analysis, both *SCR* fragments were assembled as a transcriptional fusion in pCR2.1 (Invitrogen) and subcloned as a 1.7-kb Hind III-Sac I fragment into pCAM-BIA1300 upstream of an Eco RI-Sac I nos promoter. After mobilization into *Agrobacterium tumefaciens* strain GV3101, the construct was used for transformation of flower stem disks of the *B. oleracea*  $S_2S_2$  strain, as described [K. Toriyama, J. C. Stein, M. E. Nasrallah, J. B. Nasrallah, *Theor. Appl. Genet.* 81, 769 (1991)], applying hygromycin selection. The independent origin of the transformants was verified by DNA gel blot analysis.
15. Pollen was manually transferred onto stigmas of open flowers. After 7 to 9 hours, pollen tube growth was observed by ultraviolet fluorescence microscopy [Y. O. Kho and J. Baer, *Euphytica* 17, 298 (1968)].
16. Open reading frames encoded by the three cDNAs *SCR<sub>6</sub>*, *SCR<sub>13</sub>*, and *SCR<sub>6</sub>* were identified on the basis of sequence similarity of the cysteine-rich reading frame, as well as the presence of stop codons upstream of the ATG initiation codon.
17. G. von Heijne, *Nucleic Acids Res.* 14, 4683 (1986).
18. A. G. Stephenson et al., *Plant J.* 12, 1351 (1997).
19. J. Doughty et al., *Plant Cell* 10, 1333 (1998).
20. B. S. Stanchev, J. Doughty, C. P. Scutt, H. G. Dickinson, R. R. D. Croy, *Plant J.* 10, 303 (1996).
21. W. F. Broekaert et al., *Crit. Rev. Plant Sci.* 16, 297 (1997); W. F. Broekaert, F. R. G. Terras, B. P. A. Cammue, R. W. Osborn, *Plant Physiol.* 108, 1353 (1995); F. R. G. Terras et al., *J. Biol. Chem.* 267, 15301 (1992).
22. SI in *Brassica* is under sporophytic control, whereby pollen phenotype in *S*-locus heterozygotes is determined by the two *S* alleles carried by the diploid parent plant and not by the single *S* allele carried by the haploid pollen grain.
23. Supported by NIH grant GM57527, NSF grant IBN-9631921, and U.S. Department of Agriculture grant 98-358301-6072.

13 September 1999; accepted 26 October 1999

## Molecular Architecture of the Rotary Motor in ATP Synthase

Daniela Stock,<sup>1</sup> Andrew G. W. Leslie,<sup>2</sup> John E. Walker<sup>1\*</sup>

Adenosine triphosphate (ATP) synthase contains a rotary motor involved in biological energy conversion. Its membrane-embedded  $F_0$  sector has a rotation generator fueled by the proton-motive force, which provides the energy required for the synthesis of ATP by the  $F_1$  domain. An electron density map obtained from crystals of a subcomplex of yeast mitochondrial ATP synthase shows a ring of 10 c subunits. Each c subunit forms an  $\alpha$ -helical hairpin. The interhelical loops of six to seven of the c subunits are in close contact with the  $\gamma$  and  $\delta$  subunits of the central stalk. The extensive contact between the c ring and the stalk suggests that they may rotate as an ensemble during catalysis.

ATP is the universal biological energy currency. ATP synthase produces ATP from adenosine diphosphate (ADP) and inorganic phosphate with the use of energy from a transmembrane proton-motive force generated by respiration or photosynthesis [for reviews, see (1–3)]. The enzyme consists of an extramembranous  $F_1$  catalytic domain linked by means of a central stalk to an intrinsic membrane domain called  $F_0$ . The globular  $F_1$  domain is an assembly of five different subunits with the stoichiometry  $\alpha_3\beta_3\gamma_1\delta_1\epsilon_1$ . In the atomic structure of bovine  $F_1$ , the  $\alpha$  and  $\beta$  subunits are arranged alternately around a coiled coil of two antiparallel  $\alpha$  helices in the  $\gamma$  subunit. The catalytic sites are in the  $\beta$

subunits at the  $\alpha/\beta$  subunit interface (4). The remainder of the  $\gamma$  subunit protrudes from the  $\alpha_3\beta_3$  assembly and can be cross linked to the polar loop region of the c subunits in  $F_0$  (5, 6). In mitochondria, the  $\delta$  and  $\epsilon$  subunits are associated with the  $\gamma$  subunit in the central stalk assembly (7–10), as are the bacterial and chloroplast  $\epsilon$  subunits, the counterparts of mitochondrial  $\delta$ . ATP-dependent rotation of  $\gamma$  and  $\epsilon$  within an immobilized  $\alpha_3\beta_3$  complex from the thermophilic bacterium *Bacillus* PS3 has been observed directly (11, 12). The rotation of the  $\gamma$  subunit in ATP synthase is thought to be generated by the passage of protons through  $F_0$ . Because there is only one intrinsically asymmetric  $\gamma$  subunit, it interacts differently with each of the three catalytic  $\beta$  subunits in  $F_1$ , endowing them with different nucleotide affinities (4). Rotation of the central stalk is accompanied by conformational changes in the  $\beta$  subunits, which cycle sequentially through structural states corresponding to low, medium, and high nu-

cleotide affinities. These three states are probably associated with release of product (ATP), binding of substrates (ADP and inorganic phosphate), and ATP formation, respectively. The cycle is known as the "binding change mechanism" of ATP synthesis (13). In eubacteria, the procedure is reversible, and hydrolysis of ATP in  $F_1$  generates rotation of  $\gamma$ , resulting in the pumping of protons back across the membrane through  $F_0$  (2).

In contrast to the detailed structural model established for most of the bovine  $F_1$  domain (4, 14–16) and additional structural information in other species (17, 18), little is known about the structural details of  $F_0$ . All species contain three common subunits known as a, b, and c. In *Escherichia coli*, the experimentally determined ratio of these subunits is  $a_1b_2c_{9-11}$  (19, 20). Cross-linking and genetic experiments (21, 22), as well as evolutionary arguments (23), have been interpreted as showing the presence of 12 c subunits per  $F_0$ . From biochemical studies and mutational analysis in bacteria (2, 24) and fungi (25), it is known that both a and c subunits contain functional groups that are essential for proton translocation through the membrane. A nuclear magnetic resonance (NMR) structure of a monomer of the *E. coli* c subunit in a chloroform:methanol:water mixture shows that the protein is folded into two  $\alpha$  helices (presumed to be transmembrane in the intact enzyme), linked by a loop (presumed to be extramembranous) (26). The COOH-terminal  $\alpha$  helix contains a conserved side chain carboxylate (Asp<sup>61</sup> in *E. coli* and Glu<sup>59</sup> in *Saccharomyces cerevisiae*) essential for proton translocation (2). Models have been proposed in which the a and b subunits are on the

<sup>1</sup>Medical Research Council Dunn Human Nutrition Unit, Hills Road, Cambridge CB2 2XY, UK. <sup>2</sup>Medical Research Council Laboratory of Molecular Biology, Hills Road, Cambridge CB2 2QH, UK.

\*To whom correspondence should be addressed. E-mail: walker@mrc-dunn.cam.ac.uk



## RESEARCH ARTICLES

outside of a multimeric ring of c subunits within the membrane, with the interface between a and c subunits providing the pathway for proton translocation (Fig. 1) (27–31). Protonation and deprotonation events in this interface have been proposed as part of a mechanism for generating conformational changes in  $F_1$  (32), possibly through rotation of the c ring (33). Because the generation of each ATP requires rotation of the  $\gamma$  subunit through  $120^\circ$ , a link has been made between the number of protons that must be translocated per ATP synthesized [estimated to be three or four in different systems (34, 35)] and the number of c subunits in the ring. The required rotation of  $\gamma$  through  $120^\circ$  can be achieved with either 9 c subunits in the ring and 3 translocated protons or 12 c subunits in the ring and 4 translocated protons (36). It has also been proposed that a rotary mechanism would require a peripheral “stator” to counter the tendency of  $\alpha_3\beta_3$  to follow the rotation of  $\gamma$  (36). It has been suggested that the b subunits of  $F_0$  may form part of such a stator, and evidence from reconstitution and cross-linking studies provides support for this hypothesis (37, 38). A feature connecting the periphery of  $F_0$  to  $F_1$  (the peripheral stalk) that might represent the stator has been visualized by single-particle electron microscopy of ATP synthase from bacteria, chloroplasts, and mitochondria (39–41).

**Structure analysis.** In this study, we purified ATP synthase from *S. cerevisiae* mitochondria and carried out crystallization experiments (42). The enzyme from this source consists of at least 13 different types of subunits: the  $F_1$  subunits  $\alpha$ ,  $\beta$ ,  $\gamma$ ,  $\delta$ , and  $\epsilon$ ; the  $F_0$  subunits a, b, and c, plus f and d; OSCP and ATP8, which have homologs in other mitochondrial ATP synthases; and the unique yeast subunit h (43–46). Other possible yeast subunits have been discussed as being involved in dimer formation (47). According to analyses by SDS–polyacrylamide gel electrophoresis (SDS–PAGE), high-performance liquid chromatography (HPLC) analysis, and  $\text{NH}_2$ -terminal sequencing, the purified complex used here for crystallization consists of subunits  $\alpha$ ,  $\beta$ ,  $\gamma$ ,  $\delta$ ,  $\epsilon$ , b, OSCP, d, a, h, f, ATP8, and c (in diminishing apparent molecular weight order for  $F_1$  and  $F_0$  on SDS gels) and is similar to other preparations (46, 48, 49). Crystals were grown in the presence of both ADP and the nonhydrolyzable ATP analog 5'-adenylyl-imidodiphosphate (AMP-PNP) by the microbatch technique (50) with polyethylene glycol 6000 as precipitant (42). Subunits  $\alpha$ ,  $\beta$ ,  $\gamma$ ,  $\delta$ ,  $\epsilon$ , and c were detected in the crystals by SDS–PAGE, and there was no evidence for the presence of the other subunits. It appears that they have dissociated from the complex during crystallization, leaving a subcomplex consisting of  $F_1$  and 10 copies of subunit c. A similar  $F_1c_{10}$  complex

has been isolated previously from spinach chloroplasts (51).

The structure was solved by molecular replacement with the “stand-alone” version of the program AMoRe (52) with data from 15 to 5 Å resolution and the bovine  $F_1$ –adenosine triphosphatase  $\text{Ca}$  coordinates [Protein Data Bank (PDB) accession code 1bmf (4)] as a search model (Table 1). The complete bovine model, positioned according to the results of the molecular replacement, was used to calculate phases to 3.9 Å resolution. After solvent density modification with the program Solomon/CCP4 (53, 54) assuming a solvent content of 60%, the  $\alpha$  helices of the c subunits and extensive additional density in the central stalk region could be seen in the electron density map (Fig. 2). Because of the limited resolution of the x-ray data, the side chain density is not clear, but the main chain density is generally unambiguous.

The crystal packing (Fig. 3) is atypical for membrane proteins and belongs to neither of the types described previously (55). The main crystal contacts are between the bottom of a ring of 10 c subunits and the pseudo-three-fold top of an adjacent  $F_1$  assembly. The hydrophobic external regions of the c oligomers, which are normally in contact with phospholipid, are not involved in any crystal contacts and are probably covered by unresolved molecules of detergent.

**Molecular architecture of the  $F_1c_{10}$  complex.** The  $\alpha$  and  $\beta$  subunits (73 and 79% conserved, respectively, between cow and yeast) are well defined in the electron density and have similar conformations and nucleotide compositions to their bovine counterparts. The  $\text{NH}_2$ - and  $\text{COOH}$ -terminal  $\alpha$  helices of the  $\gamma$  subunit (40% sequence identity to the bovine subunit) extend  $\sim 25$  Å farther than in the bovine model toward the c subunits, where they make a sharp bend. In the

bovine  $F_1$  structure, this part of the  $\gamma$  subunit and also subunits  $\delta$  and  $\epsilon$  were disordered. There is additional density adjacent to the lower segment of the  $\text{NH}_2$ -terminal  $\alpha$  helix of the  $\gamma$  subunit that extends over the c subunits (Fig. 2B), which can be interpreted with the crystal structure of the *E. coli*  $\epsilon$  subunit (26% sequence identity to the yeast  $\delta$  subunit) (56) (PDB accession code 1aqt). The 10 strands of the  $\beta$  barrel are visible in the yeast electron density, with  $\beta$  strand 4 and the following loop (residues 31 to 39 in *E. coli* numbering) packing against the c subunits and  $\beta$  strands 5, 8, 9, and the loop between  $\beta$  strands 1 and 2 (residues 39 to 42, 68 to 73, 74 to 79, and 9 to 14, respectively) in contact with the  $\gamma$  subunit. The lower  $\alpha$  helix ( $\text{COOH}$ -terminal) lies about 5 Å above the c subunits, and the upper  $\alpha$  helix is closer to the  $\alpha_3\beta_3$  subcomplex, extending into the solvent. This interpretation of the yeast electron density is in general agreement with a previous model of the *E. coli*  $F_1c$  complex (56) and with cross-linking studies (57), although it cannot explain cross linking between the *E. coli*  $\epsilon$  subunit and the DELSEED region of a  $\beta$  subunit (9).

The electron densities of individual c subunits show that they consist of two  $\alpha$  helices, linked by a loop. There is no interpretable side chain density, and the density could not be improved by modeling the subunits as polyaniline or by averaging. Therefore, it is not yet possible to build an unambiguous atomic model. The electron density is consistent with the NMR structure of the *E. coli* monomer determined in a chloroform:methanol:water mixture (26) (PDB accession code 1a91). Although the overall shape of the *E. coli* and the yeast c monomers is similar, the *E. coli* structure is not a perfect match to the yeast density (Fig. 2B). This could be due to the low sequence conservation (23% identity)

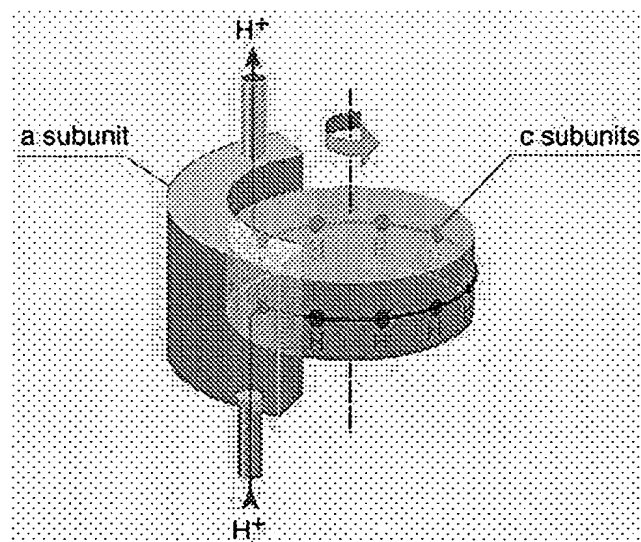


Fig. 1. Hypothetical model for the generation of rotation by proton transport through the  $F_0$  domain of ATP synthase [according to Junge (33)]. The central cylinder (blue) consists of c subunits; the external part (green) corresponds to a single a subunit. The red line indicates the proton path. [Reproduced with kind permission of the Swedish Academy of Sciences.]

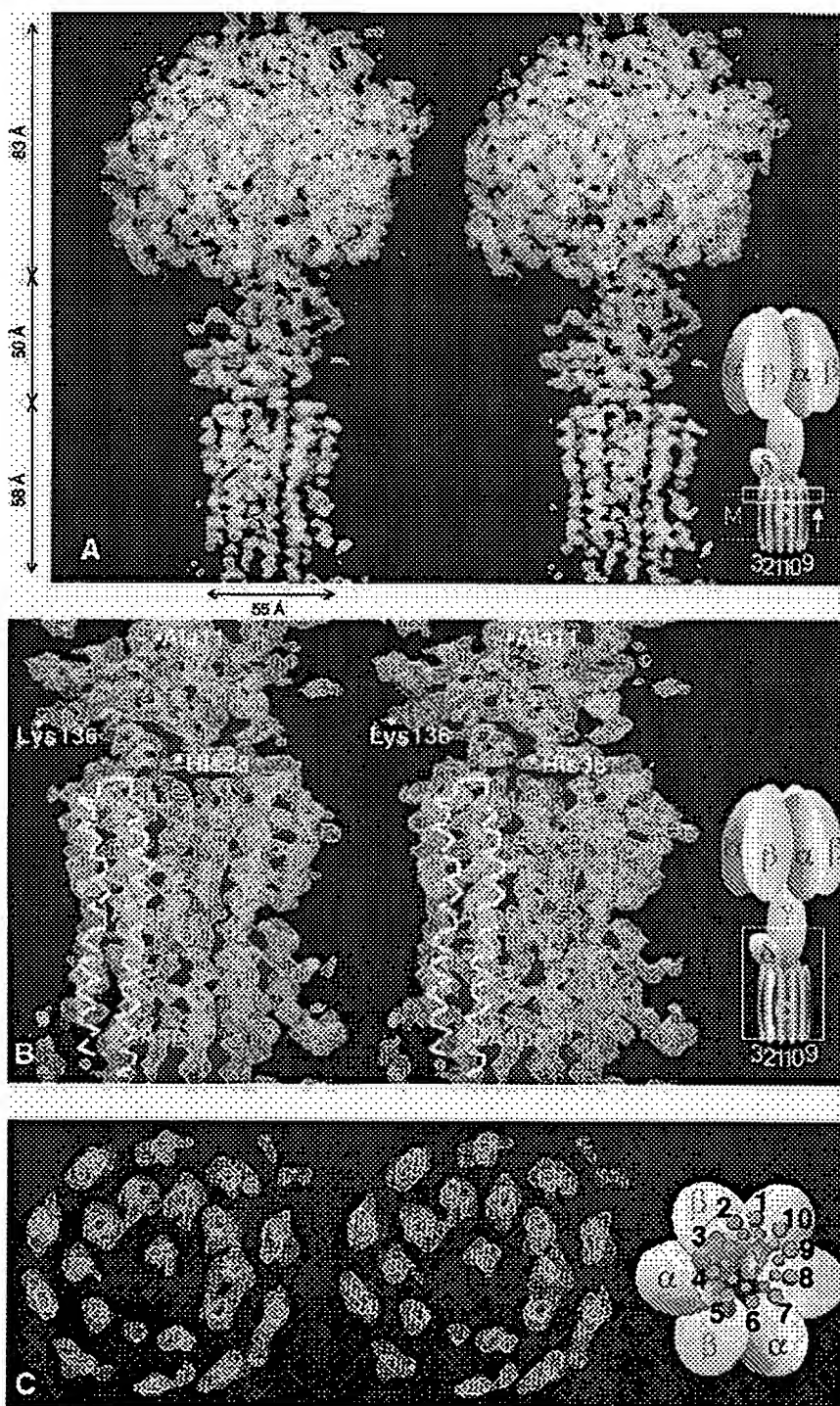
# RESEARCH ARTICLES

between the two species, or it could, at least in part, arise from the contacts between neighboring protomers. The 10 c protomers are packed tightly against each other, forming two rings of single  $\alpha$  helices (see Fig. 2C). The outer  $\alpha$  helices are kinked in the middle, making the cylindrical outer surface of the oligomer slightly concave. Despite the absence of clear side chain density, it is possible to assign the  $\alpha$

helices forming the inner and outer rings to the  $\text{NH}_2$ -terminal and  $\text{COOH}$ -terminal regions, respectively, as follows. Cysteine residues introduced at positions 40, 42, and 44 of the *E. coli* c subunit (equivalent to 38, 40, and 42 in yeast) can be cross linked to the  $\epsilon$  subunit in the *E. coli* enzyme and are therefore thought to lie in the polar loop between the two  $\alpha$  helices (57). The density for the inner  $\alpha$  helix is 58 Å long and

would accommodate 39 residues in an  $\alpha$ -helical conformation, consistent with residues 40 to 44 forming the polar loop. The density for the outer  $\alpha$  helix is 47 Å long. This would accommodate 31 residues in an  $\alpha$ -helical conformation, which is in excellent agreement with the total of 76 residues in the yeast c subunit. The kink of about  $23^\circ$  in the  $\text{COOH}$ -terminal  $\alpha$  helix is around Gly<sup>62</sup> (equivalent to Pro<sup>64</sup> in *E.*

**Fig. 2.** Stereo views of an electron density map of the yeast  $\text{F}_1\text{F}_0$  complex. The solvent flattened map was calculated at 3.9 Å resolution and contoured at 1.5  $\sigma$ . (A) Side view containing the bovine  $\text{F}_1$   $\text{C}\alpha$  model (with  $\alpha$  in orange,  $\beta$  in yellow, and  $\gamma$  in green). The density of symmetry-related molecules in the crystal is masked out. The inset indicates the location of the subunits within the complex. The location of the section shown in (C) is indicated by the white box; the direction of the view is indicated by the arrow. The presumed membrane region (M) (2) is marked by the two dotted lines. The c subunits are numbered 3, 2, 1, 10, and 9 (the best ordered c subunit was chosen as number 1). The overall height of the complex is  $\sim 190$  Å, of which the  $\alpha_3\beta_3$  subcomplex accounts for 83 Å, the stalk for 50 Å, and the c subunits for 58 Å. (B) Enlarged view of the  $\delta/\gamma$ -c contact region with the model (and numbering) of the *E. coli*  $\epsilon$  subunit (in red) and the *E. coli* c subunit (in white) fitted into the density, contoured at 1.0  $\sigma$ . The white box in the inset indicates the location of the displayed section within the complex. (C) End-on view of the density of the c ring. The inset shows the location of the  $\alpha$ ,  $\beta$ ,  $\gamma$ , and  $\delta$  subunits in relation to the c subunits. The helices of the c subunit are drawn as blue circles, the larger outer circles accounting for the larger side chains in the  $\text{COOH}$ -terminal helix. The outer diameter of the c ring is 55 Å (top) to 42 Å (equator) to 45 Å (bottom), and the inner diameter is 27 Å (top) to 17 Å (equator) to 22 Å (bottom). The dimensions exclude consideration of unresolved regions of density, including amino acid side chains and detergent or lipid molecules. The two regions of density near subunit 10 are not extensive and are likely to be noise.



# RESEARCH ARTICLES

*coli*). This arrangement would also place the glycine/alanine-rich NH<sub>2</sub>-terminal  $\alpha$  helix in the inner ring and accommodate the larger side chains of the COOH-terminal  $\alpha$  helix in the outer ring. Because of the lack of side chain density, the conserved carboxylate (Glu<sup>59</sup>) cannot be placed with certainty, but it would lie about halfway along the outer COOH-terminal  $\alpha$  helix. The resulting model shares many features in common with that proposed for the *E. coli* ring of c subunits (58), except that the latter contains 12 rather than 10 copies. It differs from an alternative model (59, 60), which placed the NH<sub>2</sub>-terminal helices on the outside. A model for the c subunit of the sodium-driven enzyme from *Propionigenium modestum* based on NMR data consists of four distinct  $\alpha$ -helical segments with the conserved carboxylate located near the cytoplasmic membrane surface (61). There is no evidence for four distinct  $\alpha$  helices in the yeast density, and the conserved carboxylate would appear to lie more centrally within the membrane, although the position of the

membrane boundary cannot be defined with certainty.

The 10 c subunits form an almost symmetrical ring, although the density for subunits 6, 7, and 8 is weaker, as seen from the asymmetrical appearance of the electron density (Fig. 2C). The central cavity of the c oligomer contains a region of elongated electron density, which is stronger in the upper and lower thirds of the cylinder than in the center (Fig. 2C). The origin of this density is not clear, but the need to maintain a semipermeable membrane *in vivo* suggests that the cavity might be filled with phospholipid.

The polar loop regions of five of the c subunits (c1 to c5) are covered by the  $\delta$  subunit (Fig. 2B). Two loops (c2 and c3) are in intimate contact, probably involving hydrogen bonds between pairs of main chain atoms, and another three (c1, c4, and c5) could form side chain contacts to either the  $\beta$  barrel of the  $\delta$  subunit or the lower of its two  $\alpha$  helices. The  $\gamma$  subunit probably makes side chain contacts to one or

two further c subunits (c9 and c10) and to one subunit (c1) that is also in contact with the  $\beta$  barrel of the  $\delta$  subunit. Therefore, six or seven consecutive c subunits or about two-thirds of the top surface of the ring are in contact with the foot of the stalk. These c subunits are much better defined in the electron density than the exposed ones, in which the density is weaker and discontinuous. The 62 residues of the yeast  $\epsilon$  subunit could not be assigned unambiguously to the density, and about 100 residues of the  $\gamma$  subunit remain unassigned, although there is extensive uninterpreted electron density both on top of the  $\delta$  subunit and next to the COOH-terminal  $\alpha$  helix of  $\gamma$ .

The extent of the interface between the c subunits and the  $\gamma$  and  $\epsilon$  subunits apparent in the electron density map of the yeast F<sub>1</sub>c<sub>10</sub> oligomer supports the hypothesis that the complex consisting of the  $\gamma$ ,  $\delta$  (*E. coli*  $\epsilon$ ),  $\epsilon$ , and c subunits rotates as an ensemble during catalysis, but other interpretations are still possible.

**Functional implications of the c ring stoichiometry.** An unexpected feature of the electron density map is that the ring of c subunits contains 10 protomers and not, as widely anticipated, 12 (21–23, 58–60). At this stage of the analysis, it is possible that some c subunits have been lost from the ring during crystallization. However, the extent of the interaction between adjacent c subunits within the ring makes this unlikely, particularly as there is no evidence to suggest a strong association between subunit c and any of the other components of F<sub>0</sub>. In addition, it is likely that the crystal contact between the ring of c subunits and the pseudo-three-fold F<sub>1</sub> domain would have selected for a population of complexes with 12 c subunits, if present. In consequence, the three-fold symmetry of the F<sub>1</sub> sector and the 10-fold symmetry of the c ring within one complex do not match. The principle of symmetry mismatch in

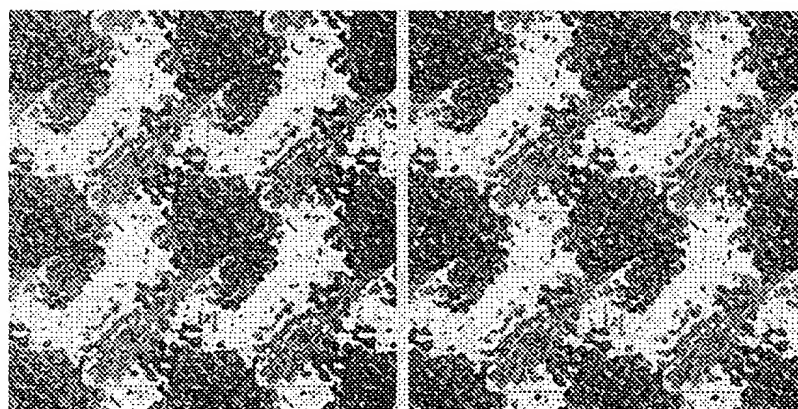


**Fig. 3.** Stereo view of the crystal packing of the yeast F<sub>1</sub>c<sub>10</sub> complex. A 45 Å thick section through the crystal perpendicular to the crystallographic y axis is shown. The electron density is contoured at 1.2  $\sigma$ . The red lines mark the x and z axes of the crystal lattice. All figures were prepared with the program MAIN (72).

**Table 1.** Statistics of data collection and structure determination. For data collection, the crystals were harvested in a buffer containing 20% glycerol as cryo-protectant and then frozen rapidly in liquid nitrogen. The crystals are small (up to 150  $\mu$ m in the largest dimension) and diffract x-rays weakly. They belong to the monoclinic space group P2<sub>1</sub> with unit cell dimensions  $a = 135.9$  Å,  $b = 175.3$  Å,  $c = 139.2$  Å, and  $\beta = 91.6^\circ$ . Assuming one F<sub>1</sub>c<sub>10</sub>

complex with 453.2 kD per asymmetric unit, the estimated solvent content is 66%. A data set was collected to 3.6 Å resolution at beamline ID02B ( $\lambda = 0.99$  Å), at the ESRF, Grenoble, France, with a Mar Research image plate detector (1600 pixel mode). The data were processed with MOSFLM (73) and SCALA/CCP4 (54). Because of anisotropic diffraction and slight radiation damage, the final data set was restricted to 3.9 Å resolution.

Resolution shell (Å)	12.33	8.72	7.12	6.17	5.52	5.03	4.66	4.36	4.11	3.90	Overall (15–3.9)
Number of observations	1343	3207	4159	4934	5600	6229	6765	7312	7756	8288	55593
Completeness (%)	69.8	92.2	92.8	93.3	93.5	94.1	94.1	94.8	94.5	95.5	93.3
$R_{\text{merge}}^*$ (%)	5.8	5.6	6.7	8.7	10.4	11.9	12.0	14.3	22.1	37.2	10.0
$I/\sigma$	7.2	6.6	7.4	6.7	6.3	5.5	5.4	4.7	3.3	1.3	4.0
Resolution range	15.0–5.0 Å										
Molecular replacement correlation coefficient	54.1 (44.0)†										
Molecular replacement R factor (%)‡	46.7 (50.6)										

\* $R_{\text{merge}} = \sum_h \sum_i |I_{h,i} - \langle I_h \rangle| / \sum_h \sum_i I_{h,i}$  where  $I_{h,i}$  is the intensity value of the  $i$ th measurement of  $h$  and  $\langle I_h \rangle$  is the corresponding mean value of  $h$  for all  $i$  measurements of  $h$ . The summation runs over all measurements. †Values for the second highest solution are given in parentheses. ‡R factor:  $\sum |F_{\text{obs}}| - |F_{\text{calc}}| / \sum |F_{\text{obs}}|$ , where  $F_{\text{obs}}$  and  $F_{\text{calc}}$  are the observed and calculated structure factor amplitudes, respectively.

# RESEARCH ARTICLES

molecular rotary engines has been discussed in relation to the DNA translocating machinery of bacteriophages (62, 63). During phage assembly, DNA is injected through the sixfold symmetrical tail into its head (fivefold symmetry axis of an icosahedron). The dodecameric head-tail connector is believed to rotate with respect to the head during DNA packaging (64). The symmetry mismatch between the head and the connector is thought to facilitate rotation by avoiding deeper energy minima that would accompany matching symmetries. Symmetry mismatch also appears to be important in the bacterial flagellar motor, which, similar to ATP synthase, is driven by the proton-motive force (65). A further example of symmetry mismatch is found in some ATP-dependent proteases (66), where a rotational mechanism has been suggested to contribute to protein unfolding. The arrangement of the components of the molecular motor in ATP synthase is rather different than that in either the bacteriophage or ATP-dependent proteases. In the latter cases, there are direct interactions between two rings of subunits with different symmetries. In the ATP synthase, there are two quite distinct regions of interaction. The first, in  $F_1$ , involves the  $\gamma$  subunit and the  $\alpha_3\beta_3$  subcomplex, whereas the second, in  $F_0$ , involves the ring of c subunits and the a subunit.

The number of c subunits in the ring has profound implications for the number of protons translocated by  $F_0$  for each ATP molecule synthesized in  $F_1$ . Each ATP synthetic event requires that the  $\gamma$  subunit rotates through  $120^\circ$ . This rotation is generated in  $F_0$  either by rotation of the c ring with  $\gamma$  (as the  $F_1c_{10}$  structure appears to indicate) or by some other mechanism in which the c subunits impart rotation to  $\gamma$  without themselves rotating. A c stoichiometry of 9 or 12 has been considered to require translocation of three or four protons per ATP synthesized to impart a  $120^\circ$  rotation to the c ring (see Fig. 1). A ring with 10 c subunits in it suggests that the  $H^+$ /ATP ratio is probably nonintegral and that its value lies between 3 and 4. Many of the experimentally measured  $H^+$ /ATP ratios lie in this range (34, 35).

Assuming that the c ring and  $\gamma$  subunit rotate as an ensemble, a nonintegral  $H^+$ /ATP ratio also makes it more likely that there is some degree of elasticity in the  $\gamma$  subunit itself, so that the stepping of the c ring (10 steps per rotation) can be matched to the stepping in  $F_1$  (three steps per rotation). Elasticity in the  $\gamma$  subunit is an explicit feature of two models for ATP synthase (67, 68), whereas in a third model (69) it is not required.

It has been suggested that the number of c subunits in *E. coli* varies depending on the carbon source (70, 71). More c subunits appear to be assembled into the complex if cells are grown in glucose than with succinate. Therefore, in the latter case, the c ring would be

smaller with an accompanying reduced gearing ratio. Changing gears and therefore the membrane potential required for ATP synthesis could be a regulatory mechanism. A variable number of c subunits could also explain the observation that covalently linked trimers of *E. coli* c subunit can form an active complex (22).

The electron density shown here provides direct proof that c protomers form a ring that is in close contact with the  $\gamma$  and  $\delta$  subunits. Our interpretation is consistent with previous ones, in which subunits  $\gamma$ ,  $\delta$ , and  $\epsilon$  form a rotating ensemble. It strongly supports the idea that the c oligomer is part of a rotary motor, converting electrochemical energy into chemical energy stored in ATP. To understand the mechanism of the generation of rotation, it will be necessary to establish the nature of the interaction between the c subunit oligomer found here and the remaining subunits in  $F_0$ .

## References and Notes

- P. D. Boyer, *Annu. Rev. Biochem.* **66**, 717 (1997).
- R. H. Fillingame, *Bacteria* **12**, 345 (1990).
- A. E. Senior, *Annu. Rev. Biophys. Biophys. Chem.* **19**, 7 (1990).
- J. P. Abrahams, A. G. W. Leslie, R. Lutter, J. E. Walker, *Nature* **370**, 621 (1994).
- S. D. Watts, C. L. Tang, R. A. Capaldi, *J. Biol. Chem.* **271**, 28341 (1996).
- S. D. Watts, Y. Zhang, R. H. Fillingame, R. A. Capaldi, *FEBS Lett.* **368**, 235 (1995).
- K. Sawada, H. Watanabe, C. Moritani-Otsuka, H. Kanazawa, *Arch. Biochem. Biophys.* **348**, 183 (1997).
- G. B. Cox et al., *J. Mol. Biol.* **229**, 1159 (1993).
- R. Aggeler, M. A. Haughton, R. A. Capaldi, *J. Biol. Chem.* **270**, 9185 (1995).
- G. L. Orriss et al., *Biochem. J.* **314**, 695 (1996).
- H. Noji, R. Yasuda, M. Yoshida, K. Kinoshita, *Nature* **386**, 299 (1997).
- Y. Kato-Yamada, H. Noji, R. Yasuda, K. Kinoshita, M. Yoshida, *J. Biol. Chem.* **273**, 19375 (1998).
- P. D. Boyer, *Biochim. Biophys. Acta* **1140**, 215 (1993).
- J. P. Abrahams et al., *Proc. Natl. Acad. Sci. U.S.A.* **93**, 9420 (1996).
- M. Van Raaij, J. P. Abrahams, A. G. W. Leslie, J. E. Walker, *Proc. Natl. Acad. Sci. U.S.A.* **93**, 6913 (1996).
- G. L. Orriss, A. G. W. Leslie, K. Braig, J. E. Walker, *Structure* **6**, 831 (1998).
- M. A. Bianchet, J. Hüllihen, P. L. Pedersen, L. M. Amzel, *Proc. Natl. Acad. Sci. U.S.A.* **95**, 11065 (1998).
- Y. Shirakihara et al., *Structure* **5**, 825 (1997).
- D. L. Foster and R. H. Fillingame, *J. Biol. Chem.* **257**, 2009 (1982).
- R. H. Fillingame, P. C. Jones, W. Jiang, F. I. Valiyaveetil, O. Y. Dmitriev, *Biochim. Biophys. Acta* **1365**, 135 (1998).
- P. C. Jones, W. Jiang, R. H. Fillingame, *J. Biol. Chem.* **273**, 17178 (1998).
- P. C. Jones and R. H. Fillingame, *J. Biol. Chem.* **273**, 29701 (1998).
- C. Ruppert et al., *J. Biol. Chem.* **274**, 25281 (1999).
- F. I. Valiyaveetil and R. H. Fillingame, *J. Biol. Chem.* **272**, 32635 (1997).
- R. J. Devenish et al., *Ann. N.Y. Acad. Sci.* **671**, 403 (1992).
- M. E. Givrin, V. K. Rastogi, F. Abildgaard, J. L. Markley, R. H. Fillingame, *Biochemistry* **37**, 8817 (1998).
- W. P. Jiang and R. H. Fillingame, *Proc. Natl. Acad. Sci. U.S.A.* **95**, 6607 (1998).
- G. Kaim, U. Matthey, P. Dimroth, *EMBO J.* **17**, 688 (1998).
- S. B. Vik, A. R. Patterson, B. J. Antonio, *J. Biol. Chem.* **273**, 16229 (1998).
- K. Takeyasu et al., *FEBS Lett.* **392**, 110 (1996).
- S. Singh, P. Turina, C. J. Bustamante, D. J. Keller, R. Capaldi, *FEBS Lett.* **397**, 30 (1996).
- R. H. Fillingame, *Biochim. Biophys. Acta* **1101**, 240 (1992).
- W. Junge, H. Lill, S. Engelbrecht, *Trends Biochem. Sci.* **22**, 420 (1997).
- D. G. Nicholls and S. J. Ferguson, *Bioenergetics 2* (Academic Press, London, 1992).
- S. Berry and B. Rumberg, *Biochim. Biophys. Acta* **1276**, 51 (1996).
- J. E. Walker, *Angew. Chem.* **37**, 2308 (1998).
- I. R. Collinson et al., *J. Mol. Biol.* **242**, 408 (1994).
- S. Engelbrecht and W. Junge, *FEBS Lett.* **414**, 485 (1997).
- S. Wilkens and R. A. Capaldi, *Nature* **393**, 29 (1998).
- B. Böttcher, L. Schwarz, P. Gräber, *J. Mol. Biol.* **281**, 757 (1998).
- S. Karrasch and J. E. Walker, *J. Mol. Biol.* **290**, 379 (1999).
- A portion (100 g) of a block of commercial baker's yeast (*S. cerevisiae*) was suspended in 250 ml of buffer containing 20 mM Tris (pH 8.0), 1 mM ethylenediaminetetraacetic acid, 1 mM dithiothreitol (DTT), 0.5 M D-sorbitol, 0.001% phenylmethylsulfonyl fluoride (PMSF), and 2.5 ml of protease inhibitor cocktail (Sigma, catalog number P-8215). Cells were broken in a bead beater (Biospec) by four treatments each of 1-min duration. Cell debris was removed by centrifugation several times at 1500g, and mitochondria were collected by centrifugation for 1 hour at 24,000g. The mitochondrial pellet was resuspended in 250 ml of buffer A [20 mM Tris (pH 8.0), 50 mM trehalose, 10% glycerol, 2 mM magnesium chloride, 1 mM ethylenediaminetetraacetic acid, 0.001% PMSF, 0.1% dodecylmaltoside, 1 mM DTT, and 0.02% sodium azide]. Protease inhibitor cocktail (2.5 ml, Sigma), deoxyribonuclease I (100 mg, Sigma), and dodecylmaltoside (2.5 g, Sigma) were added. Insoluble material was removed by centrifugation (1 hour, 142,000g), and the supernatant was applied to a 70-ml Q-Sepharose column. ATP synthase was eluted in a step gradient from 140 to 200 mM sodium chloride in buffer A. The concentrated enzyme was applied to a Sephacryl 300 column (320 ml, equilibrated in buffer A, 100 mM sodium chloride). Fractions containing ATP synthase (~20 mg typical yield) were pooled and concentrated to a protein concentration of 10 mg/ml. Disruption of the cells and all steps of the purification were performed at 4°C. Crystals were grown at 4°C under paraffin oil by the microbatch method by adding 2  $\mu$ l of buffer containing 0.1 M Tris (pH 8.0), 12% polyethylene glycol 6000, 150 mM sodium chloride, 1 mM AMP-PNP, 40  $\mu$ M ADP, 1 mM DTT, and 0.02% sodium azide to 2  $\mu$ l of protein solution.
- M. Bateson, R. J. Devenish, P. Nagley, M. Prescott, *J. Biol. Chem.* **274**, 7462 (1999).
- M. Prescott et al., *FEBS Lett.* **411**, 97 (1997).
- C. Spannagel, J. Vaillier, G. Arselin, P. V. Graves, J. Velours, *Eur. J. Biochem.* **247**, 1111 (1997).
- G. Arselin, J. Vaillier, P. V. Graves, J. Velours, *J. Biol. Chem.* **271**, 20284 (1996).
- I. Arnold, K. Pfeiffer, W. Neupert, R. A. Stuart, H. Schagger, *EMBO J.* **17**, 7170 (1998).
- R. H. P. Law, S. Manon, R. J. Devenish, P. Nagley, *Methods Enzymol.* **260**, 133 (1995).
- M. Bateson, R. J. Devenish, P. Nagley, M. Prescott, *Anal. Biochem.* **238**, 14 (1996).
- N. E. Chayen, P. D. S. Stewart, D. M. Blow, *J. Crystal Growth* **122**, 176 (1992).
- C. M. Wetzel and R. E. McCarty, *Plant Physiol.* **102**, 241 (1993).
- J. Navaza, *Acta Crystallogr. Sect. A* **50**, 157 (1994).
- J. P. Abrahams and A. G. W. Leslie, *Acta Crystallogr. Sect. D* **52**, 30 (1996).
- Collaborative Computational Project Number 4, *Acta Crystallogr. Sect. D* **50**, 760 (1994).
- H. Michel, *Trends Biochem. Sci.* **8**, 56 (1983).
- U. Uhlin, G. B. Cox, J. M. Guss, *Structure* **5**, 1219 (1997).
- J. Hermolin, O. Y. Dmitriev, Y. Zhang, R. H. Fillingame, *J. Biol. Chem.* **274**, 17011 (1999).
- O. Y. Dmitriev, P. C. Jones, R. H. Fillingame, *Proc. Natl. Acad. Sci. U.S.A.* **96**, 7785 (1999).
- G. Groth and J. E. Walker, *FEBS Lett.* **410**, 117 (1997).
- G. Groth, Y. Tilg, K. Schirwitz, *J. Mol. Biol.* **281**, 49 (1998).
- U. Matthey, G. Kaim, D. Braun, K. Wüthrich, P. Dimroth, *Eur. J. Biochem.* **261**, 459 (1999).

62. R. W. Hendrix, *Proc. Natl. Acad. Sci. U.S.A.* **75**, 4779 (1978).  
 63. ———, *Cell* **94**, 147 (1998).  
 64. J. M. Valpuesta, J. J. Fernandez, J. M. Carazo, J. L. Carrascosa, *Structure* **7**, 289 (1999).  
 65. D. R. Thomas, D. G. Morgan, D. J. DeRosier, *Proc. Natl. Acad. Sci. U.S.A.* **96**, 10134 (1999).  
 66. F. Beuron et al., *J. Struct. Biol.* **123**, 248 (1998).  
 67. D. A. Cherepanov, A. Y. Mulkidjanian, W. Junge, *FEBS Lett.* **449**, 1 (1999).  
 68. O. Pänke and B. Rumberg, *Biochim. Biophys. Acta* **1412**, 118 (1999).

69. T. Elston, H. Y. Wang, G. Oster, *Nature* **391**, 510 (1998).  
 70. R. A. Schemidt, J. Qu, J. R. Williams, W. S. A. Brusilow, *J. Bacteriol.* **180**, 3205 (1998).  
 71. R. A. Schemidt, D. K. W. Hsu, G. Deckers-Hebestreit, K. Altendorf, W. S. A. Brusilow, *Arch. Biochem. Biophys.* **323**, 423 (1995).  
 72. D. Turk, thesis, Technische Universität München, Munich, Germany (1992).  
 73. A. G. W. Leslie, *Joint CCP4 and ESF-EACMB Newsletter Protein Crystallography* (Daresbury Laboratory, Warrington, UK, 1992).

74. We thank R. Henderson for comments on the manuscript, S. Y. Peak-Chew and L. M. Fearnley for NH<sub>2</sub>-terminal sequencing and HPLC analysis, and the staff of beamline ID02B at European Synchrotron Radiation Facility (ESRF), Grenoble, for help with data collection. D.S. was supported during part of this work by an European Molecular Biology Organization Fellowship. The coordinates of an unrefined Ca model based on the bovine F<sub>1</sub> (1bmff) and the *E. coli* c (1a91) and *e* (1aqt) coordinates have been deposited in the Protein Data Bank (accession code 1qo1).

27 September 1999; accepted 1 November 1999

## First-Principles Determination of Elastic Anisotropy and Wave Velocities of MgO at Lower Mantle Conditions

B. B. Karki,<sup>1</sup> R. M. Wentzcovitch,<sup>1</sup> S. de Gironcoli,<sup>2</sup> S. Baroni<sup>2</sup>

The individual elastic constants of magnesium oxide (MgO) have been determined throughout Earth's lower mantle (LM) pressure-temperature regime with density functional perturbation theory. It is shown that temperature effects on seismic observables (density, velocities, and anisotropy) are monotonically suppressed with increasing pressure. Therefore, at realistic LM conditions, the isotropic wave velocities of MgO remain comparable to seismic velocities, as previously noticed in athermal high-pressure calculations. Also, the predicted strong pressure-induced anisotropy is preserved toward the bottom of the LM, so lattice-preferred orientations in MgO may contribute substantially to the observed seismic anisotropy in the D'' layer.

The last few years have seen rapid progress in our understanding of the behavior of the major mineral phases of Earth's mantle. Recent advances in theory and computation have made it possible to predict from first principles the structural and elastic properties of these materials throughout the entire pressure regime of the mantle (1). Experimental studies are now also possible over considerable ranges of pressure (*P*) and temperature (*T*) (2–5). However, the challenge of experimentally or theoretically determining the mineral properties at simultaneous *P* and *T* conditions of geophysical magnitudes is still enormous. Such studies will provide the basis for an improved analytical treatment of fundamental issues in Earth sciences, such as (i) constraining the mineralogy of the deep interior by directly comparing the seismic velocities (6) with predicted velocities for various mineral aggregates; (ii) describing Earth's thermal state by distinguishing thermal versus compositional effects on wave velocities; and (iii) understanding the sources of seismic anisotropies such as

those observed at D'' (7). It has been suggested that mantle flow and the accompanying stress field (in the vicinity of boundaries) could align crystalline axes along preferred directions and create anisotropic fabrics carrying the signature of the flow pattern (8).

The possibility of calculating with high accuracy and computational efficiency the entire vibrational spectrum of a crystal with the use of density functional perturbation theory (9) allows us to determine from first principles the crystal free energy,  $F(V, T)$ , from which we can extract all measurable thermodynamic quantities for the mineral, including the elastic moduli. Here we chose to start with the pressure and temperature dependence of the elastic constants of MgO (10), which exists as (Mg<sub>0.8</sub>Fe<sub>0.2</sub>)O-magnesiowüstite in the lower mantle (LM) with 20 to 30% abundance according to a typical pyrolytic model (11). A previous first principles study of high-pressure (athermal) elasticity (12) showed that MgO is strongly anisotropic at D'' pressures (125 to 135 GPa) and its wave velocities are higher than seismic velocities throughout the LM pressure regime (23 to 135 GPa). Although *T*-induced effects at ambient *P* or so are known to be substantial and to counteract those of pressure

(4, 5), the effects at high *P*'s are unknown.

The results presented below were obtained within the quasi-harmonic approximation (QHA). It is a good approximation for MgO at ambient *P* up to  $\approx 1000$  K (13), as can be seen by comparing calculated and measured thermal expansivities,  $\alpha$  (14) (see Fig. 1). The deviation of  $\alpha$  from linearity at ambient *P* and high *T*'s is related to the inadequacy of the QHA and can be traced back to the behavior of the mode Grüneisen parameters with volume (15). The agreement with experiments at about 1800 K and 180 GPa (16), as well as the predicted linear behavior at high *P*'s and *T*'s, indicate that the QHA is valid at geophysically relevant conditions.

The adiabatic elastic constants ( $c_{11}$ ,  $c_{12}$ , and  $c_{44}$ ) were obtained as a function of *P* and *T* to 150 GPa and 3000 K, respectively, by calculating the free energies for the strained lattices (17). The predicted ambient values and their initial pressure (at 300 K) and temperature (at 0 GPa) dependencies agree with

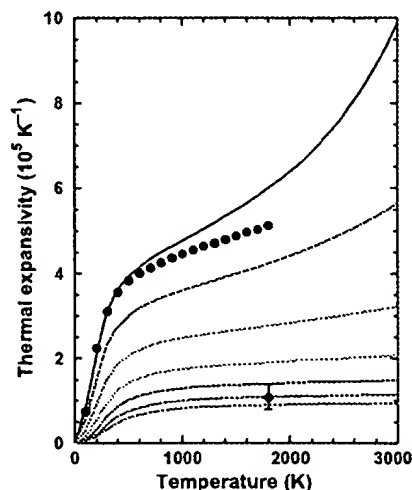


Fig. 1. Temperature dependence of thermal expansivity of MgO along several isobars at 0, 10, 30, 60, 100, 150, and 200 GPa (solid lines from top to bottom). The experimental data at zero pressure (14) are denoted by circles. The average value of  $\alpha$  between 300 and  $\sim 3300$  K at 169 to 196 GPa derived from shock-wave experiments (16) is denoted by the diamond.

<sup>1</sup>Department of Chemical Engineering and Materials Science, Minnesota Supercomputing Institute, University of Minnesota, Minneapolis, MN 55455, USA.

<sup>2</sup>Scuola Internazionale Superiore di Studi Avanzati (SISSA), I-34014 Trieste, Italy.







My NC  
[Sign In] [Regis

All Databases PubMed Nucleotide Protein Genome Structure OMIM PMC Journals Book

Search PubMed for

Go Clear

Limits Preview/Index History Clipboard Details

Display Abstract Show 20 Sort by Send to

[About Entrez](#)[Text Version](#)

[Entrez PubMed](#)  
[Overview](#)  
[Help | FAQ](#)  
[Tutorial](#)  
[New/Noteworthy](#)  
[E-Utilities](#)

[PubMed Services](#)  
[Journals Database](#)  
[MeSH Database](#)  
[Single Citation Matcher](#)  
[Batch Citation Matcher](#)  
[Clinical Queries](#)  
[Special Queries](#)  
[LinkOut](#)  
[My NCBI \(Cubby\)](#)

[Related Resources](#)  
[Order Documents](#)  
[NLM Catalog](#)  
[NLM Gateway](#)  
[TOXNET](#)  
[Consumer Health](#)  
[Clinical Alerts](#)  
[ClinicalTrials.gov](#)  
[PubMed Central](#)

☐ 1: Novartis Found Symp. 1999;221:218-29; discussion 229-34.

[Related Articles](#)  
[Links](#)

## Proton ATPases in bacteria: comparison to Escherichia coli F1F0 as the prototype.

Fillingame RH, Divall S.

Department of Biomolecular Chemistry, University of Wisconsin Medical School, Madison 53706, USA.

The F1F0 ATP synthase complex of Escherichia coli functions reversibly in coupling proton translocation to ATP synthesis or hydrolysis. The structural organization and subunit composition corresponds to that seen in many other bacteria, i.e. a membrane extrinsic F1 sector with five subunits in an alpha 3 beta 3 gamma delta epsilon stoichiometry, and a membrane-traversing F0 sector with three subunits in an a1b2c12 stoichiometry. The structure of much of the F1 sector is known from a X-ray diffraction model. During function, The gamma subunit is known to rotate within a hexameric ring of alternating alpha and beta subunits to promote sequential substrate binding and product release from catalytic sites on the three beta subunits. Proton transport through F0 must be coupled to this rotation. Subunit c folds in the membrane as a hairpin to two alpha helices to generate the proton-binding site in F0. Its structure was determined by NMR, and the structure of the c oligomer was deduced by cross-linking experiments and molecular mechanics calculations. The implications of the oligomeric structure of subunit c will be considered and related to the H<sup>+</sup>/ATP pumping ratio, P/O ratios and the cation-binding site in other types of F0. The possible limits of the structure in changing the ion-binding specificity, stoichiometry and routes of proton entrance/exit to the binding site will be considered.

### Publication Types:

- Review
- Review, Tutorial

PMID: 10207922 [PubMed - indexed for MEDLINE]

Display  Show  Sort by  Send to

[Write to the Help Desk](#)

[NCBI](#) | [NLM](#) | [NIH](#)

[Department of Health & Human Services](#)

[Privacy Statement](#) | [Freedom of Information Act](#) | [Disclaimer](#)

May 2 2005 17:45:08

## Purification and Reconstitution into Proteoliposomes of the $F_1F_0$ ATP Synthase from the Obligately Anaerobic Gram-Positive Bacterium *Clostridium thermoautotrophicum*

AMARESH DAS, D. MACK IVEY,<sup>†</sup> AND LARS G. LJUNGDAHL\*

Center for Biological Resource Recovery and Department of Biochemistry and Molecular Biology,  
University of Georgia, Athens, Georgia 30602

Received 24 July 1996/Accepted 13 December 1996

The proton-translocating  $F_1F_0$  ATP synthase from *Clostridium thermoautotrophicum* was solubilized from cholate-washed membranes with Zwittergent 3-14 at 58°C and purified in the presence of octylglucoside by sucrose gradient centrifugation and ion-exchange chromatography on a DEAE-5PW column. The purified enzyme hydrolyzed ATP at a rate of  $12.6 \mu\text{mol min}^{-1} \text{mg}^{-1}$  at 58°C and pH 8.5. It was composed of six different polypeptides with molecular masses of 60, 50, 32, 19, 17, and 8 kDa. These were identified as  $\alpha$ ,  $\beta$ ,  $\gamma$ ,  $\delta$ ,  $\epsilon$ , and  $c$  subunits, respectively, as their N-terminal amino acid sequences matched the deduced N-terminal amino acid sequences of the corresponding genes of the *atp* operon sequenced from *Clostridium thermoautotrophicum* (GenBank accession no. U64318), demonstrating the close similarity of the  $F_1F_0$  complexes from *C. thermoautotrophicum* and *C. thermoacetatum*. Four of these subunits,  $\alpha$ ,  $\beta$ ,  $\gamma$ , and  $\epsilon$ , constituted the  $F_1$ -ATPase purified from the latter bacterium. The  $\delta$  subunit could not be found in the purified  $F_1$  although it was present in the  $F_1F_0$  complex, indicating that the  $F_0$  moiety consisted of the  $\delta$  and the  $c$  subunits and lacked the  $a$  and  $b$  subunits found in many aerobic bacteria. The  $c$  subunit was characterized as  $N,N'$ -dicyclohexylcarbodiimide reactive. The  $F_1F_0$  complex of *C. thermoautotrophicum* consisting of subunits  $\alpha$ ,  $\beta$ ,  $\gamma$ ,  $\delta$ ,  $\epsilon$ , and  $c$  was reconstituted with phospholipids into proteoliposomes which had ATP- $P_i$  exchange, carbonylcyanide  $p$ -trifluoromethoxyphenylhydrazone-stimulated ATPase, and ATP-dependent proton-pumping activities. Immunoblot analyses of the subunits of ATP synthases from *C. thermoautotrophicum*, *C. thermoacetatum*, and *Escherichia coli* revealed antigenic similarities among the  $F_1$  subunits from both clostridia and the  $\beta$  subunit of  $F_1$  from *E. coli*.

*Clostridium thermoautotrophicum* and *Clostridium thermoacetatum* are gram-positive, thermophilic, obligately anaerobic bacteria that can utilize and grow on various carbon sources including sugars (e.g., glucose, fructose, xylose) and one-carbon compounds (e.g.,  $\text{CO}_2/\text{H}_2$ , CO, and methanol) (11, 34, 46, 55, 57). They are also called homoacetogens because they produce acetate as the principal metabolic end product. Although isolated from different sources these two bacteria are virtually indistinguishable with respect to their physiology and metabolism (34, 55, 57), 16S rRNA sequence (3), and genomic DNA composition (55). A major feature of the acetogenic clostridia is that they synthesize acetate from  $\text{CO}_2$  by the reductive autotrophic acetyl-coenzyme A pathway (34, 35, 46, 56, 57). The acetyl-coenzyme A pathway does not yield any net gain of energy (ATP synthesis) at the substrate level. Thus, during autotrophic growth the acetogens must generate energy from electron transport-coupled phosphorylation. The presence of an electron transport chain and a proton-translocating  $F_1$ -ATPase and their involvement in the generation of proton motive force, ATP synthesis, and amino acid uptake have been demonstrated in membranes of acetogenic clostridia (8, 24–29, 35, 39).

Proton-translocating  $F_1F_0$  ATP synthases have been characterized from bacteria, chloroplasts, and mitochondria (15, 17, 21, 43, 49, 51). They have similar structures consisting of two

parts, a cytosolic or membrane-extrinsic  $F_1$  and a membrane-intrinsic  $F_0$ . The  $F_1$  part of the enzyme has the catalytic domain which is responsible for the synthesis and hydrolysis of ATP, and the  $F_0$  part translocates protons across the membranes during catalysis. In *Escherichia coli*, the  $F_1$  part has five subunits with a composition of  $\alpha_3\beta_3\gamma\delta\epsilon$ , and the  $F_0$  part has three subunits with a composition of  $a b_2 c_{10-12}$  (15). The five subunit structure of  $F_1$  is commonly found in bacteria, mitochondria, or chloroplasts (43) although only four subunits were found in the  $F_1$  of *C. thermoacetatum* (29). In contrast, significant variations have been observed in the structure of  $F_0$ . Thus the number of subunits found in the  $F_0$  of mitochondrial ATP synthases ranges from five to eight (43, 51), while that for chloroplast and cyanobacterial ATP synthases is four (43) and that for bacterial ATP synthases ranges from one to three (4, 5, 15, 47). Among anaerobic bacteria, the simplest subunit structure of  $F_0$  has been described for *Clostridium pasteurianum*, which is comprised of only one type of subunit (4, 5).

In this study we describe the purification and characterization of the  $F_1F_0$  ATP synthase from *C. thermoautotrophicum*. The purified enzyme contains the six subunits  $\alpha$ ,  $\beta$ ,  $\gamma$ ,  $\delta$ ,  $\epsilon$ , and  $c$ , of which the  $\alpha$ ,  $\beta$ ,  $\gamma$ , and  $\epsilon$  subunits constitute the  $F_1$ -ATPase. Although the  $a$  and  $b$  subunits found in many aerobic bacteria are missing, the clostridial ATP synthase is fully functional.

### MATERIALS AND METHODS

**Bacteria and growth conditions.** *C. thermoautotrophicum* JW 701/5 and *C. thermoacetatum* ATCC 39073 were grown on 0.5% (vol/vol) methanol or 1.0% (wt/vol) glucose as carbon source at 58°C under 100%  $\text{CO}_2$  (36, 37). *E. coli* TG1 was grown in a minimal medium as previously described (9) with 0.5% (wt/vol) ammonium succinate as the energy source. Cells from both cultures were harvested at mid-log phase (after 16 to 18 h of growth) and stored at  $-20^\circ\text{C}$  until used.

\* Corresponding author. Mailing address: Department of Biochemistry and Molecular Biology, A214 Life Sciences Bldg., University of Georgia, Athens, GA 30602-7229. Phone: (706) 542-7640. Fax: (706) 542-2222. E-mail: ljungdah@bscr.uga.edu.

<sup>†</sup> Present address: Department of Biological Sciences, University of Arkansas, Fayetteville, AR 72701.



## The ATP Synthase $\gamma$ Subunit

### SUPPRESSOR MUTAGENESIS REVEALS THREE HELICAL REGIONS INVOLVED IN ENERGY COUPLING\*

(Received for publication, February 9, 1995, and in revised form, March 20, 1995)

Robert K. Nakamoto† and Marwan K. Al-Shawi

From the Department of Molecular Physiology and Biological Physics, University of Virginia,  
Charlottesville, Virginia 22908

Masamitsu Futai

From the Institute for Scientific and Industrial Research, Osaka University, Ibaraki, Osaka 567, Japan

A role in coupling proton transport to catalysis of ATP synthesis has been demonstrated for the *Escherichia coli*  $F_0F_1$  ATP synthase  $\gamma$  subunit. Previously, functional interactions between the terminal regions that were important for coupling were shown by finding several mutations in the carboxyl-terminal region of the  $\gamma$  subunit (involving residues at positions 242 and 269–280) that restored efficient coupling to the mutation,  $\gamma$ Met-23  $\rightarrow$  Lys (Nakamoto, R. K., Maeda, M., and Futai, M. (1993) *J. Biol. Chem.* 268, 867–872). In this study, we used suppressor mutagenesis to establish that the terminal regions can be separated into three interacting segments. Second-site mutations that cause pseudo reversion of the primary mutations,  $\gamma$ Gln-269  $\rightarrow$  Glu or  $\gamma$ Thr-273  $\rightarrow$  Val, map to an amino-terminal segment with changes at residues 18, 34, and 35, and to a segment near the carboxyl terminus with changes at residues 236, 238, 242, and 246. Each second-site mutation suppressed the effects of both  $\gamma$ Gln-269  $\rightarrow$  Glu and  $\gamma$ Thr-273  $\rightarrow$  Val, and restored efficient coupling to enzyme complexes containing either of the primary mutations. Mapping of these residues in the recently reported x-ray crystallographic structure of the  $F_1$  complex (Abrahams, J. P., Leslie, A. G., Lutter, R., and Walker, J. E. (1994) *Nature* 370, 621–628), reveals that the second-site mutations do not directly interact with  $\gamma$ Gln-269 and  $\gamma$ Thr-273 and that the effect of suppression occurs at a distance. We propose that the three  $\gamma$  subunit segments defined by suppressor mutagenesis, residues  $\gamma$ 18–35,  $\gamma$ 236–246, and  $\gamma$ 269–280, constitute a domain that is critical for both catalytic function and energy coupling.

In the  $F_0F_1$  ATP synthase, energy coupling between proton transport and catalysis of ATP synthesis occurs via conformational changes transmitted through a complex made up of at least eight different subunits (for reviews see Refs. 1–7). A key subunit in the coupling mechanism is the  $\gamma$  subunit, which appears as a single copy in the complex. Changes in chemical cross-linking patterns (8–13), protease sensitivity (14), inten-

sities of fluorescence probes (15), and immunoelectron micrographic images (16) have demonstrated that the  $\gamma$  subunit undergoes conformation changes in response to catalysis or proton motive force. A structural model of bovine  $F_1$  based on x-ray diffraction verifies that the  $\gamma$  subunit has specific interactions with the  $\alpha$  and  $\beta$  subunits that contain the catalytic sites and suggests that these interactions may be critical for function (17).

Through the use of mutagenesis, we established that the conserved terminal regions of the  $\gamma$  subunit are involved in coupling. By changing conserved residue Met-23 of the *Escherichia coli*  $\gamma$  subunit (286 amino acids in length) to lysine, energy coupling was rendered extremely inefficient (18). Functional interactions between terminal regions were realized by identification of several second-site mutations near the carboxyl terminus that restored efficient coupling to the  $\gamma$ Met-23  $\rightarrow$  Lys mutant (19). Two such second-site mutations were the replacements,  $\gamma$ Gln-269  $\rightarrow$  Arg and  $\gamma$ Thr-273  $\rightarrow$  Ser. Other replacements of these two conserved residues invariably caused reduced turnover and coupling efficiency (20); the most severe mutations were  $\gamma$ Gln-269  $\rightarrow$  Glu and  $\gamma$ Thr-273  $\rightarrow$  Val. In this paper, we describe the identification of several intragenic second-site mutations that suppress  $\gamma$ Gln-269  $\rightarrow$  Glu and  $\gamma$ Thr-273  $\rightarrow$  Val. Taken together, the suppressor mutations reveal three  $\gamma$  subunit regions that functionally interact to mediate energy coupling.

#### EXPERIMENTAL PROCEDURES

**Materials**—Oligonucleotides were synthesized with a Pharmacia LKB Gene Assembler Plus. [ $\alpha$ - $^{32}$ P]dCTP (3000 Ci/mmol) and [ $^{32}$ P]P<sub>i</sub> were from Amersham Corp. Restriction endonucleases and other DNA modifying enzymes were from Takara Shuzo Co., Nippon Gene Co., Toyobo Co., or New England Biolabs. *Taq* polymerase and deoxynucleotides were from Perkin-Elmer. For all other chemicals and enzymes, the highest grades commercially available were used.

**Bacterial Strains, Plasmids, and Growth Conditions**—The  $\gamma$  subunit-deficient *E. coli* strain, KF10rA (*thi*, *thy*, *recA1*, *uncG10* (Gln-14  $\rightarrow$  end)), was described previously (21) and grown as before (20). Unless otherwise indicated, all strains were grown at 37 °C. To assure that mutations in chromosomal or plasmid-borne copies of *uncG* did not revert during an experiment, the phenotype of all strains were checked after growths and plasmids were isolated and sequenced. Expression and mutagenesis of *uncG* were performed in derivatives of plasmid pBMG15 (18).

**Random Mutagenesis, Selection of Pseudo Revertants, and Manipulation of pBMG15**—The  $\gamma$ Gln-269  $\rightarrow$  Glu and  $\gamma$ Thr-273  $\rightarrow$  Val mutations first described by Iwamoto *et al.* (20) were moved to plasmid pBMG15 to facilitate replacement of the entire *uncG* coding sequence with the randomly mutagenized gene as was done by Nakamoto *et al.* (19). *uncG* (Gln-269  $\rightarrow$  Glu or Thr-273  $\rightarrow$  Val) was randomly mutagenized using a modified polymerase chain reaction (19, 22). Transformation of KF10rA with mutagenized plasmids, genetic selection and analysis of isolates able to grow on succinate minimal medium (*suc*<sup>+</sup>)

\* This research was supported by Grant GM50957 from the National Institutes of Health (to R. K. N.) and grants from the Japan Society for the Promotion of Science (to R. K. N.), the Ministry of Education, Science and Culture of Japan (to M. F.), and the Human Frontiers in Science Program (to M. F.). The costs of publication of this article were defrayed in part by the payment of page charges. This article must therefore be hereby marked "advertisement" in accordance with 18 U.S.C. Section 1734 solely to indicate this fact.

† To whom correspondence should be addressed: Dept. of Molecular Physiology and Biological Physics, University of Virginia, Jordan Hall, Box 449, Charlottesville, VA 22908. Tel.: 804-982-0279; Fax: 804-982-1616; E-mail: rkn3c@virginia.edu.

were done as before (19).

To assure that no extraneous mutations accompanied the identified suppressor mutations, each suppressor mutation was isolated on a restriction fragment and ligated into the original pBMG15 (Gln-269  $\rightarrow$  Glu) and pBMG15 (Thr-273  $\rightarrow$  Val). Second-site mutations near the amino terminus were isolated on the *Nco*I to *Xba*I fragment, mutations between codons 233 and 246 were isolated on the *Rsa*II to *Pst*I fragment, and mutations of codon 269 were isolated on the *Pst*I to *Bgl*II fragment. Reconstructed plasmids were sequenced to assure both mutations were present.

Molecular biological manipulations (23) and DNA sequencing (24) were done by standard protocols.

**Biochemical Procedures**—Membrane vesicles were prepared from strains grown at 37 °C in minimal medium containing 0.2% glucose. Logarithmic phase cells were passed through a French press at 16,000 p.s.i. and membranes isolated by differential centrifugation as described previously (25). Protein (26), ATPase activity (25, 27), and ATP synthesis (28, 32) were assayed as described previously.

For immunoblotting, membrane proteins were prepared as described by Nakamoto *et al.* (29) and separated on a 12.5% SDS-polyacrylamide gel (30). Proteins were then transferred to nitrocellulose (31) and re-

acted with polyclonal antibodies raised against *E. coli* F<sub>1</sub>  $\alpha$  and  $\beta$  subunits (obtained from Dr. Alan Senior, University of Rochester) or the  $\gamma$  subunit. Immunoreactive bands were detected using the TMB membrane peroxidase system (Kirkegaard & Perry Laboratories, Inc.).

## RESULTS

**Suppression of  $\gamma$ Met-23  $\rightarrow$  Lys by Various Amino Acids at Positions 269 and 273 of the  $\gamma$  Subunit**—Previously, residues  $\gamma$ Gln-269 and  $\gamma$ Thr-273 were implicated in energy coupling because mutations  $\gamma$ Gln-269  $\rightarrow$  Arg and  $\gamma$ Thr-273  $\rightarrow$  Ser were able to suppress the effects of the primary mutation,  $\gamma$ Met-23  $\rightarrow$  Lys, and restored efficient energy coupling (19). Interestingly, a number of other mutations at these same positions also suppressed  $\gamma$ Met-23  $\rightarrow$  Lys and resulted in oxidative phosphorylation-dependent growth when succinate was used as the sole carbon source (*suc*<sup>+</sup>). In addition to the original suppressor mutations, replacement of  $\gamma$ Gln-269 with Leu and Glu, and  $\gamma$ Thr-273 with Gly and Val conferred intragenic suppression of  $\gamma$ Met-23  $\rightarrow$  Lys (Table I). Of these,  $\gamma$ Gln-269  $\rightarrow$  Glu and  $\gamma$ Thr-273  $\rightarrow$  Val were the most deleterious and, as single mutations, did not allow growth on solid succinate medium at 37 °C. Clearly, the suppression between either of these mutations and  $\gamma$ Met-23  $\rightarrow$  Lys was mutual. Similar to previously described mutations at these positions (19),  $\gamma$ Gln-269  $\rightarrow$  Glu and  $\gamma$ Thr-273  $\rightarrow$  Val mutant strains were temperature-sensitive and were able to grow on succinate at 30 °C.

**$\gamma$  Subunit Mutations That Suppress  $\gamma$ Gln-269  $\rightarrow$  Glu and  $\gamma$ Thr-273  $\rightarrow$  Val**—In turn, we searched for second-site mutations that would suppress the effects of  $\gamma$ Gln-269  $\rightarrow$  Glu and  $\gamma$ Thr-273  $\rightarrow$  Val. Random mutations were generated in *uncG* ( $\gamma$ Gln-269  $\rightarrow$  Glu or  $\gamma$ Thr-273  $\rightarrow$  Val) and screened for the ability to grow by oxidative phosphorylation. Twelve stable *suc*<sup>+</sup> colonies arose, and plasmids were isolated and sequenced. As listed in Table II, six different mutations that resulted in amino acid changes were found as single second-site mutations. Two other second-site mutations,  $\gamma$ Glu-233  $\rightarrow$  Gly and  $\gamma$ Ala-240  $\rightarrow$  Val, were accompanied by changes of  $\gamma$ Gln-269. Finally, two second-site mutations,  $\gamma$ Asp-36  $\rightarrow$  Gly and  $\gamma$ Met-246  $\rightarrow$  Leu, were found on the same plasmid with  $\gamma$ Thr-273  $\rightarrow$  Val. To

TABLE I  
Oxidative phosphorylation-dependent growth of  $\gamma$ Gln-269 and  $\gamma$ Thr-273 mutations with or without  $\gamma$ Met-23  $\rightarrow$  Lys

Mutation(s) <sup>a</sup>	Colony formation on solid succinate medium <sup>b</sup>	
	30 °C	37 °C
$\gamma$ Met-23 $\rightarrow$ Lys	+	—
$\gamma$ Gln-269 $\rightarrow$ Leu	+	+
$\gamma$ Met-23 $\rightarrow$ Lys/ $\gamma$ Gln-269 $\rightarrow$ Leu	+	+
$\gamma$ Gln-269 $\rightarrow$ Glu	+	—
$\gamma$ Met-23 $\rightarrow$ Lys/ $\gamma$ Gln-269 $\rightarrow$ Glu	+	+
$\gamma$ Thr-273 $\rightarrow$ Gly	+	+
$\gamma$ Met-23 $\rightarrow$ Lys/ $\gamma$ Thr-273 $\rightarrow$ Gly	+	+
$\gamma$ Thr-273 $\rightarrow$ Val	+	—
$\gamma$ Met-23 $\rightarrow$ Lys/ $\gamma$ Thr-273 $\rightarrow$ Val	+	+

<sup>a</sup> Mutations were harbored on plasmid pBMG15 and tested in strain KF10rA (see "Experimental Procedures").

<sup>b</sup> Colony formation on minimal plates containing 0.4% sodium succinate was judged 5 days after streaking and incubation at the stated temperature.

TABLE II  
Second-site mutations found in plasmid-borne *uncG* ( $\gamma$ Gln-269  $\rightarrow$  Glu or  $\gamma$ Thr-273  $\rightarrow$  Val)

Controls		Growth at 37 °C in liquid succinate medium		
		% of wild type		
Wild type		100 <sup>a</sup>		
<i>uncG</i> <sup>b</sup>		1.2		
$\gamma$ Gln-269 $\rightarrow$ Glu		2.9		
$\gamma$ Thr-273 $\rightarrow$ Val		4.4		
Second-site mutations	Codon change	Primary mutation in screening	Growth when combined with:	
			$\gamma$ Glu-269	$\gamma$ Val-273
$\gamma$ Lys-18 $\rightarrow$ Met	AAG $\rightarrow$ ATG	$\gamma$ Val-273	15	7.1
$\gamma$ Ser-34 $\rightarrow$ Leu	TCG $\rightarrow$ TTG	$\gamma$ Glu-269	24	16
$\gamma$ Gln-35 $\rightarrow$ Arg	CAG $\rightarrow$ CGG	$\gamma$ Val-273	19	15
$\gamma$ Glu-233 $\rightarrow$ Gly	GAA $\rightarrow$ GGA	$\gamma$ Glu-269 $\rightarrow$ Lys <sup>c</sup>	7.6	9.5
$\gamma$ Ala-236 $\rightarrow$ Thr	GCC $\rightarrow$ ACC	$\gamma$ Glu-269	58	63
$\gamma$ Glu-238 $\rightarrow$ Gly <sup>d</sup>	GAG $\rightarrow$ GGG	$\gamma$ Glu-269	51	63
		$\gamma$ Val-273		
$\gamma$ Ala-240 $\rightarrow$ Val	GCC $\rightarrow$ GTC	$\gamma$ Glu-269 $\rightarrow$ Gly <sup>c</sup>	3.6	3.1
$\gamma$ Arg-242 $\rightarrow$ His	CGT $\rightarrow$ CAT	$\gamma$ Val-273	25	61
$\gamma$ Asp-36 $\rightarrow$ Gly	GAT $\rightarrow$ GGT	$\gamma$ Val-273	ND <sup>e</sup>	ND
+ $\gamma$ Met-246 $\rightarrow$ Leu	ATG $\rightarrow$ CTG			
$\gamma$ Asp-36 $\rightarrow$ Gly			9.7	8.5
$\gamma$ Met-246 $\rightarrow$ Leu			19	49

<sup>a</sup> Growth at 37 °C in succinate minimal medium was followed as described under "Experimental Procedures." Strain KF10rA harboring wild-type *uncG* on plasmid pBWG15 grew to an optical density of 0.59 measured at a wavelength of 650 nm.

<sup>b</sup> No *uncG* on plasmid.

<sup>c</sup> This plasmid had the indicated change at position 269 in addition to the second-site mutation. The growth data is for the second-site mutation combined with the original primary mutation.

<sup>d</sup> Second-site mutation,  $\gamma$ Glu-238  $\rightarrow$  Gly, was found with both  $\gamma$ Glu-269 and  $\gamma$ Val-273.

<sup>e</sup> ND, not determined for the triple mutants  $\gamma$ Asp-36  $\rightarrow$  Gly/ $\gamma$ Met-246  $\rightarrow$  Leu/ $\gamma$ Glu-269 or  $\gamma$ Asp-36  $\rightarrow$  Gly/ $\gamma$ Met-246  $\rightarrow$  Leu/ $\gamma$ Val-273.

TABLE III  
 Activities of mutant  $F_0F_1$  in membrane vesicles from strains grown at 37 °C

Mutation	ATPase activity <sup>a</sup>	H <sup>+</sup> pumping <sup>b</sup>	ATP synthesis <sup>c</sup>	Coupling efficiency <sup>d</sup>
	$\mu\text{mol P}_i/\text{min}/\text{mg}$	% quenching relative to wild type	$\mu\text{mol ATP}/\text{min}/\text{mg}$	Synthesis/Hydrolysis
Wild type (pBWG15)	0.31	100	0.22	0.71
<i>uncG</i> <sup>-</sup> (pBR322)	0.042	5	0.00	
$\gamma\text{Gln-269} \rightarrow \text{Glu}$	0.060	60	0.037	0.62
$\gamma\text{Thr-273} \rightarrow \text{Val}$	0.054	42	0.015	0.28
$\gamma\text{Ser-34} \rightarrow \text{Leu}$	0.20	93		
$\gamma\text{Leu-34} + \gamma\text{Glu-269}$	0.047	79		
$\gamma\text{Leu-34} + \gamma\text{Val-273}$	0.038	84		
$\gamma\text{Gln-35} \rightarrow \text{Arg}$	0.20	69	0.058	0.29
$\gamma\text{Arg-35} + \gamma\text{Glu-269}$	0.046	71	0.056	1.2
$\gamma\text{Arg-35} + \gamma\text{Val-273}$	0.037	81	0.046	1.2
$\gamma\text{Ala-236} \rightarrow \text{Thr}$	0.15	84		
$\gamma\text{Thr-236} + \gamma\text{Glu-269}$	0.057	83		
$\gamma\text{Thr-236} + \gamma\text{Val-273}$	0.060	95		
$\gamma\text{Glu-238} \rightarrow \text{Gly}$	0.21	82		
$\gamma\text{Gly-238} + \gamma\text{Glu-269}$	0.052	70		
$\gamma\text{Gly-238} + \gamma\text{Val-273}$	0.056	75		
$\gamma\text{Arg-242} \rightarrow \text{His}$	0.15	75	0.099	0.66
$\gamma\text{His-242} + \gamma\text{Glu-269}$	0.040	80	0.063	1.6
$\gamma\text{His-242} + \gamma\text{Val-273}$	0.056	90	0.062	1.1

<sup>a</sup> ATPase activities were measured in a buffer consisting of 40 mM HEPES, 5 mM  $\text{MgCl}_2$ , 300 mM KCl, and 4 mM ATP, pH 7.5, with 0.1 mg/ml membrane protein at 37 °C.

<sup>b</sup> Formation of an electrochemical gradient of protons at 37 °C as monitored by acridine orange fluorescence quenching was measured in the same buffer as the ATPase assay except HEPES was 10 mM and ATP, 1 mM. In addition, 1  $\mu\text{g}/\text{ml}$  valinomycin and 1  $\mu\text{M}$  acridine orange were present. The level of quenching was calculated by taking the difference between the maximum level of fluorescence quenching after addition of ATP, and the level after addition of 1  $\mu\text{M}$  carbonylcyanide-*m*-chlorophenylhydrazone, then dividing by the value obtained for wild-type membranes (see Fig. 1).

<sup>c</sup> NADH-driven ATP synthesis was measured as previously described (32) using a buffer consisting of 25 mM TES, 200 mM KCl, 5 mM  $\text{MgSO}_4$ , 10 mM glucose, 1 mM ADP, 10 mM [ $^{32}\text{P}$ ]P<sub>i</sub>, 100 units of hexokinase, 2 mM NADH, and 0.1–0.2 mg/ml membrane protein, pH 7.5, at 37 °C with vigorous shaking. Control experiments to determine background rates contained 5  $\mu\text{M}$  carbonylcyanide-*m*-chlorophenylhydrazone.

<sup>d</sup> Coupling efficiency is indicated by dividing the rate of ATP synthesis by the rate of ATP hydrolysis.

assure that the clustering of suppressor mutations near the ends of the gene was not due to a bias of the mutagenesis system, several randomly selected plasmids were sequenced. Mutations were found distributed throughout the mutagenized segment which included the entire *uncG* coding sequence (data not shown). These observations indicated that mutations were randomly introduced throughout the gene.

The suppression behavior of each second-site mutation was tested by isolating it on a restriction fragment and ligating into the original plasmid with either  $\gamma\text{Gln-269} \rightarrow \text{Glu}$  or  $\gamma\text{Thr-273} \rightarrow \text{Val}$ . Based on increased growth yields in liquid succinate medium, we confirmed that  $\gamma\text{Ser-34} \rightarrow \text{Leu}$ ,  $\gamma\text{Gln-35} \rightarrow \text{Arg}$ ,  $\gamma\text{Ala-236} \rightarrow \text{Thr}$ ,  $\gamma\text{Glu-238} \rightarrow \text{Gly}$ ,  $\gamma\text{Arg-242} \rightarrow \text{His}$ , and  $\gamma\text{Met-246} \rightarrow \text{Leu}$  partially suppressed the effects of the original primary mutation. In addition, we found that each of these mutations suppressed both  $\gamma\text{Gln-269} \rightarrow \text{Glu}$  and  $\gamma\text{Thr-273} \rightarrow \text{Val}$ . Although the growth yield was lower than the others,  $\gamma\text{Lys-18} \rightarrow \text{Met}$  was able to suppress  $\gamma\text{Gln-269} \rightarrow \text{Glu}$ , but only imparted a slight increase in growth to  $\gamma\text{Thr-273} \rightarrow \text{Val}$ . The remaining mutations listed in Table II were unable to suppress; however, strains carrying  $\gamma\text{Glu-269} \rightarrow \text{Lys}$  or  $\text{Gly}$  as single mutations grew on succinate (data not shown).

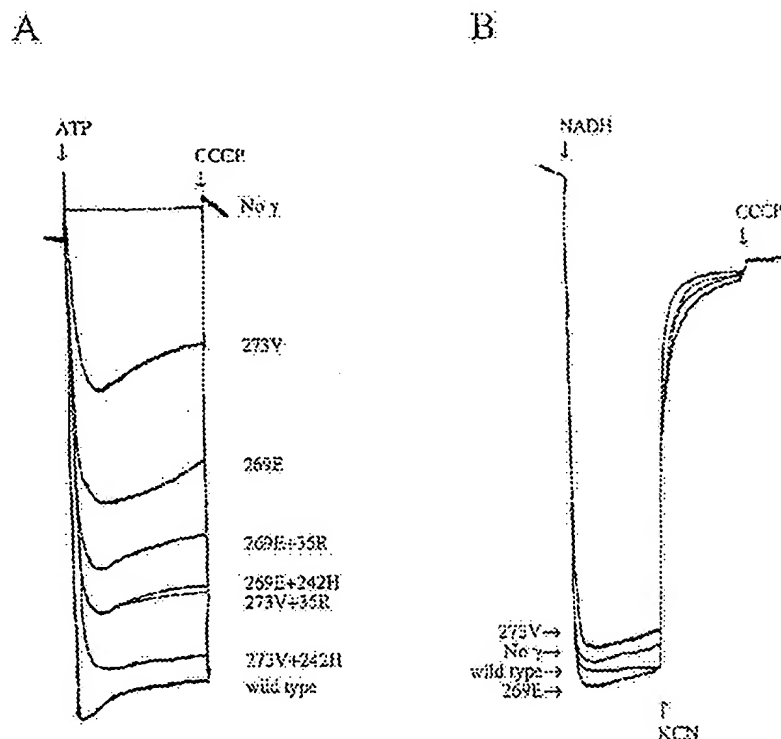
In summary, the suppressor mutations fell into two groups: three were found in the conserved amino-terminal region between positions 18 and 35, and four in the conserved carboxyl-terminal region between positions 236 and 246. The mutations near the amino terminus changed residues that are conservatively replaced in the known  $\gamma$  subunit sequences and are adjacent to residues that are completely conserved, while those near

the carboxyl terminus changed residues that are conserved or nearly so. In general, the second-site mutations near the amino terminus were not as effective as ones near the carboxyl terminus in suppressing effects of the primary mutations.

**Suppressor Mutations Restore Efficient Coupling**—The ATPase activities of  $\gamma\text{Gln-269} \rightarrow \text{Glu}$  or  $\gamma\text{Thr-273} \rightarrow \text{Val}$  mutant enzymes were greatly reduced compared to wild-type enzyme (Table III), as were ATP-dependent proton pumping (Fig. 1A) and NADH-dependent ATP synthesis rates (Table III). The  $\gamma\text{Val-273}$  enzyme generated a smaller electrochemical gradient of protons and had a lower rate of ATP synthesis than the  $\gamma\text{Glu-269}$  enzyme despite having similar ATPase activities. Both properties suggested that the  $\gamma\text{Val-273}$  enzyme was less efficient at coupling proton transport to catalysis. As an indicator of coupling efficiency, ATP synthesis and ATP hydrolysis rates were compared. Assuming that hydrolysis rates represent the catalytic competence of the enzyme, we can use synthesis:hydrolysis ratios to indicate the ability of the  $F_0F_1$  complex to couple energy between proton transport and catalysis. The synthesis:hydrolysis ratios listed in Table III suggest that the coupling efficiency of the  $\gamma\text{Glu-269}$  mutant enzyme was similar to wild type, whereas the  $\gamma\text{Val-273}$  mutant enzyme was significantly lower.

When the  $\gamma\text{Glu-269}$  and  $\gamma\text{Val-273}$  mutations were combined with each of the second-site mutations, the ATPase hydrolysis rates were essentially unchanged; however, proton pumping and ATP synthesis rates were increased (Fig. 1A and Table III). Significantly, the ATP synthesis:hydrolysis ratios for the double mutant enzymes ( $\gamma\text{Glu-269}$  or  $\gamma\text{Val-273}$  plus a suppressor

FIG. 1. Effect of  $\gamma$  subunit mutations on formation of ATP- or NADH-dependent electrochemical gradients of protons in membrane vesicles. 100  $\mu$ g of membrane vesicle protein from strain KF10rA harboring the indicated mutant  $\gamma$  subunits were suspended in 1.0 ml of the buffer described in Table III. Fluorescence intensity at 530 nm (excitation at 460 nm) was monitored at 37 °C. A, ATP-driven quenching. At the indicated times (arrows), 5  $\mu$ l of 0.2 M ATP (1 mM final concentration) or 1  $\mu$ l of 1 mM carbonylcyanide-*m*-chlorophenylhydrazine (CCCP) (1  $\mu$ M final) were added. B, NADH-driven quenching. At the indicated times (arrows), 20  $\mu$ l of 0.1 M NADH (2 mM final), 10  $\mu$ l of 0.3 M KCN (3 mM final), or 1  $\mu$ l of 1 mM carbonylcyanide-*m*-chlorophenylhydrazine (CCCP) were added.



mutation) were 2–4-fold higher than for the single mutants. These data indicate that coupling between proton transport and catalysis became more efficient and even exceeded that of wild-type enzyme.

Interestingly, the differences in activity between the  $\gamma$ Glu-269 and  $\gamma$ Val-273 mutant enzymes and wild type were not as striking as the differences in oxidative phosphorylation-dependent growth (Table II). A possible reason was that activities were measured in conditions optimal for the  $\gamma$ Glu-269 and  $\gamma$ Val-273 enzymes (pH 7.5 and 200–300 mM KCl),<sup>1</sup> and that *in vivo* conditions, especially during oxidative phosphorylation-dependent growth, may have caused the  $\gamma$ Glu-269 and  $\gamma$ Val-273 mutations to perturb enzyme function to a greater extent.

The behavior of the  $\gamma$ Glu-269 and  $\gamma$ Val-273 mutant complexes could be explained by loosely associated or unstable  $F_1$ , which readily dissociates from the membrane leaving  $F_0$  to passively conduct protons. Mutant membranes were tested for the ability to generate a proton motive force from NADH via electron transport (Fig. 1B). Similar electrochemical gradients of protons were generated regardless of the mutation present; therefore, the mutant  $F_1$  complexes appear to remain bound to the membranes and no free  $F_0$  exposed under our experimental conditions. In fact, immunoblot analysis of membranes using polyclonal antibodies against  $\alpha$ ,  $\beta$ , and  $\gamma$  subunits demonstrated that the  $F_1$  subunits were membrane-associated in all mutant complexes except when  $\gamma$  was not synthesized (Fig. 2). Interestingly, a small but significant amount of  $\alpha$  and  $\beta$  subunits were membrane-associated even in the case of strain KF10rA harboring plasmid pBR322, which lacks *uncG* and expresses no  $\gamma$  subunit.

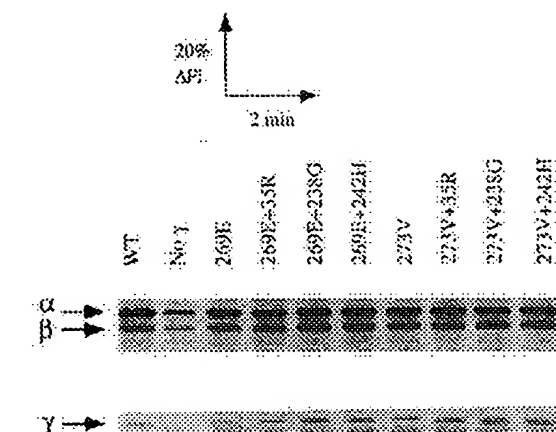


Fig. 2. Immunoblot detection of  $\alpha$ ,  $\beta$ , and  $\gamma$  subunits in membrane preparations from strain KF10rA harboring pBMG( $\gamma$ Glu-269 or  $\gamma$ Val-273) with selected suppressor mutations ( $\gamma$ Ser-34  $\rightarrow$  Leu,  $\gamma$ Glu-238  $\rightarrow$  Gly, and  $\gamma$ Arg-242  $\rightarrow$  His). 25  $\mu$ g of membrane protein from strains grown at 37 °C were separated on a 12.5% SDS-polyacrylamide gel and  $\alpha$ ,  $\beta$ , and  $\gamma$  subunit polypeptides detected by immunoblotting (see "Experimental Procedures"). Lane 1, wild type (pBWG15); lane 2, no  $\gamma$  subunit (no *uncG* on plasmid pBR322); lane 3,  $\gamma$ Glu-269; lane 4,  $\gamma$ Glu-269/ $\gamma$ Ser-34  $\rightarrow$  Leu; lane 5,  $\gamma$ Glu-269/ $\gamma$ Glu-238  $\rightarrow$  Gly; lane 6,  $\gamma$ Glu-269/ $\gamma$ Arg-242  $\rightarrow$  His; lane 7,  $\gamma$ Val-273; lane 8,  $\gamma$ Val-273/ $\gamma$ Ser-34  $\rightarrow$  Leu; lane 9,  $\gamma$ Val-273/ $\gamma$ Glu-238  $\rightarrow$  Gly; lane 10,  $\gamma$ Val-273/ $\gamma$ Arg-242  $\rightarrow$  His.

#### DISCUSSION

The multiplicity of second-site mutations that suppress  $\gamma$ Glu-269  $\rightarrow$  Glu and  $\gamma$ Thr-273  $\rightarrow$  Val, in addition to those that suppress  $\gamma$ Met-23  $\rightarrow$  Lys (19), reveals three regions of the  $\gamma$  subunit that are involved in coupling (Fig. 3). One region is between residues 269–280 near the carboxyl terminus and was defined by a series of second-site mutations that suppressed  $\gamma$ Met-23  $\rightarrow$  Lys (19). The other two regions encompassing residues 18–35 and 236–246 were described in this study. We further note that changes at position  $\gamma$ Arg-242 suppressed

<sup>1</sup> M. K. Al-Shawi and R. K. Nakamoto, unpublished results.

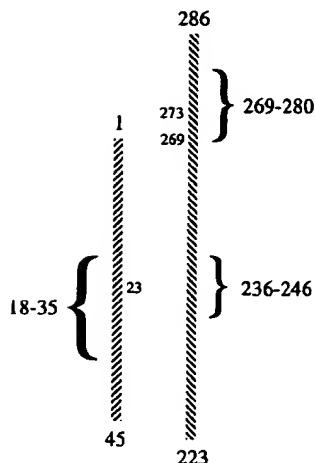


FIG. 3. Three interacting regions of the  $\gamma$  subunit involved in energy coupling. The  $\alpha$ -helical termini of the *E. coli*  $\gamma$  subunit (residues 1–45 and 223–286) are indicated by the striped vertical bars. The position of the helices relative to one another was approximated from the structural model of Abrahams *et al.* (17) based on x-ray crystallographic analysis. In the model, the two helices are in a coiled-coil conformation. The three interacting regions involved in coupling and defined by suppressor mutagenesis are indicated by the brackets (see "Discussion"). The position of the three primary mutations,  $\gamma$ Met-23  $\rightarrow$  Lys,  $\gamma$ Gln-269  $\rightarrow$  Glu, and  $\gamma$ Thr-273  $\rightarrow$  Val, are indicated by the small numbers.

$\gamma$ Met-23  $\rightarrow$  Lys as well as  $\gamma$ Gln-269  $\rightarrow$  Glu and  $\gamma$ Thr-273  $\rightarrow$  Val. We conclude that the three regions functionally interact because each shares primary mutation/suppressor mutation combinations with the other two regions. Moreover, because the primary mutations,  $\gamma$ Met-23  $\rightarrow$  Lys,  $\gamma$ Gln-269  $\rightarrow$  Glu, and  $\gamma$ Thr-273  $\rightarrow$  Val, affect coupling and the second-site mutations restore coupling to varying degrees, we propose that the three regions are directly involved in coupling transport to catalysis. Interestingly, the three regions coincide with the conserved portions of the  $\gamma$  subunit (see Ref. 5).

We are fortunate that the three  $\gamma$  subunit regions are found in the partial x-ray crystallographic structure of bovine  $F_1$  that was recently presented by Abrahams *et al.* (17). Two important features of the structural model apply to our mutagenesis results. First, the structure shows that  $\gamma$ Gln-269 (*E. coli* numbering; equivalent of bovine residue  $\gamma$ Gln-255) forms a hydrogen bond with one of the  $\beta$  subunits near its nucleotide binding site (17). The effect of replacing this residue confirms its significance. Although formation of the hydrogen bond is not essential (Arg, Gly, Leu, and Lys replacements retain function), turnover of the enzyme is greatly reduced as evidenced by low membrane ATPase and ATP synthesis rates (Table III and Refs. 19–20). Because the coupling efficiency of the  $\gamma$ Gln-269  $\rightarrow$  Glu mutant enzyme was the same as wild type, this mutation appears to disrupt catalytic turnover in both hydrolysis and synthesis directions. One turn of the helix away, replacement of the conserved  $\gamma$ Thr-273 with valine caused the same decrease in ATP hydrolysis rate and, in addition, a proportionally larger decrease in ATP synthesis rate. These results suggest that changes of  $\gamma$ Thr-273 can influence catalysis and coupling, possibly by perturbing the conformational changes involved in linking proton transport to catalysis.

The second important feature derived from the crystal structure is the relative position of the three  $\gamma$  subunit regions identified by suppressor mutagenesis. Even though the coordinates of the structure are not yet available (17), the model

clearly shows that the amino acid side chains of residues 269–280 do not directly contact those of residues 236–246 or 18–35 (see Fig. 3). Instead, the 18–35 segment appears to be adjacent to residues 236–246 in the coiled coil and interaction with the 269–280 segment is through the intervening  $\alpha$ -helix. Considering the structure and the functional interactions, we propose that the three regions of the  $\gamma$  subunit defined by the suppressor mutations constitute a domain responsible for transmitting energy between proton transport and catalytic sites.

Our results also suggest that the structural integrity of the domain is extremely important for efficient energy coupling. We base this notion on two observations. First, several different amino acid changes were able to suppress the same primary mutations. These results indicate that suppression is not the repair of a single, specific interaction between two residues, but the restabilization of interactions between segments of the  $\gamma$  subunit and possibly the  $\beta$  subunit as well. Second, the temperature sensitivity caused by the three primary mutations suggests that the structural stability of the complex was perturbed. Further structural and mutagenesis studies are required to decipher the mechanism by which the mutations affect coupling and catalysis. This information should provide an understanding of the mechanism by which proton transport is coupled to catalysis.

**Acknowledgments**—We thank Dr. Alan Senior of the University of Rochester for the gift of anti- $\alpha/\beta$  antiserum and Alistair Erskine for technical assistance.

#### REFERENCES

1. Futai, M., Noumi, T., and Maeda, M. (1989) *Annu. Rev. Biochem.* **58**, 111–136
2. Fillingame, R. H. (1990) in *The Bacteria* (Kruschwitz, T. A., ed) pp. 345–391, Academic Press, New York
3. Senior, A. E. (1990) *Annu. Rev. Biophys. Chem.* **19**, 7–41
4. Penefsky, H. S., and Cross, R. L. (1991) *Adv. Enzymol.* **64**, 173–213
5. Nakamoto, R. K., Shin, K., Iwamoto, A., Omote, H., Maeda, M., and Futai, M. (1992) *Ann. N. Y. Acad. Sci.* **671**, 335–344
6. Capaldi, R. A., Aggeler, R., Turina, P., and Wilkens, S. (1994) *Trends Biol. Sci.* **19**, 284–289
7. Walker, J. E., and Collinson, I. R. (1994) *FEBS Lett.* **346**, 39–43
8. Weias, M. A., and McCarty, R. E. (1977) *J. Biol. Chem.* **252**, 8007–8012
9. Moroney, J. V., and McCarty, R. E. (1979) *J. Biol. Chem.* **254**, 8951–8955
10. Moroney, J. V., Andreo, C. S., Vallejos, R. H., and McCarty, R. E. (1980) *J. Biol. Chem.* **255**, 6670–6674
11. Aggeler, R., and Capaldi, R. A. (1992) *J. Biol. Chem.* **267**, 21355–21359
12. Aggeler, R., Cai, S. X., Keana, J. F. W., Koike, T., and Capaldi, R. A. (1993) *J. Biol. Chem.* **268**, 20831–20837
13. Aggeler, R., and Capaldi, R. A. (1993) *J. Biol. Chem.* **268**, 14576–14578
14. Moroney, J. V., and McCarty, R. E. (1982) *J. Biol. Chem.* **257**, 6915–6920
15. Turina, P., and Capaldi, R. A. (1994) *J. Biol. Chem.* **269**, 13465–13471
16. Gogol, E. P., Johnston, E., Aggeler, R., and Capaldi, R. A. (1990) *Proc. Natl. Acad. Sci. U. S. A.* **87**, 9585–9589
17. Abrahams, J. P., Leslie, A. G. W., Luttrell, R., and Walker, J. E. (1994) *Nature* **370**, 621–628
18. Shin, K., Nakamoto, R. K., Maeda, M., and Futai, M. (1992) *J. Biol. Chem.* **267**, 20835–20839
19. Nakamoto, R. K., Maeda, M., and Futai, M. (1993) *J. Biol. Chem.* **268**, 867–872
20. Iwamoto, A., Miki, J., Maeda, M., and Futai, M. (1990) *J. Biol. Chem.* **265**, 5043–5048
21. Miki, J., Takeyama, M., Noumi, T., Kanazawa, H., Maeda, M., and Futai, M. (1986) *Arch. Biochem. Biophys.* **251**, 458–464
22. Saiki, R. K., Gelfand, D. H., Stoffel, S., Scharf, S. J., Higuchi, R., Horn, G. T., Mullis, K. B., and Erlich, H. A. (1988) *Science* **239**, 487–491
23. Sambrook, J., Fritsch, E. F., and Maniatis, T. (1989) *Molecular Cloning: A Laboratory Manual*, 2nd Ed., Cold Spring Harbor Laboratory, Cold Spring Harbor, NY
24. Sanger, F., Coulson, A. R., Barrell, B. G., Smith, A. J. H., and Roe, B. A. (1980) *J. Mol. Biol.* **143**, 161–178
25. Futai, M., Sternweis, P. C., and Heppel, L. A. (1974) *Proc. Natl. Acad. Sci. U. S. A.* **71**, 2725–2729
26. Lowry, O. H., Rosebrough, N. J., Farr, A. C., and Randall, R. J. (1951) *J. Biol. Chem.* **193**, 265–275
27. Tausaky, H. H., and Shorr, E. (1953) *J. Biol. Chem.* **202**, 675–685
28. Sugino, Y., and Miyoshi, Y. (1964) *J. Biol. Chem.* **239**, 2360–2364
29. Nakamoto, R. K., Rao, R., and Slayman, C. W. (1991) *J. Biol. Chem.* **266**, 7940–7949
30. Laemmli, U. K. (1970) *Nature* **227**, 680–685
31. Towbin, H., Staehelin, T., and Gordon, J. (1979) *Proc. Natl. Acad. Sci. U. S. A.* **76**, 4350–4354
32. Wise, J. G., and Senior, E. (1985) *Biochemistry* **24**, 6949–6954

Biochim Biophys Acta. 1995 Jun 1;1230(1-2):86-90.

[Related Articles, Links](#)

**Sequence of the gamma-subunit of *Spirulina platensis*: a new principle of thiol modulation of F<sub>0</sub>F<sub>1</sub> ATP synthase?**

**Steinemann D, Lill H.**

Universitat Osnabruck, Fachb, Biologie/Chemie, Abt. Biophysik, Germany.

The gene encoding the gamma subunit of *Spirulina platensis* F<sub>0</sub>F<sub>1</sub>, the relative of the chloroplast F<sub>1</sub> subunit responsible for thiol activation, has been cloned and sequenced. As in other cyanobacteria, a specific couple of cysteines like those involved in thiol modulation of the chloroplast enzyme was not found. Instead, two cysteine residues were identified in the *Spirulina* subunit at positions unique amongst all so far sequenced gamma subunits. Involvement of these cysteines in the thiol-modulation of the *Spirulina* enzyme reported before (Hicks and Yocum (1986) Arch. Biochem. Biophys. 245, 230-237, and Lerma and Gomez-Lojero (1987) Photosynth. Res. 11, 265-277) would manifest a re-invention of a regulatory mechanism.

PMID: 7612646 [PubMed - indexed for MEDLINE]

## F<sub>0</sub>F<sub>1</sub>-ATPase $\gamma$ Subunit Mutations Perturb the Coupling between Catalysis and Transport\*

(Received for publication, June 26, 1992)

Kouichirou Shin, Robert K. Nakamoto†, Masatomo Maeda, and Masamitsu Futai

From the Department of Organic Chemistry and Biochemistry, The Institute of Scientific and Industrial Research, Osaka University, Ibaraki, Osaka 567, Japan

We introduced mutations to test the function of the conserved amino-terminal region of the  $\gamma$  subunit from the *Escherichia coli* ATP synthase (F<sub>0</sub>F<sub>1</sub>-ATPase). Plasmid-borne mutant genes were expressed in an *uncG* strain which is deficient for the  $\gamma$  subunit ( $\gamma$ Gln-14  $\rightarrow$  end). Most of the changes, which were between  $\gamma$ Ile-19 and  $\gamma$ Lys-33,  $\gamma$ Asp-83 and  $\gamma$ Cys-87, or at  $\gamma$ Asp-165, had little effect on growth by oxidative phosphorylation, membrane ATPase activity, or H<sup>+</sup> pumping. Notable exceptions were  $\gamma$ Met-23  $\rightarrow$  Arg or Lys mutations. Strains carrying these mutations grew only very slowly by oxidative phosphorylation. Membranes prepared from the strains had substantial levels of ATPase activity, 100% compared with wild type for  $\gamma$ Arg-23 and 65% for  $\gamma$ Lys-23, but formed only 32 and 17%, respectively, of the electrochemical gradient of protons. In contrast, other mutant enzymes with similar ATPase activities (including  $\gamma$ Met-23  $\rightarrow$  Asp or Glu) formed H<sup>+</sup> gradients like the wild type. Membranes from the  $\gamma$ Arg-23 and  $\gamma$ Lys-23 mutants were not passively leaky to protons and had functional F<sub>0</sub> sectors. These results suggested that substitution by positively charged side chains at position 23 perturbed the energy coupling. The catalytic sites of the mutant enzymes were still regulated by the electrochemical H<sup>+</sup> gradient but were inefficiently coupled to H<sup>+</sup> translocation in both ATP-dependent H<sup>+</sup> pumping and  $\Delta\mu_{H^+}$  driven ATP synthesis.

The *Escherichia coli* F<sub>0</sub>F<sub>1</sub> ATPase is a reversible H<sup>+</sup> pump which plays two metabolically defined roles; in aerobic conditions, it utilizes the proton motive force from the respiratory chain to synthesize ATP, and in anaerobic conditions, it utilizes ATP from glycolysis to pump protons out of the cell forming an electrochemical H<sup>+</sup> gradient which supplies energy for secondary transport systems. The pump is composed of eight subunits divided into the membrane extrinsic F<sub>1</sub> portion ( $\alpha$ ,  $\beta$ ,  $\gamma$ ,  $\delta$ , and  $\epsilon$  subunits), which contains the catalytic sites for ATP hydrolysis or synthesis, and the membrane intrinsic F<sub>0</sub> portion ( $a$ ,  $b$  and  $c$  subunits), which contains the H<sup>+</sup> pore (reviewed in Refs. 1-5). Assembly of the functional pump requires all eight subunits, and reconstitution of ATP hydrolysis activity needs at least  $\alpha$ ,  $\beta$ , and  $\gamma$  subunits in a stoichiometry of 3:3:1 (6, 7).

The  $\gamma$  subunit occupies a central position between the

catalytic sites found in the  $\alpha$  and  $\beta$  subunits and the H<sup>+</sup> pore through the F<sub>0</sub> subunits (8, 9). Extensive use of sulfhydryl reagents led the McCarty laboratory to conclude that the chloroplast  $\gamma$  subunit both regulates ATPase catalytic activity and couples this activity to proton translocation (10-12). Recently, a mutagenesis approach was used by Iwamoto *et al.* (13) to demonstrate that the conserved carboxyl-terminal region of the *E. coli*  $\gamma$  subunit is important for ATPase catalytic activity. Of special interest, the  $\gamma$ Gln-269  $\rightarrow$  Leu mutant had ATPase activity similar to other mutant proteins (e.g.  $\gamma$ Glu-275  $\rightarrow$  Lys and  $\gamma$ Thr-277  $\rightarrow$  end, about 14% of wild type), but formed a much weaker electrochemical gradient of protons. These reports taken together suggest that the  $\gamma$  subunit participates in energy coupling, as well as regulation of ATPase activity.

In addition to the carboxyl terminus, the only other well conserved region of the  $\gamma$  subunit is found near the amino terminus. The importance of this region was suggested by the deletion of residues  $\gamma$ Lys-21 to  $\gamma$ Ala-27, which resulted in failure of the F<sub>1</sub> complex to assemble (14). In this paper, we describe the effects of site-specific mutations introduced in the amino-terminal region of the  $\gamma$  subunit. Whereas the carboxyl terminus was found to be important for catalysis, we report here that replacement of amino-terminal residue  $\gamma$ Met-23 to arginine or lysine had profound effects on the coupling between ATPase catalysis and H<sup>+</sup> translocation.

### EXPERIMENTAL PROCEDURES

**Materials**—Oligonucleotides were synthesized with Applied Biosystems (Foster City, CA) DNA synthesizer model 381A. [ $\alpha$ -<sup>32</sup>P]dCTP (3000 Ci/mmol) was from Amersham-Japan (Tokyo). Restriction endonucleases, Klenow fragment, T4 DNA ligase and *Taq* polymerase were from Takara Shuzo Co., Kyoto; Nippon Gene Co., Toyama; Toyobo Co., Osaka; or New England Biolabs, Beverly, MA.

**Bacterial Strains and Growth Conditions**—The  $\gamma$  subunit-deficient *E. coli* strain, KF10rA (*thi*, *thy*, *recA1*, *uncG10* ( $\gamma$ Gln-14  $\rightarrow$  end), was previously described and grown as before (13, 15). Minimal medium supplemented with thymine (50  $\mu$ g/ml), thiamine (2  $\mu$ g/ml), and a carbon source (either 0.2% glucose or 0.4% sodium succinate) or a rich medium (L broth) were used for genetic analysis. Minimal medium with 0.2% glucose was used for preparation of membranes. All strains were grown at 37 °C.

**Construction of Expression Plasmids Carrying Mutant Genes for the  $\gamma$  Subunit**—pBWG11 (Ref. 13, Fig. 1A) coding the entire wild-type  $\gamma$  subunit was engineered to introduce new restriction sites which are unique in the plasmid (Fig. 1B): *NcoI* at base -2, *NruI* at base 34, *AsuII* at base 88, *XbaI* at base 124, and *AseI* at base 278 (nucleotides were numbered from the first letter of the initiation codon). For these constructions, the *SmaI*-*PstI* segment of pBWG11 was ligated into pBluescript II SK(+) (Stratagene, La Jolla, CA), whose *XbaI* site was destroyed previously, to create pSKWG'. Polymerase chain reactions were performed using this plasmid as the template and the following oligonucleotides containing the altered sequences for primers: to create *NcoI*, the 21 base, 5'-GAGGAG-AAGCCATGGCCGGG-3'; for *XbaI*, the 26 base, 5'-CATGGC-GGCCCTaGaCCTTATGCAG-3'; and for *AseI*, the 27 base, 5'-GTT-

\* This research was supported in part by grants from the Ministry of Education, Science and Culture of Japan and the Human Frontier Science Program. The costs of publication of this article were defrayed in part by the payment of page charges. This article must therefore be hereby marked "advertisement" in accordance with 18 U.S.C. Section 1734 solely to indicate this fact.

† Supported by the Japan Society for the Promotion of Science.







TABLE I

Growth yields, membrane ATPase activities, and ATP-dependent  $H^+$  pumping of strain KF10rA ( $\gamma$ Gln-14  $\rightarrow$  end) harboring mutant *uncG* genes

Growth yields, ATPase activities and  $\Delta\mu_{H^+}$  were measured as described previously (13). Growth yields in succinate minimal medium are reported as percentages of that obtained from KF10rA harboring pBWG15 (wild-type  $\gamma$  gene). ATPase activities are reported in units of micromoles of  $P_i$ /min/mg protein. The ability of each strain to form  $\Delta\mu_{H^+}$  was estimated by ATP-dependent acridine orange fluorescence quenching and is reported in percent relative to that obtained from the wild type. For each mutation, the wild-type amino acid, position, and codon are listed followed by the changes made. Residues conserved in all the  $\gamma$  genes so far sequenced are underlined. Asp-165 changes to Ala, Glu, or Lys gave results identical to the listed Asn change.

Mutation	Growth yield	ATPase activity	$\Delta\mu_{H^+}$
	%	units/mg	%
Wild type	100	1.7	100
No $\gamma$ gene	1.7	0.018	0
Ile-19 (ATC) $\rightarrow$ Glu (GAA)	69	0.71	57
Thr-20 (ACT) $\rightarrow$ Val (GTT)	99	1.7	100
Lys-21 (AAA) $\rightarrow$ Leu (CTG)	98	1.6	98
Glu-24 (GAG) $\rightarrow$ Leu (CTG)	99	1.5	100
Met-25 (ATG) $\rightarrow$ Lys (AAA)	97	1.2	94
Val-26 (GTC) $\rightarrow$ Glu (GAA)	94	1.6	93
Lys-30 (AAA) $\rightarrow$ Glu (GAA)	99	0.86	94
$\rightarrow$ Leu (CTT)	95	0.91	99
Lys-33 (AAA) $\rightarrow$ Glu (GAA)	98	1.6	98
$\rightarrow$ Leu (CTT)	101	1.8	100
Asp-83 (GAC) $\rightarrow$ Lys (AAA)	100	1.5	98
$\rightarrow$ Val (GTT)	101	1.6	100
Arg-84 (CGT) $\rightarrow$ Glu (GAA)	95	1.1	100
$\rightarrow$ Leu (CTT)	94	2.3	94
Leu-86 (TTG) $\rightarrow$ Glu (GAA)	83	0.79	100
Cys-87 (TGC) $\rightarrow$ Ala (GCA)	101	1.7	98
Asp-165 (GAC) $\rightarrow$ Asn (AAC)	102	1.5	94

TABLE II

Growth yields, membrane ATPase activities, and ATP-dependent  $H^+$  pumping of  $\gamma$ Met-23 mutants

Mutation*	Growth yield	ATPase activity	$\Delta\mu_{H^+}$
	%	units/mg	%
Lys (AAA)	15	1.1	17
Arg (CGT)	28	1.7	32
Asp (GAC)	57	0.94	71
Glu (GAA)	86	1.0	78
Leu (CTG)	87	1.8	89

\* Each amino acid change is followed by the codon used to encode the mutation. See Table I for explanations of table headings.

ATPase activities similar to the wild type: 100 and 65%, respectively. In addition, the assembly of these mutants appeared normal as the relative amount of the mutant  $\gamma$  subunits was similar to wild type when visualized on immunoblots using purified anti- $\gamma$  antibodies (data not shown).

**ATP-driven  $H^+$  Gradients in Mutant Membrane Vesicles—**Membranes isolated from most of the mutants showed essentially the same degree of ATP-dependent acridine orange quenching (Tables I and II and Fig. 2A). These experiments indicated the ability of these mutants to form an electrochemical gradient of protons dependent on ATP hydrolysis which was consistent with their ability to grow by oxidative phosphorylation. In sharp contrast, the  $\gamma$ Arg-23 and  $\gamma$ Lys-23 mutant membranes formed greatly reduced gradients of 32 and 17%, respectively (Fig. 2B). As indicated above,  $\gamma$ Arg-23 and  $\gamma$ Lys-23 mutants had substantial membrane ATPase activities. Clearly, the degree of the  $H^+$  gradients formed did not correlate with the ATPase activities. Not as dramatic, membranes from  $\gamma$ Ile-19  $\rightarrow$  Glu also formed a smaller  $H^+$

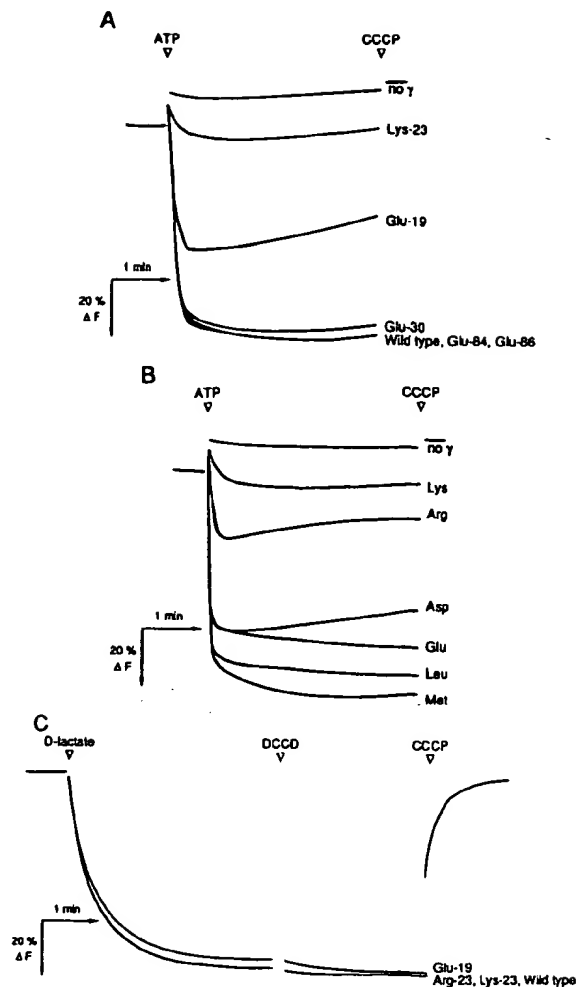


FIG. 2. Formation of an electrochemical gradient of protons in membrane vesicles from strain KF10rA ( $\gamma$ Gln-14  $\rightarrow$  end) harboring mutant *uncG* genes. A, ATP-dependent fluorescence quenching (ATP-dependent formation of an electrochemical  $H^+$  gradient) in membranes from the indicated *uncG* mutants which had similar ATPase activities (0.7–1.1  $\mu$ mol/min/mg protein). The mutant enzymes tested were  $\gamma$ Ile-19  $\rightarrow$  Glu (Glu-19),  $\gamma$ Met-23  $\rightarrow$  Lys (Lys-23),  $\gamma$ Lys-30  $\rightarrow$  Glu (Glu-30),  $\gamma$ Arg-84  $\rightarrow$  Glu (Glu-84), and  $\gamma$ Leu-86  $\rightarrow$  Glu (Glu-86). Membranes from strains harboring pBWG15 (wild type) or pBR322 (no  $\gamma$ ) are shown for comparison. 100  $\mu$ g of membrane vesicles were suspended in 1.0 ml of 10 mM Tricine (*N*-[2-hydroxy-1,1-bis(hydroxymethyl)ethyl]glycine)-choline, 140 mM KCl, 5 mM MgCl<sub>2</sub>, 1  $\mu$ g/ml valinomycin, and 1  $\mu$ M acridine orange, pH 8.0. Fluorescence at 530 nm (excitation at 490 nm) was monitored at 25  $^{\circ}$ C. At the indicated times (arrows), 5  $\mu$ l of 0.2 M ATP (Tris salt, 1 mM final concentration) or 1.5  $\mu$ l of 1 mM carbonylcyanide-*m*-chlorophenylhydrazide (1.5  $\mu$ M) was added. Traces for wild-type,  $\gamma$ Arg-84  $\rightarrow$  Glu, and  $\gamma$ Leu-86  $\rightarrow$  Glu membranes were identical. B, ATP-dependent fluorescence quenching in membranes from strains with  $\gamma$ Met-23 changed to the indicated residue or lacking the plasmid *uncG* gene (no  $\gamma$ ). Conditions were the same as in A. C, respiratory fluorescence quenching. Membrane vesicles from wild-type or  $\gamma$ Ile-19  $\rightarrow$  Glu (Glu-19),  $\gamma$ Met-23  $\rightarrow$  Arg (Arg-23), and  $\gamma$ Met-23  $\rightarrow$  Lys (Lys-23) mutant strains were incubated as described in A, except that the fluorescence of 1  $\mu$ M quinacrine was monitored (420-nm excitation and 500-nm emission). At the indicated times, 10  $\mu$ l of 0.5 M D-lactate (5 mM, final concentration), 1  $\mu$ l of 20 mM ethanolic dicyclohexylcarbodiimide (20  $\mu$ M), or 1.5  $\mu$ l of 1 mM carbonylcyanide-*m*-chlorophenylhydrazide (1.5  $\mu$ M) were added. Traces for  $\gamma$ Met-23  $\rightarrow$  Arg,  $\gamma$ Met-23  $\rightarrow$  Lys, and wild-type membranes were identical.

gradient than indicated by its ATPase activity. For comparison, we point out that membranes from  $\gamma$ Met-23  $\rightarrow$  Asp or Glu,  $\gamma$ Lys-30  $\rightarrow$  Glu or Leu,  $\gamma$ Arg-84  $\rightarrow$  Glu, or  $\gamma$ Leu-86  $\rightarrow$  Glu each had lower ATPase activities than wild type (46–65%) but formed electrochemical gradients of protons similar to wild type (71–100%, Fig. 2, A and B). It is noteworthy that replacing the neighboring Met at position 25 with Lys had little effect on ATPase activity and  $H^+$  pumping (Table I), suggesting that the behavior of a basic residue at position 23 was unique in its effect on  $H^+$  translocation.

The formation of weak  $H^+$  gradients by the mutants at position 23 was not due to the passive leakage of protons through  $F_0$ , which may have been exposed during membrane preparations; membranes of  $\gamma$ Arg-23 and  $\gamma$ Lys-23 mutants displayed the same degree of respiratory fluorescence quenching as the wild type (Fig. 2C). Furthermore, treatment with dicyclohexylcarbodiimide, which seals the  $H^+$  pathways of the  $F_0$  portion (which is open when  $F_1$  dissociates), had no effect. Importantly, we found that the assembly and function of the  $F_0$  sectors in the mutant enzymes appeared normal. Membranes from mutants or wild type in which the  $F_1$  portion was depleted by washing with dilute buffer containing EDTA showed no respiratory or ATP-dependent fluorescence quenching (Fig. 3). Subsequent incubation with wild-type  $F_1$  reestablished the ability of wild-type and mutant membrane preparations to form electrochemical  $H^+$  gradients.

#### DISCUSSION

Even though the amino terminus of the  $\gamma$  subunit appears well conserved through evolution, 13 residues between  $\gamma$ Ile-19 to  $\gamma$ Lys-33,  $\gamma$ Asp-83 to  $\gamma$ Cys-87, and at  $\gamma$ Asp-165 could be changed with little or no effect on ATPase function. Only changes at position 23 (Met  $\rightarrow$  Arg or Lys) significantly affected the function of the enzyme. Even then, the conserved  $\gamma$ Met-23 residue is not essential, because it can be changed without complete loss of function. However,  $\gamma$ Met-23 is clearly important in the energy coupling between ATPase catalysis and  $H^+$  translocation.

Because of the dramatically weaker pumping by the  $\gamma$ Arg-23 or  $\gamma$ Lys-23 mutant enzymes compared with their ATP hydrolysis activity, we could easily distinguish their effects from trivial explanations. The mutant membranes showed normal respiratory-driven quenching, indicating that they were not  $H^+$  leaky. The  $F_0$  segment from the mutant strains were functionally normal. Finally, the assembly of the mutant

$F_1$  also seemed normal as detected by the membranes which were not leaky to protons, by membrane ATPase activities which were similar to wild type, and by immunoblot analysis. Clearly, the weak ATP-dependent  $H^+$  gradients of the  $\gamma$ Arg-23 and  $\gamma$ Lys-23 mutants were due solely to a perturbation in the altered  $\gamma$  subunit.

The data strongly indicate that the  $\gamma$ Arg-23 and  $\gamma$ Lys-23 mutants were profoundly inefficient in  $H^+$  pumping. Likewise, the very slow growth on succinate indicated that  $\Delta\mu_{H^+}$ -driven ATP synthesis was also very inefficient. However, we point out that the ability to grow by oxidative phosphorylation demonstrates another important characteristic, the mutants were capable of net synthesis of ATP. This observation establishes that the ATPase catalytic sites were still regulated by  $\Delta\mu_{H^+}$ , which is in contrast to the expectation if the mutant enzymes were uncoupled in the same sense as free  $F_1$ , not regulated by  $\Delta\mu_{H^+}$  and freely hydrolyzing ATP. Mutants of this type have been described; for example, the enzyme with the subunit c Asp-61  $\rightarrow$  Gly mutation had ATPase activity similar to wild type, even though its  $H^+$  pore was blocked (33). Furthermore, we note that the effect of the  $\gamma$ Arg-23 and  $\gamma$ Lys-23 mutants was not due to a strict change in coupling ratio. In this event, the enzyme would remain efficiently coupled but pump fewer protons per ATP hydrolyzed. This type of enzyme is expected to form a stronger  $H^+$  gradient and not be readily reversible (34). We conclude, then, that the  $\gamma$ Arg-23 and  $\gamma$ Lys-23 mutants cause a slippage in the energy coupling between ATPase catalysis and  $H^+$  translocation and that these mutations perturb a function which is distinct from  $\Delta\mu_{H^+}$  regulation of ATPase hydrolysis and synthesis.

Discussions in recent reviews (1, 4) suggest that transport in the  $F_0F_1$ -ATPase is coupled via a conformational link. Several pieces of evidence indicate that the  $\gamma$  subunit participates in such a linkage by interacting with other subunits. First, the  $\gamma$  subunit intimately interacts with the catalytic subunits as demonstrated by chemical cross-linking to  $\beta$  (35, 36) and by the requirement of the  $\gamma$  subunit for reconstitution of the minimal assembly capable of ATP hydrolysis (6, 7). Second,  $\gamma$  subunit mutations, which delete either the carboxyl terminus (13, 15) or amino terminus (14),<sup>1</sup> cause the failure of the  $F_1$  complex to assemble, suggesting that both ends interact with other subunits. Third, residues in these terminal regions are involved in energy coupling (Ref. 13 and this study). This hypothesis suggests a search for second-site mutations which would suppress the perturbation caused by  $\gamma$ Arg-23 and  $\gamma$ Lys-23. Such changes of amino acids elsewhere in the enzyme complex would indicate residues which interact with  $\gamma$ Met-23 and therefore indicate the energy link between catalysis and  $H^+$  translocation.

#### REFERENCES

1. Fillingame, R. H. (1990) in *The Bacteria* (Kruswicz, T. A., ed) Vol. XII, pp. 345–391, Academic Press Inc., New York
2. Futai, M., Noumi, T., and Maeda, M. (1989) *Annu. Rev. Biochem.* 58, 111–136
3. Futai, M., and Kanazawa, H. (1983) *Microbiol. Rev.* 47, 285–312
4. Senior, A. E. (1990) *Annu. Rev. Biophys. Biophys. Chem.* 19, 7–41
5. Walker, J. E., Saraste, M., and Gay, N. J. (1984) *Biochim. Biophys. Acta* 768, 164–200
6. Futai, M. (1977) *Biochem. Biophys. Res. Commun.* 103, 604–612
7. Dunn, S. D., and Futai, M. (1980) *J. Biol. Chem.* 255, 113–118
8. Gogol, E. P., Aggeler, R., Sagermann, M., and Capaldi, R. A. (1989) *Biochemistry* 28, 4717–4724
9. Boekema, E. J., Xiao, J., and McCarty, R. E. (1990) *Biochim. Biophys. Acta* 1020, 49–56
10. Weiss, M. A., and McCarty, R. E. (1977) *J. Biol. Chem.* 252, 8007–8012
11. Moroney, J. V., and McCarty, R. E. (1979) *J. Biol. Chem.* 254, 8951–8955
12. Moroney, J. V., Andreo, C. S., Vallejos, R. H., and McCarty, R. E. (1980) *J. Biol. Chem.* 255, 6670–6674
13. Iwamoto, A., Miki, J., Maeda, M., and Futai, M. (1990) *J. Biol. Chem.* 265, 5043–5048

<sup>1</sup> K. Shin, M. Maeda, and M. Futai, unpublished results.

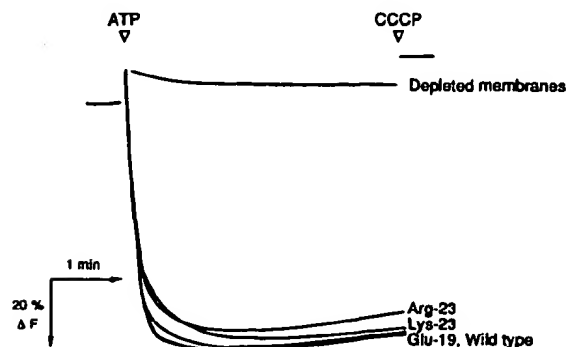


FIG. 3. Reconstitution of functional  $F_0F_1$  from  $F_1$ -depleted mutant membranes.  $\gamma$ Ile-19  $\rightarrow$  Glu (Glu-19),  $\gamma$ Met-23  $\rightarrow$  Arg (Arg-23),  $\gamma$ Met-23  $\rightarrow$  Lys (Lys-23), and wild-type membranes were depleted of the  $F_1$  sector and reconstituted with purified wild-type  $F_1$  as described earlier (18). These membranes were then subjected to ATP-dependent fluorescence quenching measurements as described in the legend to Fig. 2A. The traces for depleted membranes of the wild-type and three mutants were identical.

14. Kanazawa, H., Hama, H., Rosen, B. P., and Futai, M. (1985) *Arch. Biochem. Biophys.* **241**, 364-370
15. Miki, J., Takeyama, M., Noumi, T., Kanazawa, H., Maeda, M., and Futai, M. (1986) *Arch. Biochem. Biophys.* **251**, 458-464
16. Higuchi, R., Krummel, B., and Saiki, R. K. (1988) *Nucleic Acids Res.* **16**, 7351-7367
17. Sanger, F., Coulson, A. R., Barrell, B. G., Smith, A. J. H., and Roe, B. A. (1980) *J. Mol. Biol.* **143**, 161-178
18. Futai, M., Sternweis, P. C., and Heppel, L. A. (1974) *Proc. Natl. Acad. Sci. U. S. A.* **71**, 2725-2729
19. Kanazawa, H., Miki, T., Tamura, F., Yura, T., and Futai, M. (1979) *Proc. Natl. Acad. Sci. U. S. A.* **76**, 1126-1130
20. Lowry, O. H., Rosebrough, N. J., Farr, A. L., and Randall, R. J. (1951) *J. Biol. Chem.* **193**, 265-275
21. Towbin, H., Staehelin, T., and Gordon, J. (1979) *Proc. Natl. Acad. Sci. U. S. A.* **76**, 4250-4354
22. Miki, J., Maeda, M., Mukohata, Y., and Futai, M. (1988) *FEBS Lett.* **232**, 221-226
23. Yu, L. M., and Selman, B. R. (1988) *J. Biol. Chem.* **263**, 19342-19345
24. Inohara, N., Iwamoto, A., Moriyama, Y., Shimomura, S., Maeda, M., and Futai, M. (1991) *J. Biol. Chem.* **266**, 7333-7338
25. Kanazawa, H., Kayano, T., Mabuchi, K., and Futai, M. (1981) *Biochem. Biophys. Res. Commun.* **103**, 604-612
26. Brusilow, W. S. A., Scarpetta, M. A., Hawthorne, C. A., and Clark, W. P. (1989) *J. Biol. Chem.* **264**, 1528-1533
27. Falk, G., Hampe, A., and Walker, J. E. (1985) *Biochem. J.* **228**, 391-407
28. Tybulewicz, V. L. J., Falk, G., and Walker, J. E. (1984) *J. Mol. Biol.* **179**, 185-214
29. Cozens, A. L., and Walker, J. E. (1987) *J. Mol. Biol.* **194**, 359-383
30. McCarn, D. F., Whitaker, R. A., Alam, J., Vrba, J. M., and Curtis, S. E. (1988) *J. Bacteriol.* **170**, 3448-3458
31. Ohta, S., Yohda, M., Ishizuka, M., Hirata, H., Hamamoto, T., Otawara-Hamamoto, Y., Matsuda, K., and Kagawa, Y. (1988) *Biochim. Biophys. Acta* **933**, 141-155
32. Walker, J. E., Fearnley, I. M., Gay, N. J., Gibson, B. W., Northrop, F. D., Powell, S. J., Runswick, M. J., Saraste, M., and Tybulewicz, V. L. J. (1985) *J. Mol. Biol.* **184**, 677-701
33. Fillingame, R. H., Peters, L. K., White, L. K., Mosher, M. E., and Paule, C. R. (1984) *J. Bacteriol.* **158**, 1078-1083
34. Slayman, C. L., and Zuckier, G. R. (1989) *Ann. N. Y. Acad. Sci.* **574**, 233-245
35. Bragg, P. D., and Hou, C. (1980) *Eur. J. Biochem.* **106**, 495-503
36. Aris, J. P., and Simoni, R. D. (1983) *J. Biol. Chem.* **258**, 14599-14609

## ATPase Activity of a Highly Stable $\alpha_3\beta_3\gamma$ Subcomplex of Thermophilic $F_1$ Can Be Regulated by the Introduced Regulatory Region of $\gamma$ Subunit of Chloroplast $F_1$ \*

(Received for publication, December 6, 1999, and in revised form, January 24, 2000)

Dirk Bald†§, Hiroyuki Noji§, Michael T. Stumpp†, Masasuke Yoshida†§, and Toru Hisabori†¶

From the ‡Chemical Resources Laboratory, Tokyo Institute of Technology, Nagatsuta 4259, Midori-ku, Yokohama 226-8503 and §CREST "Genetic Programming" Team 13, Teikyo Biotechnology Center, Nogawa 907, Miyamae-ku, Kawasaki 216-0001, Japan

A mutant  $F_1$ -ATPase  $\alpha_3\beta_3\gamma$  subcomplex from the thermophilic *Bacillus* PS3 was constructed, in which 111 amino acid residues (Val<sup>92</sup> to Phe<sup>202</sup>) from the central region of the  $\gamma$  subunit were replaced by the 148 amino acid residues of the homologous region from spinach chloroplast  $F_1$ -ATPase  $\gamma$  subunit, including the regulatory stretch, and were designated as  $\alpha_3\beta_3\gamma_{(TCF)}$  (Thermophilic-Chloroplast-Thermophilic). By the insertion of this regulatory region into the  $\gamma$  subunit of thermophilic  $F_1$ , we could confer the thiol modulation property to the thermophilic  $\alpha_3\beta_3\gamma$  subcomplex. The overexpressed  $\alpha_3\beta_3\gamma_{(TCF)}$  was easily purified in large scale, and the ATP hydrolyzing activity of the obtained complex was shown to increase up to 3-fold upon treatment with chloroplast thioredoxin-*f* and dithiothreitol. No loss of thermostability compared with the wild type subcomplex was found, and activation by dithiothreitol was functional at temperatures up to 80 °C.  $\alpha_3\beta_3\gamma_{(TCF)}$  was inhibited by the  $\epsilon$  subunit from chloroplast  $F_1$ -ATPase but not by the one from the thermophilic  $F_1$ -ATPase, indicating that the introduced amino acid residues from chloroplast  $F_1$ - $\gamma$  subunit are important for functional interaction with the  $\epsilon$  subunit.

$F_0F_1$ -ATP synthases ubiquitously occur in eucaryotic and procaryotic cells and synthesize ATP from ADP and inorganic phosphate at the expense of a trans-membrane electrochemical proton gradient (1–4). The bacterial enzyme consists of a hydrophilic  $F_1$  part with a subunit composition of  $\alpha_3\beta_3\gamma\delta\epsilon$  (5) and a hydrophobic  $F_0$  part with a subunit composition of  $a_1b_2c_{10-12}$  (6). The subcomplex  $\alpha_3\beta_3\gamma^1$  is the minimum complex that is

capable of hydrolyzing ATP (7). A high resolution x-ray structure of a major part of the bovine heart mitochondrial  $F_1$  revealed an alternating hexagonal arrangement of the three  $\alpha$  and the three  $\beta$  subunits with two  $\alpha$ -helices of the  $\gamma$  subunit forming a coiled-coil in the central cavity (8). The crystal structure of an  $\alpha_3\beta_3$  complex from the thermophilic *Bacillus* PS3 is completely symmetric (9), but the incorporation of the  $\gamma$  subunit into this complex induces a functional asymmetry among the three catalytic sites (10) residing on the  $\beta$  subunits at the interface to the  $\alpha$  subunits. Rotation of the  $\gamma$  subunit relative to  $\alpha_3\beta_3$  had been suggested from kinetic analyses (11), biochemical experiments (12), and biophysical measurements (13). Finally, by a single molecular observation technique, rotation of the  $\gamma$  subunit during the ATP hydrolysis reaction in the  $\alpha_3\beta_3$  hexamer (14–17) was shown.

The molecular structure of the  $F_0F_1$ -ATP synthase of chloroplasts may be basically the same as those of other  $F_0F_1$ , but this enzyme has a unique regulation system. The activity of chloroplast  $F_0F_1$  and  $F_1$  ( $CF_1$ ) is strongly regulated by the reduction and the oxidation of a disulfide bridge in the  $\gamma$  subunit formed between the two cysteines Cys<sup>199</sup> and Cys<sup>205</sup> (spinach chloroplast) (18); this regulation system is called thiol modulation (19). Reduction of the disulfide bond elicits the latent ATP hydrolyzing activity of the isolated  $CF_1$ . *In vitro* reduction can be achieved by dithiothreitol (DTT) or other dithiols, but the natural reductant is reduced thioredoxin-*f* (Trx-*f*) (20–22). Introduction of nine amino acids comprising the regulatory sequence into the cyanobacterial  $\gamma$  subunit induced thiol modulation in *Synechocystis* (23, 24). Conversely, replacement of the two cysteines by serines in  $\gamma$  subunit of  $CF_0CF_1$  from *Chlamydomonas reinhardtii* (25, 26) resulted in a non-modulated enzyme. However, due to the lack of suitable overexpression systems for the subunits of  $CF_1$  and because of its insufficient ability for the reconstitution of the complete enzyme complex, little information is available about the details of this regulation mechanism. Recently we have succeeded in the reconstitution of a chimeric complex from recombinant  $\alpha$  and  $\beta$  subunits of  $F_1$  of the thermophilic *Bacillus* PS3 ( $TF_1$ ) and the recombinant  $\gamma$  subunit from spinach  $CF_1$  (27). The resulting chimeric  $\alpha_3\beta_3\gamma$  complex, which had substantial ATPase activity, was clearly regulated by the disulfide/dithiol state of the two regulatory cysteine residues. We could demonstrate the importance of the region around the disulfide bridge of  $\gamma$  subunit for the regulatory interaction with  $\epsilon$  subunit which is known to inhibit activity (28). However, stability of this chimeric complex was still lower than that of wild type thermophilic  $\alpha_3\beta_3\gamma$ , and large scale preparation was difficult.

In order to understand the molecular mechanism of thiol regulation, we engineered a chimeric  $\alpha_3\beta_3\gamma$  subcomplex of  $TF_1$  in which the central half of the  $\gamma$  subunit was replaced by the

\* This work was supported in part by a Grant-in-aid for Scientific Research in Priority Areas 11151209 and Grant 11640643 from the Japanese Ministry of Education, Science, Sports, and Culture (to T. H.) and Core Research for Evolutional Science and Technology (to M. Y.). The costs of publication of this article were defrayed in part by the payment of page charges. This article must therefore be hereby marked "advertisement" in accordance with 18 U.S.C. Section 1734 solely to indicate this fact.

¶ To whom correspondence should be addressed: Chemical Resources Laboratory, Tokyo Institute of Technology, Nagatsuta 4259, Midori-ku, Yokohama 226-8503, Japan. Tel.: 81-45-924-5234; Fax: 81-45-924-5277; E-mail: thisabori@res.titech.ac.jp.

<sup>1</sup> The abbreviations used are:  $\alpha_3\beta_3\gamma$  ( $\beta$ -His,  $\gamma$ S106C),  $\alpha_3\beta_3\gamma$  subcomplex of  $TF_1$  containing histidine tag on the N terminus of the  $\beta$  subunit and the substitution of Ser<sup>106</sup> of the  $\gamma$  subunit to Cys;  $CF_1$ , chloroplast coupling factor 1; DTT, dithiothreitol; Trx-*f*, spinach chloroplast thioredoxin-*f*;  $TF_1$ ,  $F_1$ -ATPase from thermophilic *Bacillus* PS3 plasma membrane; MOPS, 3-[N-morpholinol]propanesulfonic acid; TNP-ATP (or TNP-ADP), 2',3'-O-(2,4,6-trinitrophenyl) ATP (or ADP); Ni-NTA, nickel nitrilotriacetic acid;  $\alpha_3\beta_3\gamma_{TC}$ , chimeric  $\alpha_3\beta_3\gamma$  complex formed by the recombinant  $\alpha$  and  $\beta$  subunits of  $TF_1$  and the recombinant  $\gamma$  subunit of  $CF_1$ ; HPLC, high pressure liquid chromatography.

Fig. 1. Amino acid sequence of  $\gamma_{\text{CF}_1}$ . Residues 1–91 (1–95 by CF<sub>1</sub>- $\gamma$  numbering) are derived from the  $\gamma$  subunit of TF<sub>1</sub> (TF<sub>1</sub>- $\gamma$ ), residues 92–239 (bold letters) including the additional regulatory stretch (190–226) from the  $\gamma$  subunit of CF<sub>1</sub> (CF<sub>1</sub>- $\gamma$ ), and residues 240–319 again from the  $\gamma$  subunit of TF<sub>1</sub>. For comparison the domains resolved in a high resolution x-ray structure of bovine heart mitochondria F<sub>1</sub>-ATPase (MF<sub>1</sub>- $\gamma$ ) are shown (8). The long N-terminal and C-terminal helices form a coiled-coil interacting with the  $\alpha_3\beta_3$  hexagon. The closed boxes show the position of binding regions of the  $\epsilon$  subunit reported in Ref. 51.

CF <sub>1</sub> - $\gamma$	ANLRELDRIGSVKNTQKITEAMKLVAAKVRRAQEAIVNGRPFSETLVEVLYNMNEQLQTEVDVPLTK	10	20	30	40	50	60	70
TF <sub>1</sub> - $\gamma$	ASLRDIKTRINATKTSQITKAMEMVLTSKLNRAEKREI-VRPYMEKIQEVANVALAARASH---PMLV							
$\gamma$ (TCT)	ASLRDIKTRINATKTSQITKAMEMVLTSKLNRAEKREI-VRPYMEKIQEVANVALAARASH---PMLV							
MF <sub>1</sub> - $\gamma$	ASLRDIKTRINATKTSQITKAMEMVLTSKLNRAEKREI-VRPYMEKIQEVANVALAARASH---PMLV							
CF <sub>1</sub> - $\gamma$	IRTVKKVALMVVTGURGLCGGFNNMLLKKAESRIAEKKGVDVYTIISIGKKGNTYFIRREPEIPVDRIYD	80	90	100	110	120	130	140
TF <sub>1</sub> - $\gamma$	SRPVKKTGYLVITSDRGLAGAYNSNVLRLVYQTIQKRHASPEDEYAIIVIGRVGLSFFRKRNMPVILDIYR							
$\gamma$ (TCT)	SRPVKKTGYLVITSDRGLAGAYNSNVLRLVYQTIQKRHASPEDEYAIIVIGRVGLSFFRKRNMPVILDIYR							
MF <sub>1</sub> - $\gamma$	SRPVKKTGYLVITSDRGLAGAYNSNVLRLVYQTIQKRHASPEDEYAIIVIGRVGLSFFRKRNMPVILDIYR							
CF <sub>1</sub> - $\gamma$	GTNLPATAEAQAIADVVFSLFVSEEVKVEMLYTKFVSLVKSDFVHTLPLSPKGEICDINGKCVDAAE	150	160	170	180	190	200	210
TF <sub>1</sub> - $\gamma$	LDPQSPFADIKELARKTVGLFADGTFDELIMYNNHYVSAIQQEVTERKLLPLT-----PMLV							
$\gamma$ (TCT)	GTNLPATAEAQAIADVVFSLFVSEEVKVEMLYTKFVSLVKSDFVHTLPLSPKGEICDINGKCVDAAE							
MF <sub>1</sub> - $\gamma$	GTNLPATAEAQAIADVVFSLFVSEEVKVEMLYTKFVSLVKSDFVHTLPLSPKGEICDINGKCVDAAE							
CF <sub>1</sub> - $\gamma$	DELFLRTTKGKLTVERDMIKTETPAFSPILFEQDPAQILDALLPLYLNSQIIIRALQESLASELAARMT	220	230	240	250	260	270	280
TF <sub>1</sub> - $\gamma$	-----DLAENKQRTVYEFEPSPQEEILDVLLPQYAESLYGALLDAKASEHAARMT							
$\gamma$ (TCT)	DELFLRTTKGKLTVERDMIKTETPAFSPILFEQDPAQILDALLPLYLNSQIIIRALQESLASELAARMT							
MF <sub>1</sub> - $\gamma$	DELFLRTTKGKLTVERDMIKTETPAFSPILFEQDPAQILDALLPLYLNSQIIIRALQESLASELAARMT							
CF <sub>1</sub> - $\gamma$	AMSNATDNANELKKTLSINYNRRAQAKITGEILEIVAGANACV	290	300	310	320			
TF <sub>1</sub> - $\gamma$	AMKNATDNANELIKMTLSYNRRAQAATQETIIVAGANALQ							
$\gamma$ (TCT)	AMKNATDNANELIKMTLSYNRRAQAATQETIIVAGANALQ							
MF <sub>1</sub> - $\gamma$	AMKNATDNANELIKMTLSYNRRAQAATQETIIVAGANALQ							

equivalent part of the  $\gamma$  subunit from CF<sub>1</sub> including the regulatory cysteines (Fig. 1). The remaining parts derived from the TF<sub>1</sub>- $\gamma$  subunit mainly consists of the N-terminal and C-terminal  $\alpha$ -helices forming the coiled-coil and a small additional  $\alpha$ -helix. The chimeric  $\alpha_3\beta_3\gamma$  subcomplex was successfully overexpressed in *Escherichia coli* and purified as an active ATPase. Then we investigated the enzymatic property of this complex under reduced and oxidized conditions.

#### MATERIALS AND METHODS

**Chemicals**—Restriction enzymes were purchased from Toyobo Co., Tokyo, Japan. DTT and MOPS were from Nacalai Tesque, Kyoto, Japan. TNP-ATP was synthesized and purified by the method as described (29, 30). All other chemicals were of the highest grade commercially available.

**Bacterial Strains**—Plasmid amplification was carried out with *E. coli* strain JM 109, and single-stranded uracil-containing DNA was obtained from *E. coli* strain CJ 236, and for protein overexpression *E. coli* strain JM 103  $\Delta$ uncB-D was used.

**Plasmid Construction**—A DNA fragment coding for  $\alpha$ ,  $\gamma$  (S106C), and  $\beta$  (carrying an N-terminal tag of 10 histidine residues) subunits of TF<sub>1</sub> on the expression plasmid, pkkHisCys5 (14), was cloned into the multicloning site of the M13mp18 vector, and single-stranded uracil-containing DNA was obtained by the method of Ref. 31. The location for two silent mutations to construct NspV restriction sites was determined with the program MOTOJMAN provided by Fumihito Motojima, Tokyo Institute of Technology, and introduced by the method as described (31) using the primers 5'-CACGAGGCGCAGCAGTTCGAATTG-TACGCGCCAGC and 5'-TTCTTCTTGGCAGCGTTCCGAATTCGTACACCGTGCG. Then the DNA fragment coding the deduced  $\gamma$  subunit was cut out with the restriction enzymes *NheI* and *BglII* and cloned into the equivalent position between the genes for the  $\alpha$  and  $\beta$  subunits on the pkkHisCys5 vector.

A fragment of spinach chloroplast DNA coding for amino acid residues Leu<sup>96</sup>-Phe<sup>243</sup> of the  $\gamma$  subunit of CF<sub>1</sub> was amplified by the polymerase chain reaction method using the phosphorylated primers 5'-CGG-GATCCCGTTAGAAGTTGCTGAAGAAGGCTGAGTCTAGG and 5'-CGGGATCCCGTTTCCGAATTCAGAAATGGGGAAAATGCTGG with the vector containing the gene for the  $\gamma$  subunit of spinach CF<sub>1</sub> (27) as a template. The obtained DNA fragment was inserted by blunt-end ligation into pBluescript vector, which was previously digested with *SmaI*. Then the vector was digested with *NspV* to obtain a cohesive-end DNA fragment. Finally the above described pkkHisCys5 vector with two introduced *NspV* sites was digested with *NspV* and ligated with the cohesive-end DNA fragment to obtain the expression plasmid for  $\alpha_3\beta_3\gamma_{\text{TCT}}$  (pkkTCT vector). The correct orientation of the DNA fragment inserted into pkkTCT was confirmed by digestion with *NheI* and *AflII*.

**Overexpression and Protein Purification of  $\alpha_3\beta_3\gamma_{\text{TCT}}$  and  $\alpha_3\beta_3\gamma$  ( $\beta$ -His,  $\gamma$ S106C)**—pkkTCT was transformed into *E. coli* JM 103 strain, cultivated on LB medium agar plates containing 100  $\mu$ g/ml ampicillin, and then inoculated into the liquid culture. A 2-liter liquid culture in the same medium was harvested after 9 h cultivation. Cells were collected by centrifugation and disrupted by sonication. The superna-

tant was directly applied to a nickel-NTA (nitrilotriacetic acid) superflow column (Qiagen, Hilden, Germany) equilibrated with 50 mM MOPS-KOH, pH 7.0, 100 mM KCl, 5 mM MgCl<sub>2</sub>, and 10 mM imidazole. The column was washed with the same buffer containing 25 mM imidazole and then the enzyme was eluted with the same buffer containing 250 mM imidazole.

The recombinant  $\alpha_3\beta_3\gamma$  subcomplex of TF<sub>1</sub> containing a histidine tag on the N terminus of the  $\beta$  subunit and the substitution of Ser<sup>106</sup> of the  $\gamma$  subunit to Cys ( $\alpha_3\beta_3\gamma$  ( $\beta$ -His,  $\gamma$ S106C)) was expressed by using the pkkHisCys5 vector and purified by the method described (11).

**Preparation of the  $\epsilon$  Subunits**— $\epsilon$  subunit of TF<sub>1</sub> was overexpressed in *E. coli* and isolated as described (32). The recombinant  $\epsilon$  subunit of CF<sub>1</sub> was expressed as an inclusion body and purified (27). Prior to use, the folded  $\epsilon$  subunit of CF<sub>1</sub> was prepared as follows: the inclusion body was solved with 8 M urea, 50 mM Tris-Cl, pH 8.0, 1 mM EDTA, and 0.5 mM DTT and dialyzed against 50 mM MOPS-KOH, pH 7.0, 100 mM KCl, and 5 mM MgCl<sub>2</sub> for 6 h.

**Preparation of the Recombinant Trx-f**—Spinach chloroplast Trx-f was overexpressed in *E. coli* and isolated as described (21). The concentration of the purified Trx-f was determined by the measurement of the absorbance at 278 nm using the published molar absorption coefficient value of 16,830 M<sup>-1</sup>cm<sup>-1</sup> (33).

**ATP Hydrolysis Activity**—ATP hydrolysis activity was measured in the presence of an ATP regenerating system (34) with a spectrophotometer model U-3100 (Hitachi, Tokyo, Japan) equipped with a stirrer. The reaction mixture containing 50 mM MOPS-KOH, 100 mM KCl, 5 mM MgCl<sub>2</sub>, 2 mM phosphoenolpyruvate, 2 mM ATP, 50  $\mu$ g/ml pyruvate kinase, 50  $\mu$ g/ml lactate dehydrogenase, and 0.2 mM NADH was used. After a base line was monitored for 1–2 min, the reaction was initiated by the addition of 5–10  $\mu$ g of  $\alpha_3\beta_3\gamma_{\text{TCT}}$ , and the activity was measured by monitoring the decrease of NADH absorption at 340 nm at 25 °C.

In the case where the ATP regenerating system was not applicable, the activity was measured by quantifying the amount of produced phosphate (35). 80  $\mu$ l of 50 mM MOPS-KOH, pH 7.0, 100 mM KCl, 5 mM MgCl<sub>2</sub>, and 2 mM ATP were incubated in a water bath for 2 min, and then the reaction was started by the addition of 20  $\mu$ l (2  $\mu$ g) of  $\alpha_3\beta_3\gamma_{\text{TCT}}$ . After 2 min, the reaction was quenched by the addition of 100  $\mu$ l of 2.4% (w/v) trichloroacetic acid. The reaction was carried out at 25 °C unless stated otherwise.

**Inhibition by the  $\epsilon$  Subunit- $\alpha_3\beta_3\gamma_{\text{TCT}}$  or  $\alpha_3\beta_3\gamma$  ( $\beta$ -His,  $\gamma$ S106C)** were mixed with the  $\epsilon$  subunit of CF<sub>1</sub> or TF<sub>1</sub> and incubated for 1 h at room temperature. The mixture was then directly applied to the ATP hydrolysis assay using an ATP regenerating system as described above.

**ATP Hydrolysis Under Uni-site Conditions**— $\alpha_3\beta_3\gamma_{\text{TCT}}$  was oxidized with 50  $\mu$ M CuCl<sub>2</sub> or reduced with 15 mM DTT for 1 h at 30 °C. DTT in the sample was removed by an HPLC gel filtration column (TSK 3000SW<sub>XL</sub>, Tosoh Co., Tokyo, Japan) equilibrated with 50 mM MOPS-KOH, pH 7.0, 100 mM KCl, and 5 mM MgCl<sub>2</sub> because DTT directly affected the following quantitative measurement of nucleotides. This step also reduced the amount of intrinsically bound nucleotides from 0.8 mol ADP/mol  $\alpha_3\beta_3\gamma_{\text{TCT}}$  to <0.1 mol ADP/mol  $\alpha_3\beta_3\gamma_{\text{TCT}}$ . Each of the complexes was diluted to a protein concentration of 700 nM. A 50- $\mu$ l aliquot was preincubated in a 25 °C water bath and then mixed with the same volume of 150 nM TNP-ATP. At the indicated period the reaction was terminated by addition of 5  $\mu$ l of 24% (w/v) trichloroacetic acid. The

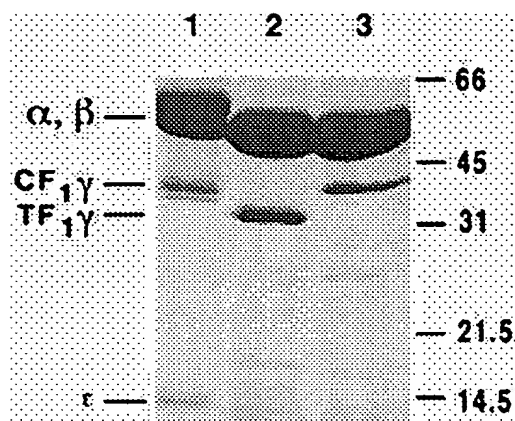


FIG. 2. Gel electrophoresis of purified  $\alpha_3\beta_3\gamma_{(TCT)}$ . Purity and the subunit composition of the complex  $\alpha_3\beta_3\gamma_{(TCT)}$  was analyzed by SDS-gel electrophoresis. A 15% (w/v) polyacrylamide gel was used. Each lane contained 15  $\mu$ g of proteins. Lane 1, CF<sub>1</sub>; lane 2,  $\alpha_3\beta_3\gamma$  ( $\beta$ -His,  $\gamma$ S106C); lane 3,  $\alpha_3\beta_3\gamma_{(TCT)}$ . Bars indicate positions of molecular mass markers (kDa).

amounts of TNP-ATP and TNP-ADP were determined by reversed-phase HPLC (35). In case of chase acceleration experiments, 10  $\mu$ l of 100  $\mu$ M ATP was added instead of trichloroacetic acid and incubated for further 10 s. Then the reaction was stopped by the addition of trichloroacetic acid as stated above.

**Gel Electrophoresis**—Polyacrylamide gel electrophoresis in the presence of SDS was performed according to Laemmli (36). Protein bands were visualized by the staining with Coomassie Brilliant Blue R-250.

## RESULTS

**Preparation and Purification of  $\alpha_3\beta_3\gamma_{(TCT)}$** — $\alpha_3\beta_3\gamma_{(TCT)}$  was overexpressed in *E. coli* JM 103 and purified by Ni-NTA affinity chromatography. The purity of the protein and the occurrence of the individual subunits in the complex were confirmed by SDS-gel electrophoresis (Fig. 2). The yield of  $\alpha_3\beta_3\gamma_{(TCT)}$  complex was about 80 mg of protein from a 2-liter *E. coli* culture, comparable to the yield of wild type  $\alpha_3\beta_3\gamma$  (7) or  $\alpha_3\beta_3\gamma$  ( $\beta$ -His,  $\gamma$ S106C) (14).

The molecular mass of the  $\gamma$  subunit in the  $\alpha_3\beta_3\gamma_{(TCT)}$  complex was about 35 kDa, clearly larger than the  $\gamma$  subunit of  $\alpha_3\beta_3\gamma$  ( $\beta$ -His,  $\gamma$ S106C) but very similar to the  $\gamma$  subunit of CF<sub>1</sub> (Fig. 2), indicating the successful expression and the formation of the complex with the mutant  $\gamma$  subunit.

**Modulation of Activity by Oxidation and Reduction**—The activity of ATP hydrolysis catalyzed by the purified  $\alpha_3\beta_3\gamma_{(TCT)}$  was measured spectrophotometrically by the pyruvate kinase/lactate dehydrogenase assay that provides continuous regeneration of ATP. Upon addition of oxidized and reduced  $\alpha_3\beta_3\gamma_{(TCT)}$  to the reaction mixture, ATP hydrolysis proceeded in a linear manner for at least 10 min without time-dependent inactivation (Fig. 3A), but the rates were different as follows:  $\alpha_3\beta_3\gamma_{(TCT)}$  was clearly activated by preincubation with DTT. When DTT alone was used for reduction, up to 2-fold activation was obtained (Fig. 3, A and B). Activation was saturated at 15 mM DTT (Fig. 3B). Extension of the preincubation time for more than 1 h did not significantly increase activation. Interestingly, the activation was higher if reduction was carried out with a combination of DTT and Trx-f (Fig. 3, A and B). When ATP hydrolysis reaction was initiated by addition of oxidized  $\alpha_3\beta_3\gamma_{(TCT)}$  and 15 mM DTT plus 500 nM Trx-f (final concentration) was added to the reaction mixture after 5 min, remarkable activation could be observed within several minutes (Fig. 3A, inset). The concentration of Trx-f for half-maximal activation was about 200 nM (Fig. 3B, inset), considerably lower than that for authentic CF<sub>1</sub>, which was more than 1  $\mu$ M (21). The specific activity of  $\alpha_3\beta_3\gamma_{(TCT)}$  in the oxidized state was 1.0–1.2

units/mg, and upon reduction with 15 mM DTT it increased to 2.2–2.6 units/mg, and with 15 mM DTT plus 500 nM Trx-f 3.0–3.3 units/mg were measured. Quantification of thiol groups indicated additional 1.6–1.9 mol of SH/mol of  $\alpha_3\beta_3\gamma_{(TCT)}$  after reduction with 15 mM DTT and additional 1.7–2.0 mol of SH/mol of  $\alpha_3\beta_3\gamma_{(TCT)}$  after reduction with 15 mM DTT plus 500 nM Trx-f.

The specific activity of  $\alpha_3\beta_3\gamma_{(TCT)}$  in the fully reduced state under the reaction conditions above (pH 7.0) was comparable to that of  $\alpha_3\beta_3\gamma$  ( $\beta$ -His,  $\gamma$ S106C) under the same conditions (4.5 units/mg). The pH optimum was between 8.5 and 9.0, similar to the values reported for wild type  $\alpha_3\beta_3\gamma$  (7), for TF<sub>1</sub> (37), and for CF<sub>1</sub> (38).

**Thermostability of  $\alpha_3\beta_3\gamma_{(TCT)}$** —The optimum temperature of the ATPase activity of oxidized and reduced  $\alpha_3\beta_3\gamma_{(TCT)}$  was at 70 °C, the same as that of  $\alpha_3\beta_3\gamma$  ( $\beta$ -His,  $\gamma$ S106C) (Fig. 4) and comparable to the values reported for wild type TF<sub>1</sub> and  $\alpha_3\beta_3\gamma$  (7). The ratio between the activities of oxidized and reduced  $\alpha_3\beta_3\gamma_{(TCT)}$  did not change significantly over the whole temperature range investigated.

**Interaction with the  $\epsilon$  Subunit**—The effect of the inhibitory  $\epsilon$  subunit of CF<sub>1</sub> and that of TF<sub>1</sub> on  $\alpha_3\beta_3\gamma_{(TCT)}$  was investigated (Fig. 5A). ATPase activity of  $\alpha_3\beta_3\gamma_{(TCT)}$  in its oxidized state was inhibited to 50–60% by the  $\epsilon$  subunit of CF<sub>1</sub>. Interestingly,  $\alpha_3\beta_3\gamma_{(TCT)}$  in its reduced state was nearly insensitive to the CF<sub>1</sub>- $\epsilon$  subunit, resulting in about a 4-fold higher activity compared with  $\alpha_3\beta_3\gamma_{(TCT)}$  in the oxidized state in the presence of the CF<sub>1</sub>- $\epsilon$  subunit. As reported previously, neither the CF<sub>1</sub>- $\epsilon$  subunit nor the TF<sub>1</sub>- $\epsilon$  subunit had any significant effect on the activity of  $\alpha_3\beta_3\gamma$  ( $\beta$ -His,  $\gamma$ S106C) when the ATP concentration was relatively high (32). However, a slight but significant increase of activity was observed upon incubation of oxidized  $\alpha_3\beta_3\gamma_{(TCT)}$  with the TF<sub>1</sub>- $\epsilon$  subunit (Fig. 5A). Again, this effect was less pronounced for  $\alpha_3\beta_3\gamma_{(TCT)}$  in the reduced form.

To clarify the cause of the weakly stimulating effect of the  $\epsilon$  subunit of TF<sub>1</sub> on ATPase activity of  $\alpha_3\beta_3\gamma_{(TCT)}$ , we examined its binding to the complex. After incubation with  $\epsilon$  subunit of TF<sub>1</sub>, the complex was separated from unbound  $\epsilon$  subunit by gel filtration HPLC. The  $\alpha_3\beta_3\gamma_{(TCT)}$  fraction was then applied to SDS-PAGE (Fig. 5B).  $\alpha_3\beta_3\gamma_{(TCT)}$  in the oxidized state as well as in the reduced state could bind the  $\epsilon$  subunit of TF<sub>1</sub> in an approximately stoichiometric ratio, comparable to  $\alpha_3\beta_3\gamma$  ( $\beta$ -His,  $\gamma$ S106C) under identical conditions.

**ATP Hydrolysis Under Uni-site Conditions**—When a stoichiometric molar ratio of TNP-ATP was added to the oxidized or reduced  $\alpha_3\beta_3\gamma_{(TCT)}$  complexes, the ATP analogue was slowly hydrolyzed. With both complexes it took 20 s to hydrolyze 50% of added TNP-ATP (Fig. 6). An interesting difference was observed upon the addition of chase ATP. Whereas hydrolysis of TNP-ATP by reduced  $\alpha_3\beta_3\gamma_{(TCT)}$  was greatly accelerated by ATP, comparable to wild type  $\alpha_3\beta_3\gamma$  (32) and  $\alpha_3\beta_3\gamma$  ( $\beta$ S1389C) (39), chase promotion was obviously lower in the case of the oxidized  $\alpha_3\beta_3\gamma_{(TCT)}$ .

## DISCUSSION

In this study, an expression plasmid for an  $\alpha_3\beta_3\gamma$  subcomplex of TF<sub>1</sub> containing a TF<sub>1</sub>/CF<sub>1</sub> chimeric  $\gamma$  subunit ( $\alpha_3\beta_3\gamma_{(TCT)}$ ) was constructed, and the desired protein complex was successfully overexpressed and purified with a yield comparable to those of wild type  $\alpha_3\beta_3\gamma$  (7) or  $\alpha_3\beta_3\gamma$  ( $\beta$ -His,  $\gamma$ S106C) (14). This proves that combining two halves of  $\gamma$  subunits from different organisms and the insertion of additional amino acid residues from the  $\gamma$  subunit of CF<sub>1</sub> into the central part of the  $\gamma$  subunit of TF<sub>1</sub> are no major obstacles for biosynthesis and *in vivo* stability of this protein complex in the employed expression system. Thus, although the homology between the transferred part of CF<sub>1</sub>- $\gamma$  subunit and the replaced part of the TF<sub>1</sub>- $\gamma$  sub-

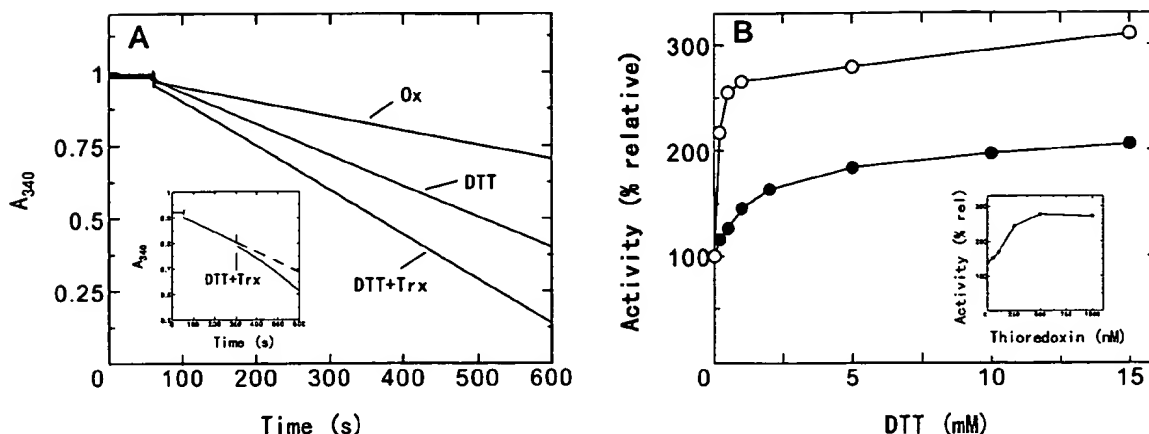


FIG. 3. Effect of DTT and Trx on ATPase activity of  $\alpha_3\beta_3\gamma_{(TCT)}$ . A, ATPase activity was measured using an ATP regenerating system monitoring the decrease of NADH absorption at 340 nm. Samples were preincubated for 1 h with 50  $\mu$ M CuCl<sub>2</sub> (Ox), 15 mM DTT (DTT), or with 15 mM DTT + 500 nM Trx-f (DTT+Trx) in 50 mM MOPS-KOH, pH 7.0, supplemented with 100 mM KCl and 5 mM MgCl<sub>2</sub>. The ATPase activity without incubation with DTT or Trx was 1.1 unit/mg and set as 100%. Inset, real time activation of oxidized  $\alpha_3\beta_3\gamma_{(TCT)}$  by addition of 15 mM DTT + 500 nM Trx-f at the indicated time. The dashed line shows the time course without addition of DTT and Trx-f. B, dependence of ATPase activity of  $\alpha_3\beta_3\gamma_{(TCT)}$  on the DTT concentration. Closed circles, X mM DTT; open circles, X mM DTT + 500 nM Trx-f. Inset, dependence of activation on Trx-f concentration in the presence of 1 mM DTT. For details see under "Materials and Methods."

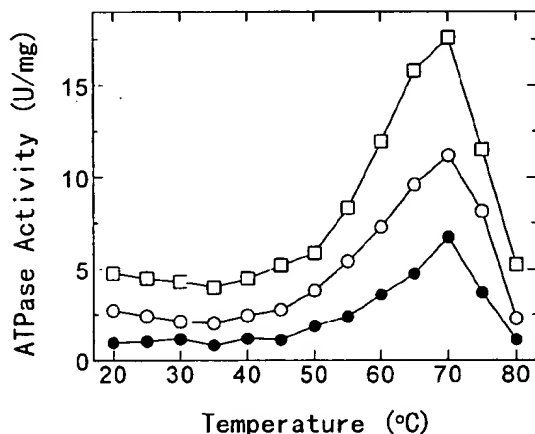


FIG. 4. Thermostability of  $\alpha_3\beta_3\gamma_{(TCT)}$ . ATPase activity was measured in the absence of an ATP regenerating system at the indicated temperatures in 50 mM MOPS-KOH, pH 7.0, supplemented with 100 mM KCl and 5 mM MgCl<sub>2</sub>. Produced phosphate was quantified by the method described (21). Closed circles,  $\alpha_3\beta_3\gamma_{(TCT)}$  oxidized with 50  $\mu$ M CuCl<sub>2</sub>; open circles,  $\alpha_3\beta_3\gamma_{(TCT)}$  reduced with 15 mM DTT; open squares,  $\alpha_3\beta_3\gamma$  ( $\beta$ -His,  $\gamma$ S106C).

unit was only about 15% on the amino acid level, proper folding of the  $\gamma$  subunit and insertion into the  $\alpha_3\beta_3$  hexagon appears to be unaffected. This is consistent with a recently published intermediate-resolution x-ray structure of *E. coli* F<sub>1</sub>, which indicated that four  $\alpha$ -helices, thought to be comprised by the central amino acid residues of the  $\gamma$  subunit (roughly *E. coli* F<sub>1</sub>  $\gamma$ 100–200, corresponding to residues 100–235 of  $\gamma_{(TCT)}$ ) are located at the tip of the enzyme and not in interaction with the  $\alpha_3\beta_3$  hexagon (40).

The ATPase activity of the  $\alpha_3\beta_3\gamma_{(TCT)}$  complex was modulated by the reduction or oxidation of the two cysteines that were introduced by the insertion of the respective part of the CF<sub>1</sub>- $\gamma$  subunit. An up to 3-fold activation could be observed by the complete reduction of these cysteines (Fig. 3). As this activation ratio is in the same range as that reported for CF<sub>1</sub> (3–7-fold) (19–22), most likely the mechanism of thiol activation is the same in the  $\alpha_3\beta_3\gamma_{(TCT)}$  complex. Sokolov *et al.* (41) recently proposed that the conformation of the  $\gamma$  subunit of CF<sub>1</sub> may be different from other F<sub>1</sub>- $\gamma$  subunits. Their conclusion is based on former results of energy transfer measurements be-

tween  $\gamma$  subunit and the catalytic sites on  $\beta$  subunits (42, 43) and their investigation of the ATPase activity of a complex formed from the isolated CF<sub>1</sub>  $\alpha_3\beta_3$  subcomplex and recombinant  $\gamma$  subunit of which the C terminus was partially deleted. In their model, the tip of the C terminus of the  $\gamma$  subunit does not act as a spindle for rotation. However, our results indicate that a bacterial  $\gamma$  subunit can be transformed into a functional chloroplast-like  $\gamma$  subunit. Thus the essential structural features and basic functions of both types of  $\gamma$  subunits should be the same. This is also consistent with previous reports that upon introduction of the chloroplast  $\gamma$ -like regulatory stretch into the  $\gamma$  subunit of cyanobacterial F<sub>1</sub> conferred thiol modulation on this enzyme (23, 24). In this mutant both ATP hydrolysis and ATP synthesis are controlled by thiol modulation. Furthermore, ATP hydrolysis activity of a reconstituted chimeric complex containing the  $\alpha$  and  $\beta$  subunits of TF<sub>1</sub>, and the  $\gamma$  subunit of CF<sub>1</sub> ( $\alpha_{T3}\beta_{T3}\gamma_C$ ), was regulated by thiol modulation (27, 28) although the complex showed reduced stability.

Interestingly, a higher degree of activation of the complex  $\alpha_3\beta_3\gamma_{(TCT)}$  could be achieved with a mixture of DTT and Trx-f than with DTT alone (Fig. 3B), although we could not detect a significant difference in the amount of reduced thiol groups. This is consistent with our recently proposed model that a conformational change, which affects the enzyme activity, is induced by the interaction with Trx-f (21).

The measurement of the temperature optimum of ATPase activity shows that  $\alpha_3\beta_3\gamma_{(TCT)}$ , similar to  $\alpha_3\beta_3\gamma$  ( $\beta$ -His,  $\gamma$ S106C), is more stable than a chimeric  $\alpha_{T3}\beta_{T3}\gamma_C$ , which displayed the highest activity at 55–60 °C (Fig. 4, compare with Fig. 2 of Ref. 27). This result implies that the introduction of the 148 amino acid residues from a mesophilic enzyme does not affect thermostability of the complex significantly. The most probable explanation is that the interaction between the coiled-coil structure of  $\gamma$  subunit and the inner surface of the cavity of  $\alpha_3\beta_3$  hexagon is especially important for the stability of the complex. Although the homology of this coiled-coil region of the  $\gamma$  subunit is relatively high (27), some varying amino acid residues in the coiled-coil region might be very important for the stability of the complex. Activation by DTT was not affected by the temperature, so although thiol modulation *in vivo* usually occurs at temperatures <30 °C in plants, it is also functional at temperatures as high as 80 °C.

The  $\epsilon$  subunit is known to be an inhibitory subunit of F<sub>1</sub>-



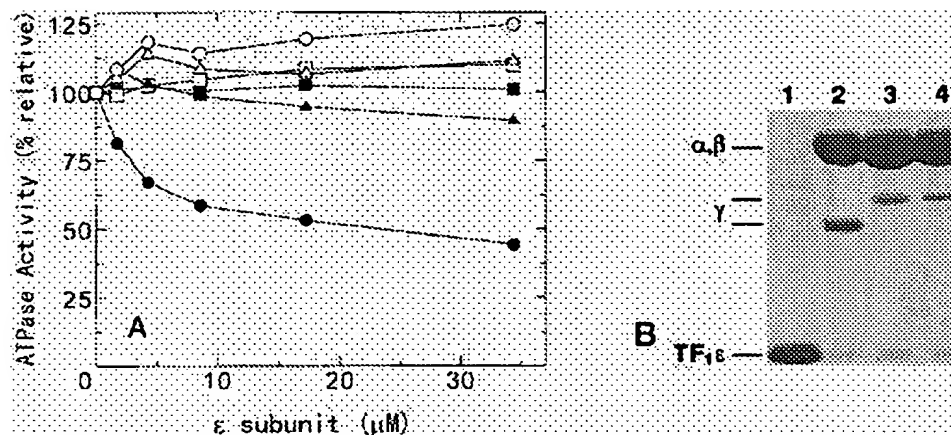


FIG. 5. Interaction of  $\alpha_3\beta_3\gamma_{TCT}$  with the  $\epsilon$  subunit of F<sub>1</sub>-ATPase. A, influence of the  $\epsilon$  subunits on ATP hydrolysis activity. Samples were oxidized with 50  $\mu$ M CuCl<sub>2</sub> (circles) or reduced with 15 mM dithiothreitol (triangles) and then mixed with the indicated amounts of the  $\epsilon$  subunit either from CF<sub>1</sub> (closed symbols) or from TF<sub>1</sub> (open symbols). ATPase activity was measured by an ATP regenerating system; the ATPase activities of  $\alpha_3\beta_3\gamma_{TCT}$  in the absence of any  $\epsilon$  subunit were 1.1 and 2.3 units/mg for  $\alpha_3\beta_3\gamma_{TCT}$  oxidized by CuCl<sub>2</sub> and reduced by DTT, respectively, and were set as 100%.  $\alpha_3\beta_3\gamma$  ( $\beta$ -His,  $\gamma$ S106C) (squares) was used as control. B, binding of TF<sub>1</sub>- $\epsilon$  to  $\alpha_3\beta_3\gamma_{TCT}$  was examined. B, isolated  $\alpha_3\beta_3\gamma_{TCT}$  and  $\alpha_3\beta_3\gamma$  ( $\beta$ -His,  $\gamma$ S106C) were mixed with TF<sub>1</sub>- $\epsilon$ , passed through a gel filtration HPLC, and then applied to 12% (w/v) SDS-PAGE. Lane 1, TF<sub>1</sub>- $\epsilon$ ; lane 2,  $\alpha_3\beta_3\gamma$  ( $\beta$ -His,  $\gamma$ S106C) + TF<sub>1</sub>- $\epsilon$ ; lane 3,  $\alpha_3\beta_3\gamma_{TCT}$  (oxidized) + TF<sub>1</sub>- $\epsilon$ ; lane 4,  $\alpha_3\beta_3\gamma_{TCT}$  (reduced) + TF<sub>1</sub>- $\epsilon$ .

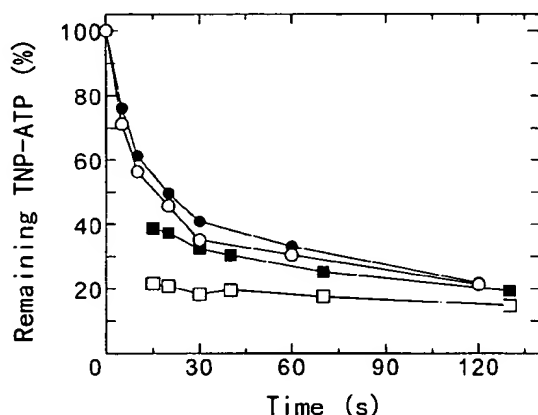


FIG. 6. Time course of hydrolysis of TNP-ATP by  $\alpha_3\beta_3\gamma_{TCT}$ .  $\alpha_3\beta_3\gamma_{TCT}$  was oxidized with 50  $\mu$ M CuCl<sub>2</sub> (closed symbols) or reduced with 15 mM DTT plus 500 nM Trx (open symbols). 350 nM  $\alpha_3\beta_3\gamma_{TCT}$  was incubated with 75 nM TNP-ATP at 25 °C for the indicated reaction period. The results of acid quench (circles) and chase acceleration (squares) were obtained from the measurement of remaining TNP-ATP and produced TNP-ADP by reversed-phase HPLC as described (35).

ATPases. It has been proposed that the C-terminal helical domain of the  $\epsilon$  subunit is mainly responsible for the inhibitory function (44–48). As the  $\epsilon$  subunit could be cross-linked to the  $\beta$  subunit (49, 50), the inhibition may be achieved by binding to the DELSEED region of the  $\beta$  subunit. We found that the  $\epsilon$  subunit of CF<sub>1</sub> can efficiently inhibit the ATPase activity of  $\alpha_3\beta_3\gamma_{TCT}$  but not that of  $\alpha_3\beta_3\gamma$  ( $\beta$ -His,  $\gamma$ S106C), although the  $\alpha$  and  $\beta$  subunits are identical (Fig. 5). This induces the conclusion that an interaction of the  $\epsilon$  subunit with the  $\gamma$  subunit may be more crucial for inhibition, possibly by providing proper binding and orientation of the  $\epsilon$  subunit. As the sequence of the amino acid residues 92–239 of the  $\gamma$  subunit of  $\alpha_3\beta_3\gamma_{TCT}$  is different from  $\alpha_3\beta_3\gamma$  ( $\beta$ -His,  $\gamma$ S106C), it can be concluded that this region confers the sensitivity to inhibition by the  $\epsilon$  subunit. Consistent with this finding, *E. coli* F<sub>1</sub> residue  $\gamma$ 106 and the region  $\gamma$ 202–212 have previously been found to be involved in binding of the  $\epsilon$  subunit by cross-linking and chemical labeling experiments (51). *E. coli* F<sub>1</sub>- $\gamma$ 106 corresponds to  $\gamma_{TCT}$ 101, near the N-terminal part of the insertion from CF<sub>1</sub>,  $\gamma$ 202–212 corresponds to  $\gamma_{TCT}$  234–244, located at the C terminus of the insertion (Fig. 1). Taken together, the part of the  $\gamma$  subunit that

is of chloroplast origin in  $\gamma_{TCT}$  appears to be crucial for binding of and inhibition by the  $\epsilon$  subunit.

As supposed from the suggested mechanism for the uni-site catalysis (29, 30), no significant differences could be detected in the rate of uni-site hydrolysis by oxidized or by reduced  $\alpha_3\beta_3\gamma_{TCT}$ . However, we found a difference in chase acceleration of hydrolysis of TNP-ATP by the addition of excess amounts of ATP (Fig. 6). The range of the chase acceleration for the reduced  $\alpha_3\beta_3\gamma_{TCT}$  was comparable to that published for TF<sub>1</sub> (35), wild type  $\alpha_3\beta_3\gamma$  (32), and  $\alpha_3\beta_3\gamma$  ( $\beta$ I389C) (39). However, significantly lower acceleration was observed for the oxidized  $\alpha_3\beta_3\gamma_{TCT}$ , indicating an impaired interplay between the catalytic sites in the suppressed activity state caused by the formation of the disulfide bridge between Cys<sup>199</sup> and Cys<sup>205</sup> of the  $\gamma$  subunit. The regulation of the enzyme activity might be attributed to this difference observed at the chase acceleration level.

The chimeric subcomplex  $\alpha_3\beta_3\gamma_{TCT}$  combines the property of thiol modulation, a unique feature of CF<sub>1</sub>-ATPase, with the stability and relative ease of genetic manipulation of the TF<sub>1</sub>-ATPase. It is therefore a very promising tool to investigate the structural basis and functional analyses of thiol modulation more in detail. Further experiments in this direction are under way in our laboratory.

**Acknowledgments**—We thank E. Munezaki, T. Suzuki, Y. Kato-Yamada, F. Motojima, T. Masaike, S. P. Tsunoda, and K. Hara for their technical assistance and helpful discussions. We particularly thank Prof. H. Strotmann (Heinrich-Heine University, Düsseldorf, Germany) and Prof. K. Kinoshita (Keio University) for critically reading the manuscript.

#### REFERENCES

1. Futai, M., and Kanazawa, H. (1983) *Microbiol. Rev.* 47, 285–312
2. Strotmann, H., and Bickel-Sandkötter, S. (1984) *Annu. Rev. Plant Physiol.* 35, 97–120
3. Senior, A. E. (1990) *Annu. Rev. Biophys. Chem.* 19, 7–41
4. Boyer, P. D. (1997) *Annu. Rev. Biochem.* 66, 717–749
5. Yoshida, M., Sone, N., Hirata, H., and Kagawa, Y. (1977) *J. Biol. Chem.* 252, 3480–3485
6. Fillingame, R. H. (1990) in *The Bacteria: A Treatise on Structure and Function* (Kruschwitz, T. A., ed) Vol. 12, pp. 345–391, Academic Press, New York
7. Matsui, T., and Yoshida, M. (1995) *Biochim. Biophys. Acta* 1231, 139–146
8. Abrahams, J. P., Leslie, A. G. W., Lutter, R., and Walker, J. E. (1994) *Nature* 370, 621–628
9. Shirakihara, Y., Leslie, A. G., Abrahams, J. P., Walker, J. E., Ueda, T., Sekimoto, Y., Kambara, M., Saika, K., Kagawa, Y., and Yoshida, M. (1997) *Structure* 15, 825–836
10. Kaibara, C., Matsui, T., Hisabori, T., and Yoshida, M. (1996) *J. Biol. Chem.* 271, 2433–2438

11. Boyer, P. D. (1993) *Biochim. Biophys. Acta* **1088**, 215-250
12. Duncan, T. M., Bulygin, V. V., Zhou, Y., Hutcheon, M. L., and Cross, R. L. (1995) *Proc. Natl. Acad. Sci. U. S. A.* **92**, 10964-10968
13. Sabbert, D., Engelbrecht, S., and Junge, W. (1996) *Nature* **381**, 623-625
14. Noji, H., Yasuda, R., Yoshida, M., and Kinosita, K., Jr. (1997) *Nature* **388**, 299-302
15. Noji, H., Häslar, K., Junge, W., Kinosita, K., Jr., Yoshida, M., and Engelbrecht, S. (1999) *Biochem. Biophys. Res. Commun.* **260**, 597-599
16. Omote, H., Sambonmatsu, N., Saito, K., Sambongi, Y., Iwamoto-Kihara, A., Yanagida, T., Wada, Y., and Futai, M. (1999) *Proc. Natl. Acad. Sci. U. S. A.* **96**, 7780-7784
17. Hisabori, T., Kondoh, A., and Yoshida, M. (1999) *FEBS Lett.* **463**, 35-38
18. Miki, J., Maeda, M., Mukohata, Y., and Futai, M. (1988) *FEBS Lett.* **232**, 221-226
19. Nalin, C. M., and McCarty, R. E. (1984) *J. Biol. Chem.* **259**, 7275-7280
20. Schwarz, O., Schürmann, P., and Strotmann, H. (1997) *J. Biol. Chem.* **272**, 16924-16927
21. Stumpp, M. T., Motohashi, K., and Hisabori, T. (1999) *Biochem. J.* **341**, 157-163
22. Creczynski-Pasa, T. B., and Graber, P. (1994) *FEBS Lett.* **350**, 195-198
23. Werner-Grüne, S., Gunkel, D., Schürmann, J., and Strotmann, H. (1994) *Mol. Gen. Genet.* **244**, 144-150
24. Krenn, B. E., Ardewijn, P., Van Walraven, H. S., Werner-Grüne, S., and Strotmann, H. (1995) *Biochem. Soc. Trans.* **23**, 757-760
25. Ross, S. A., Zhang, M. X., and Selman, B. R. (1995) *J. Biol. Chem.* **270**, 9813-9818
26. Ross, S. A., Zhang, M. X., and Selman, B. R. (1996) *J. Bioenerg. Biomembr.* **28**, 49-57
27. Hisabori, T., Kato, Y., Motohashi, K., Kroth-Pancic, P., Strotmann, H., and Amano, T. (1997) *Eur. J. Biochem.* **247**, 1158-1165
28. Hisabori, T., Motohashi, K., Kroth, P., Strotmann, H., and Amano, T. (1998) *J. Biol. Chem.* **273**, 15901-15905
29. Hiratsuka, A., and Uchida, K. (1973) *Biochim. Biophys. Acta* **320**, 635-647
30. Grubmeyer, C., and Penefsky, H. S. (1981) *J. Biol. Chem.* **256**, 3718-3727
31. Kunkel, T. A., Bebenk, K., and McClary, J. (1991) *Methods Enzymol.* **204**, 125-139
32. Kato, Y., Matsui, T., Tanaka, N., Muneyuki, E., Hisabori, T., and Yoshida, M. (1997) *J. Biol. Chem.* **272**, 24906-24912
33. Schürmann, P. (1995) *Methods Enzymol.* **252**, 274-283
34. Stiggal, D. L., Galante, Y. M., and Hatefi, Y. (1979) *Methods Enzymol.* **55**, 308-315
35. Hisabori, T., Muneyuki, E., Odaka, M., Yokoyama, K., Mochizuki, K., and Yoshida, M. (1992) *J. Biol. Chem.* **267**, 4551-4556
36. Laemmli, U. K. (1970) *Nature* **227**, 680-685
37. Yoshida, M., Sone, N., Hirata, H., and Kagawa, Y. (1975) *J. Biol. Chem.* **250**, 7910-7916
38. Sakurai, H., Shinohara, K., Hisabori, T., and Shinohara, K. (1981) *J. Biochem. (Tokyo)* **90**, 95-102
39. Tsunoda, S. P., Muneyuki, E., Amano, T., Yoshida, M., and Noji, H. (1999) *J. Biol. Chem.* **274**, 5701-5706
40. Hausrath, A. C., Gruber, G., Matthews, B. W., and Capaldi, R. A. (1999) *Proc. Natl. Acad. Sci. U. S. A.* **96**, 13697-13702
41. Sokolov, M., Lu, L., Tucker, W., Gao, F., Gegenheimer, P. A., and Richter, M. L. (1999) *J. Biol. Chem.* **274**, 13824-13829
42. Moroney, J. V., and McCarty, R. E. (1979) *J. Biol. Chem.* **254**, 8951-8955
43. Richter, M. L., Snyder, B., McCarty, R. E., and Hanmes, G. G. (1985) *Biochemistry* **24**, 5755-5763
44. Kuki, M., Noumi, T., Maeda, M., Amemura, A., and Futai, M. (1988) *J. Biol. Chem.* **263**, 17437-17442
45. Xiong, H., Zhang, D., and Vik, S. B. (1998) *Biochemistry* **37**, 16423-16429
46. Kato-Yamada, Y., Bald, D., Koike, M., Motohashi, K., Hisabori, T., and Yoshida, M. (1999) *J. Biol. Chem.* **274**, 33991-33994
47. Cruz, J. A., Harfe, B., Radkowski, C. A., Dann, M. S., and McCarty, R. E. (1995) *Plant Physiol. (Bethesda)* **109**, 1379-1388
48. Hisabori, T., Motohashi, K., Koike, M., Kroth, P., Strotmann, H., and Amano, T. (1998) in *Photosynthesis: Mechanisms and Effects* (Garab, G., ed) Vol. 3, pp. 1711-1714, Kluwer Academic Publishers Group, Dordrecht, Netherlands
49. Dallmann, H. G., Flynn, T. G., and Dunn, S. D. (1992) *J. Biol. Chem.* **267**, 18953-18960
50. Aggeler, R., Haughton, M. A., and Capaldi, R. A. (1995) *J. Biol. Chem.* **270**, 9185-9191
51. Tang, C., and Capaldi, R. A. (1996) *J. Biol. Chem.* **271**, 3018-3024

# The $\gamma$ subunit in chloroplast $F_1$ -ATPase can rotate in a unidirectional and counter-clockwise manner

Toru Hisabori<sup>a,\*</sup>, Aiko Kondoh<sup>a</sup>, Masasuke Yoshida<sup>a,b</sup>

<sup>a</sup>Research Laboratory of Resources Utilization, Tokyo Institute of Technology, Nagatsuta 4259, Midori-ku, Yokohama 226-8503, Japan

<sup>b</sup>CREST (Core Research for Evolutional Science and Technology) 'Genetic Programming' Team 13, Teikyo University Biotechnology Research center, Miyamae-ku, Kawasaki 216-0001, Japan

Received 9 November 1999

Edited by Ulf-Ingo Flügge

**Abstract** Rotation of the  $\gamma$  subunit in chloroplast  $F_1$ -ATPase ( $CF_1$ ) was investigated by using a single molecule observation technique, which is developed by Noji et al. to observe the rotation of a central  $\gamma$  subunit portion in the  $\alpha_3\beta_3\gamma$  sub-complex of  $F_1$ -ATPase from thermophilic *Bacillus* PS3 ( $TF_1$ ) during ATP hydrolysis [Noji, H. et al. (1997) *Nature* 386, 299–302]. We used two cysteines of the  $\gamma$  subunit (Cys-199 and Cys-205) of  $CF_1$ -ATPase, which are involved in the regulation of this enzyme, to fix the fluorochrome-labeled actin filament. Then we successfully observed a unidirectional, counter-clockwise rotation of the actin filament with the fluorescent microscope indicating the rotation of the  $\gamma$  subunit in  $CF_1$ -ATPase. We conclude that the rotation of the  $\gamma$  subunit in the  $F_1$ -motor is a ubiquitous phenomenon in all  $F_1$ -ATPases in prokaryotes as well as in eukaryotes.

© 1999 Federation of European Biochemical Societies.

**Key words:**  $F_1$ -ATPase; Rotation;  $\gamma$  Subunit; Chloroplast; Regulation

## 1. Introduction

$F_0F_1$ -ATP synthase of bacteria, mitochondria and chloroplasts synthesizes ATP from ADP and  $P_i$  at the expense of a proton-motive force [1–3]. The enzyme consists of the membrane-embedded sector  $F_0$  responsible for proton translocation, and the extrinsic catalytic part  $F_1$ . The architecture of  $F_1$  is very similar in various kinds of cells or organelles, respectively, and composed of five different subunits,  $\alpha_3\beta_3\gamma_1\delta_1\epsilon_1$ . Rotation of the central  $\gamma$  subunit in the  $\alpha_3\beta_3$  headpiece of  $F_1$  during the hydrolysis of ATP as suggested by Boyer [4], was experimentally supported by a biochemical approach [5], and by polarization anisotropy relaxation measurement of the fluorophore-labeled  $\gamma$  subunit of  $CF_1$  [6]. Noji et al. directly observed the rotation of the  $\gamma$  subunit in an  $\alpha_3\beta_3\gamma$  complex of

$TF_1$  by means of a fluorochrome-labeled actin filament fixed to this subunit [7]. They reported a unidirectional, counter-clockwise, and continuous rotation driven by ATP hydrolysis. It suggests that the  $\gamma$  subunit may interact with three  $\alpha/\beta$  couples sequentially step by step according to the catalytic reaction occurring at each of three catalytic sites. At very low concentration of ATP Yasuda et al. recently succeeded to observe this step-wise motion of the subunit with 120 degree steps [8], suggesting that the stepping observed by the actin filament directly reflects the catalysis occurring on each of three catalytic sites resides on  $\gamma$  subunits. Furthermore, Noji et al. [9] and Omote et al. [10] independently reported the rotation of the  $\gamma$  subunit in *E. coli*  $F_1$ -ATPase by using essentially the same kind of experimental approach.

On the other hand, Hartog and Berden [11] proposed a different catalytic mechanism which might exclude a simple rotation of the  $\gamma$  subunit in  $F_1$ -ATPase. Based on the results from energy transfer experiments between the  $\gamma$  subunit and catalytic sites on  $\gamma$  subunits [12,13] and on the ATPase activity of a complex formed from the isolated  $CF_1$   $\alpha_3\beta_3$  subcomplex and recombinant  $\gamma$  subunit of which the C-terminus was partially deleted, Sokolov et al. recently proposed a conformation of the  $\gamma$  subunit of  $CF_1$  in which the tip of the C-terminus of the  $\gamma$  subunit does not act as a spindle for rotation [14]. However, large differences in the conformations of the  $\gamma$  subunits of  $CF_1$  and bacterial  $F_1$  are not very likely as we succeeded to form an ATPase active chimeric complex with the  $\alpha$  and  $\beta$  subunits from  $TF_1$  and the recombinant  $\gamma$  subunit of  $CF_1$  [15,16]. The resulting complex mostly maintained the features of  $TF_1$  but was regulated like  $CF_1$  by the formation and the reduction of a disulfide bridge located in this  $\gamma$  subunit.

To clarify whether the rotation of the  $\gamma$  subunit in  $F_1$ -ATPase is ubiquitous in nature, we here tried to demonstrate it in  $CF_1$  by employing the method of Noji et al. [7]. As the actin filament was fixed to the  $\gamma$  subunit via a naturally occurring cysteine, the  $CF_1$ /actin derivative could be produced without any gene engineering technique. With this molecule we successfully observed a unidirectional, counter-clockwise rotation of the  $\gamma$  subunit in  $CF_1$  with the fluorescent microscope.

## 2. Materials and methods

### 2.1. Chemicals

6-{*N'*-[2-(*N*-maleimide)ethyl]-*N*-piperazinylamido}hexyl D-biotinamide (biotin-PEAC<sub>5</sub>-maleimide) was purchased from Dojindo laboratories (Japan). *N,N*-bis[2-hydroxyethyl]glycine (Bicine), 3-[*N*-morpholino]propanesulfonic acid (MOPS), *N*-ethyl-maleimide (NEM), dithiothreitol (DTT), and streptavidin were from Sigma (USA). All of other reagents were the highest grade commercially available.

\*Corresponding author. Fax: (81)-45-9245277.  
E-mail: thisabor@res.titech.ac.jp

**Abbreviations:** Bicine, *N,N*-bis[2-hydroxyethyl]glycine; biotin-PEAC<sub>5</sub>-maleimide, 6-{*N'*-[2-(*N*-maleimide)ethyl]-*N*-piperazinylamido}hexyl D-biotinamide;  $CF_1$ , chloroplast coupling factor 1;  $CF_1(-\delta)$ ,  $\delta$ -subunit deficient  $CF_1$ ; DTT, dithiothreitol;  $EF_1$ ,  $F_1$ -ATPase from *Escherichia coli* plasma membrane;  $TF_1$ ,  $F_1$ -ATPase from thermophilic *Bacillus* PS3 plasma membrane; MK buffer, 10 mM MOPS-NaOH buffer (pH 7.0) and 50 mM KCl; NEM, *N*-ethyl-maleimide; MKB buffer, MK buffer plus 10 mg/ml bovine serum albumin; MKR buffer, MK buffer containing 50 mM Na<sub>2</sub>SO<sub>3</sub>, 6 mM glucose, 0.5% 2-mercaptoethanol, 30 U/ml catalase, and 0.4 mg/ml glucose oxidase; MOPS, 3-[*N*-morpholino]propanesulfonic acid; NEM, *N*-ethyl-maleimide

## 2.2. Preparation of CF<sub>1</sub> from spinach

CF<sub>1</sub> was directly extracted with chloroform from thylakoid membranes prepared from market spinach [17] as previously described [18]. For the further purification, an Econo-Pac cartridge, *t*-butyl HIC (5 ml, Bio-Rad, USA) which was previously equilibrated with 50 mM Tris-HCl (pH 8.0), 1 mM ATP, 0.5 mM EDTA and 0.5 M (NH<sub>4</sub>)<sub>2</sub>SO<sub>4</sub> was used [19]. The crude extract dissolved in the same buffer was loaded on the column and the proteins were eluted from the column by the gradient of (NH<sub>4</sub>)<sub>2</sub>SO<sub>4</sub> from 0.5 M to 0 M. The major peak fraction eluted from the column was the  $\delta$ -subunit deficient CF<sub>1</sub> (CF<sub>1</sub>( $-\delta$ )) (Fig. 1, lane 1). It was stored as ammonium sulfate precipitation at 4°C. Before use, the preparation was desalted by passage through a gel filtration column (TSK G-3000XL, 14 mm  $\times$  300 mm, Tosoh, Japan) equilibrated with 10 mM MOPS-NaOH buffer (pH 7.0) and 50 mM KCl (MK buffer).

## 2.3. Biotin-streptavidin label of CF<sub>1</sub>( $-\delta$ )

The desalted CF<sub>1</sub>( $-\delta$ ) was first incubated with the equivalent molar ratio of NEM for 20 min at room temperature and unreacted NEM was removed by gel filtration chromatography as described above. The NEM-treated CF<sub>1</sub>( $-\delta$ ) was then reduced by the incubation with 20 mM DTT for 20 min at 37°C. After the removal of DTT in the solution by gel filtration with the same column, five-fold molar ratio of biotin-PEAC<sub>5</sub>-maleimide was added to CF<sub>1</sub>( $-\delta$ ) solution and was incubated for 20 min at room temperature. Unreacted biotin-PEAC<sub>5</sub>-maleimide was removed by gel filtration and streptavidin was attached to biotin on CF<sub>1</sub>( $-\delta$ ) by the addition of 10-fold molar excess streptavidin. Free streptavidin was then removed by a gel filtration column and the peak fraction containing streptavidin-labeled CF<sub>1</sub>( $-\delta$ ) was collected.

## 2.4. Measurement of the ATPase activity

The ATPase activity of CF<sub>1</sub>( $-\delta$ ) was measured according to the method described in [19]. The reaction mixture contained 4 mM ATP, 1 mM MgCl<sub>2</sub>, 100 mM Na<sub>2</sub>SO<sub>3</sub>. The buffers used were 50 mM MOPS-KOH (pH 7.0), Tricine-KOH (pH 8.0), or Bicine-NaOH (pH 9.0).

## 2.5. Rotation assay

A flow chamber was constructed of two coverslips (bottom, 24  $\times$  36 mm<sup>2</sup>, top, 18  $\times$  18 mm<sup>2</sup>) separated by 50  $\mu$ m spacers [7]. One chamber volume (about 10  $\mu$ l) of 20 nM CF<sub>1</sub> solution was infused into the flow chamber and allowed to adhere to the glass surface for 2 min. The chamber was washed twice with three volumes of MK buffer plus 10 mg/ml bovine serum albumin (MKB buffer). Then, 160 nM fluorescently labeled actin filament in MKB buffer was infused and incubated for 15 min. After the washing with MKB buffer, the solution in the chamber was replaced with MK buffer containing 50 mM Na<sub>2</sub>SO<sub>3</sub>, 6 mM glucose, 0.5% 2-mercaptoethanol, 30 U/ml catalase, and 0.4 mg/ml glucose oxidase (MKB buffer) plus 20 mM ATP and 5 mM MgCl<sub>2</sub> to initiate ATP hydrolysis reaction. The chamber was observed on an inverted fluorescence microscope (IX70, Olympus, Japan). Fluorescence images were recorded with an intensified CCD camera (ICCD-350F, Video Scope, USA) on an 8 mm video tape and was analyzed by the image analysis software provided by Dr. Yasuda, R.

## 3. Results and discussion

### 3.1. Biotin label of CF<sub>1</sub>- $\gamma$ subunit

Spinach CF<sub>1</sub> has altogether 11 cysteines ( $\alpha$ : 3  $\times$  1;  $\beta$ : 3  $\times$  1;  $\gamma$ : 4;  $\epsilon$ : 1). All of these cysteines are potential candidates for the biotin-PEAC<sub>5</sub>-maleimide labeling. However, the most reactive cysteine is Cys-322 on the  $\gamma$  subunit (see figure 1 of Ref. [6]). This cysteine is the penultimate amino acid from the C-terminus and should be located on the top of the molecule according to the MF<sub>1</sub> structure [20]. In order to get the filament fixed to the opposite pole of the  $\gamma$  subunit, we first treated CF<sub>1</sub>( $-\delta$ ) with NEM to block this cysteine. After the treatment, CF<sub>1</sub>( $-\delta$ ) was reduced by DTT. This reduction converts a disulfide group between Cys-199 and Cys-205 to the respective dithiol groups [21]. By the subsequent treatment

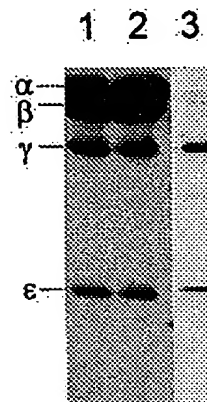


Fig. 1. Biotinylation of the  $\gamma$  subunit of CF<sub>1</sub>. SDS-PAGE was performed on 15% (w/v) polyacrylamide gel. Samples were as follows: 20  $\mu$ g of non-treated CF<sub>1</sub>( $-\delta$ ) (lane 1), 20  $\mu$ g of biotinylated CF<sub>1</sub>( $-\delta$ ) (lane 2) and 3  $\mu$ g of biotinylated CF<sub>1</sub>( $-\delta$ ) (lane 3). Proteins in lane 1 and 2 were stained with Coomassie brilliant blue R-250. Lane 3 was visualized by streptavidin-conjugated alkaline phosphatase.

with biotin-PEAC<sub>5</sub>-maleimide the biotin label could be introduced at Cys-199 or Cys-205. Both positions are in the portion of the  $\gamma$  subunit that remained unresolved in the MF<sub>1</sub> structure [20] and located at the bottom pole of the F<sub>1</sub> molecule. Biotin labeled CF<sub>1</sub>( $-\delta$ ) was then analyzed by SDS-PAGE and the bands were visualized by streptavidin conjugated alkaline-phosphatase (Fig. 1, lane 3). Biotin was only incorporated into the  $\gamma$  and  $\epsilon$  subunit. Kato et al. already reported that the  $\epsilon$  subunit in TF<sub>1</sub> rotates together with the  $\gamma$  subunit [22]. Therefore we did not try to separate possible different CF<sub>1</sub>/biotin derivatives from each other.

### 3.2. ATPase activity of the modified CF<sub>1</sub>

ATPase activity of streptavidin-labeled CF<sub>1</sub>( $-\delta$ ) was examined in the presence of 100 mM Na<sub>2</sub>SO<sub>3</sub>, which stimulates the ATPase activity of CF<sub>1</sub> [23], and compared with that of unlabeled CF<sub>1</sub>( $-\delta$ ). The ATPase activity of CF<sub>1</sub>( $-\delta$ ) labeled with streptavidin was 0.83 s<sup>-1</sup> at 37°C, i.e. about 40% lower than that of unlabeled CF<sub>1</sub> but suitable for the rotation assay. The ATPase activity of the streptavidin-labeled CF<sub>1</sub>( $-\delta$ ) measured at 25°C (as for the rotation assay) was 1.31 s<sup>-1</sup> at pH 8 and 1.97 s<sup>-1</sup> at pH 9, i.e. six to seven-fold higher than that measured at pH 7 (0.21 s<sup>-1</sup>). These rates are similar to those reported previously [24], but much slower than those obtained for the  $\alpha_3\beta_3\gamma$  complex of TF<sub>1</sub> [7,8].

### 3.3. Observation of the rotation of CF<sub>1</sub>- $\gamma$

The CF<sub>1</sub>( $-\delta$ ) derivative spontaneously fixed to the glass surface when it was infused into the flow chamber. When streptavidin-labeled CF<sub>1</sub>( $-\delta$ ) was employed and the fluorochrome labeled actin filament was infused, lots of actin filaments were observed under the fluorescence microscope but no filament was observed when biotin-labeled CF<sub>1</sub>( $-\delta$ ) was used instead of streptavidin-labeled CF<sub>1</sub>( $-\delta$ ), implying that the actin-filament was bound to CF<sub>1</sub>( $-\delta$ ) via streptavidin. Adhesion of CF<sub>1</sub>( $-\delta$ ) on the glass surface was disturbed when MKB buffer, which contains 10 mg/ml bovine serum albumin, was infused previously, and no binding of actin filaments was observed in this case.

As shown in Figs. 2 and 3, we could find a few filaments

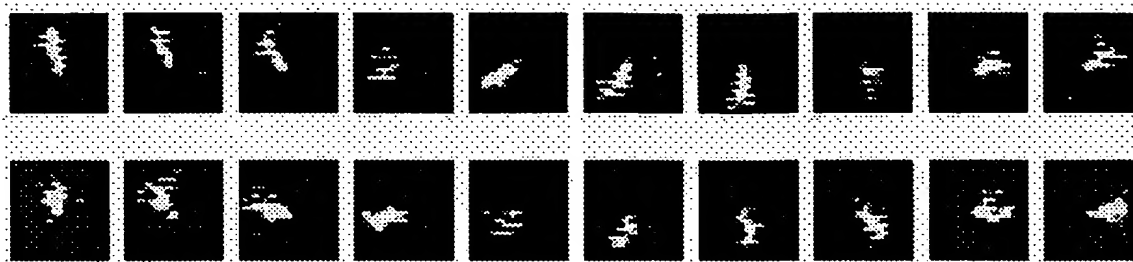


Fig. 2. Sequential images of a rotating actin filament attached to the  $\gamma$  subunit on  $CF_1$  at 20 mM ATP, 5 mM  $MgCl_2$ . The filament length was 1.26  $\mu m$  and the averaged rotational speed was 3.2 rounds/s; time interval between images was 33 ms. This figure can be viewed as a time-lapse movie sequence at our web site (<http://www.res.titech.ac.jp/seibutu/hisabori/index-e.htm>).

which showed unidirectional, counter-clockwise rotation like those on  $\alpha_3\beta_3\gamma$  from  $TF_1$  and  $EF_1$  [7–10], when MKR buffer with 8 mM ATP and 2 mM  $MgCl_2$ , or MKR buffer with 20 mM ATP and 5 mM  $MgCl_2$  was infused. At the same time vigorous movements of actin filaments which did not show the continuous rotation were observed. In the midst of the observation, we found that an actin filament suddenly divided into three sections and the middle fragment started wobbling.

The frequency to find the filament which showed the continuous rotation was lower than that for  $\alpha_3\beta_3\gamma$  complex of  $TF_1$  [7]. One of the possible reasons might be that the number of the  $CF_1$  derivatives with the top fixed on the glass surface was lower than was the case for  $TF_1$ . In the case of  $TF_1$  the

orientation of the molecule was controlled by the combination of histidine-tag connected to the  $\beta$  subunit and Ni-nitrilotriacetic acid coated beads on the glass surface [7]. In the case of the  $CF_1$  derivative the orientation was not regular because of the spontaneous adhesion of the molecules on the glass surface.

### 3.4. The characteristics of rotation of $CF_1$ - $\gamma$

As the ATPase activity of  $CF_1$ (- $\delta$ ) was influenced by the pH of the reaction medium (see above), we tried to observe differences in the rotational speed under various pH conditions. However, we could not find significant differences under our experimental conditions (Fig. 3). One obvious difference to the previous findings on  $TF_1$ - $\alpha_3\beta_3\gamma$  [7–10] was a frequently

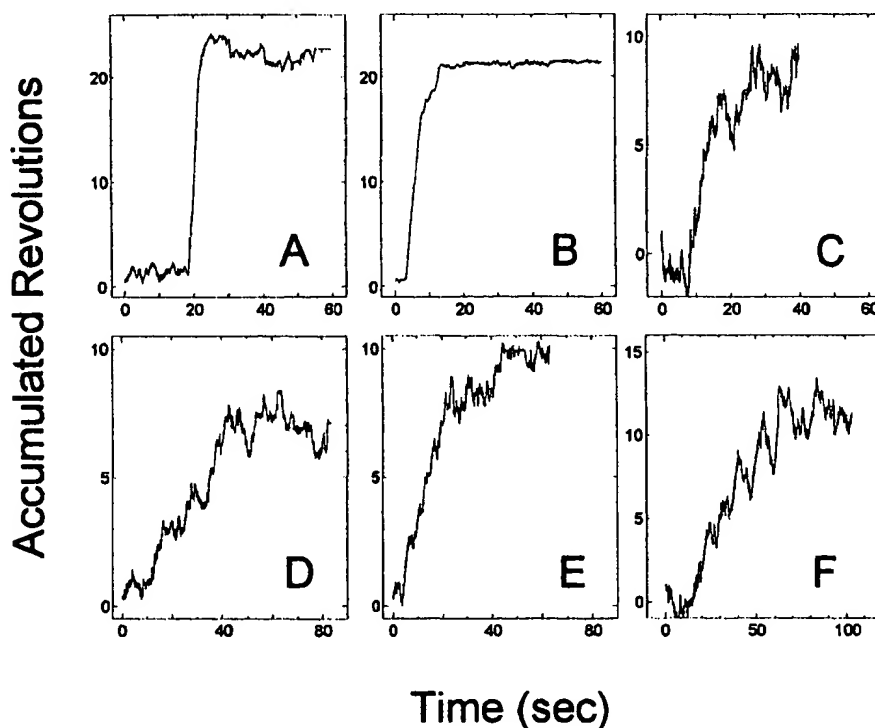


Fig. 3. Time course of the rotation of the  $\gamma$  subunit. Images of the rotating actin filaments were recorded with the intensified CCD camera, and the motion of the centroids was analyzed. The increase of the accumulated revolutions represents the counter-clockwise rotation of the filament. A–C: The rotation of the  $\gamma$  subunit was recorded in the presence of 20 mM ATP, 5 mM  $MgCl_2$  at pH 7.0. D and E: The rotation was recorded in the presence of 8 mM ATP, 2 mM  $MgCl_2$  at pH 7.0. F: The rotation was recorded in the presence of 8 mM ATP, 2 mM  $MgCl_2$  at pH 8.0. The lengths of the observed filaments were 1.26  $\mu m$  (A), 1.55  $\mu m$  (B), 1.55  $\mu m$  (C), 1.58  $\mu m$  (D), 1.92  $\mu m$  (E) and 1.46  $\mu m$  (G), respectively. The filament shown in (E) was propeller type, of which centroid is at the middle of the filament. The filament motion of (E) can be viewed as a time-lapse movie sequence at our web site (<http://www.res.titech.ac.jp/seibutu/hisabori/index-e.htm>).

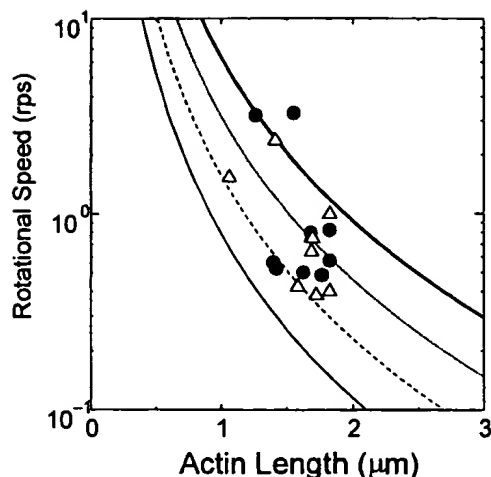


Fig. 4. Rotational speed in revolutions per second versus the length of the actin filament. Filaments that rotated around one end for  $> 5$  revolutions without an unusual intermission in the presence of (●) 20 mM ATP or (Δ) 8 mM ATP were used for the calculation of the rotational speed. Lines show the rotational speed under a constant torque of 40 pNnm (thick line), 20 pNnm (dotted line), 10 pNnm (dashed line) and 5 pNnm (thin line), respectively.

observed vigorous wobble movement of the filaments, which rotated one to two rounds in one and then in opposite direction. Even filament moving in a continuous counter-clockwise rotation (Fig. 3A) suddenly started clockwise movement for a short period. It is not clear yet whether this 'unusual' movement reflects a specific attribute of  $CF_1(-\delta)$  compared with the subcomplex of  $TF_1$ , or a kind of artifact derived from the different procedure to bind the actin filament on the  $\gamma$  subunit. The different procedure to fix the enzyme molecule on the glass surface may also be the reason.

The highest rotational speed of filaments observed in our experiments was 3.3 rounds/s. As the three catalytic sites on the enzyme are involved in the ATP hydrolysis reaction, this rotational speed implies an ATP hydrolysis reaction with a turnover rate of  $10 \text{ s}^{-1}$ . This value is 5 to 50-fold higher than the rate obtained by the measurement of ATP hydrolysis activity. The discontinuous motion of the filaments shown in Fig. 3 may explain this apparent discrepancy. Furthermore inhomogeneity of the enzyme preparation, including active and inactive molecules, may also be a possible reason.

By using the highest rotational speed of each of the filaments, we plotted the speed of rotation as a function of the lengths of the actin filaments to roughly estimate the torque (Fig. 4). As in the case of  $TF_1$  [7,8] and  $EF_1$  [9,10], longer actin filaments rotated more slowly than shorter ones. The torque values obtained from the experimental data were within the range of 20–40 pNnm and thus are consistent with the results of previous reports [7–10].

Hence we could observe that the  $\gamma$  subunit of  $CF_1$  can rotate in a similar manner as  $\gamma$  in  $TF_1$  and  $EF_1$  when hydrolyzing ATP. The rotation of the  $CF_1-\gamma$  was already suggested

on the basis of fluorescence anisotropy measurements by Sabbert et al. [6]. Our report is, to our knowledge, the first direct observation of  $\gamma$  rotation in an  $F_1$  from a eukaryotic cell although plastids are supposed to be of bacterial origin.

**Acknowledgements:** This work was supported in parts by a Grant-in-aid for Scientific Research in Priority Areas (no. 11151209) and a Grant (no. 11640643) from the Japanese Ministry of Education, Science, Sports and Culture to T.H., and CREST (Core Research for Evolutionary Science and Technology, Japan) to M.Y. We thank Kinoshita, K., Jr., Muneyuki, E., Taguchi, H., Noji, H., Bald, D., Kato-Yamada, Y., Konno, H., Hara, K., Masaike, T., Tsunoda, P. S., Hirano, Y. and Kroth, P. for their technical assistance and helpful discussion. Thanks to Yasuda, R. for providing us with the excellent image analysis program. Special thanks to Prof. Strotmann, H. (Heinrich-Heine University, Düsseldorf) for his critically reading the manuscript.

## References

- [1] Futai, M. and Kanazawa, H. (1983) *Microbiol. Rev.* 47, 285–312.
- [2] Senior, A.E. (1990) *Annu. Rev. Biophys. Chem.* 19, 7–41.
- [3] Groth, G. and Strotmann, H. (1999) *Physiol. Plant.* 106, 142–148.
- [4] Boyer, P.D. (1993) *Biochim. Biophys. Acta* 1140, 215–250.
- [5] Duncan, T.M., Bulvin, V.V., Zhou, Y., Hutcheon, M.L. and Cross, R.L. (1995) *Proc. Natl. Acad. Sci. USA* 92, 10964–10968.
- [6] Sabbert, D., Engelbrecht, S. and Junge, W. (1996) *Nature* 381, 623–625.
- [7] Noji, H., Yasuda, R., Yoshida, M. and Kinoshita Jr., K. (1997) *Nature* 386, 299–302.
- [8] Yasuda, R., Noji, H., Kinoshita Jr., K. and Yoshida, M. (1998) *Cell* 93, 1117–1124.
- [9] Noji, H., Häslar, K., Junge, W., Kinoshita Jr., K., Yoshida, M. and Engelbrecht, S. (1999) *Biochem. Biophys. Res. Commun.* 260, 597–599.
- [10] Omote, H., Sambonmatsu, N., Saito, K., Sambongi, Y., Iwamoto-Kihara, A., Yanagida, T., Wada, Y. and Futai, M. (1999) *Proc. Natl. Acad. Sci. USA* 96, 7780–7784.
- [11] Hartog, A.F. and Berden, J.A. (1999) *Biochim. Biophys. Acta* 1412, 79–93.
- [12] Richter, M.L., Snyder, B., McCarty, R.E. and Hammes, G.G. (1985) *Biochemistry* 24, 5755–5763.
- [13] Moroney, J.V. and McCarty, R.E. (1979) *J. Biol. Chem.* 254, 8951–8955.
- [14] Sokolov, M., Lu, L., Tucker, W., Gao, F., Gegenheimer, P.A. and Richter, M.L. (1999) *J. Biol. Chem.* 274, 13824–13829.
- [15] Hisabori, T., Kato, Y., Motohashi, K., Kroth-Pancic, P., Strotmann, H. and Amano, T. (1997) *Eur. J. Biochem.* 247, 1158–1165.
- [16] Hisabori, T., Motohashi, K., Kroth, P., Strotmann, H. and Amano, T. (1998) *J. Biol. Chem.* 273, 15901–15905.
- [17] Beechey, R.B., Hubbard, S.A., Linnett, P.E., Mitchell, A.D. and Munn, E.A. (1975) *Biochem. J.* 148, 533–537.
- [18] Hisabori, T. and Sakurai, H. (1984) *Plant Cell Physiol.* 25, 483–493.
- [19] Stumpp, M.T., Motohashi, K. and Hisabori, T. (1999) *Biochem. J.* 341, 157–163.
- [20] Abrahams, J.P., Leslie, A.G.W., Lutter, R. and Walker, J.E. (1994) *Nature* 370, 621–628.
- [21] Nalin, C. and McCarty, R.E. (1984) *J. Biol. Chem.* 259, 7275–7280.
- [22] Kato-Yamada, Y., Noji, H., Yasuda, R., Kinoshita Jr., K. and Yoshida, M. (1998) *J. Biol. Chem.* 273, 19375–19377.
- [23] Malyan, A.N. and Akulova, E.A. (1978) *Biokhimiia* 43, 1206–1211.
- [24] Sakurai, H., Shinohara, K., Hisabori, T. and Shinohara, K. (1981) *J. Biochem. (Tokyo)* 90, 95–102.

## The 20 C-terminal Amino Acid Residues of the Chloroplast ATP Synthase $\gamma$ Subunit Are Not Essential for Activity\*

(Received for publication, October 26, 1998, and in revised form, February 2, 1999)

Maxim Sokolov‡, Lu Lu, Ward Tucker, Fei Gao§, Peter A. Gegenheimer, and Mark L. Richter¶

From the Department of Molecular Biosciences, The University of Kansas, Lawrence, Kansas 66045

It has been suggested that the last seven to nine amino acid residues at the C terminus of the  $\gamma$  subunit of the ATP synthase act as a spindle for rotation of the  $\gamma$  subunit with respect to the  $\alpha\beta$  subunits during catalysis (Abrahams, J. P., Leslie, A. G. W., Lutter, R., and Walker, J. E. (1994) *Nature* 370, 621–628). To test this hypothesis we selectively deleted C-terminal residues from the chloroplast  $\gamma$  subunit, two at a time starting at the sixth residue from the end and finishing at the 20th residue from the end. The mutant  $\gamma$  genes were overexpressed in *Escherichia coli* and assembled with a native  $\alpha_3\beta_3$  complex. All the mutant forms of  $\gamma$  assembled as effectively as the wild-type  $\gamma$ . Deletion of the terminal 6 residues of  $\gamma$  resulted in a significant increase (>50%) in the Ca-dependent ATPase activity when compared with the wild-type assembly. The increased activity persisted even after deletion of the C-terminal 14 residues, well beyond the seven residues proposed to form the spindle. Further deletions resulted in a decreased activity to ~19% of that of the wild-type enzyme after deleting all 20 C-terminal residues. The results indicate that the tip of the  $\gamma$  C terminus is not essential for catalysis and raise questions about the role of the C terminus as a spindle for rotation.

The ATP synthase enzymes of the inner membranes of mitochondria, chloroplasts and of the bacterial cytoplasmic membrane, couple the energy of a transmembrane electrochemical proton gradient to the synthesis of ATP from ADP and inorganic phosphate. The general structural features of the enzyme are highly conserved from one organism to another. It is comprised of an integral membrane-spanning  $H^+$ -translocating segment ( $F_0$  or factor O) and a peripheral membrane segment ( $F_1$  or factor 1) which contains the catalytic sites for ATP synthesis and hydrolysis. The  $F_1$  segment is comprised of five different polypeptide subunits designated  $\alpha$  to  $\epsilon$  in order of decreasing molecular weight. The subunit stoichiometry is  $\alpha_3\beta_3\gamma_1\delta_1$  and  $\epsilon_1$ . Nucleotide binding is associated with the  $\alpha$  and  $\beta$  subunits, whereas the  $\gamma$  and  $\epsilon$  subunits play regulatory and/or structural roles. The  $\delta$  subunit is likely to be involved in binding the  $F_1$  segment to the  $F_0$  segment (reviewed in Ref. 1).

A high resolution crystal structure of the core catalytic por-

tion of the mitochondrial  $F_1$  enzyme was reported recently (2). The  $\alpha$  and  $\beta$  subunits alternate with each other to form a hexameric ring with one nucleotide binding site located at each of the six  $\alpha\beta$  subunit interfaces. Part of the structure of the  $\gamma$  subunit was also solved, including well conserved regions of the N and C termini. The C terminus, from residues 209 to 272 forms a single  $\alpha$  helix that stretches from below the base to the top of the  $\alpha\beta$  hexamer (see Fig. 5). The last nine residues of this remarkably long helix are predominantly hydrophobic in nature and pass through a greasy sleeve formed by a ring of hydrophobic residues provided by interacting N-terminal  $\beta$  barrel domains of all six of the  $\alpha$  and  $\beta$  subunits. On the basis of this unusual asymmetric structure, it was suggested that the C-terminal helix of the  $\gamma$  subunit forms a spindle around which the  $\alpha\beta$  hexamer rotates, rotation being facilitated by the hydrophobic (greasy) nature of the amino acids involved. That is, the  $\alpha\beta$  subunits provide a bearing through which the tip of the  $\gamma$  subunit passes and within which the  $\gamma$  subunit rotates. Although the amino acid sequences of  $\gamma$  subunits from different organisms show little overall homology, segments near the N and C termini are quite well conserved suggesting that they may be involved in forming important contacts with other  $F_1$  subunits (3, 4).

The crystal structure of  $F_1$  indicated that the three  $\alpha\beta$  pairs of the  $\alpha\beta$  hexamer also make direct contact with other regions of the  $\gamma$  subunit to induce different conformational states of the nucleotide binding sites at the  $\alpha\beta$  subunit interfaces. During rotation, each nucleotide binding site would sequentially alternate between three different conformational states, each state dictated by a different type of interaction with the  $\gamma$  subunit. Such rotation has been predicted from kinetic studies (5, 6), has been supported by several recent experiments (7–9), and is now widely considered to be a general mechanistic feature of all of the  $F_1$  enzymes (reviewed in Ref. 10).

In this study we have tested the “bearing” hypothesis specifically suggested by the crystal structure, by selectively deleting amino acid residues from the extreme C-terminal end of the  $\gamma$  subunit, which, in the mitochondrial enzyme, extends through the greasy sleeve of the  $\alpha\beta$  hexamer. To do this we utilized an efficient reconstitution system reported earlier (11) in which the native  $\gamma$  subunit isolated from CF<sub>1</sub><sup>1</sup> was reconstituted with an isolated  $\alpha\beta$  subunit complex. The cloned  $\gamma$  subunit could effectively replace the native  $\gamma$  subunit in reconstitution of the core enzyme complex.<sup>2</sup> Eight genetically engineered  $\gamma$  subunits, lacking between 6 and 20 of the C-terminal amino acids, were tested for assembly with the  $\alpha\beta$  subunits, and the catalytic activities of the assembled complexes were examined. The re-

\* This work was supported by National Science Foundation Grant OSR-9255223 and United States Department of Agriculture Grant 93-37306-9633. The costs of publication of this article were defrayed in part by the payment of page charges. This article must therefore be hereby marked “advertisement” in accordance with 18 U.S.C. Section 1734 solely to indicate this fact.

‡ Current address: Massachusetts Eye and Ear Infirmary, Harvard Medical School, Cambridge, MA 02114.

§ Current address: Dept. of Physiology, University of California at Los Angeles, Los Angeles, CA 90095-1662.

¶ To whom correspondence should be addressed. Tel.: 785-864-3334; Fax: 785-864-5321; E-mail: markl@kuhub.cc.ukans.edu.

<sup>1</sup> The abbreviations used are: CF<sub>1</sub>, chloroplast coupling factor 1; CF<sub>1</sub>( $-\delta\epsilon$ ), CF<sub>1</sub> deficient in the  $\delta$  and  $\epsilon$  subunits; PCR, polymerase chain reaction; Tricine, N-[2-hydroxy-1,1-bis(hydroxymethyl)ethyl]glycine; WT, wild type.

<sup>2</sup> M. Sokolov, L. Lu, W. Tucker, F. Gao, P. A. Gegenheimer, and M. L. Richter, manuscript in preparation.



sults demonstrate that the tip of the C terminus of the  $\gamma$  subunit, from residues 304 to 323 (chloroplast numbering), is not essential for rapid turnover by CF<sub>1</sub>.

#### EXPERIMENTAL PROCEDURES

**Materials**—CF<sub>1</sub> and CF<sub>1</sub> lacking the  $\delta$  and  $\epsilon$  subunits, CF<sub>1</sub>( $-\delta\epsilon$ ), were prepared from fresh market spinach as described previously (12) and stored as ammonium sulfate precipitates. Prior to use the proteins were desalted on Sephadex G-50 centrifuge columns (13). The isolated  $\epsilon$  subunit (14) was stored in the isolation buffer at 4 °C. An  $\alpha\beta$  complex and the  $\gamma$  subunit were isolated from CF<sub>1</sub>( $-\delta\epsilon$ ) as described previously (11). The  $\alpha\beta$  subunit complex was recycled through the isolation procedure to ensure that trace amounts of contaminating  $\gamma$  subunit were removed.

ATP (grade I and II) and antibiotics (ampicillin, chloramphenicol, and tetracycline) were purchased from Sigma. Stock solutions of tetracycline were prepared by dissolving the inhibitor in ethanol to a final concentration of 5 mM and stored at -70 °C. *Pfu* DNA polymerase and its reaction buffer were purchased from Strategene. T4 DNA ligase and its reaction buffer were obtained from Promega. DNase I was from Roche Molecular Biochemicals. Tryptone and yeast extract were obtained from Difco. Urea (ultra pure) was purchased from Fluka and hydroxylapatite from Bio-Rad. All other chemicals were of the highest quality reagent grade available.

**Plasmid Construction**—Most of the recombinant DNA methods used in this study have been described elsewhere (15, 16). *Escherichia coli* transformation protocols were as described by Hanahan (17). Plasmid pSG101 (4), generously supplied by Dr. M. Futai, contains the full-length cDNA for the spinach (*Spinacia oleracea*) chloroplast *atpC* gene encoding the ATP synthase  $\gamma$  subunit. A 1.1-kilobase pair *BsaI*-*Bam*HI fragment of pSG101 was subcloned into the *NcoI* and *Bam*HI cleaved expression vector pET8c (18) via an *NcoI*-*BsaI* adaptor.<sup>2</sup> The resulting plasmid pET8cgam bb1 was transformed into the expression host *E. coli* BL21(DE3)/pLysS (19). Plasmid DNA for sequencing was prepared by alkaline-SDS lysis and polyethylene glycol precipitation (20).

**Generation of *atpC* Gene Mutants**—Eight deletion mutants of  $\gamma$  were generated by "inverse" PCR with a forward primer that was complementary to the termination codon of the *atpC* gene and the downstream sequence of the pET8cgam bb1 plasmid. The reverse primer was complementary to the required C-terminal amino acid and its adjacent upstream sequence. PCR primers were 24–31 base pairs long and were 5'-phosphorylated. Oligonucleotides were synthesized by Macromolecular Resources, Colorado State University. Plasmid DNA for PCR was prepared by ethanol precipitation after phenol:chloroform extraction (17). PCR was carried out in 50  $\mu$ l of cloned *Pfu* DNA polymerase reaction buffer, which also contained 60 ng of the pET8cgambb1 plasmid, 4 mM total MgSO<sub>4</sub>, 22 pmol of each primer, 0.4 mM dNTPs, and 2.5 units of cloned *Pfu* DNA polymerase. The components were mixed on ice and placed in a GenAmp PCR System 2400 (Perkin-Elmer) prewarmed to 94 °C. Cycling parameters were: 94 °C for 1 min, 56 °C for 1 min, 72 °C for 12 min, for 20 cycles. The PCR product was purified by agarose gel electrophoresis followed by electroelution into an ISCO micro-trap. The eluted DNA was precipitated with ethanol and circularized (14). For this 100–200 ng of the DNA was incubated with 3 units of T4 DNA ligase in the T4 DNA ligase buffer overnight at room temperature (~22 °C). The resulting plasmid was transformed into *E. coli* XL1-Blue cells for amplification. The amplified plasmid was isolated using boiling lysis followed by isopropanol and ethanol precipitation and transformed into the expression host *E. coli* BL21(DE3)/pLysS (19).

Each mutant gene was isolated from the expression clone by alkaline-SDS lysis followed by ethanol precipitation after phenol:chloroform extraction (20) and sequenced by an automated fluorescence dideoxy technique (21).

**Solubilization and Folding of Overexpressed  $\gamma$  Mutants**—*E. coli* cells containing the *atpC* gene were grown at 37 °C in LB medium containing 100 mg/ml ampicillin and chloramphenicol (34 mg/ml). In mid-exponential phase growth, cells were induced with 0.1 mM isopropyl- $\beta$ -D-thiogalactopyranoside for up to 5 h. Cells were harvested by centrifugation at 4000  $\times g$  for 10 min, washed once with TE50/2 buffer (50 mM Tris-HCl, 2 mM EDTA, pH 8.0), and resuspended in a small volume (10–15 ml) of TE50/2. Cells were lysed by one to three cycles of freezing (at -70 °C or in a dry ice/ethanol bath) and thawing (15). 10 mM MgCl<sub>2</sub> and 10 mg of DNase I were added to the lysed cells, which were incubated on ice for 20 min. DNA was then sheared by sonication with a Branson 250 sonifier for 2  $\times$  15 s at an output of 4 and a duty cycle of 10. After the sonication cells were kept on ice for additional 20 min. Inclusion bodies, together with some cell debris, were sedimented at

4000  $\times g$  for 10 min. The pellet, containing mostly insoluble  $\gamma$  polypeptide, was washed three times with 25 ml of TE50/2 before solubilization.

The insoluble  $\gamma$  polypeptide was dissolved in a solution containing 4 M urea, 50 mM NaHCO<sub>3</sub>-NaOH, pH 9.5, 1 mM EDTA, 5 mM dithiothreitol, 20% (v/v) glycerol, and slowly dialyzed for 24 h against a solution containing 0.3 M LiCl, 50 mM NaHCO<sub>3</sub>-NaOH, pH 9.5, 1 mM EDTA, 5 mM dithiothreitol, 20% (v/v) glycerol. The final concentration of protein was approximately 1 mg/ml. The protein was stored at -70 °C.

**Assembly of  $\gamma$  Mutants**—The purified  $\alpha\beta$  mixture was diluted to about 100  $\mu$ g/ml with a solution containing 20% glycerol, 50 mM Hepes-NaOH, pH 7.0, 2 mM MgCl<sub>2</sub>, 2 mM ATP, and 2 mM dithiothreitol and kept on ice. The  $\gamma$  subunit preparation was added dropwise to the  $\alpha\beta$  mixture to give a final molar ratio of 3 $\gamma$ :1 $\alpha\beta$ . The mixture was gently mixed and left to sit at room temperature (~22 °C) for 2 h. Unreconstituted subunits were separated from the reconstituted  $\alpha\beta\gamma$  by anion exchange chromatography as described previously (11).

**Other Procedures**—ATPase activities were determined by measuring phosphate release (22) for 5 min at 37 °C. The assay was carried out in 0.5-ml volumes of assay mixture containing 50 mM Tricine-NaOH, pH 8.0, and 5 mM ATP. The calcium-dependent ATPase activity was assayed in the presence of 5 mM CaCl<sub>2</sub>. Magnesium-dependent ATPase was carried out in the presence of 2.5 mM MgCl<sub>2</sub> and 25 mM Na<sub>2</sub>SO<sub>4</sub>, and manganese-dependent ATPase activity was carried out in the presence of 2.5 mM MnCl<sub>2</sub> and 100 mM Na<sub>2</sub>SO<sub>4</sub>. The reaction was started by addition of 1–6  $\mu$ g of enzyme into the assay mixture and terminated by addition of 0.5 ml of cold trichloroacetic acid. Protein concentrations were determined by the Bradford method (23). Absorbance measurements were obtained using a Beckman DU-70 spectrophotometer. Gel electrophoresis was performed on NOVEX Pre-Cast 10–20% gradient gels.

#### RESULTS

**Overexpression of the Spinach *atpC* Gene in *E. coli***—The *atpC* gene encoding the full-length  $\gamma$  subunit of the spinach chloroplast ATP synthase was inserted into the pET8c expression vector and overexpressed at high levels (>100 mg/liter of cells at the end of log-phase growth). The overexpressed protein was solubilized from insoluble inclusion bodies into 4 M urea and recovered by slow dialysis. The cloned protein was identical to the native protein (11) in its ability to reconstitute with native  $\alpha\beta$  subunits to form a fully active core enzyme complex.<sup>2</sup> Eight deletion mutants of the *atpC* gene were prepared and transformed into the overexpression host and the deletions verified by sequencing each entire gene. The truncated polypeptides were designated  $\gamma_{D6}$  to  $\gamma_{D26}$ , according to the number of amino acid residues missing from the C terminus. Amino acid sequences of the C-terminal fragment of the full-length  $\gamma$  subunit and the eight deletion mutants are shown in Fig. 1. Also shown in Fig. 1 is the corresponding sequence at the C terminus of the bovine mitochondrial F<sub>1</sub>  $\gamma$  subunit. The sequence underlined corresponds to that part of the  $\gamma$  subunit that is in the immediate vicinity of the hydrophobic sleeve, the last seven residues (267–273) actually passing through the sleeve (2). Deletion of all ten C-terminal residues would arguably be sufficient to test the bearing hypothesis. The C-terminal segment of  $\gamma$  shown in Fig. 1 is one of the most highly conserved regions among  $\gamma$  subunits from different species. This is evident from the more than 50% direct sequence identity between the bovine mitochondrial and chloroplast subunits (Fig. 1).

**Assembly of the  $\gamma$  Mutants**—Each of the  $\gamma$  constructs was tested for its ability to organize the  $\alpha\beta$  subunits into a stable  $\alpha\beta\gamma$  core enzyme complex. For this, folded  $\gamma$  polypeptide was incubated with the isolated  $\alpha\beta$  complex, and the resulting  $\alpha\beta\gamma$  assembly was purified by DEAE-cellulose column chromatography as described earlier for purifying  $\alpha\beta\gamma$  assembled using the native F<sub>1</sub> subunits (11). Incubation of each of the  $\gamma$  constructs with the  $\alpha\beta$  subunits resulted in formation of an  $\alpha\beta\gamma$  complex, which is eluted from DEAE-cellulose at the same salt concentration as the native complex and which is significantly higher than that required to elute unassembled subunits (11).

GAMMA SUBUNIT C-TERMINAL DELETIONS		
	252	273
MF1- $\gamma$	-FNRTQAVITKELIELISGAAA	
	301	323
CF1- $\gamma_{WT}$	-YNRRQAKITGEILEAVAGANACV	
CF1- $\gamma_{D6}$	-YNRRQAKITGEILEAVA	
CF1- $\gamma_{D8}$	-YNRRQAKITGEILEA	
CF1- $\gamma_{D10}$	-YNRRQAKITGEIL	
CF1- $\gamma_{D12}$	-YNRRQAKITGE	
CF1- $\gamma_{D14}$	-YNRRQAKIT	
CF1- $\gamma_{D16}$	-YNRRQAK	
CF1- $\gamma_{D18}$	-YNRRQ	
CF1- $\gamma_{D20}$	-YNRA	

FIG. 1. Amino acid sequences of the C-terminal fragments of the  $\gamma$  subunits of the ATP synthases from bovine heart mitochondria (MF1- $\gamma$ , Ref. 14), wild-type spinach chloroplast (CF1- $\gamma_{WT}$ ), and C terminus deletion mutants of spinach chloroplast  $\gamma$  subunit beginning with deletion of 6 residues from the C terminus ( $\gamma_{D6}$ ) continuing with successive deletion of 2 residues up to 20 residues ( $\gamma_{D20}$ ).

The polypeptide profiles of all of the assemblies were very similar to each other as indicated for the  $\alpha\beta\gamma_{D12}$  and  $\alpha\beta\gamma_{D20}$  assemblies, which are compared with the  $\alpha\beta\gamma_{WT}$  assembly in Fig. 2. This suggests that all of the  $\gamma$  mutants were capable of assembling with the  $\alpha\beta$  subunits.

The results shown in Table I compare the ATPase activities of protein assemblies reconstituted with the first two mutants,  $\gamma_{D6}$  and  $\gamma_{D8}$  with the wild-type  $\gamma$ . Remarkably, both mutant assemblies were significantly more active than the wild-type assembly in calcium-dependent ATP hydrolysis. The magnesium-dependent activities of the two mutants, however, were significantly reduced. The apparent  $K_m$  and  $K_{cat}$  for Ca-ATP hydrolysis of the  $\gamma_{D6}$  mutant were measured and compared with the wild-type assembly (Table I). Only the  $K_{cat}$  exhibited a measurable change in the mutant.

Fig. 3 compares the relative rates of ATP hydrolysis of the remaining mutants,  $\gamma_{D10}$  through  $\gamma_{D20}$ , in the presence of either  $Ca^{2+}$ ,  $Mg^{2+}$ , or  $Mn^{2+}$  as the divalent cation substrate. The  $\gamma_{D10}$ ,  $\gamma_{D12}$ , and  $\gamma_{D14}$  mutant assemblies all showed similar responses to those of the  $\gamma_{D6}$  and  $\gamma_{D8}$  mutant assemblies in that their Ca-ATPase activities were significantly higher than that of the wild-type enzyme. The maximum activity was obtained with the  $\gamma_{D14}$  mutant, which had a specific activity of 55  $\mu\text{mol}\cdot\text{min}^{-1}\cdot\text{mg}^{-1}$ , which is the highest rate of Ca-ATP hydrolysis that we have ever observed with the chloroplast enzyme. However, deletion of 16 residues from the  $\gamma$ C terminus resulted in a sharp decrease in Ca-ATPase activity, which continued upon deletion of additional residues ending with an activity that was  $\sim 19\%$  of the wild-type control at  $\gamma_{D20}$ . In contrast to the Ca-ATPase activity, the Mg-ATPase and Mn-ATPase activities declined continuously with each additional pair of residues deleted. Nevertheless, even after deleting 20 residues from the C terminus, the enzyme exhibited significant rates of catalysis: 17% of the wild-type Mg-ATPase activity and 20% of the wild-type Mn-ATPase activity.

Activation of the latent Mg-ATPase and Mn-ATPase activities of CF1 normally requires, in addition to removing the inhibitory  $\epsilon$  subunit (14), the presence of oxyanions such as ethanol, carbonate, or sulfite, which overcome a strong inhibition caused by free metal ions binding to and stabilizing bound ADP at the catalytic site(s) (24). The degree of stimulation by oxyanions usually varies between 10- and 100-fold depending

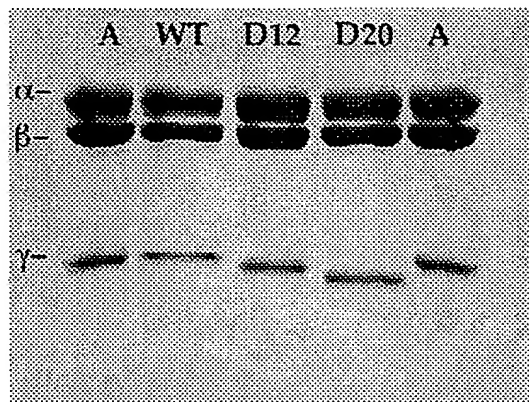


FIG. 2. Gel electrophoresis profile of the reconstituted, purified  $\alpha\beta\gamma$  assemblies and isolated CF1(- $\delta\epsilon$ ). Wild-type and mutant  $\gamma$  subunits were reconstituted with the native  $\alpha\beta$  subunits and the protein assemblies purified by ion exchange chromatography as described previously (9). Electrophoresis was performed on a 10–20% Tris-glycine gel, and proteins were stained with Coomassie Brilliant Blue R. Each lane contained 4  $\mu\text{g}$  of protein. A, isolated CF1, lacking the two small subunits,  $\delta$  and  $\epsilon$  (CF1(- $\delta\epsilon$ )); WT, D12 and D20, the  $\alpha\beta\gamma$  assemblies containing the wild-type  $\gamma$ ,  $\gamma_{D12}$ , and  $\gamma_{D20}$  mutants, respectively.

on the divalent cation and the oxyanion concentrations. The Ca-ATPase activity, however, is already high once  $\epsilon$  is removed and is slightly inhibited by oxyanions (25). So the magnesium- and manganese-dependent ATPase activities listed in Table I and shown in Fig. 3 were measured in the presence of high concentrations (25 mM) of sulfite ions. It was of interest to examine the effects of the  $\gamma$  deletions on the Mg-ATPase activities in the absence of the stimulatory oxyanions. The results of this study are shown in Table II. The Mg-ATPase activity in the absence of sulfite was, like the Ca-ATPase activity, stimulated by deletion of residues from the  $\gamma$ C terminus and was highest in the  $\gamma_{D14}$  mutant. The activity of this mutant was almost 4-fold that of the wild-type enzyme, and in parallel to the Ca-ATPase activity, it decreased markedly upon deletion of 16 or more residues. The  $\gamma_{D20}$  mutant still retained a readily measurable activity, which was  $\sim 45\%$  of that of the wild-type enzyme (Table II).

**Sensitivity of the Mutant Assemblies to Inhibitors**—The responses of the different assemblies to the inhibitory  $\epsilon$  subunit and to the fungal inhibitor tentoxin were examined, in part to evaluate the effect of the deletions on the ability of the two inhibitors to block activity and in part to verify that the observed activities are representative of the normal activity of CF1, which responds to these inhibitors with absolute specificity. The inhibitory responses of the Ca-ATPase activities of the different constructs to a fixed concentration (10-fold molar excess) of added  $\epsilon$  subunit are summarized in Table III. All of the enzyme assemblies, including the enzyme assembled with the  $\gamma_{D20}$  mutant, were strongly inhibited by  $\epsilon$ , although there was a significant variation (between 64 and 83%) in the extent of inhibition observed, and all were less inhibited than the wild-type assembly (91%). The  $\gamma_{D14}$  mutant, which exhibited the highest activity, was the least inhibited in the presence of a 10-fold molar excess of  $\epsilon$ . However, in the presence of a 30-fold molar excess of the  $\epsilon$  subunit, the  $\gamma_{D14}$  mutant was inhibited by the same extent as the wild-type enzyme (results not shown), indicating that the deletion had reduced the apparent affinity of the enzyme for  $\epsilon$  but not the maximal extent of inhibition.

The results of titrating the  $\alpha\beta\gamma$  assemblies with tentoxin are shown in Fig. 4. All of the assemblies, with the exception of the  $\gamma_{D20}$  mutant, were sensitive to inhibition by tentoxin. There were, however, significant differences among the mutant en-

TABLE I  
ATPase activities of wild-type and mutant assemblies

Protein assembly <sup>a</sup>	Ca-ATPase				Mg-ATPase	
	Units · mg <sup>-1</sup>	%	$K_{\text{cat}}$ s <sup>-1</sup>	$K_m$ (app) mM	Units · mg <sup>-1</sup>	%
$\alpha\beta\gamma_{\text{WT}}$	24.1 ± 2.0	100	149	1.2	42.8 ± 6.9	100
$\alpha\beta\gamma_{\text{D6}}$	35.3 ± 7.6	147	218	1.2	29.6 ± 8.3	70
$\alpha\beta\gamma_{\text{D8}}$	42.7 ± 8.4	177	ND <sup>b</sup>	ND	27.3 ± 5.0	64

<sup>a</sup>  $\alpha\beta\gamma$  assemblies were purified by anion exchange chromatography (11) prior to assay. ATPase values listed are the averages and standard deviations for three separate determinations.

<sup>b</sup> ND, not determined.

TABLE II  
Stimulation by sodium sulfite of the ATPase activities of the  $\alpha\beta\gamma$  assemblies

Protein preparation <sup>a</sup>	Mg-ATPase activity <sup>b</sup>	
	No additions	+ 25 mM Na <sub>2</sub> SO <sub>3</sub>
	units · mg <sup>-1</sup>	
$\alpha\beta\gamma_{\text{WT}}$	2.2	47.2
$\alpha\beta\gamma_{\text{D10}}$	5.8	34.6
$\alpha\beta\gamma_{\text{D12}}$	5.6	21.2
$\alpha\beta\gamma_{\text{D14}}$	8.5	14.8
$\alpha\beta\gamma_{\text{D16}}$	4.7	9.4
$\alpha\beta\gamma_{\text{D18}}$	1.7	6.2
$\alpha\beta\gamma_{\text{D20}}$	1.0	8.6

<sup>a</sup> Complexes were reconstituted and purified by anion exchange chromatography according to Ref. 11. The values listed are averages of three independent measurements.

<sup>b</sup> Mg-ATPase activity was determined in an assay mixture containing 50 mM Tricine-NaOH, pH 8.0, 5 mM ATP, 2.5 mM MgCl<sub>2</sub>, 5  $\mu$ g of enzyme, and sodium sulfite as indicated.

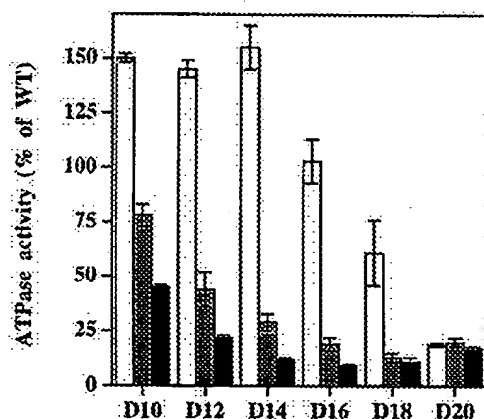


FIG. 3. Relative ATPase activity of the reconstituted, purified  $\alpha\beta\gamma$  constructs. All of the assays were carried out as described under "Experimental Procedures." The columns represent the relative ATPase activities of the different  $\alpha\beta\gamma$  assemblies in the presence of calcium chloride; white, magnesium chloride; gray, manganese chloride; black, D10 to D20 are designations for  $\alpha\beta\gamma_{\text{D10}}$  to  $\alpha\beta\gamma_{\text{D20}}$  assemblies. Activities of the  $\alpha\beta\gamma_{\text{WT}}$  (100% controls) were: Ca-ATPase, 35.5 ± 1.1; Mg-ATPase, 47.5 ± 1.5; and Mn-ATPase, 67.9 ± 5.4  $\mu$ mol·min<sup>-1</sup>·mg<sup>-1</sup>. Values shown are the averages and S.D. for five separate determinations.

zymes in the concentrations of tentoxin required to reach maximum inhibition. The most obvious differences were with the longer deletions. For example, a greater than 20-fold higher concentration was required for 90% inhibition of the activities of the  $\gamma_{\text{D16}}$  and  $\gamma_{\text{D18}}$  mutants than that required to inhibit the  $\gamma_{\text{WT}}$  to the same extent.

#### DISCUSSION

A cross-sectional view through the structure of the beef heart mitochondrial F<sub>1</sub> is shown in Fig. 5. The tip of the C terminus of the  $\gamma$  subunit, more specifically the last 7–10 residues, is surrounded by a sleeve of residues formed by part of the tightly packed  $\beta$  barrel domains of the six  $\alpha$  and  $\beta$  subunits. The sleeve

TABLE III  
Inhibition by the  $\epsilon$  subunit of the activity of the  $\alpha\beta\gamma$  assemblies

Protein preparation <sup>a</sup>	Ca-ATPase activity	
	No additions	+ $\epsilon$ subunit
	units · mg <sup>-1</sup>	
$\alpha\beta\gamma_{\text{WT}}$	20.6	1.9 (9%)
$\alpha\beta\gamma_{\text{D12}}$	34.3	10.1 (29%)
$\alpha\beta\gamma_{\text{D14}}$	39.2	14.0 (36%)
$\alpha\beta\gamma_{\text{D16}}$	31.0	9.6 (31%)
$\alpha\beta\gamma_{\text{D18}}$	20.6	4.6 (22%)
$\alpha\beta\gamma_{\text{D20}}$	4.8	0.8 (17%)

<sup>a</sup> Assemblies were incubated with a 10-fold molar excess of the  $\epsilon$  subunit or an identical volume of the buffer (control) used to isolate the  $\epsilon$  subunit (7). Samples were incubated for 8 min at room temperature and 2 min at 37 °C immediately prior to assay. Other conditions are the same as described in Table I.

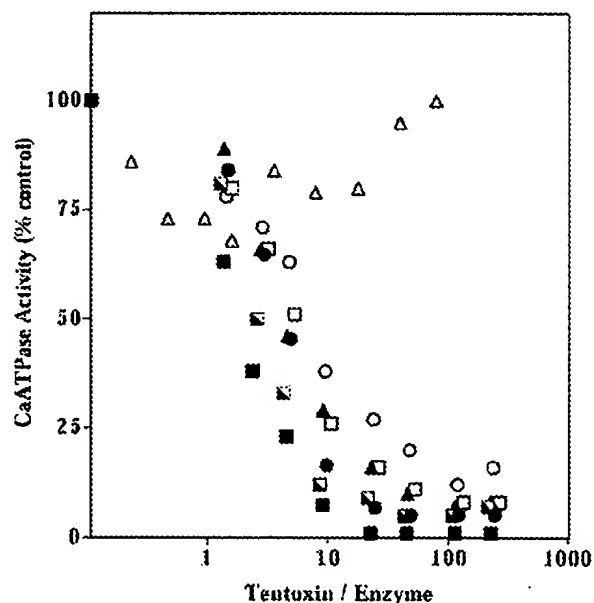


FIG. 4. The effect of tentoxin on the Ca-ATPase activities of the reconstituted, purified  $\alpha\beta\gamma$  assemblies. Ca-ATPase activity was measured as described under "Experimental Procedures." Each assembly was incubated with tentoxin to give the indicated tentoxin/enzyme ratios in the ATPase assay medium for 10 min at room temperature (~22 °C) then 2 min at 37 °C. The reactions were started by addition of 5 mM CaCl<sub>2</sub>. The ATPase activities in the absence of tentoxin were:  $\alpha\beta\gamma_{\text{WT}}$ , 16.9  $\mu$ mol·min<sup>-1</sup>·mg<sup>-1</sup> (■);  $\alpha\beta\gamma_{\text{D10}}$ , 35.1  $\mu$ mol·min<sup>-1</sup>·mg<sup>-1</sup> (●);  $\alpha\beta\gamma_{\text{D12}}$ , 25.9  $\mu$ mol·min<sup>-1</sup>·mg<sup>-1</sup> (□);  $\alpha\beta\gamma_{\text{D14}}$ , 33.9  $\mu$ mol·min<sup>-1</sup>·mg<sup>-1</sup> (▲);  $\alpha\beta\gamma_{\text{D16}}$ , 24.9  $\mu$ mol·min<sup>-1</sup>·mg<sup>-1</sup> (□);  $\alpha\beta\gamma_{\text{D18}}$ , 15.0  $\mu$ mol·min<sup>-1</sup>·mg<sup>-1</sup> (○);  $\alpha\beta\gamma_{\text{D20}}$ , 3.1  $\mu$ mol·min<sup>-1</sup>·mg<sup>-1</sup> (△).

residues, located in the region marked A on the  $\beta$  subunit in Fig. 5, have an overall hydrophobic character as do the nearby residues on the  $\gamma$  subunit. A hydrophobic contact between  $\gamma$  and the surrounding sleeve could allow the  $\gamma$  subunit to act as a spindle around which the  $\alpha\beta$  hexamer could rotate with minimum frictional resistance (2). The base of the C-terminal helix

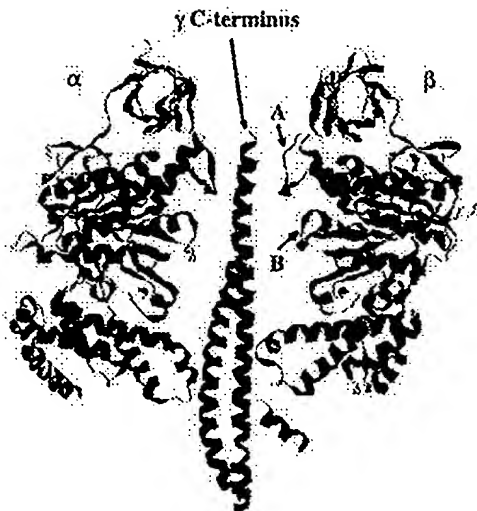


FIG. 5. Cross-section through part of the beef heart mitochondrial  $F_1$  structure indicating sites of interaction between the  $\alpha$ ,  $\beta$ , and  $\gamma$  subunits. The  $\gamma$  subunit contacts a hydrophobic sleeve formed by the structures marked A on all six of the  $\alpha$  and  $\beta$  subunits. A second site of contact involves a salt link between the  $\gamma$  subunit and the structure marked B on an adjacent  $\beta$  subunit (2).

of  $\gamma$  is offset from the central axis of the hexamer by  $\sim 7$  Å, so that, provided it remained rigid, it would sequentially and reversibly come into contact with regions of the  $\alpha$  and  $\beta$  subunits during rotation to create the required asymmetry among the nucleotide binding sites.

The remarkably high amino acid sequence conservation among the  $\alpha$  and  $\beta$  subunits of  $F_1$  enzymes from different species, together with the fact that the structures of the  $\alpha$  and  $\beta$  subunits of a thermophilic bacterium can be essentially superimposed upon those of the mitochondrial  $F_1$  subunits (26), are cogent reasons for assuming that all of the  $F_1$  enzymes have a very similar overall structure and utilize the same basic mechanism for ATP synthesis. There is, however, some evidence suggesting that there may be some minor structural differences among the  $F_1$  enzymes. For example, site mapping studies of the chloroplast  $F_1$  using fluorescence resonance energy transfer (27) as well as chemical cross-linking experiments (28) have indicated that cysteine 322, which is the second last amino acid residue at the C terminus of the  $CF_1$   $\gamma$  subunit, is located near the base of the  $\alpha\beta$  hexamer, more than 60 Å away from its position in the mitochondrial  $F_1$ . The reason for this difference is not understood at this time but is particularly intriguing given the significant amino acid sequence homology which is apparent in the C-terminal domains of  $\gamma$  subunits from different organisms (Ref. 4; also see Fig. 1). Moreover, a different location for the  $\gamma$ C terminus implies that the idea that the C-terminal helix of  $\gamma$  acts as a spindle for rotation is probably not correct, at least not as originally envisioned based on the mitochondrial  $F_1$  structure (2).

We have selectively deleted part of  $\gamma$ C terminus reasoning that if this region of  $\gamma$  was indeed acting as the tip of a spindle for rotation, or if it was in any way critical for catalysis by  $CF_1$ , the deletion should result in a complete loss of catalytic activity. However, the enzyme containing mutant  $\gamma$  subunits missing up to 20 amino acids from the C terminus was still capable of significant catalytic activity, which, with the exception of the D20 mutant, was sensitive to specific allosteric inhibitors of  $CF_1$ ; a strong indication that the mutant enzymes followed the usual cooperative catalytic pathway and that their activities were not artifactual. It is noteworthy that a similar result was obtained for *E. coli*  $F_1$  (29). In that case, membranes containing

the mutant enzyme retained a limited catalytic activity ( $\sim 10\%$  of both ATP hydrolysis and synthesis) following deletion of 10 residues from the C terminus. Deletion more than 10 residues from the C terminus resulted in a complete loss of activity in that case, although the enzyme still apparently correctly assembled on the membrane. The greater sensitivity of the *E. coli* enzyme to deletion of the C terminus may reflect a different structural requirement for catalysis by the  $F_0$ - $F_1$  complex than for the isolated  $F_1$ . The activity of the *E. coli*  $F_1$  mutants following isolation from the membrane was not investigated in that study.

The initial activation of enzyme turnover upon deletion of up to 14 residues from the C terminus of  $\gamma$  occurred for both the calcium- and the magnesium-dependent ATPase activities. One likely explanation for this effect is that the deletions resulted in a partial loosening of the structure of the enzyme to a point where it weakened binding of the cation-ADP reaction product at the catalytic site(s) in the interfacial region between  $\alpha$  and  $\beta$  subunits. Since the off-rate of the cation-ADP limits the overall reaction rate, the end result is to increase the  $K_{cat}$  of the enzyme. This would also explain why the sulfite-stimulated activity is inhibited rather than stimulated by the deletions. Assuming that the presence of high concentrations of sulfite maximally reduce the off-rate of cation-ADP so that the on-rate of the cation-ATP now becomes rate-limiting, a further reduction in nucleotide affinity at the catalytic site caused by the  $\gamma$  deletions would result in a reduction in the on-rate for the cation-ATP substrate and thus a reduction in the  $K_{cat}$ . This could also explain the reduced apparent affinities for the  $\epsilon$  subunit and for tentoxin, which resulted from the C-terminal deletions. Both inhibitors are known to block cooperative release of bound nucleotides, probably by stabilizing a rigid inhibited conformation of  $CF_1$  (1, 12). Thus a loosening of the  $F_1$  structure might favor the activated conformation over the inhibited conformation. The structural change resulting in altered inhibitor affinity does not necessarily have to be large, since small perturbations of  $\gamma$  structure, such as reduction of the  $\gamma$  disulfide bond or single-site cleavage of  $\gamma$  by trypsin, are known to markedly decrease the affinity of  $CF_1$  for the  $\epsilon$  subunit (30).

The chloroplast  $\gamma$  subunit has a glycine residue at position 310, 14 residues in from the C-terminal end (Fig. 1). Most secondary structural prediction algorithms predict a break in the C-terminal helix of  $\gamma$  at Gly-310. If the  $CF_1$   $\gamma$  were to turn back on itself at this point, the cysteine at position 322 would face toward the bottom part of  $CF_1$  (i.e. toward the membrane in  $CF_1$ - $F_0$ ) and come close to the position of this residue determined by fluorescence distance mapping (27). This would create a three-helix bundle in the central cavity of the enzyme rather than the two-helix bundle identified in the mitochondrial enzyme (2). If this is the case, the important binding interactions between  $\gamma$  and the  $\alpha\beta$  subunits identified in the mitochondrial enzyme, and which are likely to be primarily responsible for creating asymmetry among the different catalytic sites, might also be preserved in  $CF_1$ . Deleting the 14 C-terminal residues from  $CF_1$   $\gamma$  would remove the third helix from the central bundle, possibly decreasing the number of contacts between  $\gamma$  and the  $\alpha\beta$  subunits. This could feasibly have the effect of loosening the structure, thereby weakening the nucleotide affinity. The sharp decrease in catalytic activity, which occurred upon deleting residues beyond the first 14, may have resulted from an interference with the important  $\gamma$ - $\alpha\beta$  interactions. For example, the arginines at positions 254 and 256 in  $MF_1$  are surrounded by a ring of 9 charged residues located on six loop segments of the  $\alpha$  and  $\beta$  subunits marked "B" on one of the  $\beta$  subunits in Fig. 5. In the  $MF_1$  structure,

Arg-254 and Gln-255 form hydrogen bonds with adjacent residues in the  $\beta$  subunit loop to form one of the few sites of direct contact between  $\gamma$  and the  $\alpha$  and  $\beta$  subunits (2). Assuming that CF<sub>1</sub> has the same arrangement in this region of  $\gamma$ , deleting residues in the near vicinity of the site of contact would be expected to significantly compromise catalytic function as was observed.

Interestingly, an earlier study of the *E. coli* enzyme (31) showed that mutations near the C terminus of the  $\gamma$  subunit were able to restore catalytic function to functionally impaired enzymes which contained mutations near the N terminus. The original interpretation of these results was that the two mutations are in close proximity to each other. If this is true it would place the C terminus of the *E. coli*  $\gamma$  in a location very close to that of the chloroplast  $\gamma$  as determined by the fluorescence mapping experiments, assuming of course that the position of the N terminus of the *E. coli*  $\gamma$  is similar to that of the mitochondrial enzyme.

In conclusion, the results of this study have demonstrated that the extreme C-terminal 20 residues of the  $\gamma$  subunit of CF<sub>1</sub> are not essential for normal cooperative catalytic turnover by the isolated enzyme. The results eliminate the possibility of a catalytic mechanism that is universal to all F<sub>1</sub> enzymes in which the tip of the C terminus of the  $\gamma$  subunit must act as a spindle for rotational catalysis. The lack of functional importance of this part of the  $\gamma$  subunit for rapid turnover by CF<sub>1</sub> is consistent with earlier work indicating that the conformation of the C-terminal portion of the  $\gamma$  subunit of the chloroplast ATP synthase may differ from that of the mitochondrial enzyme. The results further suggest that the contacts between the  $\alpha$ ,  $\beta$ , and  $\gamma$  subunits of the enzyme, which are essential for rotational catalysis must be provided by regions of the  $\gamma$  subunit other than the extreme C terminus.

## REFERENCES

1. Richter, M. L., and Mills, D. A. (1996) in *Advances in Photosynthesis* (Yocum, C., and Ort, D. eds) Vol. IV, pp. 453–468, Elsevier Science Publishers B. V., Amsterdam
2. Abrahams, J. P., Leslie, A. G. W., Lutter, R., and Walker, J. E. (1994) *Nature* **370**, 621–628
3. Walker, J. E., Fearnley, I. M., Gay, N. J., Gibson, B. W., Northrop, F. D., Powell, S. J., Runswick, M., Saraste, M., and Tybulewicz, V. L. T. (1985) *J. Mol. Biol.* **184**, 677–701
4. Miki, J., Maeda, M., Mukohata, Y., and Futai, M. (1988) *FEBS Lett.* **232**, 221–226
5. Boyer, P. D. (1989) *FASEB J.* **3**, 2164–2178
6. Boyer, P. D. (1993) *Biochim. Biophys. Acta* **1140**, 215–250
7. Duncan, T. M., Bulygin, V., Zhou, Y., Hutcheon, M. L., and Cross, R. L. (1995) *Proc. Natl. Acad. Sci. U. S. A.* **92**, 10964–10968
8. Sabert, D., Engelbrecht, S., and Junge, W. (1996) *Nature* **381**, 623–625
9. Nogi, H., Yasuda, R., Yoshida, M., and Kinosita, K., Jr. (1997) *Nature* **388**, 299–302
10. Boyer, P. D. (1997) *Annu. Rev. Biochem.* **66**, 717–749
11. Gao, F., Lipscomb, B., Wu, L., and Richter, M. L. (1995) *J. Biol. Chem.* **270**, 9763–9769
12. Hu, N., Mills, D. A., Huchzermeyer, B., & Richter, M. L. (1993) *J. Biol. Chem.* **268**, 8536–8540
13. Penefsky, H. S. (1977) *J. Biol. Chem.* **252**, 2891–2899
14. Richter, M. L., Patrie, W. J., and McCarty, R. E. (1984) *J. Biol. Chem.* **259**, 7371–7373
15. Chen, Z., Wu, L., Richter, M. L., and Gegenheimer, P. A. (1992) *FEBS Lett.* **298**, 69–73
16. Chen, Z., Spies, A., Hein, R., Zhu, X., Thomas, B. C., Richter, M. L., and Gegenheimer, P. A. (1995) *J. Biol. Chem.* **270**, 17124–17132
17. Hanahan, D. (1985) in *DNA Cloning, A Practical Approach* (Glover, D. M., ed) pp. 109–135, Vol. I, IRL Press, Oxford
18. Studier, F. W., Rosenberg, A. H., Dunn, J. J., and Dubendorf, J. W. (1990) *Methods Enzymol.* **185**, 60–89
19. Studier, F. W., and Moffatt, B. A. (1986) *J. Mol. Biol.* **189**, 113–130
20. Sambrook, J., Fritsch, E. F., and Maniatis, T. (1989) *Molecular Cloning: A Laboratory Manual*, 2nd Ed., Cold Spring Harbor Laboratory, Cold Spring Harbor, NY
21. Averboukh, L., Douglas, S. A., Zhao, S., Lowe, K., Mahler, J., & Pardee, A. B. (1996) *BioTechniques* **20**, 918–921
22. Taussky, H. H., and Shorr, E. (1953) *J. Biol. Chem.* **202**, 675–685
23. Bradford, M. M. (1976) *Anal. Biochem.* **72**, 248–254
24. Guerrero, K. J., Xue, Z., and Boyer, P. D. (1990) *J. Biol. Chem.* **265**, 16280–16287
25. Anthon, G. E., and Jagendorf, A. T. (1986) *Biochim. Biophys. Acta* **848**, 92–98
26. Kato, Y., Matsui, T., Tanaka, N., Muneyuki, E., Hisabori, T., and Yoshida, M. (1997) *J. Biol. Chem.* **272**, 24906–24912
27. Richter, M. L., Snyder, B., McCarty, R. E., and Hammes, G. G. (1985) *Biochemistry* **24**, 5755–5763
28. Moroney, J. V., and McCarty, R. E. (1979) *J. Biol. Chem.* **254**, 8951–8955
29. Iwamoto, A., Miki, J., Maeda, M., and Futai, M. (1990) *J. Biol. Chem.* **265**, 5043–5048
30. Soteropoulos, P., Suss, K.-H., and McCarty, R. E. (1992) *J. Biol. Chem.* **267**, 10348–10354
31. Nakamoto, R. K., Maeda, M., and Futai, M. (1993) *J. Biol. Chem.* **268**, 867–882

Eur J Biochem. 1997 Oct 1;249(1):134-41.

Related Articles, Links

**Cross-linking of chloroplast F0F1-ATPase subunit epsilon to gamma without effect on activity. Epsilon and gamma are parts of the rotor.****Schulenberg B, Wellmer F, Lill H, Junge W, Engelbrecht S.**

Biophysik, Fachbereich Biologie/Chemie, Universitat Osnabruck, Germany.

Cys residues were directed into positions 17, 28, 41 and 85 of a Cys6-->Ser mutant of subunit epsilon of spinach chloroplast F0F1 ATP synthase. Wild-type and engineered epsilon were expressed in *Escherichia coli*, purified in the presence of urea, refolded and reassembled with spinach chloroplast F1 lacking the epsilon subunit [F1(-epsilon)]. Cys-containing epsilon variants were modified with a sulfhydryl-reactive photolabile cross-linker. Photocross-linking of epsilon to F1(-epsilon) yielded the same SDS gel pattern of cross-link products independent of the presence or absence of Mg<sup>2+</sup> x ADP, phosphate and Mg<sup>2+</sup> x ATP. Epsilon (wild type) [Ser6,Cys28] epsilon and [Ser6,Cys41]epsilon were cross-linked with subunit gamma. With chloroplast F0F1 the same cross-link pattern was obtained, except for one extra cross-link, probably between [Ser6,Cys28]epsilon and F0 subunit III. [Ser6,Cys17]epsilon and [Ser6,Cys85]epsilon did not produce cross-links. Cross-linking of epsilon, [Ser6,Cys28]epsilon, [Ser6,Cys41]epsilon to gamma in soluble chloroplast F1 impaired the ability of epsilon to inhibit Ca<sup>2+</sup>-ATPase activity. The Mg<sup>2+</sup>-ATPase activity of soluble F1 (measured in the presence of 30% MeOH) was not affected by cross-linking epsilon with gamma. Functional reconstitution of photophosphorylation in F1-depleted thylakoids was observed with F1 in which gamma was cross-linked to [Ser6,Cys28]epsilon or [Ser6,Cys41]epsilon but not with wild-type epsilon. In view of the intersubunit rotation of gamma relative to (alpha<sub>3</sub>beta<sub>3</sub>), which is driven by ATP hydrolysis, gamma and epsilon would seem to act concertedly as parts of the 'rotor' relative to the 'stator' (alpha<sub>3</sub>beta<sub>3</sub>).

PMID: 9363764 [PubMed - indexed for MEDLINE]

## COUPLING H<sup>+</sup> TRANSPORT AND ATP SYNTHESIS IN F<sub>1</sub>F<sub>0</sub>-ATP SYNTHASES: GLIMPSES OF INTERACTING PARTS IN A DYNAMIC MOLECULAR MACHINE

ROBERT H. FILLINGAME\*

*Department of Biomolecular Chemistry, University of Wisconsin Medical School, Madison, WI 53706, USA*

### Summary

Reversible, F<sub>1</sub>F<sub>0</sub>-type ATPases (also termed F-ATP synthases) catalyze the synthesis of ATP during oxidative phosphorylation. In animal cells, the enzyme traverses the inner mitochondrial membrane and uses the energy of an H<sup>+</sup> electrochemical gradient, generated by electron transport, in coupling H<sup>+</sup> translocation to ATP formation. Closely related enzymes are found in the plasma membrane of bacteria such as *Escherichia coli*, where the enzymes function reversibly depending upon nutritional circumstance. The F<sub>1</sub>F<sub>0</sub>-type enzymes are more distantly related to a second family of H<sup>+</sup>-translocating ATPases, the vacuolar-type or V-ATPases. Recent structural information has provided important hints as to how these enzymes couple H<sup>+</sup> transport to the chemical work of ATP synthesis. The simplest F<sub>1</sub>F<sub>0</sub>-type enzymes, e.g. as in *E. coli*, are composed of eight types of subunits in an unusual stoichiometry of  $\alpha_3\beta_3\gamma\delta\epsilon$  (F<sub>1</sub>) and  $a_1b_2c_{12}$  (F<sub>0</sub>). F<sub>1</sub> extends from the membrane, with the  $\alpha$  and  $\beta$  subunits alternating around a central subunit  $\gamma$ . ATP synthesis occurs alternately in different  $\beta$  subunits, the cooperative tight binding of ADP+P<sub>i</sub> at one catalytic site being coupled to

ATP release at a second. The differences in binding affinities appear to be caused by rotation of the  $\gamma$  subunit in the center of the  $\alpha_3\beta_3$  hexamer. The  $\gamma$  subunit traverses a 4.5 nm stalk connecting the catalytic subunits to the membrane-traversing F<sub>0</sub> sector. Subunit *c* is the H<sup>+</sup>-translocating subunit of F<sub>0</sub>. Protonation/deprotonation of Asp61 in the center of the membrane is coupled to structural changes in an extramembranous loop of subunit *c* which interacts with both the  $\gamma$  and  $\epsilon$  subunits. Subunits  $\gamma$  and  $\epsilon$  appear to move from one subunit *c* to another as ATP is synthesized. The torque of such movement is proposed to cause the rotation of  $\gamma$  within the  $\alpha_3\beta_3$  complex. Four protons are translocated for each ATP synthesized. The movement of  $\gamma$  and  $\epsilon$  therefore probably involves a unit of four *c* subunits. The organization of subunits in F<sub>0</sub> remains a mystery; it will have to be understood if we are to understand the mechanism of torque generation.

Key words: oxidative phosphorylation, proton translocation, F<sub>1</sub>F<sub>0</sub>-ATP synthase, molecular mechanism, subunit *c*, membrane and stalk sectors, interacting subunits.

### Introduction

Reversible, H<sup>+</sup>-transporting F<sub>1</sub>F<sub>0</sub>-type ATPases (also termed F-ATP synthases) catalyze the synthesis of ATP during oxidative phosphorylation. In animal cells, the enzyme traverses the inner mitochondrial membrane, where it uses the energy of an H<sup>+</sup> electrochemical gradient ( $\Delta\bar{\mu}_{\text{H}^+}$ ) generated by an H<sup>+</sup>-pumping electron transport system. Closely related F<sub>1</sub>F<sub>0</sub>-ATP synthases are found in the thylakoid membrane of chloroplasts, where the enzyme functions in electron-transport-driven photophosphorylation, and in the plasma membrane of bacteria, such as *Escherichia coli*, where the enzyme can function reversibly depending upon the nutritional circumstance. Under aerobic growth conditions, electron transport systems generate a  $\Delta\bar{\mu}_{\text{H}^+}$  across the bacterial plasma membrane by pumping of protons from the cytoplasm to the outside of the cell, and the H<sup>+</sup> gradient is then used to drive ATP synthesis. A plasma membrane  $\Delta\bar{\mu}_{\text{H}^+}$  is also required in other cellular processes such as H<sup>+</sup>-coupled nutrient transport and flagellar rotation. Under anaerobic conditions, the required  $\Delta\bar{\mu}_{\text{H}^+}$  is generated by the hydrolysis of glycolytically derived ATP by the F<sub>1</sub>F<sub>0</sub>-ATPase, protons being pumped from the cytoplasm to the outside of the

cell. The mitochondrial, chloroplast and bacterial F<sub>1</sub>F<sub>0</sub>-ATP synthases are closely related in structure and mechanism, as I shall review in greater detail below. The enzymes are regulated somewhat differently because of the diversity of physiological circumstances under which they function (Walker, 1994; Harris, 1995; Mills *et al.* 1995). In this essay, I will focus on recent work that is beginning to provide structural insights into how the enzyme works in coupling H<sup>+</sup>-transport to ATP synthesis. I will emphasize that the enzyme functions as a molecular machine in utilizing the energy of  $\Delta\bar{\mu}_{\text{H}^+}$  to make ATP. If we are to understand the mechanism, we will need to define the movements of interacting parts. A few glimpses of the total picture may now be at hand.

### Composition and general structure of F<sub>1</sub>F<sub>0</sub>-ATP synthases

F<sub>1</sub>F<sub>0</sub>-ATP synthases are composed of two structurally and functionally distinct sectors termed F<sub>1</sub> and F<sub>0</sub>. The F<sub>1</sub> portion of the enzyme extends from the surface of the membrane and in electron micrographs projects as a knob-like image. F<sub>1</sub> is

\*e-mail: fillingam@mac.wisc.edu.



easily removed from the membrane as a water-soluble complex which hydrolyzes ATP.  $F_1$  is connected to the membrane-traversing  $F_0$  sector via a narrow stalk. On removal of  $F_1$ , the transmembrane  $F_0$  sector mediates the passive transport of protons across the membrane. When the two sectors are properly associated, the complex reversibly couples ATP hydrolysis to  $H^+$  transport. The simplest  $F_1F_0$ -type enzymes, e.g. as in *E. coli*, are composed of eight types of subunits in an unusual stoichiometry of  $\alpha_3\beta_3\gamma\delta\epsilon$  ( $F_1$ ) and  $a_1b_2c_{12}$  ( $F_0$ ).

The atomic resolution structure of the  $\alpha_3\beta_3\gamma$  portion of beef heart mitochondrial  $F_1$ , recently published by Abrahams *et al.* (1994), confirms many features predicted from decades of study. A representation is given in Fig. 1. The  $\alpha$  and  $\beta$  subunits, with approximate molecular masses of 55 kDa each, alternate in an almost symmetrical hexameric arrangement around a central core. The catalytic ATP binding sites are known to lie within the  $\beta$  subunit at  $\alpha\beta$  subunit interfaces. Extended  $\alpha$ -helical segments of the partially resolved 30 kDa  $\gamma$  subunit extend through the center and protrude from the bottom of the  $\alpha_3\beta_3$  hexamer as an

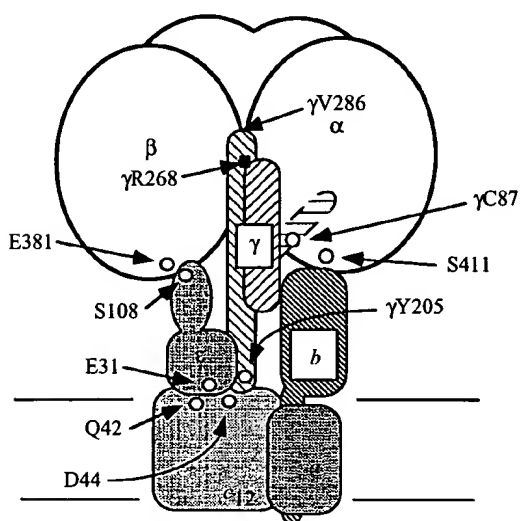


Fig. 1. Cross-sectional view of *Escherichia coli*  $F_1F_0$  ATPase emphasizing the stalk subunits. The  $\delta$  subunit is not depicted in this representation. The three  $\alpha$  and three  $\beta$  subunits alternate around a central core formed by the  $\gamma$  subunit. The three extended  $\alpha$ -helices of the  $\gamma$  subunit resolved in the X-ray structure of Abrahams *et al.* (1994) are depicted. The C-terminal residue ( $\gamma$ V286), at the end of the longest helix, is indicated; the position of the 'catch' formed between the empty  $\beta$  subunit and residues 268–269 in the  $\gamma$  C-terminal helix is indicated by the filled square labeled  $\gamma$ R268. The short helix with residue  $\gamma$ C87 projects horizontally towards a  $\beta$  subunit at the back of the structure, where it forms a second 'catch' with the  $\beta$  subunit binding the nonhydrolyzable ATP analog AMP-PNP. This 'catch', including residue  $\gamma$ C87, is adjacent to residue E381 in the DELSEED sequence of  $\beta$ , and  $\epsilon$ S108 is adjacent to  $\alpha$ S411, when  $Mg^{2+}$  AMP-PNP occupy catalytic sites; when  $Mg^{2+}$  (ADP+ $P_i$ ) occupy catalytic sites,  $\epsilon$ S108 lies close to the  $\beta$  subunit DELSEED sequence (Aggeler and Capaldi, 1996). The sites of Cys substitution used in cross-linking studies are indicated by small circles and by the wild-type residue and number; the numbers used correspond to residues in the *E. coli* enzyme. The subunit pairs formed by cross-linking of these Cys residues are discussed in the text.

extended and gently curved coiled coil. The  $\alpha$ -helix at the C-terminal end of the  $\gamma$  subunit extends 9 nm from the top of  $F_1$  to the surface of  $F_0$ , traversing the entire length of the 4.5 nm stalk (Abrahams *et al.* 1993, 1994; Watts *et al.* 1995; S. D. Watts, C. Tang and R. A. Capaldi, in preparation). The  $\epsilon$  subunit is also known to traverse the length of the stalk from the bottom of  $F_1$  to the surface of  $F_0$  (Zhang and Fillingame, 1995b). The  $\delta$  and  $b$  subunits are thought to be the other major components of the stalk in *E. coli* and chloroplasts. The components of the stalk in mitochondria are somewhat different (Collinson *et al.* 1994a,b; Belogradov *et al.* 1995; reviewed in Fillingame, 1996).

*E. coli*  $F_0$  is composed of three subunits in an experimentally determined stoichiometry of  $a_1b_2c_{10\pm1}$  (Foster and Fillingame, 1982). The content of subunit  $c$  is sufficiently uncertain that we now favor a number of 12 for reasons that are discussed below. The organization of subunits in  $F_0$  remains to be determined, although recent electron microscopic imaging experiments suggest that subunits  $a$  and  $b$  may associate at the periphery of a complex of  $c$  subunits (Birkenhäger *et al.* 1995), as is suggested in the cartoon of Fig. 1. This arrangement contrasts with previous suggestions that subunits  $a$  and  $b$  may be centrally located and rotate within a ring of  $c$  subunits (Hatch *et al.* 1995). Some information is available on the folding of individual subunits (Fillingame, 1990). The 79-residue subunit  $c$  spans the membrane as a hairpin of two extended hydrophobic  $\alpha$ -helices, with a more polar loop region which directly contacts subunits  $\gamma$  and  $\epsilon$  at the bottom of the stalk (see Fig. 2). Asp61, centered in the second transmembrane helix of subunit  $c$ , is known to be the site of  $H^+$  binding, as will be discussed below. The 156-residue subunit  $b$  is anchored to the membrane by a single hydrophobic  $\alpha$ -helix with the charged, protease-sensitive bulk of the protein extending from the membrane to form part of the stalk interacting with  $F_1$ . Proteolytic cleavage of the exposed region of subunit  $b$  abolishes  $F_1$  binding. The 271-residue subunit  $a$  is generally hydrophobic and is predicted to fold through the membrane with five or six transmembrane helices. A compelling, experimentally based model for the folding of subunit  $a$  in the membrane is still lacking. The composition of the chloroplast enzyme is easily related to that of *E. coli* with apparent substitution of  $b$  and  $b'$  subunits for the  $b_2$  dimer of *E. coli*. The bovine heart mitochondrial  $F_0$  is considerably more complex, with at least nine polypeptides present (Collinson *et al.* 1994a). Homologs of the *E. coli*  $a$  and  $c$  subunits are clearly present in bovine  $F_0$ ; the relationship of the other bovine  $F_0$  subunits with *E. coli* subunit  $b$  is less clear (Fillingame, 1996).

#### Relationship between F-ATP synthases and V-ATPases

The  $F_1F_0$ -type ATP synthases are distantly related to a second family of  $H^+$ -translocating ATPases, termed V (for vacuolar-type) or  $V_1V_0$ -ATPases (Harvey and Nelson, 1992). These enzymes are found in a variety of intracellular vesicles including plant and fungal vacuoles, clathrin-coated vesicles, secretory vesicles, Golgi bodies and lysosomes. The vesicles share the common feature of having an interior whose acidity is controlled by the  $H^+$ -pumping ATPase. V-ATPases are also widely distributed in the plasma membrane of cells specialized in  $H^+$

secretion, such as osteoclasts, where the enzyme plays a role in bone resorption (Chatterjee *et al.* 1992; Mattsson *et al.* 1994), and in kidney intercalated cells, where it functions in urinary acidification (Gluck and Nelson, 1992; Gluck *et al.* 1992). The diversity of distribution is exemplified by the tobacco hornworm midgut plasma membrane  $H^+$ -ATPase, which energizes membrane potential formation via  $K^+/H^+$  antiport (Wieczorek *et al.* 1991; see also Merzendorfer *et al.* 1997), and the distribution in cells specialized in alkalization (Harvey, 1992).  $V_1V_0$ -ATPases are composed of three types of subunits that bear obvious sequence similarity with the  $\alpha$ ,  $\beta$  and  $c$  subunits of  $F_1F_0$  and 5–6 other types of subunits bearing no obvious relationship. The stoichiometric ratio of subunits also appears to be similar, i.e.  $A_3B_3...c_6$  (Forgacs, 1992). The vacuolar subunit  $c$  is predicted to fold through the membrane with four transmembrane helices, with the first and second halves of the molecule bearing some sequence relationship to each other. The V-type gene is thought to have arisen by duplication and fusion of a primitive, bacterial-like ancestral gene (Nelson, 1992; Kibak *et al.* 1992). The  $c$  subunits of  $F_0$  and  $V_0$  could be organized similarly if there are 12  $c$  subunits per bacterial  $F_0$  and 6 vacuolar-type  $c$  subunits per  $V_0$ . Each unit would then be composed of 24 transmembrane helices. Closely related ATPases are also found in the archaeobacterial kingdom. In at least some cases, the  $A$  and  $B$  subunits most closely resemble the V-type enzyme, whereas the  $c$  subunit resembles the F-type subunit, folding with two transmembrane helices (Denda *et al.* 1989; Nelson, 1992).

#### Mechanism of coupling ATP hydrolysis with $H^+$ transport

$Mg^{2+}$ -ATP substrate binds with strong negative cooperativity to three potentially catalytic sites in  $F_1$ - and  $F_1F_0$ -ATPase complexes (Weber *et al.* 1994). Binding of the second and third nucleotide strongly promotes catalysis. Evidence from a direct binding study (Weber *et al.* 1993) and from an independent hybridization approach with mutant  $\beta$  subunits (Amano *et al.* 1996) now strongly indicates that all three catalytic sites must be occupied and catalytically competent for optimal catalysis. Boyer's postulated 'binding change mechanism' for the enzyme was based upon these assumed and other properties (Boyer, 1993; Cross, 1981). The proposed ATPase mechanism envisages three alternating and cooperatively interacting sites with varying affinities for ATP and the  $[ADP+P_i]$  products, i.e. tight (T), loose (L) and open (O). The binding of ATP at an open site would lead to an  $O \rightarrow T$  transition, with subsequent formation of tightly bound  $[ADP+P_i]$ ; simultaneously, at a second site with bound  $[ADP+P_i]$ , a  $T \rightarrow L$  transition would occur; and simultaneously, at a third site,  $[ADP+P_i]$  would be released following an  $L \rightarrow O$  transition. The energy released with the changes in binding affinity would be used to drive  $H^+$  translocation. ATP synthesis driven by  $\Delta\mu_H$  would occur in the reverse order, i.e. binding of  $[ADP+P_i]$  substrate at an open site followed by sequential  $O \rightarrow L \rightarrow T$  transitions and ultimately release of ATP from the tight site. Although cooperative interactions between catalytic sites in the binding of substrates appear to be essential to the function of the enzyme, the

$\Delta\mu_H$  generated by electron transport is the primary driving force leading to release of ATP (Souid and Penefsky, 1995).

The atomic resolution model of bovine  $F_1$  ( $\alpha_3\beta_3\gamma$ ) provides an obvious structural scenario for the binding change mechanism of ATP synthesis. The enzyme was crystallized in the presence of the nonhydrolyzable ATP analog AMP-PNP, along with ADP and  $Mg^{2+}$ . Nucleotide occupancy at each of the three catalytic sites differs, i.e. AMP-PNP is bound at one site (the triphosphate or  $\beta$ TP site), ADP is bound at the second site ( $\beta$ DP) and the third site is empty ( $\beta$ E). The structures of each of the sites differ, as does the juxtaposition of each of the three  $\beta$  subunits to the asymmetrical  $\gamma$  subunit. The nucleotide binding site is literally opened in the empty  $\beta$  subunit by movements of  $\beta$ -strands proximal to the binding site and a more global movement of the largely  $\alpha$ -helical, C-terminal third of the subunit by distances of up to 2 nm. Hydrogen-bonding rearrangements in the displaced loop of  $\beta$ E, near the nucleotide binding site, result in the formation of a 'catch' with the long C-terminal helix of the  $\gamma$  subunit (see Fig. 1). A second 'catch' is formed between the short, horizontally inclined helix of  $\gamma$  and the conserved DELSEED loop sequence in the C-terminal helical domain of the  $\beta$ TP subunit. Abrahams *et al.* (1994) propose that the conformational changes predicted in the binding change mechanism occur as a consequence of the rotation of the  $\gamma$  subunit relative to the three structurally asymmetrical  $\beta$  subunits. Subunit  $\gamma$  is proposed to rotate within a hydrophobic sleeve which surrounds the C-terminal end of the long  $F_1$ -traversing  $\alpha$ -helix. During oxidative phosphorylation, rotation would be driven by  $\Delta\mu_H$  to cause a conformational change at a tight ATP site, thus opening that site and releasing ATP. Direct evidence for rotation between all three catalytic sites is still minimal. In experiments designed to test the rotational model, Duncan *et al.* (1995) demonstrated that the  $\beta$  subunit neighboring Cys87 of subunit  $\gamma$  moved during catalytic turnover. The extent of subunit repositioning was consistent with the alternating three-site model. Sabbert *et al.* (1996) have concluded that eosin-labeled subunit  $\gamma$  rotates by more than  $200^\circ$  within an immobilized  $\alpha_3\beta_3$  core during the hydrolysis of ATP, based upon polarized absorption relaxation measurements following photobleaching.

In the  $F_1F_0$  complex, the  $\alpha$  and  $\beta$  subunits lie well above the plane of the lipid bilayer, while the  $\gamma$  subunit extends from the crown of  $F_1$  to the membrane surface. In further considering the mechanism of coupling  $H^+$  translocation to ATP synthesis, I will first review the evidence defining the  $H^+$ -binding site in  $F_0$  and then return to consider the subunit-subunit interactions which couple events in  $F_0$  to those in  $F_1$ .

#### $H^+$ -translocating unit of $F_0$

Asp61 in the second transmembrane helix of subunit  $c$  has long been thought to be the  $H^+$ -binding site in  $F_0$  and to undergo protonation-deprotonation as each  $H^+$  is transported (Fillingame, 1990), although compelling kinetic evidence for this hypothesis was lacking prior to the recent work of Dimroth and coworkers with a structurally related,  $Na^+$ -transporting  $F_1F_0$ -ATPase in the bacterium *Propionigenium modestum* (Dimroth, 1995). Asp61 is the site of reaction with

dicyclohexylcarbodiimide (DCCD), which covalently modifies the carboxyl side-chain in a very specific reaction that blocks  $H^+$  translocation. Substitution of Gly or Asn for Asp61 abolishes  $H^+$  translocation, suggesting a requirement for an ionizable group at this position. Surprisingly, the essential carboxyl can be moved from position 61 in helix-2 to position 24 in transmembrane helix-1 with retention of function (Miller *et al.* 1990; Zhang and Fillingame, 1994). These findings suggest that the essential carboxyl can be anchored in essentially the same position in the center of the membrane from either of the two transmembrane helices and, further, that the two helices may act together as a structural unit during the protonation-deprotonation cycle.

Subunits of the *E. coli* and *P. modestum* enzymes show high degrees of sequence homology, and hybrid enzymes have been constructed both biochemically (Laubinger *et al.* 1990) and genetically (Kaim and Dimroth, 1994). The *P. modestum* enzyme transports  $Na^+$  but, at low concentrations of  $Na^+$ , it has also been shown to transport  $H^+$  (Laubinger and Dimroth, 1989).  $Na^+$  and  $H^+$  apparently compete for the same site. The homologous, DCCD-reactive residue in the *P. modestum* subunit *c* is Glu65.  $Na^+$  protects Glu65 from reaction with DCCD, providing further evidence that the Glu65 carboxylate is the  $Na^+$ - and  $H^+$ -binding site (Kluge and Dimroth, 1993, 1994). On the basis of sequence comparisons of the *E. coli* and *P. modestum* subunits, we constructed mutants of the *E. coli* subunit *c* in the hope that the ion binding specificity could be changed (Zhang and Fillingame, 1995a). One combination of four mutations, Val-Asp61-Ala-Ile $\rightarrow$ Ala-Glu61-Ser-Thr did generate an  $F_0$  that binds  $Li^+$ , as evidenced by  $Li^+$  inhibition of both  $H^+$  transport and  $F_1F_0$ -ATPase activity. Thr at position 63 could be substituted by Ala or Gly with retention of the  $Li^+$ -sensitive phenotype, which suggested a requirement for a flexible but not necessarily polar residue at this position. We have suggested that the Glu61 carboxylate together with the Ser62 hydroxyl and perhaps a peptide carbonyl may provide the oxygens of the  $Li^+$ -liganding pocket. We predict that the Ser residue will be essential for  $Na^+$  binding and translocation in the *P. modestum* enzyme. In combination, these studies provide compelling evidence that Asp61 in *E. coli* and Glu65 in *P. modestum* are the site of  $H^+$  binding.

Nuclear magnetic resonance (NMR) studies of purified subunit *c* have recently provided information about its folding and the structure around Asp61. The protein was shown to fold as a hairpin of two extended  $\alpha$ -helices in a single-phase solvent mixture of chloroform-methanol-water (4:4:1) made 50 mmol  $l^{-1}$  in NaCl (Girvin and Fillingame, 1993). The protein can be purified in this solvent and reconstituted with other  $F_0$  subunits with full retention of activity (Dmitriev *et al.* 1995). Further, while in this solvent, it retains some of the properties and structural features expected of the protein in native  $F_0$  (Girvin and Fillingame, 1993, 1994). As indicated in Fig. 2, a high-resolution NMR structure has been proposed for the interacting helices from the region around Asp61 to the N- and C-terminal ends (Girvin and Fillingame, 1995). One of the most interesting features of this model is the close proximity of Ala24 in helix-1 to Asp61 in helix-2. The side-chains are within Van der Waals contact with a distance of 0.32 nm between  $\beta$ -

carbons. This proximity might, of course, be predicted from the genetic experiments discussed above in which the essential carboxyl is exchanged from position 61 to position 24 with retention of function. In looking at the model, it is easy to see how the carboxyl could be moved from one residue to the other with little effect on the structure of the bihelical unit.

Asp61 exhibits another remarkable property in the solvent system being used for NMR. The carboxyl side-chain has a pKa of 7.1, which is 1.5 units higher than that of any of the other carboxyls in the protein (Assadi-Porter and Fillingame, 1995). The other carboxyls exhibit pKa values close to that expected for solvent-exposed residues. These results suggest that the protein must be folded with the Asp61 carboxyl inaccessible to solvent and, indeed, the structural model predicts that the group should lie buried in a pocket of hydrophobic side-chains

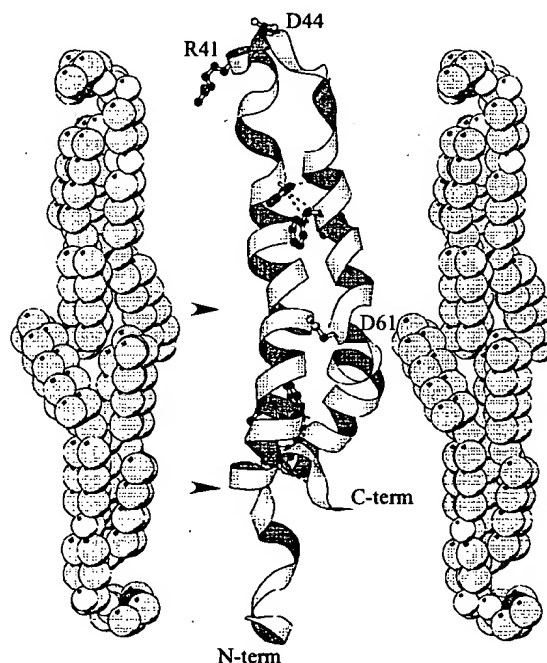


Fig. 2. Suggested folding of subunit *c* based upon current distance constraints between transmembrane  $\alpha$ -helices (drawing modified from Fillingame *et al.* 1995). The arrowheads indicate the well-defined region of helical-helical interaction (Girvin and Fillingame, 1995), i.e. from residues Tyr10 to Ala25 in helix-1 and Val60 to Ala77 in helix-2. The side-chain of Ala24 is shown juxtaposed to the Asp61 side-chain. The distance restraints from Girvin and Fillingame (1993) were combined with those in the well-defined region (Girvin and Fillingame, 1995) and used as input for modeling the whole subunit. The model was generated by distance geometry and dynamic simulated annealing using the program XPLOR. The restraints between aromatic clusters at the top and bottom of the structure are emphasized since they limit possible folding regimens. The loop region in the model shown is very similar to that in the other low-energy structures generated in this exercise, but all structural details in this region are speculative. The protein model has been placed in a bilayer of dioleoylphosphatidylethanolamine, modeled according to Peitzsch *et al.* (1995), to emphasize that the polar loop region of subunit *c* (at the top) cannot extend much beyond the plane of the membrane.

(Girvin and Fillingame, 1995). In the double mutant Ala24→Asp/Asp61→Asn, the functional Asp24 carboxyl shows a similarly elevated pKa of 6.9, a finding consistent with the structural model which shows that a carboxyl from either residue 24 or residue 61 could extend into the same hydrophobic pocket. A mutant with aspartyls at both position 24 and position 61 has also been examined and both carboxyls show pKa values close to 7.0. The function of this mutant is pH-sensitive, with one of the carboxyls predicted to have a pKa in the range 7–7.4 *in situ* (Zhang and Fillingame, 1994). The environment around Asp61 in the isolated protein may thus correlate very well with that in native  $F_0$ . During an active proton-pumping cycle, the structure around Asp61 of subunit *c* is predicted to change from a high-pKa form to a low-pKa form as protons are pumped from low concentration to high concentration (Fillingame, 1990). The structure of subunit *c* being determined by NMR may correspond to the high-pKa form of the protein.

The stoichiometry of  $H^+$  pumped per ATP hydrolyzed/synthesized is generally estimated to be at least three and more probably four (Fillingame, 1990; van Walraven *et al.* 1996). The  $H^+$ /ATP stoichiometry may explain the presence of multiple subunits *c* in the  $F_0$  complex, i.e. four subunits *c* may undergo protonation and deprotonation per ATP synthesized. At a stoichiometry of four, a change in pKa for Asp61 of 2–3 pH units would provide changes in binding energy of 40–60 kJ mol<sup>-1</sup>, which is within the range of the free energy change ( $\Delta G$ ) estimated as necessary for ATP synthesis under varying conditions (Souid and Penefsky, 1995). If three different sets of four subunits *c* protonate and deprotonate as the three  $\beta$  subunits alternate in ATP synthesis, a functional explanation for the stoichiometry of 12 subunit *c* per  $F_0$  would be at hand.

Subunit *a* is also likely to play a role in  $H^+$  translocation and perhaps in the coupling of  $H^+$  translocation to ATP synthesis. A number of subunit *a* mutants have been described, but the phenotypes are still difficult to interpret owing to the lack of a structural model (Fillingame, 1990). The number of transmembrane helices and the sidedness of the protein in the membrane are still not defined with certainty. Arg210 is generally thought to play a critical role in  $H^+$  transport, but that role is not clear. In its protonated form, it could form a transient salt bridge with Asp61 of subunit *c* to lower the pKa during the part of the  $H^+$  translocation cycle involving interaction of a single copy of subunit *c* with the single copy of subunit *a*, as I have suggested previously (Fillingame, 1990). If this hypothesis were correct, a class of Arg210 mutants might be found that retain the capacity to function in passive  $H^+$  transport not involving pKa changes, while being inactive in active  $H^+$  transport cycles where the pKa changes are required. Indeed the Arg210→Ala mutant shows hints of such a phenotype, i.e. the mutant lacks ATP synthase and ATPase-coupled  $H^+$  transport activities but shows significant indications of passive  $H^+$  conductance activity (Hatch *et al.* 1995). Arg210 could also serve in either more or less direct roles.

Hatch *et al.* (1995) have now generated functional pseudorevertants to the Arg210→Gln mutant where the essential Arg is replaced by a Gln252→Arg mutation. This

functional double mutant is unusual in that oxidative phosphorylation clearly takes place, whereas ATP-driven  $H^+$  transport was not demonstrable. These results are difficult to rationalize since the two activities are presumed to represent a reversal of the same process. The studies of Hatch *et al.* (1995) most simply suggest a proximity of residues 210 and 252 in the membrane, which would occur with Arg210 on transmembrane helix-4 and Gln252 on transmembrane helix-5 in the five-helix model they propose. Such folding would also bring Gly218 and Glu219 into close proximity of His245, as predicted by other genetic studies (Cain and Simoni, 1988; Hartzog and Cain, 1994). The idea of an extended transmembrane helix with a continuous functional face from residues 212 to 222 is supported by Ala insertion mutagenesis experiments (Wang and Vik, 1994). Other genetic studies suggest that a face of this putative helix, including residues 217, 221 and 224, may interact with the essential carboxyl group of subunit *c* during ATPase-coupled  $H^+$  transport (Fraga *et al.* 1994a). In these studies, the function of the Ala24→Asp/Asp61→Gly double mutant was shown to be optimized by third-site mutations in residues 217, 221 or 224. Since passive proton conductance is not disrupted in the Asp24Gly61 double mutant (Zhang and Fillingame, 1994), the optimizing mutations may facilitate the movements between subunits which lead to changes in pKa or which couple to conformational changes linked to ATP synthesis.

#### Coupling of $H^+$ transport to ATP synthesis

The protonation/deprotonation of Asp61 in subunit *c* was initially proposed to be linked with conformational changes in the polar loop region on the basis of the phenotype of an 'uncoupled' mutant (Mosher *et al.* 1985). Mutation of Gln42→Glu in the conserved Arg-Gln-Pro sequence of the polar loop gave rise to an  $F_1F_0$  complex with normal ATPase activity that was uncoupled from  $H^+$  translocation. The  $F_1$  moiety was bound by the mutant  $F_0$  with normal affinity, and the mutant  $F_0$  was shown to promote normal passive proton conductance. However, in contrast to the case of wild-type  $F_1F_0$ , when  $F_1$  was bound it did not block the intrinsic proton conductance of  $c$ Gln42→Glu  $F_0$ . We have more recently described a very similar phenotype for the Arg41→Lys polar loop mutant (Fraga *et al.* 1994b). Other mutations in Gln42 and Pro43 give rise to  $F_1F_0$  showing varying degrees of uncoupling (Fraga and Fillingame, 1989; Miller *et al.* 1989).

In an attempt to define the subunit in  $F_1$  that interacted with the polar loop to couple ATPase and  $H^+$  translocation, we selected suppressor mutations to the  $c$ Gln42→Glu mutation. All four of the extragenic suppressors isolated proved to lie in the Glu31 codon of subunit  $\epsilon$ ; the suppressor mutations being Glu31→Lys (found twice), Glu31→Gly and Glu31→Val (Zhang *et al.* 1994). To test whether there was a direct interaction between residue 31 of subunit  $\epsilon$  and the polar loop of subunit *c*, Cys residues were introduced into both regions and crosslinking attempted by oxidation. Cross-links were found with the  $\epsilon$ Cys31/ $c$ Cys40,  $\epsilon$ Cys31/ $c$ Cys42 and  $\epsilon$ Cys31/ $c$ Cys43 pairs, but not with the  $\epsilon$ Cys31/ $c$ Cys39 pair (Zhang and Fillingame, 1995b).

A cAsp44→Cys mutant was also generated. The Cys in this mutant proved to be hyper-reactive, crosslinking with other subunits by mechanisms other than Cys–Cys oxidation. In collaboration with R. Capaldi's laboratory (University of Oregon, Eugene), the region of crosslinking in subunit  $\gamma$  was defined by peptide mapping (Watts *et al.* 1995). S. D. Watts, C. Tang and R. A. Capaldi (in preparation) have now introduced Cys at position 205 in subunit  $\gamma$  and shown crosslinking with Cys42, Cys43 and Cys44 of subunit  $c$ . In sum, these results suggest that the conformational coupling between the loop region of subunit  $c$  and the stalk of  $F_1$  is likely to occur *via* direct interactions between loop residues of subunit  $c$  and residues in regions surrounding Glu31 of subunit  $\epsilon$  and Tyr205 of subunit  $\gamma$ .

The structure of the loop region of subunit  $c$  is not yet known but, on the basis of known NMR distance constraints, it is not likely to extend beyond the head group region of the phospholipid bilayer (Fig. 2; Fillingame *et al.* 1995). We do know that the structure of the loop region around Pro43 changes as Asp61 is titrated in the chloroform–methanol–water solvent used for NMR (Assadi-Porter and Fillingame, 1995), adding further support for the idea of  $H^+$  binding causing global changes in loop structure. The atomic resolution X-ray model of  $F_1$  does not resolve the region of subunit  $\gamma$  around Tyr205, but it can be assumed that the C-terminal  $\alpha$ -helical structure protruding from the bottom of  $F_1$  extends to the surface of the membrane. Crosslinking studies indicate that subunit  $\epsilon$  must also extend the entire length of the stalk as it can be crosslinked to both the  $F_0$  and  $F_1$  domains (Zhang and Fillingame, 1995b; Aggeler and Capaldi, 1996). Wilkens *et al.* (1995) have recently reported an NMR-derived structure for isolated subunit  $\epsilon$  (Fig. 3). It is a protein of two distinct domains, where the N-terminal domain of 84 residues forms a flattened 10-stranded  $\beta$ -barrel and the C-terminal 48 residues fold as an antiparallel hairpin of two extended  $\alpha$ -helices. Although the C-terminal domain interacts with important regions of the  $\beta$  or  $\alpha$  subunits, the interaction depending upon the nucleotide bound at catalytic sites (Capaldi *et al.* 1995; Aggeler and Capaldi, 1996), this interaction appears to be unimportant in coupling since the entire domain can be deleted without loss of function (Kuki *et al.* 1988). Subunits  $\epsilon$  and  $\gamma$  are known to bind to each other *in vitro* (Dunn, 1982), and regions of interaction have been defined by crosslinking, including interactions around residue Tyr205 of  $\gamma$  and within the N-terminal  $\beta$ -barrel domain of subunit  $\epsilon$  (Tang and Capaldi, 1996; see Fig. 3). As protons are translocated, the  $\gamma\epsilon$  complex is hypothesized to move as a unit from one subunit  $c$  to another to generate torque on  $\gamma$  that would cause it to rotate as an axle within the  $\alpha_3\beta_3$  hexamer of  $F_1$  (Tang and Capaldi, 1996).

How might ATP synthesis be driven by such a molecular machine? The  $\gamma$  subunit inside the  $\alpha_3\beta_3$  complex would be predicted to rotate by  $120^\circ$  as each tightly bound ATP is released, and each  $120^\circ$  rotation would be expected to break and establish new 'catches' with the  $\beta E$  and  $\beta TP$  subunits. The  $120^\circ$  rotation would be driven by the translocation of 4  $H^+$  and the unidirectional movement of the  $\gamma\epsilon$  complex across the loop regions of four subunits  $c$ . Such a molecular machine could be

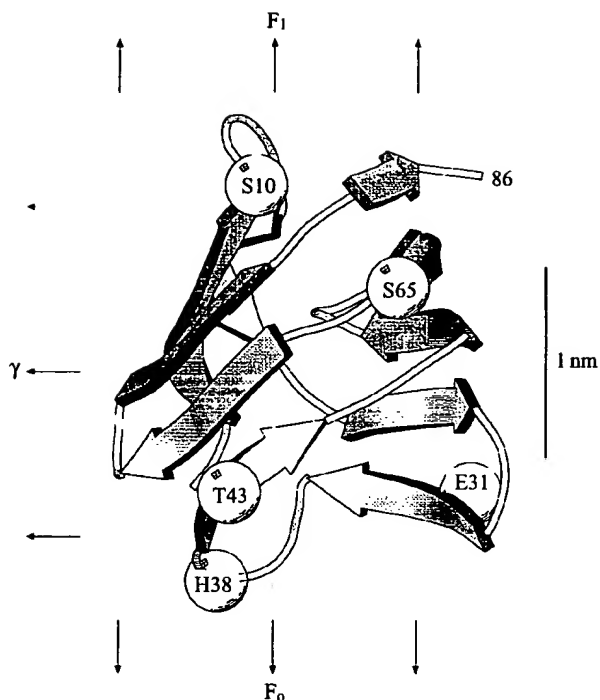


Fig. 3. Structure of the  $\beta$ -barrel domain of subunit  $\epsilon$ , determined by nuclear magnetic resonance, emphasizing the sites of interaction with  $F_0$  and with subunit  $\gamma$  of  $F_1$  (Wilkens *et al.* 1995). The distance between the  $\alpha$ -carbons of His38 and Glu31 at the bottom the structure is 1.8 nm. The coordinates and figure were provided by Dr S. Wilkens and Dr R. Capaldi (University of Oregon).

designed by the following rules. Formation of the  $\gamma\epsilon$ -c complex would require a loop structure, as seen only in the low-pKa form of subunit  $c$ , i.e. the form that accepts  $H^+$  from the high  $H^+$  activity side (outer surface) of the membrane. The association of the single-copy, subunit  $a$  with subunit  $c$  might be required to generate the low-pKa Asp61, as was discussed above. Movement of subunit  $a$  away from subunit  $c$  would be coupled to a pKa shift and translocation of the carboxyl group to the low  $H^+$  activity side (inner surface) of the membrane. The release of  $H^+$  from the high-pKa form of subunit  $c$ , or the conformational change accompanying the pKa shift, would result in changes in subunit  $c$  loop structure causing disassociation of the  $\gamma\epsilon$  complex. An asymmetry in association of the  $\gamma\epsilon$  pair with  $F_0$  subunits  $a$  or  $b$  could unidirectionally restrict movement of  $\gamma\epsilon$  to the loop of the next low-pKa subunit  $c$ , i.e. force movement in a clockwise or counter-clockwise direction. As the fourth  $H^+$  was translocated on completion of the  $120^\circ$  rotation, sufficient torque would be generated to drive the  $120^\circ$  rotation of subunit  $\gamma$  within the  $\alpha_3\beta_3$  hexamer, by the breaking and reformation of the  $\beta E$  and  $\beta TP$  'catches', with a cooperative alteration of nucleotide binding site structure in the three  $\beta$  subunits and release of ATP from the 'tight' site.

In evaluating such a model, one needs to know whether the  $\gamma$  subunit moves smoothly in four isoenergetic steps over each  $120^\circ$  of rotation, as it moves from one  $\beta$  to the next, or in contrast,

whether most of the energy is spent in a single event such as driving 'catch' breaking and/or 'catch' reformation and the associated conformational changes. On the basis of the X-ray crystal structure, the latter seems more likely. If the energy is consumed in a single event, then the sequential release of four protons in isoenergetic translocations steps, as suggested in the paragraph above, is problematic. That is, how would the energy be stored over the interval between the first and fourth translocation event? A solution to the problem is to make the release of  $H^+$  from the high-pKa form of subunit *c* dependent upon the position of  $\gamma$  within the  $\alpha_3\beta_3$  core, e.g. to permit  $H^+$  release only when  $\gamma$  is in position to form a new catch. In such a model, the association of  $\gamma$  with the loop of subunit *c* would still be dependent upon formation of the low-pKa form of the protein, and transition to the high-pKa form would still cause  $\gamma$  disassociation, but  $H^+$  would not be released from the high-pKa sites before simultaneous completion of the 120° movement of subunit  $\gamma$ .

The work described from my own laboratory was supported by US Public Health Service Grant GM23105. I thank Dr Rod Capaldi and Dr Stephen Wilkens of the University of Oregon, Eugene, for providing coordinates of subunit  $\epsilon$ , for the drawing shown in Fig. 3 and for providing timely access to information prior to publication.

### References

- ABRAHAMS, J. P., LESLIE, A. G. W., LUTTER, R. AND WALKER, J. E. (1994). Structure at 2.8 Å resolution of  $F_1$ -ATPase from bovine heart mitochondria. *Nature* **370**, 621–628.
- ABRAHAMS, J. P., LUTTER, R., TODD, R. J., VAN RAAIJ, M. L., LESLIE, A. G. W. AND WALKER, J. E. (1993). Inherent asymmetry of the structure of  $F_1$ -ATPase from bovine heart mitochondria at 6.5 Å resolution. *EMBO J.* **12**, 1775–1780.
- AGGELER, R. AND CAPALDI, R. A. (1996). Nucleotide dependent movement of the  $\epsilon$  subunit between  $\alpha$  and  $\beta$  subunits in the *Escherichia coli*  $F_1F_0$  type ATPase. *J. biol. Chem.* **271**, 13888–13891.
- AMANO, T., HISABORI, T., MUNAYUKI, E. AND YOSHIDA, M. (1996). Catalytic activities of  $\alpha_3\beta_3\gamma$  complexes of  $F_1$ -ATPase with one, two or three incompetent catalytic sites. *J. biol. Chem.* **271**, 18128–18133.
- ASSADI-PORTER, A. M. AND FILLINGAME, R. H. (1995). Proton-translocating carboxyl of subunit *c* of  $F_1F_0$   $H^+$ -ATP synthase: Unique environment suggested by the pK<sub>a</sub> determined by  $^1H$ -NMR. *Biochemistry, N.Y.* **34**, 16186–16193.
- BELOGRUDOV, G. I., TOMICH, J. M. AND HATEFI, Y. (1995). ATP synthase complex: Proximities of subunits in bovine submitochondrial particles. *J. biol. Chem.* **270**, 2053–2060.
- BIRKENHÄGER, R., HOPPERT, M., DECKERS-HEBESTREIT, G., MAYER, F. AND ALTENDORF, K. (1995). The  $F_0$  complex of the *Escherichia coli* ATP synthase: Investigation by electron spectroscopic imaging and immunoelectron microscopy. *Eur. J. Biochem.* **230**, 58–67.
- BOYER, P. D. (1993). The binding change mechanism for ATP synthase – some probabilities and possibilities. *Biochim. biophys. Acta* **1140**, 215–250.
- CAIN, B. D. AND SIMONI, R. D. (1988). Interaction between Glu-219 and His-245 within the *a* subunit of  $F_1F_0$ -ATPase in *Escherichia coli*. *J. biol. Chem.* **263**, 6606–6612.
- CAPALDI, R. A., AGGELER, R. AND WILKENS, S. (1995). Conformational changes in the  $\gamma$  and  $\epsilon$  subunits are integral to the functioning of the *Escherichia coli*  $H^+$ -pumping ATPase (ECF<sub>1</sub> $F_0$ ). *Biochem. Soc. Trans.* **23**, 767–770.
- CHATTERJEE, D., CHAKRABORTY, M., LEIT, M., NEFF, L., JAMSAKELLOKUMPU, S., FUCHS, R., BARTKIEWICZ, M., HERNANDO, N. AND BARON, R. (1992). The osteoclast proton pump differs in its pharmacology and catalytic subunits from other vacuolar  $H^+$ -ATPases. *J. exp. Biol.* **172**, 193–204.
- COLLINSON, I. R., RUNSWICK, M. J., BUCHANAN, S. K., FEARNLEY, I. M., SKEHEL, J. M., VANRAAIJ, M. J., GRIFFITHS, D. E. AND WALKER, J. E. (1994a).  $F_0$  membrane domain of ATP synthase from bovine heart mitochondria: Purification, subunit composition and reconstitution with  $F_1$ -ATPase. *Biochemistry, N.Y.* **33**, 7971–7978.
- COLLINSON, I. R., VAN RAAIJ, M. J., RUNSWICK, M. J., FEARNLEY, I. M., SKEHEL, J. M., ORRIS, G. L., MIROUX, B. AND WALKER, J. E. (1994b). ATP synthase from bovine heart mitochondria: *In vitro* assembly of a stalk complex in the presence of  $F_1$ -ATPase and in its absence. *J. molec. Biol.* **242**, 408–421.
- CROSS, R. L. (1981). The mechanism and regulation of ATP synthesis by  $F_1$ -ATPases. *A. Rev. Biochem.* **50**, 681–714.
- DENDA, K., KONISHI, J., OSHIMA, T., DATE, T. AND YOSHIDA, M. (1989). A gene encoding the proteolipid subunit of *Sulfolobus acidocaldarius* ATPase complex. *J. biol. Chem.* **264**, 7119–7121.
- DIMROTH, P. (1995). On the way towards the  $Na^+$ -binding site within the  $F_1F_0$  ATPase of *Propionigenium modestum*. *Biochem. Soc. Trans.* **23**, 770–775.
- DMITRIEV, O. Y., ALTENDORF, K. AND FILLINGAME, R. H. (1995). Reconstitution of  $F_0$  complex of *Escherichia coli* ATP synthase from isolated subunits: varying the number of essential carboxylates by co-incorporation of wild type and mutant subunit *c* after purification in organic solvent. *Eur. J. Biochem.* **233**, 478–483.
- DUNCAN, T. M., BULYGIN, V. V., ZHOU, Y., HUTCHEON, M. L. AND CROSS, R. L. (1995). Rotation of subunits during catalysis of *Escherichia coli*  $F_1$ -ATPase. *Proc. natn. Acad. Sci. U.S.A.* **92**, 10964–10968.
- DUNN, S. D. (1982). The isolated  $\gamma$  subunit of *Escherichia coli*  $F_1$  ATPase binds the  $\epsilon$  subunit. *J. biol. Chem.* **257**, 7354–7359.
- FILLINGAME, R. H. (1990). Molecular mechanics of ATP synthesis by the  $F_1F_0$  type  $H^+$  transporting ATP synthases. *The Bacteria* **12**, 345–391.
- FILLINGAME, R. H. (1996). Membrane sectors of F and V type  $H^+$  transporting ATPases. *Curr. Opin. struct. Biol.* **6** (in press).
- FILLINGAME, R. H., GIRVIN, M. E. AND ZHANG, Y. (1995). Correlations of structure and function in subunit *c* of *Escherichia coli*  $F_1F_0$  ATP synthase. *Biochem. Soc. Trans.* **23**, 760–766.
- FORGAC, M. (1992). Structure and properties of the coated vesicle ( $H^+$ )-ATPase. *J. Bioenerg. Biomembr.* **24**, 341–350.
- FOSTER, D. L. AND FILLINGAME, R. H. (1982). Stoichiometry of subunits in the  $H^+$ -ATPase complex of *Escherichia coli*. *J. biol. Chem.* **257**, 2009–2015.
- FRAGA, D. AND FILLINGAME, R. H. (1989). Conserved polar loop region of *Escherichia coli* subunit *c* of the  $F_1F_0$   $H^+$ -ATPase: glutamine 42 is not absolutely essential, but substitutions alter binding and coupling of  $F_1$  to  $F_0$ . *J. biol. Chem.* **264**, 6797–6803.
- FRAGA, D., HERMOLIN, J. AND FILLINGAME, R. H. (1994a). Transmembrane helix-helix interactions in  $F_0$  suggested by suppressor mutations to Asp24Gly61 mutant of ATP synthase subunit *c*. *J. biol. Chem.* **269**, 2562–2567.
- FRAGA, D., HERMOLIN, J., OLDENBURG, M., MILLER, M. AND FILLINGAME, R. H. (1994b). Arginine 41 of subunit *c* of *Escherichia coli*  $H^+$ -ATP synthase is essential in binding and coupling of  $F_1$  to  $F_0$ . *J. biol. Chem.* **269**, 7532–7537.
- GIRVIN, M. E. AND FILLINGAME, R. H. (1993). Helical structure and folding of subunit *c* of  $F_1F_0$  ATP synthase:  $^1H$  nmr resonance assignments and NOE analysis. *Biochemistry, N.Y.* **32**, 12167–12177.
- GIRVIN, M. E. AND FILLINGAME, R. H. (1994). Hairpin-like folding of subunit *c* of  $F_1F_0$  ATP synthase:  $^1H$  distance measurements to nitroxide-derivatized aspartyl-61. *Biochemistry, N.Y.* **33**, 665–674.



- GIRVIN, M. E. AND FILLINGAME, R. H. (1995). Determination of local protein structure by spin label difference 2D nmr: The region neighboring Asp61 of subunit *c* of the  $F_1F_0$  ATP synthase. *Biochemistry, N.Y.* **34**, 1635–1645.
- GLUCK, S. AND NELSON, R. (1992). The role of the V-ATPase in renal epithelial  $H^+$  transport. *J. exp. Biol.* **172**, 205–218.
- GLUCK, S., NELSON, R. D., LEE, B. S., WANG, Z. Q., GUO, X. L., FU, J. Y. AND ZHANG, K. (1992). Biochemistry of the renal V-ATPase. *J. exp. Biol.* **172**, 219–229.
- HARRIS, D. A. (1995). Protein and peptide inhibitors of the  $F_1$ -ATPase. *Biochem. Soc. Trans.* **23**, 790–793.
- HARTZOG, P. E. AND CAIN, B. D. (1994). Second-site suppressor mutations at glycine 218 and histidine 245 in the  $\alpha$  subunit of  $F_1F_0$  ATP synthase in *Escherichia coli*. *J. biol. Chem.* **269**, 32313–32317.
- HARVEY, W. R. (1992). Physiology of V-ATPases. *J. exp. Biol.* **172**, 1–17.
- HARVEY, W. R. AND NELSON, N. (1992). V-ATPases. *J. exp. Biol.* **172**, 1–485.
- HATCH, L. P., COX, G. B. AND HOWITT, S. M. (1995). The essential arginine residue at position 210 in the  $\alpha$  subunit of the *Escherichia coli* ATP synthase can be transferred to position 252 with partial retention of activity. *J. biol. Chem.* **270**, 29407–29412.
- KAIM, G. AND DIMROTH, P. (1994). Construction, expression and characterization of a plasmid-encoded  $Na^+$ -specific ATPase hybrid consisting of *Propionigenium modestum*  $F_0$ -ATPase and *Escherichia coli*  $F_1$ -ATPase. *Eur. J. Biochem.* **222**, 615–623.
- KIBAK, H., TAIZ, L., STARKE, T., BERNASCONI, P. AND GOGARTEN, J. P. (1992). Evolution of structure and function of V-ATPases. *J. Bioenerg. Biomembr.* **24**, 415–424.
- KLUGE, C. AND DIMROTH, P. (1993). Kinetics of inactivation of the  $F_1F_0$  ATPase of *Propionigenium modestum* by dicyclohexylcarbodiimide in relationship to  $H^+$  and  $Na^+$  concentration: Probing the binding site for the coupling ions. *Biochemistry, N.Y.* **32**, 10378–10386.
- KLUGE, C. AND DIMROTH, P. (1994). Modification of isolated subunit *c* of the  $F_1F_0$ -ATPase from *Propionigenium modestum* by dicyclohexylcarbodiimide. *FEBS Lett.* **340**, 245–248.
- KUKI, M., NOUMI, T., MAEDA, M., AMEMURA, A. AND FUTAI, M. (1988). Functional domains of  $\epsilon$  subunit of *Escherichia coli*  $H^+$ -ATPase ( $F_0F_1$ ). *J. biol. Chem.* **263**, 17437–17442.
- LAUBINGER, W., DECKERS-HEBESTREIT, G., ALTENDORF, K. AND DIMROTH, P. (1990). A hybrid adenosinetriphosphatase composed of  $F_1$  of *Escherichia coli* and  $F_0$  of *Propionigenium modestum* is a functional sodium ion pump. *Biochemistry, N.Y.* **29**, 5458–5463.
- LAUBINGER, W. AND DIMROTH, P. (1989). The sodium ion translocating adenosine triphosphatase of *Propionigenium modestum* pumps protons at low sodium ion concentrations. *Biochemistry, N.Y.* **28**, 7194–7198.
- MATTSSON, J. P., SCHLESINGER, P. H., KEELING, D. J., TEITELBAUM, S. L., STONE, D. K. AND XIE, X.-S. (1994). Isolation and reconstitution of a vacuolar-type proton pump of osteoclast membranes. *J. biol. Chem.* **269**, 24979–24982.
- MERZENDORFER, H., GRÄF, R., HUSS, M., HARVEY, W. AND WIECZOREK, H. (1997). Regulation of proton-translocating V-ATPases. *J. exp. Biol.* **200**, 225–235.
- MILLER, M. J., FRAGA, D., PAULE, C. R. AND FILLINGAME, R. H. (1989). Mutations in the conserved proline-43 residue of the *uncE* protein (subunit *c*) of *Escherichia coli*  $F_1F_0$  ATPase alter the coupling of  $F_1$  to  $F_0$ . *J. biol. Chem.* **264**, 305–311.
- MILLER, M. J., OLDENBURG, M. AND FILLINGAME, R. H. (1990). The essential carboxyl group in subunit *c* of the  $F_1F_0$  ATP synthase can be moved and  $H^+$ -translocating function retained. *Proc. natn. Acad. Sci. U.S.A.* **87**, 4900–4904.
- MILLS, J. D., AUSTIN, P. A. AND TURTON, J. S. (1995). Thioredoxin and control of  $F_0F_1$ : function and distribution. *Biochem. Soc. Trans.* **23**, 775–780.
- MOSHER, M. E., WHITE, L. K., HERMOLIN, J. AND FILLINGAME, R. H. (1985).  $H^+$ -ATPase of *Escherichia coli*: An *uncE* mutation impairing coupling between  $F_1$  and  $F_0$  but not  $F_0$ -mediated  $H^+$ -translocation. *J. biol. Chem.* **260**, 4807–4814.
- NELSON, N. (1992). Structural conservation and functional diversity of V-ATPases. *J. Bioenerg. Biomembr.* **24**, 407–414.
- PEITZSCH, R. M., EISENBER, M., SHARP, K. A. AND MCLAUGHLIN, S. (1995). Calculations of the electrostatic potential adjacent to model phospholipid bilayers. *Biophys. J.* **68**, 729–738.
- SABBERT, D., ENGELBRECHT, S. AND JUNGE, W. (1996). Intersubunit rotation in active F-ATPase. *Nature* **381**, 623–625.
- SQUID, A.-K. AND PENEFSKY, H. S. (1995). Energetics of ATP dissociation from the mitochondrial ATPase during oxidative phosphorylation. *J. biol. Chem.* **270**, 9074–9082.
- TANG, C. AND CAPALDI, R. A. (1996). Characterization of the interface between  $\gamma$  and  $\epsilon$  subunits of *Escherichia coli*  $F_1$ -ATPase. *J. biol. Chem.* **271**, 3018–3024.
- VAN WALRAVEN, H. S., STROTMANN, H., SCHWARZ, O. AND RUMBERG, B. (1996). The  $H^+$ /ATP coupling ratio of the ATP synthase from thiol-modulated chloroplasts and two cyanobacterial strains is four. *FEBS Lett.* **379**, 309–313.
- WALKER, J. E. (1994). The regulation of catalysis in ATP synthase. *Curr. Opin. struct. Biol.* **4**, 912–918.
- WANG, S. AND VIK, S. B. (1994). Single amino acid insertions probe the  $\alpha$  subunit of the *Escherichia coli*  $F_1F_0$ -ATP synthase. *J. biol. Chem.* **269**, 3095–3099.
- WATTS, S. D., ZHANG, Y., FILLINGAME, R. H. AND CAPALDI, R. A. (1995). The gamma subunit in the *Escherichia coli* ATP synthase complex ( $ECF_1F_0$ ) extends through the stalk and contacts the  $c$  subunits of the  $F_0$  part. *FEBS Lett.* **368**, 235–238.
- WEBER, J., WILKE-MOUNTS, S. AND SENIOR, A. E. (1994). Cooperativity and stoichiometry of substrate binding to the catalytic sites of *Escherichia coli*  $F_1$ -ATPase: Effects of magnesium, inhibitors and mutation. *J. biol. Chem.* **269**, 20462–20467.
- WEBER, J., WILKE-MOUNTS, S., LEE, R. S.-F., GRELL, E. AND SENIOR, A. E. (1993). Specific placement of tryptophan in the catalytic sites of *Escherichia coli*  $F_1$ -ATPase provides a direct probe of nucleotide binding: Maximal ATP hydrolysis occurs with three sites occupied. *J. biol. Chem.* **268**, 20126–20133.
- WIECZOREK, H., PUTZENLECHNER, M., ZEISKE, W. AND KLEIN, U. (1991). A vacuolar-type proton pump energizes  $K^+/H^+$  antiport in an animal plasma membrane. *J. biol. Chem.* **266**, 15340–15347.
- WILKENS, S., DAHLQUIST, F. M., MCINTOSH, L. P., DONALDSON, L. W. AND CAPALDI, R. A. (1995). Structural features of the  $\epsilon$  subunit of the *Escherichia coli* ATP synthase determined by nmr spectroscopy. *Nature Struct. Biol.* **2**, 961–967.
- ZHANG, Y. AND FILLINGAME, R. H. (1994). Essential aspartate in subunit *c* of  $F_1F_0$  ATP synthase: Effect of position 61 substitutions in helix-2 on function of Asp24 in helix-1. *J. biol. Chem.* **269**, 5473–5479.
- ZHANG, Y. AND FILLINGAME, R. H. (1995a). Changing the ion binding specificity of the *Escherichia coli*  $H^+$ -transporting ATP synthase by directed mutagenesis of subunit *c*. *J. biol. Chem.* **270**, 87–93.
- ZHANG, Y. AND FILLINGAME, R. H. (1995b). Subunits coupling  $H^+$  transport and ATP synthesis in the *Escherichia coli* ATP synthase: Cys–Cys crosslinking of  $F_1$  subunit  $\epsilon$  to the polar loop of  $F_0$  subunit *c*. *J. biol. Chem.* **270**, 24609–24614.
- ZHANG, Y., OLDENBURG, M., AND FILLINGAME, R. H. (1994). Suppressor mutations in  $F_1$  subunit  $\epsilon$  recouple ATP-driven  $H^+$ -translocation in uncoupled Q42E subunit *c* mutant of the *Escherichia coli*  $F_1F_0$  ATP synthase. *J. biol. Chem.* **269**, 10221–10224.



## $\beta$ - $\gamma$ Subunit Interaction Is Required for Catalysis by $H^+$ -ATPase (ATP Synthase)

$\beta$  SUBUNIT AMINO ACID REPLACEMENTS SUPPRESS A  $\gamma$  SUBUNIT MUTATION HAVING A LONG UNRELATED CARBOXYL TERMINUS\*

(Received for publication, May 31, 1995, and in revised form, July 10, 1995)

Catherine Jeanteur-De Beukelaer, Hiroshi Omote†, Atsuko Iwamoto-Kihara‡, Masatomo Maeda§, and Masamitsu Futai||

From the Division of Biological Science, the Institute of Scientific and Industrial Research, Osaka University, Ibaraki, Osaka 567, Japan

The mechanisms of energy coupling and catalytic cooperativity are not yet understood for  $H^+$ -ATPase (ATP synthase). An *Escherichia coli*  $\gamma$  subunit frameshift mutant (downstream of Thr- $\gamma$ 277) could not grow by oxidative phosphorylation because both mechanisms were defective (Iwamoto, A., Miki, J., Maeda, M., and Futai, M. (1990) *J. Biol. Chem.* 265, 5043–5048). The defect(s) of the  $\gamma$  frameshift was obvious, because the mutant subunit had a carboxyl terminus comprising 16 residues different from those in the wild type. However, in this study, we surprisingly found that an Arg- $\beta$ 52  $\rightarrow$  Cys or Gly- $\beta$ 150  $\rightarrow$  Asp replacement could suppress the deleterious effects of the  $\gamma$  frameshift. The membranes of the two mutants ( $\gamma$  frameshift/Cys- $\beta$ 52 with or without a third mutation, Val- $\beta$ 77  $\rightarrow$  Ala) exhibited increased oxidative phosphorylation, together with 70–100% of the wild type ATPase activity. Similarly, the  $\gamma$  frameshift/Asp- $\beta$ 150 mutant could grow by oxidative phosphorylation, although this mutant had low membrane ATPase activity. These results suggest that the  $\beta$  subunit mutation suppressed the defects of catalytic cooperativity and/or energy coupling in the  $\gamma$  mutant, consistent with the notion that conformational transmission between the two subunits is pertinent for this enzyme.

$H^+$ -ATPase (ATP synthase,  $F_0F_1$ ) synthesizes ATP coupled with an electrochemical gradient of protons (for reviews see Refs. 1–3). The catalytic site of the enzyme is located in the  $\beta$  subunit of the  $F_1$  sector ( $\alpha_3\beta_3\gamma\delta\epsilon$ ). The membrane-intrinsic  $F_0$  sector ( $ab_2c_6-10$ ) functions as a proton pathway. Studies on a negatively stained specimen labeled with maleimidogold established that the central mass of  $F_1$  contains the amino-terminal part of the  $\gamma$  subunit (4). The x-ray structures of the mitochondrial  $F_1$  sector of bovine heart and rat liver have been studied by two groups independently (5–7). In the crystal structure of bovine  $F_1$ , the  $\alpha$  and  $\beta$  subunits are arranged alternatively

around the amino and carboxyl-terminal  $\alpha$  helices of the  $\gamma$  subunit (7). Consistent with its central location in the  $F_1$  sector, the active role of the  $\gamma$  subunit in catalysis and its energy coupling with proton transport have been supported by biochemical and molecular biological studies (8–12).

Mutational studies on the *Escherichia coli* enzyme suggested the importance of the amino- and carboxyl-terminal regions of the  $\gamma$  subunit (286 total residues) in catalysis and energy coupling. Amino acid substitutions in the region between Gln- $\gamma$ 269 and Thr- $\gamma$ 277 decreased the membrane ATPase activity and growth by oxidative phosphorylation (8, 10). The amino-terminal mutants, Met- $\gamma$ 23  $\rightarrow$  Lys and Met- $\gamma$ 23  $\rightarrow$  Arg, exhibited substantial ATPase activities (65 and 100%, respectively, of the wild type level), although they grew only very slowly by oxidative phosphorylation (9). The uncoupled phenotype of the Met- $\gamma$ 23  $\rightarrow$  Lys mutant was suppressed by eight different amino acid replacements mapped between residues 269 and 280 in the carboxyl-terminal domain (10, 13). These results suggest that the two terminal regions functionally interact to mediate efficient energy coupling. The  $\gamma$  subunit with the Ser- $\gamma$ 8  $\rightarrow$  Cys mutation cross-linked with a different  $\beta$  subunit region in the presence of  $Mg^{2+}$ -ADP or  $Mg^{2+}$ -ATP, suggesting that conformational changes related to the catalytic site event occur around Ser- $\gamma$ 8 (11). Furthermore, a fluorescence probe introduced into the  $\gamma$  subunit changed its spectrum on the addition of ATP or AMPPNP<sup>1</sup> (12). However, it is unknown which region(s) of the  $\beta$  subunit interacts functionally with the  $\gamma$  subunit.

The interaction(s) between different subunits within the  $F_1$  sector can be clearly shown by mutation studies (14); suppression of the defective energy coupling of the Ser- $\beta$ 174  $\rightarrow$  Phe mutation by an Arg- $\alpha$ 296  $\rightarrow$  Cys replacement indicated the importance of the functional  $\alpha$ - $\beta$  interaction in energy coupling. In this study, a similar approach was adopted for the  $\beta$  subunit- $\gamma$  subunit interaction. We previously isolated an interesting frameshift mutant that had 16 unrelated residues due to a nucleotide deletion from the Gln- $\gamma$ 278 codon (8); the  $\gamma$  subunit frameshift has 7 additional residues at its carboxyl terminus together with 9 altered residues downstream of Thr- $\gamma$ 277. The mutant cells exhibited low membrane ATPase activity and could not grow by oxidative phosphorylation. Thus, the long altered carboxyl-terminal domain may interact deleteriously with the  $\beta$  subunit leading to lower catalytic cooperativity and defective energy coupling. The defect of the  $\gamma$  frameshift mutation was suppressed by  $\beta$ R52C (Arg- $\beta$ 52  $\rightarrow$  Cys) with or without a  $\beta$ V77A (Val- $\beta$ 77  $\rightarrow$  Ala) or  $\beta$ C150D (Gly- $\beta$ 150  $\rightarrow$  Asp)

\* This work was supported by grants from the Japanese Ministry of Education, Science, and Culture and the Human Frontier Science Program. The costs of publication of this article were defrayed in part by the payment of page charges. This article must therefore be hereby marked "advertisement" in accordance with 18 U.S.C. Section 1734 solely to indicate this fact.

† Supported by a Postdoctoral Fellowship from the Japan Society for the Promotion of Science.

§ Present address: Dept. of Biology, College of Arts and Sciences, The University of Tokyo, Komaba, Meguro-ku, Tokyo 153, Japan.

|| Present address: Laboratory of Biochemistry, Faculty of Pharmaceutical Sciences, Osaka University, Suita, Osaka 565, Japan.

|| To whom correspondence should be addressed. Tel.: 81-6-879-8480; Fax: 81-6-875-5724; E-mail: m-futai@sanken.osaka-u.ac.jp.

<sup>1</sup> The abbreviations used are: AMPPNP, 5'-adenylyl- $\beta$ , $\gamma$ -imidodiphosphate; PCR, polymerase chain reaction; MES, 2-(*N*-morpholino)ethanesulfonic acid; MOPS, 3-(*N*-morpholino)propanesulfonic acid.

replacement in the  $\beta$  subunit, suggesting that the deleterious  $\beta$ - $\gamma$  interaction in the  $\gamma$  frameshift was suppressed by the second  $\beta$  subunit mutation. It is surprising that growth of the three mutants can be supported by oxidative phosphorylation.

#### EXPERIMENTAL PROCEDURES

***E. coli* and Growth Conditions**—Strains DK8 ( $\Delta uncB-C$ , *ilv::Tn10*, *thi*) (15) lacking the entire *unc* (ATP synthase) operon and KF10rA (*thi*, *thy*, *recA1*, *uncG10* (Gln- $\gamma$ 14  $\rightarrow$  end)) carrying pBMG293fs (frameshift in the *uncG* gene for the  $\gamma$  subunit) (8) were also used. The rich medium (L broth) supplemented with 50  $\mu$ g/ml thymine with or without ampicillin and the minimal medium (16) containing 2  $\mu$ g/ml thiamine, 50  $\mu$ g/ml thymine, 50  $\mu$ g/ml isoleucine, 50  $\mu$ g/ml valine, and a carbon source (10 mM glucose, 15 mM succinate, or 0.5% glycerol) were described previously.

**Construction of pBMUG15fs Carrying the Entire *unc* Operon with the  $\gamma$  Subunit Frameshift Mutation**—The  $\gamma$  frameshift mutation was introduced into a recombinant plasmid, pBWU1 (17), carrying the entire wild type *unc* operon (see Fig. 1). A unique *SpeI* site was introduced into the noncoding region (9 base pairs downstream of the last letter of the *uncG* end codon) by mutagenesis of pBWU1 using polymerase chain reaction (PCR) (Perkin-Elmer); the combinations of primers I and III and primers II and IV were used for the first PCR, and then primers I and II were used for the second PCR (see Fig. 1a). The primers used were: I, 5'-TGCCAGGTCACCGGCATGG-3'; II, 5'-TAACCGGAGT-GCTCGATCGC-3'; III and IV, as shown in Fig. 1. After removing the *NdeI* segment from the resulting plasmid, pBWU15 carrying the entire *unc* operon was constructed. pBMG293fs (8) carrying *uncG* with the  $\gamma$  frameshift mutation was subjected to PCR using primers I and FS (see Fig. 1b). The *RsaI*-*SpeI* fragment was isolated from the amplified product and ligated with pBWU15 digested with the same endonucleases. The resulting recombinant plasmid, pBMUG15fs, was used for further studies.

**Random Mutagenesis of the  $\beta$  Subunit Gene (*uncD*)**—The *SpeI*-*SacI* fragment corresponding to the amino-terminal half of the *uncD* gene was isolated and introduced into pBluescript II SK+ (see Fig. 1c). A modified PCR (18) was employed to generate random mutations using universal primers (vector segments), and the *SpeI*-*SacI* fragment was isolated and ligated with pBMUG15fs treated with the same enzymes. The resulting plasmids were transformed into strain DK8, and cells showing positive growth on succinate by oxidative phosphorylation were isolated. These cells harbored recombinant plasmids carrying the  $\gamma$  frameshift mutation and  $\beta$  subunit mutation(s). A plasmid, pBMUD13-G150D, having a single mutation, Gly- $\beta$ 150  $\rightarrow$  Asp (GGT  $\rightarrow$  GAT) was constructed as described previously (17).

**Other Procedures**—Membrane vesicles were prepared from logarithmic phase cells (19) and suspended in a TKDG buffer (10 mM Tris-HCl, pH 8.0, 140 mM KCl, 0.5 mM dithiothreitol, and 10% glycerol). The formation of an electrochemical  $H^+$  gradient (8), ATPase activity (19), the amount of protein (20), and the rate of ATP synthesis in the presence of 10 mM NADH (14) were assayed by the published procedures. DNA manipulation and sequencing were performed as described previously (21). Immunoblotting was carried out using an Amersham ECL Western blotting detection kit.

**Materials**—Oligonucleotides were synthesized with a Pharmacia LKB (Uppsala) Gene Assembler Plus. The restriction and modifying enzymes for DNA were from Takara Shuzo Co. (Kyoto, Japan), Nippon Gene Co. (Toyama, Japan), or New England Biolabs (Beverly, MA). *Taq* polymerase and deoxynucleotides were from Perkin-Elmer.

#### RESULTS

**Construction of a Recombinant Plasmid, pBMUG15fs, Carrying the *unc* Operon with the  $\gamma$  Subunit Frameshift Mutation**—A plasmid, pBMG293fs, carrying the frameshift  $\gamma$  subunit gene was derived from a mutant recombinant plasmid, pBMG278Q (Glu- $\gamma$ 278  $\rightarrow$  Gln) by one nucleotide deletion from the Gln- $\gamma$ 278 codon (CAG  $\rightarrow$  AG) (8). The frameshift  $\gamma$  subunit was 7 residues longer than the wild type (286 total residues) and had 16 different residues. Plasmid pBMG293fs could not support the growth of the  $\gamma$  mutant, KF10rA (Gln- $\gamma$ 14  $\rightarrow$  end), by oxidative phosphorylation, although membranes of KF10rA/pBMG293fs exhibited substantial ATPase activity (8).

For further studies, the frameshift  $\gamma$  subunit gene was transferred from pBMG293fs into pBWU15 (Fig. 1, a and b). The resulting plasmid, pBMUG15fs, carried all cistrons of the *unc*

operon for  $H^+$  ATPase with the  $\gamma$  frameshift mutation. Similar to KF10rA/pBMG293fs, DK8 harboring pBMUG15fs could not grow by oxidative phosphorylation and exhibited about 23% of the membrane ATPase activity of the same strain with wild type plasmid pBWU15 (Table I). As shown previously (22), DK8 harboring pBWU15 had 10-fold more enzyme than the regular *E. coli* strain. Thus, mutant cells even with enzyme having 10% of the specific activity of the wild type can grow by oxidative phosphorylation, if they can couple  $H^+$  transport and ATP synthesis properly. The Ser- $\beta$ 174  $\rightarrow$  Leu mutant is an example of such cells; this mutant exhibited 10% membrane ATPase activity and a 50% growth yield on oxidative phosphorylation (14). Therefore, it is clear that DK8/pBMUG15fs (with 23% membrane ATPase activity) is defective in energy coupling because no growth by oxidative phosphorylation could be observed. Consistent with no growth, the rate of ATP synthesis by DK8/pBMUG15fs membrane vesicles was less than 5% of the wild type level (Table I).

**$\beta$  Subunit Amino Acid Substitutions Suppressed the  $\gamma$  Frameshift Mutation**—A DNA fragment corresponding to the amino-terminal half of the  $\beta$  subunit (Ala- $\beta$ 1 to Leu- $\beta$ 162) was randomly mutagenized by PCR and ligated into pBMUG15fs (Fig. 1c). Surprisingly, three plasmids could confer the ability of oxidative phosphorylation-dependent growth on strain DK8 (Table I). DNA sequencing of the two plasmids (pBMUG15fsR1 and pBMUG15fsR2) revealed different  $\beta$  subunit mutations,  $\beta$ R52C and  $\beta$ G150D, respectively (Table I). The third plasmid (pBMUG15fsR3) had two mutations,  $\beta$ R52C and  $\beta$ V77A. The amounts of enzyme ( $F_1$  sector) found in membranes of the  $\gamma$  frameshift with or without the  $\beta$  subunit mutation(s) were similar to those in the wild type (Fig. 2a). Consistent with the 7 additional residues attached to the carboxyl terminus, the mobilities of the frameshift  $\gamma$  subunits on electrophoresis were significantly lower than that of the wild type. This was clear with partially purified  $F_1$  (Fig. 2b). Essentially the same amounts of the mutant and wild type  $\gamma$  subunits were also identified on Western blotting (data not shown).

**Second Site Mutations Restored Oxidative Phosphorylation and Energy Coupling**—Growth by oxidative phosphorylation was substantially recovered in DK8 harboring recombinant plasmids with the  $\gamma$  frameshift and the  $\beta$  subunit mutation, whereas no growth was observed for the  $\gamma$  frameshift (Table I). DK8 harboring pBMUG15fsR1 ( $\beta$ R52C) and pBMUG15fs R2 ( $\beta$ G150D) gave about 70% of the growth yield of the wild type. The *unc* operon carried by pBMUG15fsR3 had two amino acid substitutions ( $\beta$ R52C and  $\beta$ V77A) in the  $\beta$  subunit together with the  $\gamma$  frameshift. We think that both the  $\beta$ R52C and  $\beta$ V77A mutations suppressed the  $\gamma$  frameshift mutation because DK8/pBMUG15fsR3 always gave a higher growth yield and rate than DK8/pBMUG15fsR1 having only a  $\beta$ R52C replacement in the  $\beta$  subunit. The growth rate of DK8/pBMUG15fsR1 was about 40% of the wild type level, whereas those of other mutants were essentially the same as that of the wild type (data not shown).

Membrane vesicles from the  $\gamma$  frameshift/ $\beta$ R52C mutant and that with  $\beta$ V77A exhibited high membrane ATPase activities (70 and 100% of the wild type level, respectively) and could synthesize ATP at about 15 ( $\gamma$  frameshift/ $\beta$ R52C) and 30% ( $\gamma$  frameshift/ $\beta$ R52C/ $\beta$ V77A) of the wild type rate (Table I). These results suggest that the  $\beta$  subunit mutations suppressed the defective catalytic cooperativity of the  $\gamma$  frameshift and increased the membrane ATPase activity. Consistent with higher growth by oxidative phosphorylation, the  $\gamma$  frameshift/ $\beta$ R52C/ $\beta$ V77A mutant exhibited higher ATPase activity and ATP synthesis than the  $\gamma$  frameshift/ $\beta$ R52C. Membrane vesicles from the  $\gamma$  frameshift with  $\beta$  subunit mutations exhibited lower ATP

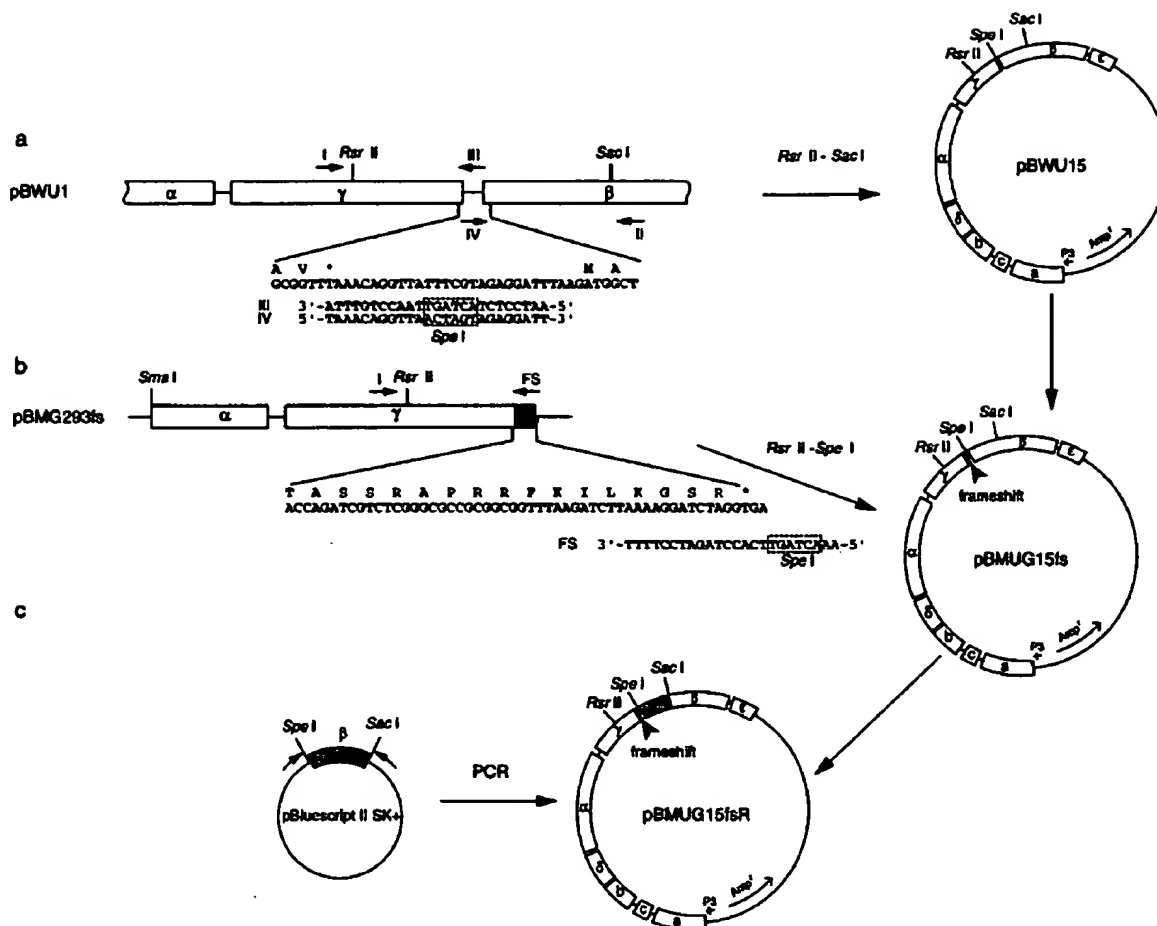


FIG. 1. Construction of a recombinant plasmid (pBMUG15fs) carrying the *unc* ( $H^+$ -ATPase) operon with the  $\gamma$  subunit frameshift mutation and introduction of random mutations into the  $\beta$  subunit. *a*, an *Spe*I site was introduced by PCR between the  $\gamma$  and  $\beta$  subunit genes carried by pBWU1; primers I/III and II/IV were used. The product was subjected to a second PCR (primer I/II). The resulting amplified fragment was digested with *Rsr*II and *Sac*I and then inserted into the corresponding site of pBWU1. The *Nde*I fragment was deleted from the resulting plasmid, and the final construct was named pBWU15. *b*, an *Spe*I site was also introduced downstream of the  $\gamma$  subunit gene of pBMUG293fs using primers I and FS. The *Rsr*II-*Spe*I fragment was obtained and introduced into the corresponding site of the derivative of pBWU15 constructed in *a*. The derivative was named pBMUG15fs. It should be noted that five restriction sites were introduced previously into the carboxyl-terminal region without changes in the amino acid residues coded (8). *c*, the *Spe*I-*Sac*I fragment of pBMUG15fs was transferred to pBluescript II SK+ and then subjected to PCR mutagenesis with sequence primers. The amplified products were digested with *Spe*I and *Sac*I and then ligated with the large *Spe*I-*Sac*I fragment of pBMUG15fs. Three plasmids conferred the ability of oxidative phosphorylation-dependent growth on strain DK8 lacking the *unc* operon.

synthesis than the wild type, suggesting that they are still defective in energy coupling.

The membrane ATPase activity of  $\gamma$  frameshift/ $\beta$ G150D was found to be low when assayed by the standard procedure. The  $\gamma$  frameshift/ $\beta$ G150D enzyme was unstable under these conditions. As shown previously (14), the Arg- $\alpha$ 296  $\rightarrow$  Cys/Ser- $\beta$ 174  $\rightarrow$  Phe enzyme was quickly inactivated but stabilized with high concentration of KCl (14). Similar to this mutant enzyme, the  $\gamma$  frameshift/ $\beta$ G150D enzyme was stabilized by KCl, and ATPase activity was found to be highest (2.6 units/mg protein, about 10% of the wild type level) when assayed in the presence of 70 mM KCl (Fig. 3a). The optimal pH values of the mutant enzyme with and without KCl were 7.0–8.0 and 6.5, respectively, whereas that of the wild type was 8.5 regardless of the presence of KCl (Fig. 3, *a* and *b*); the specific activity of the mutant ATPase was found to be about 40% of the wild type level when assayed at pH 6.5. Thus the high growth yield of the mutant by oxidative phosphorylation may be due to the restored energy coupling because the mutant exhibited lower ATPase activity than the wild type even assayed under different conditions. Repeated trials to obtain membrane vesicles with ATP synthe-

sis from the double mutant were not successful; we tried buffers with different pH values and ionic strengths for the preparation of membranes and assaying ATP synthesis, but the mutant membranes were always leaky to protons. The altered properties of the mutant were due to the combination of the  $\gamma$  frameshift and  $\beta$ G150D; as separate mutants, the  $\gamma$  frameshift and  $\beta$ G150D exhibited 23 and 17% of the membrane ATPase activity of the wild type, respectively, when assayed at pH 8.0, and membranes of the  $\beta$ G150D single mutant were not leaky to protons, showing 13% of the ATP synthesis level of the wild type (Table I).

#### DISCUSSION

Protons transported through  $F_0$  may cause a series of conformational changes in different subunits and finally drive ATP synthesis in the  $\beta$  subunit. Similarly in the reverse reaction, ATP hydrolysis causes the  $\beta$  subunit conformational change(s), which is transmitted through other subunits and finally to the  $H^+$  transport pathway in the  $F_0$  sector. The  $\gamma$  frameshift mutant had two defects: a defect in catalytic cooperativity, giving low ATPase activity, and one in energy cou-

TABLE I  
Properties of mutants carrying the  $\gamma$  subunit frameshift  
and  $\beta$  subunit amino acid replacements

Strain DK8 harboring plasmids with the  $\gamma$  frameshift and  $\beta$  subunit mutations were tested for growth by oxidative phosphorylation (growth yield on 15 mM succinate), membrane ATPase activity, and *in vitro* ATP synthesis. The plasmids carrying  $\beta/\gamma$  mutations were:  $\gamma$  frameshift/ $\beta$ R52C (CGT  $\rightarrow$  TGT), pBMUG15fsR1;  $\gamma$  frameshift/ $\beta$ R52C (CGT  $\rightarrow$  TGT)/ $\beta$ V77A (GTC  $\rightarrow$  GCC), pBMUG15fsR3; and  $\gamma$  frameshift/ $\beta$ G150D (GCT  $\rightarrow$  GAT), pBMUG15fsR2. The wild type (DK8/pBWU15) was also tested as a control. pBMUG15fsR3 also carried a synonymous change in the Leu- $\beta$ 38 codon. Membrane ATPase activities were assayed at pH 8.0 and 6.5 under standard conditions. The relative growth yields are shown: wild type, 0.80 (absorbance at 650 nm).

Mutation	Growth on succinate	Membrane ATPase		ATP synthesis <i>in vitro</i>
		pH 8.0	pH 6.5	
	%	units/mg protein		nmoles/mg/min
None (wild type)	100	28.4	5.0	149
$\gamma$ frameshift	<2	6.5		7.2
$\gamma$ frameshift/ $\beta$ R52C	75	20.5	3.2	22
$\gamma$ frameshift/ $\beta$ R52C/ $\beta$ V77A	83	28.4	4.5	43
$\gamma$ frameshift/ $\beta$ G150D	67	2.6 <sup>a</sup>	2.1	ND <sup>b</sup>
$\beta$ G150D	80	4.8	1.6	20
No <i>unc</i> operon	0	0.16	$\leq 0.1$	2.9

<sup>a</sup> The membrane ATPase activity value determined in the presence of 70 mM KCl is shown for the frameshift/ $\beta$ G150D (see Fig. 3 for the effect of KCl). The wild type activity was about 18 units/mg protein under the modified conditions.

<sup>b</sup> ND, not detected. Stable mutant membranes exhibiting substantial ATP synthesis activity could not be obtained, although we changed the pH and ionic strength of the buffers for preparation of membranes and for assaying of ATP synthesis. The assay with dicyclohexylcarbodiimide also gave no synthesis.

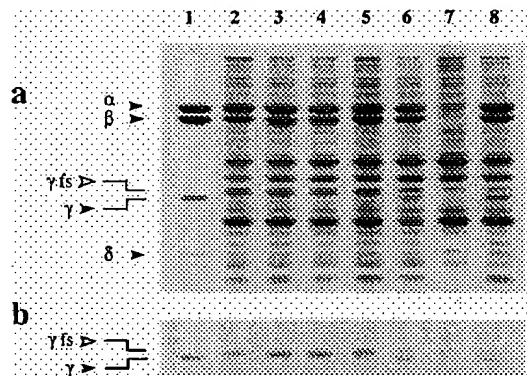


FIG. 2. Polyacrylamide gel electrophoresis of  $F_1$ -ATPase fractions from DK8 harboring various mutant plasmids. Cells were grown in a synthetic medium with glycerol as the sole carbon source. Their membranes (40  $\mu$ g of protein) were subjected to polyacrylamide gel electrophoresis (12%) in the presence of sodium dodecyl sulfate and then stained with Coomassie Brilliant Blue (a). The solubilized  $F_1$  sectors (EDTA extract, 15  $\mu$ g of protein) were also subjected to electrophoresis, and portions of the gel are shown to indicate mobility differences between the wild type and frameshift  $\gamma$  subunits (b). The positions of  $F_1$  subunits are indicated by arrows, together with the frameshift  $\gamma$  ( $\gamma$ fs). Lane 1, purified  $F_1$  (15  $\mu$ g); lane 2,  $\gamma$  frameshift; lane 3,  $\gamma$  frameshift/R52C; lane 4,  $\gamma$  frameshift/R52C/V77A; lane 5,  $\gamma$  frameshift/G150D; lane 6, wild type; lane 7, DK8/pBR322 (no *unc* operon); lane 8, G150D.

pling, resulting in low efficiency in ATP synthesis. The frameshift  $\gamma$  subunit had a longer altered sequence downstream of Thr- $\gamma$ 277. With two methods (23, 24), it was predicted that the mutant carboxyl-terminal forms a  $\beta$ -strand, whereas with the same methods a wild type  $\alpha$  helix similar to the x-ray structure was predicted (7). The  $\beta$ -strand may possibly extend about 60 Å from Thr- $\gamma$ 277 and interact with the upper  $\beta$ -barrel and/or a part of the catalytic domain of the  $\beta$  subunit (Fig. 4). Thus, the mutant enzyme became defective in energy coupling and cata-

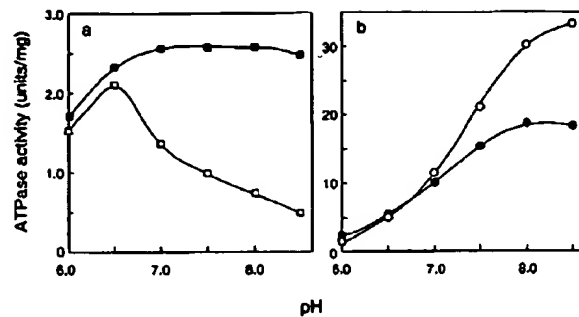


FIG. 3. Effects of pH and KCl on the membrane ATPase activity of the  $\gamma$  frameshift/ $\beta$ G150D mutant. pH activity profiles of the  $\gamma$  frameshift/ $\beta$ G150D (a) and wild type (b) membrane enzymes are shown. Membranes were diluted with TKDG buffer and then ATPase activity was measured with (closed symbols) and without (open symbols) 70 mM KCl. The standard assay conditions were used except that different buffers were used: pH 6 and 6.5, 20 mM MES-NaOH; pH 7 and 7.5, MOPS-NaOH; pH 8 and 8.5, Tris-HCl.

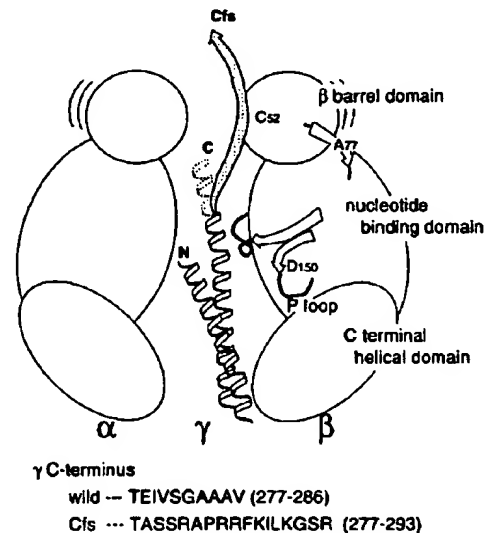


FIG. 4. A model of  $F_1$  with the  $\gamma$  frameshift mutation and suppression by the  $\beta$  subunit mutations. A model was drawn based on the x-ray structure of bovine  $F_1$  (7). The  $\gamma$  frameshift has an unrelated sequence of 16 residues (additional 7 residues at the carboxyl terminus together with 9 altered residues downstream of Thr- $\gamma$ 277). With two methods (23, 24), it was predicted that the carboxyl-terminal region of the  $\gamma$  frameshift forms a  $\beta$ -strand of about 60 Å (shaded arrow). The  $\beta$ R52C (with or without  $\beta$ V77A) and  $\beta$ G150D mutations restored membrane ATPase activity and ATP synthesis. Mutant residues ( $C_{52}$ ,  $A_{77}$ , and  $D_{150}$ ) are located following the bovine  $F_1$  structure. The amino (N) and carboxyl (C) termini of the wild type and the frameshift (Cfs)  $\gamma$  subunit are shown. The glycine-rich phosphate loop (25, 26) containing the catalytic residues is also shown (P loop).

lytic cooperativity, possibly because the long carboxyl-terminal  $\beta$ -strand inhibited the proper conformational transmission between the  $\beta$  and  $\gamma$  subunit. It may also be possible that the transmission is carried out through the rotation of the  $\gamma$  subunit (7) and such mechanical movement was inhibited in the  $\gamma$  frameshift by the interaction of its carboxyl  $\beta$ -strand with the  $\beta$  subunit.

The defective energy coupling and catalytic cooperativity of the  $\gamma$  frameshift mutant were suppressed by amino acid replacements in the  $\beta$  subunit, indicating that the altered  $\beta$ - $\gamma$  interaction in the  $\gamma$  frameshift was restored by the  $\beta$  subunit mutations. Two different replacements,  $\beta$ R52C with or without  $\beta$ V77A and  $\beta$ G150D, suppressed the  $\gamma$  frameshift, possibly through different mechanisms. The Arg- $\beta$ 52 residue is con-

served in all the  $\beta$  subunit so far sequenced (57 different species; SWISS PROT rel. 30), and the corresponding bovine residue is located in the  $\beta$ -barrel domain (7). Val- $\beta$ 77 corresponds to bovine Ile-84, which is located in the  $\beta$ -sheet connecting the  $\beta$ -barrel and nucleotide binding domains. Therefore, the deleterious interaction between the putative  $\beta$ -strand of the carboxyl-terminal domain of the  $\gamma$  frameshift and the  $\beta$ -barrel was restored by the second mutation ( $\beta$ R52C) in the same domain. This is further supported by an additional suppressing effect of the  $\beta$ V77A mutation.

Gly- $\beta$ 150 is located in the phosphate loop containing the catalytic residues (25, 26). The corresponding bovine loop may show a large conformational change during catalysis, because structures of this region in the nucleotide-bound and empty  $\beta$  subunit are strikingly different (7). Thus, the  $\beta$ G150D mutation may affect the orientation of another loop located above the glycine-rich sequence or that of the carboxyl-terminal  $\alpha$  helical domain. These structural considerations suggest that the defective energy coupling of the  $\gamma$  frameshift was suppressed by the Asp- $\beta$ 150 mutation, possibly because the  $\beta$  subunit mutation changed the mode of conformational transmission between the  $\beta$  catalytic site and the  $\gamma$  subunit. Further studies with the present approach will be helpful for clarifying the conformational transmission among subunits during ATP synthesis.

## REFERENCES

1. Futai, M., Noumi, T., and Maeda, M. (1989) *Annu. Rev. Biochem.* **58**, 111-136
2. Fillingame, R. H. (1990) in *The Bacteria* (Kruschwitz, T. A., ed) pp. 345-391, Academic Press, New York
3. Senior, A. E. (1990) *Annu. Rev. Biophys. Biophys. Chem.* **19**, 7-41
4. Wilkens, S., and Capaldi, R. A. (1992) *Arch. Biochem. Biophys.* **299**, 105-109
5. Bianchet, M., Ysern, X., Hüllihen, J., Pedersen, P. L., and Amzel, L. M. (1991) *J. Biol. Chem.* **266**, 21197-21201
6. Abrahams, J. P., Lutter, R., Todd, R. J., van Raaij, M. J., Leslie, A. G. W., and Walker, J. E. (1993) *EMBO J.* **12**, 1775-1780
7. Abrahams, J. P., Leslie, A. G. W., Lutter, R., and Walker, J. E. (1994) *Nature* **370**, 621-628
8. Iwamoto, A., Miki, J., Maeda, M., and Futai, M. (1990) *J. Biol. Chem.* **265**, 5043-5048
9. Shin, K., Nakamoto, R. K., Maeda, M., and Futai, M. (1992) *J. Biol. Chem.* **267**, 20835-20839
10. Nakamoto, R. K., Maeda, M., and Futai, M. (1993) *J. Biol. Chem.* **268**, 867-872
11. Aggeler, R., Cai, S. X., Keana, J. F. W., Koike, T., and Capaldi, R. A. (1993) *J. Biol. Chem.* **268**, 20831-20837
12. Turina, P., and Capaldi, R. A. (1994) *J. Biol. Chem.* **269**, 13465-13471
13. Nakamoto, R. K., Al-Shawi, M. K., and Futai, M. (1995) *J. Biol. Chem.* **270**, 14042-14046
14. Omote, H., Park, M.-Y., Maeda, M., and Futai, M. (1994) *J. Biol. Chem.* **269**, 10265-10269
15. Klionsky, D. J., Brusilow, W. S. A., and Simoni, R. D. (1984) *J. Bacteriol.* **160**, 1055-1060
16. Tanaka, S., Lerner, S. A., and Lin, E. C. C. (1967) *J. Bacteriol.* **93**, 642-648
17. Takeyama, M., Ihara, K., Moriyama, Y., Noumi, T., Ida, K., Tomioka, N., Itai, A., Maeda, M., and Futai, M. (1990) *J. Biol. Chem.* **265**, 21279-21284
18. Iwamoto, A., Park, M.-Y., Maeda, M., and Futai, M. (1993) *J. Biol. Chem.* **268**, 3156-3160
19. Futai, M., Sternweis, P. C., and Heppel, L. A. (1974) *Proc. Natl. Acad. Sci. U. S. A.* **71**, 2725-2729
20. Lowry, O. H., Rosebrough, N. J., Farr, A. C., and Randall, R. J. (1951) *J. Biol. Chem.* **193**, 265-275
21. Sambrook, J., Fritsch, E. F., and Maniatis, T. (1989) *Molecular Cloning: A Laboratory Manual*, 2nd Ed., Cold Spring Harbor Laboratory, Cold Spring Harbor, NY
22. Moriyama, Y., Iwamoto, A., Hanada, H., Maeda, M., and Futai, M. (1991) *J. Biol. Chem.* **266**, 22141-22146
23. Chou, P. Y., and Fasman, G. D. (1974) *Biochemistry* **13**, 212-245
24. Garnier, J., Osguthorpe, D. J., and Robson, B. (1978) *J. Mol. Biol.* **120**, 97-120
25. Omote, H., Maeda, M., and Futai, M. (1992) *J. Biol. Chem.* **267**, 20571-20576
26. Senior, A. E., and Al-Shawi, M. K. (1992) *J. Biol. Chem.* **267**, 21471-21478

## Transcriptional Regulation of the Proton-Translocating ATPase (*atpIBEFHAGDC*) Operon of *Escherichia coli*: Control by Cell Growth Rate

ELVIN KASIMOGLU,<sup>†</sup> SOON-JUNG PARK,<sup>‡</sup> JOEL MALEK, CHING PING TSENG,<sup>§</sup>  
AND ROBERT P. GUNSALUS\*

Department of Microbiology and Molecular Genetics and the Molecular Biology Institute, University of California,  
Los Angeles, California 90095

Received 29 November 1995/Accepted 23 July 1996

The  $F_0F_1$  proton-translocating ATPase complex of *Escherichia coli*, encoded by the *atpIBEFHAGDC* operon, catalyzes the synthesis of ATP from ADP and  $P_i$  during aerobic and anaerobic growth when respiratory substrates are present. It can also catalyze the reverse reaction to hydrolyze ATP during nonrespiratory conditions (i.e., during fermentation of simple sugars) in order to maintain an electrochemical proton gradient across the cytoplasmic membrane. To examine how the *atp* genes are expressed under different conditions of cell culture, *atpI-lacZ* operon fusions were constructed and analyzed in single copy on the bacterial chromosome or on low-copy-number plasmids. Expression varied over a relatively narrow range (about threefold) regardless of the complexity of the cell growth medium, the availability of different electron acceptors or carbon compounds, or the pH of the culture medium. In contrast to prior proposals, *atp* operon expression was shown to occur from a single promoter located immediately before *atpI* rather than from within it. The results of continuous-culture experiments suggest that the cell growth rate rather than the type of carbon compound used for growth is the major variable in controlling *atp* gene expression. Together, these studies establish that synthesis of the  $F_0F_1$  ATPase is not greatly varied by modulating *atp* operon transcription.

The proton-translocating ATPase of *Escherichia coli* is a member of the  $F_0F_1$  class of ATPases that occur widely in bacteria and in the mitochondria and chloroplasts of eukaryotic organisms (7, 32). During aerobic cell growth, the ATPase of *E. coli* couples the energy derived from oxygen respiration to ATP synthesis by the process commonly known as electron transport-linked phosphorylation. During anaerobic growth, *E. coli* can also generate an electrochemical proton gradient by respiration using a variety of alternative electron acceptors, including nitrate, trimethylamine *N*-oxide (TMAO), dimethyl sulfoxide, and fumarate; the ATPase also functions to synthesize ATP under these conditions. However, when the cell performs anaerobic fermentations, it can generate ATP only by substrate-level phosphorylation reactions. During this growth mode, *E. coli* must employ the ATPase to hydrolyze ATP to generate the electrochemical proton gradient required to support other membrane functions, including solute transport and flagellar rotation (23).

The structure and function of the bacterial ATPase have been studied extensively (see reviews in references 7, 32, and 37). The ATPase of *E. coli* is composed of eight dissimilar polypeptides that are present in a stoichiometry of  $a_1:c_{12}:b_2:\delta_1:\alpha_3:\gamma_1:\beta_3:\epsilon_1$  (6). Its molecular mass is approximately 545 kDa for the combined  $F_0F_1$  complex. The *atpIBEFHAGDC* genes that encode these subunits are located at 84 min on the *E. coli*

chromosome map (2). An additional gene of unknown function, called *atpI*, precedes the other eight *atp* genes (3, 14, 37). The *atpI* gene product appears to be a hydrophobic protein, as judged from analysis of its predicted amino acid sequence. Analysis of the *atpIBEFHAGDC* mRNA revealed the location of the 5' end that initiates at a position 73 nucleotides upstream of the start of *atpI* translation (13, 14, 28). All of the genes appear to be cotranscribed from a single promoter to give a 7-kb mRNA that terminates just following the *atpC* gene (9, 13, 28). Numerous investigations have documented the differential translation of the *atp* genes such that each subunit of the ATPase is produced in the appropriate amount for assembly into the mature  $F_0F_1$  complex (1, 18, 19, 27, 29, 31, 35). This process involves an ordered endonucleolytic processing of the *atp* message to yield several stable intermediates that are then differentially translated. This processing involves the formation of complex mRNA secondary structures that allow different levels of ribosome binding and efficiencies of translation.

Given the relatively detailed understanding of *atp* mRNA translation, little is known about the control of *atp* operon transcription under the various conditions of *E. coli* growth. In this study, we examined the expression of *atpI-lacZ* operon fusions that were contained on the bacterial chromosome in a single copy or on low-copy-number plasmids and found that *atp* operon expression was remarkably constant under a variety of cell growth conditions.

### MATERIALS AND METHODS

**Bacterial strains, bacteriophages, and plasmids.** The genotypes of the *E. coli* K-12 strains, bacteriophages, and plasmids used are given in Table 1. To construct the *arcA*, *fnr*, *himA*, and *fix* strains, an MC4100/ΔEK13 lysogen was infected with a P1 lysate which had been prepared from cells containing the specified deletion or mutation (21, 25). Mutant MC4100/ΔEK13 strains were selected by the transfer of antibiotic resistance. The Δ*arcA*::Kan<sup>r</sup> phenotype was confirmed by the characteristic small colony size when cells were plated on

\* Corresponding author. Mailing address: Department of Microbiology and Molecular Genetics, 1602 Molecular Sciences Bldg., University of California, Los Angeles, CA 90095-1489. Phone: (310) 206-8201. Fax: (310) 206-5231.

<sup>†</sup> Present address: Meharry Medical School, Nashville, TN 37012.

<sup>‡</sup> Present address: Samsung Biomedical Research Institute, Kangnam-Ku Seoul, Korea 135-230.

<sup>§</sup> Present address: Institute of Biological Science and Technology, National Chiao Tung University, Taiwan, Republic of China.

TABLE 1. *E. coli* K-12 strains, plasmids, and bacteriophages used

Strain, plasmid, or phage	Origin	Genotype or phenotype	Source
<b>Strains</b>			
MC4100		F <sup>-</sup> <i>araD139</i> ( $\Delta$ <i>argF-lac</i> ) <i>U169 rpsL150 relA1 ffb5301 deoC1 ptsF25 rbsR</i>	33
PC2		$\Delta$ <i>fur</i>	25
PC35	MC4100	$\Delta$ <i>arcA</i> Kan <sup>r</sup>	25
SJP3	MC4100	<i>himA</i> $\Delta$ 82	25
SJP4	MC4100	<i>fts767</i>	25
MRi93	MC4100	<i>pcnB</i>	16
<b>Plasmids</b>			
pHJUP1		<i>atpI</i> <sup>+</sup>	13
pRS415		<i>lacZ</i> <sup>+</sup> <i>lacY</i> <sup>+</sup> <i>lacA</i> <sup>+</sup>	34
pJM1	pRS415	<i>atpI'</i> - <i>lacZ</i> <i>lacY</i> <sup>+</sup> <i>lacA</i> <sup>+</sup>	This study
pJM2	pRS415	<i>atpI</i> <sup>+</sup> B'- <i>lacZ</i> <i>lacY</i> <sup>+</sup> <i>lacA</i> <sup>+</sup>	This study
pJM3	pRS415	<i>atpI</i> <sup>+</sup> B'- <i>lacZ</i> <i>lacY</i> <sup>+</sup> <i>lacA</i> <sup>+</sup>	This study
pEK13	pRS415	<i>atpI'</i> - <i>lacZ</i> <sup>+</sup>	This study
<b>Phages</b>			
M13mp18			20
13SJP1811	M13mp18	<i>atpI</i>	This study
M13SJP18102	M13SJP1811	M13SJP1811 with an additional <i>Bam</i> HI site	This study
$\lambda$ RS45		<i>lacZ</i> <sup>+</sup> <i>lacY</i> <sup>+</sup> <i>lacA</i> <sup>+</sup>	34
$\lambda$ EK13	$\lambda$ RS45	<i>atpI'</i> - <i>lacZ</i> <sup>+</sup>	This study

toluidine blue plates (25). The *himA*::Tet<sup>r</sup> phenotype was confirmed by the inability of Mu phage to form clear plaques on a *himA* mutant (25).

**Construction of *atpI-lacZ* operon fusions.** An *atpI-lacZ* fusion (pEK13) containing the first 13 codons of *atpI* and the upstream 1.3 kb of DNA was constructed by digesting plasmid pHJUP1 (13) with *Hind*III. The resulting 1.3-kb *atpI* fragment was inserted into M13mp18 to give phage M13SJP11. A *Bam*HI restriction site was introduced into *atpI* at codon 13 by site-directed mutagenesis to give M13SJP102. The 1.2-kb *Bam*HI fragment that contains the 5' end of *atpI* and the upstream region was transferred into plasmid pRS45 (34) to give pEK13. The correct orientation of the *atpI-lacZ* fusion in pEK13 was confirmed by restriction enzyme digestions with *Sca*I and *Hind*III and by DNA sequence analysis. The fusion was then transferred onto  $\lambda$ RS45 (34) to give phage  $\lambda$ EK13. Lambda phages containing the 1.3-kb *atpI-lacZ* fusion were isolated by their ability to confer the Lac<sup>+</sup> phenotype to MC4100. A high-titer lysate of  $\lambda$ EK13 was used to lysogenize MC4100. Since  $\lambda$  phages integrate at the *att* lambda integration site, the wild-type *atp* operon is preserved intact at 84 min on the chromosome. Single lysogens were identified by  $\beta$ -galactosidase assay and stocked for subsequent analysis.

To examine if additional promoter(s) are located within the *atpI* gene, various regions of the *atp* operon (Fig. 1) were PCR amplified from DNA isolated from MC4100, to introduce an upstream *Eco*RI site and a downstream *Bam*HI site. These fragments were then inserted into the corresponding sites of plasmid pRS415 to generate the *atpI-lacZ*, *atpI'*-*B-lacZ*, and *atpI*B'-*lacZ* plasmids, pJM1,

pJM2, and pJM3, respectively. The constructions were verified by DNA sequence analysis. Expression of the plasmid-borne fusions was monitored in a *pcnB* strain to maintain the fusions at low copy number in the cell (16).

**Cell growth.** For strain, phage, and plasmid constructions, cells were grown on Luria broth (LB) or solid media (5, 25). When required, ampicillin, kanamycin, and tetracycline were added to the medium in concentrations of 80, 40, and 20 mg/liter, respectively. For  $\beta$ -galactosidase assay, cells were grown in a glucose-containing minimal medium (pH 7.0) unless otherwise indicated (4). Carbon compounds were added to the minimal medium at 40 mM. Buffered LB (5) was used to evaluate the effect of medium richness. Anaerobic cell growth was performed in 10-ml anaerobic tubes fitted with butyl rubber stoppers as previously described (5). Aerobic growth was performed by incubating 10-ml culture volumes in 150-ml flasks with loose-fitting caps shaken vigorously (380 rpm). All cultures were incubated at 37°C.

For anaerobic growth with the alternative electron acceptor nitrate, fumarate, or TMAO, a glucose- or a glycerol-containing minimal medium was supplemented with each of the respiratory compounds at a final level of 40 mM (5). Flasks were inoculated from overnight cultures of the medium grown under identical conditions, and the cultures were allowed to double four to five times to mid-exponential phase (optical density at 600 nm of 0.40 to 0.45; Kontron Uvikon 810 Spectrophotometer) before harvest. To determine the effect of pH on *atpI-lacZ* transcription, buffered media were adjusted to pH 5.7, 6.0, 6.3, 7.0, and 7.5 as previously described (4). The pH values were measured before and after cell growth; at the end of the experiment, the pH did not drop by more than 0.2 units.

Growth of cells in a continuous culture was performed as previously described (36). A Queue Mouse bioreactor (Queue Corporation, Parkersburg, W.V.) was fitted with a 2-liter vessel and operated at a 1-liter liquid working volume (36). The medium was Vogel-Bonner medium (pH 6.5) modified by addition of Casamino Acids (0.25 mg/liter) and by using glucose at a concentration of 2.25 mM to limit cell growth (i.e., a carbon-limited medium). Aerobic continuous culture conditions were maintained by saturating the culture medium with sterile air at a rate of 2.0 liters/min. Anaerobic conditions were maintained by continuously sparging the vessel with oxygen-free nitrogen at a rate of 200 ml/min. To vary cell growth rate (*k*), the medium addition rate was adjusted accordingly: the medium addition rates ranged from 2 to 16 ml/min (*k* = 0.12 to 0.96/h), which corresponded to cell doubling times of 350 and 58 min, respectively (23, 36). When cells were shifted to a new rate of growth, steady state was generally achieved in five reactor residence times.

**$\beta$ -Galactosidase assay.**  $\beta$ -Galactosidase assays were performed as previously described (5).  $\beta$ -Galactosidase values represent the values of at least four experiments. Values usually did not vary by more than 6% from the mean. Protein concentration was estimated by assuming that a cell optical density of 1.4 at 600 nm is equal to 150  $\mu$ g of protein per ml (21). Units of  $\beta$ -galactosidase are expressed as nanomoles of *o*-nitrophenyl- $\beta$ -D-galactopyranoside (ONPG) hydrolyzed per minute per milligram of protein. An extinction coefficient of 0.0045 was used for ONPG.

**Molecular biology techniques.** Transformation of *E. coli* and chromosomal and plasmid isolations were performed as described previously (17). DNA sequencing, using a Sequenase kit (version 2.0; U.S. Biochemical), and PCR am-

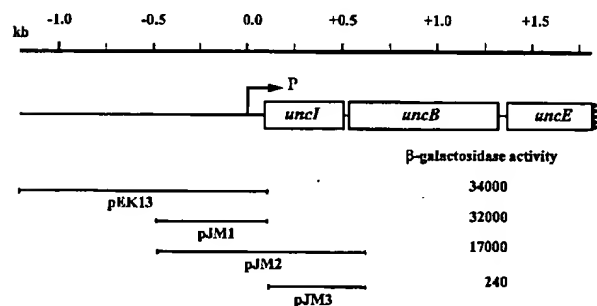


FIG. 1. Physical map of *atpI-lacZ* operon fusions used in this study. The *atpI-lacZ*<sup>+</sup> fusion plasmid pEK13 contains a 1.3-kb *Bam*HI fragment with the first 13 codons of the *atpI* gene and the associated upstream regulatory region from pHJUP1; this fragment was inserted into the *Bam*HI site of pRS415 to generate pEK13. Plasmid pJM1 is identical to pEK13 except that it contains only the 554 bp before *atpI*, while pJM2 contains *atp* DNA extending to codon 29 of *atpB*. Plasmid pJM3 contains DNA from the bp 18 of *atpI* to codon 29 of *atpB*. The boxed regions represent the indicated *atp* genes. The arrow indicates the direction of *atpI*B'-*lacZ* transcription from the *atp* promoter.  $\beta$ -Galactosidase activity is expressed as in Table 2.



TABLE 2. Effects of carbon compounds on *atpI-lacZ* expression

Addition(s) <sup>a</sup>	β-Galactosidase activity (nmol of ONPG hydrolyzed/min/mg of protein)	
	+O <sub>2</sub>	-O <sub>2</sub>
Glucose	11,300	15,000
Galactose	15,000	14,800
Xylose	16,700	17,300
Pyruvate	23,500	21,500
Glycerol	21,500	NG <sup>b</sup>
Acetate	18,100	NG
Succinate	21,700	NG
Fumarate	23,400	NG
Malate	18,700	NG
LB	9,820	11,500
LB, glucose	7,600	8,300
LB, pyruvate	8,800	8,000

<sup>a</sup> MC4100/ΔEK13 cells were grown either in a minimal medium aerobically or anaerobically or in a LB with supplements as described in the text. Carbon compounds were added at a final concentration of 40 mM.

<sup>b</sup> NG, no growth.

plification, using a GeneAmp PCR system 2400 (Perkin-Elmer Cetus), were performed according to the manufacturer's instructions.

**Materials.** ONPG, ampicillin, kanamycin, and tetracycline were purchased from Sigma Chemical Co., St. Louis, Mo.

## RESULTS AND DISCUSSION

**Effect of oxygen and carbon substrates on *atpI-lacZ* expression.** To examine how the composition of the cell culture medium affects *atp* operon expression, an *atpI-lacZ* fusion containing the first 13 codons of *atpI* and the 1.3-kb upstream region was constructed (Fig. 1, pEK13). Following its insertion into the chromosome in single copy (see Materials and Methods), cells were grown under aerobic and anaerobic conditions in rich media or in minimal salts medium that contained single carbon compounds. During aerobic cell growth, *atpI-lacZ* expression did not vary by more than threefold (Table 2). Expression was highest when the tricarboxylic acid (TCA) cycle intermediates fumarate, malate, and succinate were used or when acetate and pyruvate, metabolic precursors of the cycle, were used. Expression was lowest when a rich medium (LB or a LB plus glucose) was used. During anaerobic cell culture conditions, *atpI-lacZ* expression did not vary significantly from that seen during aerobic conditions. Anaerobic cell growth on a glucose minimal salts medium led to expression about 30% higher than that seen during aerobic growth.

In light of the findings of Futai et al. (7, 15, 22), we investigated the possibility that there were additional weak *atp* promoters located within the *atpI* gene. To do this, we constructed a series of plasmid-borne *atpI-lacZ* fusions (Fig. 1). These plasmids were then introduced into an *E. coli* strain harboring a *pcnB* (11) mutation, and the β-galactosidase activity was determined in batch cultures grown aerobically in buffered LB. The strain with plasmid pJM3 that contained all of *atpI* except its first 13 codons displayed approximately 0.7% of the activity measured from pEK13, which has 1.3 kb of DNA upstream of *atpI*. This result indicates that there is little to no transcription originating from within the *atpI* open reading frame. The levels of β-galactosidase activity in cells containing either plasmid pEK13 or plasmid pJM1 were about the same (ca. 32,000 to 34,000 U). However, the level of β-galactosidase directed from the *atpI*<sup>+</sup>*B-lacZ* fusion on pJM2, which includes all of *atpI* and the first 29 codons of *atpB*, was approximately 50% of that measured from pJM1. This difference is most likely due to the

TABLE 3. Effects of alternative electron acceptors on *atpI-lacZ* expression

Electron acceptor added <sup>a</sup>	β-Galactosidase activity (nmol of ONPG hydrolyzed/min/mg of protein)	
	Glucose	Glycerol
None	15,000	NG <sup>b</sup>
Oxygen	11,300	21,500
Nitrate	10,400	18,900
Fumarate	12,400	21,100
TMAO	13,800	23,400

<sup>a</sup> MC4100/ΔEK13 cells were grown on minimal medium as described in the text. The electron acceptors were present at 40 mM except for oxygen, in which case the medium was saturated with air by vigorous shaking.

<sup>b</sup> NG, no growth.

instability of the mRNA containing the *atpI* reading frame, since there is proposed to be a site for endonucleolytic cleavage within *atpI* (19). Thus, *atp* operon expression appears to be the result of transcription from a single promoter located 73 bp upstream of *atpI* (13, 14, 28). All subsequent studies were performed with the ΔEK13 *atpI-lacZ* operon fusion.

**Effects of respiratory substrates on *atpI-lacZ* expression.** As *E. coli* can respire by using oxygen, nitrate, TMAO, or fumarate as an electron acceptor, we tested how the presence of each of these compounds affected *atpI-lacZ* expression (Table 3). When glucose was used as a carbon source, *atpI-lacZ* expression varied by no more than about 30% with the different electron acceptors. Interestingly, expression was highest when no electron acceptor was provided (i.e., conditions in which the cell must ferment). When glycerol was used in place of glucose, *atpI-lacZ* expression was elevated by almost twofold for each respiratory condition tested. Thus, the type of carbon substrate used for cell growth appears to have a greater influence on the level of *atp* gene expression than does the presence of a respiratory substrate.

**Effect of medium pH on *atpI-lacZ* expression.** Since the cell maintains a relatively constant internal pH, we examined whether changes in the pH of the cell culture medium affect *atpI-lacZ* expression. Cells were grown in a buffered glucose minimal medium at pH values ranging from pH 5.7 to 7.5. Aerobically, *atpI-lacZ* expression was remarkably constant, not varying more than +5% (Table 4). During anaerobic cell culture, cells did not grow well below pH 6; however, above this pH value, gene expression increased modestly. Gene expression was higher under anaerobic than aerobic conditions for each pH value tested. Together, these findings suggest that the hydrogen ion concentration of the bacterial culture medium is not an important variable for control of *atp* gene expression in *E. coli*.

TABLE 4. Effect of medium pH on *atpI-lacZ* expression<sup>a</sup>

Medium pH	β-Galactosidase activity (nmol of ONPG hydrolyzed/min/mg of protein)	
	+O <sub>2</sub>	-O <sub>2</sub>
5.7	11,700	ND
6.0	11,700	ND
6.3	11,000	13,800
7.0	11,300	15,000
7.5	11,100	15,800

<sup>a</sup> MC4100/ΔEK13 cells were grown in a glucose minimal medium adjusted to different pH values as previously described (4). ND, not determined.

TABLE 5. Effects of oxygen and mutations in the *arcA*, *fnr*, *fis*, and *himA* genes on *atpI-lacZ* expression

Strain <sup>a</sup> (relevant genotype)	$\beta$ -Galactosidase activity (nmol of ONPG hydrolyzed/ min/mg of protein)	
	+O <sub>2</sub>	-O <sub>2</sub>
MC4100 (wild type)	11,300	15,000
SJP1 ( $\Delta arcA$ )	10,800	14,500
PC2 ( $\Delta fnr$ )	10,500	10,900
SJP4 ( $\Delta fis$ )	15,000	16,000
SJP3 ( $\Delta himA$ )	8,700	12,400

<sup>a</sup> Cells containing  $\lambda$ EX13 were grown in a glucose minimal medium either aerobically or anaerobically as described in the text.

**Effects of *arcA* and *fnr* mutations on *atpI-lacZ* expression.** The regulation of many of genes in *E. coli* involved with aerobic and anaerobic metabolism, including respiratory pathway genes, the TCA cycle genes, and fermentation-related genes, is modulated by the *arcA* and *fnr* gene products (8, 10, 12). We tested whether mutations in either of these two regulatory genes affect *atpI-lacZ* expression. Little to no difference was observed during either aerobic or anaerobic growth in a glucose minimal medium of *fnr*, *fnr arcA*, or *arcA* strains (Table 5). Similar results were observed when strains defective in the *himA* (encoding integration host factor) and *fis* genes were examined.

**Effect of cell growth rate on *atpI-lacZ* expression.** When cells were grown in batch culture in different types of media, we noted that *atpI-lacZ* expression was higher in a minimal medium containing two-, three-, or four-carbon compounds than in a rich medium (Table 2). Cell growth rates were determined on each type of medium, and when the generation times were graphed versus the level of *atpI-lacZ* expression, an inversely proportional relationship was seen (Fig. 2).

To determine if the variation in *atp* gene expression was due to the type of carbon used or to differences in cell growth rate, we also examined *atpI-lacZ* expression in cells grown in continuous culture (Fig. 3). Expression also varied by threefold and was higher at slow ( $k = 0.12 \text{ h}^{-1}$ ) than at fast ( $k = 0.96 \text{ h}^{-1}$ ) cell doubling times. Anaerobiosis had little effect on *atp* gene expression. Since cell growth in these experiments was

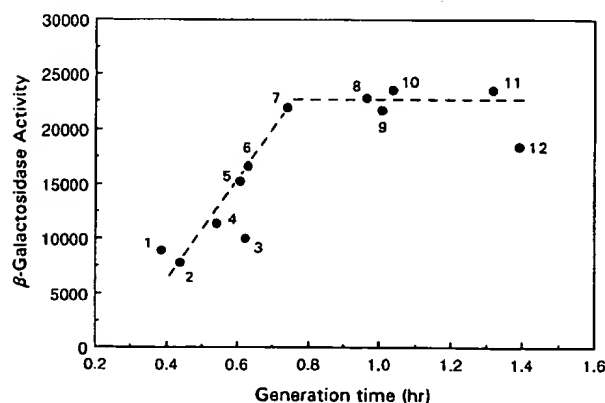


FIG. 2. Effect of cell growth rate on *atpI-lacZ* expression in batch culture. Cells were grown in the indicated medium, and the cell generation time (hours) was recorded. Medium or carbon compound used for cell growth: 1, LB plus pyruvate; 2, LB plus glucose; 3, LB; 4, glucose; 5, galactose; 6, xylose; 7, succinate; 8, malate; 9, glycerol; 10, fumarate; 11, pyruvate; 12, acetate.

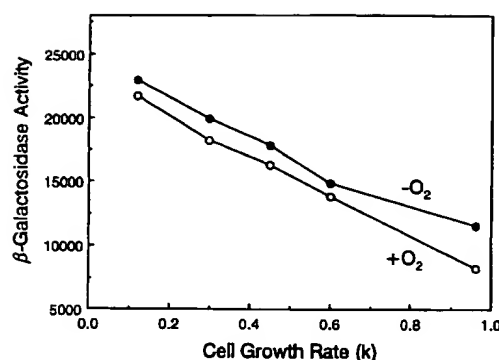


FIG. 3. Effect of cell growth rate on *atpI-lacZ* expression in continuous culture during aerobic and anaerobic growth conditions. Cells were grown at the indicated growth rates as described in Materials and Methods. For aerobic growth, air was maintained at 100% saturation in the culture medium throughout the experiment. For anaerobic growth, the vessel was sparged with O<sub>2</sub>-free nitrogen (200 ml/min).  $\beta$ -Galactosidase activity is expressed as nanomoles of ONPG hydrolyzed per minute per milligram of protein. Cells were grown aerobically (○) or anaerobically (●) as described in Materials and Methods.

carbon limited (i.e., by glucose), it appears that the rate of cell growth rather than the type of carbon used is the major determinant in controlling *atp* operon expression. In support of this proposal, Sakai-Tomita et al. (30) noted that the synthesis of the ATPase of *Vibrio parahaemolyticus* was catabolite repressed, whereas it was not in *E. coli*.

**Regulatory implications.** During most conditions, the proton-translocating ATPase of *E. coli* is used for cellular energy generation via electron transport-linked phosphorylation reactions, as is typical of the ATPases of many bacterial species and of eukaryotic cells (7, 32). Although there have been extensive studies addressing translational regulation of the *atp* operon that encodes the ATPase, little was known about how the *atp* genes are transcribed in response to cell growth under different environmental conditions. In this study, we demonstrate that *atp* operon expression, as measured by using *atpI-lacZ* fusions, remains within a remarkably narrow range regardless of the medium composition, extracellular pH, or the presence of respiratory substrates (Tables 2 and 3). Gene expression did not vary by more than threefold. Expression was highest in a medium containing carbon compounds that do not yield ATP by substrate-level phosphorylation (i.e., TCA cycle intermediates or acetate), whereas it was lowest when a glucose-containing minimal medium or a rich medium (i.e., LB) was used. The reduced level of *atpI* and *atpB* gene expression under these latter conditions correlates with a reduced need for cellular ATP synthesis when the biosynthetic intermediates are available from the LB medium.

Since the ATPase complex is involved in proton translocation across the cytoplasmic membrane, we were interested in determining whether any changes in external H<sup>+</sup> concentration or anaerobiosis affected ATPase gene expression. No effect on *atpI* expression when the medium pH was varied (Table 5). It appears that transcription of the *atp* operon in *E. coli* is not dynamically modulated as a strategy to regulate ATPase capacity within the cell. Rather, the results suggest that the number of ATPase complexes remains relatively constant under different cell culture conditions that include anaerobic respiration or fermentation (Tables 2 and 3). The ATPase capacity of the cell is apparently sufficient to maintain the electrochemical proton gradient during changes in extracellular pH encountered under different cell growth conditions.

Such conditions include those in which the cell must use the ATPase to hydrolyze ATP rather than synthesize it. Since *atp* operon expression was modestly higher under anaerobic fermentative conditions, ATP hydrolysis does not require significantly elevated levels of the ATPase complex.

Gene expression in batch cell culture correlates well with *atp* expression occurring during continuous culture (Fig. 2 and 3). An inverse pattern of *atp* gene expression was observed with cell growth rate and was similar to the pattern observed for expression of the *gluA* (citrate synthase) and *sdhCDAB* (succinate dehydrogenase) genes of the TCA cycle (24–26). Expression of the *atp*, *sdhCDAB*, *mdh*, and *gluA* genes was highest in a minimal medium when cells were grown on TCA cycle intermediates or with acetate, in which case cells grew more slowly than they did in rich medium. The cells must expend more energy in order to synthesize cellular intermediates needed for macromolecule production. Since *E. coli* only modestly varies the level of *atpBEFHAGDC* operon transcription, it will be of interest to determine whether other types of bacteria regulate ATPase genes in a similar way.

#### ACKNOWLEDGMENTS

We thank Paul McNicholas for providing assistance with PCR techniques.

This work was supported in part by Public Health Service grants AI21678 and GM49694 from the National Institutes of Health.

#### REFERENCES

- Angov, E., and W. S. A. Brusilow. 1988. Use of *lac* fusions to measure in vivo regulation of expression of *Escherichia coli* proton-translocating ATPase (*unc*) genes. *J. Bacteriol.* 170:459–462.
- Bachmann, B. J. 1990. Linkage map of *Escherichia coli* K-12, edition 8. *Microbiol. Rev.* 54:130–197.
- Brusilow, W. S. A., A. C. G. Porter, and R. D. Simoni. 1983. Cloning and expression of *uncI*, the first gene of the *unc* operon of *Escherichia coli*. *J. Bacteriol.* 155:1265–1270.
- Cotter, P. A., V. Chepur, R. B. Gennis, and R. P. Gunsalus. 1990. Cytochrome *o* (*cyoABCDE*) and *d* (*cydAB*) oxidase gene expression in *Escherichia coli* is regulated by oxygen, pH, and the *fnr* gene product. *J. Bacteriol.* 172:6333–6338.
- Cotter, P. A., and R. P. Gunsalus. 1989. Oxygen, nitrate, and molybdenum regulation of *dmsABC* gene expression in *Escherichia coli*. *J. Bacteriol.* 171:3817–3823.
- Foster, D. L., and R. H. Fillingame. 1982. Stoichiometry of subunits on the H<sup>+</sup>-ATPase complex of *Escherichia coli* ATP synthetase. *J. Biol. Chem.* 257:2009–2015.
- Futai, M., T. Noumi, and M. Maeda. 1989. ATP synthase (H<sup>+</sup>-ATPase): results by combined biochemical and molecular biological approaches. *Annu. Rev. Biochem.* 58:111–136.
- Gunsalus, R. P. 1992. Control of electron flow in *Escherichia coli*: coordinated transcription of respiratory pathway genes. *J. Bacteriol.* 174:7069–7074.
- Gunsalus, R. P., W. S. A. Brusilow, and R. D. Simoni. 1982. Gene order and gene-polypeptide relationship of the proton-translocating ATPase operon (*unc*) of *Escherichia coli*. *Proc. Natl. Acad. Sci. USA* 79:320–324.
- Gunsalus, R. P., and S.-J. Park. 1994. Aerobic-anaerobic gene regulation in *Escherichia coli*: control by the ArcAB and Fnr regulons. *Res. Microbiol.* 145:437–450.
- He, L., F. Soderbom, E. G. H. Wagner, U. Binnie, N. Binns, and M. Masters. 1993. PcnB is required for the rapid degradation of RNAI, the antisense RNA that controls the copy number of ColE1-related plasmids. *Mol. Microbiol.* 9:1131–1142.
- Iuchi, S., and E. C. C. Lin. 1993. Adaptation of *Escherichia coli* to redox environments by gene expression. *Mol. Microbiol.* 9:9–15.
- Jones, H. M., C. M. Brajkovich, and R. P. Gunsalus. 1983. In vivo 5' terminus and length of the mRNA for the proton translocating ATPase (*unc*) operon of *Escherichia coli*. *J. Bacteriol.* 155:1279–1287.
- Kanazawa, H., K. Mabuchi, and M. Futai. 1983. Nucleotide sequence of the promoter region of the gene cluster for the proton-translocating ATPase from *Escherichia coli*: identification of the active promoter. *Biochem. Biophys. Res. Commun.* 107:568–575.
- Kanazawa, H., K. Mabuchi, T. Kayano, T. Noumi, T. Sekiya, and M. Futai. 1981. Nucleotide sequence of the F<sub>0</sub> components of the proton-translocating ATPase from *Escherichia coli*: prediction of the primary structure of the F<sub>0</sub> subunits. *Biochem. Biophys. Res. Commun.* 103:613–620.
- Lapilato, J. S. Bortner, and J. Beckwith. 1986. Mutations in a new chromosomal gene of *Escherichia coli* K-12, *pcnB* reduce plasmid copy number of pBR322 and its derivatives. *Mol. Gen. Genet.* 205:285–290.
- Maniatis, T., E. F. Fritsch, and J. Sambrook. 1982. Molecular cloning: a laboratory manual. Cold Spring Harbor Laboratory, Cold Spring Harbor, N.Y.
- McCarthy, J. E. G. 1988. Expression of the *unc* genes in *Escherichia coli*. *J. Bioenerg. Biomembr.* 20:19–39.
- McCarthy, J. E. G., B. Gerstel, B. Surin, U. Wiedemann, and P. Ziemke. 1991. Differential expression from the *Escherichia coli atp* operon mediated by segmental differences in mRNA stability. *Mol. Microbiol.* 5:2447–2458.
- Messing, J., and J. Vieira. 1982. A new pair of M13 vectors for selecting either DNA strand of double digest restriction fragments. *Gene* 19:269–276.
- Miller, J. 1972. Experiments in molecular genetics. Cold Spring Harbor Laboratory, Cold Spring Harbor, N.Y.
- Moriyama, Y., A. Iwamoto, H. Hanada, M. Maeda, and M. Futai. 1991. One-step purification of the *Escherichia coli* H<sup>+</sup>-ATPase (F<sub>0</sub>F<sub>1</sub>) and its reconstitution into liposomes with neurotransmitter transporters. *J. Biol. Chem.* 266:22141–22146.
- Neidhardt, F. C., J. L. Ingraham and M. Schaecter. 1990. Physiology of the bacterial cell. p. 197–212. Sinauer Associates, Inc., Sunderland, Mass.
- Park, S.-J., P. A. Cotter, and R. P. Gunsalus. 1995. Regulation of malate dehydrogenase (*mdh*) gene expression in *Escherichia coli* in response to oxygen, carbon and heme availability. *J. Bacteriol.* 177:6652–6656.
- Park, S.-J., J. McCabe, J. Turna, and R. P. Gunsalus. 1994. Regulation of the citrate synthase (*gluA*) gene of *Escherichia coli* in response to anaerobiosis and carbon supply: role of the *arcA* gene product. *J. Bacteriol.* 176:5086–5092.
- Park, S.-J., C. P. Tseng, and R. P. Gunsalus. 1995. Regulation of the *Escherichia coli* succinate dehydrogenase (*sdhCDAB*) operon in response to anaerobiosis and medium richness: role of the ArcA and Fnr proteins. *Molec. Microbiol.* 15:473–482.
- Patel, A. M., and S. D. Dunn. 1992. RNase E-dependent cleavages in the 5' and 3' regions of the *Escherichia coli unc* mRNA. *J. Bacteriol.* 174:3541–3548.
- Porter, A. C. G., W. S. A. Brusilow, and R. D. Simoni. 1983. Promoter for the *unc* operon of *Escherichia coli*. *J. Bacteriol.* 155:1271–1278.
- Rex, G., B. Surin, G. Besse, B. Schneppe, and J. E. G. McCarthy. 1994. The mechanism of translational coupling in *Escherichia coli*. *J. Biol. Chem.* 269:18118–18127.
- Sakai-Tomita, Y., C. Moritani, H. Kanazawa, M. Tsuda, and T. Tsuchiya. 1992. Catabolite repression of the H<sup>+</sup>-translocating ATPase in *Vibrio parahaemolyticus*. *J. Bacteriol.* 174:6743–6751.
- Schneppe, B., G. Deckers-Hebestreit, J. E. G. McCarthy, and K. Altendorf. 1991. Translation of the first gene of the *Escherichia coli unc* operon. *J. Biol. Chem.* 266:21090–21098.
- Senior, A. E. 1988. ATP synthesis by oxidative phosphorylation. *Physiol. Rev.* 68:177–231.
- Silhavy, T. J., M. L. Berman, and L. W. Enquist. 1984. Experiments with gene fusions. Cold Spring Harbor Laboratory, Cold Spring Harbor, N.Y.
- Simons, R. W., R. Houman, and K. Kleckner. 1987. Improved single and multicopy *lac*-based cloning vectors for protein and operon fusions. *Gene* 53:85–96.
- Solomon, A. Kimberly, Debbie K. W. Hsu, and William S. A. Brusilow. 1989. Use of *lacZ* fusions to measure in vivo expression of the first three genes of the *Escherichia coli unc* operon. *J. Bacteriol.* 171:3039–3045.
- Tseng, C. P., A. K. Hansen, P. Cotter, and R. P. Gunsalus. 1994. Effect of cell growth rate on expression of the anaerobic respiratory pathway operons, *frdABCD*, *dmsABC*, and *narGHJI*, of *Escherichia coli*. *J. Bacteriol.* 176:6599–6605.
- Walker, J. E., M. Saraste, and N. J. Gay. 1984. The *unc* operon, nucleotide sequence, regulation, and structure of ATP-synthase. *Biochim. Biophys. Acta* 768:164–200.

Gene. 1996 Dec 12;183(1-2):87-96.

[Related Articles, Links](#)

**Cloning and nucleotide sequence analysis of the *Streptococcus mutans* membrane-bound, proton-translocating ATPase operon.**

**Smith AJ, Quivey RG Jr, Faustoferri RC.**

Department of Dental Research, School of Medicine and Dentistry, University of Rochester, NY 14642, USA.

The function of the membrane-bound ATPase in *S. mutans* is to regulate cytoplasmic pH values for the purpose of maintaining delta pH. Previous studies have shown that as part of its acid-adaptive ability, *S. mutans* is able to increase H(+)-ATPase levels in response to acidification. As part of the study of ATPase regulation in *S. mutans*, we have cloned the ATPase operon and determined its genetic organization. The structural genes from *S. mutans* were found to be in the order: c, a, b, delta, alpha, gamma, beta, and epsilon; where c and a were reversed from the more typical bacterial organization. The operon contained no I gene homologue but was preceded by a 239-bp intergenic space. Deduced aa sequences from open reading frames indicated that genes encoding homologues of glycogen phosphorylase and nonphosphorylating, NADP-dependent glyceraldehyde-3-phosphate dehydrogenase flank the H(+)-ATPase operon, 5' and 3' respectively. Sequence analysis indicated the presence of three inverted-repeat nt sequences in the glgP-uncE intergenic space. Primer extension analysis of mRNAs prepared from batch-grown or steady-state cultures demonstrated that the transcriptional start site did not change as a function of culture pH value. The data suggest that potential stem-and-loop structures in the promoter region of the operon do not function to alter the starting position of ATPase-specific mRNA transcription.

PMID: 8996091 [PubMed - indexed for MEDLINE]

## Gene Structure of *Enterococcus hirae* (*Streptococcus faecalis*) $F_1F_0$ -ATPase, Which Functions as a Regulator of Cytoplasmic pH

CHIYOKO SHIBATA, TERUYOSHI EHARA, KEIKO TOMURA, KAZUEI IGARASHI,  
AND HIROSHI KOBAYASHI\*

Faculty of Pharmaceutical Sciences, Chiba University, 1-33, Yayoi-cho, Inage-ku, Chiba, 263, Japan

Received 1 April 1992/Accepted 27 July 1992

*Enterococcus hirae* (formerly *Streptococcus faecalis*) ATCC 9790 has an  $F_1F_0$ -ATPase which functions as a regulator of the cytoplasmic pH but does not synthesize ATP. We isolated four clones which contained genes for c, b, delta, and alpha subunits of this enzyme but not for other subunit genes. It was revealed that two specific regions (upstream of the c-subunit gene and downstream of the gamma-subunit gene) were lost at a specific site in the clones we isolated, suggesting that these regions were unstable in *Escherichia coli*. The deleted regions were amplified by polymerase chain reaction, and the nucleotide sequences of these regions were determined. The results showed that eight genes for a, c, b, delta, alpha, gamma, beta, and epsilon subunits were present in this order. Northern (RNA) blot analysis showed that these eight genes were transcribed to one mRNA. The i gene was not found in the upper region of the a-subunit gene. Instead of the i gene, this operon contained a long untranslated region (240 bp) whose G+C content was only 30%. There was no typical promoter sequence such as was proposed for *E. coli*, suggesting that the promoter structure of this species is different from that of *E. coli*. Deduced amino acid sequences suggested that *E. hirae*  $H^+$ -ATPase is a typical  $F_1F_0$ -type ATPase but that its gene structure is not identical to that of other bacterial  $F_1F_0$ -ATPases.

The anaerobic bacteria enterococci (streptococci) have a unique proton-translocating ATPase ( $H^+$ -ATPase) which does not synthesize ATP but regulates the cytoplasmic pH in this species (16, 17, 29). The cytoplasmic pH is regulated by proton extrusion via the  $H^+$ -ATPase and by potassium influx via the specific transport system for this ion. The latter system is not absolutely necessary for pH regulation, but dissipation of the membrane potential generated by the former system is definitely required. In fact, maintenance of neutral cytoplasmic pH can be attained in the presence of valinomycin, which dissipates the membrane potential (28).

Biosynthesis of  $H^+$ -ATPase is stimulated at a low cytoplasmic pH (2, 31). Data from our laboratory have shown that an elevated amount of  $H^+$ -ATPase at a low pH is essential for maintaining neutral cytoplasmic pH (32, 49). Thus, it now appears that the primary factor for regulating cytoplasmic pH is the  $H^+$ -ATPase in enterococci (streptococci). Abrams and his coworkers (1, 3-5, 36) have shown that *Enterococcus hirae* (formerly *Streptococcus faecalis*)  $H^+$ -ATPase is biochemically similar to an  $F_1F_0$ -ATPase of aerobic bacteria which synthesizes ATP coupled with the proton motive force.

In this study, we examined the gene structure of this  $H^+$ -ATPase with *E. hirae* ATCC 9790. The operon for *E. hirae*  $H^+$ -ATPase contained eight genes for a, c, b, delta, alpha, gamma, beta, and epsilon subunits in that order, and the deduced amino acid sequences of *E. hirae*  $H^+$ -ATPase subunits had a high homology with those of other bacterial  $F_1F_0$ -ATPases. These results genetically support the fact that *E. hirae*  $H^+$ -ATPase is a typical  $F_1F_0$ -ATPase. However, the upper region of the a-subunit gene contained no open reading frame corresponding to the i gene. Instead of the i gene, there was a long untranslated region (240 bp).

## MATERIALS AND METHODS

**Strains and culture conditions.** *E. hirae* ATCC 9790 was generously supplied by F. M. Harold, Colorado State University. *E. hirae* was grown on either KTY or 2KTY (30) medium. *Escherichia coli* DH5 $\alpha$  (46) and MV1190 (53) were grown on L broth without glucose (37). DK8 (26), which lacks  $H^+$ -ATPase, was generously supplied by M. Futai, Osaka University.

**Western blot (immunoblot) analysis.** Cells were treated with 5% trichloroacetic acid for 20 min in boiling water. Trichloroacetic acid was extracted with a mixture of ether and ethanol (1:1), and the samples were dissolved in a buffer containing 62.5 mM Tris-HCl (pH 6.8), 2% sodium dodecyl sulfate (SDS), 10% glycerol, 5% mercaptoethanol, and 0.06% bromophenol blue. The resulting solution was heated for 5 min at 100°C. Polyacrylamide gel electrophoresis with 1% SDS was carried out as described previously (35). Proteins separated in the gel were transferred to a nitrocellulose filter (Advantec Co., Tokyo, Japan), and the membrane filter was treated with antiserum against the  $F_1$  portion of *E. hirae* ATPase for 2 h at room temperature in a mixture prepared as follows. *E. coli* DK8 was grown overnight in L broth containing 1% glucose and then was washed with buffer (10 mM Tris-HCl, 1 mM MgCl<sub>2</sub>, pH 7.5). The washed cells were suspended in the same buffer and then passed through a French pressure cell at 20,000 lb/in<sup>2</sup>. The *E. coli* lysate was added to Tris-saline buffer containing 3% bovine serum albumin at 0.1 mg/ml, and antiserum (50  $\mu$ g/ml) prepared as described previously (32) was added. The resulting mixture was incubated for 2 h at 4°C before use. The staining was carried out by the addition of 0.035% H<sub>2</sub>O<sub>2</sub> in Tris-saline buffer containing 4-chloro-naphthol (0.3 mg/ml) and methanol (1%).

**Colony hybridization.** Transformants of DH5 $\alpha$  were grown overnight on a membrane filter (GeneScreen Plus; DuPont/NEN Research Products) placed on an L-broth plate con-

\* Corresponding author.

taining ampicillin (50 µg/ml) and then on another L plate containing ampicillin (50 µg/ml) and chloramphenicol (25 µg/ml). The membrane containing the colonies was treated first with 10% SDS for 3 min, then with 0.5 N NaOH–1.5 M NaCl for 3 min, and finally with 1 M ammonium acetate–0.02 M NaOH for 3 min. The membrane was washed with 2× SSC (1× SSC consists of 0.15 M NaCl plus 0.015 M sodium citrate, pH 8.0) and then was incubated in buffer containing 75 mM sodium citrate, 50 mM NaH<sub>2</sub>PO<sub>4</sub>, 750 mM NaCl, 1% SDS, 50% formamide, and denatured salmon sperm DNA (100 µg/ml), pH 7.5, for 2 h at 42°C. After the probe (5 ng/ml; 4 × 10<sup>6</sup> cpm/ml) was added, hybridization was carried out for 12 h at 42°C. The probe was prepared by a random primed DNA-labeling method (12) with [ $\alpha$ -<sup>35</sup>S]dATP. The membrane was finally washed four times with 2× SSC for 30 min per wash.

**Southern hybridization.** Chromosomal DNA and plasmids were digested with endonuclease and separated by 0.7% agar gel electrophoresis with TBE buffer (46). After DNA fragments were transferred to a filter (GeneScreen Plus), hybridization was carried out by the addition of oligonucleotide (2 ng/ml; 4 × 10<sup>7</sup> cpm/ml) as described above. Oligonucleotides were synthesized chemically and labeled with [ $\gamma$ -<sup>32</sup>P]ATP by T<sub>4</sub> polynucleotide kinase.

**Determination of nucleotide sequence.** The nucleotide sequence was determined by the dideoxy nucleotide chain termination method (47) using Sequenase (version 2.0; United States Biochemical Corp.) and [ $\alpha$ -<sup>35</sup>S]dATP (7). DNA fragments were subcloned into either pUC118 or pUC119 (53). The subcloned fragments were partially deleted with exonuclease III and mung bean nuclease (20). Single DNA strands were prepared by using MV1190 and M13KO7 as described previously (53). Universal and custom primers were used for the sequencing. The regions which were lost in the clones were amplified by polymerase chain reaction (PCR) as described previously (11) except that Tth polymerase (Toyobo, Osaka, Japan) was used, and nucleotide sequences were determined directly by using custom primers.

**Extraction of mRNA from *E. hirae*.** mRNA was extracted from *E. hirae* as described previously (48) with the following modifications. The killing buffer containing 20 mM Tris-HCl, 5 mM MgCl<sub>2</sub>, and 20 mM sodium azide, pH 7.3, was frozen and then crushed with an ice pick without being melted. *E. hirae* was grown on 100 ml of 2KTY medium, pH 8.0. The culture medium was rapidly mixed with 100 ml of the frozen crushed killing buffer when the A<sub>540</sub> of the culture medium was 0.4 to 0.5. The mixture was centrifuged at 6,000 × g for 5 min, and the pellet was suspended in 8 ml of sucrose buffer (50 mM Tris-HCl, 25% sucrose, pH 8.0). Achropeptidase (0.63 mg/ml) and EDTA (0.3 mM) were added, and the mixture was centrifuged at 4,000 × g for 5 min. The pellet was suspended in 1.5 ml of lysis buffer (20 mM Tris-HCl, 3 mM EDTA, 0.2 M NaCl, pH 8.0). The suspension was then mixed with 1.5 mM of lysis buffer containing 1% SDS which had been preheated to 95°C. After the mixture was shaken for 1 min in a hot water bath at 95°C, 3 ml of hot phenol was added, and the mixture was agitated in a water bath at 65°C for 3 min. After centrifugation at 2,000 × g for 5 min, the suspension was treated with phenol twice and ether four times. RNA precipitated with 0.1 volume of 3 M sodium acetate and 2.5 volumes of ethanol was dissolved in sterilized H<sub>2</sub>O.

**Other procedures.** The alignment of amino acid sequences was performed according to the program of D. J. Lipman et al. (38) adapted to an NEC computer; the operating system

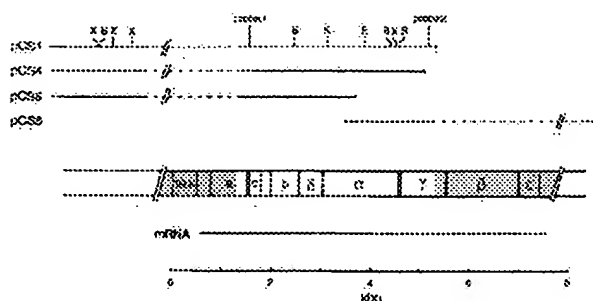


FIG. 1. Physical maps of isolated clones and proposed gene structure of the *E. hirae* H<sup>+</sup>-ATPase operon. a, c, b,  $\delta$ ,  $\alpha$ ,  $\gamma$ ,  $\beta$ , and e indicate the ATPase subunits encoded in the genes. 19k indicates the gene for an unknown 19-kDa protein. The nucleotide sequences of the shadowed regions were determined with the fragments of chromosomal DNA amplified by PCR, and the rest of the H<sup>+</sup>-ATPase operon was sequenced by using the isolated clones. Dotted lines represent the deleted regions of isolated plasmids. The proposed transcript is represented by the lower line. Restriction enzymes: B, *Bgl*II; E, *Eco*RI; K, *Kpn*I; X, *Xba*I.

was an MS-DOS. The cost file for the alignment used was PAM250 (38). Chromosomal DNA was prepared as described previously (13). Northern (RNA) blot analysis, primer extension analysis, and S1 mapping were carried out as described previously (46). The protein concentration was determined as described elsewhere (39).

**Chemicals.** [ $\alpha$ -<sup>35</sup>S]dATP, [ $\alpha$ -<sup>32</sup>P]dCTP, and [ $\gamma$ -<sup>32</sup>P]ATP were purchased from either DuPont/NEN Research Products or ICN Biomedicals, Inc. Other reagents used were of analytical grade.

**Nucleotide sequence accession number.** The nucleotide sequence data reported in this article have been deposited with GenBank under accession number M90060.

## RESULTS

**Cloning of H<sup>+</sup>-ATPase genes.** Chromosomal DNA was partially digested with endonuclease *Sau*3AI, and 5- to 15-kbp fragments were isolated from a 0.7% agar plate after gel electrophoresis. The fragments were ligated with vector pUC9 (52) cut by *Bam*HI after the vector was treated with alkaline phosphatase. *E. coli* DH5 $\alpha$  was transformed.

The clone containing genes for the H<sup>+</sup>-ATPase was isolated by Western blot analysis as follows. Twenty to 30 transformants were mixed and cultured in the same tube. After cells were incubated with isopropyl- $\beta$ -D-thiogalactopyranoside for 2 h in the culture medium, they were collected by centrifugation at 6,000 × g for 5 min, and Western blot analysis was carried out with the resulting pellet. One of about 40 samples was positive: the product of that sample reacted with antiserum against *E. hirae* H<sup>+</sup>-ATPase. All transformants in the positive sample were again checked separately by Western blot analysis, and we isolated a clone, designated pCS1, which produced the alpha subunit of enterococcal ATPase.

We next isolated other clones, designated pCS4, pCS5, and pCS6, by colony hybridization with the *Kpn*I-*Eco*RI fragment of pCS1 (Fig. 1) as a probe.

**Nucleotide sequence of pCS1.** The nucleotide sequence of pCS1 was determined in both directions. The deduced amino acid sequence of the open reading frame indicated by c in Fig. 1 was identical to the sequence of the c subunit obtained

TABLE 1. Molecular weights of *E. hirae* H<sup>+</sup>-ATPase subunits

Subunit	No. of:		Mol wt	
	Nucleotides	Amino acids	Sequence <sup>a</sup>	SDS-PAGE <sup>b</sup>
a	717	239	27,461	27,000
b	522	174	19,391	15,000
c	213	71	7,294	6,000
Alpha	1,554	518	56,548	55,000
Beta	1,404	468	51,030	50,000
Gamma	900	300	33,049	35,000
Delta	540	180	20,698	20,000
Epsilon	420	140	15,606	12,000

<sup>a</sup> As calculated from deduced amino acid sequences.<sup>b</sup> As obtained from SDS-polyacrylamide gel electrophoresis (PAGE) (taken from references 3 and 36).

by the Edman degradation method (34) except for one residue at position 31, which was serine in our data but was glycine according to previous data (34). We therefore concluded that the frame was the gene for the c subunit.

Our criteria for identifying the genes for the other subunits were based on their having homology to the same genes of other bacterial ATPases. We assumed that the gene begins with either TTG or ATG and ends with universal termination codons, because it has been proposed that the genes for a and gamma subunits in *Bacillus megaterium* begin with TTG (8). Based on these criteria, the c-, b-, delta-, and alpha-subunit genes were identified in pCS1. The molecular weights of c, b, delta, and alpha subunits calculated from the deduced amino acid sequences were close to the values proposed previously (3, 36; Table 1). These data strongly suggest that the genes located in pCS1 encode *E. hirae* H<sup>+</sup>-ATPase subunits.

**Deletion of chromosomal DNA at specific sites in isolated clones.** We determined the nucleotide sequence to be about 1.75 kbp upstream of the c-subunit gene (Fig. 1), but the region contained no open reading frame which corresponded to the a-subunit gene. Previous data (36) have shown that enterococcal H<sup>+</sup>-ATPase contains the eight subunits alpha, beta, gamma, delta, epsilon, a, b, and c.

In order to clarify this discrepancy, Southern blot analysis was carried out with probe 1 (24 bp; Fig. 1). The sizes of the *Eco*RI, *Xba*I, and *Bgl*II fragments of chromosomal DNA were not identical to those of the isolated clone pCS1 (data not shown), suggesting that a part of chromosomal DNA (over 4 kbp) was lost during the isolation of pCS1 and that the deletion site was between the initiation site of the c-subunit gene and the *Xba*I site upstream of the gene.

The clones pCS4 and pCS5 also each contained the upper region of the c-subunit gene (Fig. 1), and their physical maps were identical to that of pCS1. It is of interest that the nucleotide sequence of this region was exactly the same in the plasmids pCS1, pCS4, and pCS5, suggesting that the deletion was at a specific site.

The clone pCS6 covered the down region of pCS1 (Fig. 1) and contained the open reading frame in the down region of the alpha-subunit gene. The molecular weight calculated from the deduced amino acid sequence of this frame was 24,267, a much smaller value than that of the gamma subunit obtained previously by SDS-polyacrylamide gel electrophoresis (Table 1). However, the deduced amino acid sequence of this frame was similar to that of the amino-terminal region of the gamma subunit of *B. megaterium* ATPase (8), and the deduced amino acid sequences of the two bacteria had 45.8%

identical residues. The clone pCS6 contained two other open reading frames, but their amino acid sequences were quite different from those of the beta and epsilon subunits of other bacterial H<sup>+</sup>-ATPases. These data again suggest the loss of genes downstream of the carboxyl terminal of the gamma subunit. This suggestion was confirmed by Southern blot analysis carried out using probe 2 (24 bp; Fig. 1), and the size of the deleted region was shown to be >4 kbp.

**Nucleotide sequences of the deleted regions.** The nucleotide sequence of the deleted region was determined by PCR with a "walking" technique. To confirm the determined nucleotide sequence, several fragments (1,500 to 2,000 bp) were produced by PCR with chromosomal DNA as a template, and their nucleotide sequences were determined again in both directions.

The results showed that genes for a, gamma, beta, and epsilon subunits were located in the deleted regions (Fig. 1). The a-subunit gene was thought to start at the TTG codon instead of at the ATG codon (Fig. 2). The reasons for this assumption were, first, that the molecular weight calculated from the deduced amino acid was 27,461 (Table 1), while the value was 25,169 if it was assumed that the ATG codon (nucleotide 901 in Fig. 2) was the first codon. The molecular weight obtained from gel electrophoresis was 27,000 (Table 1). Second, the a-subunit gene also started at the TTG codon in *B. megaterium* ATPase (8).

The molecular weights of these subunits calculated by deduced amino sequences were identical to the values obtained by electrophoresis (Table 1). Only the molecular weight of the gamma subunit, for some unknown reason, was lower than the value obtained by electrophoresis (Table 1).

The order of genes for *E. hirae* ATPase was the same as that for other bacterial F<sub>1</sub>F<sub>0</sub> ATPases (Fig. 1). There was a long noncoding region (209 bp) between the c- and b-subunit genes (Fig. 2). Fourteen base pairs overlapped in the b- and delta-subunit genes, and there was a palindromic sequence in this region (Fig. 2).

**Comparison of amino acid sequences in ATPases of enterococci and other species.** The deduced amino acid sequences of *E. hirae* ATPase subunits showed homology with those of F<sub>1</sub>F<sub>0</sub>-type ATPases of other bacteria (Table 2). The homology was especially high between *E. hirae* and *B. megaterium* ATPases (Table 2). The amino acid sequences of alpha and beta subunits were greatly conserved in comparison with sequences of the other subunits. A part of the deduced amino acid sequence of the beta subunit of *Streptococcus sobrinus* (173 amino acids) has been reported (45), and the amino acids of that portion are 95% identical to those of our sequence. These data suggest that *E. hirae* H<sup>+</sup>-ATPase is a typical F<sub>1</sub>F<sub>0</sub> type of ATPase, although its function is quite different from ATP synthesis.

***E. hirae* ATPase operon does not contain the i gene.** We determined the nucleotide sequence of 2 kbp upstream of the a-subunit gene by using the PCR product. There was an open reading frame, designated the 19k gene, in the upper region of the a-subunit gene (Fig. 1 and 2). The 19k gene contained 163 deduced amino acids, and its molecular weight was 18,859. The deduced amino acid sequence of this 19k gene was quite different from that of the i gene product of other bacteria; homology was less than 20%. The content of hydrophobic amino acids was less than 40%, and the hydrophobicity profile suggested that the 19k protein was a hydrophilic protein.

The region between the 19k gene and the a-subunit gene contained 300 bp (Fig. 2). The longest open reading frame in



1 TTTTATAAGGGAATTAAGAAGAAAAAAGAAAAATAACCAATAACCACTATGAATACCACTTTGGAGGAATGTCATATGCCAAAAGGCGACGAAAGTTAATCGCCCAAAATAAAAAGGCA 120  
M N T S L E E C H M P E G D G K L I A Q N K K A  
19K proteins

274  
121 CGCCATGATTATTCGATTATCGATACGATGGAAGCAGGAATGGTCTGCAAGGAACAGAAATCAATCGATCCGAAACAGCGGAATCAATTTGAAAGATGGATTGTCCGATTTCGAAAC 240  
R H D Y S I I D T N E A G N V L Q G T E I K S I R N S R I N L K D G F V R I R N

241 GGTGAAGCATTTTGCATAATGTTTCATATCAGTCCCTATGAACAAGGCAATATTTTAAACATGATCCGTTACGAACAAGAAAGTTACTATTACACAAAAACAGATTTCACGGCTAGAG 360  
G E A F L H N V H I S P Y E Q G N I F N H D P L R T R E L L L H K K Q I S R L E

361 ACTGAAACAAAAATACCGGGGTACGATCGTACCCTTAAAGAATATATTCGTGATGGGTATGCCAAAGTTTGTGTTGCTTTCGAAAGGGAAGAAATCTTATGACAAGCGAGAAGAT 480  
T E T K N T G V T I V P L E E Y I R D G Y A K V L I G L A K G K K S Y D K R E D

481 CTAAACGAAAGATGTGGATCGTCAAAATGATCGAACATTAATAAATTTCTCTAGATAATTTTCATTATCCTTTTTTCGCATATTCGGTGCTTTTAGGTTTACTTAAATGATAAAATTTTOTT 600  
L K R E D V D R Q I D R T L E N F S R stop \*\*\*\*\*

220  
601 AGCATTTAATCTGATAAAGCATGATATCACAGGTTTTTCTGTAAAACGCCACGATGATTTTAGGAAAAGCAAACTTTTTTGACTGAAATAAAAAATTTGCTGATTTTCATGAAAT 720  
\*  
721 GTTTTGAATTTTCTGTTTCATGTTGATGATACCGTTTGGTTAGAAAACGATTTAGAAAAACAGATGTACACATGAATTTGATTTATGTGAAATTCAGGGAAGAGGTGAAATGGA 840  
721 GTTTTGAATTTTCTGTTTCATGTTGATGATACCGTTTGGTTAGAAAACGATTTAGAAAAACAGATGTACACATGAATTTGATTTATGTGAAATTCAGGGAAGAGGTGAAATGGA 840

841 TTGGATGAACGCTCGCTAACGTTCCATATTGACCGGTTTGGTTTGTATGGTACTGTTTGTATGATGGTGTATTGACCTGTTTGATTGCTTCTTCTTACTTCTTTACAAAGAAAT 960  
M D E R S L T F H I G P V W F D G T V C N M V L L T C L I V F F L V Y F F T R N  
a subunit

210  
961 CTTAAGATGAAACCAACGGGAAACAAATCGCTGGAATGGTCAATTGACTTTACCCGAGGGATCGTAACAGATAATCTGCCTAGAAAAGAATTGAATAATTTTCATTGTTGGCTTTT 1080  
L K M K P T G E Q N A L E W V I D F T R G I V T D N L P R K E L N N F H L L A F

1801 CCTTGATTCTAGTCTTTGCTGTTTAACTCAATTAAGTGTGAGGATAGGACTACTGCTCAATCTCTTTTAAATGTCAAAAAGTGAAGAAAAACCACTGATTATTTTCAAAATAATT 1920  
L I L V F A V stop  
c subunit

1921 GAGTTGTTTCATCATAATACTAGAACAAAAGCGGTTGAAGAGGCTGTTCAATCATTGAAGTCAGGATTCCTTCATCATCCATGAGATACACCTTAAAGAAAGGAAGGCTAGCCTATGCT 2040  
M L  
b subunit

2041 GAATCAATTGGCAATTGCAGAAAGTTGGTAATCCGATGTTAGGTAATATCATCGTTGTCAGCGGCTCAATTTTGATACTAATGTTTCTATTGAAACATTTTCTTGGGGAACCAATCAGCGA 2160  
N Q L A I A E V G N P M L G N I I V V S G S F L I L M P L L K H F A W G P I S D

2401 AGAAGCTGATACAGCTTTAAAGTCTGTAAAAGATGATGTAGCAGATCTTCTCTTCAAAATCGCGGCTAAAACTTGAACAAAGAAATGTCTCCAGAAATGCATGAATCTTTAATCAATCA 2520  
E R D T A L N S V K D D V A D L S L Q I A A K I L N K E L S P E M H E S L I N Q  
b subunit

2521 ATATATCGAAGGCTAGGTTCTTCAAAAGAACTAGATAAATATACTGTGCGCAGACGCTACGGTAAAGCACTATTTGAACTGGCGATCGATTCAAAATAGCGAGAAGAAATTTACCAAG 2640  
Y I E G L G S S N E T R stop  
M K L D K Y T V G R R Y G K A L F E L A I D S N S A E E I Y Q E  
delta subunit

2641 AATTACTAAGCTTACGCCAAATCTATAGTGAATACCTGGATTAGGCAACGTACTTAGTGACGTCGCTTGAACCTCACGAAAAACGAATCATTATGGATAAATTTGTCAGTGGGTTT 2760  
L L S L R Q I Y S E I P G L O N V L S D V R L E P H E K R I I M D K L V S G F D

7321 AGAGCCAAACACGTGCTGAGCGACAAATCGCAGAAAGCAAAAGAAAGAAAGATACGAATGAATTGAAACGTGCGACAGTTGCTTTGCATCGTGAATCAACCGAATCAAGGTTTCAAAA 7440  
R A E Q R A E R Q I A E A K E E D T N E L E R A T V A L H R A I N R I E V S E  
epsilon subunit

7441 CATTCTTAAAGCAACGAATGAGGACCTAACAAAGTGGCTTTAAAAATCCAAGATTCTTAAGGAGATTCTTTAGAAATTTTGGATTTTTTATCGTTTTTTTTTATGGTAGTTATATTC 7560  
H S stop

7561 TAAACATAAAAGTAAAGAACAATTACTTCTTTATTACATAAAAATATGGAACCTTTCATCATTATGATACTATGGTAAACTAATTGCAGTAAAAAGGAGGTATTATAATGCCGAAAAAG 7680  
M P K K  
ORF

FIG. 2. Part of the nucleotide sequence of the H<sup>+</sup>-ATPase operon. The transcriptional initiation site is indicated by the asterisk at position 601. The Pribnow box-like sequence is represented by the double lines. The upper arrows represent the primers used. Palindromic sequences are represented by the lower arrows. ORF indicates the open reading frame located in the downstream region of the H<sup>+</sup>-ATPase operon.

TABLE 2. Homology of deduced amino acid sequences in ATPases of enterococci, *B. megaterium*, and *E. coli*<sup>a</sup>

Species	% Homology in subunit:							
	a	b	c	Alpha	Beta	Gamma	Delta	Epsilon
<i>B. megaterium</i>	45.1	34.7	59.6	75.1	76.4	54.0	23.8	44.5
<i>E. coli</i>	32.5	21.2	41.3	52.2	66.2	32.0	25.2	25.8

<sup>a</sup> Amino acid sequences of *E. hirae* subunits and corresponding subunits of other bacterial ATPases were aligned as described in Materials and Methods, and homology was calculated by the following equation: [(no. of identical residues × 2)/(no. of residues of A + no. of residues of B)] × 100.

this region consisted of 69 bp whose molecular weight as calculated from the deduced amino acid sequence was 2,912. We therefore concluded that the operon for *E. hirae* H<sup>+</sup>-ATPase does not contain the *i* gene.

**Transcriptional initiation site.** The chromosomal DNA was amplified by PCR using 5'-<sup>32</sup>P-labeled primer 210 (position 956, Fig. 2) and primer 274 (position 147, Fig. 2), and the resulting product was used for S1 mapping analysis. The main spot was located approximately 300 bp upstream of primer 210. The major spot obtained by primer extension analysis was located at the same position when primer 210 was used. To determine the position precisely, we next used primer 220 (position 646, Fig. 2) for primer extension analysis and the PCR product of chromosomal DNA amplified with primers 220 and 274 for S1 mapping. The data suggested that the transcriptional initiation site is A, located 240 bp upstream of the  $\alpha$ -subunit gene (Fig. 2 and 3). This result supports our conclusion that the H<sup>+</sup>-ATPase operon does not contain the *i* gene. The size of the mRNA was determined by Northern blot analysis, which revealed the mRNA

to be approximately 7 kb (Fig. 4), suggesting that the eight subunit genes are transcribed to one mRNA.

**Promoter sequence.** There was a sequence of TAAAAT upstream of the transcriptional initiation site (Fig. 2) which was similar to the -10 region of the promoter suggested for *E. coli*. However, the typical -35 region was not found in this region. The noncoding region between the 19k gene and the  $\alpha$ -subunit gene consisted of 70% A and T. Therefore, there were many Pribnow box-like sequences in the noncoding region downstream of the transcriptional initiation site. These results indicate that the promoter structure of the *E. hirae* gene is different from that of the *E. coli* gene.

There are several palindromic sequences in the 5' untranslated region (Fig. 2). Since *E. hirae* H<sup>+</sup>-ATPase is inducible at a low pH (2, 31, 32), the palindromic sequences may be involved in the regulation of gene expression by cytoplasmic pH.

**End of the mRNA of this operon.** There was a noncoding region of 219 bp between the epsilon-subunit gene and the next open reading frame (Fig. 2). Two palindromic sequences, one small and one large, were found in this noncoding region (Fig. 2). At the end of the large palindromic sequence was a T-rich sequence that was similar to the transcriptional termination signal sequence proposed for *E. coli* (44).

We tried to determine the end of the mRNA by S1 mapping with the PCR product as a probe. However, we obtained multiple spots, perhaps because of the heterogeneity of the 3' ends of the PCR products we used. Since these multiple spots were located before the palindromic sequence downstream of the epsilon-subunit gene, the *E. hirae* signal for the transcriptional termination may be different from that

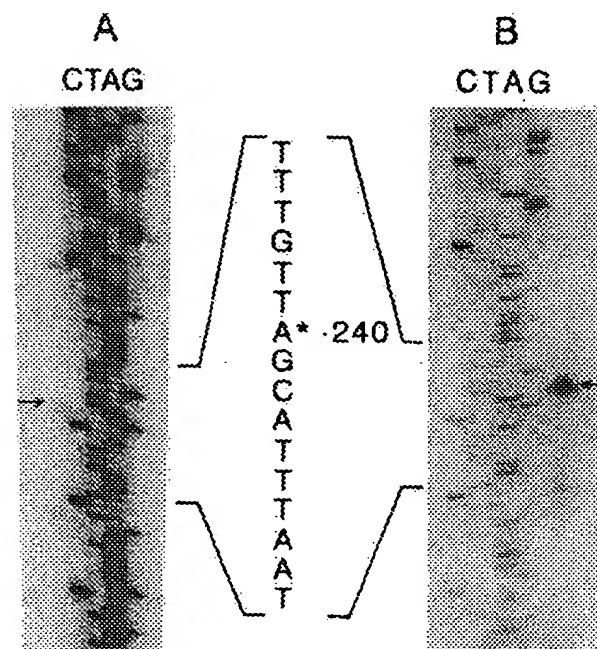


FIG. 3. Determination of transcriptional initiation site. Primer extension analysis (A) was carried out using primer 220 (Fig. 2) labeled by [ $\gamma$ -<sup>32</sup>P]ATP as described in Materials and Methods. The fragment of chromosomal DNA was amplified by PCR with primers 220 and 274 (Fig. 2), and S1 mapping (B) was carried out as described in Materials and Methods. The spot indicated by arrows is marked with an asterisk.

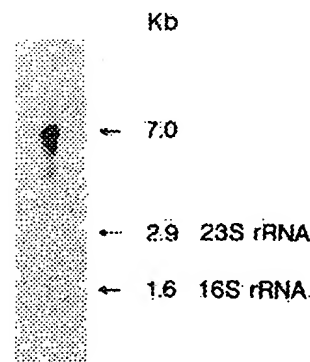


FIG. 4. Northern blot analysis. mRNA was extracted from *E. hirae*, and Northern blot analysis was carried out as described in Materials and Methods. The DNA fragment of chromosomal DNA containing the  $\epsilon$ -subunit gene and a part of the  $\alpha$ -subunit gene was produced by PCR and labeled with a multiprimer labeling kit (Amersham International plc.) using [ $\alpha$ -<sup>32</sup>P]dCTP.

of *E. coli*. In the case of *E. coli*, it has been proposed that the rho factor-independent termination occurs at the T-rich region located at the end of the palindromic sequence (44).

## DISCUSSION

The operon for *E. hirae*  $H^+$ -ATPase contained eight genes in the subunit order a, c, b, delta, alpha, gamma, beta, and epsilon. The deduced amino acid sequences of these subunits have a high homology with those of other  $F_1F_0$ -ATPases. In particular, over 70% of the residues of the alpha and beta subunits in *E. hirae* are identical to those of the subunits in the gram-positive bacterium *B. megaterium*.

Our present data are in good agreement with the previous proposal by Abrams and his coworkers (1, 3-5, 36) that *E. hirae*  $H^+$ -ATPase is a typical  $F_1F_0$ -ATPase. However, its function is quite different from those of other  $F_1F_0$ -ATPases (16, 17, 29). Thus, it appears that  $F_1F_0$ -ATPase has dual functions: one is to synthesize ATP coupled with the respiratory chain in organisms containing this chain, and the other is to act as a pH regulator in microorganisms without the respiratory chain.

The  $F_1F_0$ -ATPase operons of other bacteria contain the *i* gene as a first structure gene. However, the first gene of the *E. hirae*  $H^+$ -ATPase operon is the a-subunit gene rather than the *i* gene. It remains an open question as to why the  $F_1F_0$ -ATPase operons of most bacteria contain the *i* gene, and the function of this gene is also still unknown. *E. hirae*  $H^+$ -ATPase can synthesize ATP when the proton motive force is imposed artificially (9, 40, 41, 51). These data may suggest that the product of the *i* gene is not required for either enzyme assembly or enzyme function. However, the possibility does remain that the *i* gene is located outside of the  $H^+$ -ATPase operon.

It is of interest that mRNA of the operon contains a long noncoding region upstream of the a subunit gene. There are several palindromic sequences in this region (Fig. 2), and the region may be related to the regulation of gene expression of *E. hirae*  $H^+$ -ATPase. Nakayama et al. (43) recently reported that the gene for pheromone-inducible protein has a palindromic sequence upstream of the reading frame. Since  $H^+$ -ATPase is inducible at a low pH, the palindromic sequence could be involved in the regulation of gene expression by the cytoplasmic pH. The method for mRNA preparation from *E. hirae* has already been established (48), but its yield was very low when cells were growing at a low cytoplasmic pH. Therefore, it is not known whether the amount of mRNA of the  $H^+$ -ATPase operon is increased at a low pH or not. New methods for mRNA preparation will need to be developed in order to perform further analyses of the gene expression.

There is another palindromic sequence at the downstream region of the gene cluster for  $F_0$  subunits (Fig. 2). The mutant in which the synthesis of the  $F_0$  portion is not coupled with that of the  $F_1$  portion has been isolated (50), and therefore this palindromic sequence may be related to the regulation of gene expression of this operon.

The A+T contents of enterococci (streptococci) are very high (42). In particular, the A+T contents of noncoding regions are as high as 70%. Therefore, there are many Pribnow box-like sequences. However, there is no typical promoter sequence in front of the transcriptional initiation site such as has been proposed for *E. coli*. Our present results suggest that the promoter sequence of *E. hirae* is different from that of *E. coli*. In this regard, the difference in

the promoter sequences of *Streptococcus pneumoniae* and *E. coli* has recently been discussed (10).

Our present data also suggest that the transcriptional termination signal is different from that of *E. coli*. This may be related to the fact that *E. hirae* contains a large amount of A+T, with the region between the epsilon-subunit gene and the next open reading frame containing 74% A+T.

Our findings indicated that some parts of chromosomal DNA may be unstable in *E. coli*. We tried to isolate clones of the deleted regions by using the fragment amplified by PCR, but this was not successful. It has been observed that the introduction of the a-subunit gene of *E. coli*  $H^+$ -ATPase into *E. coli* is lethal (24). These regions of *E. hirae* may also be harmful for *E. coli*. However, the region around the beta subunit of *E. coli* is not toxic. The deletion of *E. hirae* chromosomal DNA was often observed when the DNA was inserted into a cloning vector and transformed *E. coli* (unpublished observation). Furthermore, the nucleotide sequence of the upper region of the c-subunit gene was the same in all the clones isolated independently, suggesting a site-specific deletion. Thus, many genes of *E. hirae* seem to be harmful for *E. coli*, and *E. coli* may possess some system(s) to remove these genes at specific sites. A common sequence was not found in the two regions which were lost in the present study. Further analysis will be required to resolve this problem.

Our present data support the concept that *E. hirae*  $H^+$ -ATPase is evolutionarily close to that of the gram-positive bacterium *B. megaterium*. However, only the enterococcal operon has no *i* gene. The energy metabolism of enterococci is different from that of other bacteria; *E. hirae* has no respiratory chain. It now appears that *E. hirae*  $H^+$ -ATPase extrudes protons and that the physiological role of this proton extrusion is to maintain a neutral cytoplasmic pH (17, 28-32, 49). Hence, the activity of proton extrusion is negligible in neutral and alkaline environments; the proton motive force is generated only at a low pH (28). This unique metabolism may be related to the lack of the *i* gene.

*E. hirae* has many cation transport systems which are driven by ATP rather than by the proton motive force (6, 18, 19, 21-23, 25, 27, 33), while cation transport systems are mainly driven by the proton motive force in bacteria with the respiratory chain (15). Eukaryotes have cation transport ATPases, sodium/potassium ATPase, calcium ATPase, etc. Similarities between *E. hirae* ion-translocating ATPases and eukaryotic ATPases have been suggested before (14, 21). Our data support the idea that *E. hirae* is phylogenetically close to eubacteria but not to eukaryotes. It can be assumed that *E. hirae* lost its respiratory chain after it separated from other gram-positive bacteria. Thus, we suppose that similar cation-translocating ATPases evolved independently in eukaryotes and enterococci after a powerful system for proton extrusion was lost.

## ACKNOWLEDGMENTS

We express our appreciation to D. B. Clewell for introducing the genetic techniques for enterococci and to Y. Anraku for synthesizing the oligonucleotides. We thank A. Gerz for his help with preparation of the manuscript. We are grateful to F. M. Harold and M. Futai for the bacterial strains and to S. F. Altschul for the alignment program.

This work was supported in part by a Grant-in-Aid for Scientific Research on Priority Areas of Bioenergetics (to H.K.) from the Ministry of Education, Science and Culture, Japan.

## REFERENCES

- Abrams, A. 1985. The proton-translocating membrane ATPase (F<sub>1</sub>F<sub>0</sub>) in *Streptococcus faecalis* (faecium), p. 177-193. In A. N. Martonosi (ed.), *Enzymes in biological membranes*, 2nd ed., vol. 4. Plenum Press, New York.
- Abrams, A., and C. Jensen. 1984. Altered expression of the H<sup>+</sup> ATPase in *Streptococcus faecalis* membranes. *Biochem. Biophys. Res. Commun.* 122:151-157.
- Abrams, A., C. Jensen, and D. H. Morris. 1976. Role of Mg<sup>2+</sup> ions in the subunit structure and membrane binding properties of bacterial energy transducing ATPase. *Biochem. Biophys. Res. Commun.* 69:804-811.
- Abrams, A., and R. M. Leimgruber. 1982. The N, N'-dicyclo-carbodiimide-sensitive ATPase in *Streptococcus faecalis* membranes, p. 465-471. In A. N. Martonosi (ed.), *Membranes and transport*, vol. 1. Plenum Press, New York.
- Abrams, A., and J. B. Smith. 1974. Bacterial membrane ATPase, p. 395-429. In P. D. Boyer (ed.), *The enzymes*, 3rd ed., vol. 10. Academic Press, Inc., New York.
- Bakker, E. P., and F. M. Harold. 1980. Energy coupling to potassium transport in *Streptococcus faecalis*: interplay of ATP and the protonmotive force. *J. Biol. Chem.* 255:433-440.
- Biggin, M. D., T. J. Gibson, and G. F. Hong. 1983. Buffer gradient gels and <sup>35</sup>S label as an aid to rapid DNA sequence determination. *Proc. Natl. Acad. Sci. USA* 80:3963-3965.
- Brusilow, W. S. A., M. A. Scarpetta, C. A. Hawthorne, and W. P. Clark. 1989. Organization and sequence of the genes coding for the proton-translocating ATPase of *Bacillus megaterium*. *J. Biol. Chem.* 264:1528-1533.
- Clarke, D. J., and J. G. Morris. 1979. The proton-translocating adenosine triphosphatase of the obligatory anaerobic bacterium *Clostridium pasteurianum*. *Eur. J. Biochem.* 98:613-620.
- Dillard, J. P., and J. Yother. 1991. Analysis of *Streptococcus pneumoniae* sequences cloned into *Escherichia coli*: effect of promoter strength and transcription terminators. *J. Bacteriol.* 173:5105-5109.
- Ertlich, H. A. 1989. PCR technology: principles and applications for DNA amplification. Stockton Press, New York.
- Feinberg, A. P., and B. Vogelstein. 1983. A technique for radiolabeling DNA restriction endonuclease fragments to high specific activity. *Anal. Biochem.* 132:6-13.
- Franke, A. E., and D. B. Clewell. 1981. Evidence for a chromosome-borne resistance transposon (Tn916) in *Streptococcus faecalis* that is capable of "conjugal" transfer in the absence of a conjugative plasmid. *J. Bacteriol.* 145:494-502.
- Furst, P., and M. Solioz. 1985. Formation of a β-aspartyl phosphate intermediate by the vanadate-sensitive ATPase of *Streptococcus faecalis*. *J. Biol. Chem.* 260:50-52.
- Harold, F. M. 1977. Membranes and energy transduction in bacteria. *Curr. Top. Bioenerg.* 6:83-149.
- Harold, F. M., and K. Altendorf. 1974. Cation transport in bacteria: K<sup>+</sup>, Na<sup>+</sup>, and H<sup>+</sup>. *Curr. Top. Membr. Transp.* 5:1-50.
- Harold, F. M., and J. Van Brunt. 1977. Circulation of H<sup>+</sup> and K<sup>+</sup> across the plasma membrane is not obligatory for bacterial growth. *Science* 197:372-373.
- Heefner, D. L., and F. M. Harold. 1980. ATP-linked sodium transport in *Streptococcus faecalis*. I. The sodium circulation. *J. Biol. Chem.* 255:11396-11402.
- Heefner, D. L., H. Kobayashi, and F. M. Harold. 1980. ATP-linked sodium transport in *Streptococcus faecalis*. II. Energy coupling in everted membrane vesicles. *J. Biol. Chem.* 255:11403-11407.
- Henikoff, S. 1984. Unidirectional digestion with exonuclease III creates targeted breakpoints for DNA sequencing. *Gene* 28:351-359.
- Hugentobler, G., I. Heid, and M. Solioz. 1983. Purification of a putative K<sup>+</sup>-ATPase from *Streptococcus faecalis*. *J. Biol. Chem.* 258:7611-7617.
- Kakinuma, Y., and F. M. Harold. 1985. ATP-driven exchange of Na<sup>+</sup> and K<sup>+</sup> ions by *Streptococcus faecalis*. *J. Biol. Chem.* 260:2086-2091.
- Kakinuma, Y., and K. Igarashi. 1988. Active potassium extrusion regulated by intracellular pH in *Streptococcus faecalis*. *J. Biol. Chem.* 263:14166-14170.
- Kanazawa, H., T. Kiyasu, T. Noumi, and M. Futai. 1984. Overproduction of subunit a of the F<sub>0</sub> component of proton-translocating ATPase inhibits growth of *Escherichia coli* cells. *J. Bacteriol.* 158:300-306.
- Kinoshita, N., T. Unemoto, and H. Kobayashi. 1984. Sodium-stimulated ATPase in *Streptococcus faecalis*. *J. Bacteriol.* 158:844-848.
- Klionsky, D. J., W. S. A. Brusilow, and R. D. Simoni. 1984. In vivo evidence for the role of the ε subunit as an inhibitor of the proton-translocating ATPase of *Escherichia coli*. *J. Bacteriol.* 160:1055-1060.
- Kobayashi, H. 1982. Second system for potassium transport in *Streptococcus faecalis*. *J. Bacteriol.* 150:506-511.
- Kobayashi, H. 1985. A proton-translocating ATPase regulates pH of the bacterial cytoplasm. *J. Biol. Chem.* 260:72-76.
- Kobayashi, H. 1987. Regulation of cytoplasmic pH in streptococci, p. 255-269. In J. Reizer and A. Peterkofsky (ed.), *Sugar transport and metabolism in gram-positive bacteria*. Ellis Horwood Ltd., Chichester, England.
- Kobayashi, H., N. Murakami, and T. Unemoto. 1982. Regulation of the cytoplasmic pH in *Streptococcus faecalis*. *J. Biol. Chem.* 257:13246-13252.
- Kobayashi, H., T. Suzuki, N. Kinoshita, and T. Unemoto. 1984. Amplification of the *Streptococcus faecalis* proton-translocating ATPase by a decrease in cytoplasmic pH. *J. Bacteriol.* 158:1157-1160.
- Kobayashi, H., T. Suzuki, and T. Unemoto. 1986. Streptococcal cytoplasmic pH is regulated by changes in amount and activity of a proton-translocating ATPase. *J. Biol. Chem.* 261:627-630.
- Kobayashi, H., J. Van Brunt, and F. M. Harold. 1978. ATP-linked calcium transport in cells and membrane vesicles of *Streptococcus faecalis*. *J. Biol. Chem.* 253:2085-2092.
- Kocherginskaya, S. A., M. I. Shakhparonov, N. A. Aldanova, N. N. Modyanov, and Y. A. Ovchinnikov. 1982. Proton-translocating adenosinetriphosphatase from *Streptococcus faecalis*. Structure of the dicyclohexylcarbodiimide-binding subunit. *Bioorg. Chem.* 8:1569-1571.
- Laemmli, U. K. 1970. Cleavage of structural proteins during the assembly of the head of bacteriophage T4. *Nature (London)* 227:680-685.
- Leimgruber, R. M., C. Jensen, and A. Abrams. 1981. Purification and characterization of the membrane adenosine triphosphatase complex from the wild-type and N, N'-dicyclohexylcarbodiimide-resistant strains of *Streptococcus faecalis*. *J. Bacteriol.* 147:363-372.
- Lennox, E. S. 1955. Transduction of linked genetic characters of the host by bacteriophage P1. *Virology* 1:190-206.
- Lipman, D. J., S. F. Altschul, and J. D. Kececioglu. 1989. A tool for multiple sequence alignment. *Proc. Natl. Acad. Sci. USA* 86:4412-4415.
- Lowry, O. H., N. J. Rosebrough, A. L. Farr, and R. J. Randall. 1951. Protein measurement with the Folin phenol reagent. *J. Biol. Chem.* 193:265-275.
- Maloney, P. C., E. R. Kashket, and T. H. Wilson. 1974. A protonmotive force drives ATP synthesis in bacteria. *Proc. Natl. Acad. Sci. USA* 71:3896-3900.
- Maloney, P. C., and T. H. Wilson. 1975. ATP synthesis driven by a protonmotive force in *Streptococcus lactis*. *J. Membr. Biol.* 25:285-310.
- Marmur, J., and P. Doty. 1962. Determination of the base composition of deoxyribonucleic acid (DNA) from its thermal denaturation temperature. *J. Mol. Biol.* 5:109-118.
- Nakayama, J., H. Nagasawa, A. Isogai, D. B. Clewell, and A. Suzuki. 1990. Amino acid sequence of pheromone-inducible surface protein in *Enterococcus faecalis*, that is encoded on the conjugative plasmid pPD1. *FEBS Lett.* 267:81-84.
- Platt, T. 1986. Transcription termination and the regulation of gene expression. *Annu. Rev. Biochem.* 55:339-372.
- Quivey, R. G., Jr., R. C. Faustorferri, W. A. Belli, and J. S. Flores. 1991. Polymerase chain reaction amplification, cloning, sequence determination and homologies of streptococcal

- ATPase-encoding DNAs. *Gene* 97:63-68.
46. Sambrook, J., E. F. Fritsch, and T. Maniatis. 1989. Molecular cloning: a laboratory manual, 2nd ed. Cold Spring Harbor Laboratory, Cold Spring Harbor, N.Y.
  47. Sanger, F., S. Nicklen, and A. R. Coulson. 1977. DNA sequencing with chain-terminating inhibitors. *Proc. Natl. Acad. Sci. USA* 74:5463-5467.
  48. Shaw, J. H., and D. B. Clewell. 1985. Complete nucleotide sequence of macrolide-lincosamide-streptogramin B-resistance transposon Tn917 in *Streptococcus faecalis*. *J. Bacteriol.* 164: 782-796.
  49. Suzuki, T., and H. Kobayashi. 1989. Regulation of the cytoplasmic pH by a proton-translocating ATPase in *Streptococcus faecalis* (*faecium*). A computer simulation. *Eur. J. Biochem.* 180:467-471.
  50. Suzuki, T., T. Unemoto, and H. Kobayashi. 1988. Novel streptococcal mutants defective in the regulation of H<sup>+</sup>-ATPase biosynthesis and in F<sub>0</sub> complex. *J. Biol. Chem.* 263:11840-11843.
  51. Van der Drift, C., D. B. Janssen, and P. M. G. F. Van Wezenbeek. 1978. Hydrolysis and synthesis of ATP by membrane-bound ATPase from a motile *Streptococcus*. *Arch. Microbiol.* 119:31-36.
  52. Vieira, J., and J. Messing. 1982. The pUC plasmids, an M13mp7-derived system for insertion mutagenesis and sequencing with synthetic universal primers. *Gene* 19:259-268.
  53. Vieira, J., and J. Messing. 1987. Production of single-stranded plasmid DNA. *Methods Enzymol.* 153:3-11.

GENE 08462

## The ATP synthase ( $F_1F_o$ ) of *Streptomyces lividans*: sequencing of the *atp* operon and phylogenetic considerations with subunit $\beta$ \*

( $F_1F_o$ -ATPase; Actinomycetes; secondary metabolites; membrane)

Michael Hensel<sup>a,\*\*</sup>, Holger Lill<sup>b</sup>, Roland Schmid<sup>a</sup>, Gabriele Deckers-Hebestreit<sup>a</sup> and Karlheinz Altendorf<sup>a</sup>

<sup>a</sup>Arbeitsgruppe Mikrobiologie, Fachbereich Biologie/Chemie, Universität Osnabrück, D-49069 Osnabrück, Germany; and <sup>b</sup>Arbeitsgruppe Biophysik, Fachbereich Biologie/Chemie, Universität Osnabrück, D-49069 Osnabrück, Germany

Received by C.R. Hutchinson: 8 April 1994; Revised/Accepted: 6 June/7 July 1994; Received at publishers: 26 September 1994

### SUMMARY

The DNA encoding the subunits of the ATP synthase ( $F_1F_o$ ) of *Streptomyces lividans* 66 strain 1326 was identified using oligodeoxyribonucleotide probes derived from the N-terminal sequence of subunit  $\gamma$  of the  $F_1$  complex. The complete nucleotide sequence of the operon was determined. The *atp* operon contains nine genes, *atpIBEFHAGDC*, encoding the eight structural components of the ATP synthase complex and the *i* protein, a polypeptide of unknown function. The gene order found is identical to that in other non-photosynthetic eubacteria. The determination of the N-terminal amino acid (aa) sequences of the  $F_1$  subunits  $\alpha$ ,  $\beta$ ,  $\gamma$ ,  $\delta$  and  $\epsilon$  allowed us to identify the translational start points and to define the primary structures of the proteins. The aa sequence deduced for subunit  $\delta$  revealed an N-terminal extension of about 90 aa, which is not present in any  $\delta$  subunit or OSCP (oligomycin sensitivity-conferral protein) of other species studied so far. The phylogenetic relationship of eu- and archaebacteria was investigated using sequencing data of the highly conserved  $\beta$  subunit of different ATP synthases including that of *S. lividans*. The calculations revealed that *S. lividans*  $\beta$  does not form a phylogenetic group together with the Gram<sup>+</sup> taxa of low G+C contents, but is more closely related to the  $\beta$  subunit of Rhodobacteria.

### INTRODUCTION

Unique features like the production of secondary metabolites and the distinct life cycle gave rise to the investigation of biochemical pathways of Streptomyces. Although many pathways for the biosynthesis of antibiotics have already been established, the knowledge about the primary metabolism, and its conjunction to second-

ary metabolism or events in the life cycle is still limited. The ATP synthase ( $F_1F_o$ ) is a key enzyme in energy transduction in all kingdoms of life and has, therefore, been well characterized in a variety of species, thus offering the possibility of detailed comparative studies. The enzyme is composed of a water-soluble, catalytic  $F_1$  moiety, and a membrane-integrated, ion-translocating  $F_o$  moiety (Senior, 1990; Fillingame, 1990). As a first step

Correspondence to: Dr. K. Altendorf, Universität Osnabrück, Fachbereich Biologie/Chemie, D-49069 Osnabrück, Germany. Tel. (49-541) 969-2864; Fax (49-541) 969-2870.

\*This article is dedicated to Prof. Achim Trebst on the occasion of his 65th birthday.

\*\*Present address: Department of Infectious Diseases and Bacteriology, Royal Postgraduate Medical School, Hammersmith Hospital, Du Cane Road, London W12 0NN, UK. Tel. (44-81) 740-3222.

Abbreviations: aa, amino acid(s); bp, base pair(s); DIG, digoxigenin; GCG, Genetics Computer Group (Madison, WI, USA); kb, kilobase(s) or 1000 bp; nt, nucleotide(s); oligo, oligodeoxyribonucleotide; ORF, open reading frame; OSCP, oligomycin sensitivity-conferral protein; PA, polyacrylamide; PVDF, polyvinylidene difluoride; *R.*, *Rhodospirillum*; RBS, ribosome-binding site; *S.*, *Streptomyces*;  $SLF_1F_o$ , ATP synthase of *S. lividans*;  $SLF_1$ ,  $F_1$  complex of *S. lividans* ATP synthase.

we set out to characterize the  $F_1$  portion of the ATP synthase of *Streptomyces lividans* (SLF<sub>1</sub>) and compared its properties to the well-established counterpart of *Escherichia coli* (Hensel et al., 1991). Furthermore, the properties of the membrane-bound ATP synthase (SLF<sub>1</sub>F<sub>0</sub>) were studied in detail followed by its isolation and reconstitution. The ATP-hydrolyzing activity of the membrane-bound ATP synthase of *S. lividans* revealed oligomycin sensitivity, a feature only shared by the ATP synthases of Rhodobacteria and mitochondria. Furthermore, the effects of divalent cations on the enzyme activity resemble that of the ATP synthases of *Rhodospirillum rubrum* and *Bacillus* spp. (M.H., H. Bernsau, G.D.-H. and K.A., data not shown). These distinct features merit further detailed analysis of the ATP synthase of Streptomyces.

## RESULTS AND DISCUSSION

### (a) Cloning and sequencing of the *atp* operon of *S. lividans*

The individual subunits  $\alpha$ ,  $\beta$ ,  $\gamma$ ,  $\delta$  and  $\epsilon$  of the SLF<sub>1</sub> complex were isolated, transferred onto a PVDF membrane, and subjected to automated N-terminal sequencing (Table I). As expected, in each case the N-terminal N-formylMet residue was removed, since small aa, like Ala, Ser, Gly or Thr, are known to favour cleavage of the initiator Met (Flinta et al., 1986). The oligos MH008 (5'-GGIGCICAICTICGIGTSTACAAG) and MH012 (5'-CTTGATASACICGAGITGIGCICC) (where S=G or C) were deduced from the N-terminal aa 1 to 8 of subunit  $\gamma$  of SLF<sub>1</sub> taking into consideration the specific codon

TABLE I

N-terminal aa sequences of the  $F_1$  subunits of the *S. lividans* ATP synthase\*

Subunit	N-terminal aa sequence
$\alpha$	AELTIRPEEIRDALENFVQXYK
$\beta$	TTTVETATATGRVA
$\gamma$	GAQLRVYKRRIRXV
$\delta$	SGMHGASREALAAARERLDA
$\epsilon$	AAELHVALVAADR

\* The SLF<sub>1</sub> complex was isolated as described previously (Hensel et al., 1991) and separated on 13% PA/0.3% SDS gels in the presence of 6 M urea (Schägger and von Jagow, 1987). Bands corresponding to subunits  $\alpha$  and  $\gamma$  were excised, electroeluted and transferred onto PVDF membranes (0.45  $\mu$ m; Millipore, Eschborn, Germany) according to Sheer (1990). Subunits  $\beta$ ,  $\delta$  and  $\epsilon$  were electrophoretically transferred onto membranes according to Dunn (1986) using a carbonate buffer system (10 mM NaHCO<sub>3</sub>/3 mM Na<sub>2</sub>CO<sub>3</sub> pH 9.9/20% (v/v) methanol). The N-terminal aa sequences of SLF<sub>1</sub> subunits were determined on a 473A sequencer (Applied Biosystems, Weiterstadt, Germany) with pulsed liquid phase chemistry using a modified standard cycle (R.S., unpublished).

usage of Streptomyces (Wada et al., 1992). These probes hybridized to a chromosomal *Pst*I fragment of about 2.2 kb (data not shown) which was cloned to yield plasmid p3ID8 (see Fig. 1B). The use of this *Pst*I insert as hybridization probe allowed the selection of clones containing *atp* genes from a genomic DNA library of *S. lividans* constructed in  $\lambda$ Charon35 (Betzler et al., 1987). Of about 20 000 recombinant phages screened by plaque hybridization, 19 positive clones could be identified and clone  $\lambda$ 102 was selected for further analyses (see Fig. 1B). *Kpn*I fragments of the insert of clone  $\lambda$ 102 of about 3.9, 3.2 and 2.2 kb were subcloned to yield plasmids pC100, pC200 and pC300, respectively. A vector portion of  $\lambda$ Charon35 present in pC300, was excised to obtain pC320 (compare Fig. 1B). Sequence analysis revealed that the insert of clone  $\lambda$ 102 contained the genes *atpI'BEFHAGDC* (Fig. 1A,B). The 5' end of *atpI*, as well as the promoter sequence of the *atp* operon were missing. Since a clone containing this region could not be selected from the  $\lambda$ Charon35 library the *Bam*HI-*Kpn*I insert of pC320 was used as a probe for hybridization to the *Kpn*I digest of *S. lividans* 66 chromosomal DNA. Hybridizing fragments of about 5.2 kb were cloned, and sequencing of a subcloned *Sall*-*Kpn*I fragment (pF450) allowed completion of the sequence of the 5' region of the *atp* operon.

### (b) Structure of the *atp* operon of *S. lividans*

The determination of the nt sequence of the *atp* operon revealed that the genes encoding the ATP synthase are organized in one operon (*atpI'BEFHAGDC*) (Figs. 1A and 2), comparable to *atp* operons of other non-photosynthetic bacteria. Codon preference analysis revealed a very high third position G + C bias of protein-encoding regions of the operon (data not shown), a feature characteristic for Streptomyces genes (Wright and Bibb, 1992). The large intergenic regions of the operon exhibit only a moderate third position G + C bias and no ORFs.

The transcription terminator of the *atp* operon was detected by analysis of the sequence with the TERMINATOR program of the GCG package. This putative, factor-independent terminator is located immediately downstream the *atpC* gene. Due to the third position G + C bias, the region upstream from the *atpI* gene does not seem to contain polypeptide-encoding regions. Therefore, this region was analyzed for the presence of a promoter. A region with limited similarity to the 'E. coli-like' group of *Streptomyces* promoters, with the consensus TTGaca(N<sub>18</sub>)TAGGaT (Bibb, 1985) is located about 100 bp in 5' direction of the *atpI* start codon (nt 210 to 250 in Fig. 2). It has to be mentioned that this promoter designation is putative and awaits experimental proof.



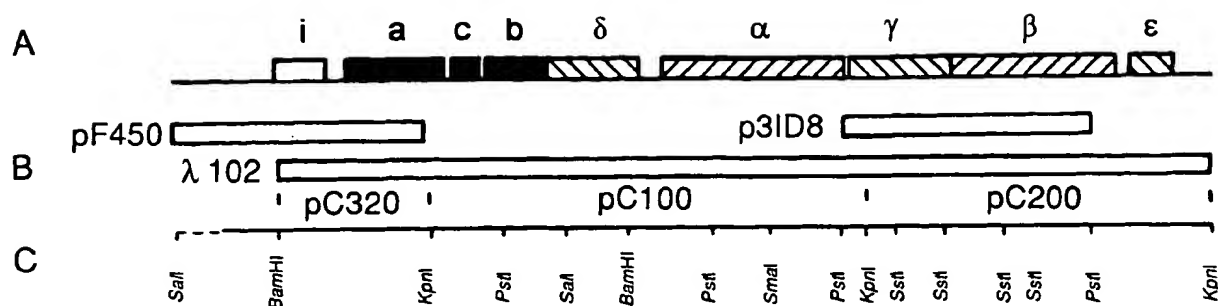


Fig. 1. Organization for the *atp* operon of *S. lividans*. For sequencing of the *atp* operon of *S. lividans*, restriction fragments of the chromosomal DNA (B) were cloned and analyzed (p3ID8, pF450). Furthermore, the insert of a phage selected from a  $\lambda$ Charon35 library ( $\lambda$ 102) was subcloned (pC100, pC200, pC320) and sequenced. Restriction sites relevant for the cloning of *atp* are marked (C). The order of the individual genes of the operon is given by the designations of the respective gene products (A). Genes encoding the subunits of the  $F_0$  complex and the  $F_1$  complex are represented by filled and hatched boxes, respectively. **Methods:** *S. lividans* 66 strain 1326 kindly donated by Dr. H. Schrempf (Universität Osnabrück) was grown in Difco tryptic soy broth media (30 g/l; Nordwald, Hamburg, Germany) at 30°C with vigorous aeration. Chromosomal DNA of *S. lividans* was prepared by the hexadecyltrimethyl ammonium bromide method (Ausubel et al., 1987). As a modification of the method, washed mycelia (1 g) were resuspended in 5 ml 10 mM Tris-HCl pH 8.0/1 mM EDTA/2 mg per ml lysozyme and incubated for 30 min at 30°C in order to weaken the streptomycetal cell wall prior to the extraction of DNA. The plating of a  $\lambda$ Charon35 library of chromosomal DNA of *S. lividans* (Betzler et al., 1987) and the transfer of plaques onto membranes (Hybond N<sup>+</sup>, pore size 0.45  $\mu$ m, Amersham, Braunschweig, Germany) was performed according to standard procedures (Ausubel et al., 1987). Labeling of oligos and DNA fragments, hybridization with transferred plaques and Southern blots, and the subsequent detection was performed using the non-radioactive DIG system (Boehringer-Mannheim, Mannheim, Germany). Other DNA manipulations were carried out according to standard methods (Ausubel et al., 1987; Sambrook et al., 1989) using DNA-modifying enzymes from Boehringer-Mannheim and Gibco-BRL (Eggenstein-Leopoldsdorf, Germany).

Furthermore, the promoter of the *S. lividans atp* operon might be not '*E. coli*-like' and due to the large intergenic sequences, the presence of additional promoter sequences as has been also shown for the *E. coli atp* operon is possible (Walker et al., 1984).

Since the N-terminal aa sequences of all SLF<sub>1</sub> subunits have been determined (Table I), the start codons for *atpHAGDC* could be identified. However, the *atpC* gene does not contain an ATG start codon. From N-terminal sequencing, a TTG start codon has to be favored. Compared to the alternative start codon GTG, TTG start codons are rarely used in *Streptomyces*, but have been reported (Th  berge et al., 1992). For the other *atp* genes, *atpIBEF*, the translational start is putative. In the case of more than one possible start codon, e.g., *atpB* and *atpF*, the putative regions were aligned to the 3' region of the 16S rRNA of *S. lividans* using BESTFIT in order to locate RBS (data not shown). The *atpF* gene possesses three possible translational starts with only minute distances apart, as has been also observed for *atpF* in other *atp* operons, like that of *E. coli* (Walker et al., 1984) or *Propionigenium modestum* (Esser et al., 1990).

### (c) Features of the deduced aa sequences

The molecular masses calculated from the deduced aa sequences of the ATP synthase subunits are in good agreement with biochemical data (data not shown; for SLF<sub>1</sub> subunits, compare Hensel et al., 1991). A significant feature is the primary structure of subunit  $\delta$ , which exhib-

its a molecular mass of 28 941 Da. The start codon of the corresponding ORF was confirmed by aa sequencing of the N-terminal region of subunit  $\delta$ . In addition, the apparent molecular mass for subunit  $\delta$  has been shown to be 28 kDa (Hensel et al., 1991). However, the corresponding subunits, i.e., subunit  $\delta$  of other eubacterial ATP synthases and the mature OSCP of mitochondrial ATP synthases, exhibit molecular masses of about 18–20 kDa. An alignment revealed that the higher molecular mass of *S. lividans*  $\delta$  is reflected by an N-terminal extension of about 90 aa (data not shown). An analysis of the secondary structure by various computational methods indicated two additional  $\alpha$ -helical regions with a moderate amphipathic character. Due to the conserved character of the secondary structures of ATP synthase subunits, a functional importance of the N-terminal extension has to be postulated.

The subunits of the  $F_0$  complex in general are known to exhibit only limited homology in the primary sequence. However, the similarity in the secondary structure and the appearance of, although few, conserved residues in alignments of subunits  $\alpha$  and  $\gamma$  of *S. lividans* and various other species, stressed the identity of the SLF<sub>0</sub> subunits. These sequence alignments revealed that a remarkable high degree of homology exists between the  $\alpha$  subunits of *S. lividans* and *R. rubrum*. The overall identity between both species is 36.5%, compared to about 25% identity to subunit  $\alpha$  of other species (data not shown). In addition, the aa residues of *E. coli* subunit  $\alpha$ , e.g., Arg<sup>210</sup>,

1  
 2  
 3  
 4  
 5  
 6  
 7  
 8  
 9  
 10  
 11  
 12  
 13  
 14  
 15  
 16  
 17  
 18  
 19  
 20  
 21  
 22  
 23  
 24  
 25  
 26  
 27  
 28  
 29  
 30  
 31  
 32  
 33  
 34  
 35  
 36  
 37  
 38  
 39  
 40  
 41  
 42  
 43  
 44  
 45  
 46  
 47  
 48  
 49  
 50  
 51  
 52  
 53  
 54  
 55  
 56  
 57  
 58  
 59  
 60  
 61  
 62  
 63  
 64  
 65  
 66  
 67  
 68  
 69  
 70  
 71  
 72  
 73  
 74  
 75  
 76  
 77  
 78  
 79  
 80  
 81  
 82  
 83  
 84  
 85  
 86  
 87  
 88  
 89  
 90  
 91  
 92  
 93  
 94  
 95  
 96  
 97  
 98  
 99  
 100  
 101  
 102  
 103  
 104  
 105  
 106  
 107  
 108  
 109  
 110  
 111  
 112  
 113  
 114  
 115  
 116  
 117  
 118  
 119  
 120  
 121  
 122  
 123  
 124  
 125  
 126  
 127  
 128  
 129  
 130  
 131  
 132  
 133  
 134  
 135  
 136  
 137  
 138  
 139  
 140  
 141  
 142  
 143  
 144  
 145  
 146  
 147  
 148  
 149  
 150  
 151  
 152  
 153  
 154  
 155  
 156  
 157  
 158  
 159  
 160  
 161  
 162  
 163  
 164  
 165  
 166  
 167  
 168  
 169  
 170  
 171  
 172  
 173  
 174  
 175  
 176  
 177  
 178  
 179  
 180  
 181  
 182  
 183  
 184  
 185  
 186  
 187  
 188  
 189  
 190  
 191  
 192  
 193  
 194  
 195  
 196  
 197  
 198  
 199  
 200  
 201  
 202  
 203  
 204  
 205  
 206  
 207  
 208  
 209  
 210  
 211  
 212  
 213  
 214  
 215  
 216  
 217  
 218  
 219  
 220  
 221  
 222  
 223  
 224  
 225  
 226  
 227  
 228  
 229  
 230  
 231  
 232  
 233  
 234  
 235  
 236  
 237  
 238  
 239  
 240  
 241  
 242  
 243  
 244  
 245  
 246  
 247  
 248  
 249  
 250  
 251  
 252  
 253  
 254  
 255  
 256  
 257  
 258  
 259  
 260  
 261  
 262  
 263  
 264  
 265  
 266  
 267  
 268  
 269  
 270  
 271  
 272  
 273  
 274  
 275  
 276  
 277  
 278  
 279  
 280  
 281  
 282  
 283  
 284  
 285  
 286  
 287  
 288  
 289  
 290  
 291  
 292  
 293  
 294  
 295  
 296  
 297  
 298  
 299  
 300  
 301  
 302  
 303  
 304  
 305  
 306  
 307  
 308  
 309  
 310  
 311  
 312  
 313  
 314  
 315  
 316  
 317  
 318  
 319  
 320  
 321  
 322  
 323  
 324  
 325  
 326  
 327  
 328  
 329  
 330  
 331  
 332  
 333  
 334  
 335  
 336  
 337  
 338  
 339  
 340  
 341  
 342  
 343  
 344  
 345  
 346  
 347  
 348  
 349  
 350  
 351  
 352  
 353  
 354  
 355  
 356  
 357  
 358  
 359  
 360  
 361  
 362  
 363  
 364  
 365  
 366  
 367  
 368  
 369  
 370  
 371  
 372  
 373  
 374  
 375  
 376  
 377  
 378  
 379  
 380  
 381  
 382  
 383  
 384  
 385  
 386  
 387  
 388  
 389  
 390  
 391  
 392  
 393  
 394  
 395  
 396  
 397  
 398  
 399  
 400  
 401  
 402  
 403  
 404  
 405  
 406  
 407  
 408  
 409  
 410  
 411  
 412  
 413  
 414  
 415  
 416  
 417  
 418  
 419  
 420  
 421  
 422  
 423  
 424  
 425  
 426  
 427  
 428  
 429  
 430  
 431  
 432  
 433  
 434  
 435  
 436  
 437  
 438  
 439  
 440  
 441  
 442  
 443  
 444  
 445  
 446  
 447  
 448  
 449  
 450  
 451  
 452  
 453  
 454  
 455  
 456  
 457  
 458  
 459  
 460  
 461  
 462  
 463  
 464  
 465  
 466  
 467  
 468  
 469  
 470  
 471  
 472  
 473  
 474  
 475  
 476  
 477  
 478  
 479  
 480  
 481  
 482  
 483  
 484  
 485  
 486  
 487  
 488  
 489  
 490  
 491  
 492  
 493  
 494  
 495  
 496  
 497  
 498  
 499  
 500  
 501  
 502  
 503  
 504  
 505  
 506  
 507  
 508  
 509  
 510  
 511  
 512  
 513  
 514  
 515  
 516  
 517  
 518  
 519  
 520  
 521  
 522  
 523  
 524  
 525  
 526  
 527  
 528  
 529  
 530  
 531  
 532  
 533  
 534  
 535  
 536  
 537  
 538  
 539  
 540  
 541  
 542  
 543  
 544  
 545  
 546  
 547  
 548  
 549  
 550  
 551  
 552  
 553  
 554  
 555  
 556  
 557  
 558  
 559  
 560  
 561  
 562  
 563  
 564  
 565  
 566  
 567  
 568  
 569  
 570  
 571  
 572  
 573  
 574  
 575  
 576  
 577  
 578  
 579  
 580  
 581  
 582  
 583  
 584  
 585  
 586  
 587  
 588  
 589  
 590  
 591  
 592  
 593  
 594  
 595  
 596  
 597  
 598  
 599  
 600  
 601  
 602  
 603  
 604  
 605  
 606  
 607  
 608  
 609  
 610  
 611  
 612  
 613  
 614  
 615  
 616  
 617  
 618  
 619  
 620  
 621  
 622  
 623  
 624  
 625  
 626  
 627  
 628  
 629  
 630  
 631  
 632  
 633  
 634  
 635  
 636  
 637  
 638  
 639  
 640  
 641  
 642  
 643  
 644  
 645  
 646  
 647  
 648  
 649  
 650  
 651  
 652  
 653  
 654  
 655  
 656  
 657  
 658  
 659  
 660  
 661  
 662  
 663  
 664  
 665  
 666  
 667  
 668  
 669  
 670  
 671  
 672  
 673  
 674  
 675  
 676  
 677  
 678  
 679  
 680  
 681  
 682  
 683  
 684  
 685  
 686  
 687  
 688  
 689  
 690  
 691  
 692  
 693  
 694  
 695  
 696  
 697  
 698  
 699  
 700  
 701  
 702  
 703  
 704  
 705  
 706  
 707  
 708  
 709  
 710  
 711  
 712  
 713  
 714  
 715  
 716  
 717  
 718  
 719  
 720  
 721  
 722  
 723  
 724  
 725  
 726  
 727  
 728  
 729  
 730  
 731  
 732  
 733  
 734  
 735  
 736  
 737  
 738  
 739  
 740  
 741  
 742  
 743  
 744  
 745  
 746  
 747  
 748  
 749  
 750  
 751  
 752  
 753  
 754  
 755  
 756  
 757  
 758  
 759  
 760  
 761  
 762  
 763  
 764  
 765  
 766  
 767  
 768  
 769  
 770  
 771  
 772  
 773  
 774  
 775  
 776  
 777  
 778  
 779  
 780  
 781  
 782  
 783  
 784  
 785  
 786  
 787  
 788  
 789  
 790  
 791  
 792  
 793  
 794  
 795  
 796  
 797  
 798  
 799  
 800  
 801  
 802  
 803  
 804  
 805  
 806  
 807  
 808  
 809  
 810  
 811  
 812  
 813  
 814  
 815  
 816  
 817  
 818  
 819  
 820  
 821  
 822  
 823  
 824  
 825  
 826  
 827  
 828  
 829  
 830  
 831  
 832  
 833  
 834  
 835  
 836  
 837  
 838  
 839  
 840  
 841  
 842  
 843  
 844  
 845  
 846  
 847  
 848  
 849  
 850  
 851  
 852  
 853  
 854  
 855  
 856  
 857  
 858  
 859  
 860  
 861  
 862  
 863  
 864  
 865  
 866  
 867  
 868  
 869  
 870  
 871  
 872  
 873  
 874  
 875  
 876  
 877  
 878  
 879  
 880  
 881  
 882  
 883  
 884  
 885  
 886  
 887  
 888  
 889  
 890  
 891  
 892  
 893  
 894  
 895  
 896  
 897  
 898  
 899  
 900  
 901  
 902  
 903  
 904  
 905  
 906  
 907  
 908  
 909  
 910  
 911  
 912  
 913  
 914  
 915  
 916  
 917  
 918  
 919  
 920  
 921  
 922  
 923  
 924  
 925  
 926  
 927  
 928  
 929  
 930  
 931  
 932  
 933  
 934  
 935  
 936  
 937  
 938  
 939  
 940  
 941  
 942  
 943  
 944  
 945  
 946  
 947  
 948  
 949  
 950  
 951  
 952  
 953  
 954  
 955  
 956  
 957  
 958  
 959  
 960  
 961  
 962  
 963  
 964  
 965  
 966  
 967  
 968  
 969  
 970  
 971  
 972  
 973  
 974  
 975  
 976  
 977  
 978  
 979  
 980  
 981  
 982  
 983  
 984  
 985  
 986  
 987  
 988  
 989  
 990  
 991  
 992  
 993  
 994  
 995  
 996  
 997  
 998  
 999  
 1000

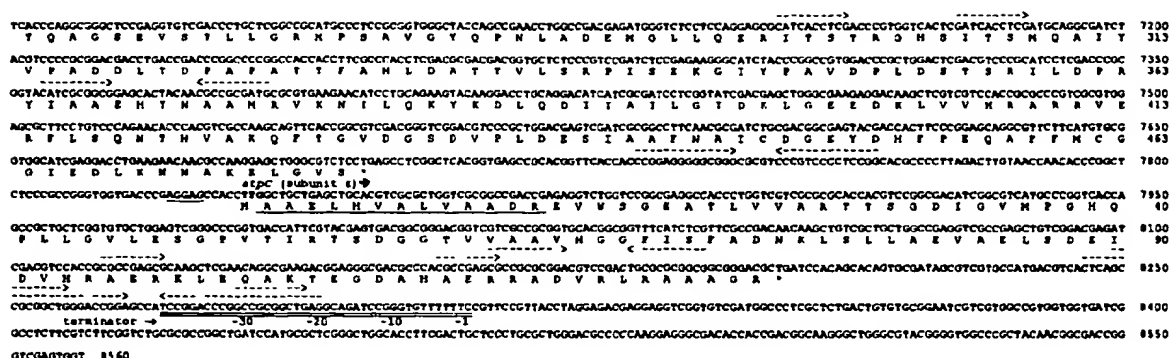


Fig. 2. Sequence of the *S. lividans atp* operon. The complete nt sequence was determined by sequencing both strands of DNA. The N-terminal sequences determined by aa sequencing are indicated by underlining the aa deduced from nt sequencing. Putative and confirmed start codons of the genes are printed bold, whereas putative RBS of individual genes are underlined. As functional elements of the operon, the putative promoter and terminator sequences are double underlined. The digits -35 and -10 indicate functional elements of the putative promoter, while the digit -1 at the terminator sequence indicates the last transcribed nt. Regions containing inverted or direct repeats are indicated by arrows. The nt sequence was submitted to the EMBL data library and is available under accession No. Z22606. Methods: For DNA sequencing a combination of the exonuclease III method of Henikoff (1984) and the primer walking approach was applied. DNA sequencing of single-strand templates was performed with Sequenase version 2.0 kits for standard applications, and with Taquenase version 2.0 kits for the resolution of regions containing strong secondary structures (both US Biochemical, Bad Homburg, Germany). For the resolution of compressions arising from stable secondary structures due to the high G+C content of 75%, each sequence position was determined at least twice with control reactions employing base analogues (dITP for Sequenase and deazaGTP for Taquenase). Sequence fragments were assembled and analyzed by means of the GCG software package version 7.2 running on a  $\mu$ VAX 3800.

Glu<sup>219</sup> and His<sup>245</sup>, shown to be essential for proton translocation through  $F_0$  (Senior, 1990; Fillingame, 1990), are conserved in subunit  $\alpha$  of *S. lividans*, although the positions of Glu and His have been inverted (Fig. 2; Arg<sup>209</sup>, His<sup>218</sup>, Glu<sup>254</sup>). From site-directed mutagenesis experiments with *E. coli* subunit  $\alpha$  it is known that both residues can be exchanged against each other yielding an  $F_0$  complex with higher rates of proton translocation than that of either single mutation (Cain and Simoni, 1988).

#### (d) Phylogenetic analysis

Due to their ubiquity and highly conserved structure, the sequences of rRNAs have been postulated as molecular chronometers and the great number of known rRNA sequences allowed the generation of phylogenetic trees (Woese, 1987). ATP synthase subunits involved in nucleotide binding, i.e., subunits  $\alpha$  and  $\beta$ , also show highly conserved primary structures in all species investigated so far. Furthermore, these polypeptides are ubiquitous, and, therefore, also allow the generation of phylogenetic trees. As a result, this calculation resembles the grouping of previously analyzed species (Amann et al., 1988; Klugbauer et al., 1992; Xie et al., 1993). The Gram<sup>+</sup> group with a low G+C content of the DNA presents a single line of descent. Rhodobacteria, Cyanobacteria and the *Bacteriodes/Cytophaga* group appear as phylogenetically coherent groups. In contrast, *Propionigenium modestum* and *Mycoplasma gallisepticum* show an individual line of descent (Fig. 3).

The phylogenetic position of *S. lividans* distant to other members of the Gram<sup>+</sup> line of descent, but in juxtaposition to Rhodobacteria, is a rather unexpected result. Recent analysis of 16S rRNA (Woese, 1987; Olsen et al., 1994) has shown a coherent grouping of Gram<sup>+</sup> taxa with high and low G+C content. The analysis of the sequences of subunit  $\beta$ , however, revealed a split in the Gram<sup>+</sup> branch of decline between *S. lividans* as a member of the high-G+C Gram<sup>+</sup> group and other Gram<sup>+</sup> taxa of the low-G+C branch. Similar to the phylogenetic calculations shown here, an analysis by Schleifer and Ludwig (1989) indicated a position of the high-G+C Gram<sup>+</sup> group distant from the low-G+C Gram<sup>+</sup> group, although *Streptomyces* was not analyzed. Furthermore, the outstanding phylogenetic position of the high-G+C Gram<sup>+</sup> group was recently supported by analysis of the 23S rRNA, which has been characterized by an insertion unique for this group of bacteria (Roller et al., 1992). The phylogenetic proximity of *S. lividans* and Rhodobacteria, which is also supported by biochemical evidences (see INTRODUCTION), might be a consequence of the high G+C content of both species. The G+C content of the *atp* operon of *S. lividans* (68%) is close to the values for the *atp* operons of *R. rubrum* (66%) and *Rhodopseudomonas blautica* (65%) (Falk et al., 1985; Tybulewicz et al., 1984), whereas the sequences of other species exhibit lower G+C contents. Therefore, it has to be considered whether the high G+C content in the species mentioned is the result of an analogous evolution or whether it is a primary feature.

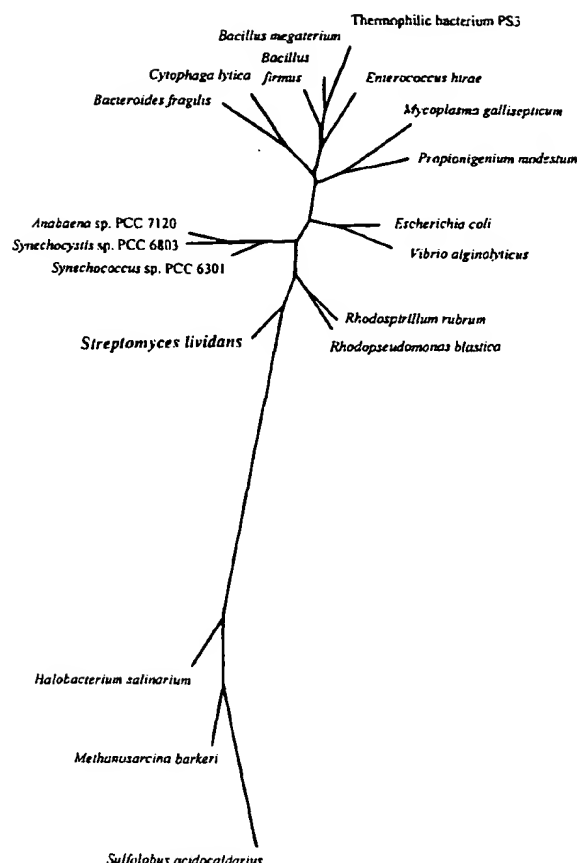


Fig. 3. Phylogenetic tree calculated with nt sequences of *atpD* (subunit  $\beta$ ). The phylogenetic tree presented is the result of several runs of the DNAML program of the PHYLIP package, versions 3.2 and 3.5. The nt sequences for the genes of the subunit  $\beta$  of *Anabaena* sp. PCC 7120, *Bacillus firmus*, *Bacillus megaterium*, *Bacteroides fragilis*, *Cytophaga hutchinsonii*, *Enterococcus hirae*, *Escherichia coli*, *Mycoplasma gallisepticum*, *Propionigenium modestum*, *Rhodopseudomonas blautica*, *R. rubrum*, *Synechococcus* sp. PCC 6301, *Synechocystis* sp. PCC 6803, thermophilic bacterium PS3, *Vibrio alginolyticus* and the subunit A of *Halobacterium salinarum*, *Methanosarcina barkeri* and *Sulfolobus acidocaldarius* were obtained from the EMBL database release 33 (see database entries for references). The deduced aa sequences of subunits  $\beta$  and A of eu- and archaeobacteria, respectively, were aligned in order to minimize gaps (data not shown). The resulting alignment was translated into an alignment of the corresponding nt sequences, which was used for the calculations of the phylogenetic relationship. In this form, the sum of the branch lengths between species of the phylogenetic tree corresponds to the evolutionary distance. In order to provide an outgroup for the phylogenetic analysis, sequences of genes for the archaeobacterial ATPase subunit A, which is related to the eubacterial subunit  $\beta$ , were included. No considerations about the sequence of the catalytic subunit of the common ancestor of archae- and eubacteria are allowed, thus the tree remains unrooted.

#### (e) Conclusions

(1) Oligos derived from N-terminal aa sequences of ATP synthase subunits allowed the identification and

cloning of nt fragments encoding the ATP synthase of *S. lividans*.

(2) Sequence analyses revealed that the ATP synthase genes are organized in one operon (*atpIBEFHAGDC*).

(3) Subunit  $\delta$  possesses a unique N-terminal extension of 90 aa.

(4) Amino-acid residues shown to be essential for proton translocation through  $F_o$  are conserved in subunits  $\alpha$  and  $\gamma$  of *S. lividans*.

(5) Phylogenetic analyses performed with subunit  $\beta$  indicated a position of *S. lividans* distant from other Gram<sup>+</sup> bacteria but close to Rhodobacteria.

#### ACKNOWLEDGEMENTS

We are grateful to Dr. M. Betzler (Universität Osnabrück, Germany) for providing the  $\lambda$ Charon35 library of *S. lividans* chromosomal DNA, to Dr. H. Schrepf (Universität Osnabrück) for introducing M.H. into the handling of Streptomyces and for helpful discussion, to Dr. U. Kunze (Universität Osnabrück) for computational support, and to E.M. Uhlemann for excellent technical assistance. This work was supported by the Deutsche Forschungsgemeinschaft (SFB 171) and the Fonds der Chemischen Industrie (fellowship to M.H.).

#### REFERENCES

- Amann, R., Ludwig, W. and Schleifer, K.H.:  $\beta$ -subunit of ATP-synthase: a useful marker for studying the phylogenetic relationship of eubacteria. *J. Gen. Microbiol.* 134 (1988) 2815–2821.
- Ausubel, F.M., Brent, R., Kingston, R.E., Moore, D.D., Seidman, J.G., Smith, J.A. and Struhl, K.: *Current Protocols in Molecular Biology*. Wiley, New York, NY, 1987 (updated 1992).
- Betzler, M., Dyson, P. and Schrepf, H.: Relationship of an unstable *argG* gene to a 5.7-kilobase amplifiable DNA sequence in *Streptomyces lividans* 66. *J. Bacteriol.* 169 (1987) 4804–4810.
- Bibb, M.J.: Gene expression in *Streptomyces* – nucleotide sequences involved in the initiation of transcription and translation. In: Szabó, G., Biró, S. and Goodfellow, M. (Eds.), *Sixth International Symposium on Actinomycetes Biology*. Akadémiai Kiadó, Budapest, 1985, pp. 25–33.
- Cain, B.D. and Simoni, R.D.: Interaction between Glu-219 and His-245 within the  $\alpha$  subunit of  $F_1F_o$ -ATPase in *Escherichia coli*. *J. Biol. Chem.* 263 (1988) 6606–6612.
- Dunn, S.D.: Effects of the modification of transfer buffer composition and the renaturation of proteins in gels on the recognition of proteins on Western blots by monoclonal antibodies. *Anal. Biochem.* 157 (1986) 144–153.
- Esser, U., Krumholz, L.R. and Simoni, R.D.: Nucleotide sequence of the  $F_o$  subunits of the sodium dependent  $F_1F_o$  ATPase of *Propionigenium modestum*. *Nucleic Acids Res.* 18 (1990) 5887.
- Falk, G., Hampe, A. and Walker, J.E.: Nucleotide sequence of the *Rhodospirillum rubrum atp* operon. *Biochem. J.* 228 (1985) 391–407.
- Fillingame, R.H.: Molecular mechanics of ATP synthesis by  $F_1F_o$  type  $H^+$ -translocating ATP synthases. In: Krulwich, T.A. (Ed.), *The*

- Bacteria: A Treatise on Structure and Function, Vol. XII. Academic Press, New York, NY, 1990, pp. 345–391.
- Flinta, C., Persson, B., Jönvall, H. and von Heijne, G.: Sequence determinants of cytosolic N-terminal protein processing. *Eur. J. Biochem.* 154 (1986) 193–196.
- Henikoff, S.: Unidirectional digestion with exonuclease III creates targeted breakpoints for DNA sequencing. *Gene* 28 (1984) 351–359.
- Hensel, M., Deckers-Hebestreit, G. and Altendorf, K.: Purification and characterization of the  $F_1$  portion of the ATP synthase ( $F_1F_0$ ) of *Streptomyces lividans*. *Eur. J. Biochem.* 202 (1991) 1313–1319.
- Klugbauer, N., Ludwig, W., Bauerlein, E. and Schleifer, K.H.: Subunit  $\beta$  of adenosine triphosphate synthase of *Pectinatus frisingensis* and *Lactobacillus casei*. *Syst. Appl. Microbiol.* 15 (1992) 323–330.
- Olsen, G.J., Woese, C.R. and Overbeek, R.: The winds of (evolutionary) change: breathing new life into microbiology. *J. Bacteriol.* 176 (1994) 1–6.
- Roller, C., Ludwig, W. and Schleifer, K.H.: Gram-positive bacteria with a high DNA G + C content are characterized by a common insertion within their 23S rRNA genes. *J. Gen. Microbiol.* 138 (1992) 1167–1175.
- Sambrook, J., Fritsch, E.F. and Maniatis, T.: *Molecular Cloning. A Laboratory Manual*, 2nd ed. Cold Spring Harbor Laboratory Press, Cold Spring Harbor, NY, 1989.
- Schägger, H. and von Jagow, G.: Tricine-sodium dodecyl sulfate-polyacrylamide gel electrophoresis for the separation of proteins in the range from 1 to 100 kDa. *Anal. Biochem.* 166 (1987) 368–379.
- Schleifer, K.H. and Ludwig, W.: Phylogenetic relationship among bacteria. In: Fernholm, B., Bremer, K. and Jönvall, H. (Eds.), *The Hierarchy of Life*. Elsevier Science Publishers, Amsterdam, 1989, pp. 103–117.
- Senior, A.E.: The proton-translocating ATPase of *Escherichia coli*. *Annu. Rev. Biophys. Biophys. Chem.* 19 (1990) 7–41.
- Sheer, D.: Sample centrifugation onto membranes for sequencing. *Anal. Biochem.* 187 (1990) 76–83.
- Théberge, M., Lacaze, P., Shareck, F., Morosoli, R. and Kluepfel, D.: Purification and characterization of an endoglucanase from *Streptomyces lividans* 66 and DNA sequence of the gene. *Appl. Environ. Microbiol.* 58 (1992) 815–820.
- Tybulewicz, V.L.J., Falk, G. and Walker, J.E.: *Rhodospseudomonas blautia* *atp* operon: nucleotide sequence and transcription. *J. Mol. Biol.* 179 (1984) 185–214.
- Wada, K.N., Wada, Y., Ishibashi, F., Gojobori, T. and Ikemura, T.: Codon usage tabulated from the GenBank genetic sequence data. *Nucleic Acids Res.* 20 (1992) 2111–2118.
- Walker, J.E., Saraste, M. and Gay, N.J.: The *unc* operon. Nucleotide sequence, regulation and structure of ATP-synthase. *Biochim. Biophys. Acta* 768 (1984) 164–200.
- Woese, C.R.: Bacterial evolution. *Microbiol. Rev.* 51 (1987) 221–271.
- Wright, F. and Bibb, M.J.: Codon usage in the G + C-rich *Streptomyces* genome. *Gene* 113 (1992) 55–65.
- Xie, D.L., Lill, H., Hauska, G., Maeda, M., Futai, M. and Nelson, N.: The *atp2* operon of the green bacterium *Chlorobium limicola*. *Biochim. Biophys. Acta* 1172 (1993) 267–273.

## The Abundance of *atp* Gene Transcript and of the Membrane $F_1F_0$ -ATPase as a Function of the Growth pH of Alkaliphilic *Bacillus firmus* OF4

D. MACK IVEY,<sup>†</sup> MICHAEL G. STURR, TERRY A. KRULWICH, AND DAVID B. HICKS\*

Department of Biochemistry, Mount Sinai School of Medicine of City University  
of New York, New York, New York 10029

Received 15 April 1994/Accepted 6 June 1994

**Molecular biological and biochemical studies of the  $F_1F_0$ -ATP synthase of alkaliphilic *Bacillus firmus* OF4 show that the enzyme used at pH 7.5 and pH 10.5 is a unique product of the *atp* operon, expressed at the same levels and yielding an enzyme with the same subunit properties and c-subunit/holoenzyme stoichiometry.**

The bioenergetics of oxidative phosphorylation in extremely alkaliphilic *Bacillus* species is difficult to describe according to a strictly chemiosmotic model. The maintenance of a cytoplasmic pH below pH 8.5 during growth at pH values of 10.5 and higher reduces the net electrochemical proton gradient ( $\Delta p$ ) that is available to energize proton-coupled bioenergetic work. The surprising observation is that the small  $\Delta p$  at pH 10.5, for example, supports similar or higher phosphorylation potentials ( $\Delta G_p$  values) in alkaliphilic *Bacillus firmus* OF4 as observed with cells growing at pH 7.5, although the total  $\Delta p$  is almost three times higher in pH 7.5-grown cells (7, 19). The discordance is even greater when the external pH is elevated above 11 (19). Since neither the use of  $Na^+$  as a coupling ion nor the sequestration of oxidative phosphorylation in organelles accounts for these observations with extreme alkaliphiles, the possibility of a highly variable  $H^+$ /ATP coupling stoichiometry has been considered as a way of fitting the data to a chemiosmotic model (13). In a completely chemiosmotic coupling mode, the  $\Delta G_p/\Delta p$  ratio should be equal to the  $H^+$ /ATP ratio so that a higher  $H^+$ /ATP ratio would compensate for a lower  $\Delta p$ . In order to account for the bioenergetic parameters measured in a rigorously controlled chemostat study, the  $H^+$ /ATP ratio would have to vary from just above 3 to 13 over the organism's pH range for rapid growth (19). Such a variability in stoichiometry is difficult to envision if a single species of synthase operates over the entire range of growth pH. Prokaryotic ATP synthases, including those of the *Bacillus* species studied to date, are F-type ATPases encoded by operons in which the first cistron is generally a gene (*atpI*) of unknown function, which is followed by the three genes (*atpBEF*) encoding the subunits of the integral membrane  $F_0$  part of the complex and then the five genes (*atpHAGDC*) encoding the catalytic  $F_1$  part (3, 6, 10). Earlier PCR studies failed to indicate more than one *atp* operon or multiple *atpE* genes encoding the c-subunit, even though the degenerate primers used were able to amplify the alkaliphile genes, which have specific sequence motifs (10, 11), as well as conventional *atp* genes from unrelated *Bacillus* species (11). However, previous studies did not include a characterization of the actual enzyme found at different pH values or whether there was a

pH-dependent change in the level of the synthase, in its subunit structure, or in the c-subunit/holoenzyme ratio. In *Enterococcus faecalis*, an increase in the amount of the ATPase was found to be an adaptation to a low external pH (12), making it of interest to examine the possibility of up-regulation by the alkaliphile at high external pH values for growth. No evidence has been presented for a discrete change in c-subunit/holoenzyme stoichiometry in connection with physiological or environmental challenges. However, the presence of approximately 9 to 12 copies of this subunit per F-ATPase assembly and the importance of this subunit in the pathway for the coupling ion have led to proposals directly relating a synthetic function and the  $H^+$ /ATP stoichiometry to the c-subunit/holoenzyme stoichiometry of different classes of ATPases (4).

In this study, total RNA (14) from *B. firmus* OF4 cultures grown at pH 7.5 and pH 10.5 was analyzed by Northern (RNA) blots, using methods described previously (15). A probe consisting of the entire c-subunit gene and upstream region hybridized to the full-length (7-kb) transcript of the *atp* operon, giving signals of approximately equal intensity with RNA samples obtained from cells grown at the two pH values (Fig. 1). If anything, in the particular set shown, there was slightly more hybridizing RNA in cells grown at the lower pH. No other bands were detectable, suggesting that transcription from an internal promoter upstream of the *atpE* gene does not occur at either growth pH. Identical results were obtained with a probe containing an internal region of the a-subunit gene (data not shown). Primer extension analysis was used to determine the transcriptional start site of the *atp* operon. A single extended product of the same size was obtained with samples of RNA isolated from either pH 7.5- or pH 10.5-grown cells, and the intensities of bands were approximately the same at both pH values, consistent with the results of the Northern blot analyses (data not shown).

Membranes from *B. firmus* OF4 grown at either pH 7.5 or pH 10.5 were isolated, fractionated on denaturing gels, and probed by Western (immunoblot) analysis with antibody against the  $\beta$ -subunit of *Escherichia coli*, using procedures comparable to those described earlier (9). As shown in Fig. 2, there was no difference in the amount of this major  $F_1F_0$ -ATPase subunit in membranes from cells grown at the two pH values. The synthase represented 2.2% of membrane protein, being present at 44 pmol/mg of membrane protein in sets of preparations from cells grown at the two pH values. The  $F_1F_0$ -ATPase was purified from membranes of pH 7.5- and pH 10.5-grown cells; although not shown, the initial membranes

\* Corresponding author. Mailing address: Box 1020, Department of Biochemistry, Mount Sinai School of Medicine, 1 G. Levy Pl., New York, NY 10029. Phone: (212) 241-7466. Fax: (212) 996-7214.

<sup>†</sup> Present address: Department of Biological Sciences, University of Arkansas, Fayetteville, AR 72701.

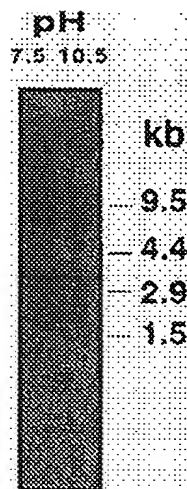


FIG. 1. Northern blot analysis of the *atp* operon of *B. firmus* OF4. Five-microgram samples of total RNA from cells of *B. firmus* OF4 grown at pH 7.5 and pH 10.5 were denatured, electrophoresed, transferred to nylon membranes, and probed with a radiolabeled fragment containing the *atpE* gene. The probe consisted of a 499-bp *NheI*-*SspI* fragment of pRC3. pRC3 was isolated from a *B. firmus* OF4 *EcoRI*-*ClaI* genomic DNA library constructed in pSPT19 (Boehringer Mannheim) and contains the genes encoding the subunits *i*, *a*, *c*, *b*, and  $\delta$  of the ATP synthase downstream of the T7 RNA polymerase promoter. Standard molecular biological procedures used in this and other manipulations were conducted as described previously (1, 16). Positions and sizes of RNA standards (Gibco/BRL) are shown on the right.

had comparable ATPase activities and the pattern observed upon gel electrophoresis of the two purified preparations was identical to that found earlier for enzyme from pH 10.5-grown cells (8). The relative amounts and sizes of the subunits were

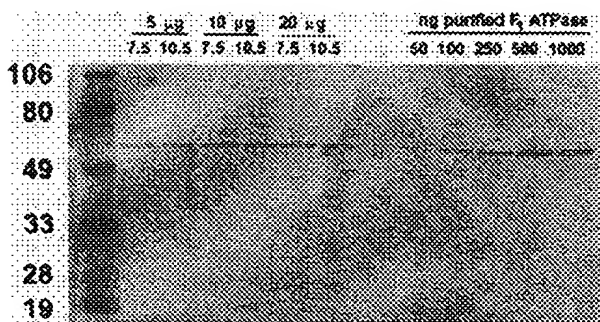


FIG. 2. Quantitative immunoblot of  $\beta$ -subunit ( $F_1F_0$ -ATPase) content in membrane vesicles of *B. firmus* OF4. Everted membrane vesicles were prepared essentially as described previously (8). Five-, ten-, and twenty-microgram samples of total membrane protein from *B. firmus* OF4 grown at pH 7.5 and pH 10.5 were subjected to SDS-PAGE, transferred to nitrocellulose, and probed with a mono-specific polyclonal antibody against the  $\beta$ -subunit of *E. coli*  $F_1$ . After densitometric analysis of the bands formed from the indicated concentrations of purified *B. firmus* OF4  $F_1$  (the right half of the blot), a standard curve, from which the concentration of enzyme in membrane samples was calculated, was prepared. Molecular weight standards (in thousands) are on the left.

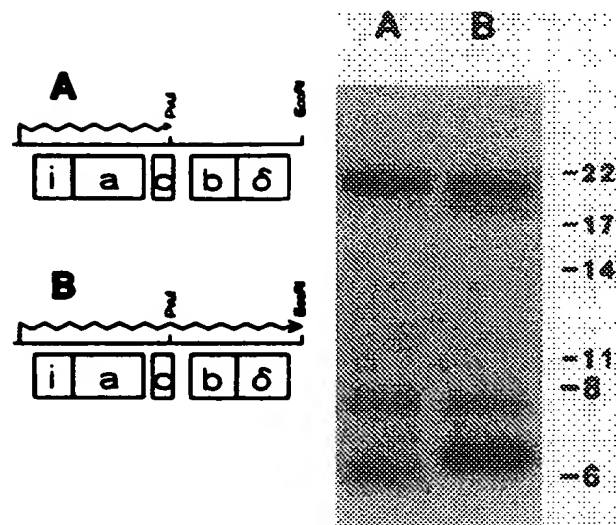


FIG. 3. In vitro transcription and translation of the genes of the *B. firmus* OF4 *atp* operon encoding the  $F_0$  subunits and  $\delta$ . *PvuI* (A) and *EcoRI* (B) digests of pRC3 were used for in vitro transcription and translation, which were carried out by using the protocols provided by Promega. Following transcription with T7 RNA polymerase, plasmid DNA was digested with RQ1 DNase and the products of transcription reactions were added directly to an *E. coli* S30 translation system (Promega) containing [ $^{35}$ S]methionine. Translation products were separated by SDS-PAGE and visualized by autoradiography. Molecular masses (in kilodaltons) of marker proteins are given on the right.

comparable for the two preparations and were reproducible among independent preparations.

The *c*-subunit was only barely discernible or in some cases not detectable in Coomassie-stained gels. To definitively identify the position of this subunit, as well as that of the *a*-subunit, in the gel system, in vitro transcription and translation of the 5' portion of the *atp* operon of *B. firmus* OF4 were carried out. A 2.9-kb *ClaI*-*EcoRI* fragment of *B. firmus* OF4 DNA containing the *atpIBEFH* genes was placed behind the T7 RNA polymerase promoter of pSPT19. *PvuI* digestion of this construct results in such a truncation of the *atpE* gene that the *c*-subunit lacks its final nine amino acid residues and the *b*- and  $\delta$ -subunits are not made. *EcoRI* digestion of the construct leaves all of the genes intact. As shown in Fig. 3, transcription and translation of these digests, followed by sodium dodecyl sulfate-polyacrylamide gel electrophoresis (SDS-PAGE) and autoradiography, allowed unambiguous identification of the products of the *atpIBEFH* genes, the subunits *i*, *a*, *c*, and  $\delta$ , respectively. The smallest product of the *PvuI*-digested construct (Fig. 3A) was smaller than that of the *EcoRI*-digested construct (Fig. 3B), confirming that this was the *c*-subunit in truncated and untruncated forms, respectively. Not detectable in this experiment was the product of the *atpF* gene, the *b*-subunit. This may reflect the use of GUG as the start codon for this gene; the S30 translation system employed in this experiment may not recognize and translate this region appropriately. Having established the electrophoretic mobility of the authentic *c*-subunit, quantitative comparison of the *c*-subunit content of membranes from pH 7.5- and pH 10.5-grown cells of *B. firmus* OF4 was carried out by analysis of gel fractionation of membranes that had been treated with radioactive *N,N'*-dicyclohexylcarbodiimide (DCCD). In Fig. 4, the pattern of membrane proteins from one of several independent sets of



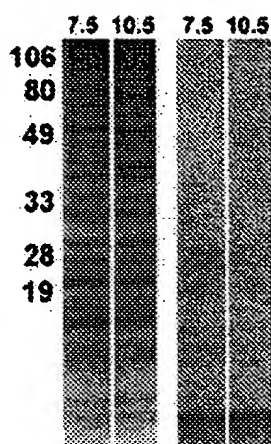


FIG. 4. [ $^{14}\text{C}$ ]DCCD labeling of everted membrane vesicles of *B. firmus* OF4 grown at pH 7.5 and pH 10.5. Everted membrane vesicles were incubated with [ $^{14}\text{C}$ ]DCCD overnight and washed twice as described by others (2, 5). Radiolabeled vesicles were extracted with chloroform-methanol (2:1) and ether precipitated. Ether precipitates were solubilized in SDS sample buffer, loaded on an SDS-PAGE gel (17), and stained for total protein by Coomassie brilliant G (first two lanes), and the gel was dried and exposed to a phosphorimager screen (last two lanes) to detect radiolabeled proteins. The molecular mass of the band corresponding to the c-subunit was approximately 7 kDa. Prestained molecular weight standards (in thousands) are indicated on the left.

such membranes is shown side by side with an autoradiogram of the same gel. Although there were some differences in overall membrane protein patterns, some of which are not reproducible in independent sets, the autoradiograms consistently indicated no pH-dependent change in the c-subunit content of the membranes. Given the observations that both an  $F_1$  subunit and the c-subunit were present in the same amounts in membranes from pH 7.5- and pH 10.5-grown cells, the ratio of c-subunit to holoenzyme must also be the same at the two pH values.

Previous studies indicated that the *B. firmus* OF4 c-subunit and that of another, unrelated, extremely alkaliphilic *Bacillus* sp. differed from homologs of several nonalkaliphilic bacteria in the regions of the c- and a-subunits (11, 13). The c-subunit was purified by chloroform-methanol extraction (5) of membranes from *B. firmus* OF4 grown at pH 7.5 and pH 10.5 to determine whether partial analysis by microsequencing would indicate that both or only one of the preparations contained the unusual sequence features that had been deduced from the gene sequence. Preparations of the c-subunit in chloroform-methanol (2:1) were applied to a polyvinylidene difluoride membrane and subjected to cyanogen bromide cleavage (18); N-terminal amino acid sequencing was performed on a gas-phase sequencer by using standard Edman degradative chemistry. Microsequencing from the N terminus proceeded much more efficiently after treatment of the samples with cyanogen bromide, indicating that a blocked N-terminal methionine is probably present in purified c-subunit samples. Subsequent to cyanogen bromide treatment, it was possible to identify 23 residues of sequence from the N terminus and an additional 5 residues that followed the single internal cleavage and appeared as a minor sequence set. Both of these sequences were identical in samples from cells grown at the two pH values; moreover, they conformed precisely to the sequence deduced

from the gene sequence. The determined sequence included many residues that are thus far specific to two alkaliphilic c-subunits. For example, in the first putative transmembrane helix, sequencing identified the following residues (presented as residue and position number): G-5, G-17, A-20, I-21, and A-22. In addition, the unusual second proline (at position 58), near the important carboxylate in the second putative transmembrane helix, was identified in both samples. Thus, the ATP synthase from *B. firmus* OF4 grown at pH 7.5 and pH 10.5 appears to be a unique enzyme that is neither present in unusual or pH-dependent amounts in the membrane nor variable in its ratio or in the species of c-subunit. If the alkaliphile uses the enormously variable  $\text{H}^+/\text{ATP}$  stoichiometry required to account for the phosphorylation potentials generated at different values of growth pH, then it does so with a single enzyme. The unlikelihood of this is compounded by the finding that the molar growth yield of *B. firmus* OF4 on limiting malate in continuous culture is actually higher at pH 10.5 than at pH 7.5, the reverse of what would be expected if more protons had to be translocated inward to produce the same amount of ATP (19). Moreover, there are qualitative observations in connection with alkaliphilic oxidative phosphorylation that would not be accounted for simply by a variable stoichiometry of coupling (13).

We are grateful to Nathan Nelson for the gift of antibody prepared against the  $\beta$ -subunit of the *E. coli*  $F_1F_0$ -ATPase.

This work was supported by research grant GM28454 from the National Institutes of Health. Protein sequence analysis was provided by The Rockefeller University Protein Sequencing Facility, which is supported in part by NIH shared instrumentation grants and by funds provided by the U.S. Army and Navy for purchase of equipment.

#### REFERENCES

1. Ausubel, F. M., R. Brent, R. E. Kingston, D. D. Moore, J. A. Smith, J. G. Seidman, and K. Struhl (ed.). 1987. Current protocols in molecular biology. John Wiley & Sons, Inc., New York.
2. Beechey, R. B., P. E. Linnett, and R. H. Fillingame. 1979. Isolation of carbodiimide-binding proteins from mitochondria and *Escherichia coli*. *Methods Enzymol.* 55:426-434.
3. Brusilow, W. S. A., M. A. Scarpetta, C. A. Hawthorne, and W. P. Clark. 1989. Organization and sequence of the genes encoding the proton-translocating ATPase of *Bacillus megaterium*. *J. Biol. Chem.* 264:1528-1533.
4. Cross, R. L., and L. Taiz. 1990. Gene duplication as a means for altering  $\text{H}^+/\text{ATP}$  ratios during the evolution of  $F_0F_1$  ATPases and synthases. *FEBS Lett.* 259:227-229.
5. Fillingame, R. H. 1976. Purification of the carbodiimide-reactive protein component of the ATP energy-transducing system of *Escherichia coli*. *J. Biol. Chem.* 251:6630-6637.
6. Futai, M., T. Noumi, and M. Maeda. 1988. Molecular genetics of  $F_1$ -ATPase from *Escherichia coli*. *J. Bioenerg. Biomembr.* 20:41-58.
7. Guffanti, A. A., O. Finkelthal, D. B. Hicks, L. Falk, A. Sidhu, A. Garro, and T. A. Krulwich. 1986. Isolation and characterization of new facultatively alkaliphilic strains of *Bacillus* species. *J. Bacteriol.* 167:766-773.
8. Hicks, D. B., and T. A. Krulwich. 1990. Purification and reconstitution of the  $F_1F_0$ -ATP synthase from alkaliphilic *Bacillus firmus* OF4: evidence that the enzyme translocates  $\text{H}^+$  but not  $\text{Na}^+$ . *J. Biol. Chem.* 265:20547-20554.
9. Hicks, D. B., R. J. Plass, and P. G. Quirk. 1991. Evidence for multiple terminal oxidases, including cytochrome *d*, in facultatively alkaliphilic *Bacillus firmus* OF4. *J. Bacteriol.* 173:5010-5016.
10. Ivey, D. M., and T. A. Krulwich. 1991. Structure and nucleotide sequence of the genes encoding the ATP synthase from alkaliphilic *Bacillus firmus* OF4. *Mol. Gen. Genet.* 229:292-300.
11. Ivey, D. M., and T. A. Krulwich. 1992. Two unrelated alkaliphilic *Bacillus* species possess identical deviations in sequence from those of conventional prokaryotes in regions of  $F_0$  genes implicated in proton translocation through the ATP synthase. *Res.*

- Microbiol. 143:467-470.
12. Kobayashi, H., T. Suzuki, and T. Unemoto. 1986. Streptococcal cytoplasmic pH is regulated by changes in amount and activity of a proton-translocating ATPase. *J. Biol. Chem.* 261:627-630.
  13. Krulwich, T. A., and A. A. Guffanti. 1992. Proton-coupled bioenergetic processes in extremely alkaliphilic bacteria. *J. Bioenerg. Biomembr.* 24:587-599.
  14. Ladin, B. F., E. M. Accuroso, J. R. Mielenz, and C. R. Wilson. 1992. A rapid procedure for isolating RNA from small-scale *Bacillus* cultures. *BioTechniques* 12:672-676.
  15. Quirk, P. G., D. B. Hicks, and T. A. Krulwich. 1993. Cloning of the *cta* operon from alkaliphilic *Bacillus firmus* OF4 and characterization of the pH-regulated cytochrome *caa*<sub>3</sub> oxidase it encodes. *J. Biol. Chem.* 268:678-685.
  16. Sambrook, J., E. F. Fritsch, and T. Maniatis. 1989. Molecular cloning: a laboratory manual, 2nd ed. Cold Spring Harbor Laboratory, Cold Spring Harbor, N.Y.
  17. Schagger, H., and G. von Jagow. 1987. Tricine-sodium dodecyl sulfate-polyacrylamide gel electrophoresis for the separation of proteins in the range from 1 to 100 kDa. *Anal. Biochem.* 166:368-379.
  18. Simpson, R. J., and E. C. Nice. 1984. *In situ* cyanogen bromide cleavage of N-terminally blocked proteins in a gas-phase sequencer. *Biochem. Int.* 8:787-791.
  19. Sturr, M. G., A. A. Guffanti, and T. A. Krulwich. 1994. Growth and bioenergetics of alkaliphilic *Bacillus firmus* OF4 in continuous culture at high pH. *J. Bacteriol.* 176:3111-3116.

# Complete genomic sequence of *Pasteurella multocida*, Pm70

Barbara J. May\*, Qing Zhang\*, Ling Ling Li\*, Michael L. Paustian\*, Thomas S. Whittam†, and Vivek Kapur\*\*

\*Department of Veterinary Pathobiology, University of Minnesota, St. Paul, MN 55108; and National Food Safety and Toxicology Center, Michigan State University, East Lansing, MI 48824

Communicated by Harley W. Moon, Iowa State University, Ames, IA, December 29, 2000 (received for review November 14, 2000)

We present here the complete genome sequence of a common avian clone of *Pasteurella multocida*, Pm70. The genome of Pm70 is a single circular chromosome 2,257,487 base pairs in length and contains 2,014 predicted coding regions, 6 ribosomal RNA operons, and 57 tRNAs. Genome-scale evolutionary analyses based on pairwise comparisons of 1,197 orthologous sequences between *P. multocida*, *Haemophilus influenzae*, and *Escherichia coli* suggest that *P. multocida* and *H. influenzae* diverged ~270 million years ago and the  $\gamma$  subdivision of the proteobacteria radiated about 680 million years ago. Two previously undescribed open reading frames, accounting for ~1% of the genome, encode large proteins with homology to the virulence-associated filamentous hemagglutinin of *Bordetella pertussis*. Consistent with the critical role of iron in the survival of many microbial pathogens, *in silico* and whole-genome microarray analyses identified more than 50 Pm70 genes with a potential role in iron acquisition and metabolism. Overall, the complete genomic sequence and preliminary functional analyses provide a foundation for future research into the mechanisms of pathogenesis and host specificity of this important multispecies pathogen.

It has been more than a century since Louis Pasteur conducted experiments with *Pasteurella multocida* (*Pm*), first demonstrating that laboratory attenuated bacteria could be used for the development of vaccines (1). Despite this seminal discovery, the molecular mechanisms for infection and virulence of *Pm* have remained largely undetermined, and this organism has continued to cause a wide range of diseases in animals and humans. It is the causative agent of fowl cholera in domesticated and wild birds, hemorrhagic septicemia in cattle, atrophic rhinitis in swine, and is the most common source of infection in humans because of dog and cat bites (2, 3).

Because the genomic DNA sequence encodes all of the heritable information responsible for microbial replication, virulence, host specificity, and ability to evade the immune system, a comprehensive knowledge of a pathogen's genome provides all of the necessary information required for cost-effective and targeted research into disease prevention and treatment. To better understand the molecular basis for *Pm*'s virulence, pathogenicity, and host specificity, we sequenced the genome of a common avian isolate recovered from a recent case of fowl cholera in chickens. The analysis identified a total of 2,014 open reading frames, including several encoding putative virulence factors. In particular, *Pm* has two genes with significant homology to the filamentous hemagglutinin gene in *Bordetella pertussis*, as well as more than 50 genes with a potential role in iron uptake and metabolism. The analysis also provides strong evidence that *Pm* and its close relative, *Haemophilus influenzae* (*Hi*), diverged ~270 million years ago (mya) and that the  $\gamma$  subdivision of the proteobacteria, a group that contains many of the pathogenic Gram-negative organisms, radiated ~680 mya.

## Materials and Methods

**Multilocus Enzyme Electrophoresis (MLEE).** MLEE was used to determine the population genetic structure of *Pm* from avian

sources. Methods for MLEE have been described in detail elsewhere (4). Briefly, 271 *Pm* isolates recovered from 14 wild and domesticated avian species from throughout the world were grown and sonicated for the collection of the enzyme-containing supernatant. Histochemical staining for 13 metabolic enzymes [mannose phosphate isomerase, glutamate dehydrogenase, shikimic acid, glucose-6-phosphate dehydrogenase, nucleoside phosphorylase, phosphoenol pyruvate, malate dehydrogenase, fumarase (two isoforms), phosphoglucose isomerase, adenylate kinase, 6-phosphogluconate dehydrogenase, and mannitol-1 phosphate dehydrogenase] was conducted to determine distinct mobility variants of each enzyme. Each isolate was characterized by its combination of alleles at 13 enzyme loci, and electrophoretic type designations were assigned by computer analysis as described (4).

**Sequencing and Assembly.** A shotgun strategy (5) was adopted to sequence the genome of Pm70 (capsular type A; serotype 3). To create a small (1.8- to 3.0-kb) insert library, genomic DNA was initially isolated by using a chloroform/cetyltrimethylammonium bromide-based method, as described (6). Next, the DNA was sheared by nebulization (<http://www.genome.ou.edu>) and cloned into pUC18 for isolation and sequencing. Approximately 25,000 clones were sequenced from both ends by using Dye-terminator chemistry on ABI 377 (Applied Biosystems) and Megabace (Molecular Dynamics) sequencing machines. A total of 53,265 sequences were used to generate the final assembly, giving about a 10-fold coverage of the genome. Sequence assembly and verification were accomplished by using PHRED-PHAP (P. Green, <http://genome.washington.edu>). To close the approximately 100 gaps at the end of the shotgun phase, several methods were used, including primer walking, homology-based comparisons of gap ends, and multiplex PCR. Primer walking was performed on genomic DNA or on a large-insert  $\lambda$  library (15–20 kb). The final assembly was compared to a previously published genetic map of *Pm* (7).

Potential coding sequences (CDSs) were predicted by using ORPHEUS, GLIMMER, and ARTEMIS, and the results were compared and verified manually in ARTEMIS (8, 9). Homology studies were completed with BLASTP analysis by using a database constructed by the Computational Biology Center at the University of Minnesota (<http://www.cbc.umn.edu>). Transfer RNAs were predicted by TRNASCAN-SE (10).

Abbreviations: mya, million years ago; CDS, coding sequence; *Pm*, *Pasteurella multocida*; *Hi*, *Haemophilus influenzae*; *Ec*, *Escherichia coli*; MLEE, multilocus enzyme electrophoresis; D, distance.

Data deposition: The sequence reported in this paper has been deposited in the GenBank database (accession no. AE004439).

\*To whom reprint requests should be addressed at: Department of Veterinary Pathobiology, University of Minnesota, 1971 Commonwealth Avenue, St. Paul, MN 55108. E-mail: vkapur@umn.edu.

The publication costs of this article were defrayed in part by page charge payment. This article must therefore be hereby marked "advertisement" in accordance with 18 U.S.C. §1734 solely to indicate this fact.

**Microarray Analysis and Isolation of Total RNA.** A flask of brain-heart infusion (BHI) media (Becton Dickinson) was inoculated with *Pm* Pm70 and grown to log phase ( $OD_{600} = 0.7$ ) at 37°C. The culture was then split into two 180-ml volumes, which were pelleted at 4°C, washed with 1× PBS, and pelleted again. One pellet was resuspended in 180 ml BHI and the other in 180 ml BHI containing the iron-chelator 2,2'-dipyridyl (200  $\mu$ M). The cultures were incubated on a rotary shaker at 37°C, and 30-ml volumes were removed at time points of 15, 30, 60, and 120 min after resuspension. The cultures were briefly centrifuged, and the pellets were flash frozen in dry ice and ethanol. Total RNA extractions were performed with RNeasy maxi columns (Qiagen, Chatsworth, CA), with DNase digestions done on-column by adding 82 Kunitz units of enzyme (Qiagen) and incubating at room temperature for 15 min. Ten micrograms of each RNA sample was used in two separate hybridization experiments on identical arrays.

**cDNA Synthesis and Labeling Conditions.** Construction of cDNA and DNA microarray hybridization approaches were performed as described at our web site (<http://www1.umn.edu/agac/microarray/protocols.html>). In brief, 30  $\mu$ g of random hexamers (Amersham) and 10  $\mu$ g of total RNA were initially preheated at 70°C for 10 min, quick-cooled on ice for 10 min, and incubated for 2 h at 42°C with the following reverse transcription-PCR reaction mix: first-strand buffer, 10 mM DTT; 380 units of Superscript II RT; and 500  $\mu$ M dATP, dCTP, dGTP; 100  $\mu$ M dTTP, all from Life Technologies-GIBCO/BRL; and 400  $\mu$ M amino-allyl-labeled dUTP (Sigma; 4:1 ratio). After hydrolysis with 10  $\mu$ l 1 M NaOH and 10  $\mu$ l 0.5 M EDTA for 15 min at 65°C, the samples were neutralized with the addition of 25  $\mu$ l of 1 M Tris-HCl (pH 7.4) and cleanup was performed with Microcon 30 filters (Millipore). The fluorescent monofunctional *N*-hydroxysuccinimide-ester dyes Cy3 and Cy5 were coupled with the cDNAs from control and iron-depleted bacteria, respectively for 1 hour, quenched with 4.5  $\mu$ l hydroxylamine (4 M; Sigma), and cleaned with the Qia-Quick PCR Purification Kit (Qiagen). The samples were then dried down and stored for no longer than 24 h at 4°C before use.

**DNA Microarray Hybridization and Analysis.** Preparation of DNA microarrays (including primer sequences and PCR protocols), and hybridization techniques are also described at our web site mentioned above. Briefly, a library of targets representing all 2,014 open reading frames (ORFs) from *Pm* Pm70 was constructed with primers designed to amplify fragments  $\leq 500$  base pairs from each ORF from genomic DNA template. Two rounds of PCR were performed to minimize genomic DNA contamination, and the final 100- $\mu$ l reactions were checked for quality on agarose gels and purified with MultiScreen PCR plates (Millipore). Arrays of 1,936 ORF segments representing the successful amplifications and >95% of the *Pm* CDSs were printed by using a Total Array System robot (BioRobotics, Cambridge, UK). Samples containing no DNA were also spotted as a negative controls.

Hybridization was conducted by resuspending our cDNA-labeled probes in dH<sub>2</sub>O, 3× SSC, along with SDS and salmon sperm to be used as blockers. The probe was then added to the array and incubated at 63°C for 6 hours. Images of the hybridized arrays were obtained with a ScanArray 5000 microarray scanner, and fluorescent intensities were analyzed by using the program QuantArray (GSI Lumonics, Watertown, MA). Hybridization experiments were repeated two times to ensure reproducibility of the results. To obtain a Cy3/Cy5 intensity ratio for each spot, the intensities for each spot were first standardized by subtracting local background and normalizing individual spot intensities against the total spot intensity for both channels. Spots with a 2-fold or greater intensity ratio were further analyzed for their

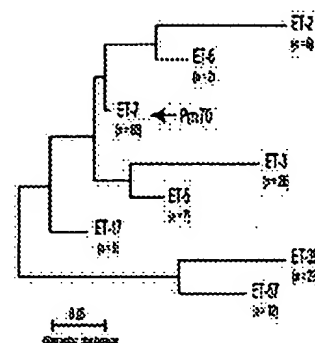


Fig. 1. Genetic relationships among the eight common clones of *Pm* recovered from avian sources. A total of 271 independent isolates of *Pm* recovered from 14 avian species were characterized for differences in electrophoretic mobility at 13 loci by MLEE. Of the 82 electrophoretic types that were identified, more than two-thirds of the isolates were represented by the eight clones shown in the dendrogram. Furthermore, a total of 31% of the isolates were represented by a single group, electrophoretic type 07 (arrow) that included the isolate Pm70.

differences in gene expression. Hierarchical clustering and analysis were performed by using the publicly available programs CLUSTER and TREEVIEW (<http://www.microarrays.org/software>; ref. 11).

## Results and Discussion

***Pm* Population Genetic Structure.** To identify the bacterial clones responsible for most infections in avian hosts, we first determined the genetic diversity and population structure of *Pm* strains collected from a wide range of wild and domesticated birds. A total of 271 independent isolates recovered from 14 avian species were characterized for protein polymorphisms at 13 enzyme loci by multilocus enzyme electrophoresis (4). The analysis revealed 72 electrophoretic types (ETs), with an average genetic diversity (*H*) of  $0.474 \pm 0.049$ , indicating that considerable genetic variation exists within *Pm*. However, more than two-thirds (69%) of all isolates were accounted for by only eight clones (ETs), and 31% of the isolates were of a single clone designated ET-7 (Fig. 1). Strain Pm70, isolated in 1995 from a case of fowl cholera in chickens, is a member of this *Pm* clone and was thus targeted for genome sequence analysis.

**Characteristics of the Pm70 Genome.** We used the random shotgun approach to generate more than 53,000 sequence fragments from strain Pm70, which were then assembled into a single circular sequence of 2,257,487 base pairs (Fig. 2). The putative origin of replication of the chromosome was identified on the basis of the presence of *dnaA* boxes, characteristic oligomer skew, and G-C skew immediately before the first putative coding sequence, *gidA* (12, 13). The entire sequence specifies 2,014 potential CDSs with an average size of 998 base pairs, which in sum account for 89% of the entire chromosome (Fig. 7, which is published as supplemental data on the PNAS web site, [www.pnas.org](http://www.pnas.org)). The remaining 11% of the sequence consists of 6 complete rRNA operons (16S-23S-5S), 57 rRNA genes representing all 20 amino acids, and a relatively small number of noncoding elements (Table 1). Sequence comparisons identified 200 CDSs (10%) unique to *Pm* and 1,197 CDSs with orthologs in both the *Hi* and *Escherichia coli* (*Ec*) genomes. These results are consistent with an overall close relationship and support the classification of these bacteria in the  $\gamma$  subdivision of the proteobacteria. Because 26% of the CDSs are most similar to hypothetical proteins of unknown functions, as is seen in other

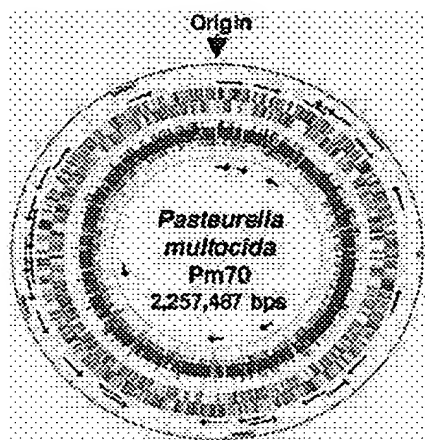


**Fig. 2.** Circular representation of the genome of *Pm*, Pm70. The *Pm* genome and its coding regions with homologies, the tRNA and rRNA operons, and the overall G-C content are presented. The outer circle represents the scale in base pairs with the origin noted. The outer arrows represent the 57 tRNAs and the inner arrows represent the 6 complete rRNA operons (165–235–55). The 2,014 potential coding sequences are represented by colors depicting homology to both *Ec* and *Hi* (green), *Ec* alone (purple), *Hi* alone (light blue), or to organisms other than *Hi* or *Ec* or unique to *Pm* (red). The G-C % of each coding sequence is represented in the interior circle by different shades of pink in increments of 5%: the lightest pink represents a G-C % of 25–30% whereas the darkest pink represents 45–50%. The figure was generated by using GENESCOPE software (DNASTar, Madison, WI).

completed microbial genomes, a substantial portion of *Pm*'s biochemistry and cell biology remains to be discovered (14).

The *Pm* genome encodes complete sets of enzymes for the oxidative pentose phosphate and Entner–Doudoroff pathways, glycolysis, gluconeogenesis, and the trichloroacetic acid cycle [trichloroacetic acid (TCA) cycle; see Table 3, which is published as supplemental data on the PNAS web site]. These pathways are also present in both *Ec* (15) and *Hi* (5), except for the absence of a complete TCA cycle in *Hi*. The *Pm* genome, like *Hi* and *Ec*, encodes a complete set of instructions for the synthesis of all 20 amino acids and purine and pyrimidine nucleotides. In contrast to *Ec*, catabolic pathways for several amino acids, including those for asparagine, histidine, leucine, lysine, and phenylalanine, are missing in both *Pm* and *Hi*. Pathways involved in sulfur uptake and metabolism as well as nitrogen and folic acid metabolism are present in the bacterium. Strains of *Pm* are known to use a number of carbohydrates, including sucrose, fructose, galactose, mannose, sorbitol, and ethanol, which is consistent with the

**Table 1.** Summary of the complete genome of *P. multocida*

	No. of CDS	%
Number of CDS	2,014	
Homologues to peptides	1,814	90
Homologues to hypothetical proteins	531	26
CDS unique to <i>Pm</i>	200	10
Homologues to <i>Hi</i>	1,421	71
Homologues to <i>Ec</i>	1,392	69
Orthologues to <i>Ec</i> but not <i>Hi</i>	223	11
Orthologues to <i>Hi</i> but not <i>Ec</i>	195	10
CDS genome coverage		89
Overall GC%		41
Average molecular weight of proteins	37,081 K <sub>d</sub>	
Average gene size	997 bp	
tRNAs	57	
rRNA operons	6	

**Table 2.** Evolutionary distances between *P. multocida*, *H. influenzae*, and *E. coli*

Comparison	D* values for CDSs	
	Conserved (n = 774)	Divergent (n = 243)
Pm–Hi	24.0 ± 11.9	68.4 ± 13.8
Pm–Ec	59.1 ± 31.0	162.4 ± 79.9
Hi–Ec	61.3 ± 31.8	170.7 ± 80.6

\*D, evolutionary distance for each pairwise comparison.

presence of corresponding genes identified in our analysis (16). On the basis of the presence of identifiable orthologs, several additional carbohydrates, such as maltotriose, fucose, ribose, and sorbose, are also likely to be used by *Pm*.

**Evolutionary Relationships of *Pm*.** Members of the *Pasteurella*, *Haemophilus*, and *Escherichia* genera belong to the  $\gamma$  subdivision of the proteobacteria and include many of the most pathogenic Gram-negative bacteria. The availability of the complete genome sequence from three members of this subdivision provided us with the ability to examine the comparative evolution of these organisms at a genomic scale. To determine evolutionary relationships between *Pm*, *Hi*, and *Ec*, the 1,197 CDSs represented in all three organisms were aligned by CLUSTALW, and the percentage of identical amino acids in aligned sequences was determined. We next calculated evolutionary distance (D) per Grishin (17) and tabulated the distribution of D for each pairwise comparison of *Pm*, *Hi*, and *Ec* for the 1,197 orthologs. The mean ( $\pm$  standard deviation) of the pairwise distances were: *Pm*–*Hi* 56.6  $\pm$  83.6; *Pm*–*Ec* 104.0  $\pm$  89.1; and *Hi*–*Ec* 114.5  $\pm$  103.6. All three distributions were J-shaped with long tails, and separation of the orthologs outside the 1.5 interquartile range resulted in the identification of 243 divergent and 774 conserved CDSs (Table 2). Scatter plots of pairwise D values show near linear relationships (Fig. 3), indicating remarkable consistency in the rate of divergence of orthologous genes among these genera. Feng and Doolittle (18) calibrated Grishin's D against the fossil

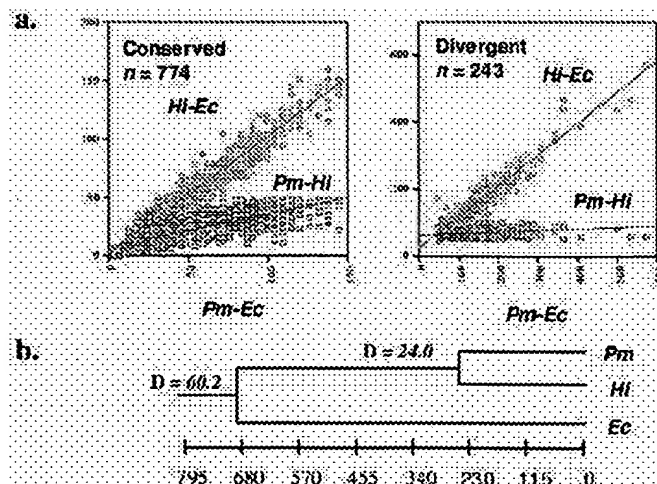


**Fig. 3.** Genome-scale evolutionary comparisons between *Pm*, *Hi*, and *Ec*. Scatter plots were created from pairwise evolutionary distance (D) values, as described. The x axis represents the pairwise D value for *Pm* and *Ec* and the y axis represents the pairwise D value for either *Hi* and *Ec* or *Pm* and *Hi* as indicated. (a) Scatterplot for the 774 conserved sequences and 243 divergent sequences. (b) Dendrogram showing the evolutionary distance in millions of years between *Pm*, *Hi*, and *Ec*. D values for each of the branch points are also presented.

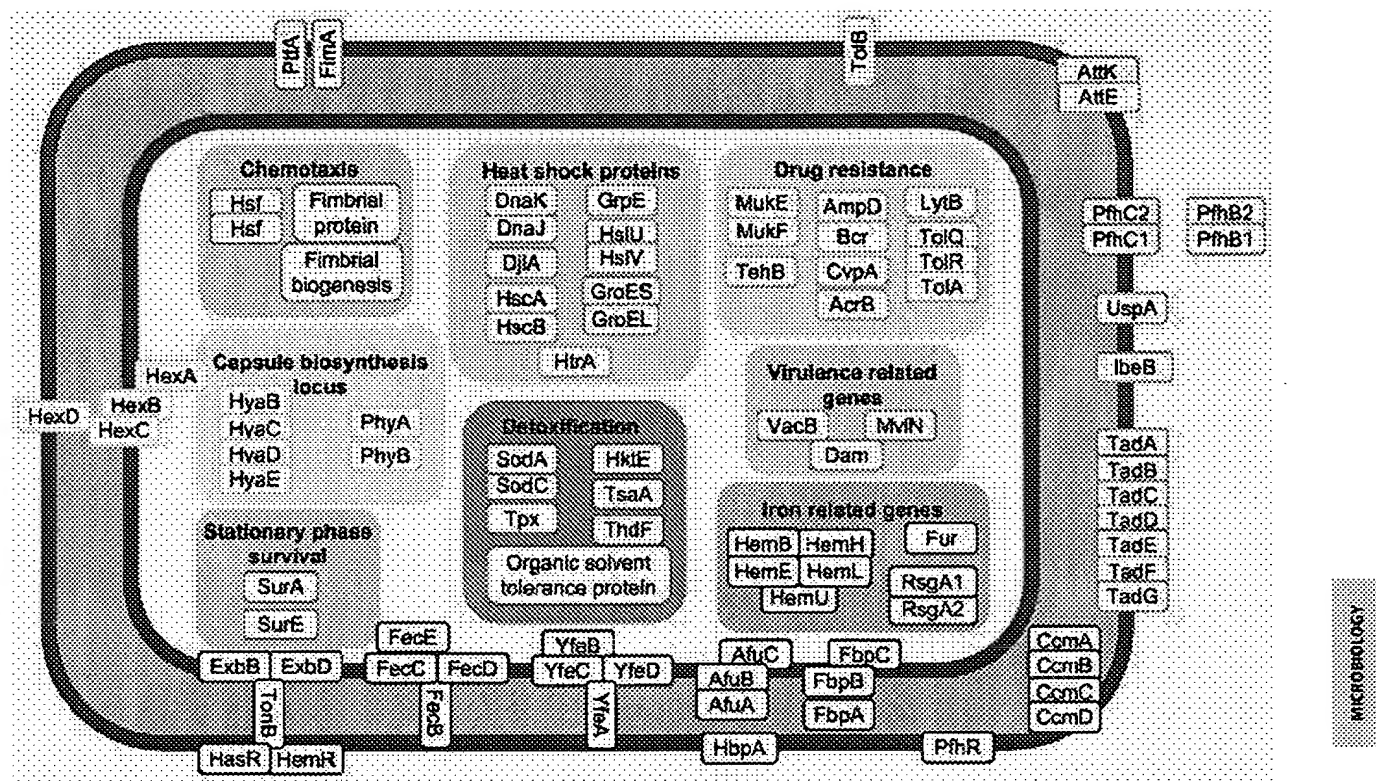


Fig. 4. A comprehensive view of the biochemical processes involved in *Pm* pathogenicity. Orthologs previously identified as virulence factors in other organisms are represented. Principal functional categories are shown in bold. Potential coding sequences related to these functions are arranged within each correspondingly colored category.

record for groups of vertebrates by plotting D versus time of divergence and obtained a slope of 0.088 that can be used to extrapolate evolutionary distance to time in millions of years. Applying this calibration to the 774 conserved genes, we estimate that *Pm* diverged from *Hi*  $\approx$  270 mya (range, 138–407 mya) and separated from a common ancestor with *Ec*  $\approx$  680 mya (range, 319–1,024 mya) (Fig. 3b). Together, these results place the root

of the  $\gamma$  division of the proteobacteria at  $\approx$ 680 mya, and confirm the relatively close relationship between the *Pasteurella* and *Haemophilus* genera (Fig. 3b).

**Virulence Factors of *Pm*.** The molecular basis for *Pm*'s pathogenicity and host specificity is not well understood. Our genomic analysis identified a total of 104 putative virulence-associated

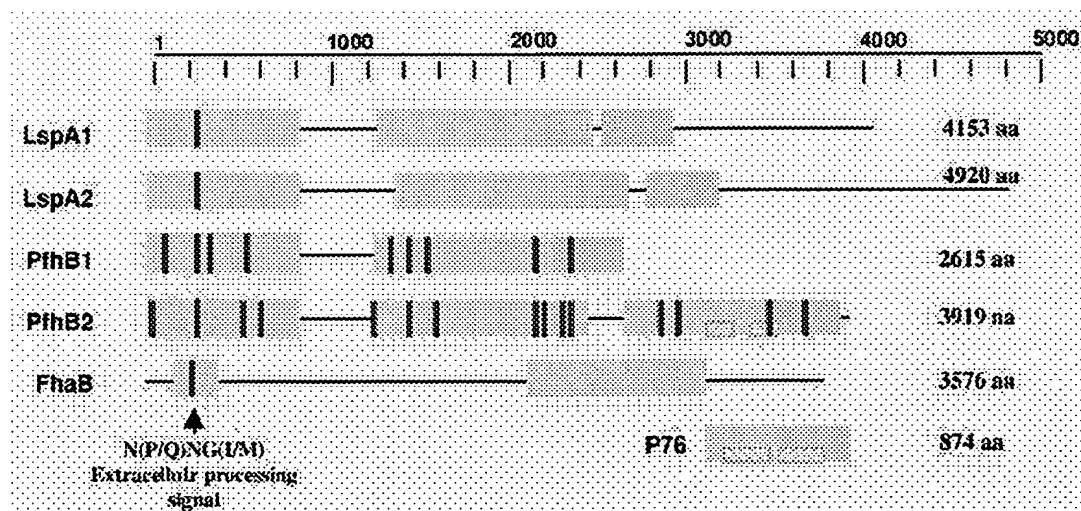


Fig. 5. Analysis of PfhB domains. Homology comparisons among PfhB1, PfhB2, from *Pm*, LspA1, LspA2, from *H. ducreyi*, FhaB from *B. pertussis*, and P76 from *Haemophilus somnus* are presented. Homologous domains are represented with the same colored boxes and the direct repeats in p76 and PfhA2 are patterned in blue. The N(P/Q)NG(I/M) extracellular processing motif is indicated and the integrin-binding protein motifs are shown as dark purple lines.



genes in *Pm*, which account for  $\approx 7\%$  of the coding density of the genome (Fig. 4). In particular, we discovered a 24-kb region with two new potential *Pm* virulence factors and their accessory genes. The two potential virulence CDSs, here termed *Pasteurella* filamentous hemagglutinin (*pfhB1*) and *pfhB2*, are 7,845 and 11,757 base pairs, respectively, and are virtually identical in sequence with the exception of a large deletion in the central region of *pfhB1* (Fig. 5). Both *PfhB1* and *PfhB2* contain domains with strong homology to the filamentous hemagglutinin (FhaB) of *B. pertussis* (19–21). FhaB governs the adherence of *B. pertussis* to host cells and is a major component of the acellular vaccines used to protect humans against whooping cough (22). Orthologs of this large protein have also been recently described in several other pathogens including *Haemophilus ducreyi* (LspA1 and LspA2), *Neisseria meningitidis*, *Serratia marcescens*, *Proteus mirabilis*, and *Pseudomonas aeruginosa* (23–27).

Several lines of evidence suggest that *PfhB1* and *PfhB2* play a role in the virulence of *Pm*. First, the amino-terminal ends of *PfhB1* and *PfhB2* have a conserved motif N(P/Q)NG(I/M) that is present in all members of this large protein family and is involved in posttranslational processing and extracellular signaling (Fig. 5; ref. 28). Second, the central region contains several integrin-binding motifs that also are characteristic of this family (29). The presence of these conserved motifs suggests that, similar to *FhaB* of *B. pertussis*, both *PfhB1* and *PfhB2* are involved in adherence of bacterial cells to host cell surfaces. Third, the carboxy terminus contains regions with significant homology (66% amino acid identity) to the serum-resistance protein p76 of *Haemophilus somnus* (30). Expression of p76 confers resistance to opsonization in *H. somnus*, thereby enhancing pathogen survival in the host. Two approximately 400-aa direct repeats found in p76 are also present in *PfhB2* (30). Interestingly, the carboxyl-terminal region of p76 shows homology to LspA1 and LspA2 of *H. ducreyi*, the causative agent of chancroid ulcers in humans (23). Taken together, these studies provide compelling evidence that the *PfhB* protein plays a major role in the virulence of *Pm* and that its inactivation may enable the development of well-defined live attenuated vaccines.

**Iron Uptake and Acquisition in *Pm*.** Because of its central role in electron transport, iron is an essential nutrient for most organisms. The low solubility of iron at neutral pH leads to a relative paucity of free iron within hosts and creates a major barrier to microbial growth *in vivo*. To compete for this limiting nutrient, microbes have evolved a variety of novel strategies for acquiring iron (31). More than 2.5% (53 CDSs) of the *Pm* genome is devoted to genes encoding proteins homologous to known proteins involved in iron uptake or acquisition (Fig. 6). Furthermore, several of these genes have undergone recent duplications (68–72% similar) in the *Pm* genome. For instance, *Pm* has a cluster of genes closely related to those encoding an iron transport system of *Actinobacillus pleuropneumoniae* (*afuA*, *afuB*, and *afuC*), but there are three copies of the *afuA* ortholog (Pm0953, 0954, and 0955; ref. 32) in the Pm70 genome. A second region (base pairs 520,397–528,389) of the *Pm* genome is rich in genes with homology to those linked to iron transport in the 102-kb pigmentation locus in *Yersinia pestis* (33). The 102-kb region of *Y. pestis* contains, for example, the *ybt* locus involved in siderophore uptake and the *hms* locus involved in hemin storage. Although the orthologs for *ybt* and *hms* are not found in strain Pm70, 8 other CDSs located between these genes in *Y. pestis* are present in the Pm70 genome. The predicted proteins of these eight CDSs contain transmembrane domains, and several are hypothesized to be members of the abc transporter family. One putative membrane CDS (Pm0446) contains a cytochrome *c* motif that provides a heme-binding site and another transmembrane CDS (Pm0453) contains a high-affinity iron permease motif. Because this region is not present in the *Ec*

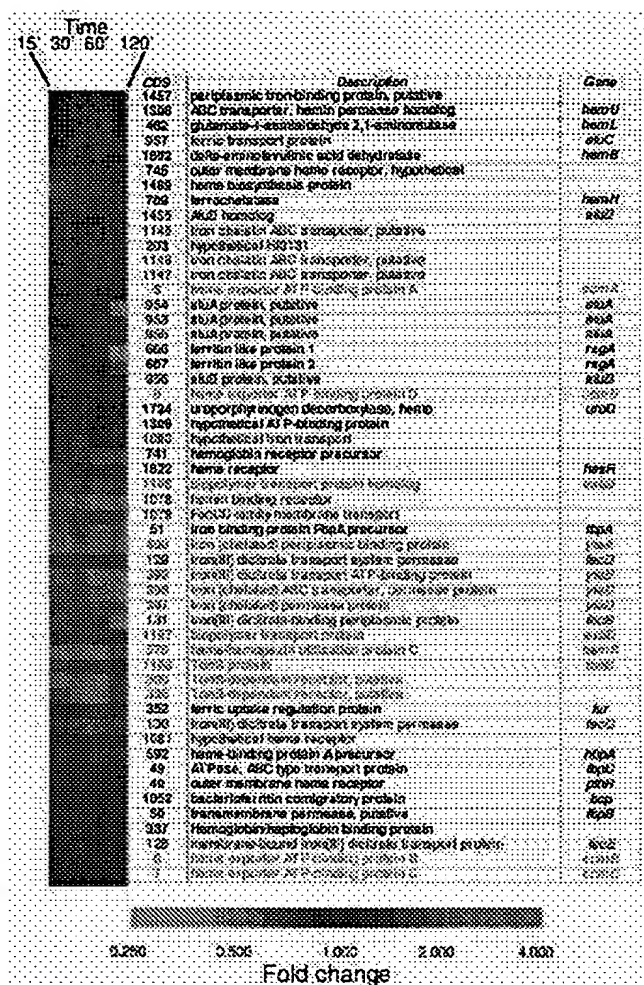


Fig. 6. Hierarchical clustering of 53 *Pm* CDSs identified based on sequence comparisons to be involved in iron metabolism or to require iron as a co-factor. Fluorescent ratios representing relative expression profiles of *Pm* CDSs at 15, 30, 60, and 120 min time points are shown in (Left). The red and green colors represent fold increase and decrease, respectively, in gene expression in response to low iron conditions (addition of the iron chelator, 2,2'-dipyridyl). Their corresponding open reading frames numbers and CDS descriptions are also shown. CDSs depicted in the same color are in close proximity to each other on the genome and may be a part of potential operons.

or *Hi* genomes, it has either been deleted in those genomes or acquired by *Pm* through horizontal transfer.

To elucidate other genetic systems involved in iron acquisition and metabolism, we used microarray technology to study patterns of gene expression in the *Pm* genome under iron depleted conditions. The results show that 174 of the CDSs showed a 2-fold or greater change in expression for at least one of four time points (15', 30', 60', and 120') after growth under iron-limiting conditions. Hierarchical clustering of these 174 CDSs on the basis of their expression patterns revealed that 53% decreased in expression in response to low-iron conditions, and 47% increased in expression relative to the control. Among these, reduced expression was seen for orthologs to the *frd* and *fdx* operons, both of which are involved in anaerobic energy metabolism and require iron to function (34, 35). In addition, 11 homologues involved in glycolysis or electron transport were decreased in expression under low-iron conditions. Of the CDSs that increased in expression, 16 were homologous to iron-specific cation transport proteins. Other orthologs in this group include



the surface polysaccharide biosynthesis enzymes GmhA and Skp. Thirty-one percent of the 174 CDSs whose expression was significantly altered by low-iron levels are previously undescribed or have close homology only to hypothetical proteins. The remaining 1,760 CDSs were either poorly measured or did not change significantly over the course of the experiment. Additional data, including the original hybridization images, a list of the genes represented on the array, as well as all primary datasets can be found at our web site (<http://www.cbc.umn.edu/ResearchProjects/AGAC/Pm/Pmarraydata.html>).

To specifically examine the behavior of known iron-related genes, we performed a second hierarchical cluster analysis focused on 53 CDSs with homology to iron-binding or uptake genes (Fig. 6). Several iron-related families of genes tended to cluster close to each other in terms of their expression profiles. Especially notable was the overall increase in expression of the *fec*, *yfe*, and *tonB* gene families. *Yfe* was previously identified in *Yersinia pestis* as an abc iron transport system (36), whereas *fec* and *tonB* were characterized as periplasmic-binding-protein-dependent iron transporters (37). Similarly, Pm0451 and 0452, which are orthologs to genes in the 102-kb pigmentation locus, were also up-regulated. In contrast, genes homologous to the *afu* family of periplasmic-binding-protein-dependent iron transport genes showed an overall decrease in expression (34). Taken together, these findings indicate that whole-genome expression studies made possible with the knowledge of the complete genome sequence provide a rich source of new hypotheses and

insights for future research into the molecular basis of pathogenesis of *Pm*.

**Concluding Statement.** In summary, the entire genome sequence and preliminary functional analyses have identified a variety of virulence factors for possible investigation in this major animal and human pathogen. Furthermore, the availability of the genome sequence provides a foundation for future research into the epidemiology, evolution, and mechanisms of pathogenesis and host specificity of *Pm*.

We gratefully acknowledge Caroline Hoellrich and Alongkorn Amonsri for assistance with MLEE analysis. We appreciate the support of Judy Laber, Megan Lillihei, and Daniel Strom at the Advanced Genetics Analysis Center at the University of Minnesota, as well as Jun Yu at the University of Washington Genome Center (Seattle, WA) and his colleagues at the Beijing Human Genome Center (Beijing, China) for assistance during the sequencing phase of our project. We also gratefully acknowledge the support of Bruce Roe (Department of Chemistry and Biochemistry, University of Oklahoma, Norman, OK) and Ernest Retzel (Computational Biology Centers, University of Minnesota) for providing technical facilities and protocols during various phases of the project. This project was made possible by the continued encouragement of our colleagues, Larry Schook, Michael Murtaugh, Mitchell Abrahamsen, and Sagarika Kanjilal, to whom we are forever grateful. Funding for this project was provided by research grants from the Minnesota Turkey Growers Association, the Minnesota Agricultural Experimentation Center, the University of Minnesota Academic Health Center, and the U. S. Department of Agriculture's National Research Initiative (to V.K.) and by the National Institutes of Health (to T.S.W.).

- Pasteur, L. (1998) in *Milestones in Microbiology: 1156 to 1940*, trans. and ed. Brock, T. D. (Am. Soc. Microbiol., Washington, DC), pp. 126–131.
- Rhoades, K. R. & Rimler, R. B. (1989) in *Pasteurella and Pasteurellosis*, eds. Adlam, C. & Rutter, J. M. (Academic, San Diego, CA), pp. 95–114.
- Rhoades, K. R. & Rimler, R. B. (1991) in *Diseases of Poultry*, eds. Calnek, B. W., Barnes, H. J., Beard, C. W., Reid, W. M. & Yoder, H. W. J. (Iowa State Univ. Press, Ames, IA) pp. 145–162.
- Selander, R. K., Caugant, D. A., Ochman, H., Musser, J. M., Gilmour, M. N. & Whittam, T. S. (1986) *Appl. Environ. Microbiol.* **51**, 873–884.
- Fleischmann, R. D., Adams, M. D., White, O., Clayton, R. A., Kirkness, E. F., Kerlavage, A. R., Bult, C. J., Tomb, J.-F., Dougherty, B. A., Merrick, J. M., et al. (1995) *Science* **269**, 496–512.
- Ausubel, F. M., Brent, R., Kingston, R. E., Moore, D. D., Seidman, J. G., Smith, J. A. & Struhl, K. (1999) in *Current Protocols in Molecular Biology* (Greene and Wiley-Interscience, New York) pp. 2.4.3–2.4.4.
- Hunt, M. L., Ruffolo, C. G. & Rajakumar, K. (1998) *J. Bacteriol.* **180**, 6054–6058.
- Frishman, D., Mironov, A., Mewes, H. W. & Gelfand, M. (1998) *Nucleic Acids Res.* **26**, 2941–2947.
- Salzberg, S. L., Delcher, A. L., Kasif, S. & White, O. (1998) *Nucleic Acids Res.* **26**, 544–548.
- Lowe, T. M. & Eddy, S. R. (1997) *Nucleic Acids Res.* **25**, 955–964.
- Eisen, M. B. & Brown, P. O. (1999) *Methods Enzymol.* **303**, 179–205.
- Salzberg, S. L., Salzberg, A. J., Kerlavage, A. R. & Tomb, J. F. (1998) *Gene* **217**, 56–67.
- Lobry, J. R. (1996) *Mol. Biol. Evol.* **13**, 660–665.
- Fraser, C. M., Eisen, J., Fleischmann, R. D., Ketchum, K. A. & Peterson, S. (2000) *Emerg. Infect. Dis.* **6**, 505–512.
- Blattner, F. R., Plunkett, G., Bloch, C. A., Perna, N. T., Burland, V., Riley, M., Collado-Vides, J., Glasner, J. D., Rode, C. K., Mayhew, G. F., et al. (1997) *Science* **277**, 1453–1474.
- Rimler, R. B. & Rhoades, K. R. (1989) in *Pasteurella and pasteurellosis*, eds. Adlam, C. & Rutter, J. M. (Academic, San Diego, CA) pp. 37–73.
- Grishin, N. V. (1995) *J. Mol. Evol.* **41**, 675–679.
- Feng, D. & Doolittle, R. F. (1997) *J. Mol. Evol.* **44**, 361–370.
- Relman, D. A., Domenighini, M., Tuomanen, E., Rappuoli, R. & Falkow, S. (1989) *Proc. Natl. Acad. Sci. USA* **86**, 2637–2641.
- Locht, C., Bertin, P., Menozzi, F. D. & Renauld, G. (1993) *Mol. Microbiol.* **9**, 653–660.
- Domenighini, M., Relman, D., Capiou, C., Falkow, S., Prugnola, A., Scarlato, V. & Rappuoli, R. M. (1990) *Mol. Microbiol.* **15**, 787–800.
- Sato, H. & Sato, Y. (1999) *Biologicals* **27**, 61–69.
- Ward, C. K., Lumbley, S. R., Latimer, J. L., Cope, L. D. & Hansen, E. J. (1998) *J. Bacteriol.* **180**, 6013–6022.
- Parkhill, J., Achtman, M., James, K. D., Bentley, S. D., Churcher, C., Klee, S. R., Morelli, G., Basham, D., Brown, D., Chillingworth, T., et al. (2000) *Nature (London)* **404**, 502–506.
- Poole, K., Schiebel, E. & Braun, V. (1988) *J. Bacteriol.* **170**, 3177–3188.
- Uphoff, T. S. & Welch, R. A. (1990) *J. Bacteriol.* **172**, 1206–1216.
- Stover, C. K., Pham, X. Q., Erwin, A. L., Mizoguchi, S. D., Warrenner, P., Hickey, M. J., Brinkman, F. S., Hufnagle, W. O., Kowalik, D. J., Lagrou, M., et al. (2000) *Nature (London)* **406**, 959–964.
- Braun, V., Hobbie, S. & Ondracek, R. (1992) *FEMS Microbiol. Lett.* **79**, 299–305.
- Ruoslahti, E. (1996) *Annu. Rev. Cell. Dev. Biol.* **12**, 697–715.
- Cole, S. P., Guiney, D. G. & Corbeil, L. B. (1993) *J. Gen. Microbiol.* **139**, 2135–2143.
- Wandersman, C. & Stojiljkovic, I. (2000) *Curr. Opin. Microbiol.* **3**, 215–220.
- Chen, N., Frey, J., Chang, C. F. & Chang, Y. F. (1996) *FEMS Microbiol. Lett.* **143**, 1–6.
- Buchrieser, C., Rusniok, C., Frangeul, L., Couve, E., Billault, A., Kunst, F., Carniel, E. & Glaser, P. (1999) *Infect. Immun.* **67**, 4851–4861.
- Imlay, J. A. (1995) *J. Biol. Chem.* **270**, 19767–19777.
- Ta, D. T. & Vickery, L. E. (1992) *J. Biol. Chem.* **267**, 11120–11125.
- Bearden, S. W. & Perry, R. D. (1999) *Mol. Microbiol.* **32**, 403–414.
- Moeck, G. S. & Coulton, J. W. (1998) *Mol. Microbiol.* **28**, 675–681.

[ExPASy Home page](#)[Site Map](#)[Search ExPASy](#)[Contact us](#)[ENZYME](#)[Swiss-Prot](#)Search for 

## NiceZyme View of ENZYME: EC 3.6.3.14

### Official Name

H(+)-transporting two-sector ATPase.

### Alternative Name(s)

ATP synthase.

F(1)-ATPase.

F(o)F(1)-ATPase.

F(0)F(1)-ATPase.

H(+)-transporting ATP synthase.

H(+)-transporting ATPase.

Mitochondrial ATPase.

Chloroplast ATPase.

### Reaction catalysed

ATP + H(2)O + H(+)(In) <=> ADP + phosphate + H(+)(Out)

### Comment(s)

- A multisubunit non-phosphorylated ATPase that is involved in the transport of ions.
- Large enzymes of mitochondria, chloroplasts and bacteria with a membrane sector (F(o)) and a cytoplasmic-compartment sector (F(1), V(1), A(1)).
- The F-type enzymes of the inner mitochondrial and thylakoid membranes act as ATP synthases.
- All of the enzymes included here operate in a rotational mode, where the extramembral sector (F(1), V(1), A(1) subunits) is connected via the delta-subunit to the membrane sector subunits.
- Within this complex, the gamma- and epsilon-subunits, as well as the 9-12 c subunits rotate at different degree angles and perform parts of ATP synthesis.
- This movement is driven by the H(+) electrochemical potential gradient.
- The V-type (in vacuoles and clathrin-coated vesicles) and A-type (archaeal) enzymes have a different mechanism. Under physiological conditions, they pump H(+) rather than synthesize ATP.
- Formerly EC 3.6.1.34.

### Human Genetic Disease(s)

Neuropathy, ataxia, and retinitis pigmentosa [MIM:551500](#)

Distal renal tubular acidosis with deafness [MIM:267300](#)

### Cross-references

PROSITE	<a href="#">PDOC00137</a> ; <a href="#">PDOC00138</a> ; <a href="#">PDOC00327</a> ; <a href="#">PDOC00328</a>
BRENDA	<a href="#">3.6.3.14</a>
PUMA2	<a href="#">3.6.3.14</a>
PRIAM enzyme-specific profiles	<a href="#">3.6.3.14</a>
Kyoto University LIGAND chemical database	<a href="#">3.6.3.14</a>
IUBMB Enzyme Nomenclature	<a href="#">3.6.3.14</a>
IntEnz	<a href="#">3.6.3.14</a>
MEDLINE	<a href="#">Find literature relating to 3.6.3.14</a>

[P13619](#), [AT5F1\\_BOVIN](#); [Q94516](#), [AT5F1\\_DROME](#)  
[Q9CQ07](#), [AT5F1\\_MOUSE](#); [P19511](#), [AT5F1\\_RAT](#);  
[P05496](#), [AT5G1\\_HUMAN](#); [P48202](#), [AT5G1\\_MOUSE](#)  
[P17605](#), [AT5G1\\_SHEEP](#); [P07926](#), [AT5G2\\_BOVIN](#)  
[P56383](#), [AT5G2\\_MOUSE](#); [Q06646](#), [AT5G2\\_RAT](#);  
[P48201](#), [AT5G3\\_HUMAN](#); [P56384](#), [AT5G3\\_MOUSE](#)  
[Q12349](#), [ATP14\\_YEAST](#); [Q13931](#), [ATP18\\_SCHPO](#)  
[P81451](#), [ATP19\\_YEAST](#); [Q96252](#), [ATP4\\_ARATH](#);  
[Q41000](#), [ATP4\\_PEA](#); [P80085](#), [ATP4\\_SPIOL](#);  
[P05632](#), [ATP5E\\_BOVIN](#); [P34539](#), [ATP5E\\_CAEEL](#)  
[Q06450](#), [ATP5E\\_IPOBA](#); [Q41898](#), [ATP5E\\_MAIZE](#)  
[P29418](#), [ATP5E\\_RAT](#); [P87316](#), [ATP5E\\_SCHPO](#)  
[P13620](#), [ATP5H\\_BOVIN](#); [Q24251](#), [ATP5H\\_DROME](#)  
[Q9DCX2](#), [ATP5H\\_MOUSE](#); [P31399](#), [ATP5H\\_RAT](#);  
[P12633](#), [ATP5I\\_CRILLO](#); [P56385](#), [ATP5I\\_HUMAN](#)  
[Q9MYT8](#), [ATP5I\\_PIG](#); [P29419](#), [ATP5I\\_RAT](#);  
[Q24407](#), [ATP5J\\_DROME](#); [P18859](#), [ATP5J\\_HUMAN](#)  
[P97450](#), [ATP5J\\_MOUSE](#); [P13618](#), [ATP5J\\_PIG](#);  
[P21571](#), [ATP5J\\_RAT](#); [Q28852](#), [ATP5L\\_BOVIN](#)  
[Q9CPQ8](#), [ATP5L\\_MOUSE](#); [Q5RFH0](#), [ATP5L\\_PONPY](#)  
[P92547](#), [ATP62\\_ARATH](#); [Q37385](#), [ATP6\\_ACACA](#);  
[P50363](#), [ATP6\\_ALLAR](#); [P50364](#), [ATP6\\_ALLMA](#);  
[P50654](#), [ATP6\\_ANAPL](#); [P12404](#), [ATP6\\_ANASP](#);  
[P33507](#), [ATP6\\_ANOQU](#); [Q00275](#), [ATP6\\_APILI](#);  
[Q37708](#), [ATP6\\_ARTSF](#); [P24876](#), [ATP6\\_ASCSU](#);  
[P00853](#), [ATP6\\_ASPAM](#); [Q33823](#), [ATP6\\_ASTPE](#);  
[P41013](#), [ATP6\\_BACCA](#); [P20600](#), [ATP6\\_BACME](#);  
[P22476](#), [ATP6\\_BACPF](#); [P42010](#), [ATP6\\_BACST](#);  
[P41291](#), [ATP6\\_BALMU](#); [P24945](#), [ATP6\\_BALPH](#);  
[Q47426](#), [ATP6\\_BRAFL](#); [Q21004](#), [ATP6\\_BRALA](#);  
[Q9MIY5](#), [ATP6\\_BRARE](#); [Q31721](#), [ATP6\\_BRATO](#);  
[Q51878](#), [ATP6\\_BUCAP](#); [Q89B45](#), [ATP6\\_BUCBP](#);  
[Q9ZZ62](#), [ATP6\\_CANFA](#); [Q85Q99](#), [ATP6\\_CANGA](#);  
[Q32644](#), [ATP6\\_CAPHI](#); [Q78684](#), [ATP6\\_CARAU](#);  
[P14092](#), [ATP6\\_CHICK](#); [P48878](#), [ATP6\\_CHOCR](#);  
[P14862](#), [ATP6\\_COCHE](#); [P50681](#), [ATP6\\_COTJA](#);  
[P34191](#), [ATP6\\_CROLA](#); [P24946](#), [ATP6\\_CYPCA](#);  
[P41313](#), [ATP6\\_DIDMA](#); [Q79551](#), [ATP6\\_DINSE](#);  
[P50269](#), [ATP6\\_DROSI](#); [P00851](#), [ATP6\\_DROYA](#);  
[P00855](#), [ATP6\\_ECOLI](#); [P00852](#), [ATP6\\_EMENI](#);  
[P92480](#), [ATP6\\_EQUAS](#); [P48894](#), [ATP6\\_FELCA](#);

<u>Q9T9Y7</u> , ATP6_GORGO;	<u>P43719</u> , ATP6_HAEIN;
<u>Q9ZL15</u> , ATP6_HELPJ;	<u>P56085</u> , ATP6_HELPY;
<u>P48662</u> , ATP6_HORSE;	<u>P00846</u> , ATP6_HUMAN;
<u>Q6DN61</u> , ATP6_KLULA;	<u>O03169</u> , ATP6_LATCH;
<u>P14569</u> , ATP6_LOCFI;	<u>Q34946</u> , ATP6_LUMTE;
<u>P07925</u> , ATP6_MAIZE;	<u>P26853</u> , ATP6_MARPO;
<u>P00848</u> , ATP6_MOUSE;	<u>P63655</u> , ATP6_MYCBO;
<u>P47645</u> , ATP6_MYCGE;	<u>P45829</u> , ATP6_MYCLE;
<u>P63654</u> , ATP6_MYCTU;	<u>Q00224</u> , ATP6_MYTED;
<u>P22067</u> , ATP6_NAEFO;	<u>P37212</u> , ATP6_NEUCR;
<u>Q36964</u> , ATP6_ONCMA;	<u>P48178</u> , ATP6_ONCMY;
<u>Q9T9W9</u> , ATP6_PANPA;	<u>Q9T9W0</u> , ATP6_PANTR;
<u>P12696</u> , ATP6_PARLI;	<u>O79675</u> , ATP6_PELSU;
<u>Q35538</u> , ATP6_PETMA;	<u>Q00521</u> , ATP6_PHOVI;
<u>Q35915</u> , ATP6_PIG;	<u>P25005</u> , ATP6_PISOC;
<u>Q95913</u> , ATP6_POLOR;	<u>P92695</u> , ATP6_PONPA;
<u>P25761</u> , ATP6_PSEPU;	<u>Q37601</u> , ATP6_PYLLI;
<u>P05504</u> , ATP6_RAT;	<u>Q99821</u> , ATP6_RHISA;
<u>Q9B6H6</u> , ATP6_RHOPD;	<u>P15012</u> , ATP6_RHORU;
<u>Q9ZEC1</u> , ATP6_RICPR;	<u>Q35920</u> , ATP6_SALSA;
<u>P21535</u> , ATP6_SCHPO;	<u>O79406</u> , ATP6_SCYCA;
<u>P80086</u> , ATP6_SPIOL;	<u>Q9ZZ49</u> , ATP6_SQUAC;
<u>P50012</u> , ATP6_STRLI;	<u>P95784</u> , ATP6_STRMU;
<u>P15995</u> , ATP6_STRPU;	<u>P0A2Y9</u> , ATP6_STRR6;
<u>P08444</u> , ATP6_SYNP6;	<u>P27178</u> , ATP6_SYNY3;
<u>P05499</u> , ATP6_TOBAC;	<u>Q36835</u> , ATP6_TRIRU;
<u>O03570</u> , ATP6_TROHI;	<u>O03359</u> , ATP6_TROMO;
<u>P12984</u> , ATP6_VIBAL;	<u>Q04654</u> , ATP6_VICFA;
<u>P00849</u> , ATP6_XENLA;	<u>Q36258</u> , ATP6_YARLI;
<u>Q9SJI2</u> , ATP7_ARATH;	<u>O13350</u> , ATP7_KLULA;
<u>O94390</u> , ATP7_SCHPO;	<u>P80496</u> , ATP7_SOLTU;
<u>P30902</u> , ATP7_YEAST;	<u>P48895</u> , ATP8_ALBCO;
<u>O47871</u> , ATP8_ALLMI;	<u>P50655</u> , ATP8_ANAPL;
<u>P33506</u> , ATP8_ANOQU;	<u>Q00276</u> , ATP8_APILI;
<u>O99598</u> , ATP8_ARTJA;	<u>Q37707</u> , ATP8_ARTSF;
<u>P00858</u> , ATP8_ASPAM;	<u>Q33822</u> , ATP8_ASTPE;
<u>P41292</u> , ATP8_BALMU;	<u>P24947</u> , ATP8_BALPH;
<u>P03929</u> , ATP8_BOVIN;	<u>O47427</u> , ATP8_BRAFL;
<u>Q9MIY6</u> , ATP8_BRARE;	<u>Q9ZZ63</u> , ATP8_CANFA;
<u>P17345</u> , ATP8_CANPA;	<u>Q32643</u> , ATP8_CAPHI;
<u>O78683</u> , ATP8_CARAU;	<u>Q9TEG7</u> , ATP8_CAVPO;
<u>Q9MQJ9</u> , ATP8_CEREH;	<u>O03199</u> , ATP8_CERSI;
<u>Q9XPI2</u> , ATP8_CHEMY;	<u>P14093</u> , ATP8_CHICK;
<u>Q9MDB7</u> , ATP8_COLPA;	<u>Q9TBI6</u> , ATP8_CORCN;
<u>P50682</u> , ATP8_COTJA;	<u>P14414</u> , ATP8_CRIGR;
<u>P24948</u> , ATP8_CYPCA;	<u>O21329</u> , ATP8_DASNO;
<u>P41314</u> , ATP8_DIDMA;	<u>O79550</u> , ATP8_DINSE;
<u>P84345</u> , ATP8_DROME;	<u>Q9MGM1</u> , ATP8_DROSE;
<u>P03933</u> , ATP8_DROYA;	<u>Q8W9N2</u> , ATP8_DUGDU;
<u>P92479</u> , ATP8_EQUAS;	<u>P48896</u> , ATP8_FELCA;
<u>Q34571</u> , ATP8_GORGO;	<u>Q9TBJ1</u> , ATP8_GUIGU;
<u>Q9ZZY7</u> , ATP8_HIPAM;	<u>P48663</u> , ATP8_HORSE;
<u>Q95705</u> , ATP8_HYLLA;	<u>Q34801</u> , ATP8_HYLSY;
<u>Q9TA07</u> , ATP8_LAMFL;	<u>Q9MEI6</u> , ATP8_LAMPA;
<u>Q8LX28</u> , ATP8_LEMCA;	<u>Q9MLQ5</u> , ATP8_LIMPO;
<u>Q9MDJ1</u> , ATP8_LOXNO;	<u>Q34942</u> , ATP8_LUMTE;
<u>O47493</u> , ATP8_METSE;	<u>P24949</u> , ATP8_MICPE;
<u>Q9TBI8</u> , ATP8_MUSVO;	<u>O63902</u> , ATP8_MYOGL;

<u>Q08656</u> , ATP8_NEUCR;	<u>P07513</u> , ATP8_OENBE;
<u>Q9TBI5</u> , ATP8_OPIHO;	<u>Q36453</u> , ATP8_ORNAN;
<u>Q35587</u> , ATP8_PANPA;	<u>Q35647</u> , ATP8_PANTR;
<u>P12697</u> , ATP8_PARLI;	<u>Q9T9D5</u> , ATP8_PAROL;
<u>Q9MGD7</u> , ATP8_PENMO;	<u>Q35537</u> , ATP8_PETMA;
<u>Q9MET2</u> , ATP8_PHYCA;	<u>P48882</u> , ATP8_PICCA;
<u>P25004</u> , ATP8_PISOC;	<u>Q02653</u> , ATP8_PODAN;
<u>P92694</u> , ATP8_PONPA;	<u>P92896</u> , ATP8_PONPP;
<u>Q35416</u> , ATP8_PRODO;	<u>O79431</u> , ATP8_RABIT;
<u>O79396</u> , ATP8_RHEAM;	<u>O99820</u> , ATP8_RHISA;
<u>Q9XN27</u> , ATP8_SALAL;	<u>Q9XN35</u> , ATP8_SALFO;
<u>P21536</u> , ATP8_SCHPO;	<u>Q9MEV6</u> , ATP8_SCIVU;
<u>O78751</u> , ATP8_SHEEP;	<u>Q9ZZ50</u> , ATP8_SQUAC;
<u>P15997</u> , ATP8_STRPU;	<u>Q9MJB2</u> , ATP8_TALEU;
<u>Q9ME31</u> , ATP8_VIRAL;	<u>P03931</u> , ATP8_XENLA;
<u>P00856</u> , ATP8_YEAST;	<u>Q37377</u> , ATP9_ACACA;
<u>Q75G38</u> , ATP9_ASHGO;	<u>P14571</u> , ATP9_BETVU;
<u>Q85Q98</u> , ATP9_CANGA;	<u>P48880</u> , ATP9_CHOCH;
<u>P16000</u> , ATP9_EMENI;	<u>P17254</u> , ATP9_HELAN;
<u>P60117</u> , ATP9_LYCES;	<u>P00840</u> , ATP9_MAIZE;
<u>Q9U505</u> , ATP9_MANSE;	<u>P26855</u> , ATP9_MARPO;
<u>P60115</u> , ATP9_OENBI;	<u>P14863</u> , ATP9_ORYSA;
<u>P69420</u> , ATP9_PEA;	<u>P60118</u> , ATP9_PETHY;
<u>P48881</u> , ATP9_PICCA;	<u>Q06838</u> , ATP9_PICPJ;
<u>P61828</u> , ATP9_SACDO;	<u>P21537</u> , ATP9_SCHPO;
<u>P69421</u> , ATP9_SOYBN;	<u>P60116</u> , ATP9_TOBAC;
<u>P69422</u> , ATP9_VICFA;	<u>P13547</u> , ATP9_WHEAT;
<u>Q37695</u> , ATP9_YARLI;	<u>P61829</u> , ATP9_YEAST;
<u>P80021</u> , ATPA1_PIG;	<u>P19482</u> , ATPA2_BOVIN
<u>Q37380</u> , ATPAM_ACACA;	<u>P92549</u> , ATPAM_ARATH
<u>P68542</u> , ATPAM_BRACM;	<u>P22201</u> , ATPAM_BRANA
<u>P05494</u> , ATPAM_MAIZE;	<u>P26854</u> , ATPAM_MARPO
<u>P05492</u> , ATPAM_OENBI;	<u>P15998</u> , ATPAM_ORYSA
<u>P24459</u> , ATPAM_PHAVU;	<u>P68541</u> , ATPAM_RAPSA
<u>P80082</u> , ATPAM_SPIOL;	<u>P12862</u> , ATPAM_WHEAT
<u>Q85AU2</u> , ATPA_ANTFO;	<u>Q02848</u> , ATPA_ANTSP;
<u>P56757</u> , ATPA_ARATH;	<u>Q9K6H3</u> , ATPA_BACHD;
<u>P09219</u> , ATPA_BACP3;	<u>P22477</u> , ATPA_BACPF;
<u>P37808</u> , ATPA_BACSU;	<u>P26965</u> , ATPA_BRYMA;
<u>O51874</u> , ATPA_BUCAP;	<u>Q89B41</u> , ATPA_BUCBP;
<u>P56294</u> , ATPA_CHLVU;	<u>Q9Z689</u> , ATPA_CLOAB;
<u>Q9TM26</u> , ATPA_CYACA;	<u>P48080</u> , ATPA_CYAPA;
<u>P00822</u> , ATPA_ECOLI;	<u>P26679</u> , ATPA_ENTHR;
<u>P35009</u> , ATPA_GALSU;	<u>O78475</u> , ATPA_GUITH;
<u>Q9ZK79</u> , ATPA_HELPJ;	<u>P55987</u> , ATPA_HELPY;
<u>P49375</u> , ATPA_KLULA;	<u>Q9CER8</u> , ATPA_LACLA;
<u>Q9BBS3</u> , ATPA_LOTJA;	<u>P05022</u> , ATPA_MAIZE;
<u>Q9MUT2</u> , ATPA_MESVI;	<u>Q03265</u> , ATPA_MOUSE;
<u>P33252</u> , ATPA_MYCGA;	<u>P47641</u> , ATPA_MYCGE;
<u>Q50329</u> , ATPA_MYCPN;	<u>Q98QB7</u> , ATPA_MYCPU;
<u>Q07405</u> , ATPA_MYXXA;	<u>Q9TL16</u> , ATPA_NEPOL;
<u>Q40611</u> , ATPA_OCHNE;	<u>Q00820</u> , ATPA_ODOSI;
<u>P12084</u> , ATPA_ORYSA;	<u>Q9CKW2</u> , ATPA_PASMU;
<u>P41602</u> , ATPA_PINTH;	<u>P51242</u> , ATPA_PORPU;
<u>P05439</u> , ATPA_RHOB1;	<u>P72245</u> , ATPA_RHOCA;
<u>Q92G86</u> , ATPA_RICCN;	<u>O50288</u> , ATPA_RICPR;
<u>P06450</u> , ATPA_SPIOL;	<u>P63675</u> , ATPA_STAAM;
<u>Q6GEX0</u> , ATPA_STAAR;	<u>Q6G7K5</u> , ATPA_STAAS;

<u>Q8CNJ5</u> , ATPA_STAEP;	<u>P50001</u> , ATPA_STRLI;
<u>Q05372</u> , ATPA_SYNPI;	<u>P08449</u> , ATPA_SYNPI6;
<u>P41167</u> , ATPA_THIFE;	<u>P00823</u> , ATPA_TOBAC;
<u>Q9KNH3</u> , ATPA_VIBCH;	<u>P12112</u> , ATPA_WHEAT;
<u>P07251</u> , ATPA_YEAST;	<u>P43395</u> , ATPBM_ACTCH
<u>P38482</u> , ATPBM_CHLRE;	<u>P37399</u> , ATPBM_DAUCA
<u>P19023</u> , ATPBM_MAIZE;	<u>P17614</u> , ATPBM_NICPL
<u>P81663</u> , ATPBM_PINPS;	<u>P80083</u> , ATPBM_SPIOL
<u>O03062</u> , ATPB_ADICA;	<u>O03064</u> , ATPB_ADIRA;
<u>P62614</u> , ATPB_AEGCR;	<u>P06540</u> , ATPB_ANASP;
<u>Q31794</u> , ATPB_ANTFO;	<u>O67828</u> , ATPB_AQUAE;
<u>P19366</u> , ATPB_ARATH;	<u>O03063</u> , ATPB_ASPND;
<u>P41009</u> , ATPB_BACCA;	<u>P25075</u> , ATPB_BACFI;
<u>Q9K6H5</u> , ATPB_BACHD;	<u>P12698</u> , ATPB_BACME;
<u>P22478</u> , ATPB_BACPF;	<u>P42006</u> , ATPB_BACST;
<u>Q9TMV0</u> , ATPB_BEARE;	<u>O03066</u> , ATPB_BLEOC;
<u>P83505</u> , ATPB_BRARA;	<u>Q9MRR9</u> , ATPB_BRASC;
<u>Q07232</u> , ATPB_BUCAP;	<u>Q89B39</u> , ATPB_BUCBP;
<u>P46561</u> , ATPB_CAEEL;	<u>P99504</u> , ATPB_CANFA;
<u>Q9MU80</u> , ATPB_CHASI;	<u>P35110</u> , ATPB_CHLLI;
<u>Q8KAC9</u> , ATPB_CHLTE;	<u>P42465</u> , ATPB_CHLVI;
<u>Q9Z687</u> , ATPB_CLOAB;	<u>Q8XID4</u> , ATPB_CLOPE;
<u>P30399</u> , ATPB_CUSRE;	<u>Q9TM41</u> , ATPB_CYACA;
<u>Q9PTY0</u> , ATPB_CYPCA;	<u>P13357</u> , ATPB_CYTLY;
<u>O03067</u> , ATPB_DICAN;	<u>P30158</u> , ATPB_DICDH;
<u>Q24751</u> , ATPB_DROVI;	<u>P00824</u> , ATPB_ECOLI;
<u>O03069</u> , ATPB_EQUAR;	<u>P31476</u> , ATPB_EUGGR;
<u>Q08807</u> , ATPB_GALSU;	<u>Q9LA80</u> , ATPB_GEOTH;
<u>P43715</u> , ATPB_HAEIN;	<u>Q9ZK81</u> , ATPB_HELPJ;
<u>Q25117</u> , ATPB_HEMPU;	<u>P42466</u> , ATPB_HERAU;
<u>P06576</u> , ATPB_HUMAN;	<u>Q9BA84</u> , ATPB_HYOLA;
<u>P07137</u> , ATPB_IPOBA;	<u>P49376</u> , ATPB_KLULA;
<u>Q9CES0</u> , ATPB_LACLA;	<u>Q9RAU0</u> , ATPB_LACLC;
<u>Q9BBU0</u> , ATPB_LOTJA;	<u>P00827</u> , ATPB_MAIZE;
<u>Q9TKI7</u> , ATPB_MEDSA;	<u>Q9MUT5</u> , ATPB_MESVI;
<u>O03075</u> , ATPB_MICSZ;	<u>Q8MBF7</u> , ATPB_MONCA;
<u>P63678</u> , ATPB_MYCBO;	<u>P33253</u> , ATPB_MYCGA;
<u>P45823</u> , ATPB_MYCLE;	<u>Q50331</u> , ATPB_MYCPN;
<u>P63677</u> , ATPB_MYCTU;	<u>Q9TL34</u> , ATPB_NEPOL;
<u>P69369</u> , ATPB_NICBI;	<u>P69370</u> , ATPB_NICPL;
<u>P26531</u> , ATPB_NICSP;	<u>P49647</u> , ATPB_ODOSI;
<u>P12085</u> , ATPB_ORYSA;	<u>O03077</u> , ATPB_OSMCI;
<u>P05037</u> , ATPB_PEA;	<u>Q03235</u> , ATPB_PECFR;
<u>P80658</u> , ATPB_PHYPA;	<u>Q47037</u> , ATPB_PICAB;
<u>P51259</u> , ATPB_PORPU;	<u>P50003</u> , ATPB_PRODI;
<u>O03079</u> , ATPB_PTEAQ;	<u>O03080</u> , ATPB_PTEES;
<u>Q9MTG8</u> , ATPB_RAPSA;	<u>P10719</u> , ATPB_RAT;
<u>P72247</u> , ATPB_RHOCA;	<u>P05038</u> , ATPB_RHORU;
<u>O50290</u> , ATPB_RICPR;	<u>Q07233</u> , ATPB_SCHGA;
<u>Q9MTX9</u> , ATPB_SCHSP;	<u>P00825</u> , ATPB_SPIOL;
<u>P99112</u> , ATPB_STAAN;	<u>Q6GEX2</u> , ATPB_STAAR;
<u>P63680</u> , ATPB_STAAW;	<u>Q8CNJ7</u> , ATPB_STAEP;
<u>P0A300</u> , ATPB_STRCO;	<u>P21933</u> , ATPB_STRDO;
<u>P95789</u> , ATPB_STRMU;	<u>Q05373</u> , ATPB_SYNPI;
<u>P26527</u> , ATPB_SYNY3;	<u>O50550</u> , ATPB_THEMA;
<u>P00826</u> , ATPB_TOBAC;	<u>O03085</u> , ATPB_VANDA;
<u>Q9KNH5</u> , ATPB_VIBCH;	<u>P20858</u> , ATPB_WHEAT;
<u>P00830</u> , ATPB_YEAST;	<u>Q92196</u> , ATPD_AGABI;

## Swiss-Prot

<u>Q02849</u> , ATPD_ANTSP;	<u>Q757N0</u> , ATPD_ASHGO;
<u>Q9K6H2</u> , ATPD_BACHD;	<u>P17675</u> , ATPD_BACME;
<u>P22479</u> , ATPD_BACPF;	<u>P42008</u> , ATPD_BACST;
<u>P05630</u> , ATPD_BOVIN;	<u>P57121</u> , ATPD_BUCAI;
<u>Q89B42</u> , ATPD_BUCBP;	<u>Q09544</u> , ATPD_CAEEL;
<u>Q9TM27</u> , ATPD_CYACA;	<u>P48082</u> , ATPD_CYAPA;
<u>P26680</u> , ATPD_ENTHR;	<u>P35010</u> , ATPD_GALSU;
<u>P43717</u> , ATPD_HAEIN;	<u>P30049</u> , ATPD_HUMAN;
<u>P80285</u> , ATPD_MICLU;	<u>Q9D3D9</u> , ATPD_MOUSE;
<u>P33254</u> , ATPD_MYCGA;	<u>P47642</u> , ATPD_MYCGE;
<u>Q50328</u> , ATPD_MYCPN;	<u>Q98QU2</u> , ATPD_MYCPU;
<u>P56525</u> , ATPD_NEUCR;	<u>Q40610</u> , ATPD_OCHNE;
<u>Q02758</u> , ATPD_PEA;	<u>Q95312</u> , ATPD_PIG;
<u>P35434</u> , ATPD_RAT;	<u>P05437</u> , ATPD_RHOBL;
<u>P05438</u> , ATPD_RHORU;	<u>Q92G85</u> , ATPD_RICCN;
<u>Q9P6R6</u> , ATPD_SCHPO;	<u>Q07300</u> , ATPD_SORBI;
<u>P63658</u> , ATPD_STAAM;	<u>P99109</u> , ATPD_STAAN;
<u>Q6G7K4</u> , ATPD_STAAS;	<u>P63659</u> , ATPD_STAAW;
<u>O50156</u> , ATPD_STRBO;	<u>P50008</u> , ATPD_STRLI;
<u>P0A2Z4</u> , ATPD_STRPN;	<u>P0A2Z5</u> , ATPD_STRR6;
<u>P08448</u> , ATPD_SYNP6;	<u>P27180</u> , ATPD_SYNY3;
<u>P32980</u> , ATPD_TOBAC;	<u>P12987</u> , ATPD_VIBAL;
<u>Q8XU77</u> , ATPE1_RALSO;	<u>Q8XRM1</u> , ATPE2_RALSO
<u>P69445</u> , ATPE_AEGCO;	<u>P69446</u> , ATPE_AEGCR;
<u>Q70XZ7</u> , ATPE_AMBTC;	<u>P06542</u> , ATPE_ANASP;
<u>Q66903</u> , ATPE_AQUAE;	<u>P09468</u> , ATPE_ARATH;
<u>Q72XE9</u> , ATPE_BACC1;	<u>P41012</u> , ATPE_BACCA;
<u>Q630U4</u> , ATPE_BACCZ;	<u>Q9K6H6</u> , ATPE_BACHD;
<u>P12699</u> , ATPE_BACME;	<u>P07678</u> , ATPE_BACP3;
<u>Q5WB79</u> , ATPE_BACSK;	<u>P42009</u> , ATPE_BACST;
<u>Q6G1X0</u> , ATPE_BARHE;	<u>Q6FYM4</u> , ATPE_BARQU;
<u>Q7WEN0</u> , ATPE_BORBR;	<u>Q7W3B1</u> , ATPE_BORPA;
<u>Q89X75</u> , ATPE_BRAJA;	<u>P63660</u> , ATPE_BRUME;
<u>P57125</u> , ATPE_BUCAI;	<u>O51871</u> , ATPE_BUCAP;
<u>Q62FR4</u> , ATPE_BURMA;	<u>Q63PI1</u> , ATPE_BURPS;
<u>Q9PJ18</u> , ATPE_CAMJE;	<u>Q7VQV5</u> , ATPE_CANBF;
<u>Q8M9X7</u> , ATPE_CHAGL;	<u>P35111</u> , ATPE_CHLLI;
<u>Q8KAC8</u> , ATPE_CHLTE;	<u>P32979</u> , ATPE_CHLVU;
<u>Q9Z686</u> , ATPE_CLOAB;	<u>Q8XID5</u> , ATPE_CLOPE;
<u>Q6NHS8</u> , ATPE_CORDI;	<u>Q8FQ19</u> , ATPE_COREF;
<u>Q83AF4</u> , ATPE_COXBU;	<u>P30400</u> , ATPE_CUSRE;
<u>Q85FT3</u> , ATPE_CYAME;	<u>P48083</u> , ATPE_CYAPA;
<u>Q72E05</u> , ATPE_DESVH;	<u>Q9S5B5</u> , ATPE_DESVM;
<u>P58646</u> , ATPE_ECO57;	<u>P00832</u> , ATPE_ECOLI;
<u>P43453</u> , ATPE_ENTHR;	<u>Q6CYJ6</u> , ATPE_ERWCT;
<u>Q8RGE3</u> , ATPE_FUSNN;	<u>Q08808</u> , ATPE_GALSU;
<u>Q7NHG9</u> , ATPE_GLOVI;	<u>Q6B8S5</u> , ATPE_GRATL;
<u>Q7VPN9</u> , ATPE_HAEDU;	<u>P43718</u> , ATPE_HAEIN;
<u>Q9ZK82</u> , ATPE_HELPJ;	<u>P56084</u> , ATPE_HELPY;
<u>P07138</u> , ATPE_IPOBA;	<u>Q9RGY0</u> , ATPE_LACAC;
<u>Q9RAT9</u> , ATPE_LACLC;	<u>Q88UU4</u> , ATPE_LACPL;
<u>Q8F2J6</u> , ATPE_LEPIN;	<u>Q927W5</u> , ATPE_LISIN;
<u>Q8Y4C2</u> , ATPE_LISMO;	<u>Q9BBT9</u> , ATPE_LOTJA;
<u>Q65Q08</u> , ATPE_MANSM;	<u>P06285</u> , ATPE_MARPO;
<u>Q9MUT4</u> , ATPE_MESVI;	<u>P80286</u> , ATPE_MICLU;
<u>P63663</u> , ATPE_MYCBO;	<u>P33255</u> , ATPE_MYCGA;
<u>P45822</u> , ATPE_MYCLE;	<u>Q6KI83</u> , ATPE_MYCMO;
<u>Q50332</u> , ATPE_MYCPN;	<u>Q98QU6</u> , ATPE_MYCPU;



<u>Q9JW69</u> , ATPE_NEIMA;	<u>Q9JXQ3</u> , ATPE_NEIMB;
<u>Q820S4</u> , ATPE_NITEU;	<u>Q5Z0Y0</u> , ATPE_NOCFA;
<u>Q8EM84</u> , ATPE_OCEIH;	<u>P49648</u> , ATPE_ODOSI;
<u>Q6ENG8</u> , ATPE_ORYNI;	<u>P12086</u> , ATPE_ORYSA;
<u>Q9CKW0</u> , ATPE_PASMU;	<u>P05039</u> , ATPE_PEA;
<u>O47036</u> , ATPE_PICAB;	<u>Q85X21</u> , ATPE_PINKO;
<u>P51260</u> , ATPE_PORPU;	<u>Q6A8C8</u> , ATPE_PROAC;
<u>Q7VA75</u> , ATPE_PROMA;	<u>Q7TUS2</u> , ATPE_PROMM;
<u>Q9TJR8</u> , ATPE_PROWI;	<u>Q9HT21</u> , ATPE_PSEAE;
<u>Q87TT5</u> , ATPE_PSESM;	<u>Q8WI12</u> , ATPE_PSINU;
<u>Q98EV9</u> , ATPE_RHILO;	<u>Q92LK9</u> , ATPE_RHIME;
<u>P05441</u> , ATPE_RHOBL;	<u>P72248</u> , ATPE_RHOCa;
<u>P05442</u> , ATPE_RHORU;	<u>Q92G89</u> , ATPE_RICCN;
<u>Q68VU9</u> , ATPE_RICTY;	<u>O50143</u> , ATPE_RUMAL;
<u>P0A1B8</u> , ATPE_SALTI;	<u>P0A1B7</u> , ATPE_SALTY;
<u>P00833</u> , ATPE_SPIOL;	<u>P63664</u> , ATPE_STAAM;
<u>Q6GEX3</u> , ATPE_STAAR;	<u>Q6G7K8</u> , ATPE_STAAS;
<u>Q8CNJ8</u> , ATPE_STAEP;	<u>Q8E5U7</u> , ATPE_STRA3;
<u>Q82J85</u> , ATPE_STRAW;	<u>O50160</u> , ATPE_STRBO;
<u>P0A2Z7</u> , ATPE_STRLI;	<u>P95790</u> , ATPE_STRMU;
<u>Q5XCX9</u> , ATPE_STRP6;	<u>P63670</u> , ATPE_STRP8;
<u>Q9A0I6</u> , ATPE_STRPY;	<u>P63668</u> , ATPE_STRR6;
<u>Q67TB6</u> , ATPE_SYMTH;	<u>Q8DLG7</u> , ATPE_SYNEL;
<u>P0A2Z9</u> , ATPE_SYNP6;	<u>P0A2Z8</u> , ATPE_SYNP7;
<u>P26533</u> , ATPE_SYNY3;	<u>Q9X1U5</u> , ATPE_THEMA;
<u>P41171</u> , ATPE_THIFE;	<u>P00834</u> , ATPE_TOBAC;
<u>P12988</u> , ATPE_VIBAL;	<u>Q9KNH6</u> , ATPE_VIBCH;
<u>Q8DDG7</u> , ATPE_VIBVU;	<u>Q7MGI1</u> , ATPE_VIBVY;
<u>Q8D3J2</u> , ATPE_WIGBR;	<u>Q7MSF4</u> , ATPE_WOLSU;
<u>Q8PCZ4</u> , ATPE_XANCP;	<u>Q9PE86</u> , ATPE_XYLFA;
<u>P58647</u> , ATPE_YERPE;	<u>Q663Q9</u> , ATPE_YERPS;
<u>Q85AL8</u> , ATPF_ANTFO;	<u>Q02850</u> , ATPF_ANTSP;
<u>Q758L2</u> , ATPF_ASHGO;	<u>P41014</u> , ATPF_BACCA;
<u>P20601</u> , ATPF_BACME;	<u>P09221</u> , ATPF_BACP3;
<u>P37814</u> , ATPF_BACSU;	<u>P57120</u> , ATPF_BUCAI;
<u>Q89B43</u> , ATPF_BUCBP;	<u>Q6FRW0</u> , ATPF_CANGA;
<u>P56296</u> , ATPF_CHLVU;	<u>O05098</u> , ATPF_CLOAB;
<u>P48084</u> , ATPF_CYAPA;	<u>P00859</u> , ATPF_ECOLI;
<u>P30393</u> , ATPF_EUGGR;	<u>P35011</u> , ATPF_GALSU;
<u>P43720</u> , ATPF_HAEIN;	<u>Q9ZK77</u> , ATPF_HELPJ;
<u>O13349</u> , ATPF_KLULA;	<u>P0A2Z0</u> , ATPF_LACLA;
<u>Q9BBS4</u> , ATPF_LOTJA;	<u>P48186</u> , ATPF_MAIZE;
<u>Q9MUT1</u> , ATPF_MESVI;	<u>P63657</u> , ATPF_MYCBO;
<u>P47643</u> , ATPF_MYCGE;	<u>P45827</u> , ATPF_MYCLE;
<u>P63656</u> , ATPF_MYCTU;	<u>Q9TL15</u> , ATPF_NEPOL;
<u>Q40609</u> , ATPF_OCHNE;	<u>Q00822</u> , ATPF_ODOSI;
<u>P12087</u> , ATPF_ORYSA;	<u>Q870C4</u> , ATPF_PARBR;
<u>O62939</u> , ATPF_PINTH;	<u>P51244</u> , ATPF_PORPU;
<u>Q92JP3</u> , ATPF_RICCN;	<u>Q9ZEC4</u> , ATPF_RICPR;
<u>P06453</u> , ATPF_SPIOL;	<u>P50013</u> , ATPF_STRLI;
<u>P0A2Z2</u> , ATPF_STRPN;	<u>P0A2Z3</u> , ATPF_STRR6;
<u>P08447</u> , ATPF_SYNP6;	<u>P27181</u> , ATPF_SYNY3;
<u>P06290</u> , ATPF_TOBAC;	<u>P12989</u> , ATPF_VIBAL;
<u>Q87KA4</u> , ATPF_VIBPA;	<u>Q8DDH2</u> , ATPF_VIBVU;
<u>P05626</u> , ATPF_YEAST;	<u>Q01908</u> , ATPG1_ARATH
<u>Q96250</u> , ATPG3_ARATH;	<u>P26360</u> , ATPG3_IPOBA
<u>P12408</u> , ATPG_ANASP;	<u>P41010</u> , ATPG_BACCA;
<u>P20602</u> , ATPG_BACME;	<u>P09222</u> , ATPG_BACP3;

<u>P42007</u> , ATPG_BACST;	<u>P37810</u> , ATPG_BACSU;
<u>P57123</u> , ATPG_BUCAI;	<u>O51873</u> , ATPG_BUCAP;
<u>P12113</u> , ATPG_CHLRE;	<u>O01666</u> , ATPG_DROME;
<u>P43452</u> , ATPG_ENTHR;	<u>F43716</u> , ATPG_HAEIN;
<u>P56082</u> , ATPG_HELPHY;	<u>P36542</u> , ATPG_HUMAN;
<u>Q9CER9</u> , ATPG_LACLA;	<u>Q60189</u> , ATPG_METMA;
<u>P63672</u> , ATPG_MYCBO;	<u>P33257</u> , ATPG_MYCGA;
<u>P45824</u> , ATPG_MYCLE;	<u>Q50330</u> , ATPG_MYCPN;
<u>Q06908</u> , ATPG_ODOSI;	<u>Q91686</u> , ATPG_PASMU;
<u>Q41075</u> , ATPG_PHATR;	<u>P35435</u> , ATPG_RAT;
<u>P72246</u> , ATPG_RHOCA;	<u>P07227</u> , ATPG_RHORU;
<u>O74754</u> , ATPG_SCHPO;	<u>P05435</u> , ATPG_SPIOL;
<u>P50007</u> , ATPG_STRLI;	<u>P95788</u> , ATPG_STRMU;
<u>P08450</u> , ATPG_SYNP6;	<u>P17253</u> , ATPG_SYNY3;
<u>P29790</u> , ATPG_TOBAC;	<u>P12990</u> , ATPG_VIBAL;
<u>P61172</u> , ATPH_ANTFO;	<u>Q02851</u> , ATPH_ANTSP;
<u>Q37304</u> , ATPH_CHLRE;	<u>P56297</u> , ATPH_CHLVU;
<u>P48086</u> , ATPH_CYAPA;	<u>P10603</u> , ATPH_EUGGR;
<u>O78479</u> , ATPH_GUIITH;	<u>P69194</u> , ATPH_LOTJA;
<u>P62481</u> , ATPH_MARPO;	<u>Q9MUT0</u> , ATPH_MESVI;
<u>Q42969</u> , ATPH_OCHNE;	<u>Q00824</u> , ATPH_ODOSI;
<u>P69450</u> , ATPH_ORYSA;	<u>P28530</u> , ATPH_PAVLU;
<u>P41603</u> , ATPH_PINTH;	<u>P51246</u> , ATPH_PORPU;
<u>P69447</u> , ATPH_SPIOL;	<u>P06286</u> , ATPH_TOBAC;
<u>Q85AE6</u> , ATPI_ANTFO;	<u>Q02847</u> , ATPI_ANTSP;
<u>P69371</u> , ATPI_ATRBE;	<u>O63075</u> , ATPI_CHLRE;
<u>Q9TM31</u> , ATPI_CYACA;	<u>P30391</u> , ATPI_EUGGR;
<u>O78480</u> , ATPI_GUIITH;	<u>Q9BBS5</u> , ATPI_LOTJA;
<u>P06289</u> , ATPI_MARPO;	<u>Q9MUS9</u> , ATPI_MESVI;
<u>Q40607</u> , ATPI_OCHNE;	<u>Q00825</u> , ATPI_ODOSI;
<u>P12083</u> , ATPI_ORYSA;	<u>P28529</u> , ATPI_PAVLU;
<u>P41604</u> , ATPI_PINTH;	<u>P51247</u> , ATPI_PORPU;
<u>P69372</u> , ATPI_TOBAC;	<u>Q9XPT0</u> , ATPI_WHEAT;
<u>Q28851</u> , ATPK_BOVIN;	<u>Q22021</u> , ATPK_CAEEL;
<u>P56134</u> , ATPK_HUMAN;	<u>P56135</u> , ATPK_MOUSE;
<u>O94377</u> , ATPK_SCHPO;	<u>Q06405</u> , ATPK_YEAST;
<u>O66564</u> , ATPL_AQUAE;	<u>P25966</u> , ATPL_BACAO;
<u>P20603</u> , ATPL_BACME;	<u>P00845</u> , ATPL_BACP3;
<u>P42011</u> , ATPL_BACST;	<u>P37815</u> , ATPL_BACSU;
<u>O51877</u> , ATPL_BUCAP;	<u>Q89B44</u> , ATPL_BUCBP;
<u>P68701</u> , ATPL_ECO57;	<u>P68700</u> , ATPL_ECOL6;
<u>P26682</u> , ATPL_ENTHR;	<u>P43721</u> , ATPL_HAEIN;
<u>P56087</u> , ATPL_HELPHY;	<u>Q57674</u> , ATPL_METJA;
<u>P33258</u> , ATPL_MYCGA;	<u>P47644</u> , ATPL_MYCGE;
<u>Q59550</u> , ATPL_MYCPN;	<u>P63691</u> , ATPL_MYCTU;
<u>P15014</u> , ATPL_RHORU;	<u>Q92JP1</u> , ATPL_RICCN;
<u>P68703</u> , ATPL_SALTI;	<u>P68704</u> , ATPL_SALTY;
<u>P0A304</u> , ATPL_STRCO;	<u>P0A305</u> , ATPL_STRLI;
<u>P50017</u> , ATPL_STROR;	<u>P0A306</u> , ATPL_STRPN;
<u>P62020</u> , ATPL_SULAC;	<u>P62021</u> , ATPL_SULTO;
<u>P08445</u> , ATPL_SYNP6;	<u>P27182</u> , ATPL_SYNY3;
<u>Q9PR08</u> , ATPL_UREPA;	<u>P0A309</u> , ATPL_VIBAL;
<u>P68706</u> , ATPL_YERPE;	<u>Q18803</u> , ATPN_CAEEL;
<u>Q96251</u> , ATPO_ARATH;	<u>Q75EZ3</u> , ATPO_ASHGO;
<u>P90921</u> , ATPO_CAEEL;	<u>Q6FSD5</u> , ATPO_CANGA;
<u>P48047</u> , ATPO_HUMAN;	<u>P22778</u> , ATPO_IPOBA;
<u>Q9DB20</u> , ATPO_MOUSE;	<u>Q9P602</u> , ATPO_NEUCR;
<u>Q06647</u> , ATPO_RAT;	<u>O74479</u> , ATPO_SCHPO;

<u>P80087</u> , ATPO_SPIOL;	<u>P09457</u> , ATPO_YEAST;
<u>P12410</u> , ATPX_ANASP;	<u>Q02852</u> , ATPX_ANTSP;
<u>P48085</u> , ATPX_CYAPA;	<u>P35012</u> , ATPX_GALSU;
<u>Q40608</u> , ATPX_OCHNE;	<u>Q00823</u> , ATPX_ODOSI;
<u>P15015</u> , ATPX_RHORU;	<u>P31853</u> , ATPX_SPIOL;
<u>P08446</u> , ATPX_SYNP6;	<u>P27183</u> , ATPX_SYNY3;
<u>O34171</u> , FLII_AGRT5;	<u>O67531</u> , FLII_AQUAE;
<u>P52607</u> , FLII_BORBU;	<u>P57178</u> , FLII_BUCAI;
<u>Q89AZ7</u> , FLII_BUCBP;	<u>Q05528</u> , FLII_CAUCR;
<u>Q9ZJJ3</u> , FLII_HELPJ;	<u>Q07025</u> , FLII_HELPY;
<u>P26465</u> , FLII_SALTY;	<u>O83417</u> , FLII_TREPA;
<u>Q887B5</u> , HRCN_PSESM;	<u>Q52371</u> , HRCN_PSESY;
<u>P62018</u> , MTPE_SULAC;	<u>P62019</u> , MTPE_SULTO;
<u>P43436</u> , NTPF_ENTHR;	<u>P43437</u> , NTPF_ENTHR;
<u>P43438</u> , NTPH_ENTHR;	<u>P43440</u> , NTPJ_ENTHR;
<u>P0A1C0</u> , SPAL_SALTI;	<u>P0A1B9</u> , SPAL_SALTY;
<u>P0A1C2</u> , SPAL_SHISO;	<u>P74857</u> , SSAN_SALTY;
<u>Q9W4P5</u> , VOD1_DROME;	<u>Q9LHA4</u> , VOD2_ARATH;
<u>P61420</u> , VA0D_BOVIN;	<u>P54641</u> , VA0D_DICDI;
<u>Q25531</u> , VA0D_MANSE;	<u>P51863</u> , VA0D_MOUSE;
<u>O13753</u> , VA0D_SCHPO;	<u>P32366</u> , VA0D_YEAST;
<u>Q20591</u> , VA0H_CAEEL;	<u>Q9BDP4</u> , VA0H_CANFA;
<u>P40682</u> , VAS1_BOVIN;	<u>Q15904</u> , VAS1_HUMAN;
<u>O54715</u> , VAS1_RAT;	<u>Q38676</u> , VATA1_ACEAT
<u>P48602</u> , VATA1_DROME;	<u>Q04236</u> , VATA1_EQUAR
<u>P50516</u> , VATA1_MOUSE;	<u>Q29048</u> , VATA1_PIG;
<u>O83441</u> , VATA1_TREPA;	<u>Q38677</u> , VATA2_ACEAT
<u>Q04238</u> , VATA2_EQUAR;	<u>P38607</u> , VATA2_HUMAN
<u>O83541</u> , VATA2_TREPA;	<u>O16109</u> , VATA_AEDAE;
<u>Q23654</u> , VATA_ARATH;	<u>Q29101</u> , VATA_ARCFU;
<u>Q39442</u> , VATA_BETVU;	<u>O51121</u> , VATA_BORBU;
<u>P38078</u> , VATA_CANTR;	<u>Q822J8</u> , VATA_CHLCV;
<u>Q9Z993</u> , VATA_CHLPN;	<u>O84310</u> , VATA_CHLTR;
<u>P48414</u> , VATA_CYACA;	<u>P09469</u> , VATA_DAUCA;
<u>O06504</u> , VATA_DESSY;	<u>P54647</u> , VATA_DICDI;
<u>Q9HNE3</u> , VATA_HALN1;	<u>P25163</u> , VATA_HALSA;
<u>Q40002</u> , VATA_HORVU;	<u>P49087</u> , VATA_MAIZE;
<u>Q8TIJ1</u> , VATA_METAC;	<u>P22662</u> , VATA_METBA;
<u>Q8TWL6</u> , VATA_METKA;	<u>Q60186</u> , VATA_METMA;
<u>P11592</u> , VATA_NEUCR;	<u>P13548</u> , VATA_PHAAU;
<u>Q03498</u> , VATA_PLAFA;	<u>Q9UXU7</u> , VATA_PYRAB;
<u>Q8U4A6</u> , VATA_PYRFU;	<u>O57728</u> , VATA_PYRHO;
<u>Q8K8T1</u> , VATA_STRP3;	<u>P09639</u> , VATA_SULAC;
<u>Q971B7</u> , VATA_SULTO;	<u>Q9P997</u> , VATA_THEAC;
<u>Q56403</u> , VATA_THET8;	<u>Q97CQ0</u> , VATA_THEVO;
<u>P17255</u> , VATA_YEAST;	<u>Q38681</u> , VATB1_ACEAT
<u>Q43432</u> , VATB1_GOSHI;	<u>Q40078</u> , VATB1_HORVU
<u>O83442</u> , VATB1_TREPA;	<u>Q38680</u> , VATB2_ACEAT
<u>Q43433</u> , VATB2_GOSHI;	<u>Q40079</u> , VATB2_HORVU
<u>P62814</u> , VATB2_MOUSE;	<u>P62815</u> , VATB2_RAT;
<u>Q9YF36</u> , VATB_AERPE;	<u>P11574</u> , VATB_ARATH;
<u>O51120</u> , VATB_BORBU;	<u>Q19626</u> , VATB_CAEEL;
<u>P49712</u> , VATB_CHICK;	<u>Q822J9</u> , VATB_CHLCV;
<u>Q9Z992</u> , VATB_CHLPN;	<u>O84309</u> , VATB_CHLTR;
<u>Q9RWG7</u> , VATB_DEIRA;	<u>O06505</u> , VATB_DESSY;
<u>Q9HNE4</u> , VATB_HALN1;	<u>P25164</u> , VATB_HALSA;
<u>P31410</u> , VATB_HELVI;	<u>P31401</u> , VATB_MANSE;
<u>P22663</u> , VATB_METBA;	<u>Q57669</u> , VATB_METJA;

<u>Q27035</u> , VATB_METTH;	<u>P20022</u> , VATB_METTL;
<u>Q25691</u> , VATB_PLAFA;	<u>Q9UXU8</u> , VATB_PYRAB;
<u>Q8U4A5</u> , VATB_PYRFU;	<u>O57729</u> , VATB_PYRHO;
<u>P13052</u> , VATB_SULAC;	<u>Q9UWW8</u> , VATB_SULSO;
<u>Q9HM64</u> , VATB_THEAC;	<u>O32467</u> , VATB_THESI;
<u>Q97CP9</u> , VATB_THEVO;	<u>Q26976</u> , VATB_TRYCO;
<u>Q9SDS7</u> , VATC_ARATH;	<u>O29103</u> , VATC_ARCFU;
<u>P21282</u> , VATC_BOVIN;	<u>Q9XXU9</u> , VATC_CAEEL;
<u>O06502</u> , VATC_DESSY;	<u>P54648</u> , VATC_DICDI;
<u>Q9HNE1</u> , VATC_HALN1;	<u>Q48330</u> , VATC_HALVO;
<u>P21283</u> , VATC_HUMAN;	<u>Q9U5N1</u> , VATC_MANSE;
<u>Q57672</u> , VATC_METJA;	<u>Q60184</u> , VATC_METMA;
<u>Q9Z1G3</u> , VATC_MOUSE;	<u>Q9UXU5</u> , VATC_PYRAB;
<u>O57726</u> , VATC_PYRHO;	<u>Q9HDW6</u> , VATC_SCHPO;
<u>P74902</u> , VATC_THET8;	<u>Q97CQ2</u> , VATC_THEVO;
<u>Q9V7D2</u> , VATD1_DROME;	<u>O83443</u> , VATD1_TREPA;
<u>O83539</u> , VATD2_TREPA;	<u>Q9YF38</u> , VATD_AERPE;
<u>O29099</u> , VATD_ARCFU;	<u>O51119</u> , VATD_BORBU;
<u>P34462</u> , VATD_CAEEL;	<u>P87220</u> , VATD_CANAL;
<u>Q9Z991</u> , VATD_CHLPN;	<u>O84308</u> , VATD_CHLTR;
<u>O06506</u> , VATD_DESSY;	<u>Q9HNE7</u> , VATD_HALN1;
<u>Q9U0S4</u> , VATD_MANSE;	<u>Q8TII9</u> , VATD_METAC;
<u>Q60188</u> , VATD_METMA;	<u>O27034</u> , VATD_METTH;
<u>O59941</u> , VATD_NEUCR;	<u>Q9UXU9</u> , VATD_PYRAB;
<u>O57731</u> , VATD_PYRHO;	<u>O97755</u> , VATD_RABIT;
<u>P57747</u> , VATD_SUBDO;	<u>P62016</u> , VATD_SULAC;
<u>P62017</u> , VATD_SULTO;	<u>Q9HM63</u> , VATD_THEAC;
<u>Q97CP8</u> , VATD_THEVO;	<u>P32610</u> , VATD_YEAST;
<u>O29104</u> , VATE_ARCFU;	<u>O51123</u> , VATE_BORBU;
<u>O94072</u> , VATE_CANAL;	<u>Q9PK83</u> , VATE_CHLMU;
<u>O84312</u> , VATE_CHLTR;	<u>Q9SWE7</u> , VATE_CITLI;
<u>Q9RWH1</u> , VATE_DEIRA;	<u>O06501</u> , VATE_DESSY;
<u>P54611</u> , VATE_DROME;	<u>O23948</u> , VATE_GOSHI;
<u>Q48329</u> , VATE_HALVO;	<u>Q9U1G5</u> , VATE_HETSC;
<u>P31402</u> , VATE_MANSE;	<u>Q40272</u> , VATE_MESCR;
<u>Q57673</u> , VATE_METJA;	<u>Q8TWL9</u> , VATE_METKA;
<u>O27039</u> , VATE_METTH;	<u>P50518</u> , VATE_MOUSE;
<u>Q9UXU4</u> , VATE_PYRAB;	<u>Q8U4A9</u> , VATE_PYRFU;
<u>O13687</u> , VATE_SCHPO;	<u>Q41396</u> , VATE_SPIOL;
<u>Q9UWW5</u> , VATE_SULSO;	<u>Q971B8</u> , VATE_SULTO;
<u>P74901</u> , VATE_THET8;	<u>Q97CQ3</u> , VATE_THEVO;
<u>P22203</u> , VATE_YEAST;	<u>Q24583</u> , VATF1_DROME;
<u>Q9VNL3</u> , VATF2_DROME;	<u>Q17029</u> , VATF_ANOGA;
<u>O29102</u> , VATF_ARCFU;	<u>Q26029</u> , VATF_BOVIN;
<u>Q8XJW4</u> , VATF_CLOPE;	<u>O06503</u> , VATF_DESSY;
<u>Q9HNE2</u> , VATF_HALN1;	<u>Q48331</u> , VATF_HALVO;
<u>P31478</u> , VATF_MANSE;	<u>Q8TIJ2</u> , VATF_METAC;
<u>Q60185</u> , VATF_METMA;	<u>O27037</u> , VATF_METTH;
<u>Q9Y756</u> , VATF_NEUCR;	<u>Q9UXU6</u> , VATF_PYRAB;
<u>O57727</u> , VATF_PYRHO;	<u>P50408</u> , VATF_RAT;
<u>Q9HM66</u> , VATF_THEAC;	<u>P74903</u> , VATF_THET8;
<u>Q9I8H3</u> , VATF_XENLA;	<u>P39111</u> , VATF_YEAST;
<u>P79251</u> , VATG1_BOVIN;	<u>Q5WR09</u> , VATG1_CANFA;
<u>Q9CR51</u> , VATG1_MOUSE;	<u>Q862Z6</u> , VATG1_PANTR;
<u>O82629</u> , VATG2_ARATH;	<u>O95670</u> , VATG2_HUMAN;
<u>Q9TSV6</u> , VATG2_PIG;	<u>O82703</u> , VATG2_TOBAC;
<u>Q96LB4</u> , VATG3_HUMAN;	<u>P91303</u> , VATG_CAEEL;
<u>Q9XZH6</u> , VATG_DROME;	<u>Q25532</u> , VATG_MANSE;

<a href="#">O74174</a> , VATG_SCHPO;	<a href="#">P46836</a> , VATG_YEAST;
<a href="#">Q22494</a> , VATH2_CAEEL;	<a href="#">Q9LX65</a> , VATH_ARATH;
<a href="#">Q9V3J1</a> , VATH_DROME;	<a href="#">Q9UI12</a> , VATH_HUMAN;
<a href="#">Q9TVC1</a> , VATH_PIG;	<a href="#">O14265</a> , VATH_SCHPO;
<a href="#">O83444</a> , VATI1_TREPA;	<a href="#">O83544</a> , VATI2_TREPA
<a href="#">O29106</a> , VATI_ARCFU;	<a href="#">O51118</a> , VATI_BORBU;
<a href="#">Q9Z990</a> , VATI_CHLPN;	<a href="#">O84307</a> , VATI_CHLTR;
<a href="#">Q9HND8</a> , VATI_HALN1;	<a href="#">Q57675</a> , VATI_METJA;
<a href="#">O27041</a> , VATI_METTH;	<a href="#">Q9UXU2</a> , VATI_PYRAB;
<a href="#">Q9UWW3</a> , VATI_SULSO;	<a href="#">Q9HM61</a> , VATI_THEAC;
<a href="#">Q21898</a> , VATL1_CAEEL;	<a href="#">P25515</a> , VATL1_YEAST
<a href="#">P34546</a> , VATL2_CAEEL;	<a href="#">P32842</a> , VATL2_YEAST
<a href="#">O16110</a> , VATL_AEDAE;	<a href="#">Q17046</a> , VATL_ASCSU;
<a href="#">P68162</a> , VATL_BETVU;	<a href="#">P23956</a> , VATL_BOVIN;
<a href="#">P54642</a> , VATL_DICDI;	<a href="#">P23380</a> , VATL_DROME;
<a href="#">Q24810</a> , VATL_ENTHI;	<a href="#">Q43434</a> , VATL_GOSHI;
<a href="#">P27449</a> , VATL_HUMAN;	<a href="#">Q96473</a> , VATL_KALDA;
<a href="#">Q41773</a> , VATL_MAIZE;	<a href="#">P31403</a> , VATL_MANSE;
<a href="#">P63082</a> , VATL_MOUSE;	<a href="#">Q26250</a> , VATL_NEPNO;
<a href="#">Q40635</a> , VATL_ORYSA;	<a href="#">O22552</a> , VATL_PHAAU;
<a href="#">P63081</a> , VATL_RAT;	<a href="#">P50515</a> , VATL_SCHPO;
<a href="#">Q40585</a> , VATL_TOBAC;	<a href="#">Q03105</a> , VATL_TORMA;
<a href="#">Q91V37</a> , VATO_MOUSE;	<a href="#">O14046</a> , VATO_SCHPO;
<a href="#">P55717</a> , Y4YI_RHISN;	<a href="#">P40290</a> , YSCN_YEREN;

[View entry in original ENZYME format](#)

[All Swiss-Prot entries referenced in this entry](#), with possibility to download in different formats, align etc.

[All ENZYME/Swiss-Prot entries corresponding to 3.6.3.-](#)

[All ENZYME/Swiss-Prot entries corresponding to 3.6.-](#)

[All ENZYME/Swiss-Prot entries corresponding to 3.-](#)

 [ExPASy Home page](#)

[Site Map](#)

[Search ExPASy](#)

[Contact us](#)

[ENZYME](#)

[Swiss-Prot](#)

Hosted by  [NCSC](#)  
[US](#)

Mirror  
sites:

[Australia](#)

[Bolivia](#)

[Brazil](#)

[Canada](#)

[Korea](#)

[Switzerland](#)

[Taiwan](#)

## The Formation or the Reduction of a Disulfide Bridge on the $\gamma$ Subunit of Chloroplast ATP Synthase Affects the Inhibitory Effect of the $\epsilon$ Subunit\*

(Received for publication, March 12, 1998)

Toru Hisabori<sup>‡§</sup>, Ken Motohashi<sup>‡</sup>, Peter Kroth<sup>¶</sup>, Heinrich Strotmann<sup>¶</sup>, and Toyoki Amano<sup>‡</sup>

From the <sup>‡</sup>Research Laboratory of Resources Utilization, Tokyo Institute of Technology, Nagatsuta 4259, Midori-ku, Yokohama 226–8503, Japan and the <sup>¶</sup>Institut für Biochemie der Pflanzen, Heinrich-Heine Universität Düsseldorf, Universitätsstraße 1, D-40225 Düsseldorf, Germany

We have studied the change of the catalytic activity of chimeric complexes that were formed by chloroplast coupling factor 1 (CF<sub>1</sub>)  $\gamma$ ,  $\alpha$  and  $\beta$  subunits of thermophilic bacterial F<sub>1</sub> after formation or reduction of the disulfide bridge of different  $\gamma$  subunits modified by oligonucleotide-directed mutagenesis techniques. For this purpose, three mutant  $\gamma$  subunits were produced:  $\gamma_{\Delta 194-230}$ , here 37 amino acids from Pro-194 to Ile-230 are deleted,  $\gamma_{C199A}$ , Cys-199 is changed to Ala, and  $\gamma_{\Delta 200-204}$ , amino acids from Asp-200 to Lys-204 are deleted. All of the chimeric subunit complexes produced from each of these mutant CF<sub>1</sub>- $\gamma$  subunits and  $\alpha$  and  $\beta$  subunits from thermophilic bacterial F<sub>1</sub> lost the sensitivity against thiol reagents when compared with the complex containing wild-type CF<sub>1</sub>- $\gamma$ . The pH optimum (pH 8.5–9.0) and the concentration of methanol to stimulate ATPase activities were not affected by these mutations. These indicate that the introduction of the mutations did not change the main features of ATPase activity of the chimeric complex.

However, the interaction between  $\gamma$  subunit and  $\epsilon$  subunit was strongly influenced by the type of  $\gamma$  subunit itself. Although the ATPase activity of the chimeric complex that contained  $\gamma_{\Delta 200-204}$  or  $\gamma_{C199A}$  was inhibited by the addition of recombinant  $\epsilon$  subunit from CF<sub>1</sub> similarly to complexes containing the reduced wild-type  $\gamma$  subunit, the recombinant  $\epsilon$  subunit did not inhibit the ATPase of the complex, which contained the oxidized form of  $\gamma$  subunit. Therefore the affinity of the  $\epsilon$  subunit to the  $\gamma$  subunit may be dependent on the state of the  $\gamma$  subunit or the  $\epsilon$  subunit may bind to the oxidized form of  $\gamma$  subunit in a mode that does not inhibit the activity. The ATPase activity of the complex that contains  $\gamma_{\Delta 194-230}$  was not efficiently inhibited by  $\epsilon$  subunit. These results show that the formation or reduction of the disulfide bond on the  $\gamma$  subunit may induce a conformational change in the region that directly affects the interaction of this subunit with the adjacent  $\epsilon$  subunit.

F<sub>0</sub>F<sub>1</sub>-ATP synthase synthesizes ATP from ADP and P<sub>i</sub> at the expense of a proton-motive force (1–3). The enzymes consist of

the membrane-embedded sector F<sub>0</sub> responsible for proton translocation and the extrinsic catalytic part F<sub>1</sub>. The architecture of F<sub>1</sub> is very similar in various kinds of cells or organelles. The F<sub>1</sub> part is composed of five different subunits designated as  $\alpha$ ,  $\beta$ ,  $\gamma$ ,  $\delta$ , and  $\epsilon$ , and their molecular stoichiometry is 3:3:1:1:1. Nucleotide binding sites reside on each of the  $\alpha$  and  $\beta$  subunits, i.e. there are altogether 6 nucleotide binding sites per F<sub>1</sub>. The catalytic sites are located at the interfaces between  $\alpha$  and  $\beta$  subunits. The high resolution x-ray structure of bovine heart mitochondrial F<sub>1</sub> confirmed that most of the amino acid residues that form this site are provided from the  $\beta$  subunit (4). The  $\alpha$  and  $\beta$  subunits, which have a similar three-dimensional structure, alternate in a hexagonal arrangement around a central cavity containing the  $\gamma$  subunit as already expected from previous electron microscopic studies (5). The crystal structure of an  $\alpha_3\beta_3$  complex from the thermophilic *Bacillus* PS3 was completely symmetric (6), but the incorporation of the  $\gamma$  subunit into this complex induced a functional asymmetry among the three catalytic sites (7).

Rotation of the  $\gamma$  subunit related with catalysis was suggested from kinetic results (8), the exchange of a disulfide bridge formed between  $\gamma$  and  $\beta$  subunits (9), and polarization anisotropy relaxation measurement of the fluorophore-labeled  $\gamma$  subunit of chloroplast F<sub>1</sub> (CF<sub>1</sub>)<sup>1</sup> (10). Recently, Noji *et al.* (11) directly observed that this  $\gamma$  subunit rotates in the central cavity formed by  $\alpha$  and  $\beta$  subunits like a motor axis during the ATP hydrolysis reaction. This experiment clearly shows that the interaction between the part of coiled-coil of the  $\gamma$  subunit and the inner surface of the central cavity formed by  $\alpha$  and  $\beta$  subunits is not tight, and the interaction between the  $\gamma$  subunit and one of  $\alpha$  or  $\beta$  subunit can alternate step by step in one direction according to the catalytic reaction occurring sequentially at each of three catalytic sites.

The CF<sub>0</sub>CF<sub>1</sub>-ATP synthase of chloroplasts is regulated by the proton gradient, which activates the enzyme and by the reduction or the oxidation of a disulfide bridge in the  $\gamma$  subunit, which modulates activity. The latter regulation is known as thiol modulation (12). The structural basis for the thiol modulation is assigned to the sequence motif of 9 amino acids comprising two cysteines in the  $\gamma$  subunit (13). *In vitro* reduction can be achieved by dithiothreitol (DTT) or other dithiols, but the natural reductant is a reduced thioredoxin *f* (14), which was

\* This work was supported by grants from Yamada Science Foundation (Japan) (to T. H.), by a Grant-in-aid for Science Research (to T. H.) (08640822 and 09044209) from the Ministry of Education, Science, Sports and Culture of Japan, and by Deutsche Forschungsgemeinschaft (SFB 189) (to H. S.). The costs of publication of this article were defrayed in part by the payment of page charges. This article must therefore be hereby marked "advertisement" in accordance with 18 U.S.C. Section 1734 solely to indicate this fact.

§ To whom correspondence should be addressed. Tel.: 81-45-924-5234; Fax: 81-45-924-5277; E-mail: thisabor@res.titech.ac.jp.

<sup>1</sup> The abbreviations used are: CF<sub>1</sub>, chloroplast-coupling factor 1; DTT, dithiothreitol; CF<sub>1</sub>(- $\epsilon$ ), CF<sub>1</sub> with the  $\epsilon$  subunit removed; EF<sub>1</sub>, F<sub>1</sub> from the plasma membrane of *E. coli*; TF<sub>1</sub>, F<sub>1</sub> from the plasma membrane of thermophilic *Bacillus* PS3;  $\gamma_{\Delta 194-230}$ ,  $\gamma$  subunit of CF<sub>1</sub> with 37 amino acids from Pro-194 to Ile-230 deleted;  $\gamma_{C199A}$ ,  $\gamma$  subunit of CF<sub>1</sub> with Cys-199 changed to Ala;  $\gamma_{\Delta 200-204}$ ,  $\gamma$  subunit of CF<sub>1</sub> with the amino acids from Asp-200 to Lys-204 deleted;  $\gamma_c$  and  $\epsilon_c$ , recombinant  $\gamma$  and  $\epsilon$  subunits of CF<sub>1</sub> from spinach chloroplast; Tricine, N-[2-hydroxy-1,1-bis(hydroxymethyl)ethyl]glycine.

reduced by the photosynthetic electron transport chain via ferredoxin. Recently, Ross *et al.* (15) have succeeded in constructing a mutant  $\gamma$  subunit with one or two cysteines substituted by serine in the green algae *Chlamydomonas reinhardtii*. By these substitutions,  $CF_1$  became a DTT-insensitive enzyme. On the other hand, Gabrys *et al.* (16) selected a couple of mutants with chloroplast ATPase redox responses that were different from that of the wild-type plant by screening the *Arabidopsis* grown from the seeds that were previously treated with mutagen. They selected some mutant plants that might contain mutations within the  $\gamma$  subunit of  $CF_1$ .

The  $\epsilon$  subunit of  $CF_1$  is known as an intrinsic inhibitor protein. Recently, Cruz *et al.* (17, 18) produced recombinant mutant  $\epsilon$  subunits and tested their effects on the ATPase activity of  $\epsilon$ -deficient  $CF_1$  ( $CF_1(-\epsilon)$ ). They determined that the most important part of the  $\epsilon$  subunit as an inhibitor was the  $NH_2$ -terminal region. Similar experiments were reported for the  $\epsilon$  subunit of  $F_1$  from *Escherichia coli* ( $EF_1$ ) (19). These studies suggested that about 15 amino acid residues from the  $NH_2$  terminus were necessary for the inhibition. Wilkens *et al.* (20) reported the three-dimensional structure of the isolated  $\epsilon$  subunit from  $EF_1$  solved in solution by NMR spectroscopy. The structure shows that the  $NH_2$ -terminal 90 amino acids form so-called  $\beta$ -sandwich structure with two five-stranded  $\beta$  sheets. The C-terminal domain, on the other hand, is formed by two  $\alpha$ -helices. Recently, Uhlin *et al.* (21) solved the crystal structure of this subunit at 2.3 Å resolution. They confirmed the  $\beta$ -sandwich structure reported by Wilkens *et al.* (20) and found that the C-terminal two helices arranged in an anti-parallel coiled-coil structure. From the three-dimensional structure and cross-linking experiments employing cysteine mutants of  $\gamma$  and  $\epsilon$  subunits, it was concluded that the contact region of  $\epsilon$  subunit to  $\gamma$  subunit is at one side of the  $\beta$ -sandwich structure (20, 22).

The results of Capaldi and co-workers (20, 22) show that about 40 amino acids from the  $NH_2$  terminus of the  $\epsilon$  subunit, which form one-half of the  $\beta$ -sandwich structure, represent the region where the subunit is in direct contact with the  $\gamma$  subunit. Recently, Schulenberg *et al.* (23) also reported that the  $\epsilon$  subunit of  $CF_1$  can contact the  $\gamma$  subunit at the similar region. The characteristics of the interaction between  $\gamma$  subunit and  $\epsilon$  subunit of  $CF_1$  were investigated directly (24, 25) and indirectly (26). Andralojc and Harris (24) reported that the affinity of the  $\epsilon$  subunit to  $CF_1(-\epsilon)$  was decreased when the  $\gamma$  subunit of the complex was in a reduced state. From the inhibition of  $Ca^{2+}$ -ATPase activity, they estimated a  $K_d$  of 60 nM for the reduced  $CF_1(-\epsilon)$  and 0.14 nM for the oxidized one. Duhe and Selman (25) also reported a stimulation of dissociation of the  $\epsilon$  subunit from  $CF_1$  of *Chlamydomonas* in the presence of DTT. They suggested that the dissociation of the  $\epsilon$  subunit is an obligatory process in the DTT-induced unmasking of ATPase activity of soluble  $CF_1$ . Soteropoulos *et al.* (26) reported an activation of  $CF_1$ -ATPase by dilution of the enzyme. For the reduced  $CF_1$ , a half-maximal activation was obtained at a much lower dilution than with oxidized  $CF_1$ , and they estimated that the affinity for the  $\epsilon$  subunit would be decreased about 20-fold by the reduction of  $CF_1$ .

Recently, we reported on the reconstitution of a chimeric complex from recombinant  $\alpha$  and  $\beta$  subunits from  $F_1$  of the thermophilic *Bacillus* PS3 ( $TF_1$ ) and the recombinant  $\gamma$  subunit ( $\gamma_c$ ) from spinach  $CF_1$  (27). The complex had substantial ATPase activity and this activity was affected by the disulfide/dithiol state of the two regulatory cysteine residues on the  $\gamma$  subunits. That means that  $\gamma_c$  imposed redox control on the chimeric complex. Furthermore, the activity of the chimeric complex was suppressed by the addition of recombinant  $\epsilon$  subunit from  $CF_1$  ( $\epsilon_c$ ), but not by the addition of the  $\epsilon$  subunit from

$TF_1$ . These results suggest that the regulatory functions of  $\gamma$  and  $\epsilon$  subunits of  $CF_1$  may be linked to each other.

Here, we prepared three modified  $\gamma$  subunits of  $CF_1$  by oligonucleotide-directed mutagenesis. We investigated the effects of the mutations on the enzyme activity and its regulation in chimeric complexes formed by these  $\gamma$  subunits,  $\epsilon_c$ , and  $\alpha_3\beta_3$  from  $TF_1$ . We found the region around the disulfide bridge of the  $\gamma$  subunit to be important for the regulatory interaction between the  $\gamma$  subunit and  $\epsilon$  subunit.

#### EXPERIMENTAL PROCEDURES

**Materials**—Restriction endonucleases were obtained from Toyobo Inc., Tokyo, Japan. The Bradford protein assay system was from Bio-Rad. Urea was purchased from Nacalai Tesque, Kyoto, Japan. DTT was from Sigma. Other chemicals were the highest grade commercially available.

**Construction of the Plasmids for the Mutant  $\gamma_c$  and Their Expression**—Recombinant plasmids carrying the gene for the  $\gamma$  subunit from spinach plastids (*atpC*) was previously constructed (27). Oligonucleotide-directed mutagenesis was carried out as described by Kunkel *et al.* (28). The oligonucleotide used to create the  $\gamma_c$  with the additional amino acid stretch of the  $\gamma$  subunit of  $CF_1$  (from Pro-194 to Ile-230) deleted ( $\gamma_{194-230}$ ) was: 5'-ATCCACACCCCTACTCCCTTAAGAAAAACCGAAACACAGCATT-3'. The one used to create the  $\gamma_c$  with Cys-199 changed to Ala ( $\gamma_{C199A}$ ) was: 5'-ACCCTACTCCCTTAAGACCCAAAGAGAAATTGCGGACATCAATGGAAAA-3'. To create  $\gamma_c$  with the amino acid sequence from Asp-200 to Lys-204 deleted ( $\gamma_{200-204}$ ), the following oligonucleotide was used: 5'-ACCCTACTCCCTTAAGACCCAAA-GGAGAAATTTGCTGTGTCGACGACGACAGAA-3'. Each of the genes was transferred to the expression vector pET23d (Novagen) and was transformed into the expression host *E. coli* strain BL21(DE3). Each of the  $\gamma_c$  proteins was expressed yielding inclusion bodies and further purified by the methods described previously (27).

**Expression and Purification of the Recombinant  $\epsilon_c$** —The plasmid pSocB149 (28), which contains the gene for the subunit  $\epsilon$  of  $CF_1$  from spinach ( $\epsilon_c$ ) was a generous gift from Dr. Whitfield, R. P., Australia. The expression plasmid for  $\epsilon_c$  was constructed according to the method described by Hisabori *et al.* (27) and transformed into *E. coli* strain BL21(DE3).  $\epsilon_c$  was over-expressed by the method used for  $\gamma_c$ . The  $\epsilon_c$  inclusion bodies were first dissolved by the addition of 8 M urea, 40 mM Tris-Cl (pH 8.0), 0.4 mM DTT, and 0.8 mM EDTA and further purified by the method described previously (27).

**Preparation of  $\alpha$  and  $\beta$  Subunits of  $TF_1$** —The recombinant  $\alpha$  and  $\beta$  subunits of  $TF_1$  were expressed in *E. coli* strain DK8 (*bglR*, *thi-1*, *rel-1*, *HfrPO1*,  $\Delta(uncB-uncC)ilv::Tn10$ ) and purified as described previously (30, 31).

**Reconstitution of the Chimeric Subunit Complex**—Reconstitution of the chimeric subunit complex was formed by the same method described previously (27). Briefly, each of the isolated  $\gamma_c$  subunits was mixed with the  $\alpha$  and  $\beta$  subunits from  $TF_1$  in a ratio of 1:1:1 (w/v), and a solution containing 8 M urea, 1 mM EDTA, 0.5 mM DTT, and 40 mM Tris-Cl (pH 8.0) was added to yield a final urea concentration of 4 M. The solution was then dialyzed against 50 mM Tris-HCl (pH 8.0), 200 mM NaCl, 0.4 mM  $MgCl_2$ , and 0.4 mM ATP at 20 °C for 3 h. After the dialysis, the unsolved  $\gamma_c$  subunits were removed from the solution by centrifugation and provided for the measurement of ATPase activity.

**Activation and Deactivation of the Complex and the Measurement of ATPase Activity**—To activate or deactivate the  $\alpha_3\beta_3\gamma_c$  complexes by the formation or reduction of disulfide bridge on the  $\gamma$  subunit, formed complexes were incubated in the presence of 2 mM DTT or 50  $\mu$ M  $CuCl_2$  for 2 h at 30 °C. Then 10  $\mu$ l of the complex solution (normally containing 2–3  $\mu$ g of protein) was added to 90  $\mu$ l of the reaction mixture containing 50 mM Tricine-KOH (pH 8.0), 2 mM ATP, and 2 mM  $MgCl_2$  to initiate the reaction. The reaction was continued for 5–10 min, and then terminated by the addition of 100  $\mu$ l of ice-cold 2.4% (v/v) perchloric acid. The amounts of liberated  $P_i$  were measured by a colorimetric method. Since the ATPase activity was measured by the mixture of the chimeric complex and the monomer proteins, which were not incorporated into the complex, the specific activity of the ATPase was calculated based on the amounts of  $\alpha$  plus  $\beta$  subunits that were used for the formation of the complex.

#### RESULTS AND DISCUSSION

**Responses of the Chimeric Complexes Containing Mutant  $\gamma_c$  to Oxidation/Reduction**—In comparison to the  $\gamma$  subunit from thermophilic bacteria, the  $\gamma$  subunit of  $CF_1$  contains a stretch of



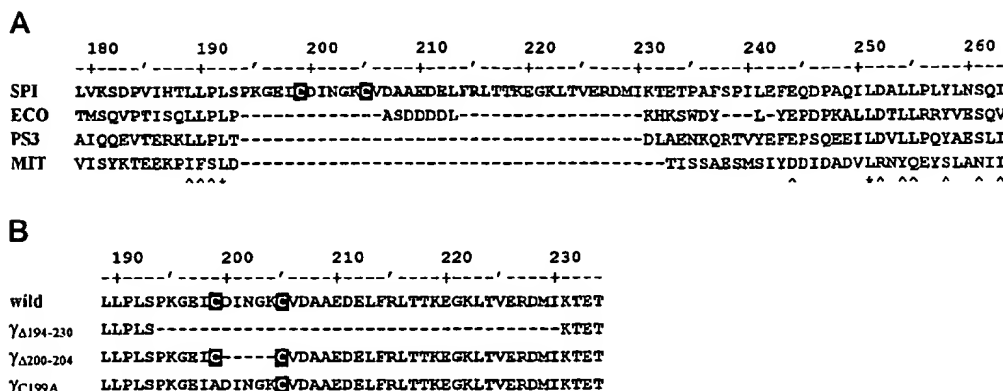


Fig. 1. Partial amino acid alignments of  $\gamma$  subunits. A, alignment of the protein sequences of the  $\gamma$  subunits of  $F_1$  complexes from spinach chloroplast (SPI) (13), *E. coli* (ECO) (38, 39), thermophilic *Bacillus* PS3 (PS3) (29), and bovine heart mitochondria (MIT) (40) was made by computer program CLUSTALW (41). The positions that are identical in three of the four sequences are marked by “^” and the identical positions in all of the sequences are marked by “\*”. Gaps are marked by broken lines. Two cysteines (Cys-199 and Cys-204), which form the disulfide bridge, were shown as reversed capitals. Only the sequences from Leu-179 to Ile-263 of spinach  $CF_1$ - $\gamma$  subunit and the corresponding region of others are shown. B, the sequences from Leu-189 to Thr-234 of spinach  $CF_1$ - $\gamma$  subunit are demonstrated. Three mutants, designated as  $\gamma_{\Delta 194-230}$ ,  $\gamma_{\Delta 200-204}$ , and  $\gamma_{C199A}$  were engineered and expressed in *E. coli*. Amino acid positions that have been deleted are shown as broken lines.

an additional 37 amino acids comprising the two cysteines (Cys-199 and Cys-205), which are responsible for the thiol modulation (Fig. 1A). To characterize the differences of the properties between bacterial  $\gamma$  and chloroplast  $\gamma$ , we designed three mutations of the  $\gamma$  subunit of  $CF_1$ . These were  $\gamma_{\Delta 194-230}$ , which is lacking the  $CF_1$ - $\gamma$  specific additional amino acid stretch (see Fig. 1B),  $\gamma_{\Delta 200-204}$ , in which the space between the two regulatory cysteines is shortened, and  $\gamma_{C199A}$ , which cannot form the disulfide bridge involved in thiol modulation. The complexes containing those mutant  $\gamma_c$  subunits were not supposed to show any responses against oxidation/reduction. As shown in Fig. 2, the ATPase activity of these chimeric complexes was not altered by the incubation with DTT or with  $CuCl_2$ , although the ATPase activity of the complex containing wild-type  $\gamma_c$  was remarkably stimulated by the incubation with DTT and suppressed by the incubation with  $CuCl_2$  as reported previously (27).

For further characterization of the mutant  $\gamma$  subunits, some properties of the chimeric complexes were investigated. First, we measured the pH dependence of the ATPase activity of the complexes. We could not find any change of pH dependence of ATPase activity; all four kinds of complexes showed the same pH profiles (data not shown), indicating that the property of the catalytic sites did not change by the mutation of  $\gamma_c$  subunit. Also the optimal pH (pH 8.5–9.0) was the same as that found for the authentic  $TF_1$  (32) or  $CF_1$  (33).

**Methanol Activation of the ATPase Activity of the Chimeric Subunit Complexes**—Methanol stimulation of ATPase activity is one of the unique features of isolated (33, 34) and membrane-bound  $CF_1$  (35). In a previous report, we found that the incorporation of the  $\gamma$  subunit from  $CF_1$  into the bacterial  $\alpha_3\beta_3$  hexagon conferred the property of methanol stimulation of the ATPase to the complex, whereas the  $\alpha_3\beta_3\gamma$  complex formed by the bacterial subunits only is insensitive against methanol (27). As shown in Fig. 3, the ATPase activities of all four chimeric complexes were stimulated by the addition of methanol and optimal concentrations of methanol were 25% (v/v). The most remarkable difference between the  $\gamma$  subunit from thermophilic bacteria and the  $\gamma$  subunit of  $CF_1$  is the occurrence of an intercalated amino acid stretch of more than 30 amino acids in  $CF_1$ - $\gamma$  (Fig. 1A). One may expect that the region that senses methanol would be located in this additional stretch. However, when the mutant  $\gamma$  subunit, which is lacking in this region, was used to form the chimeric complex, the methanol sensitivity was the same as for the complex that contained the wild-type  $\gamma$

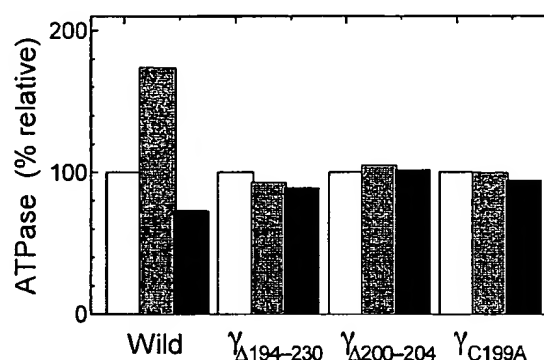


Fig. 2. Change of the ATPase activity of the chimeric  $\alpha_3\beta_3\gamma_c$  complexes by incubation with DTT or  $CuCl_2$ . The chimeric complex was reconstituted from 500  $\mu$ g of  $\gamma_c$ ,  $\alpha$  subunit, and  $\beta$  subunit according to the method described under “Experimental Procedures.” Then each of the complexes was incubated with 2 mM DTT (■) or 50  $\mu$ M  $CuCl_2$  (■) for 2 h at 30 °C, and their ATPase activities were measured. The ATPase activity ( $\mu$ mol  $P_i$  released/mg  $\alpha + \beta$ /min) of each of the complexes that were not treated with DTT or  $CuCl_2$  (□) was 0.672 with wild-type  $\gamma$ , 0.254 with  $\gamma_{\Delta 194-230}$ , 0.557 with  $\gamma_{\Delta 200-204}$ , and 0.534 with  $\gamma_{C199A}$ , and set as 100%.

subunit. Therefore, the methanol sensitivity of  $CF_1$ - $\gamma$  subunit must be attributed to some other portion of the protein.

**Inhibitory Effects of the  $\epsilon$  Subunit**—The  $\epsilon$  subunit of  $F_1$  is an intrinsic ATPase inhibitor. However, this subunit may also be involved in  $H^+$  coupling of the ATPase (36). Recently, Cruz *et al.* (17, 18) expressed the mutant  $\epsilon$  subunit of  $CF_1$  in *E. coli* and investigated their inhibitory effects on the  $CF_1$ ( $-\epsilon$ ). Similar deletion experiments were carried out for  $EF_1$  by Jounouchi *et al.* (19). They reported that the deletion of the  $NH_2$ -terminal 16 amino acids is strongly affecting the coupling between ATP hydrolysis and  $H^+$  translocation, but  $F_1$  with an  $\epsilon$  subunit lacking the 15 amino-terminal residues could bind to  $F_0$  in a functionally competent manner. However, Cruz *et al.* (17) found that the deletions of 6 amino acids from the C terminus or the deletions of 11 amino acids from the  $NH_2$  terminus decreased the inhibitory effect of this subunit on the ATPase of  $CF_1$ .

The  $Mg^{2+}$ -ATPase activity of the oxidized form of  $CF_1$  is quite low or almost zero. However, the chimeric complex displayed remarkable  $Mg^{2+}$ -ATPase activity even in its oxidized form. Therefore it was possible to investigate the interaction between the  $\epsilon$  and  $\gamma$  subunits under the reduced and oxidized

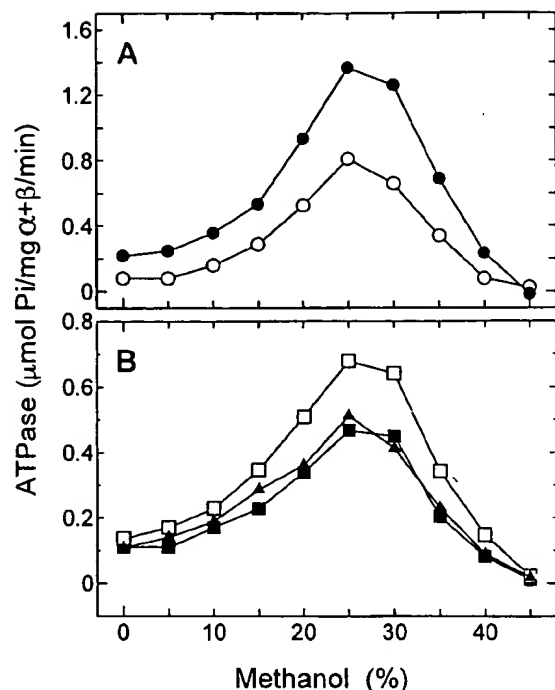


FIG. 3. Methanol dependence of the ATPase activity of the chimeric  $\alpha_3\beta_3\gamma_\epsilon$  complex. The chimeric complex was reconstituted from 500  $\mu$ g of  $\gamma_\epsilon$ , 500  $\mu$ g of  $\alpha$  subunit, and 500  $\mu$ g of  $\beta$  subunit according to the method described under "Experimental Procedures." A, the complexes with the wild-type  $\gamma$  subunit were formed and then incubated with 2 mM DTT (●) or 50  $\mu$ M  $CuCl_2$  (○) for 2 h at 30 °C, and their ATPase activities were measured under the various concentrations of methanol indicated in the figure. B, the chimeric complexes with (■)  $\gamma_{\Delta 194-230}$ , (▲)  $\gamma_{\Delta 200-204}$ , and (□)  $\gamma_{C199A}$  were formed, and their ATPase activities were measured.

conditions by measuring the inhibition of the ATPase. Surprisingly, the ATPase activity was less inhibited by the  $\epsilon$  subunit in the chimeric complex with the oxidized  $\gamma$  subunit than with the reduced  $\gamma$  subunit (Fig. 4A) (27). The addition of methanol reduced the inhibitory effect of  $\epsilon_\epsilon$  for both the reduced and oxidized state complexes, indicating the stimulation effect of methanol on  $CF_1$ -ATPase can be partially attributed to the release of the  $\epsilon$  subunit from the enzyme. A change of the responses of  $CF_1$  against the  $\epsilon$  subunit under the reduced or oxidized condition were already reported by Andralojc and Harris (24), Duhe and Selman (25), and Soteropoulos *et al.* (26). Andralojc and Harris (24) investigated the inhibition of  $Ca^{2+}$ -ATPase activity. By adding the various amounts of isolated  $\epsilon$  subunit to  $CF_1(-\epsilon)$ , they concluded that the oxidized  $CF_1(-\epsilon)$  has a higher affinity for the isolated  $\epsilon$  subunit than the reduced enzyme. Soteropoulos *et al.* (26) diluted  $CF_1$  solution to nanomolar concentration and found a difference of the activation ratio by oxidation/reduction. Activation by dilution occurred for the reduced enzyme at higher than for the reduced enzyme. From their results, they concluded that the affinity of the  $\epsilon$  subunit to the reduced  $CF_1$  is about 20-fold lower than to the oxidized one.

It is difficult to explain why the apparent affinity of the  $\epsilon$  subunit to the chimeric complex is lower when the  $\gamma$  subunit is in the oxidized state. Possibly the origin of the  $\alpha_3\beta_3$  hexamer influences the interaction, too. On the other hand, we cannot be sure that the  $\gamma_\epsilon$  really has the same conformation in the chimeric complex as the authentic  $CF_1$ .

**Relation between the Conformation of the  $\gamma$  Subunit and the Effect of the  $\epsilon$  Subunit**—If the additional amino acid stretch observed only on  $CF_1$  is responsible for the interaction between

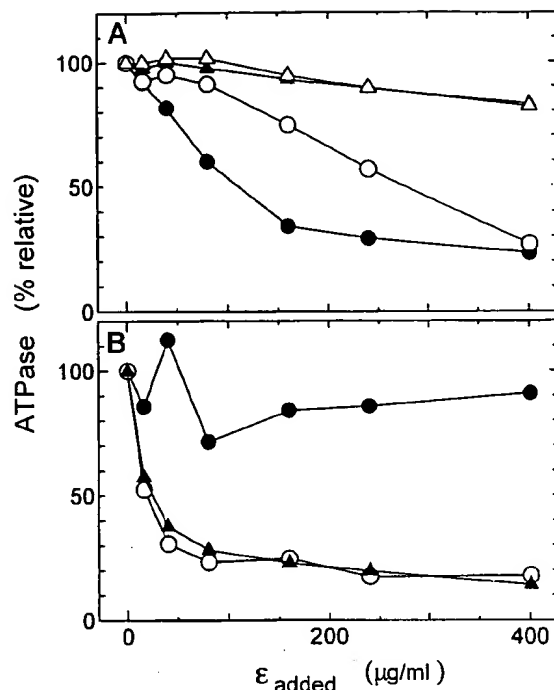


FIG. 4. The effects of  $\epsilon_\epsilon$  on the activity of the  $\alpha_3\beta_3\gamma_\epsilon$  complexes. A, the chimeric complex was formed the same way as described in the legend for Fig. 2. 100  $\mu$ g/ml of the reduced (closed symbols) or the oxidized (open symbols) complex was incubated with the indicated amounts of  $\epsilon_\epsilon$  for 1 h at room temperature. The ATPase activity of the complex was measured for 5 to 10 min in the absence (circle) or presence (triangle) of 20% methanol. B, the chimeric complexes with three kinds of mutant  $\gamma$  subunit were formed the same way as described in the legend for Fig. 2. 100  $\mu$ g/ml of each of the complexes containing  $\gamma_{\Delta 194-230}$  (●),  $\gamma_{\Delta 200-204}$  (▲), and  $\gamma_{C199A}$  (○) was incubated with the indicated amounts of  $\epsilon_\epsilon$  for 1 h at room temperature, and the ATPase activity of the complex was measured.

the  $\gamma$  and  $\epsilon$  subunits, a mutation of this segment might affect the inhibition of ATPase by the  $\epsilon$  subunit. The sensitivity of the complexes that contain  $\gamma_{C199A}$  or  $\gamma_{\Delta 200-204}$  against the  $\epsilon$  subunit was the same as that of the complex with the reduced form of the  $\gamma$  subunit (Fig. 4B), although we expected that the conformation of  $\gamma_{\Delta 200-204}$  was similar to the oxidized-form of the  $\gamma$  subunit.

On the other hand, the complex that contains  $\gamma_{\Delta 194-230}$  was not inhibited by the addition of the  $\epsilon$  subunit. From the report of Capaldi and co-workers (20, 22), the contact region between the  $\epsilon$  and  $\gamma$  subunits is located around 40 amino acids from the  $NH_2$  terminus of the  $\epsilon$  subunit. The chemical cross-linking experiments carried out by using cross-linker-labeled  $\epsilon$  subunit and  $CF_1(-\epsilon)$  gave the same conclusion (23). The contact region on the  $\gamma$  subunit is very close to the position where the additional amino acid stretch is intercalated in  $CF_1-\gamma$  (13) (see Fig. 1A). Hence, the structure of this additional amino acid stretch might be very important not only for the redox regulation but also for the interaction between the  $\gamma$  and  $\epsilon$  subunits.

Ross *et al.* (37) reported that mutation of the spacer region between the two regulatory cysteines (GEICD(K or A)VDGK-(D)CVDAA) diminished redox regulation of  $CF_1$  from *Chlamydomonas*. They used *C. reinhardtii* strain *atpC1*, which lacks the gene for the  $\gamma$  subunit, and complemented the photophosphorylation activity with mutated  $\gamma$  subunit genes. Thylakoid vesicles prepared from the mutant strain containing  $\gamma_{D199K/K203D}$  or  $\gamma_{D199A}$  did not show a remarkable change of the photophosphorylation in the presence or the absence of DTT. Accordingly the authors concluded that the spacer region be-

tween the disulfide bridge is also involved in redox regulation of  $CF_1$ . This result corresponds with our result concerning  $\gamma_{\Delta 200-204}$ . Although  $\gamma_{\Delta 200-204}$  still contains the two cysteines, the complex with this subunit did not show any difference in activity by incubation with DTT or  $CuCl_2$ , respectively (Fig. 2). Apart from this all other properties of ATPase of this complex were the same as those of the wild type. This complex appeared to have an affinity for  $\epsilon$  subunit because the ATPase of this complex was strongly inhibited by the addition of  $\epsilon_c$  subunit (Fig. 4B).

Hence, our results strongly suggest that the change in the conformation that occurred at the lower part of the  $\gamma$  subunit is drastic enough to affect the binding of the  $\epsilon$  subunit to this subunit, although the point that is different from the results of Ross *et al.* (37) as mentioned above should be further investigated.

**Acknowledgments**—We thank Prof. R. G. Herrmann for providing us with a cloned gene for the  $\gamma$  subunit of spinach  $CF_1$  (*atpC* gene), Dr. S. Werner-Grüne for preparing the *atpC* gene without transit sequence, and Dr. P. R. Whitfeld for providing us with a cloned gene for the  $\epsilon$  subunit of spinach  $CF_1$  (pSocB149). We also thank K. Saika, Dr. M.-H. Sato, and Dr. H. Noji for technical assistance. Thanks to F. Motojima for providing us with the excellent program "Motojiman" to design the appropriate primer for the mutagenesis. Special thanks to Prof. M. Yoshida for helpful discussion.

## REFERENCES

1. Futai, M., and Kanazawa, H. (1983) *Microbiol. Rev.* **47**, 285–312
2. Strotmann, H., and Bickel-Sandkötter, S. (1984) *Annu. Rev. Plant Physiol.* **35**, 97–120
3. Senior, A. E. (1990) *Annu. Rev. Biophys. Chem.* **19**, 7–41
4. Abrahams, J. P., Leslie, A. G. W., Lutter, R., and Walker, J. E. (1994) *Nature* **370**, 621–628
5. Gogol, E. P., Aggeler, R., Sagermann, M., and Capaldi, R. A. (1989) *Biochemistry* **28**, 4717–4724
6. Shirakihara, Y., Leslie, A. G., Abrahams, J. P., Walker, J. E., Ueda, T., Sekimoto, Y., Kambara, M., Saika, K., Kagawa, Y., and Yoshida, M. (1997) *Structure (Lond.)* **15**, 825–836
7. Kaubara, C., Matsui, T., Hisabori, T., and Yoshida, M. (1996) *J. Biol. Chem.* **271**, 2433–2438
8. Boyer, P. D. (1993) *Biochim. Biophys. Acta* **1098**, 215–250
9. Duncan, T. M., Bulygin, V. V., Zhou, Y., Hutcheon, M. L., and Cross, R. L. (1995) *Proc. Natl. Acad. Sci. U. S. A.* **92**, 10964–10968
10. Sabbert, D., Engelbrecht, S., and Junge, W. (1996) *Nature* **381**, 623–625
11. Noji, H., Yasuda, R., Kinoshita, K., Jr., and Yoshida, M. (1997) *Nature* **388**, 299–302
12. Nalin, C. M., and McCarty, R. E. (1984) *J. Biol. Chem.* **259**, 7275–7280
13. Miki, J., Maeda, M., Mukohata, Y., and Futai, M. (1988) *FEBS Lett.* **232**, 221–226
14. Schwarz, O., Schürmann, P., and Strotmann, H. (1997) *J. Biol. Chem.* **272**, 16924–16927
15. Ross, S. A., Zhang, M. X., and Selman, B. R. (1995) *J. Biol. Chem.* **270**, 9813–9818
16. Gabrys, H., Kramer, D. M., Crofts, A. R., and Ort, D. R. (1994) *Plant Physiol.* **104**, 769–776
17. Cruz, J. A., Harfe, B., Radkowski, C. A., Dann, M. S., and McCarty, R. E. (1995) *Plant Physiol.* **109**, 1379–1388
18. Cruz, J. A., Radkowski, C. A., and McCarty, R. E. (1997) *Plant Physiol.* **113**, 1185–1192
19. Jounouchi, M., Takeyama, M., Noumi, T., Maeda, M., and Futai, M. (1992) *Arch. Biochem. Biophys.* **292**, 87–94
20. Wilkens, S., Dahlquist, F. W., McIntosh, L. P., Donaldson, L. W., and Capaldi, R. A. (1995) *Nat. Struct. Biol.* **2**, 961–967
21. Uhlin, U., Cox, G. B., and Guss, J. M. (1997) *Structure (Lond.)* **15**, 1219–1230
22. Tang, C., and Capaldi, R. A. (1996) *J. Biol. Chem.* **271**, 3018–3024
23. Schulerberg, B., Wellmer, F., Lill, H., Junge, W., and Engelbrecht, S. (1997) *Eur. J. Biochem.* **249**, 134–141
24. Andralojc, P. J., and Harris, D. A. (1990) *Biochim. Biophys. Acta* **1016**, 55–62
25. Duhe, R. J., and Selman, B. R. (1990) *Biochim. Biophys. Acta* **1017**, 70–78
26. Soteropoulos, P., Suss, K. H., and McCarty, R. E. (1992) *J. Biol. Chem.* **267**, 10348–10354
27. Hisabori, T., Kato, Y., Motohashi, K., Strotmann, H., Kroth-Pancic, P., and Amano, T. (1997) *Eur. J. Biochem.* **247**, 1158–1165
28. Kunkel, T. A., Bebenk, K., and McClary, J. (1991) *Methods Enzymol.* **204**, 125–139
29. Munn, A. L., Whitfeld, P. R., Bottomley, W., Hudson, G. S., Jans, D. A., Gibson, F., and Cox, G. B. (1991) *Biochim. Biophys. Acta* **1060**, 82–88
30. Ohta, S., Yohda, M., Ishizuka, M., Hirata, H., Hamamoto, T., Otawara-Hamamoto, Y., Matsuda, K., and Kagawa, Y. (1988) *Biochim. Biophys. Acta* **933**, 141–155
31. Ohtsubo, M., Yoshida, M., Ohta, S., Kagawa, Y., Yohda, M., and Date, T. (1987) *Biochem. Biophys. Res. Commun.* **146**, 705–710
32. Yoshida, M., Sone, N., Hirata, H., and Kagawa, Y. (1977) *J. Biol. Chem.* **252**, 3348–3485
33. Sakurai, H., Shinohara, K., Hisabori, T., and Shinohara, K. (1981) *J. Biochem. (Tokyo)* **90**, 95–102
34. Selman-Reimer, S., Merchant, S., and Selman, B. R. (1981) *Biochemistry* **20**, 5476–5482
35. Anthon, G. E., and Jagendorf, A. T. (1984) *Biochim. Biophys. Acta* **723**, 358–365
36. Zhang, Y., Oldenburg, M., and Fillingame, R. H. (1994) *J. Biol. Chem.* **269**, 10221–10224
37. Ross, S. A., Zhang, M. X., and Selman, B. R. (1996) *J. Bioenerg. Biomembr.* **28**, 49–57
38. Kanazawa, H., Kayano, T., Mabuchi, K., and Futai, M. (1981) *Biochem. Biophys. Res. Commun.* **103**, 604–612
39. Saraste, M., Gay, N. J., Eberle, A., Runswick, M. J., and Walker, J. E. (1981) *Nucleic Acids Res.* **9**, 5287–5296
40. Walker, J. E., Fearnley, I. M., Gay, N. J., Gibson, B. W., Northrop, F. D., Powell, S. J., Runswick, M. J., Saraste, M., and Tybulewicz, V. L. J. (1985) *J. Mol. Biol.* **184**, 677–701
41. Thompson, J. D., Higgins, D. G., and Gibson, T. J. (1994) *Nucleic Acids Res.* **22**, 4673–4680

Eur J Biochem. 1997 Aug 1;247(3):1158-65.

[Related Articles, Links](#)

**The regulatory functions of the gamma and epsilon subunits from chloroplast CF1 are transferred to the core complex, alpha3beta3, from thermophilic bacterial F1.**

**Hisabori T, Kato Y, Motohashi K, Kroth-Pancic P, Strotmann H, Amano T.**

Research Laboratory of Resources Utilization, Tokyo Institute of Technology, Yokohama, Japan.  
[thisabor@res.titech.ac.jp](mailto:thisabor@res.titech.ac.jp)

The expression plasmids for the subunit gamma (gamma(c)) and the subunit epsilon (epsilon(c)) of chloroplast coupling factor (CF1) from spinach were constructed, and the desired proteins were expressed in *Escherichia coli*. Both expressed subunits were obtained as inclusion bodies. When recombinant gamma(c) was mixed with recombinant alpha and beta subunits of F1 from thermophilic *Bacillus PS3* (TF1), a chimeric subunit complex (alpha3beta3gamma(c)) was reconstituted and it showed significant ATP hydrolysis activity. The ATP hydrolysis activity of this complex was enhanced in the presence of dithiothreitol and suppressed by the addition of CuCl<sub>2</sub>, which induces formation of a disulfide bond between two cysteine residues in gamma(c). Hence, this complex has similar modulation characteristics as CF1. The effects of recombinant epsilon(c) and epsilon subunit from TF1 (epsilon(t)) on alpha3beta3gamma(c) were also investigated. Epsilon(c) strongly inhibited the ATP hydrolysis activity of chimeric alpha3beta3gamma(c) complex but epsilon(t) did not. The inhibition was abolished and the ATP hydrolysis activity was recovered when methanol was added to the assay medium. The addition of epsilon(c) or epsilon(t) to the alpha3beta3gamma(t) complex, which is the authentic subunit complex from TF1, resulted in weak stimulation of the ATP hydrolysis activity. These results suggest that (a) the specific regulatory function of gamma(c) can be transferred to the bacterial subunit complex; (b) the interaction between the gamma(c) subunit and epsilon(c) strongly affects the enzyme activity, which was catalyzed at the catalytic sites that reside on the alpha3beta3 core.

PMID: 9288943 [PubMed - indexed for MEDLINE]

Mol Cell Biochem. 1984;60(1):33-71.

Related Articles, Links

**Recent developments on structural and functional aspects of the F1 sector of H<sup>+</sup>-linked ATPases.****Vignais PV, Satre M.**

This review concerns the catalytic sector of F1 factor of the H<sup>+</sup>-dependent ATPases in mitochondria (MF1), bacteria (BF1) and chloroplasts (CF1). The three types of F1 have many similarities with respect to the structural parameters, subunit composition and catalytic mechanism. An alpha 3 beta 3 gamma delta epsilon stoichiometry is now accepted for MF1 and BF1; the alpha 2 beta 2 gamma 2 delta 2 epsilon 2 stoichiometry for CF1 remains as matter of debate. The major subunits alpha, beta and gamma are equivalent in MF1, BF1 and CF1; this is not the case for the minor subunits delta and epsilon. The delta subunit of MF1 corresponds to the epsilon subunit of BF1 and CF1, whereas the mitochondrial subunit equivalent to the delta subunit of BF1 and CF1 is probably the oligomycin sensitivity conferring protein (OSCP). The alpha beta gamma assembly is endowed with ATPase activity, beta being considered as the catalytic subunit and gamma as a proton gate. On the other hand, the delta and epsilon subunits of BF1 and CF1 most probably act as links between the F1 and F0 sectors of the ATPase complex. The natural mitochondrial ATPase inhibitor, which is a separate protein loosely attached to MF1, could have its counterpart in the epsilon subunit of BF1 and CF1. The generally accepted view that the catalytic subunit in the different F1 species is beta comes from a number of approaches, including chemical modification, specific photolabeling and, in the case of BF1, use of mutants. The alpha subunit also plays a central role in catalysis, since structural alteration of alpha by chemical modification or mutation results in loss of activity of the whole molecule of F1. The notion that the proton motive force generated by respiration is required for conformational changes of the F1 sector of the H<sup>+</sup>-ATPase complex has gained acceptance. During the course of ATP synthesis, conversion of bound ADP and Pi into bound ATP probably requires little energy input; only the release of the F1-bound ATP would consume energy. ADP and Pi most likely bind at one catalytic site of F1, while ATP is released at another site. This mechanism, which underlines the alternating cooperativity of subunits in F1, is supported by kinetic data and also by the demonstration of partial site reactivity in inactivation experiments performed with selective chemical modifiers. One obvious advantage of the alternating site mechanism is that the released ATP cannot bind to its original site. (ABSTRACT TRUNCATED AT 400 WORDS)

**Publication Types:**

- Review

Mol Microbiol. 1989 Jul;3(7):851-9.

Related Articles, Links

**Independent and coupled translational initiation of atp genes in Escherichia coli: experiments using chromosomal and plasmid-borne lacZ fusions.****Gerstel B, McCarthy JE.**

Department of Microbiology, GBF--Gesellschaft für Biotechnologische Forschung mbH, Braunschweig, FRG.

The translational initiation rates directed by the translational initiation regions (TIRs) of the atpB, atpH, atpA and atpG genes of Escherichia coli were investigated using lacZ fusions present on plasmids as well as integrated into the chromosome. This was the first investigation of the translational efficiency of the atpB gene, whose unfused product (subunit a) can be toxic to the cell. The specific mRNA levels, rates of in vivo protein synthesis and beta-galactosidase activities encoded by the atp::lacZ fusions were compared in order to obtain valid estimates of relative translation rates. The results indicate that in the E. coli atp operon, translation directed by the atpB, atpH and atpG TIRs is less efficient than that directed by the atpA TIR, and are thus consistent with earlier measurements of direct atp gene expression. Initiation is, however, to differing extents, controlled by coupling to the translation of upstream neighbours. There is particularly tight coupling between atpH and atpA. Increasing the distance between these two genes whilst maintaining the original atpA TIR structure decreased the degree of coupling. The influence of manipulations of the atpG TIR structure upon translational efficiency was quantitatively more pronounced when the atpG fusions were present as a single copy per chromosome. This is likely to be related to the mRNA binding characteristics of 30S ribosomal subunits and/or to the influence of other (trans-acting) factors. The control of independent and coupled initiation at the atp TIRs is discussed in relation to mRNA structure and possible cis and trans regulatory phenomena.

PMID: 2529415 [PubMed - indexed for MEDLINE]

J Bioenerg Biomembr. 1988 Feb;20(1):19-39.

[Related Articles, Links](#)

## **Expression of the unc genes in Escherichia coli.**

**McCarthy JE.**

Gesellschaft fur Biotechnologische Forschung mbH, Braunschweig, West Germany.

The unc (or atp) operon of Escherichia coli comprises eight genes encoding the known subunits of the proton-translocating ATP synthase (H<sup>+</sup>-ATPase) plus a ninth gene (uncI) of unknown function. The subunit stoichiometry of the H<sup>+</sup>-ATPase (alpha 3 beta 3 gamma 1 delta 1 epsilon 1 a1b2c10-15) requires that the respective unc genes be expressed at different rates. This review discusses the experimental methods applied to determining how differential synthesis is achieved, and evaluates the results obtained. It has been found that the primary level of control is translational initiation. The translational efficiencies of the unc genes are determined by primary and secondary mRNA structures within their respective translational initiation regions. The respective rates of translation are matched to the subunit requirements of H<sup>+</sup>-ATPase assembly. Finally, points of uncertainty remain and experimental strategies which will be important in future work are discussed.

Publication Types:

- Review

PMID: 2894371 [PubMed - indexed for MEDLINE]



Biochim Biophys Acta. 1996 Jun 7;1307(2):162-70.

Related Articles, Links

**The promoter-proximal, unstable IB region of the atp mRNA of Escherichia coli: an independently degraded region that can act as a destabilizing element.****Schramm HC, Schneppe B, Birkenhager R, McCarthy JE.**

Department of Gene Expression, National Biotechnology Research Centre (GBF), Braunschweig, Germany.

Differential expression of the genes in the Escherichia coli atp (unc) operon is achieved via control of the translational initiation, translational coupling and mRNA stability of the respective genes. The atpIB region of the polycistronic mRNA is less stable than the remaining seven genes. We have investigated the functional half-lives of the atp genes in reconstructed versions of the operon. In order to be able to do this reliably, we have readdressed the interpretation of the complex functional inactivation data obtained by means of transcriptional inhibition using rifampicin. Our results indicate the usable information to be gleaned from this commonly applied technique, while identifying the potential errors in their quantitative interpretation. We estimate that the functional half-life of atpB is slightly over one-half that of atpE and the other atp genes, while atpI is at least two times less stable than atpB. The instability of the atpI mRNA was also demonstrated by its rapid fragmentation. Relocation of atpIB to a position in the promoter-distal region of the operon between atpG and atpD did not change the inactivation rate of atpB. However, it did destabilize the atpG mRNA. Examination of the physical degradation of atpI mRNA shows particularly rapid cleavage in this gene, thus explaining the destabilization effect. The atpIB segment is therefore an autonomously unstable region that can act as a destabilizing element for upstream-located genes in a polycistronic environment.

Mol Microbiol. 1991 Oct;5(10):2447-58.

[Related Articles, Links](#)

**Differential gene expression from the Escherichia coli atp operon mediated by segmental differences in mRNA stability.**

**McCarthy JE, Gerstel B, Surin B, Wiedemann U, Ziemke P.**

Department of Gene Expression, GBF-Gesellschaft für Biotechnologische Forschung mbH, Braunschweig, Germany.

The atp operon of Escherichia coli directs synthesis rates of protein subunits that are well matched to the requirements of assembly of the membrane-bound H(+)-ATPase (alpha 3 beta 3 gamma 1 delta 1 epsilon 1a1b2c10-15). Segmental differences in mRNA stability are shown to contribute to the differential control of atp gene expression. The first two genes of the operon, atpI and atpB, are rapidly inactivated at the mRNA level. The remaining seven genes are more stable. It has previously been established that the translational efficiencies of the atp genes vary greatly. Thus differential expression from this operon is achieved via post-transcriptional control exerted at two levels. Neither enhancement of translational efficiency nor insertion of repetitive extragenic palindromic (REP) sequences into the atpI-B intercistronic region stabilized atpI. We discuss the implications of these results in terms of the pathway of mRNA degradation and of the role of mRNA stability in the control of gene expression.

PMID: 1838784 [PubMed - indexed for MEDLINE]

Gene. 1988 Dec 10;72(1-2):131-9.

[Related Articles, Links](#)**Post-transcriptional control in Escherichia coli: translation and degradation of the atp operon mRNA.****McCarthy JE, Schauder B, Ziemke P.**

GBF, Gesellschaft fur Biotechnologische Forschung mbH., Braunschweig, F.R.G.

An attractive subject for investigations of post-transcriptional control is the atp operon, whose nine genes are differentially expressed. The primary mode of control of atp gene expression is exercised at the translational level. It has been clearly demonstrated for almost all of the atp genes that the primary and secondary structures of their respective translational initiation regions direct translational initiation rates that correspond well to the requirements for these subunits in the cell. The relationship between the structure of the translational initiation region, including bases upstream from the Shine-Dalgarno region and downstream from the start codon, and the rates of initiation that it determines, has been investigated in more detail using various polycistronic and monocistronic systems. No evidence could be found for a role of codon usage bias in controlling overall translation rates. The functional half-lives of atpE and of the other six cistrons downstream from it are similar. The chemical stabilities of the first two cistrons of the polycistronic atp mRNA may, however, be lower, and we are investigating the possibility that there may also be control of atp gene expression exercised at the level of mRNA stability. The effects of manipulations of the intercistronic regions of at least the plasmid borne atp operon are consistent with a model of mRNA decay in which rate control is associated with endonucleolytic cleavages within individual cistrons. The experimental data are discussed in relation to the possible ways in which primary and secondary structures of the mRNA might control translational efficiency and stability.

PMID: 2907496 [PubMed - indexed for MEDLINE]

Biochim Biophys Acta. 1992 Apr 6;1130(3):297-306.

[Related Articles](#), [Links](#)

**The control of mRNA stability in *Escherichia coli*: manipulation of the degradation pathway of the polycistronic *atp* mRNA.**

**Ziemke P, McCarthy JE.**

Department of Gene Expression, GBF, Gesellschaft für Biotechnologische Forschung mbH, Braunschweig Germany.

The physical and functional stabilities of genes in the *atp* operon fall into two classes. The first two genes, *atpI* and *atpB*, are rapidly inactivated and degraded at the mRNA level. The remaining seven genes are more stable. In order to investigate how these stabilities are determined, DNA sequences encoding mRNA structures that influence degradative events in other systems, including RNase III sites and REP sequences, were subcloned or synthesized and inserted into non-coding regions of the operon. The effects of insertion of an RNase III site depended on whether cleavage left an unstable 3' end or a stabilizing stem-loop upstream of the cutting point. Generation of an unstable 3' end destabilized the neighbouring upstream *atp* gene, thus modifying the course and rate control of degradation. Removal of the *atp* transcriptional terminator attenuated expression of the last gene of the operon, *atpC*. This effect was reversed by substitution of an alternative stem-loop for the terminator. REP sequences inserted into intercistronic regions apparently could not influence rate-controlling steps. The reported data shed light on the factors controlling the inactivation and degradation of genes in the polycistronic *atp* mRNA, and are discussed in relation to the general role of degradation processes in the control of gene expression.

## Limited Differential mRNA Inactivation in the *atp* (*unc*) Operon of *Escherichia coli*

OLE R. LAGONI,<sup>1</sup> KASPER VON MEYENBURG,<sup>2</sup> AND OLE MICHELSEN<sup>1\*</sup>

Department of Microbiology, Technical University of Denmark, Building 221, DK-2800 Lyngby, Denmark,<sup>1</sup>  
and Biotechnology K-681, CIBA-GEIGY AG, 4002 Basel, Switzerland<sup>2</sup>

Received 14 April 1993/Accepted 14 July 1993

Individual subunits of ATP synthase, encoded by the eight genes of the *atp* operon (*atpA* through *atpH*), have been found to be synthesized at a 10-fold range in molar amounts (D. L. Foster and R. H. Fillingame, *J. Biol. Chem.* 257:2009-2015, 1982; K. von Meyenburg, B. B. Jørgensen, J. Nielsen, F. G. Hansen, and O. Michelsen. *Tokai J. Exp. Clin. Med.* 7:23-31, 1982). We have determined the functional half-lives at 30°C of mRNAs transcribed from these genes either during constitutive expression in a partial diploid strain or after induced expression from a plasmid. Accurate decay kinetics of the relative mRNA levels were determined by monitoring the rates of synthesis of the individual ATP synthase subunits by radioactive pulse labeling at different times after blocking transcription initiation with rifampin. The mRNA transcribed from the *atp* operon was found to be inactivated about twice as fast as the bulk mRNA in *E. coli*. Exceptions are the mRNA from the promoter-proximal *atpB* gene, which was inactivated about three times as fast as the bulk mRNA, and *atpC* mRNA, the inactivation rate of which was comparable to that of the bulk mRNA. These moderate differences in the kinetics of functional decay explain only a minor part of the differences in expression levels of the *atp* genes. We conclude, therefore, that the individual *atp* mRNAs must be translated with widely different efficiencies. The present analysis further revealed that mRNA degradation is sensitive to heat shock; i.e., after incubation at 39°C for 5 min followed by a shift back to 30°C, the decay rate of the bulk mRNA was decreased by 30%.

The eight genes that code for the subunits of the ATP synthase of *Escherichia coli* together with a ninth promoter-proximal gene, *atpI*, form an operon, *atpIBEFHAGDC*, coding for the subunits *i*, *a*, *c*, *b*,  $\delta$ ,  $\alpha$ ,  $\gamma$ ,  $\beta$ , and  $\epsilon$ , respectively (8, 11, 23). A major promoter (*atpI*<sub>p</sub>) and two minor promoters (*atpB*<sub>p1</sub>, *atpB*<sub>p2</sub>) within the *atpI* gene have been identified (24, 41). Expression of the *atp* operon as a whole does not appear to be subject to substrate or growth rate control (23, 29) or to respond to anaerobic or aerobic shifts (37).

The gene order and the amounts of subunits expressed are shown in Fig. 1 and Table 2, respectively. The ATP synthase is a multicomponent enzyme with a cytoplasmic ATPase; the coupling factor, *F*<sub>1</sub>, with the composition  $\alpha_3$ ,  $\beta_3$ ,  $\delta$ ,  $\gamma$ ,  $\epsilon$ ; and a membrane-embedded part, the proton channel, *F*<sub>0</sub>, with the composition *a*, *b*<sub>2</sub>, *c*<sub>10-12</sub> (9, 42). The stoichiometry of the *F*<sub>1</sub> part was first established by Bragg and Hou (2) from the composition of the <sup>14</sup>C-labeled, isolated enzyme. Their values were supported by measurements of the molecular ratio of the subunits synthesized in either overproducing cells (42) or from a transducing  $\lambda$  phage (9). These measurements of the production rates of the subunits gave a molecular ratio for the *F*<sub>0</sub> subunits which became the accepted stoichiometry of the *F*<sub>0</sub> part of the enzyme, although titration of isolated *F*<sub>0</sub> subunits in reconstitution experiments with active proton channels suggests that the minimal stoichiometry of *F*<sub>0</sub> is *a*<sub>1</sub>*b*<sub>2</sub>*c*<sub>8</sub> (25).

Differences in gene expression within the same operon can be accounted for either by differences in translation frequencies or by differences in mRNA availability. McCarthy et al. (20) have shown that the region between the *atpB* and the *atpE* genes has translation enhancer activity.

Several enzymes involved in mRNA decay have been identified. Two 3' exonucleases, RNase II and polynucleotide phosphorylase (6), and one broad-specificity endonuclease, RNase M (4), have been shown to be involved in mRNA decay, and four site-specific endonucleases, RNase III (7, 34), RNase E (22, 27), RNase K (18), and RNase P (21), have been shown to be involved in the processing of mRNAs, leaving new ends to be decayed by exonucleases. There is no known enzyme in *E. coli* that digests RNA from the 5' end, but the *lac* mRNA has been shown to be degraded from the 5' to the 3' end (3, 32).

Besides detection by McCarthy et al. (19), who expressed the *atp* operon on a plasmid from the  $\lambda$ P<sub>L</sub> promoter, the full-length *atp* transcript has only been detected by Jones et al. (16) (as an mRNA of approximately 7 kb) and by Patel and Dunn (28), who recently detected the full-length transcript in an *rne* mutant; on the other hand, Schaefer et al. (35) found two *atp* transcripts of 6.5 and 4.6 kb by using either an *atpG* or an *atpC* probe. They could not identify a full-length mRNA from the *atp* operon, and they noticed a possible processing site in the C-terminal end of the *atpI* gene close to the initiation site of the *atpB*<sub>p2</sub> promoter and about 6.5 kb from the transcriptional terminator. Patel and Dunn (28) also identified several RNase E processing sites in the *atp* transcript, (i) one in the 5' end of the coding sequence of the *atpC* gene, (ii) one near the 5' end of the *atpB* gene, and (iii) two in the leader region of the *atpE* gene. The latter two have also been identified by Gross (13) in the isolated leader region.

McCarthy et al. (19) have recently published that the mRNAs, which code for the *a* (*atpB*) and *c* (*atpE*) subunits of the ATP synthase, were inactivated with half-lives of 2 min and 7 to 12 min, respectively.

We have determined the functional half-lives of the tran-

\* Corresponding author.

TABLE 1. The *E. coli* K-12 strains used

Strain	Characteristics	Source or reference
BL321	<i>mc105</i>	38
BL322	<i>mc</i> <sup>+</sup>	38
CM845	<i>asnA31 asnB32 thi1 relA1 spoT</i> <i>F<sup>+</sup>Δasn105</i>	39
CM1471	<i>atp1BEFH706 asnB32 thi1</i> <i>relA1 spoT1 F<sup>+</sup></i>	41
LM1888	pBJC1888 <sup>a</sup>	
MC1000	<i>araD139 ΔaraΔeu7697 ΔlacX74</i> <i>galU galK rpsL</i>	5
OL171	pOLC40 <sup>b</sup>	
OL22	pOLC3 <sup>b</sup>	
CN489	<i>mc105 glyA:Tn5<sup>b</sup></i>	Carsten Petersen
OL264	<i>mc105<sup>b</sup></i>	This work
OL266	— <sup>b</sup>	This work
OL279	pJNC33 <sup>b</sup>	
OL283	OL266/pBJC1888	
OL285	OL264/pBJC1888	

<sup>a</sup> Genotype of strain CM1471.<sup>b</sup> Genotype of strain MC1000.

scripts for all of the subunits of the ATP synthase from an *atp* operon located on a multicopy plasmid and for the *a*, *c*, *α*, and *β* subunits from the chromosomal *atp* operon in a partially diploid strain, and we have obtained results different from those of McCarthy et al. (19). It is therefore pertinent to ask to what extent such differences in functional half-lives between gene transcripts in the same operon contribute to the relative stoichiometry of the ATP synthase

subunits of *a:b:c:α:β:γ:δ:ε* of 1:2:12:3:3:1:1. Our results actually support the finding of McCarthy et al. (19) of a difference in half-lives between the *atpB* (*a*) gene and *atpE* (*c*) gene (but only by a factor of 1.5), while the functional half-lives of all of the *atp* gene mRNAs are virtually identical but are about 50% shorter than the functional half-life of the bulk mRNA. Thus, the major part of the differences in rates of synthesis of the subunits of the ATP synthase must be due to differences in the efficiency of the translation initiations and not differences in mRNA stability.

## MATERIALS AND METHODS

**Bacterial strains and plasmids.** The strains used in this study are listed in Table 1, and the plasmids are shown in Fig. 1.

All plasmids are pBR322 derivatives, including plasmid pBJC1888 (*ci857 λpR-atpBEFHAGDC*) (40) and plasmid pOMC11 (*atpB*) (10). Plasmid pJNC33 carries the 2,137-bp fragment from the *Bgl*II site in the C-terminal end of the *gidA* gene to the *Bam*HI site in the N-terminal end of the *atpB* gene, cloned into the *Bam*HI site on pMLB1034 (36). The *atpB* gene is fused in frame with the *lacZ* gene. Plasmid pOLC3 carries the 240-bp fragment from the C-terminal *Hind*III site in the *atpI* gene to the *Bam*HI site in the N-terminal end of the *atpB* gene cloned into pMLB1034. The *atpB* gene is fused in frame with the *lacZ* gene. Plasmid pOLC40 carries the 1,106-bp fragment from the C-terminal *Hind*III site in the *atpI* gene to the *Ava*I site in the *atpE* gene cloned into pMLB1034, restricted with *Hind*III and *Bam*HI endonucleases. The protruding ends of *Ava*I and *Bam*HI

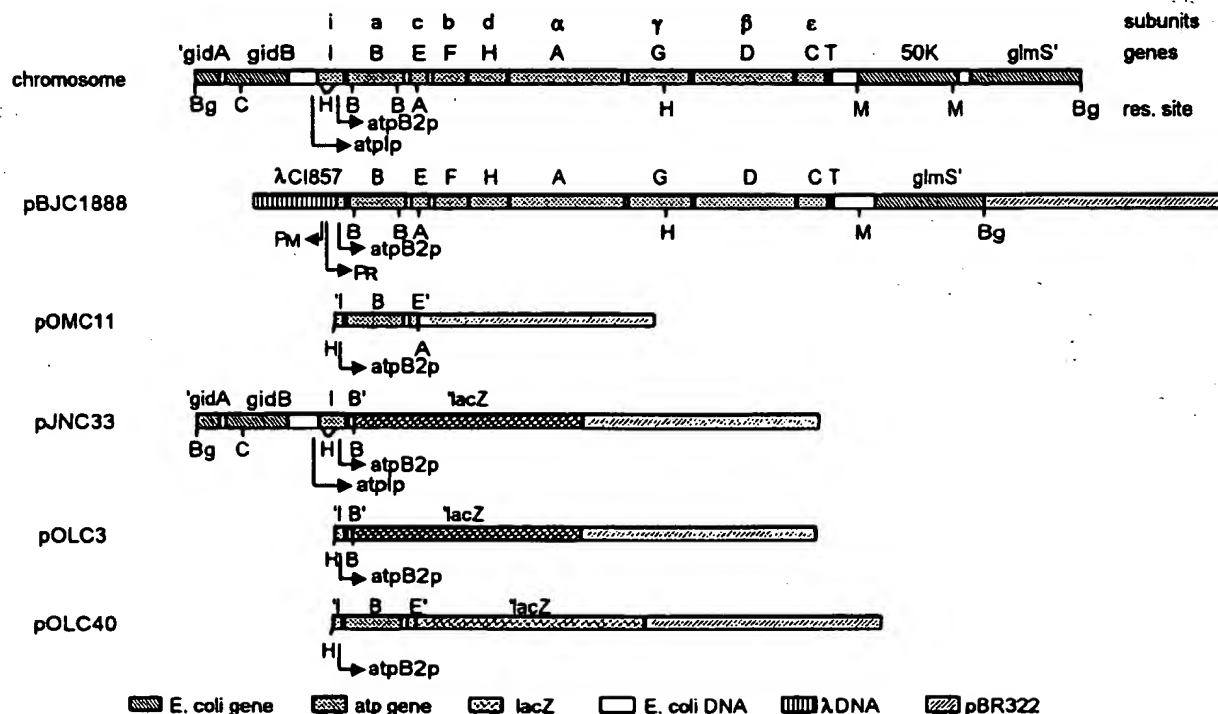


FIG. 1. Map of the *atp* operon and plasmids used in this study. Promoters: *atpIp*, major *atp* promoter; *atpB2p* (*atpB<sub>2</sub>*), minor *atp* promoter; *P<sub>M</sub>* (*p<sub>M</sub>*), promoter of the *λ CI* gene, *P<sub>R</sub>* (*p<sub>R</sub>*), *λp<sub>R</sub>* promoter. Restriction (res.) sites: Bg, *Bgl*II; C, *Cla*I; H, *Hind*III; B, *Bam*HI; A, *Ava*I; M, *Mlu*I.

sites were removed with mung bean nuclease before ligation. The *atpE* gene is fused in frame with the *lacZ* gene.

**Growth of bacterial cultures.** Growth media and measurement of growth were described earlier (40). Growth media were supplemented with the necessary amino acids, leucine and arginine at 50  $\mu\text{g/ml}$ , and plasmid-carrying strains were supplemented with ampicillin at 100  $\mu\text{g/ml}$ .

**Construction of RNase III-deficient strain.** OL264 and OL266 were constructed by transducing CN489 to GlyA<sup>+</sup> with P1 lysates from BL321 and BL322, respectively. The *rnC* phenotypes were confirmed by examining the processing of the stable RNA in the strains.

**Determination of functional mRNA half-lives.** The functional half-life of the bulk mRNA of the cells was determined from the decay in total protein synthesis measured by pulse labeling.

The functional stability of the mRNA was determined by measuring the ability of the cells to synthesize subunits of the ATP synthase or *atp::lacZ* hybrid protein after addition of rifampin.

The functional half-lives of mRNA of the *atp* genes from the partial diploid strain, CM845, were determined as follows. Cells were grown at 30°C in minimal medium (20 ml) with glucose and [<sup>3</sup>H]leucine (50  $\mu\text{g/ml}$ ; 50  $\mu\text{Ci}/\mu\text{mol}$ ). Samples were withdrawn at different times after addition of rifampin (300  $\mu\text{g/ml}$ ) and were pulse labeled for 30 s with [<sup>35</sup>S]methionine (10  $\mu\text{Ci/ml}$ ; 1,000 Ci/mmol) followed by a 2-min chase with 100 mg of methionine per ml (30). The cells were harvested by centrifugation and washed, and membranes were prepared as described earlier (39). The membrane proteins were separated by sodium dodecyl sulfate-polyacrylamide gel electrophoresis (SDS-PAGE) and autoradiographed (41) on AGFA Structurix X-ray film, which has a linear response to  $\beta$  radiation in the range used.

The functional half-lives of *atp::lacZ* fusions were determined as described above, except that because the *atp::lacZ* fusions separate well by normal SDS-PAGE, the membrane preparation could be omitted.

The functional half-lives of *atp* mRNA expressed from the  $\lambda p_R$  on a multicopy plasmid were determined as follows. The cultures were grown exponentially at 30°C then shifted to 39°C for 3 min for induction before addition of rifampin. The temperature was shifted back to 30°C at the time of rifampin addition. The radioactive labeling procedure was performed as described above for *atp* genes from strain CM845. Membrane preparation could be omitted, because this pulse induction yields a very large fraction of the radioactivity in the various *atp* subunits (e.g., the autoradiograph in Fig. 2).

Quantification of the proteins was done by optical scanning of the autoradiographs obtained after different exposure on an LKB Ultrascan Laser Densitometer 2202, and the readings were corrected for sample volume variations and membrane recovery ([<sup>3</sup>H]leucine prelabeling).

The half-lives of all of the transcripts were determined from regression analysis of the rates of synthesis of the proteins.

## RESULTS

The mRNA transcribed from the *atp* operon is inactivated faster than the inactivation of the bulk mRNA in *E. coli*. Strain LM1888 harbors plasmid pBJC1888 carrying the promoter  $p_R$  of phage  $\lambda$  fused to the eight ATP synthase genes *atpB* to *atpC* (Fig. 1). Inactivation of the heat-sensitive  $\lambda$  repressor protein, which is expressed from the *C1857* gene on the same plasmid, leads to induction of the *atp* genes. Addition of

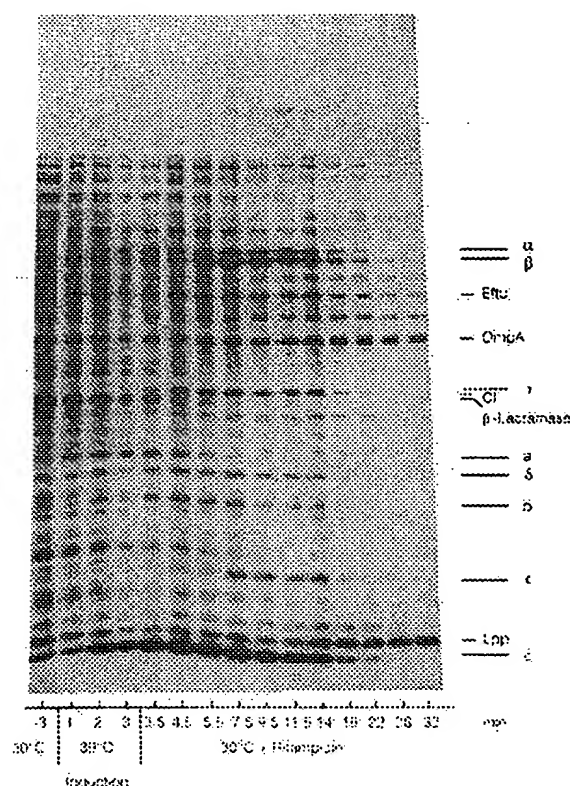


FIG. 2. Autoradiogram of total strain LM1888 pulse labeled with [<sup>35</sup>S]methionine at different times before and after addition of rifampin and separated by SDS-PAGE. The times for the different samples and the proteins measured are indicated. Rifampin, rifampin.

rifampin to induced cells enables us to measure the functional half-lives, at 30°C, of the mRNAs coding for the different subunits of the ATP synthase (Fig. 2 and 3). Furthermore, the addition of rifampin prevented the detrimental effect of induction of the ATP synthase subunits on overall protein synthesis (40). The results (Fig. 3 and Table 2) show that the transcripts from the *atp* genes were inactivated in the same sequence as they were transcribed. The functional half-lives of the mRNAs coding for the subunits of the ATP synthase were determined in parallel with the half-lives of other mRNAs, which code for distinct proteins on the same gel (Fig. 2 and Table 2), notably lipoprotein (*lpp*), outer membrane protein (*ompA*), and elongation factor Tu (*tufA* and *tufB*). The transcripts from the six genes in the middle of the operon, *atpE* to *atpD* (subunits  $c$ ,  $b$ ,  $\delta$ ,  $\alpha$ ,  $\gamma$ ,  $\beta$ ), all had functional half-lives close to 2.5 min, while the transcript from the *atpB* gene had a somewhat shorter functional half-life of about 1.6 min. The functional half-life of the transcript from the last gene in the operon, *atpC* (subunit  $\epsilon$ ), of 4 min was close to the half-life of the bulk mRNA of the cells, 4.5 min. The transcripts from *tufA* and *tufB* genes had the same half-lives of 4.5 min at 30°C as the bulk mRNA of the cells, in agreement with previously reported values at 30°C (30). The transcript from the *ompA* gene appeared to have a half-life of 10 min, while the transcript from the *lpp* gene decayed with a half-life of 35 to 40 min, as expected for these long-living mRNAs (26, 30).



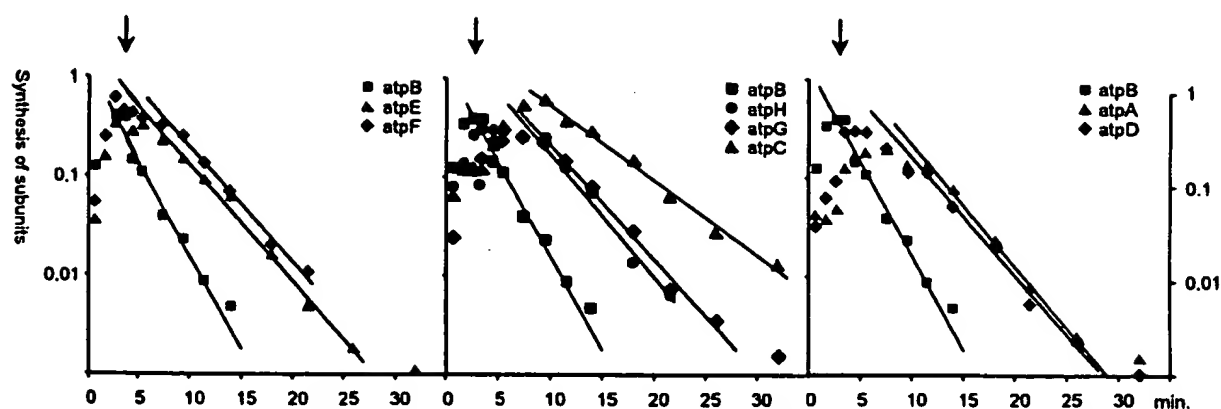


FIG. 3. Representative curves of inactivation of *atp* gene transcripts in strain LM1888. The data points show the synthesis of the different subunits before and after addition of rifampin normalized by the stoichiometry of the ATP synthase. Arrows indicate rifampin addition. Half-lives are shown in Table 2.

The mRNAs coding for the  $\lambda$  repressor and the  $\beta$ -lactamase had half-lives of 1.2 min.

The ratio of expression of subunits *a*, *c*, and *b* 0.5 min after addition of rifampin was 1:10:2 in accordance with the stoichiometry of the ATP synthase. The maximal expression of other subunits could not be used for stoichiometric calculations because of decay of the mRNA.

In plasmid pBJC1888 the *atp* mRNA is initiated in the  $\lambda$  DNA in front of the *cro* gene. The transcript is then read through approximately 80 bases from *E. coli oriC* DNA into the C-terminal end of the *atpI* gene, 156 bases in front of the *atpB* gene. In order to rule out the possibility that the shorter half-life of the *atpB* transcript is a cloning artifact caused by the different sequences joined in front of the *atp* genes, the functional half-lives of the mRNAs, which code for different subunits of ATP synthase, were therefore determined at 30°C in the partially diploid strain CM845, which carries an extra copy of the normal *atp* operon on a transducing  $\lambda$  phage. In this strain (CM845), we were only able to determine the half-lives for the mRNA coding for the *a*, *c*,  $\alpha$ , and  $\beta$  subunits. The results (Table 2) show that the half-lives for the mRNAs for all four subunits were again shorter than the half-life for the bulk mRNA in this exponentially growing

strain (3.5 min). The half-life for mRNA coding for the *a* subunit was 1 min, which was again 1.5 times shorter than the half-lives for the other three subunits (1.5 to 1.7 min). This showed that the low stability of subunit *a*-specific mRNA was not a cloning artifact introduced by the  $\lambda p_R$  promoter. The half-lives for the mRNAs coding for the OmpA and the Lpp proteins were also measured (6.6 and 22 min, respectively).

The difference in half-lives between the two strains is apparently due to the temperature induction—3 min at 39°C—used for strain LM1888; such a heat shock caused a 1.4-times increase in the functional half-life of the bulk mRNA in a control strain CM1471 (data not shown). The relative proportions between the half-lives of the different mRNAs in the two strains, LM1888 with heat induction and CM845 without heat induction, were the same.

**Location of the signal for stability of the mRNAs.** The functional half-life of mRNA coding for *lacZ* gene fusions can easily be determined because the fusion proteins are normally well separated from other proteins on SDS-PAGE. We have used two fusion plasmids, pJNC33 and pOLC3, with the same subunit *a*:: $\beta$ -galactosidase fusion, but with different 5' leader sequences (i.e., with and without the 5' leader and *atpI* gene, respectively), and plasmid pOLC40 with a subunit *c*:: $\beta$ -galactosidase fusion (structures of the plasmids are shown in Fig. 1). The half-lives of the transcripts of the *atp*::*lacZ* fusion genes of 1.2 min for the *atpB*::*lacZ* transcript (pJNC33 and pOLC3) and 3 min for the *atpE*::*lacZ* transcript (pOLC40) were close to the half-lives of the transcripts for subunits *a* and *c*, respectively, from plasmid pBJC1888. This shows that the half-life of the transcript of the *atpB*::*lacZ* fusion gene is also independent of the 5' leader and *atpI* gene sequence, as was found with the half-life of the transcript of the *atpB* gene.

Furthermore, the results show that the signals for the stability of the mRNAs coding for these fusions are located in the 5' end of the sequence of the *atp* genes, all three plasmids having the same 3' end because they are all pMLB1034 derivatives. The signals for the inactivation rate of the mRNAs specific for the *atpB* and *atpE* genes are therefore most likely located close to the translation initiation sites of these genes.

The functional inactivation rate in the operon is not caused by an RNase III site. Inspection of the sequence of the *atp*

TABLE 2. Functional half-lives of *atp* gene transcripts and other mRNAs at 30°C

Gene	Subunit	Stoichiometry <sup>a</sup>	Half-lives (min) of:			
			LM1888	OL283	OL285	CM845
<i>atpB</i>	<i>a</i>	1	1.6	1.7	1.5	1.0
<i>atpE</i>	<i>c</i>	12	2.6			1.7
<i>atpF</i>	<i>b</i>	2	2.6	2.9	3.6	
<i>atpH</i>	$\delta$	1	2.4	3	2.6	
<i>atpA</i>	$\alpha$	3	2.5	3	2.5	1.6
<i>atpG</i>	$\gamma$	1	2.6	3.2	2.5	
<i>atpD</i>	$\beta$	3	2.4	3	3	1.5
<i>atpC</i>	<i>e</i>	1	4.0	5.1	2.2	
<i>tuf</i>			4.5			
<i>ompA</i>			10			6.6
<i>lpp</i>			35–40			22
<i>cl</i>			1.2			
<i>bla</i>			1.2			
Bulk mRNA			4.5			3.5

<sup>a</sup> Derived from von Meyenburg et al. (40).

operon suggested an RNase III site in the beginning of the *atpB* gene. S1 mapping of RNA transcribed from plasmid pOMC11 in the two isogenic strains OL264 and OL266 did not reveal any differences in the two strains (results not shown). The short half-life of the transcript from the *atpB* gene is thus not caused by cleavage of the mRNA by RNase III.

The functional half-lives of the transcripts from pBJC1888 in the two strains were identical to the half-lives determined in strain LM1888, except that the transcript from the *atpC* gene had a half-life of about 2.5 min, similar to that of the transcripts from the other distal genes in the *mc* strain and in contrast to what was found in the wild-type strains (Table 2).

This also shows that the functional half-lives of the transcripts from pBJC1888 are most likely strain independent, because strain OL283 and strain LM1888 are derivatives of strain MC1000 and strain ER, respectively.

### DISCUSSION

From the *atp* operon, a polycistronic mRNA is expressed that encodes nine peptides (12, 42), eight of which are subunits of ATP synthase. We have followed the functional inactivation of the mRNA of the *atp* operon at 30°C, both from a transcriptional fusion between the phage  $\lambda p_R$  promoter and the *atp* genes, rendering them inducible, and from the intact *atp* operon in an exponentially growing strain diploid for the *atp* operon. The inactivation of the mRNAs was two times faster than the inactivation of the bulk mRNA of the cells, except for the mRNA from the promoter-proximal *atpB* gene, which was inactivated three times faster than the bulk mRNA, and the mRNA from the last gene, *atpC*, which was inactivated at the same rate as the bulk mRNA. The differences in functional decay between the mRNAs coding for the various *atp* genes thus contribute to a limited extent to the stoichiometry of the ATPase subunits. The differences in expression of the ATPase subunits must then be due to differences in the efficiencies of translational initiation.

McCarthy et al. (20) have shown that the region between the *atpB* and *atpE* genes has translation enhancer activity, and Patel and Dunn (28) and Gross (13) have found that the same region is cleaved by RNase E. Therefore, this region also appears to be the border between two parts of the *atp* transcript, with a 1.5-fold difference in functional half-lives.

McCarthy et al. (19) have recently found that the functional half-lives of the mRNAs encoding the *a* (*atpB*) and *c* (*atpE*) subunits of the ATP synthase differed by a factor of 3 to 6 (2 min and 7 to 12 min, respectively, at 42°C).

While most *E. coli* mRNAs are inactivated with half-lives of between 0.5 and 3 min at 37°C (1, 30), a few mRNAs which code for outer membrane proteins—e.g., OmpA and Lpp—have considerably longer half-lives (10 min or more) (14, 17, 26, 30). The long half-life of 7 to 12 min for the *atpE* mRNA observed by McCarthy et al. (19) is in the same range as the half-lives for the mRNAs coding for outer membrane proteins (Lpp and OmpA). It seems surprising that the *atpE* mRNA should not have been identified earlier as a semi-stable mRNA, either in minicells (17) or in the presence of rifampin (14).

The explanation for this paradox and the discrepancy between the results of McCarthy et al. (19) and those of the present analysis of the *atpB* and *atpE* mRNA stability may lie in the specific experimental procedure chosen. McCarthy et al. (19) used a plasmid with the *atp* operon expressed from the  $\lambda p_L$  promoter. The experiments were performed at 42°C

after a 20-min induction at the same temperature. We also used temperature induction, but we used the weaker  $\lambda p_R$  promoter and a lower temperature (39°C) for induction, we limited the induction to relatively short periods (3 to 5 min) in order to avoid the anticipated side effects of *atp* operon induction, and we performed the experiments at 30°C. von Meyenburg et al. (40) have shown that rapid induction of the *atp* operon induces (i) partial collapse of the membrane potential within 4 to 6 min of induction and (ii) cessation of growth and protein synthesis and concomitant loss of cell viability. It is likely that the rather extended half-lives of the *atpE* mRNA are an artifact due to a strong and prolonged temperature induction by McCarthy et al. (19). McCarthy et al. also used plasmids on which the *atp* operon was expressed from the weaker *lac* promoter, but in our experience (40), this promoter (with approximately 1.5 times the strength of the *atp* promoter) is strong enough to provoke the detrimental effects of induction of the *atp* operon on a pBR322-derived plasmid. Furthermore, it is not possible to deduce from the paper of McCarthy et al. (19) the exact experimental procedures used in the experiments with the *lac* promoter.

Our results (Fig. 3) show that the active *atpB* mRNA is reduced to 10% when the *atpG*, *atpD*, and *atpC* genes are being transcribed and translated at maximal rates. This might imply that not all of the cistrons on the 6.5-kb mRNA (*atpG* probe) identified by Schaefer et al. (35) are translated at the same time and that the mRNA might be inactivated before it is degraded, in agreement with the model suggested by Petersen (33).

The signal for the differential instability of the transcripts might be located close to the 5' ends of the *atpB* and *atpE* genes, because the transcripts of translational fusions between the *atpB* and *atpE* genes and the *lacZ* gene had the same half-lives (1.2 and 3 min, respectively) as the transcripts of the normal *atpB* and *atpE* genes (Table 2). Petersen (31) has shown that fusion of *lacZ* to a gene close to the translation initiation site might result in very short half-lives of the mRNA. In this study, the fusion points between the *atp* genes and the *lacZ* gene were separated from the initiation site by 87 to 90 bp. Because the half-lives for the transcripts of the *lacZ* fusions were very similar to the half-lives found for the normal *atpB* and *atpE* mRNAs, it is fair to assume that the decay of the gene fusion transcripts is controlled by the same rate-determining signals as the stability of the normal transcripts.

RNase III does not seem to be responsible for setting the average decay rate of *atp* mRNA or for the differential effects between *atpB* and *atpE*, because the functional half-lives of the transcripts from the *atp* operon in an *mc* mutant are virtually the same as in the wild-type strain, with the exception of that from the *atpC* gene, which in this strain had a functional half-life close to those of the transcripts from the rest of the operon.

The values for the functional half-lives of *atp* mRNA at 30°C are 1.0 min for *atpB* and 1.6 min for most of the other genes, the latter being approximately 50% of the half-life of the bulk mRNA at 30°C. Both the overall half-life and the half-lives of the transcripts of the *ompA*, *lpp*, *tufA*, and *tufB* genes are in good agreement with published results (26, 30).

Why is the *atp* mRNA less stable than other mRNA? Is this a fortuitous feature, or does it reflect a selective advantage to the cells? This question must remain open. One possible answer could be that a short half-life of an mRNA combined with more efficient transcriptional and translational initiations is a strategy that would result in a more

precisely determined amount of the product synthesized than less-efficient initiations combined with a longer half-life of the bulk mRNA. The amount of ATP synthase in *E. coli* seems to be precisely adjusted to yield a maximal growth rate (15).

#### ACKNOWLEDGMENTS

We thank Tove Atlung for carefully reading the manuscript. This work was supported by the Danish Center for Microbiology.

#### REFERENCES

- Blundell, M., E. Craig, and D. Kennell. 1972. Decay rates of different mRNA in *E. coli* and models of decay. *Nature (London)* **238**:46-49.
- Bragg, P. D., and C. Hou. 1975. Subunit composition, function, and spatial arrangement in the  $\text{Ca}^{2+}$ - and  $\text{Mg}^{2+}$ -activated adenosine triphosphatases of *Escherichia coli* and *Salmonella typhimurium*. *Arch. Biochem. Biophys.* **167**:311-321.
- Cannistraro, V. J., and D. Kennell. 1985. Evidence that the 5' end of *lac* mRNA starts to decay as soon as it is synthesized. *J. Bacteriol.* **161**:820-822.
- Cannistraro, V. J., and D. Kennell. 1989. Purification and characterization of ribonuclease M and mRNA degradation in *Escherichia coli*. *Eur. J. Biochem.* **181**:363-370.
- Casadaban, M., and S. N. Cohen. 1980. Analysis of gene control signals by DNA fusion and cloning in *Escherichia coli*. *J. Mol. Biol.* **138**:179-207.
- Donovan, W. P., and S. R. Kushner. 1986. Polynucleotide phosphorylase and ribonuclease II are required for cell viability and mRNA turnover in *Escherichia coli* K-12. *Proc. Natl. Acad. Sci. USA* **83**:120-124.
- Dunn, J. J., and F. W. Studier. 1973. T7 early mRNAs and *Escherichia coli* ribosomal RNAs are cut from large precursor RNAs in vivo by ribonuclease III. *Proc. Natl. Acad. Sci. USA* **70**:3296-3300.
- Fillingame, R. H. 1980. The proton-translocating pumps of oxidative phosphorylation. *Annu. Rev. Biochem.* **49**:1079-1113.
- Foster, D. L., and R. H. Fillingame. 1982. Stoichiometry of subunits in the  $\text{H}^+$ -ATPase complex of *Escherichia coli*. *J. Biol. Chem.* **257**:2009-2015.
- Friedl, P., J. Hoppe, R. P. Gunsalus, O. Michelsen, K. von Meyenburg, and H. U. Schaller. 1983. Membrane integration and function of the three  $\text{F}_0$  subunits of the ATP synthase of *Escherichia coli* K12. *EMBO J.* **2**:99-103.
- Futai, M., and H. Kanazawa. 1983. Structure and function of proton-translocating adenosine triphosphatase ( $\text{F}_0\text{F}_1$ ): biochemical and molecular biological approaches. *Microbiol. Rev.* **47**:285-312.
- Gibson, F., J. A. Downie, G. B. Cox, and J. Radik. 1978. Mu-induced polarity in the *unc* operon of *Escherichia coli*. *J. Bacteriol.* **134**:728-736.
- Gross, G. 1991. RNaseE cleavage in the *atpE* leader region of *atpE/interferon- $\beta$*  hybrid transcripts in *Escherichia coli* causes enhanced rates of mRNA decay. *J. Biol. Chem.* **266**:17880-17884.
- Hirashima, A., G. Childs, and M. Inouye. 1973. Differential inhibitory effects of antibiotics on biosynthesis of envelope proteins of *Escherichia coli*. *J. Mol. Biol.* **79**:373-389.
- Jensen, P. R., H. Westerhoff, and O. Michelsen. 1993. Excess capacity of  $\text{H}^+$ -ATPase and inverse respiratory control in *Escherichia coli*. *EMBO J.* **12**:1277-1282.
- Jones, H. M., C. M. Brakovich, and R. P. Gunsalus. 1983. In vivo 5' terminus and length of the mRNA for the proton-translocating ATPase (*unc*) operon of *Escherichia coli*. *J. Bacteriol.* **155**:1279-1287.
- Levy, S. B. 1975. Very stable prokaryotic messenger RNA in chromosomeless *Escherichia coli* minicells. *Proc. Natl. Acad. Sci. USA* **72**:2900-2904.
- Lundberg, U., A. von Gabain, and Ö. Melefors. 1990. Cleavages in the 5' region of the *ompA* and *bla* mRNA control stability: studies with an *E. coli* mutant altering mRNA stability and a novel endoribonuclease. *EMBO J.* **9**:2731-2741.
- McCarthy, J. E. G., B. Gerstel, B. Surin, U. Wiedemann, and P. Ziemke. 1991. Differential gene expression from the *Escherichia coli* *atp* operon mediated by segmental differences in mRNA stability. *Mol. Microbiol.* **5**:2447-2458.
- McCarthy, J. E. G., H. U. Schaller, and W. Seibald. 1985. Translational initiation frequency of *atp* genes from *Escherichia coli*: identification of an intercistronic sequence that enhances translation. *EMBO J.* **4**:519-526.
- Miczak, A., R. A. K. Srivastava, and D. Apiron. 1991. Location of the RNA-processing enzymes RNaseIII, RNaseE and RNaseP in the *Escherichia coli* cell. *Mol. Microbiol.* **5**:1801-1810.
- Mudd, E. A., P. Prentki, D. Belin, and H. M. Kirsch. 1988. Processing of bacteriophage T4 gene 32 mRNAs into a stable species requires *Escherichia coli* ribonuclease E. *EMBO J.* **7**:3601-3607.
- Nielsen, J. 1984. Structure and expression of the ATP synthase operon of *Escherichia coli*. Ph.D. thesis. Technical University of Denmark, Lyngby.
- Nielsen, J., B. B. Jørgensen, K. von Meyenburg, and F. G. Hansen. 1984. The promoters of the *atp* operon of *Escherichia coli* K12. *Mol. Gen. Genet.* **193**:64-71.
- Nielsen, J., and J. P. Rosenbusch. 1988. Purification and reconstitution of the three subunits of the membrane part ( $\text{F}_0$ ) of the ATP synthase ( $\text{F}_1\text{F}_0$ ) of *E. coli*. *European Bioenergetics Conference* **5**:216.
- Nilsson, G., J. G. Belasco, S. N. Cohen, and A. von Gabain. 1984. Growth-rate dependent regulation of mRNA stability in *Escherichia coli*. *Nature (London)* **312**:75-77.
- Nilsson, P., and B. E. Uhlin. 1991. Differential decay of a polycistronic *Escherichia coli* transcript is initiated by RNaseE-dependent endonucleolytic processing. *Mol. Microbiol.* **5**:1791-1799.
- Patel, A. M., and S. D. Dunn. 1992. RNase E-dependent cleavages in the 5' and 3' regions of the *Escherichia coli* *unc* mRNA. *J. Bacteriol.* **174**:3541-3548.
- Pedersen, S., P. L. Block, S. Reeh, and F. Neidhardt. 1978. Patterns of protein synthesis in *E. coli*: a catalog of the amount of 140 individual proteins in different growth rates. *Cell* **14**:179-186.
- Pedersen, S., S. Reeh, and J. D. Friesen. 1978. Functional mRNA half lives in *E. coli*. *Mol. Gen. Genet.* **166**:329-336.
- Petersen, C. 1987. The functional stability of the *LacZ* transcript is sensitive towards sequence alterations immediately downstream of the ribosome binding site. *Mol. Gen. Genet.* **209**:179-187.
- Petersen, C. 1991. Multiple determinants of functional mRNA stability: sequence alterations at either end of the *lacZ* gene affect the rate of mRNA inactivation. *J. Bacteriol.* **173**:2167-2172.
- Petersen, C. 1992. Control of functional mRNA stability in bacteria: multiple mechanisms of nucleolytic and non-nucleolytic inactivation. *Mol. Microbiol.* **6**:277-282.
- Portier, C., L. Dondon, M. Grunberg-Manago, and P. Regnier. 1987. The first step in the functional inactivation of the *Escherichia coli* polynucleotide phosphorylase messenger is a ribonuclease III processing at the 5' end. *EMBO J.* **6**:2165-2170.
- Schaefer, E. M., D. Hartz, L. Gold, and R. D. Simon. 1989. Ribosome-binding sites and RNA-processing sites in the transcript of the *Escherichia coli* *unc* operon. *J. Bacteriol.* **171**:3901-3908.
- Schultz, J., T. J. Silhavy, M. L. Berman, N. P. Foll, and S. D. Emer. 1982. A previously unidentified gene in the *spc* operon of *Escherichia coli* K12 specifies a component of the protein export machinery. *Cell* **31**:227-235.
- Smith, M. W., and F. C. Neidhardt. 1983. Proteins induced by anaerobiosis in *Escherichia coli*. *J. Bacteriol.* **154**:336-343.
- Studier, F. W. 1975. Genetic mapping of a mutation that causes ribonuclease III deficiency in *Escherichia coli*. *J. Bacteriol.* **124**:307-316.

39. von Meyenburg, K., F. G. Hansen, L. D. Nielsen, and E. Riise. 1978. Origin of replication, *oriC*, of the *Escherichia coli* chromosome on specialized transducing phages  $\lambda$ asn. Mol. Gen. Genet. 160:287-295.
40. von Meyenburg, K., B. B. Jørgensen, O. Michelsen, L. Sørensen, and J. E. G. McCarthy. 1985. Proton conduction by subunit *a* of the membrane-bound ATP synthase of *Escherichia coli* revealed after induced overproduction. EMBO J. 4:2357-2363.
41. von Meyenburg, K., B. B. Jørgensen, J. Nielsen, and F. G. Hansen. 1982. Promoters of the *atp* operon coding for the membrane-bound ATP synthase of *Escherichia coli* mapped by Tn10 insertion mutations. Mol. Gen. Genet. 188:240-248.
42. von Meyenburg, K., B. B. Jørgensen, J. Nielsen, F. G. Hansen, and O. Michelsen. 1982. The membrane bound ATP synthase of *Escherichia coli*: a review of structural and functional analyses of the *atp* operon. Tokai J. Exp. Clin. Med. 7:23-31.

## Genes Encoding the Alpha, Gamma, Delta, and Four F<sub>0</sub> Subunits of ATP Synthase Constitute an Operon in the Cyanobacterium *Anabaena* sp. Strain PCC 7120†

DAVID F. McCARN, RICHARD A. WHITAKER, JAWED ALAM,‡ JACQUELINE M. VRBA,  
AND STEPHANIE E. CURTIS\*

Department of Genetics, Box 7614, North Carolina State University, Raleigh, North Carolina 27695-7614

Received 26 January 1988/Accepted 21 April 1988

A cluster of genes encoding subunits of ATP synthase of *Anabaena* sp. strain PCC 7120 was cloned, and the nucleotide sequences of the genes were determined. This cluster, denoted *atpI*, consists of four F<sub>0</sub> genes and three F<sub>1</sub> genes encoding the subunits *a* (*atpI*), *c* (*atpH*), *b'* (*atpG*), *b* (*atpF*),  $\delta$  (*atpD*),  $\alpha$  (*atpA*), and  $\gamma$  (*atpC*) in that order. Closely linked upstream of the ATP synthase subunit genes is an open reading frame denoted gene 1, which is equivalent to the *uncI* gene of *Escherichia coli*. The *atpI* gene cluster is at least 10 kilobase pairs distant in the genome from *atp2*, a cluster of genes encoding the  $\beta$  (*atpB*) and  $\epsilon$  (*atpE*) subunits of the ATP synthase. This two-clustered ATP synthase gene arrangement is intermediate between those found in chloroplasts and *E. coli*. A unique feature of the *Anabaena atpI* cluster is overlap between the coding regions for *atpF* and *atpD*. The *atpI* cluster is transcribed as a single 7-kilobase polycistronic mRNA that initiates 140 base pairs upstream of gene 1. The deduced translation products for the *Anabaena* sp. strain PCC 7120 subunit genes are more similar to chloroplast ATP synthase subunits than to those of *E. coli*.

The proton-translocating ATP synthase is a multimeric membrane protein complex that couples a transmembrane gradient of electrochemical potential energy produced during electron transport to formation of ATP. This ubiquitous enzyme is found in cell membranes of bacteria, in inner mitochondrial membranes, and in thylakoid membranes of plant chloroplasts (reviewed in references 15, 18, and 30). In all examples studied the enzyme consists of two multimeric components: an extrinsic portion, F<sub>1</sub>, composed of subunits denoted  $\alpha$ ,  $\beta$ ,  $\gamma$ ,  $\delta$ , and  $\epsilon$ , and in integral membrane portion F<sub>0</sub>, composed of several subunits which vary depending on the source of the ATP synthase. In *Escherichia coli* and chloroplasts, the two systems used for comparison in this study, there are three (*a* to *c*) and four (I to IV) F<sub>0</sub> subunits, respectively.

In *E. coli*, genes encoding all eight subunits of the ATP synthase are tightly linked and cotranscribed (15). For the ATP synthase of chloroplasts, genes for some subunits are encoded in the nucleus and others are encoded in the organelle genome. The chloroplast ATP synthase genes of higher plants are organized into two separate transcriptional units: the  $\beta$  and  $\epsilon$  genes are linked and cotranscribed (35), while a second cluster containing the I, III, IV, and  $\alpha$  subunit genes map many kilobase pairs away in a second ATP synthase gene cluster (9, 19). The  $\gamma$ ,  $\delta$ , and subunit II genes are nuclear (34).

The cyanobacteria are procaryotes with an oxygen-evolving photosynthetic system nearly identical to that of plant chloroplasts. The similarity between cyanobacterial and plant photosystems, as well as the procaryotlike features of chloroplasts, lends support to the proposal (28) that

plant chloroplasts may have evolved from close relatives of the cyanobacteria. The characterization of ATP synthase genes provides an opportunity to study the evolution of an important set of genes present in bacteria, cyanobacteria, and chloroplasts. In previous work the genes encoding the  $\beta$  (*atpB*) and  $\epsilon$  (*atpE*) subunits of the ATP synthase in *Anabaena* sp. strain 7120 were shown to be linked and cotranscribed (10). In this paper the structure and arrangement of the genes encoding the  $\alpha$  (*atpA*),  $\gamma$  (*atpC*),  $\delta$  (*atpD*), *a* (*atpI*), *b* (*atpF*), *b'* (*atpG*), and *c* (*atpH*) subunits of the ATP synthase from *Anabaena* sp. strain 7120 are reported. These genes are tightly linked in the order *atpI-atpH-atpG-atpF-atpD-atpA-atpC* and form a single transcription unit. Preceding *atpI* and within the transcription unit is an eighth gene of unknown function denoted gene 1. The 7-kilobase (kb) polycistronic mRNA is initiated 140 base pairs (bp) from the start of the operon. This large ATP synthase gene cluster is at least 10 kbp from the *atpB-atpE* operon. A similar arrangement of two ATP synthase gene clusters has been reported for the cyanobacterium *Synechococcus* sp. strain PCC 6301 (8).

### MATERIALS AND METHODS

**Isolation of cyanobacterial, bacteriophage, and bacterial DNAs.** *Anabaena* sp. strain PCC 7120 total cellular DNA was isolated from 15-liter cultures as described previously (11). Lambda bacteriophage and *E. coli* strains were grown and phage and plasmid DNA were isolated as described previously (38).

**Isolation of genomic clones containing ATP synthase genes.** A recombinant phage library of *Sau3A*I partial fragments of *Anabaena* sp. strain PCC 7120 total DNA cloned in the lambda vector  $\lambda$ L47.1, obtained from James Golden, was screened by plaque hybridization (38) by using a cloned fragment of *Chlamydomonas reinhardtii* chloroplast DNA. The plasmid p86, obtained from J. Boynton, contains a 3.6-kbp *Eco*RI fragment of *C. reinhardtii* chloroplast DNA that carries the 5' end of the *atpA* gene. p86 was digested

\* Corresponding author.

† Paper no. 11394 of the Journal Series of the North Carolina Agricultural Research Service.

‡ Present address: Department of Biochemistry and Molecular Biology, Louisiana State University Medical Center, New Orleans, LA 70112.

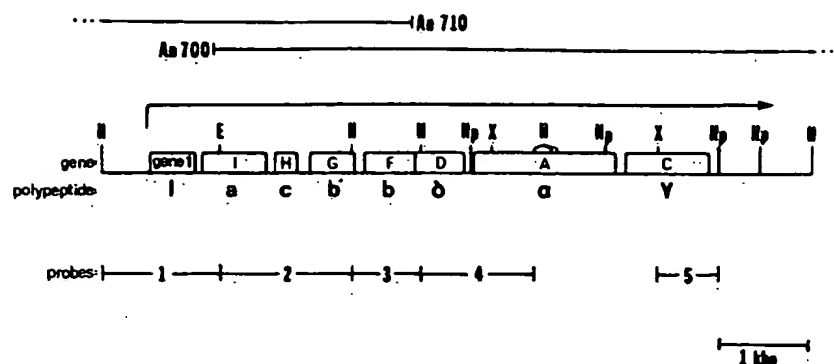


FIG. 1. Physical map of the region containing the *Anabaena* sp. strain PCC 7120 *atpI* gene cluster. The lines denoted An700 and An710 represent the inserts of *Anabaena* DNA from the recombinant clones  $\lambda$ An700 and  $\lambda$ An710, respectively. Symbol:  $\square$ , gene coding regions within which the gene (*atp*) designations are given. Gene product designations are given below the genes. The *atpF* and *atpD* coding regions overlap. *atpI* is transcribed as a polycistronic mRNA that initiates 140 bp upstream of gene 1. The numbered bars indicate specific DNA fragments used in Northern and Southern blot hybridizations. Abbreviations for restriction endonuclease sites: X, *XbaI*; Hp, *HpaI*; H, *HindIII*; E, *EcoRI*.

with *EcoRI*, and the plasmid insert was purified by electroelution from a 0.8% agarose gel. The insert was cloned into an SP6 vector (Promega Biotec, Madison, Wis.), and a  $^{32}$ P-labeled ribonucleotide probe was prepared as specified by the manufacturer. Labeled probes were purified by passage through a Sephadex G-25 spin column (27) and hybridized with plaque lifts as previously described (38). Following hybridization, the filters were washed once in  $2\times$  SSC ( $1\times$  SSC is 0.15 M NaCl plus 0.015 M sodium citrate)–0.5% sodium dodecyl sulfate at room temperature for 20 min and then a second time in  $0.1\times$  SSC–0.5% sodium dodecyl sulfate at 42°C for 2 h. A final 30-min wash was carried out under the same conditions as the second wash.

Positive clones from the screening with the *atpA* probe were rescreened with an *atpH* probe. The *atpH* probe, obtained from John Gray, contained a 140-bp *HaeIII*–*HindIII* fragment internal to the pea chloroplast *atpH* gene cloned into M13mp9 (22). The double-stranded form of the *atpH* clone was digested with *HindIII* and *BamHI*, and the insert was purified by electroelution from a 1.5% agarose gel. The fragment was cloned into an SP6 vector (Promega Biotec), and a  $^{32}$ P-labeled ribonucleotide probe was prepared as described above. One clone, denoted  $\lambda$ An700, which hybridized with both the heterologous *atpH* and *atpA* probes, was selected from the lambda library of *Anabaena* sp. strain PCC 7120 DNA and characterized further.

**Mapping and subcloning of *Anabaena* ATP synthase gene fragments.** A restriction endonuclease map of  $\lambda$ An700 was determined by using *HindIII*, *EcoRI*, and *XbaI*. Southern blots containing various restriction endonuclease digests of  $\lambda$ An700 were hybridized with the heterologous *atpA* and *atpH* probes. The *HindIII* fragments homologous to these two probes and *HindIII* fragments which mapped between them in  $\lambda$ An700 were subcloned into the M13 vectors mp18 and mp19 (Fig. 1). An *XbaI* fragment which overlapped the two *atpA*-homologous *HindIII* fragments was also subcloned into the same M13 vectors (Fig. 1).

Initial DNA sequence determinations on the cloned *HindIII* fragments indicated that  $\lambda$ An700 did not contain the entire gene cluster. A probe from near the 5' end of the  $\lambda$ An700 insert (Fig. 1, probe 3) was therefore used to screen the  $\lambda$ L47.1 recombinant library for an overlapping clone. One clone, denoted  $\lambda$ An710, which was complementary to probe 3 but not to probe 4 (Fig. 1), was selected and mapped.

A 1.3-kbp *EcoRI*–*HindIII* fragment of  $\lambda$ An710 containing the 5' end of the gene cluster and upstream sequences was subcloned into M13mp18 and M13mp19.

**Analysis of ATP synthase gene copy number.** The number of copies of the ATP synthase genes in the *Anabaena* sp. strain PCC 7120 genome was determined by hybridization of ATP synthase gene probes to Southern blots of *Anabaena* cellular DNA digested with *HindIII* or *EcoRI*. Probes 1 through 4 consisted of restriction fragments produced by digestion of  $\lambda$ An700 DNA with *HindIII* and *EcoRI*. Probe 5 was produced by digesting  $\lambda$ An700 with *XbaI* and *HpaI*. The fragments were purified by electrophoresis from agarose gels,  $^{32}$ P labeled by nick translation, and hybridized with Southern blots as described previously (38).

**DNA sequence determinations.** The sequences of the *HindIII* and *XbaI* fragments subcloned in M13 were determined by using the chain termination method (39) and site-directed oligonucleotide primers. The sequences of both strands were determined. Sequence analyses were performed by using the IBI DNA/Protein Sequence Analysis System computer software (International Biotechnologies, Inc., New Haven, Conn.).

**RNA analysis.** Total RNA was isolated as described previously (44). RNA was denatured with formaldehyde and formamide, fractionated on 1% agarose gels containing 2.2 M formaldehyde, and then transferred to nitrocellulose as described previously (27). Size markers consisting of DNA fragments of known size (1-kb ladder and lambda DNA digested with *HindIII* [Bethesda Research Laboratories, Inc., Gaithersburg, Md.]) were similarly denatured and fractionated. Northern (RNA) blots were hybridized with nick-translated probes 1 through 5 (Fig. 1) and washed as described for Southern blots.

**Oligonucleotide synthesis.** All oligonucleotides were synthesized in an automated DNA synthesizer (model 380A; Applied Biosystems, Inc., Foster City, Calif.). Oligonucleotides were prepared for DNA sequencing or primer extension as described previously (10).

**Primer extension and S1 nuclease assays.** Primer extension assays were performed as described previously (10) by using an oligonucleotide primer of 15 bases specific to the gene 1 coding region (Fig. 2).

A probe for the S1 nuclease protection assay was prepared by cloning the 1.3-kbp *HindIII*–*EcoRI* fragment (Fig. 1,

TTACACAACAGGTTGAGGAGCAATCCCTGATCTTGCCTCTCGTATCTAGCTTATCCTGAGGGTAAAGTTTCTCTAACCGTATCTCTGGGCAAGAAGT 100  
 TAATTGTTTTTTCTAAAGTATTGTTACCGGATCGTGATATGATTTCAGCTGACTGAATGTCAGTCATAATAAGTTAGCTGTACTGGTTTCAAGTCCCGT 200  
 GAGCTTGTCAGAAGAACCAATTTACCCACCCCGACAACACGACAAGATACTCAACCTGGTTTGGAGACGACAGAACCAACTCTTCCATGCAGGAG 300  
 M Q E  
 gene 1  
 TTTTATCAACTCTATCAAGAGTTGGTGTAACTCACTCTTGTCTTAAACAGGGGTTGATTATCTCTGCTGGATCTTTTATTCCTTAAACATTGCTCTGA 400  
 F Y Q L Y Q E L V L I T L V L T G V V P I S V W I P Y S L N I A L  
 ATTATTTATTAGGAGCGGTGACAGGTGTGGTTTACTTGGAGGATGTTGGCAAAAGATGTTGAGCGTTTAGGTAGAGAAAAACAGTCGCTGAGTAAACTCG 500  
 N Y L L G A C T G V V Y L R M L A K D V E R L G R E K Q S L S K T R  
 GTTGGCGTTTAAATGGCGCTGATTTTCTGGCAGCACGGTGGAAATCAATGCAATAATGCCCATCTTTTGGGATTCTCACCTACAAGCGACGCTC 600  
 L A L L M A L I L L A A R W N Q L Q I N P I P L G P L T Y K A T L  
 ATCATTATGTAGTAGGCTGGCTTTTATCTCTGACTCGCCAAAGCTCCGGCAACCTTAAAGGCTCCTCTTCTCCAGGTAAGATTGGAGAAGCAATTGA 700  
 I I Y V V R V A P I S D S P K L R Q P \*  
 AATGGAAGGAAAAATGTTGAATTTTCTGAATTTTACTCTGTTCCACTTCCGAATTTGGAAGTGGGAAAAATCTGTACTGGCAATAGGCAACTTAAAC 800  
 M L N P L N P Y S V P L A E L E V G K H L Y W Q I G N L K  
 alrI  
 TGCACGGTCAGGTGTTTCTACCTCTTGGTTTGTATTGGCTGTAGTACTAGCTTCTGTGGCTGCAAGCAGTAACGTTAAACGGATTCTAGTGGCAT 900  
 L H G Q V P L T S W P V I G V L V L A S V A A S S N V K R I P S G I  
 ACAGAACCTACTGGAGTATGCCCTGGAATTCATTCCGGGATTTGGCTAAAAACAGATTGGCGAAAAAGAAATATCGCCCTGGGTGCCTTTCTGTTGGCAT 1000  
 Q N L L E Y A L E P I R D L A K N Q I G E K E Y R P W V P P V G T  
 TTGTTTTGTTCATTTTGTGTCAAATTTGTCAGGAGCCTTAGTTCCTTCAAGCTGATTCATTGCTGAGGAGAAATTAACAGCACCAACCAGCGACA 1100  
 L P L P I P V S N W S G A L V P P K L I H L P E G E L T A P T S D  
 TCAATACAACCTGTGTCATTAGCTTTGTTGACATCTTGGCGTATTTTACCGTGGATTGAGCAAAAAAGGACTGGGGTATTTTGGTAACTACGTGCAACC 1200  
 I N T T V A L A L L T S L A Y F Y A G P S K K G L G Y F G N Y V Q P  
 TGTATCGTTCATGTGCCATTCAAAATTAAGAAGCTTCACTAAGCCCTTCCCTGAGTTTCCGTTTATTCGGTAACATCTTAGCTGATGAACCTGTA 1300  
 V S P M L P P K I I E D F T K P L S L S P R L P G N I L A D E L V  
 GTGGCCGTACTGGTATTACTAGTGCCTTTATTTGACCTTTGCCAGTAATGGCTTTCCCACTATTACAAGCGCTATCCAGGCACTAATTTTGTACTT 1400  
 V A V L V L L V P L P V P L P V M A P P L P T S A I Q A L I F A T  
 TGGCTGCGGTTCATATCGGTGAAGCGATGGAAGATCATCATGCGGAAGAGCATGAGGAACATCATTAGTCAATTAGTATTAGTTAAGTAACTGACA 1500  
 L A A A Y I G E A M E D H H G E E H E E H H \*  
 ACCGACCACTAACAAAACCATTCGTTTCATTAAAGTAAGGAAGAAATATCATGGATCCATTAGTTTCTGCTGCTTCCGTTTATAGCTGCTGCTCTAGCTGT 1600  
 M D P L V S A A S V L A A A L A V  
 alrH  
 TGGTTTGGCTGCAATCGGCCCTGGTATTGGTCAAGGTAATGCAGCAGGAACAAGCTGTAGAAGGTATTGCCCGTCAGCCGAGCAGAAGGTAATAATTCGC 1700  
 G L A A I G P G I G Q G N A A G Q A V E G I A R Q P E A E G K I R  
 GGTACATTACTACTCAGTTTGGCGTTTATGGAAGCGCTAACCATCTACGGTCTAGTAGTGTCTAGTATTGTTGTTTGTAAACCCCTTTCGATAATCAG 1800  
 G T L L L S L A P M E A L T I Y G L V V A L V L L P A N P P A \*  
 TACTGAGTACTGGGTGCTGAGTGTGAGTGAGTGAATAAGTATTAGGAGTAAAGGGTTAAGCCCTTTAACCCATAACTTATAACTCAAACTCAAACTCAAAC 1900  
 TCACAACCTCAGGACTAACATAGTAGATAGGAACAAGCAAAACATGACACATTCGATCACCTTATTGGCGGTGGAAGGTTGCCAAGGAAGCGGCGCTATT 2000  
 M T H W I T L L A V E K V A K E G G L P  
 alrG  
 TGATTTAGATGCTACCTTACCTTAATGGCAATCCAGTTCCTCTGTTAGCTCTGATATTGAATGCCACTCTCTACAAGCAATTGGGTAAAGCTATTGAT 2100  
 D L D A T L P L M A I Q P L L L A L I L H A T L Y K P L G K A I D  
 GGGCGAAATGAATATGTTCTGAACAATCAATTAGAAGCCCAAGAGCGTTTGTCAAAGCTGAGAAATTTGCAGAGGCTTACGAAACAGAGTTAGCAGGAG 2200  
 G R N E Y V R N N Q L E A Q E R L S K A E K L A E A Y E Q E L A G



CTAGACGGC<sup>•</sup>AAAGCACAAC<sup>•</sup>AAATTATTGCTGACGCTCAAG<sup>•</sup>CGGAGCCAAAA<sup>•</sup>ATTGCTGCTGAAAA<sup>•</sup>AGTAGCAGCAGCG<sup>•</sup>CAAAA<sup>•</sup>GAAAGCTCAGGCACA  
 A R R Q A Q T I I A D A Q A E A Q K I A A E K V A A A Q K E A Q A Q 2300  
 AAGAGAACA<sup>•</sup>AGCGGCCGGTGA<sup>•</sup>AAATTGAGCAGCAAAA<sup>•</sup>ACAGCAGGCTCTGG<sup>•</sup>CTTCTTAGAGCAACAAGTAGATGCCCTAAGTCGCCAAATCTTAGAAAA<sup>•</sup>G  
 R E Q A A G E I E Q Q K Q Q A L A S L E Q Q V D A L S R Q I L E K 2400  
 CTTTGGGAGCCGATCTAGTAAAGCAGCGCTAACTCAATAA<sup>•</sup>ATTAGTCATTAGTCATTGGTCATTAGTCATTAGTCAAA<sup>•</sup>AGAGAGAATGACGAAGGGCG  
 L L G A D L V K Q R \* 2500  
 AATGACACA<sup>•</sup>AACTTTGGCAGCGCAGTTGTGGATGAAAA<sup>•</sup>ATCATGGGCACTTTT<sup>•</sup>TACTGTTGATGGCGGAAGCCAGCG<sup>•</sup>CGTTGGAGGTGAATGGCAG  
 M G T F L L L M A E A S A V G G E L A  
 ALDP 2600  
 AAGGTGGGG<sup>•</sup>CGAAGGTGGTTTGGTTTAAATACCAATATTCTCGACACCA<sup>•</sup>ACTGATTAACTGGCCATTATTACTGTGCTGTTTGTCTTTGGCAGC  
 E G G A E G G P G L N T N I L D T N L I N L A I I I T V L F V P G R 2700  
 GAAGTTTGGGTAATACCTGAA<sup>•</sup>AACTCGCCGCAAAA<sup>•</sup>CAATTGAAACAGCAATTAAGAA<sup>•</sup>TGCAGAA<sup>•</sup>CAAGTGGCGCAGATGCAGCCAAGCAACTGAA<sup>•</sup>  
 K V L G N T L K T R R E N I E T A I K N A E Q R A A D A A K Q L K 2800  
 GAGGCGCAACAAAA<sup>•</sup>ACTAGAGCAAGCACAAGCAGAAGCTGAGAGAATCAAAAA<sup>•</sup>ATCAGCCCAAGACAATGCTCAAA<sup>•</sup>CCGAGGTCAAGCCATCATTTGCC<sup>•</sup>  
 E A Q Q K L E Q A Q A E A E R I K K S A Q D N A Q T A G Q A I I A 2900  
 AAGCTGCTGTAGATATTGA<sup>•</sup>ACGCTTACAAGAAGCAGGGG<sup>•</sup>CAGCAGACTTGAATGCAGAACTAGATAGAGCGATCGCTCAGTTGGCGCAGCGAGTAGTTGC  
 Q A A V D I E R L Q E A G A A D L N A B L D R A I A Q L R Q R V V A 3000  
 TTTGGCATTGCAAAAGGTGCAATCAGAACTGCAAGGTGGCATTAGTGAAGATGCTCAAAAA<sup>•</sup>ACTCTAATTGACCGTAGCATCGCACAATGGGAGGGCGGA  
 L A L Q K V E S E L Q G G I S E D A Q K T L I D R S I A Q L G G G 3100  
 GTATGACAAGTAAAGTAGCAAA<sup>•</sup>CACTGAGGTAGCTCAACCTTACGCTCAGGCAC<sup>•</sup>TGTTGTCAATCGCCAAATCGAAAAGCTTGACGGAAGAGTTCCGCAC  
 V \*  
 M T S K V A N T E V A Q P Y A Q A L L S I A K S K S L T E E P G T  
 ALDP 3200  
 AGATCGCGTACTTTGCTGA<sup>•</sup>ACCTGCTGACAGAAA<sup>•</sup>ATCAACAGCTACGCAACTTCATCGATAACCCCTTTATTGCGAGCTGAGAACAAAA<sup>•</sup>AGCTCTCATC  
 D A R T L L N L L T E N Q Q L R N P I D N P F I A A E N K K A L I 3300  
 AAACAAATATTGAGTGAAGCTAGCCCTTACCTACGTAAC<sup>•</sup>TCTTACTGTTGTTGGTAGATAAA<sup>•</sup>CGACGCA<sup>•</sup>TTTCTTCTTGCAGAGATTTTACAGCAGT  
 K Q I L S E A S P Y L R N P L L L L V D K R R I F F L P E I L Q Q 3400  
 ATTTGGCTCTCTTACGGCA<sup>•</sup>ACTGAATCAAA<sup>•</sup>CCGTATTAGCGGAAGTACTTCTGCTGTGGCTTTAACAGAA<sup>•</sup>GATCAACAGCAAGCAGTTACAGAAAAGGT  
 Y L A L L R Q L N Q T V L A E V T S A V A L T E D Q Q Q A V T E K V 3500  
 ATTTGGCACTACCAAAGCTCGTCAAGTGGAACTGGCAACCAAGGTAGACAGTACCTGATTGGTGGTGTGATCATTAAAGTAGGCTCTCAGGTAATTGAC  
 L A L T K A R Q V E L A T K V D S D L I G G V I I K V G S Q V I D 3600  
 TCTAGTATCCGGGTCAGTTGCGTGCCTCTCTTGGCGCTTAAGCAATAGCTAGAAAGTT<sup>•</sup>CAGAGGTTAAAGTTAGCGGTTT<sup>•</sup>CACATCAGGCACTTGACA  
 S S I R G Q L R R L S L R L S N S \* 3700  
 ATTAATAATTGTTGTGATTGTGGTTAACTCTTAACACCTCAAACTAAATGCAGACGCGATATTGTTTCTCGCGTCTATTAAATATCTTCCGTCTCGCAA  
 3800  
 GAAAAAAGATACACACATGAGCATTTCAAATTAGACCTGACGAAATCAGCAGTATTATT<sup>•</sup>CAGCAGCAAA<sup>•</sup>TCGAGCAATACGACCAAGAA<sup>•</sup>GTCAAAAGTTGC  
 M S I S I R P D E I S S I I Q Q Q I E Q Y D Q E V K V A  
 ALPA 3900  
 TAACGTCGGTACTGTACTACAAAGTAGGTGACGGTATCGCCCGGATCTATGGTCTAGAAAAGGCTATGGCTGGGGAAC<sup>•</sup>TTTGGAA<sup>•</sup>TTTGAAGACGGCACA  
 N V G T V L Q V G D G I A R I Y G L E K A M A G E L L E F E D G T 4000  
 GTTGGTATCGCCCAAACTTAGAAGAAGATAACGTTGGTGGGCTACTGATGGGTGAAGGCGGGAAATTCAGAAGGTAGCACCGTTACTGTACTGGCA  
 V G I A Q N L E E D N V G A V L M G E G R E I Q E G S T V T A T G 4100  
 GAATTGCTCAAAATCGGTGTCGGTGAAGCCTTAATTGGCCCGCTTGTGATGCTTTGGGTGCTGCTATTGACGGTAAAGGCGCATCAAGCCAGCGAAAG  
 R I A Q I G V G E A L I G R V V D A L G R A I D G E G D I K A S E S 4200  
 CCGCTGATTGAATCTCTCGCCCTGGTATCATCGCTCGTCTCGCTACAGAAACCGGTATCACTGCGAATTGACTCCATGATTCCTATT  
 R L I E S P A P G I I A R R S V H E P M Q T G I T A I D S M I P I 4300

4400  
 GCGCGTGGTCAACGGGAATTAATCATTTGGTACCGCTCAAAACAGGTAAACATCCGATCGGATCGACACCATCATTAACCAAAAAGTGAAGATGTAGTT  
 G R G Q R E L I I G D R Q T G K T A I A I D T I I N Q K G E D V V

4500  
 GCCTTACGTTGCCATTGTGCTCAAAAAGCTTCTACCGTTGCTAACGTAGTCCAACTCTCAAGAAAAAGTGAATGGATTACAGTAGTGTAGTGTGCTGC  
 C V Y V A I G Q K A S T V A H V V Q T L Q E K G A N D Y T V V V A A

4600  
 TGGTGCCAGTGAACCTGCTACCGTACAATTCCTGGCTCCCTACACAGGCGCTACTATTGCTGAGTACTTCATGTACAAAAGCAAGCTACCTTGGTAATT  
 G A S E P A T L Q P L A P Y T G A T I A E Y F M Y K G K A T L V I

4700  
 TACGACGACTTATCTAAGCAAGCTCAAGCTTATCCGCAAAATGCTCTGCTGTTACGTGCTCCACCAGGAGCGGAAGCTTACCGTGGAGAGCTATCTTACA  
 Y D D L S E Q A Q A Y R Q N S L L L R R P P G G S A Y P G D V F Y

4800  
 TTCACCTCTGTTTGTGGAAAGACGCAAACTCAGTGTGAAGTCTGGTAAAGTAGCATGACCGCGCTACCAATCATCGAAAGCCAAAGCTGGTGAAGT  
 I H S R L L E R A A K L S D E L G K G S N T A L P I I E T Q A G D V

4900  
 TTCTGCTACATCTCTACCAACGTAATTTCTATTACAGACGCTCAGATATCTTATCTTCTGACTTATTAAAGCTGGTATTCTGCTCGGCTGTAAACCTT  
 S A Y I P T H V I S I T D G Q I P L S S D L F N A G I R P A V H P

5000  
 GGTATCTCTGTATCCCGTGTGGGTTCTGCGGCACAAACCAAGCGATGAAGAAAGTGTCTGGTAAGATTAGCTCGAACTAGCACAGTTTACGACCTTCC  
 G I S V S R V G S A A Q T E A N K K V A G K I K L E L A Q F D D L

5100  
 AAGCCTTCGCGCAATTTGCTTCCGACCTAGATAAAGCCACCCAGACCAATTTGGCAAGAGGTCAACGCGCTCGCGGAACTCTCAACAGTCCCAAAATCA  
 Q A P A Q P A S D L D K A T Q D Q L A R G Q R L R E L L K Q S Q N Q

5200  
 GCCTCTATCCGTAGCTGAACAAAGTAGCCATCTGTATCCGAGGTATCAACGCTTACTTAGATGATATCCCTGTTGATAAAAGTCACCACTTACCAAAGGC  
 P L S V A E Q V A I L Y A G I N G Y L D D I P V D K V T T P T K G

5300  
 TTGAGAGATTACTTGAAGTCCGCGTAAACCCCTACTTCCAAGACGTACAAATCGAAGAAAGCACTGGGTGATGATGAAGAAAGCAATTGAAGCGAGCTT  
 L R D Y L K S G V N P Y F Q D V Q S K K A L G D D E E K A L K A A

5400  
 TAGAAGACTACAAAAAGACCTTCAAGCTACAGCGTAATTAGTCTATTGGTCACTGCTAGTACCAATAGACACTGACAACCTGACAACCTGACAA  
 L E D Y K K T F K A T A \*

5500  
 CTGACAACCTGACAATCAACAAATATTATGCTTAATCTCAATCAATACGGGATCGCAATTCAGTCCGTCAAAAACCAAGAAATACACAGAAAGCATGCG  
 M P N L K S I R D R I Q S V K N T K K I T E A M R  
 ALPC

5600  
 CTTGGTACGCGCGCGCGGTACGTCGCGCCCAAGAACAGTAATCGCTACTCGTCTCTTGTGCTGACCGTTTGGCACAAGTATTATACGGTTTCCAACT  
 L V A A A R V R R A Q E Q V I A T R P F A D R L A Q V L Y G L Q T

5700  
 CGTCTACGCTTTGAAGATGTAGACTTACCTCTACTGAAAAACCGGAAGTTAAATCAGTAGGCTTGTAGTTATTCTGGCGATCGTGGTTGTGCGCGG  
 R L R P E D V D L P L L K K R E V K S V G L L V I S G D R G L C G

5800  
 GTTACAATAACAAGCTATCCGTCGCGGAAAAACCGGCAAGAACTCAAGGCAGAAAGTCTAGATTACACATTGTTATTGTTGGCGAAAAAGCTGA  
 G Y N T N V I R R A E N R A K E L K A E G L D Y T F V I V G R K A E

5900  
 ACAATATTTAGACGCGCTGAACCAACCATCGATGCTAGTTACTGCTTAGAGCAAAATCCCAACCGCGATGAAGCTAATAAAATTCGACGAATTC  
 Q Y F R R R E Q P I D A S Y T G L E Q I P T A D E A N K I A D E L

6000  
 CTCTCTTATCTCTCAGAAAAAGTAGACCGCATCGAGTTAGTTACACCGCTTCTGCTCTCTTGGTTAGCTCTGCTCCGCTATCCAAACCTTGTCTAC  
 L S L P L S E K V D R I E L V Y T R P V S L V S S R P V I Q T L L

6100  
 CCCTTGACACTCAAGGTTTGAAGCAGCGGATGACGAAATATCCGTCGACAACTCGTGGCGGTCAATTCGAAGTGGAAAGCCAAACAGTACCAAGCA  
 P L D T Q G L E A A D D E I P R L T T R G G O P Q V E R O T V T S Q

6200  
 AGCTCGCCCTTTGCCCGCGACAGTATTTTGAACAAGACCCAGTACAGATTCTTGATTCACTATTCCTTGTATTTAAGCAACCAAGCTATTACGGCGG  
 A R P L P R D S I P E Q D P V O I L D S L L P L Y L S N Q L L R A

6300  
 CTGCAAGATCAGCCGCTAGTGAATTAGCCGCGCGGATGACAGCAATGAGCAACGCTAGTGAAGAAAGCTGGTGAATTAATCAAGTCTCTTCACTGTCTCT  
 L Q E S A A S E L A A R N T A N S H A S E N A G E L I K S L S L S

6400  
 ACAACAAAGCCGCTCAAGCCGCCATTACCCAAAGAACTCTTGAAGTGTGTGGTGTGTCAGAAAGCGTGTGACTTAGGAAAAAGCAATTCCTAGACATGACAA  
 Y H K A R Q A A I T Q E L L E V V G G A E A L T \*

6500  
 ATAGCTAATTGCTAGTCACTTCAACTGGCAATTAGCTATTTTAAATTTTAAAGTGTCCCGTTAACCATCTATGATTACAAATTACGAATGACGAAC

TACGAATTAATAATCCCGTACTATAATGAAATATAAAGATCATGGGTCGTCGGTTTCGACAGGTGGCGAACGCTACTCTGTGATTCAAGGTCGAGAGT 6600  
 GAGTCTCTCTGCAAAATCAAGGCTCAAAAAGTAAATGCGAATAACATCGTTAAATTTGCTCGTAAGGACGCTCTAGTAGCTGCCTAAATAGCCTCT 6700  
 TTCAGGTTTCGAGCGTCTTCGGTTTGAATCCTTAAGGACTGAAGACCAACCCCAACGGATGCTCTAGCAATGTTCTCTGGTTGGCTTGTAGCTAAGAT 6800  
 TTAATCAGAGCATCTACGTTTCGGGATAATGAACGATTCCTCCGCTTGAGGGTCAGAAAGGCTAAACCTGTGAATGAGCGGGGGTCAATACCCAATTGCG 6900  
 ACAGCAGTTCGACTCTGCTCGATCCACTAACAGTAAATATAGTTAAACAGTCCACTTCTCTACGAGGTGGACTTTTGTATTTATGGATACATTTCTCTCTG 7000

FIG. 2. Nucleotide sequence of the noncoding strand of the *atpI* gene cluster and flanking regions. Translation products are given below the nucleotide sequence. The complement to the sequence of the primer used in the primer extension assay is overlined. The arrowhead indicates the 5' end of the mRNA transcript as determined by primer extension. Clusters of direct repeat sequences are underlined by arrows. Convergent arrows mark inverted repeat sequences capable of forming stable stem-loop structures in mRNA.

probe 1) of  $\lambda$ An710 into the vector pBS M13<sup>+</sup> (Stratagene Cloning Systems, San Diego, Calif.). A full-length <sup>32</sup>P-labeled ribonucleotide probe complementary to the mRNA was prepared as specified by the manufacturer. S1 nuclease assays were performed as described previously (27) with the ribonucleotide probe and total RNA.

## RESULTS

**Cloning of the ATP synthase genes.** A lambda recombinant library of total *Anabaena* sp. strain PCC 7120 DNA was screened with a probe containing a portion of the gene for the  $\alpha$  subunit (*atpA*) of the ATP synthase from *C. reinhardtii* chloroplasts. Positive clones were rescreened with a  $c$  subunit gene (*atpH*) from pea chloroplasts. A clone denoted  $\lambda$ An700, which hybridized with both the *atpA* and *atpH* probes, was selected and characterized by restriction endonuclease mapping (Fig. 1).

Hybridization of the *atpA* and *atpH* probes to restriction endonuclease digests of  $\lambda$ An700 DNA indicated *Hind*III fragments of 1.3 and 2.8 kbp with homology to *atpA* and a 3.6-kbp *Hind*III fragment with homology to *atpH*. The *atpH*-homologous fragment contained one end of the *Anabaena* DNA insert in  $\lambda$ An700 and approximately 2.0 kbp of vector DNA. The three identified fragments and the *Hind*III fragments which mapped between them in  $\lambda$ An700 were subcloned into M13 vectors. An *Xba*I fragment which overlapped the two *atpA* homologous *Hind*III fragments was also subcloned into M13.

**DNA sequence analysis of the ATP synthase genes.** The sequences of the subcloned *Hind*III and *Xba*I fragments of  $\lambda$ An700 were determined. Translation of the DNA sequence revealed that one end of the insert in  $\lambda$ An700 fell within an open reading frame (ORF) which was followed by six closely linked ORFs on the same DNA strand (Fig. 2). To obtain the sequence of the incomplete ORF and upstream sequences, we isolated an overlapping clone, denoted  $\lambda$ An710, from the lambda recombinant library (Fig. 1). A 1.3-kbp *Hind*III-*Eco*RI fragment of  $\lambda$ An710 containing the incomplete ORF was subcloned, and its sequence was determined. This fragment contained the 5', end of the partial ORF from  $\lambda$ An700, which was preceded by an additional closely linked ORF (Fig. 1). Thus, the entire gene cluster contained eight ORFs and was denoted *atpI* in accordance with the nomenclature proposed by Cozens and Walker (8).

There are no other ORFs on either strand of the DNA in close proximity to the *atpI* cluster. The 1.3 kbp of sequence characterized downstream from *atpC* does not contain any

ORFs, nor does the 700 bp of sequence upstream from gene 1.

**Identification of F<sub>1</sub> subunit genes.** Cyanobacterial ATP synthases are similar in size to those of *E. coli* and chloroplasts (20, 26), and the F<sub>1</sub> component is composed of five subunits ( $\alpha$ ,  $\beta$ ,  $\gamma$ ,  $\delta$ , and  $\epsilon$ ), which are similar in size to those of other organisms. To identify the ATP synthase F<sub>1</sub> subunit genes in *atpI*, we compared the ORFs with the deduced translation products of F<sub>1</sub> subunit genes from other organisms. The  $\alpha$  subunit gene (*atpA*) was identified on the basis of the high similarity of the deduced translation product to the tobacco chloroplast and *E. coli*  $\alpha$  subunits (Table 1). The *atpA* gene encodes a protein of M<sub>r</sub> 57,181 or 54,301, depending on which of two in-frame methionines is used to initiate translation.

The ORFs upstream and downstream of *atpA* showed homology to the *E. coli*  $\delta$  and  $\gamma$  subunits, respectively (Fig. 1; Table 1). Their placement relative to *atpA*, which was the same as in the *E. coli* ATP synthase operon, further supported the identification of these as  $\delta$  (*atpD*) and  $\gamma$  (*atpC*) subunit genes. The *atpC* and *atpD* genes encode proteins of M<sub>r</sub> 35,213 and 20,345, respectively, in good agreement with the molecular weights determined by denaturing sodium dodecyl sulfate-gel electrophoresis for the  $\delta$  and  $\gamma$  subunits from the cyanobacterium *Spirulina platensis* (20).

TABLE 1. Similarity with *Anabaena* proteins<sup>a</sup>

ATP synthase subunit	% Similarity with proteins from:		
	<i>Synechococcus</i> sp. <sup>b</sup>	Chloroplasts <sup>c</sup>	<i>E. coli</i> <sup>d</sup>
$\alpha$	78	69	55
$\beta$	87	81	68
$\gamma$	80	N <sup>e</sup>	35
$\delta$	49	N	26
$\epsilon$	70	41	33
a (IV)	80	68	17
b (I)	41	26	26
b' (II)	58	N	NE <sup>f</sup>
c (III)	96	89	33

<sup>a</sup> *Anabaena* sp. strain PCC 7120; percent identical amino acids after alignment for maximum similarity.

<sup>b</sup> *Synechococcus* sp. strain PCC 6301 (8).

<sup>c</sup> Amino acid sequences for all subunits are from spinach chloroplasts (19, 47), except for the  $\alpha$  subunit, which is from wheat chloroplasts (23).

<sup>d</sup> Amino acid sequences from references 16, 17, and 40.

<sup>e</sup> N, Nucleus encoded in plants; complete amino acid sequences not available.

<sup>f</sup> NE, No equivalent subunit.

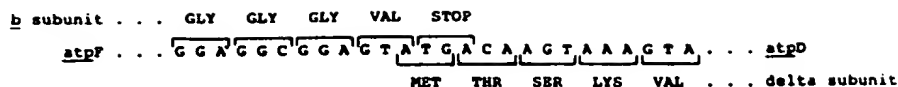


FIG. 3. Nucleotide and amino acid sequence showing the overlap between the *atpF* and *atpD* genes.

**Identification of  $F_0$  subunit genes.** Little information is available on the amino acid sequences of cyanobacterial  $F_0$  subunits or the subunit composition of the  $F_0$  component. Upstream from the three  $F_1$  genes in *atpI* are four ORFs (Fig. 1) with various degrees of similarity to  $F_0$  subunits from different sources. The third ORF in *atpI* is very similar to subunits *c* and III from *E. coli* and chloroplasts, respectively, and is identified as a *c* subunit gene (*atpH*). The second ORF downstream from *atpH* has sequence similarity to chloroplast I subunits and is therefore identified as a *b* subunit gene (*atpF*). The ORF preceding *atpF* has similarity with the partial amino acid sequence available for subunit II of chloroplasts (4). An equivalent subunit is lacking in the *E. coli*  $F_0$ . However, an analogous ORF has been characterized in *Synechococcus* sp. strain PCC 6301 and denoted *b'* (45) on the basis of the similarity of its structure to those of *b* subunits. In accordance with this suggested nomenclature, the fourth ORF in the *Anabaena atpI* cluster is identified as a *b'* (II) subunit gene (*atpG*). The *atpF*, *atpG*, and *atpH* gene sequences encode proteins of  $M_r$  19,754, 17,953, and 7,894, respectively.

Two additional ORFs map upstream of *atpH* in the *atpI* cluster. The first of these does not appear to encode an ATP synthase subunit, but has a similar hydropathy profile to the *uncI* gene product of *E. coli* (data not shown). *uncI*, which has a similar position in the *E. coli* ATP synthase gene cluster, encodes a hydrophobic polypeptide of unknown function. An analogous gene in the *Synechococcus* sp. strain PCC 6301 *atpI* cluster has been denoted gene 1 (9), and this nomenclature is also used for the first ORF in the *Anabaena* sp. strain PCC 7120 gene cluster. The gene 1 product has two potential initiator methionines and therefore has *M<sub>r</sub>* 18,766 or 14,028. Between gene 1 and *atpH* is an ORF with homology to subunits *a* and IV of *E. coli* and chloroplasts, respectively (Table 1); it is identified as an *a* subunit gene (*atpI*). The *atpI* gene encodes a protein of *M<sub>r</sub>* 27,974. The order of the genes in the *Anabaena atpI* gene cluster is thus gene 1-*atpI*-*atpH*-*atpG*-*atpF*-*atpD*-*atpA*-*atpC*.

**Features of the *atpI* DNA sequence.** Within the *atpI* cluster, the spacer regions between genes range from 60 to 170 bp in length, except for the *atpF* and *atpD* arrangement. These genes are fused such that the last two codons of *atpF* overlap the first two codons of *atpD* (Fig. 3). The other intergenic spacer regions of the *atpI* cluster contain numerous short direct repeat sequences (Fig. 2). In the *atpA-atpC* intergenic region, the two sets of direct repeats are complementary to each other (i.e., an inverted repeat), such that a stable stem-loop structure (43) could be formed in the mRNA (Fig. 4). Two other inverted repeat sequences which could form stable stem-loop structures are observed at 29 and 548 bp downstream from the *atpI* cluster (Fig. 2, positions 6399 and 6948; Fig. 4).

**Analysis of ATP synthase gene copy number.** Radiolabeled DNA probes were prepared from various regions of the ATP synthase gene cluster (Fig. 1, probes 1 to 5) and hybridized to Southern blots of total *Anabaena* sp. strain PCC 7120 DNA digested with *Hind*III or *Eco*RI (data not shown). All probes hybridized to single bands of the expected size in each digest, indicating that these genes occur as single copies in the genome.

**Analysis of transcripts.** Nick-translated probes produced from various regions of *atpI* (Fig. 1) were hybridized with Northern blots of total *Anabaena* sp. strain PCC 7120 RNA to assess the number and sizes of mRNA species derived from the gene cluster. Each probe hybridized with an mRNA species of approximately 7.0 kb (Fig. 5), suggesting that the genes are part of a large transcriptional unit. All probes showed some hybridization to RNA species in the size ranges of the rRNA bands. Probe 1 (Fig. 1) hybridized with two additional bands of approximately 2.1 and 1.2 kb. Probe 2 also hybridized with a 2.1-kb transcript (Fig. 5).

Primer extension assays performed with total RNA and a primer specific to the gene 1 coding region (Fig. 2) produced a single primer-extended product which mapped 140 bp upstream from the predicted translation start for gene 1 (Fig. 6). S1 nuclease mapping with a probe that included the 5' end of *atpI*, all of gene 1, and 500 bp 5' to gene 1 (Fig. 1, probe 1) confirmed the single mRNA endpoint identified in the primer extension assay and demonstrated that no additional RNA endpoints map between gene 1 and *atpI* (data not shown).

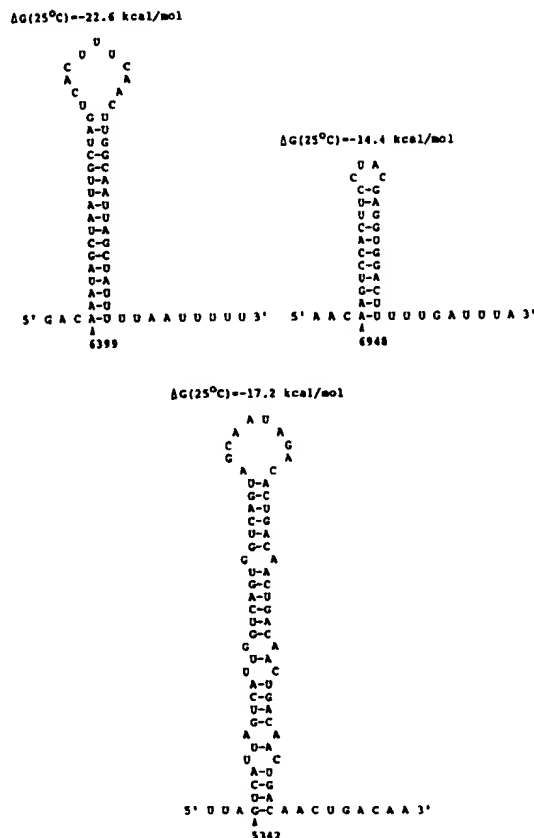


FIG. 4. Nucleotide sequences of regions theoretically capable of forming stable stem-loop structures in mRNA. Nucleotides are numbered as in Fig. 2.

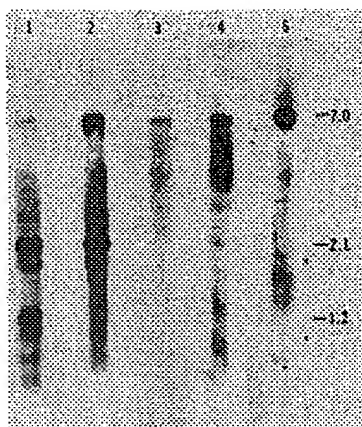


FIG. 5. Identification of *atpI* mRNA species. Total *Anabaena* sp. strain PCC 7120 RNA (20  $\mu$ g) was denatured, electrophoresed, transferred to nitrocellulose paper, and hybridized with specific probes marked in Fig. 1. Approximate sizes of hybridizing species are shown.

## DISCUSSION

**Organization of ATP synthase genes in *E. coli*, cyanobacteria, and chloroplasts.** In previous work (10) the genes encoding the  $\beta$  (*atpB*) and  $\epsilon$  (*atpE*) subunits of the ATP synthase from the filamentous cyanobacterium *Anabaena* sp. strain PCC 7120 were shown to form an operon (*atp2*) and to be unlinked to other ATP synthase genes. A cluster of the remaining eight genes encoding subunits of the ATP synthase has been isolated and characterized by nucleotide sequencing. The genes of this cluster, denoted *atp1*, were

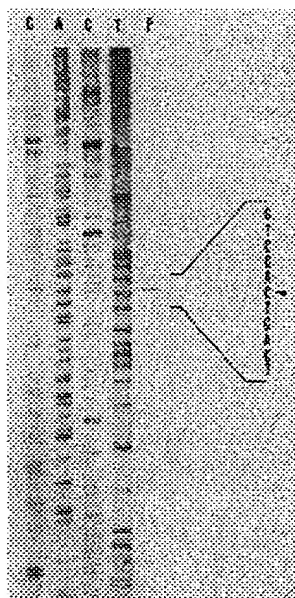


FIG. 6. Identification of the start site for transcription of the *atpI* gene cluster. A 15-nucleotide primer specific to the gene 1 coding region was used in a primer extension assay with total *Anabaena* sp. strain PCC 7120 RNA. The extended product was electrophoresed in parallel with a sequence ladder (G, A, C, T) generated by using the same primer on the noncoding strand of the DNA.

identified by comparison of their predicted translation products with amino acid sequences of ATP synthase subunits from other organisms. The organization of the *Anabaena* sp. strain PCC 7120 genes is *atpI-atpH-atpG-atpF-atpD-atpA-atpC*; in addition, a closely linked gene denoted gene 1 is found upstream of *atpI* in this cluster. Gene 1 appears to be equivalent to *E. coli uncl*, which encodes a polypeptide of unknown function. Each of the *Anabaena* sp. strain PCC 7120 ATP synthase genes is single copy. The *atpI* gene cluster is at least 10 kbp from the *atp2* cluster. The same ATP synthase gene organization is observed in the unicellular cyanobacterium *Synechococcus* sp. strain PCC 6301 (8).

In *E. coli*, eight genes for the ATP synthase subunits and *uncl* are clustered and cotranscribed (15). The two clusters of ATP synthase genes thus characterized from cyanobacteria are ordered in the same manner as in *E. coli*, but both *Synechococcus* sp. strain 6301 and *Anabaena* sp. strain PCC 7120 have an extra gene (*atpG*) relative to *E. coli*. *atpG* encodes a protein similar to the partial amino acid sequence of spinach chloroplast subunit II (4). The *atpG* product has been designated *b'* (45) on the basis of the similarity of its hydrophathy profile with those of the *b* subunit of *E. coli* and subunit I of chloroplasts. It has been hypothesized that *atpG* represents a duplicated and diverged copy of *atpF* (9). The characterization of four genes encoding  $F_0$  subunits from two cyanobacterial species suggests that cyanobacterial ATP synthases, like those of chloroplasts (36, 46), contain an  $F_0$  composed of four polypeptides.

The cyanobacterial ATP synthase gene arrangement is reminiscent of the organization in higher-plant chloroplasts. Chloroplast ATP synthase genes are found in two clusters: genes encoding subunits IV (*atpI*), III (*atpH*), I (*atpF*), and  $\alpha$  (*atpA*) are found in tandem in that order (9, 18), whereas the *atpB* and *atpE* genes are found in tandem but map elsewhere in the genome (34). Thus, chloroplasts and cyanobacteria have two clusters of ATP synthase genes, with genes within each cluster in the same order. Genes for the remaining chloroplast subunits, II (*atpG*),  $\delta$  (*atpD*), and  $\gamma$  (*atpC*), however, are encoded in the nucleus (34). The cyanobacterial ATP synthase gene organization is thus intermediate between those observed in *E. coli* and higher-plant chloroplasts.

**Features of the *atpI* DNA sequence.** A unique feature of the *Anabaena* sp. strain PCC 7120 *atpI* cluster is overlap between the *atpF* and *atpD* genes: nucleotides of the last amino acid codon and stop codons of *atpF* make up the first and part of the second codon of *atpD* (Fig. 3). A similar overlap is not observed in the cyanobacterium *Synechococcus* sp. strain PCC 6301 or in *E. coli*. The *Anabaena* sp. strain PCC 7120 *atpF-atpD* gene overlap cannot be unequivocally established until amino acid sequences for the *b* and  $\delta$  subunits are available. Two pieces of information, however, support the idea that these genes overlap. (i) All of the *Anabaena* sp. strain PCC 7120 ATP synthase gene coding regions, as well as other *Anabaena* sp. strain PCC 7120 genes thus far characterized, initiate with a methionine codon; the only methionine codon in the *atpD* reading frame is that which overlaps with the *atpF* gene. (ii) The first three amino acids of the *Synechococcus* sp. strain PCC 6301 and *Anabaena* sp. strain PCC 7120 deduced *atpD* gene translation products are identical, and the protein homologies are colinear.

The *Anabaena* sp. strain PCC 7120 *atpF-atpD* gene overlap is reminiscent of the situation found in many plant chloroplasts in which the *atpB* and *atpE* genes overlap (23, 25, 47). The *atpB-atpE* overlap in chloroplasts is similar to

that observed for *atpF* and *atpD* in that the last two codons of *atpB* overlap with the first two codons of *atpE*. *atpB-atpE* overlaps are not observed in *Anabaena* sp. strain PCC 7120 (12), *Synechococcus* sp. strain PCC 6301 (9), or *E. coli* (35). Another feature of chloroplast ATP synthase genes which is absent in *E. coli* and the cyanobacteria studied is observed in the structure of the *atpF* gene. The chloroplast *atpF* genes contain an intron (5, 19, 33, 42), whereas those of *Anabaena* sp. strain PCC 7120 and *Synechococcus* sp. strain PCC 6301 (8) do not.

Most, but not all, of the genes of the *Anabaena* sp. strain PCC 7120 *atpI* cluster are preceded by regions similar to that of *E. coli* ribosome-binding (Shine-Dalgarno) sequences (41). The sequence of the 16S rRNA from *Anabaena* sp. strain PCC 7120 has not been determined, but the 16S rRNA from the cyanobacterium *Synechococcus* sp. strain PCC 6301 has the same sequence as that of *E. coli* in the mRNA binding region (6). Thus, cyanobacterial ribosome-binding sites are expected to be similar to those of *E. coli*. The absence of Shine-Dalgarno sequences has also been observed with the *rbcS* (32) and *psbA* (12) genes of *Anabaena* sp. strain PCC 7120.

The ORFs for gene 1 and *atpA* contain two potential initiator methionines, and since no protein sequence data are available for these polypeptides from *Anabaena* sp. strain PCC 7120, it is not possible to ascertain where translation initiates. The presence of a putative ribosome-binding site near the downstream methionine in gene 1 would suggest that this is the translation start point, and comparison of homologies with the gene 1 products from *E. coli* and *Synechococcus* sp. strain PCC 6301 would support this. The *atpA* gene, however, contains no identifiable ribosome-binding site near either potential initiator methionine codon. As with the gene 1 product, the *Anabaena* sp. strain PCC 7120  $\alpha$  subunit amino acid sequence is homologous with the  $\alpha$  subunits from other organisms starting with the downstream methionine. The  $\alpha$  subunit from *S. platensis* was estimated by denaturing sodium dodecyl sulfate-gel electrophoresis to be of  $M_r$  53,400 (20). This is in closer agreement to the predicted size ( $M_r$  54,301) of the deduced translation product of *Anabaena atpA* derived from the downstream in-frame methionine.

Many of the intergenic spacer regions of *atpI* are characterized by short direct repeats (Fig. 2). Such repeats are also observed in the *atpB-atpE* spacer of the *atp2* cluster (12). The two sets of repeats in the *atpA-atpC* spacer are complementary; interestingly, these same two sets of repeats are found in the *atpB-atpE* spacer in the same position relative to each other and to the upstream gene. They are also observed downstream of the phycocyanin operon in *Anabaena* sp. strain PCC 7120 (3). The significance of these repeat sequences is not known.

**Transcription of *atpI*.** All genes of *atpI* hybridized with an mRNA transcript approximately 7.0 kb in length, indicating that genes of this cluster are cotranscribed and thus constitute an operon. Two regions at the 5' end of *atpI* hybridized to additional RNA species. Probe 1 (Fig. 1) hybridized with a 1.2-kb mRNA species that most probably originates from a gene upstream of *atpI*, whose transcription unit overlaps the 5' end of probe 1 (D. F. McCarn and S. E. Curtis, unpublished results). Probes 1 and 2 also hybridized with a 2.1-kb species. Since only one RNA endpoint was mapped within probe 1 (see below), this 2.1-kb mRNA must have the same 5' end as the 7.0-kb mRNA or originate from the opposite strand.

The polycistronic mRNA for *atpI* was shown by primer

extension and S1 nuclease assays to initiate at a single site that maps 140 bp upstream from gene 1. A sequence 10 nucleotides upstream from the *atpI* transcription start site resembles the -10 consensus sequence for *E. coli* promoters (37); however, there appears to be no sequence similar to the *E. coli* -35 promoter consensus sequence. Sequences used for the promotion of transcription during vegetative growth in *Anabaena* sp. strain PCC 7120 have not been identified. The presence of an *E. coli* -10 promoter sequence upstream from the transcription start site has also been noted for the *rbcL* (11), *psbA* (12), *petF1* (1), and *atpB* (10) genes of *Anabaena* sp. strain PCC 7120.

**Stoichiometry of ATP synthase subunits.** The ATP synthase subunits of *E. coli* and chloroplast  $F_1$  components are found in a stoichiometry of  $\alpha_3, \beta_3, \gamma_1, \delta_1, \epsilon_1$  (14, 30), and the stoichiometry of cyanobacterial  $F_1$  subunits is expected to be similar. The  $F_0$  component of *E. coli* is reported to have a stoichiometry of  $a_1, b_2, c_{10-12}$  (14). Chloroplast and cyanobacterial  $F_0$  components have not been characterized with regard to subunit ratios, but if the stoichiometries are similar to those in *E. coli*, the  $F_0$  may contain one *b* (I) and one *b'* (II) rather than two identical *b* subunits (8). The presence in *E. coli* and *Anabaena* sp. strain PCC 7120 of a single mRNA encoding proteins present in different stoichiometries in the enzyme, together with the absence of evidence for suboperon-length transcripts, suggests that a posttranscriptional mechanism(s) is required to regulate the relative stoichiometries of the subunits. There is evidence that translational control of the operon in *E. coli* is mediated through regions of potential stem-loop structures that include the ribosome-binding sites upstream of gene encoding the *b*,  $\delta$ , and  $\gamma$  subunits (7, 24).

Analysis of the *atpI* nucleotide sequence revealed several regions of possible secondary structure. As in *E. coli*, there is potential for formation of stem-loop structures in the mRNA between the  $\alpha$  and  $\gamma$  subunit genes (Fig. 4). Unlike in *E. coli*, however, no such region can be found between the *c* and *b* and between the *b* and  $\delta$  subunit genes. In *E. coli* the stem-loop structures include the Shine-Dalgarno sequence and the start codon for the downstream gene. The stem-loop structures observed in *Anabaena* sp. strain PCC 7120 are upstream of the putative ribosome-binding regions and consequently do not include start codons. Thus, it is unlikely that these regions of potential secondary structure play a role in regulating the translation of the ATP synthase subunits in this operon.

**Evolution of ATP synthase subunits.** Analysis of the derived amino acid sequences for the *Anabaena* sp. strain PCC 7120 ATP synthase genes shows that the different subunits have undergone variable rates of evolution. In general, the cyanobacterial subunits are more similar to those of higher plants than to those of *E. coli* (Table 1). The most highly conserved subunits among the species compared are  $\alpha$  and  $\beta$ . This high degree of conservation probably reflects constraints on amino acid divergence related to the proposed roles of these subunits in catalysis and nucleotide binding (30).

Although complete amino acid sequences for the nucleus-encoded  $\gamma$  and  $\delta$  subunits of chloroplast ATP synthase are not available from plants, comparisons between *E. coli* and cyanobacteria (Table 1) suggest that these subunits are not highly conserved. In *E. coli* the  $\delta$  subunit is essential for the binding of  $F_1$  to  $F_0$  in membranes (13), and in chloroplasts it has been shown to prevent proton leakage through  $CF_0$  (2). Comparison of the  $\delta$  subunit sequences from *E. coli*, cyanobacteria, and plant chloroplasts, when available, may pro-

vide information on regions of the polypeptide that are important for subunit function.

The sequence data for the  $\gamma$  subunit poses questions regarding the regulation of cyanobacterial ATP synthases. McCarty and Racker showed that  $Mg^{2+}$ -dependent ATP hydrolysis in spinach chloroplasts and  $Ca^{2+}$ -dependent ATP hydrolysis in soluble spinach  $CF_1$  can be elicited by light and/or dithiothreitol (29). Nalin and McCarty (31) found a correlation between activation of the latent  $CF_1$   $Ca^{2+}$ -ATPase potential and reduction of a disulfide bond between two cysteine residues in the  $CF_1$   $\gamma$  subunit. Two additional sulfhydryl groups were identified in the spinach  $\gamma$  subunit protein. In *Anabaena variabilis*, latent  $Mg^{2+}$ -ATPase activity in smooth vesicles can be activated by light, a -SH reductant, and an electron donor (35). Thus, the ATP synthase of an *Anabaena* species can undergo a type of activation which is similar to that found in spinach chloroplasts and which contrasts with nonoxygenic photosynthetic and heterotrophic bacteria, in which ATPase activity is not latent (35). Similar light activation is found in the *S. platensis* ATP synthase (21). Analysis of the derived amino acid sequence for the *Anabaena* sp. strain PCC 7120  $\gamma$  subunit, as well as that for *Synechococcus* sp. strain PCC 6301, however, reveals only a single cysteine residue. Thus, the activation of the latent  $Ca^{2+}$ -dependent ATPase activity must occur by a mechanism that is different from the disulfide reduction reported for spinach  $CF_1$ .

None of the  $F_0$  subunit amino acid sequences are well conserved between cyanobacteria and *E. coli*; however, the *c* and *a* subunits are well conserved between cyanobacteria and chloroplasts (Table 1). The analysis of cyanobacterial ATP synthase genes suggests that the ATP synthases of cyanobacteria, like those of chloroplasts, have two *b*-type subunits (*b* and *b'*). Neither of these subunits is particularly well conserved between the two cyanobacterial species. Although the  $F_0$  subunits have various degrees of sequence similarity, comparisons of the hydropathy profiles for each of the  $F_0$  subunits from *E. coli*, cyanobacteria, and chloroplasts (8) suggest that their structures are similar. Thus, the maintenance of subunit conformation may be important for the proposed roles of the  $F_0$  subunits in binding of the  $F_0$  to the  $F_1$  portion of the complex and formation of the proton channel (15).

In recent cross-reconstitution studies, Hicks and Yocum (20) showed that light-driven ATP synthesis could be restored by  $F_1$  from *S. platensis* in spinach thylakoid membranes depleted of  $CF_1$  with NaBr; likewise, spinach  $CF_1$  was able to restore ATP synthesis in depleted *S. platensis* membranes. The similarity of cyanobacterial and chloroplast ATP synthases has been confirmed by analysis of cyanobacterial ATP synthase genes. These studies show that the ATP synthases of cyanobacteria and chloroplasts have a similar subunit composition and that many of the subunits have a high degree of sequence similarity. In addition, the ATP synthase genes in chloroplasts and both cyanobacterial species studied display a two-clustered arrangement. The similarity between cyanobacterial and chloroplast ATP synthase structure, as well as ATP synthase gene organization, supports the hypothesis (28) that chloroplasts and cyanobacteria evolved from common ancestors.

#### ACKNOWLEDGMENTS

This work was supported by Public Health Service grant GM32766 from the National Institutes of Health, grant 84-3352 from the North Carolina Biotechnology Center, and grant DMB8614424 from the National Science Foundation. Jawed Alam and Jacqueline

Vrba were supported by a postdoctoral fellowship and graduate fellowship, respectively, provided by the North Carolina Consortium for Research and Education in Plant Molecular Biology.

We thank John Boynton and John Gray for providing chloroplast ATP synthase probes.

#### LITERATURE CITED

1. Alam, J., R. A. Whitaker, D. W. Krogmann, and S. E. Curtis. 1986. Isolation and sequence of the gene for ferredoxin I from the cyanobacterium *Anabaena* sp. strain PCC 7120. *J. Bacteriol.* 168:1265-1271.
2. Andreo, C. S., W. J. Partle, and R. E. McCarty. 1982. Effect of ATPase activation and the  $\delta$  subunit of coupling factor 1 on reconstitution of photophosphorylation. *J. Biol. Chem.* 257:9968-9975.
3. Belknap, W. R., and R. Haselkorn. 1987. Cloning and light regulation of expression of the phycocyanin operon of the cyanobacterium *Anabaena*. *EMBO J.* 6:871-884.
4. Berzborn, R. J., J. Otto, W. Finke, H. E. Meyer, and J. Block. 1987. Conclusions from N-terminal amino acid sequences of subunits delta from spinach and maize  $CF_1$  and of subunits I and II from spinach  $CF_0$ . *Biol. Chem. Hoppe-Seyler* 368:551-552.
5. Bird, C. R., B. Koller, A. D. Auffret, A. K. Huttley, C. J. Howe, T. A. Dyer, and J. C. Gray. 1985. The wheat chloroplast gene for  $CF_0$  subunit I of ATP synthase contains a large intron. *EMBO J.* 4:1381-1388.
6. Borbely, G., and A. Simoncsits. 1981. 3'-Terminal conserved loops of 16S rRNAs from the cyanobacterium *Synechococcus* PCC 6301 and maize chloroplast differ only in two bases. *Biochem. Biophys. Res. Commun.* 101:846-852.
7. Brusilow, W. S. A., D. J. Klionsky, and R. D. Simoni. 1982. Differential polypeptide synthesis of the proton-translocating ATPase of *Escherichia coli*. *J. Bacteriol.* 151:1363-1371.
8. Cozens, A. L., and J. E. Walker. 1987. The organization and sequence of the genes for ATP synthase subunits in the cyanobacterium *Synechococcus* 6301. *J. Mol. Biol.* 194:359-383.
9. Cozens, A. L., J. E. Walker, A. L. Phillips, A. K. Huttly, and J. C. Gray. 1986. A sixth subunit of ATP synthase, an  $F_0$  component, is encoded in the pea chloroplast genome. *EMBO J.* 5:217-222.
10. Curtis, S. E. 1987. Genes encoding the beta and epsilon subunits of the proton-translocating ATPase from *Anabaena* sp. strain PCC 7120. *J. Bacteriol.* 169:80-86.
11. Curtis, S. E., and R. Haselkorn. 1983. Isolation and sequence of the gene for the large subunit of ribulose-1,5-bisphosphate carboxylase from the cyanobacterium *Anabaena* 7120. *Proc. Natl. Acad. Sci. USA* 80:1835-1839.
12. Curtis, S. E., and R. Haselkorn. 1984. Isolation, sequence and expression of two members of the 32kd thylakoid membrane protein gene family from the cyanobacterium *Anabaena* 7120. *Plant Mol. Biol.* 3:249-258.
13. Dunn, S. D., and L. A. Heppel. 1981. Properties and functions of the subunits of the *Escherichia coli* coupling factor ATPase. *Arch. Biochem. Biophys.* 210:421-436.
14. Foster, D. L., and R. H. Fillingame. 1982. Stoichiometry of subunits in the  $H^+$ -ATPase of *Escherichia coli*. *J. Biol. Chem.* 257:2009-2015.
15. Futai, M., and H. Kanazawa. 1983. Structure and function of proton-translocating adenosine triphosphatase ( $F_0F_1$ ): biochemical and molecular biological approaches. *Microbiol. Rev.* 47:285-312.
16. Gay, N. J., and J. E. Walker. 1981. The *atp* operon: nucleotide sequence of the region encoding the  $\alpha$  subunit of *Escherichia coli* ATP-synthase. *Nucleic Acids Res.* 9:2187-2194.
17. Gay, N. J., and J. E. Walker. 1981. The *atp* operon: nucleotide sequence of the promoter and the genes for the membrane proteins, and the  $\alpha$  subunit of *Escherichia coli* ATP synthase. *Nucleic Acids Res.* 9:3919-3926.
18. Hatefi, Y. 1985. The mitochondrial electron transport and oxidative phosphorylation system. *Annu. Rev. Biochem.* 54:1015-1069.
19. Hennig, J., and R. G. Herrmann. 1986. Chloroplast ATP synthase of spinach contains nine nonidentical subunit species, six



- of which are encoded by plastid chromosomes in two operons in a phylogenetically conserved arrangement. *Mol. Gen. Genet.* 8: 543-549.
20. Hicks, D. B., and C. F. Yocum. 1986. Properties of the cyanobacterial coupling factor ATPase from *Spirulina platensis*. I. Electrophoretic characterization and reconstitution of photophosphorylation. *Arch. Biochem. Biophys.* 245:220-229.
  21. Hicks, D. B., and C. F. Yocum. 1986. Properties of the cyanobacterial coupling factor ATPase from *Spirulina platensis*. II. Activity of the purified and membrane-bound enzyme. *Arch. Biochem. Biophys.* 245:230-237.
  22. Howe, C. J., A. D. Auffret, A. Doherty, C. M. Bowman, T. A. Dyer, and J. C. Gray. 1982. Location and nucleotide sequence of the gene for the proton-translocating subunit of wheat chloroplast ATP synthase. *Proc. Natl. Acad. Sci. USA* 79:6903-6907.
  23. Howe, C. J., I. M. Fearnley, J. E. Walker, T. A. Dyer, and J. C. Gray. 1985. Nucleotide sequences of the genes for the alpha, beta and epsilon subunits of wheat chloroplast ATP synthase. *Plant Mol. Biol.* 4:333-345.
  24. Klionsky, D. J., D. G. Skalniak, and R. D. Simoni. 1984. Differential translation of the genes encoding the proton-translocating ATPase of *Escherichia coli*. *J. Biol. Chem.* 18:8096-8099.
  25. Krebbers, E. T., I. M. Larrinua, L. McIntosh, and L. Bogorad. 1982. The maize chloroplast genes for the  $\beta$  and  $\epsilon$  subunits of the photosynthetic coupling factor  $CF_1$  are fused. *Nucleic Acids Res.* 10:4985-5002.
  26. Lubberding, H. J., G. Zimmer, H. S. Van Walraven, J. Schrickz, and R. Kraayenhof. 1983. Isolation, purification and characterization of the ATPase complex from the thermophilic cyanobacterium *Synechococcus* 6716. *Eur. J. Biochem.* 137:95-99.
  27. Maniatis, T., E. F. Fritsch, and J. Sambrook. 1982. Molecular cloning: a laboratory manual. Cold Spring Harbor Laboratory, Cold Spring Harbor, N.Y.
  28. Margulis, L. 1981. Symbiosis in cell evolution, p. 37-62. W. H. Freeman and Co., San Francisco.
  29. McCarty, R. E., and E. Racker. 1968. Partial resolution of the enzymes catalyzing photophosphorylation. III. Activation of adenosine triphosphatase and  $^{32}P$ -labeled orthophosphate adenosine triphosphate exchange in chloroplasts. *J. Biol. Chem.* 243: 129-137.
  30. Merchant, S., and B. R. Selman. 1985. Photosynthetic ATPases: purification, properties, subunit isolation and function. *Photosynth. Res.* 6:3-31.
  31. Nalin, C. M., and R. E. McCarty. 1984. Characterization of the cysteinyl-containing peptides of the  $\gamma$  subunit of coupling factor 1. *J. Biol. Chem.* 259:7281-7285.
  32. Nierzwicki-Bauer, S. A., S. E. Curtis, and R. Haselkorn. 1984. Cotranscription of genes encoding the small and large subunits of ribulose-1,5-bisphosphate carboxylase in the cyanobacterium *Anabaena* 7120. *Proc. Natl. Acad. Sci. USA* 81:5961-5965.
  33. Ohyama, K., H. Fukuzawa, T. Kohchi, H. Shirai, T. Sano, K. Umesono, Y. Shiki, M. Takeuchi, Z. Chang, S. Aota, H. Inokuchi, and H. Ozeki. 1986. Chloroplast gene organization deduced from complete sequence of liverwort *Marchantia polymorpha* chloroplast DNA. *Nature (London)* 322:572-574.
  34. Palmer, J. D. 1985. Comparative organization of chloroplast genomes. *Annu. Rev. Genet.* 19:325-354.
  35. Petrack, B., and F. Lipmann. 1961. Photophosphorylation and photohydrolysis in cell-free preparations of blue-green algae, p. 621-630. In W. D. McElroy and B. Glass (ed.), *Light and life*. The Johns Hopkins Press, Baltimore.
  36. Pick, U., and E. Racker. 1979. Purification and reconstitution of the  $N,N'$ -dicyclohexycarbodiimide-sensitive ATPase complex from spinach chloroplasts. *J. Biol. Chem.* 254:2793-2799.
  37. Reznikoff, W. S., D. A. Siegle, D. W. Cowing, and C. A. Gross. 1985. The regulation of transcription initiation in bacteria. *Annu. Rev. Genet.* 19:355-388.
  38. Rice, D., B. J. Mazur, and R. Haselkorn. 1982. Isolation and physical mapping of nitrogen fixation genes from the cyanobacterium *Anabaena* 7120. *J. Biol. Chem.* 257:13157-13167.
  39. Sanger, F., S. Nicklen, and A. R. Coulson. 1977. DNA sequencing with chain-terminating inhibitors. *Proc. Natl. Acad. Sci. USA* 74:5463-5467.
  40. Saraste, M., N. J. Gay, A. Eberle, M. J. Runswick, and J. E. Walker. 1981. The *atp* operon: nucleotide sequence of the genes for the  $\gamma$ ,  $\beta$ , and  $\epsilon$  subunits of *Escherichia coli* ATP synthase. *Nucleic Acids Res.* 9:5286-5296.
  41. Shine, J., and L. Dalgarno. 1974. The 3'-terminal sequence of *Escherichia coli* 16S ribosomal RNA: complementarity to non-sense triplets and ribosome binding sites. *Proc. Natl. Acad. Sci. USA* 71:1342-1346.
  42. Shinozaki, K., H. Deno, T. Wakasugi, and M. Suglura. 1986. Tobacco chloroplast gene coding for subunit I of proton-translocating ATPase: comparison with the wheat subunit I and *E. coli* subunit b. *Curr. Genet.* 10:421-423.
  43. Tinoco, I., Jr., P. N. Borer, B. Dengler, M. Levine, O. C. Uhlenbeck, D. M. Crothers, and J. Gralla. 1973. Improved estimation of secondary structure in ribonucleic acids. *Nature (London) New Biol.* 246:40-41.
  44. Tumer, N. E., S. J. Robinson, and R. Haselkorn. 1983. Different promoters for the *Anabaena* glutamine synthetase gene during growth using molecular or fixed nitrogen. *Nature (London)* 306: 337-341.
  45. Walker, J. E., and V. L. J. Tybulewicz. 1985. Comparative genetics and biochemistry of light-driven ATP synthases, p. 141-153. In C. Arntzen, L. Bogorad, S. Bonitz, and K. Steinback (ed.), *Molecular biology of the photosynthetic apparatus*. Cold Spring Harbor Laboratory, Cold Spring Harbor, N.Y.
  46. Westhoff, P., J. Alt, N. Nelson, and R. G. Herrmann. 1985. Genes and transcripts for the ATP synthase  $CF_0$  subunit I and II from spinach thylakoid membranes. *Mol. Gen. Genet.* 199:290-299.
  47. Zurawski, G., W. Bottomley, and P. R. Whitfield. 1982. Structures of the genes for the  $\beta$  and  $\epsilon$  subunits of spinach chloroplast ATPase indicate a dicistronic mRNA and an overlapping translation stop/start signal. *Proc. Natl. Acad. Sci. USA* 79:6260-6264.

## Composition and Primary Structure of the $F_1F_0$ ATP Synthase from the Obligately Anaerobic Bacterium *Clostridium thermoaceticum*

AMARESH DAS AND LARS G. LJUNGDAHL\*

Center for Biological Resource Recovery and Department of Biochemistry and Molecular Biology,  
University of Georgia, Athens, Georgia 30602

Received 23 January 1997/Accepted 31 March 1997

The subunit composition and primary structure of the proton-translocating  $F_1F_0$  ATP synthase have been determined in *Clostridium thermoaceticum*. The isolated enzyme has a subunit composition identical to that of the  $F_1F_0$  ATP synthase purified from *Clostridium thermoautotrophicum* (A. Das, D. M. Ivey, and L. G. Ljungdahl, J. Bacteriol. 179:1714–1720, 1997), both having six different polypeptides. The molecular masses of the six subunits were 60, 50, 32, 17, 19, and 8 kDa, and they were identified as  $\alpha$ ,  $\beta$ ,  $\gamma$ ,  $\delta$ ,  $\epsilon$ , and  $c$ , respectively, based on their reactivity with antibodies against the  $F_1$  ATPase purified from *C. thermoautotrophicum* and by comparing their N-terminal amino acid sequences with that deduced from the cloned genes of the *C. thermoaceticum* *atp* operon. The subunits *a* and *b* found in many bacterial ATP synthases could not be detected either in the purified ATP synthase or crude membranes of *C. thermoaceticum*. The *C. thermoaceticum* *atp* operon contained nine genes arranged in the order *atpI* (*i*), *atpB* (*a*), *atpE* (*c*), *atpF* (*b*), *atpH* ( $\delta$ ), *atpA* ( $\alpha$ ), *atpG* ( $\gamma$ ), *atpD* ( $\beta$ ), and *atpC* ( $\epsilon$ ). The deduced protein sequences of the *C. thermoaceticum* ATP synthase subunits were comparable with those of the corresponding subunits from *Escherichia coli*, thermophilic *Bacillus* strain PS3, *Rhodospirillum rubrum*, spinach chloroplasts, and the cyanobacterium *Synechococcus* strain PCC 6716. The analysis of total RNA by Northern hybridization experiments reveals the presence of transcripts (mRNA) of the genes *i*, *a*, and *b* subunits not found in the isolated enzyme. Analysis of the nucleotide sequence of the *atp* genes reveals overlap of the structural genes for the *i* and *a* subunits and the presence of secondary structures (in the *b* gene) which could influence the posttranscriptional regulation of the corresponding genes.

ATP synthase is the key enzyme in the energy transduction processes which couples the transmembrane ion gradient generated by respiration (electron transport) to the synthesis of ATP from ADP and  $P_i$  (17, 39, 48, 49). The enzyme also catalyzes the hydrolysis of ATP, which generates an ion gradient. In most biological systems, the primary ions involved in the ion gradient are protons, but in some systems, sodium ions replace the protons (27, 43). ATP synthases from various sources have similar structures. They consist of two subcomplexes, a membrane-extrinsic  $F_1$  part and a membrane-intrinsic  $F_0$  part. The most investigated  $F_1F_0$  complex is that of *Escherichia coli*, in which the  $F_1$  has five subunits,  $\alpha$ ,  $\beta$ ,  $\gamma$ ,  $\delta$ , and  $\epsilon$ , and  $F_0$  has three subunits, *a*, *b*, and *c* (16). From biochemical and genetic studies, it has been demonstrated that all eight subunits are essential for the function of *E. coli* ATP synthase (12, 18, 47).

The ATPase (*atp*) operons of various organisms have been sequenced (18). In *E. coli*, alkaliphilic bacterium *Bacillus firmus* OF4, and thermophilic *Bacillus* strain PS3, the *atp* operon consists of nine structural genes, *atpIBEFHAGDC*, encoding *i*, *a*, *c*, *b*,  $\delta$ ,  $\alpha$ ,  $\gamma$ ,  $\beta$ , and  $\epsilon$  subunits (25, 38, 55). These genes are grouped together to form a single transcriptional unit. However, in the purple nonsulfur photosynthetic bacteria *Rhodospirillum rubrum* (52) and *Rhodospirillum rubrum* (14), the  $F_0$  genes (*atpBEF*) are grouped separately from the  $F_1$  genes (*atpHAGDC*). In the cyanobacteria *Synechococcus* strain PCC 6301 (6), *Synechococcus* strain 6716 (53), *Synechocystis* sp.

strain PCC 6803 (28), and *Anabaena* strain PCC 7120 (7), the structural genes are arranged in two transcriptional units, one containing the *B*, *E*, *F*, *H*, *A*, and *G* genes and the other containing the *D* and *C* genes.

The homoacetogens *Clostridium thermoaceticum* and *Clostridium thermoautotrophicum* are thermophilic anaerobic gram-positive bacteria which are strikingly similar with respect to physiology, DNA composition, and the metabolism of carbon sources (2, 13, 29, 30, 42, 57, 58). One of the most distinctive features of these bacteria is their ability to produce acetate directly from  $CO_2$  by using the acetyl coenzyme A pathway (13, 29, 42, 58). The acetyl coenzyme A pathway is also the major pathway involved during autotrophic growth on  $C_1$  compounds like CO and methanol (13, 29, 30, 42, 57, 58). This pathway does not yield any net gain of ATP at the substrate level (13, 29, 30). Thus, to support growth, acetogens must generate energy through chemiosmosis (11, 21–23, 30). Evidence for this is the presence of an electron transport system (11, 21–23) and a proton-translocating ATP synthase (8, 9, 24, 33) in membranes of *C. thermoaceticum* and *C. thermoautotrophicum*.

The  $F_1$  ATPase and ATP synthase from *C. thermoautotrophicum* (9) and the  $F_1$  ATPase from *C. thermoaceticum* (24) have been purified. The  $F_1$  ATPases from both clostridia have four subunits and identical subunit composition. The ATP synthase from *C. thermoautotrophicum* has six subunits with an apparent composition of  $\alpha_3\beta_3\gamma\delta\epsilon c_{6-8}$  (9, 10), and it lacks the *a* and *b* subunits of  $F_0$  found in many aerobic bacteria, including *E. coli* (16, 17, 48).

In this study, we describe the subunit composition of the ATP synthase from *C. thermoaceticum* and the primary structure of the *atp* operon (*Ct**atp*) encoding the subunits of this enzyme complex. The subunit composition of the *C. ther-*

\* Corresponding author. Mailing address: Department of Biochemistry and Molecular Biology, A214 Life Sciences Building, University of Georgia, Athens, GA 30602-7229. Phone: (706) 542-7640. Fax: (706) 542-2222. E-mail: Ljungdah@bscr.uga.edu.

TABLE 1. Oligonucleotide primers used in PCR for amplification of DNA probes used in Southern and Northern hybridization experiments

Primer <sup>a</sup>	Sequence (5'-3')
FP.....	GA (AG) (CA) G (TCG) AC (TCG) (CA) G (TCG) GA (AG) GG (TCG) AA (TC) GA
RP.....	GT (CGA) A (GA) (GA) TC (GA) TC (GA) GC (CGA) GGIAC (AG) TA
IFP.....	ACAGTATCTTTAGTGGAC
IRP.....	AATAGATGGGATAGGTC
BFP.....	TTGGGACTTCGGGCTCTG
BRP.....	CAGTCCCGTGGACAAAG
FFP.....	CGGTCTTATTCGCCCTTG
FRP.....	GCTCACTCATTGCAGTCG
HFP.....	CGACTGCAATGAGTGAGC
HRP.....	CTTGCCCGGAACCTCTCTT

<sup>a</sup> The nucleotide sequences of the degenerate primers FP and RP were designed from two highly conserved regions of amino acid sequences of the  $\beta$  subunit of *E. coli* F<sub>1</sub> ATPase as described in Materials and Methods. The nucleotide sequences of the remaining primers were designed directly from the DNA sequence of the *Ct*atp operon. The sequences of IFP and IRP were taken from the upstream and downstream regions of *atpI*. Similarly, the sequences of BFP and BRP, FFP and FRP, and HFP and HRP were taken from the upstream and downstream regions of *atpB*, *atpF*, and *atpH*, respectively.

*moacetivum* ATP synthase is identical with that of *C. thermoautotrophicum* (9). The *Ct*atp operon contains nine structural genes, including those encoding the *i*, *a*, and *b* subunits which are not found in the ATP synthases purified from both clostridia. Results of Western and Northern blotting experiments suggest the presence of polycistronic mRNAs, which include the transcripts of the genes encoding *i*, *a*, and *b* subunits, and the absence of the *a* and *b* subunits in membranes of *C. thermoacetivum*.

(A preliminary report of this work has been published elsewhere [10].)

#### MATERIALS AND METHODS

**Bacterial strains and growth conditions.** *C. thermoacetivum* (ATCC 39073) and *C. thermoautotrophicum* JW 701/5 were grown on 1% (wt/vol) glucose at 58°C under 100% CO<sub>2</sub> (31). *E. coli* XL1-Blue MRA and XL1-Blue MRA(P2) were used as hosts to screen the genomic library of *C. thermoacetivum* in  $\lambda$ FIX II (described below). *E. coli* XL-Blue was used as a host for plasmids in transformation experiments (described below). All *E. coli* strains were grown and maintained in LB or 2XYT medium.

**Preparation of membranes and purification of ATP synthases from *C. thermoautotrophicum* and *C. thermoacetivum*.** The membranes were prepared from whole cells after the cells were broken in a French press (24). The ATP synthase was purified from cholate-washed membranes (9).

**Antibodies against synthetic peptides.** Synthetic peptides were designed from the protein sequences of the *a*, *b*, and  $\delta$  subunits deduced from the cloned genes of *C. thermoacetivum* and used as antigens to raise antibodies in adult New Zealand White rabbits. The amino acid sequences of the synthetic peptides used were <sup>2</sup>GLRALGEIMTHVRPVEJF<sup>19</sup> (for subunit *a*), <sup>37</sup>LGKVLADREARJEG NLND<sup>54</sup> (for subunit *b*), and <sup>1</sup>MSEQNARRYARALFNIARE<sup>21</sup> (for subunit  $\delta$ ).

**DNA source and synthetic oligonucleotides.** The genomic DNA of *C. thermoacetivum* was isolated as described previously (37). The  $\lambda$  DNA was isolated by using the Wizard Lambda Preps DNA purification system (Promega Corp., Madison, Wis.). The plasmid DNA was isolated by using a QIAprep Spin Plasmid kit (Qiagen Inc., Chatsworth, Calif.).

**The ATPase probe and PCR.** The DNA probe used to screen the genomic library was a 390-bp PCR product amplified from *C. thermoacetivum* genomic DNA by using the degenerate primers FP (forward primer) and RP (reverse primer) (Table 1), designed from two highly conserved regions of amino acid sequences <sup>191</sup>ERTREGND<sup>198</sup> and <sup>311</sup>YVPADDLTD<sup>319</sup>, respectively, of the  $\beta$  subunit of *E. coli* F<sub>1</sub> ATPase (10, 50). The amplification was carried out for 30 cycles in a 480 Thermal Cycler (Perkin-Elmer Instruments Div., Norwalk, Conn.). Each cycle includes 1 min of melting at 94°C, 90 s of annealing at 49°C, and 2 min of extension at 72°C. The PCR product was cloned into pCRII vector (Invitrogen Corp., San Diego, Calif.), generating pAD1, and sequenced. The deduced amino acid sequence of the PCR product was found to be highly homologous with the corresponding sequences of the F<sub>1</sub> $\beta$  subunits from various

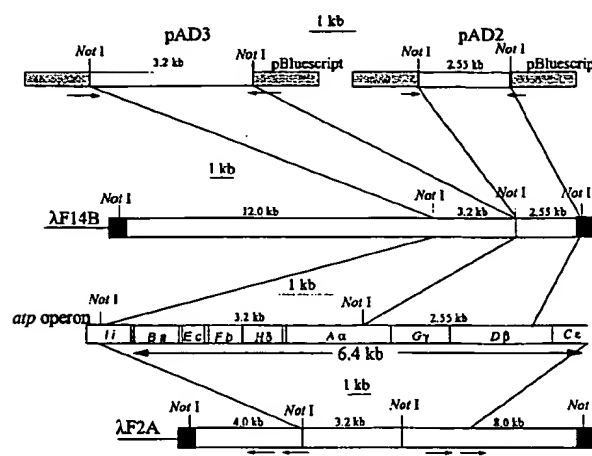


FIG. 1. Strategies used in cloning and sequencing experiments. Two ATPase-positive clones,  $\lambda$ F2A and  $\lambda$ F14B, were selected by screening the *C. thermoacetivum* genomic library in  $\lambda$ FIX II. The *NotI* sites at both ends of the insert belong to the vector's multiple cloning site. The 2.5- and 3.2-kb *NotI* fragments of  $\lambda$ F14B were cloned into pBluescript (SK-) to obtain the subclones pAD2 and pAD3, respectively. The DNAs from the two plasmids and that from  $\lambda$ F2A were used as templates for sequencing as described in Materials and Methods.

sources (10). The PCR product was labeled with digoxigenin (DIG)-11-dUTP (Boehringer Mannheim Co., Indianapolis, Ind.) under conditions similar to those described above except that the nucleotide mixture was made with 5.3 mM DIG-11-dUTP and 2.7 mM Gene Amp deoxynucleoside triphosphates (Perkin-Elmer).

**Genomic library and screening.** A genomic library of *C. thermoacetivum* was constructed in  $\lambda$ FIX II by Stratagene (La Jolla, Calif.). The library was screened for ATPase-positive clones by plaque hybridization using the 390-bp DIG-labeled PCR product (see above) as a probe. The hybridization experiments and the detection of ATPase-positive clones (plaques) were carried out by using a Genius kit (Boehringer Mannheim). The positive clones picked up after primary screening were purified by secondary or tertiary screening using the same protocol.

**Plasmids and phages.** Several ATPase-positive clones were obtained after secondary or tertiary screening of the library. Two clones,  $\lambda$ F2A and  $\lambda$ F14B, were selected and used for further study. The DNAs isolated from these clones were digested with *NotI* and subjected to electrophoresis on 1% (wt/vol) agarose gels (45). Three fragments were obtained from each clone: 3.2, 4.0, and 8.0 kb from  $\lambda$ F2A and 2.5, 3.2, and 12.0 kb from  $\lambda$ F14B. The 8.0- and 2.5-kb fragments hybridized to the 390-bp DNA probe. The 2.5- and 3.2-kb fragments were recovered from agarose gels, purified by using a GeneClean spin kit (Bio 101, Vista, Calif.), and cloned into pBluescript (SK-) (45). The resulting plasmids carrying the 2.5- and 3.2-kb *NotI* fragments were designated pAD2 and pAD3, respectively (Fig. 1). The plasmids carrying the 3.2-kb *NotI* fragment from either  $\lambda$ F2A or  $\lambda$ F14B were found to be indistinguishable with respect to restriction map and DNA sequence analysis (not shown), indicating that this fragment is common to both clones.

**Isolation of mRNA and Northern hybridization experiments.** Total RNA was isolated from freshly grown cells of *C. thermoacetivum* by using an RNeasy kit (Qiagen) and separated by electrophoresis on 1.2% (wt/vol) agarose gels under denaturing conditions in the presence of 2.3 M formaldehyde (45). The Northern (RNA) blot analyses were carried out by using a Genius kit as instructed by the manufacturer (Boehringer Mannheim). The DNA probes specific for *atpI*, *atpB*, *atpF*, and *atpH* genes were synthesized and labeled with DIG-11-dUTP by PCR using primer pairs IFP-IFP, BFP-BRP, FFP-FRP, and HFP-HRP (Table 1), respectively. The conditions for PCR were the same as used for the amplification of the 390-bp DNA fragment as described above. The DNA probes for all genes except *atpI* were amplified by using pAD3 DNA as a template. To amplify the *atpI* probe, *C. thermoacetivum* genomic DNA was used as a template; the amplified product (500 bp) was purified by using a GeneClean spin kit (Bio 101) and used as a template to reamplify the specific product by PCR.

**Other methods.** Proteins were estimated by a modified Lowry method as described previously (15). Sodium dodecyl sulfate-polyacrylamide gel electrophoresis (SDS-PAGE) was carried out by the method of Laemmli (26) in the presence of urea (51). Twelve percent (wt/vol) acrylamide in the resolving gel and 4% (wt/vol) acrylamide in the stacking gel were used, and the proteins were stained with Coomassie brilliant blue 250. The Western blotting experiments were carried out as instructed by the manufacturer (Bio-Rad, Hercules, Calif.). The synthesis of peptides and oligonucleotides and the sequencing of protein and

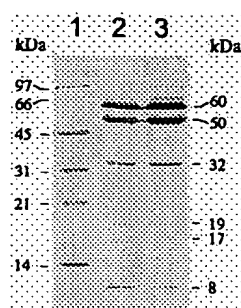


FIG. 2. SDS-PAGE with 8 M urea of the purified ATP synthases from *C. thermoaceticum* (10 µg; lane 2) and *C. thermoautotrophicum* (10 µg; lane 3) and of the protein standards (lane 1). The proteins were stained with Coomassie blue.

DNA samples were carried out at the Molecular Genetics Facility of the University of Georgia. The animal work, including the injection of antigens to rabbits and collection of blood samples, was carried out at the Animal Facility of the University of Georgia. The sequence data were analyzed with the Genetics Computer Group package (University of Wisconsin Biotechnology Center, Madison) on the VAX/VMS system of the BioScience Computing Resources at the University of Georgia.

**Nucleotide sequence accession number.** The nucleotide sequence reported here has been assigned accession no. U64318 in the GenBank, EMBL, and DDBJ libraries.

## RESULTS

**Subunit composition of the ATP synthase from *C. thermoaceticum* and comparison with that of *C. thermoautotrophicum*.** Figure 2 shows the results of SDS-PAGE of the  $F_1F_0$  ATP synthases purified from *C. thermoaceticum* and *C. thermoautotrophicum*. The enzymes from both bacteria have the same subunit composition, each having six different polypeptides with molecular masses of 60, 50, 32, 19, 17, and 8 kDa. These molecular masses are in close agreement with the calculated molecular masses of the  $\alpha$  (55,357 Da),  $\beta$  (49,863 Da),  $\gamma$  (33,305 Da),  $\delta$  (20,163 Da),  $\epsilon$  (14,518 Da), and  $c$  (7,458 Da) subunits, respectively, deduced from the cloned genes of the *Ctatp* operon (Table 2). We previously showed that the N-terminal amino acid sequences of the six ATP synthase subunits of *C. thermoautotrophicum* matched the N-terminal amino acid sequences of the  $\alpha$ ,  $\beta$ ,  $\gamma$ ,  $\delta$ ,  $\epsilon$ , and  $c$  subunits of the ATP synthase deduced from the cloned genes of the *Ctatp* operon (9). The  $F_1$  ATPases purified from *C. thermoaceticum* (24) and *C. thermoautotrophicum* (9) have the same subunit composition, and immunoblot analyses of the membranes from both clostridia revealed similarities of the  $\alpha$ ,  $\beta$ , and  $\gamma$  subunits

of the  $F_1$  ATPases (9). Determinations of the N-terminal amino acid sequences of the 32-, 19-, 17-, and 8-kDa polypeptides of the *C. thermoaceticum* ATP synthase showed a complete match with the N-terminal amino acid sequences of the  $\gamma$ ,  $\delta$ ,  $\epsilon$ , and  $c$  subunits deduced from the cloned genes of the *Ctatp* operon. Therefore, the six subunits of the purified ATP synthase from *C. thermoaceticum* are  $\alpha$ ,  $\beta$ ,  $\gamma$ ,  $\delta$ ,  $\epsilon$ , and  $c$ , and its composition is identical to that of the *C. thermoautotrophicum* ATP synthase, as shown in Fig. 2. The  $F_0$  moiety of the ATP synthase of the acetogenic clostridia is composed of the  $\delta$  and  $c$  subunits as suggested previously (9) and apparently lacks the  $a$  and  $b$  subunits present in several aerobic bacteria.

**Western blotting experiments to test the presence of  $a$  and  $b$  subunits.** Antibodies against synthetic peptides designed from the deduced protein sequences of the  $a$  and  $b$  subunits of the *C. thermoaceticum* ATP synthase failed to react with any protein in the purified  $F_1F_0$  ATP synthase or in crude membranes or whole-cell extracts of *C. thermoaceticum* or *C. thermoautotrophicum*. Antibodies against a synthetic peptide designed from the deduced protein sequence of the *C. thermoaceticum*  $\delta$  subunit used as a positive control reacted strongly with the corresponding subunit present in the ATP synthase purified from both clostridia (not shown). These results support the findings that the  $a$  and  $b$  subunits are not present in the  $F_1F_0$  complex of *C. thermoaceticum* and *C. thermoautotrophicum*.

**Cloning and sequencing of the *C. thermoaceticum* ATP synthase genes.** The entire *Ctatp* operon is present in the clone  $\lambda$ F2A, and plasmids pAD2 and pAD3 together have the complete DNA sequences for the genes encoding  $a$ ,  $c$ ,  $b$ ,  $\delta$ ,  $\alpha$ , and  $\gamma$  subunits of the ATP synthase and partial sequences of the  $i$  and  $\beta$  genes (Fig. 1). The sequences of the remaining portions of the  $i$  and  $\beta$  genes and that of the gene encoding the  $\epsilon$  subunit were obtained by primer walking on  $\lambda$ F2A DNA as template as outlined in Fig. 1.

**Identification and analysis of the *atp* genes.** Nine open reading frames (ORFs), each having a putative start codon and a ribosome binding site (Shine-Dalgarno [S/D] sequence), were identified within the 7.5-kb region sequenced (Fig. 3). The nine structural genes of the *atp* operon encoding nine subunits of the *C. thermoaceticum* ATP synthase were organized in the order *atpI* ( $i$ ), *atpB* ( $a$ ), *atpE* ( $c$ ), *atpF* ( $b$ ), *atpH* ( $\delta$ ), *atpA* ( $\alpha$ ), *atpG* ( $\gamma$ ), *atpD* ( $\beta$ ), and *atpC* ( $\epsilon$ ), which is similar to that found in most bacteria (3, 25, 38, 46, 55). The deduced protein sequences of the nine genes reveal similarities with the corresponding sequences of the nine ATP synthase subunits from different species (Table 2). The protein encoded by the first gene, *atpI*, is called the inhibitor protein or the  $i$  subunit. The  $i$  protein is the least homologous (21 to 24% identity) among

TABLE 2. Comparison of the *Ctatp* gene products with the corresponding *atp* gene products from *E. coli*, thermophilic bacterium PS3, *R. rubrum*, spinach, and *Synechococcus* strain PCC 6716<sup>a</sup>

Gene	Subunit	Mol wt	% Identity (% similarity)				
			<i>E. coli</i>	TheP3	Rhoru	Spio1	SynP1
<i>atpI</i>	<i>i</i>	14,207	24 (49)	23 (51)	21 (49)		
<i>atpB</i>	<i>a</i>	25,411	28 (63)	34 (64)	31 (65)	36 (70)	36 (69)
<i>atpE</i>	<i>c</i>	7,458	25 (65)	34 (71)	29 (61)	56 (78)	58 (80)
<i>atpF</i>	<i>b</i>	19,019	31 (58)	38 (62)	29 (51)	22 (41)	29 (52)
<i>atpH</i>	$\delta$	20,163	30 (58)	31 (56)	29 (53)	27 (54)	28 (55)
<i>atpA</i>	$\alpha$	55,357	57 (76)	67 (81)	61 (77)	60 (76)	64 (81)
<i>atpG</i>	$\gamma$	33,305	40 (62)	46 (66)	43 (66)	42 (63)	45 (66)
<i>atpD</i>	$\beta$	49,863	70 (83)	73 (84)	69 (81)	72 (84)	72 (84)
<i>atpC</i>	$\epsilon$	14,518	31 (62)	39 (62)	31 (54)	35 (55)	39 (63)

<sup>a</sup> References are as follows: *E. coli*, 55; thermophilic bacterium PS3 (TheP3), 38; *R. rubrum* (Rhoru), 14; *Synechococcus* (SynP1), 26; spinach subunits  $a$ ,  $c$ ,  $b$ ,  $\alpha$ ,  $\gamma$ ,  $\beta$ , and  $\epsilon$ , database accession no. P06451, P00843, P06453, P06450, P05435, P00825, and P00833, respectively; and the  $\delta$  subunit, 20.

the ATPase subunits of *C. thermoaceticum* compared with the corresponding subunits from *E. coli*, thermophilic bacterium PS3, and *R. rubrum* (Table 2). Cozens and Walker (6) and Brusilow et al. (3) used hydropathy profiles of the deduced amino acid sequences to characterize the inhibitor proteins of *Synechococcus* and *B. megaterium*, respectively. We performed a similar analysis of the protein encoded by the first structural gene of the *Ctatp* operon and found that it very closely resembles the inhibitor protein of thermophilic bacterium PS3 (Fig. 4), indicating that the first gene of the *Ctatp* operon is *atpI*. We did not find any ORF in the 680-bp region sequenced upstream of *atpI*.

The start codons for the genes encoding  $\alpha$ ,  $\beta$ ,  $\gamma$ ,  $\delta$ ,  $\epsilon$ , and  $c$  subunits were identified from the N-terminal amino acid sequences of the respective proteins purified from *C. thermoautotrophicum* (9). Two types of start codons were found in the *Ctatp* operon. The start codons are ATG for *atpI*, *atpE*, *atpH*, *atpG*, and *atpC* and TTG for *atpB*, *atpF*, *atpA*, and *atpD*. Previously, a conserved S/D sequence of AGGAGT/g was proposed for several genes sequenced from *C. thermoaceticum* (36, 44). This sequence matched perfectly with the proposed S/D sequences of the genes encoding the  $a$ ,  $c$ ,  $b$ ,  $\beta$ , and  $\epsilon$  subunits. The N-terminal amino acid of the  $\beta$  subunit of the *C. thermoautotrophicum* ATP synthase is methionine (9), and the start codon of the  $\beta$  gene of the *C. thermoaceticum* *atp* operon is TTG, demonstrating the use of TTG for methionine. Thus, methionine is proposed as the first amino acid in the deduced protein sequences of  $a$ ,  $b$ , and  $\alpha$  subunits, as the genes for these subunits carry the TTG start codon. The structural genes *atpI* and *atpB* overlap by 50 bases, and the structural genes *atpF* and *atpH* overlap by 4 bases.

The  $\alpha$ ,  $\beta$ , and  $\gamma$  subunits show greater similarity to the corresponding subunits from other species than do the remaining subunits (13). The  $\alpha$ ,  $\beta$ , and  $\gamma$  subunits of *C. thermoaceticum* have 40 to 73% identities with the corresponding subunits from *E. coli*, thermophilic bacterium PS3, *R. rubrum*, spinach chloroplasts, and *Synechococcus* strain PCC 6716 (Table 2). The homology is relatively poor (22 to 39% identities) for other ATPase subunits except for the  $c$  subunit. It has higher homology with the  $c$  subunits of spinach chloroplasts and *Synechococcus* (56 to 58% identities) than with that of *E. coli*, thermophilic bacterium PS3, and *R. rubrum* (25 to 29% identities), and alignment of the protein sequences shows that the most conserved region of the subunit is the DCCD-binding pocket (Fig. 5), in which 18 of 22 residues are found to be identical.

The consensus nucleotide-binding domains, Walker motifs A (GXXXXGKT/S) and B (L-hydrophobic-hydrophobic-hydrophobic-D) (1, 56), are found to be conserved in the deduced protein sequence of the  $\beta$  subunit of *C. thermoaceticum* (Fig. 3). In the  $\alpha$  subunit, the motif A sequence is conserved but the motif B sequence is altered by a single substitution of a cysteine residue for a hydrophobic residue (Fig. 3). Apparently, this difference does not affect the catalytic activity of the enzyme.

**Northern blot analysis.** The analysis of the Northern blots (Fig. 6) reveals the presence of the transcripts (mRNAs) of the genes encoding subunits  $i$ ,  $a$ , and  $b$ . It also appears that initially long transcripts were synthesized, which subsequently degraded into smaller products, as indicated by the presence of smear in the blots. Within the smear of the blots hybridized to the *atpI* and *atpB* probes were found some pronounced bands of smaller fragments. The maximum size of the transcripts was approximately 7 kb, suggesting that all nine genes are transcribed into a single polycistronic mRNA. The presence of a smear in the Northern blots of *atp* mRNA and the presence of

intense bands of smaller fragments in the Northern blots of *atpI* and *atpB* have also been reported for *E. coli* and have been suggested to be due to specific endonucleolytic cleavage of the transcripts of the corresponding genes (34, 35).

**Regulatory sequences.** The exact promoter structure of the *Ctatp* operon was not determined. Several *C. thermoaceticum* genes that have been cloned and sequenced have promoter structures similar to those of *E. coli* genes (36, 44). Two putative promoters (P1 and P2) with sequence similarities to the *E. coli* consensus promoter (41) were found in front of the first structural gene, *atpI* (Fig. 3). Due to the presence of several intergenic regions in the *Ctatp* operon, the presence of internal promoters as has been described for the *E. coli* *atp* operon (55) may be possible. A GC loop followed by a string of T residues, a structure resembling a putative terminator (40), was found immediately after the  $\epsilon$  gene. It may serve as the putative transcription terminator of the *atp* operon.

There are three long and two short intergenic regions found in the *Ctatp* operon. The long regions are *atpB-atpE* (98 bp), *atpE-atpF* (88 bp), and *atpH-atpA* (49 bp). The two long intergenic regions around *atpE* are present also in other bacterial *atp* operons, including those of *E. coli* (55), *Bacillus subtilis* (46), *B. megaterium* (3), and thermophilic bacterium PS3 (38). The remaining long intergenic region (*atpH-atpA*) is not common to any bacterial *atp* operon. A long palindromic sequence which may protect the *atpE* mRNA from nuclease attacks (35) is found downstream of *atpE* ( $c$  gene) (Fig. 3). A similar finding is also reported for the *B. subtilis* *atp* operon (46).

## DISCUSSION

The results of this study demonstrate that the ATP synthases purified from *C. thermoaceticum* and *C. thermoautotrophicum* have the same subunit composition and that they lack subunits  $i$ ,  $a$ , and  $b$ , although the structural genes encoding these subunits are present in the *Ctatp* operon. Previously we have shown that the absence of these subunits does not influence the functional integrity of the ATP synthase purified from *C. thermoautotrophicum* (9).

The  $i$  subunit is also found to be absent in the ATP synthases purified from many bacteria (12, 16, 17, 27, 38, 43), but subunits  $a$  and  $b$  are generally present. In *E. coli*, the inhibitor protein can be synthesized in vitro and in minicells, but it has never been detected in vivo (12). The mutations in *atpI* do not affect the activity of the ATPase, and so the function of this gene and its protein is unknown (19, 54). In *C. thermoaceticum*, the transcripts (mRNAs) of the genes encoding the  $i$ ,  $a$ , and  $b$  subunits are found, which shows that the absence of these subunits in the ATP synthase of this bacterium is not due to the lack of transcription. McCarthy et al. (34, 35) demonstrated that in *E. coli*, the mRNAs of *atpI* and *atpB* are comparatively less stable due to their fragmentation by endonucleolytic cleavage and have half-lives much shorter than those of the remaining genes of the *atp* operon. Fragmentation of the transcripts of *atpI* and *atpB* is also likely to occur in *C. thermoaceticum*, as is evident from the Northern hybridization experiments (Fig. 6), and could be one of the reasons for the lack of expression of these genes. It is interesting that the structural genes of subunits  $i$  and  $a$  overlap considerably in the *Ctatp* operon but are well separated in other bacteria (3, 25, 38, 46, 55).

The codon usage may also play an important role in differential expression of the *atp* genes. In *E. coli*, the presence of rare codons in *atpI* has been suggested to be one of the reasons for the poor expression of this gene (55). We have compared the codon usages of different genes in the *Ctatp* operon. A

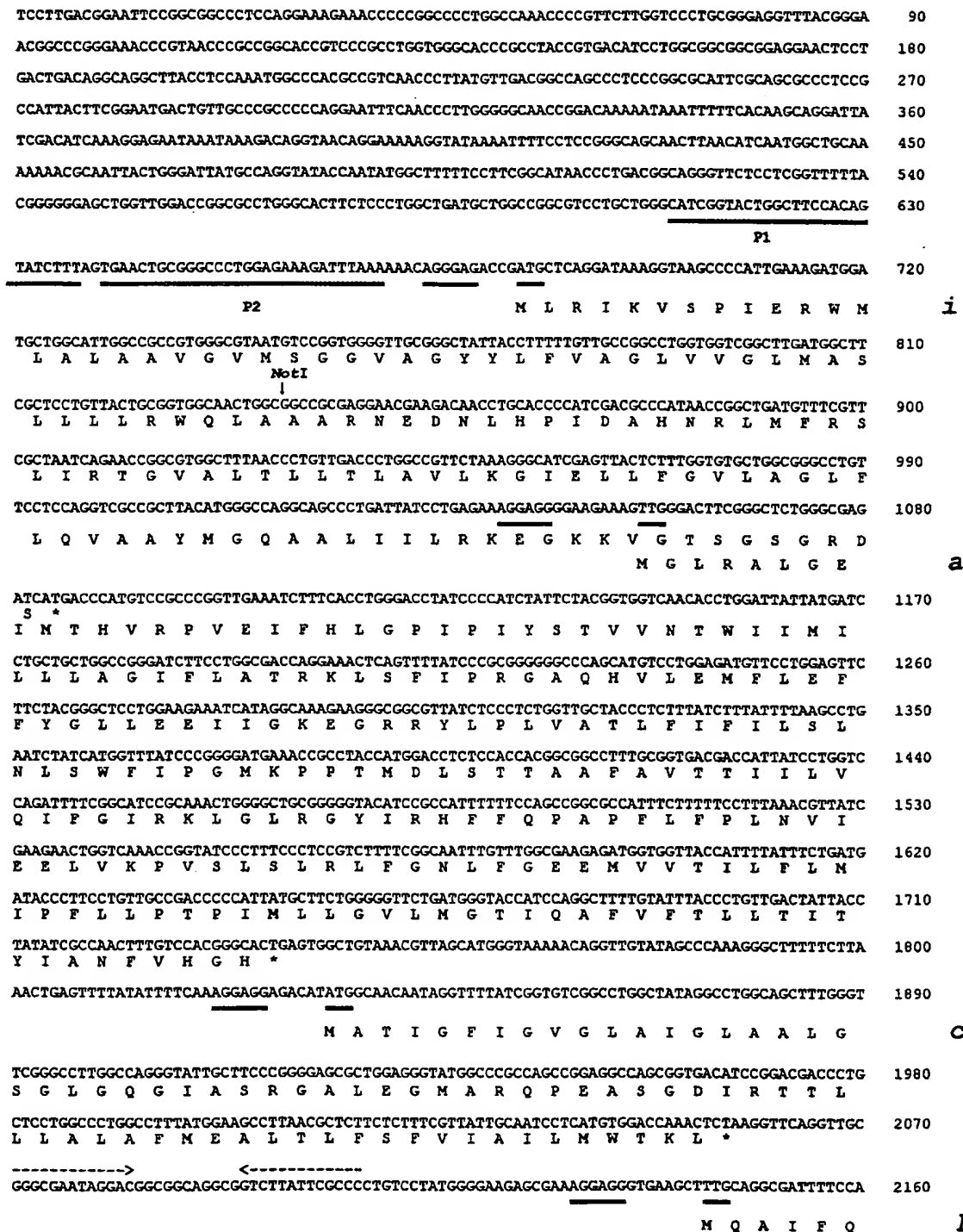


FIG. 3. Nucleotide and deduced protein sequences of the structural genes of the *Clap* operon. Putative promoters P1 and P2 are indicated by labeled thick lines below the sequence; the terminator is marked by thick arrows above the sequence; start codons and S/D sequences are marked by unlabeled thick lines below the sequence; inverted repeats are marked by dashed single-line arrows above the sequence. The nucleotide-binding motifs of the  $\alpha$  and  $\beta$  subunits are shown by underlined letters. The names of the encoded ATPase subunits are given at the right at the start of the ORFs; nucleotide numbering is also shown at the right.

GGCCCTGAATTTTAAATCCCTGGACCTTTTATTTCAGACCTTAAATTTGCTTGTGTTATGGGGTTACTGTATGTATTCCTGTATAAGCC 2250  
A L N P N P W T F L F Q T L N L L V V M G L L Y V F L Y K P  
-----> <-----  
CCTGGGCAAGGTCCTGGCCGACCGCGAGGCCAGGATTGAGGGCAACCTGAACGACGCGGCGGAGCCAGGGAAAAGCGGAAAAACATCCT 2340  
L G K V L A D R E A R I E G N L N D A A A A R E K A E N I L  
----->  
CGCCGAATACCGGCAACAGCTCCAGGGCGCCGCGCAGGAAGCCAGGCCATCCTGGACAGGGCTACGAAGATGGCCGAAGAAACCCGGGC 2430  
A E Y R Q Q L Q G A R Q E A Q A I L D R A T K M A E E T R A  
<-----  
GGAGATTATTAAACCGGCCCGGGAAGAACCGAACGGACCTGGCACAGGCCCGGAGGGAGATTGAGGGTGAGAAGAGCAAGGCCCTGGC 2520  
E I I N R A R E E A E R T L A Q A R R E I E G E K S K A L A  
AGCCATTTCGACGGAAGCCCGCAGCTTGGCGGATCCTGGCAGCCGCGCAAGTCTTGGAGCGTTCCCTGACTCCCGATGACCAAGAACGGCT 2610  
A I R S E A A S L A I L A A G K V L E R S L T P D D Q E R L  
GGCCCGGGAAGCCATTGCCGAGGTGGAGCGACTGCAATGAGTGAGCAGAACGTAGCCAGGCGCTATGCCGCGCCCTTTTAAATATTGCC 2700  
A R E A I A E V E R L Q \*  
M S E Q N V A R R Y A R A L F N I A δ  
CGGAGCAGGGTACAGCCGGCGAATTGCCCAACGGCCTGGAGGAGGTACGCCGTACCCCTGGCTGAAAACAGTGACTTCCGCCGGGTACTC 2790  
R E Q G T A G E F A N G L E E V S R T L A E N S D F R R V L  
TACCACCAAGTTGATCCCGTGGCGGAGAAACAGAACTCATCGATACCATCTTTCCCGACATTAAACCGCTCTTAAAGAACTTCTCTCCAC 2880  
Y H Q L I P V R E K Q K L I D T I F P D I N P L L K N F L H  
CTGCTCTGGCCAAAGGGCGGGGAGCGGGCGCTGCCGAGATGGCCGCCAGTTCCGCCGCTGGTGAGCAGGGCGAAACATCCTGCC 2970  
L V L A K G R E R A L P E M A A Q F R R L V D Q A E N I L P  
GTGAGGTACCTCGGCCATTACCTGCGGAGGATATCCTGGCCGCGCTGAAGGAACGCTGGCCGGAATTACAGGAGGAATATCCGA 3060  
V E V T S A I T L R E D I L A G L K E R L A G I T R R N I R  
CTCTCCAGCGGGTCAACCGGAGTTAATCGGCGGGGTGGTATCGCCCTGGGGACCGCGCTCTGGATGCCAGCGTCAAGAAAAAGCTG 3150  
L S S R V N P E L I G G V V I R L G D R V L D A S V K K K L  
GAATCTCTGGGTGAACACCTGAACAGGGCTTGAGAGAACGACAGAAAAATCGGACAGGGCGAAGGGGTGAAGGTAGATTGAGCATTCG 3240  
E L L G E H L K R A \*  
M S I R α  
ACCCGACGAGATAACAGTATTTTAAAGAACAGATTGAACAATACCACTGGAAGTAGAAATGGCCGAGGTGGGAACCGTTACCCAGGT 3330  
P D E I T S I L K N Q I E Q Y Q L E V E M A E V G T V T Q V  
CGGTGACGGTATCCCGCCATCTACGGCCTGGACCGGGCCATGGCCGGGAGCTGCTGGAGTTCCCGGGCGATATCTATGGCATGGTCT 3420  
G D G I A R I Y G L D R A M A G E L L E F P G D I Y G M V L  
GAACCTGGAAGAAGATAACGTCCGCGCCGTTATCTCGGTCCCTATACCATATCAAGAGGGCGACCAAGTCAACGTACCGGGCGTAT 3510  
N L E E D N V G A V I L G P Y T H I K E G D Q V K R T G R I  
TGTCGAGGTCCGGTGGCGGAAGCCCTCATCGGCCGGTGGTCAACGCCATGGGCCAGCCCATAGACGGCAAGGGGCTATCCAGACGGA 3600  
V E V P V G E A L I G R V V N A M G Q P I D G K G P I Q T D  
TAAATCCCGCCGGTGAATCCCGCGCGCGGGCGTGGTCTACCGCCAGCCGGTCAATACTCCCTTACAAACGGGCTCAAGGCCATTGA 3690  
K F R P V E S P A P G V V Y R Q P V N T P L Q T G L K A I D  
CTCCATGGTCCCATCGCGCGGTCAGCGGGAGCTGATTATCGGTGACCGCCAGACGGGGAAGACGGCCATTGCCGTGGACACCATCAT 3780  
S M V P I G R G Q R E L I I G D R Q T G K T A I A V D T I I  
CAACCAAAGGGGAGAACGTTATCTGCATCTATGTGGCCATCGGCCAGAGGGCTTCTACAGTGGCGGGCTAGTCCAGCGCTGGAAGA 3870  
N Q K G Q N V I C I Y V A I G Q K A S T V A G V V Q R L E E  
GGCCGAGCTATGGAATATATCATCGTCGTATGGCTACAGCCAGCGAACCGCGCCCATGCTCTACATTGCCCCCTACGCGCGCTGCAC 3960  
A G A M E Y I I V V M A T A S E P A P M L Y I A P Y A G C T  
CATGGGCGAATACCTTTATGTATGAGCAGCACCGGGACGTTCTCTGCGTTTATGACGACCTTTCCAAGCAGCAGCAGCTTACCGGGA 4050  
M G E Y F M Y E Q H R D V L C V Y D D L S K H A A A Y R E L  
NotI  
|  
CTCCCTGCTTCTCGCGCGCGCGCGGGCGGTGAGCCTTACCGGGGGATGTCTTCTATCTCCACTCCGGGTGCTGGAGCGGCGGCGCCG 4140  
S L L L R R P P G R E P Y P G D V F Y L H S G L L E R P A R  
CCTGACCGACTCCCTGGGTGGCGGTTCCCTCACTGCCCTGCGGTCATTGAGACCCAGGCTGGCGATGTCTCGCTTACATTCCGACCAA 4230  
L T D S L G G G S L T A L P V I E T Q A G D V S A Y I P T N

FIG. 3—Continued.



TGTTATCTCCATCACCAGCGCCAGATCTTCTGGAGTCTGATCTCTTATGCCGGCCAGCGTCCGGCCATTAACGTCGCCCTCTCGGT V I S I T D G Q I F L E S D L F Y A G Q R P A I N V A L S V	4320
ATCCCCGGTGGGCGGCCGCCAGATCAAGGCCATGAACAGGTGGCGCCCGCTGCCCTGGACCTGGCCAGTACCGCGAGCTGGC S R V G G A A Q I K A M K Q V A A R L R L D L A Q Y R E L A	4410
GGCCTTCGCCAGTTCGGTTCGACCTGGATAAGCCACCCAGGCGAGATTGGCCCGGCCGAGCGCATGATGGAGATTTGAAACAAGA A F A Q P G S D L D K A T Q A R L A R A E R M M E I L K Q D	4500
CCAGTACCAACCCATGCCCGTCGAAGAACAGGTGGTCTCTATGCTGCCCTCAATGGCTTCCTGGACGACCTGCCTGTAGGCCGGGT Q Y Q P M P V E E Q V V V L Y A A V N G F L D D L P V G R V	4590
GCGCGCCTTTGAAAGGACTTCTCGGCTTCTCCGCAACGAGAGGCGTGGGTCTGGCCGCGATCCGCGAAAAACGCCAGCTGGACGA R A F E K D F L R F L R N E R P E V L A G I R E K R Q L D D	4680
TAACTCCAGGAACAACTGAAAAAGAGCATTGAAGACTTCAAAGGCAGCTTTACCGCTGCCGGAATCATAAGGTGGTGAGCCGGCATG N L Q E Q L K K S I E D F K G S F T A A G E S * —————	4770
	M
GCCACATGCGTGACCTGAAGCGCCGCATCCGAGTGTCCAGATACCCAGCATATTCCAGGGCCATGAAGATGGTAGCTGCCGCCAAG A H M R D L K R R I R S V Q S T Q H I T R A M K M V A A A K	4860
CTGCGCAAGGCCAGGCCAGGTACGGCAGCGCGGCCCTATGCCGCAAGCTGGAGGAAGTGGTGGGACGCTGATGGCGGCCGTGGAT L R K A Q A Q V T A G R P Y A A K L E E V V G R L M A A V D	4950
CCGGAACCCAGCCCTGGCGGCCACCCGGAGGTAAAAAGCCGCTATGCTGATAACCGCTGACCGGGCCCTGGCCGGGGTTAT P E T Q P L A A T R E V K K A G G Y V L I T A D R G L A G G Y	5040
AACGCCAACCTCATCCGCTGACGGAGAACGCTGCCGGGAGGAAGCGCTCCCGCTGCCCTGGTAGCCGTGGGCCGCAAGGCCGGGAC N A N L I R L T E E R L R E E G R P A A L V A V G R K G R D	5130
TTTTCCGCGCGCGCGCGGTGGAGATAGTCAATCCTTACCGACATAGCGGATAACCCGGAACCTCATCCAGGCCCGGGAACCTGGCCCGC F F R R R P V E I V K S F T D I G D N P E L I Q A R E L A R	5220
CAGCTGGTGACCATGTACCTGGAGGGTACCTGGACGAGGTTAACCTGATCAATACCCGTTTCTATTCCGCCATCCGCCAGGTACCCATG Q L V T M Y L E G T L D E V N L I N T R F Y S P I R Q V P M	5310
GTGAGCGGTGCTGCCCATCGCTACCCCCGGGAAAAAGGATACCGCGGATTATATCTATGAACCTCACCAGGAGCGCTCTCGCG V E R L L P I A T P R E K K D T G D Y I Y E P S P E G V L R	5400
GTCTCTCTGCCCCGTTACTGCGAGATCAAGGTCTACCGGGCCCTCTCGGAGGCCAAGGCCAGCGAGCAGCGCCCGGATGACGGCCATG V L L P R Y C E I K V Y R A L L E A K A S E H G A R M T A M	5490
GATAACGCCACCAAGAATGTCGCGAGATGATTGACAAATTCACCTATCCTTCAACCGCGCCCGCCAGCGCGGCATCACCAACGAGATC D N A T K N A A E M I D K F T L S F N R A R Q A A I T N E I	5580
GTGGAGATCGTCGCCGGGGCAGATGCTTTGAAGTAAAGGAGGGGACAAGTTTGAACGAAGGACAGGTGGTCCAGGTTATTGGCCCGGTGG V E I V A G A D A L K * —————	5670
	M N E G Q V V Q V I G P V V
TTGACGTCGAATTCGCCAGCGACCGTCTGCCCCGACCTGTATAACGCCATCACCATTAAACCGATAAGATTAAATAACCATGGAGGCCA D V E F A S D R L P D L Y N A I T I K T D K I N I T M E A M	5760
TGCAGCACCTGGGCAACACACCGTCCGCTGTGTGGCCCTCTCTCGACCGAGCGGCTGACGAGGGATGAAGCCGTTGACACCGGCC Q H L G N N T V R C V A L S S T D G L Q R G M K A V D T G Q	5850
AGCCAATCACCGGTAGCGCGGGCTACCTGGGACGGCTCTTTAACGCTCTGGGAGAACCCATTGACAACAGGGACCGGTAGAAA P I T V P V G R A T L G R L F N V L G E P I D N Q G P V E T	5940
CCACCGAGAGGCTGCCATTACCGCGCGCGCCCTCTTTGAAGAGCAACAGCCTTCTACCGAGGTCTGGAGACTGGCATCAAGGTGG T E R L P I H R P A P S F E E Q Q P S T E V L E T G I K V V	6030
TCGACCTCTGGCGCCCTACGCCAAGGGCGGCAAGATCGGCCTCTTCGGCGCGCGGGGTCGGCAAGACGGTCTCATCATGGAACCTCA D L L A P Y A K G G K I G L F G G A G V G K T V L I M E L I	6120
TCCGCAACATCGCCTATGAACACGGCGGCTTTTCCGCTCTTCAGCGCGGTGGGCGAGCGTACCCGCGAGGGTAACGACCTTACCTGGAGA R N I A Y E H G G F S V F S G V G E R T R E G N D L Y L E M	6210
TGAAGGAATCCGGGTTCTCGAAAAGACGGCCCTGGTCTTTGGCCAGATGAACGAACCCCGGGTGGCCCGCTCGGGTGGGTCTTACAG K E S G V L E K T A L V F G Q M N E P P G A R L R V G L T G	6300
GCCTGACTATGCCGAGTACTTCCGGGACCCGAGGCCAGGACGTTCTCTCTTCATCGACAATATCTTTCGCTTCGTGCGAGCCCGGTT L T M P E Y F R D P E A Q D V L L F I D N I F R F V Q P G S	6390

γ

β

FIG. 3—Continued.

difference is observed in the relative use of codons for certain amino acids between *atpB* and the rest of the genes in the operon. These codons are TTT (Phe), GGG (Gly), CTT (Leu), and CAT (His). The numbers of these codons present in *atpB* are 14, 9, 5, and 3, which account for 40, 35, 43, and 42%,

respectively, of the total number of the corresponding codons present in the entire *Ctaip* operon. We have compared the use of these codons among other genes of *C. thermoacetica* which have been sequenced, e.g., the formyltetrahydrofolate synthetase, carbon monoxide dehydrogenase, methylenetetrahy-

```

CCGAGGTTTCCGCCCTCCTGGCCCGGATGCCCTCGCGGTGGGTTATCAGCCACCCCTGCCACAGAGATGGGGCCCTGCAGGAACGGA 6480
E V S A L L A R M P S A V G Y Q P T L P T E M G P L Q E R I

TTACCTCCACGAAAAGGGTTCATCACCTCCGTGCAAGCTATCTATGTGCCGGCGACGACCTGACCGACCGGCGCCGGCGACGACCT 6570
T S T K K G S I T S V Q A I Y V P A D D L T D P A P A T T F

TCGCCCATCTGGAGCCACACGGTTCGTCCCGGCAGATCGCTGAGCTGGGCATCTACCGGCGCTGACCCCTCGACTCCACCTCCC 6660
A H L D A T T V L S R Q I A E L G I Y P A V D P L D S T S R

GTATCCTGGACCGCGCGCTCCTGGGAGAAGAGCACTACCAGGTGGTCCGGGAGTCCAGCAGGTACTGCAGCGTTATAAAGAACTCCAGG 6750
I L D P R V L G E E H Y Q V V R G V Q Q V L Q R Y K E L Q D

ACATTATCGCCATCTCGGAATGGATGAGCTGTCCGAAGATGATAAACTCATAGTAGCCCGGCGACGCAAGATCCAGCGTTTCTCTCCC 6840
I I A I L G M D E L S E D D K L I V A R A R K I Q R F L S Q

AGCCCTTCCACGTAGCCGAGGCTTTTACCGGCCAGCCCGGGGTTTATGTGCCCTGAAGGAAACCATTCGCGGTTTCAAAGAGATCCTGG 6930
P F H V A E A F T G Q P G V Y V P L K E T I R G F K E I L E

AGGGCGCCACGACAACCTCCCCGAGCAGGCTTCTATATGGTCCGGACCATCGACGAAGCCGTCAAGAAGGCCAGGAGTTGATGTAGA 7020
G R H D N L P E Q A F Y M V G T I D E A V K K G Q E L N *

TGGCCTCCCTCAACCTGGAGATCATACTCCCGAGCGGGTGGTCTGCAGCGGAAGCCGCCAGCGTCATAGCTCCAGGTATCCAGGGCT 7110
A S L N L E I I T P E R V V L Q A E A Q S V I A P G I Q G Y

ACCTGGGTGTCTACCGGAGCAGCCCTTTGATCACTCCCTCCAGGCGGGGTCGTACCTGCCCGCGCGGGAGAGAGCGGAGGAAC 7200
L G V L P E H A R L I T P L Q A G V V T C R R R E R A E E R

GTGTGGCTGTTTCCGGCGGTTTCTGGAAGCGGCGCGGACCAGGTAATATCTGGCGGATACAGCGAAGCGTCCGAAGAGATCGACG 7290
V A V S G G F L E A G P D Q V I I L A D T A E R S E E I D V

TCGAATGGGCGCGGAGCGCGGGAGCGGGCGGAGCGGCGCTTGGCGGAGCGCCCCCGGGCTGGACGTGCCAGGGCGGAGGCGGCGCC 7380
E W A R Q A R E R A E R R L R E R P P G L D V A R A E A A L

TGCGCGAGCGGTAGCCCGCTTGAAGCGCGCGGAGCTATTTAAGTAGTCTATTTTCCAGTCCCTCGCAAGATAGGAATAACACTA 7469
R R A V A R L K A A G A I *

CCCCCTGCAAAGGGGCTTTTCTTTTGTTC 7500

```

FIG. 3—Continued.

drofolate reductase (36, 37), corrinoid/iron sulfur protein (32), and methyltetrahydrofolate corrinoid/iron-sulfur protein (44) genes. Of the four above-mentioned codons, GGG and CTT are rarely used by these genes, which suggests that the presence of the

higher number of these codons in *atpB* may reduce the translational efficiency of its mRNA in *C. thermoaceticum*.

It is not clear why the gene encoding the *b* subunit is not expressed in *C. thermoaceticum*. Computer analysis of the transcript (mRNA) of this gene reveals the presence of two appar-

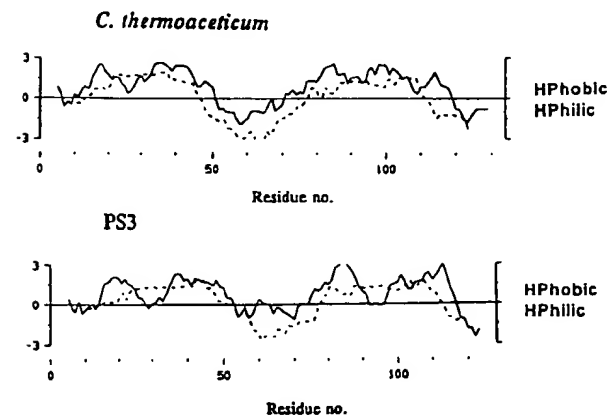


FIG. 4. Hydropathy profiles of the inhibitor protein of thermophilic bacterium PS3 and that of the predicted product (molecular weight, 14,207) of the inhibitor gene from *C. thermoaceticum*. The plots were generated by using the computer program PEPPLOT (Genetics Computer Group). The segments of the plots above the horizontal line represent hydrophobic (HPhobic) regions, and the segments below the line represent hydrophilic (HPhilic) regions. The dotted lines represent the alpha helix, and the solid lines represent the beta structures.

AtpC_cthe	1	...MATIGFIGVGLAIGLAALGSGLQGIASRGALGQARQPEASGD
AtpC_Synp1	1	MDPLVASASVLAALAIGLASLGPQIGQGNASGGQAVGQARQPEARGK
AtpC_Syny3	1	MDSTVAASVIAALAVGLGATGPGIGQGNASGGQAVGQARQPEARGK
AtpC_Spiol	1	MNPLIAASVIAAGLAVGLASIGPGVGGQTAAGQAVGQARQPEARGK
AtpC_Pea	1	MNPLIAASVIAAGLAVGLASIGPGVGGQTAAGQAVGQARQPEARGK
AtpC_Tobac	1	MNPLIAASVIAAGLAVGLASIGPGVGGQTAAGQAVGQARQPEARGK
AtpC_Eugrr	1	MNPLIAASVIAAGLAVGLASIGPGVGGQTAAGQAVGQARQPEARGK
AtpC_Thp3	1	...MSLGVLAALAVGLGALGAGIGNGLVSRITGQARQPELRPV
AtpC_Ecol1	1	MENLNMDLLYMAAVMGLAAGAAIGIGLGGKFLGQARQPDLLPL
AtpC_cthe	42	IRTTLLSLAFMELTIYGLVVALVLLFANPFAS
AtpC_Synp1	46	IRGTLTLLAFMELTIYGLVVALVLLFANPFAS
AtpC_Syny3	46	IRGTLTLLAFMELTIYGLVVALVLLFANPFAS
AtpC_Spiol	46	IRGTLTLLSLAFMELTIYGLVVALVLLFANPFV
AtpC_Pea	46	IRGTLTLLSLAFMELTIYGLVVALVLLFANPFV
AtpC_Tobac	46	IRGTLTLLSLAFMELTIYGLVVALVLLFANPFV
AtpC_Eugrr	46	IRGTLTLLSLAFMELTIYGLVVALVLLFANPFV
AtpC_Thp3	46	LQTMFIGVALVLPPIGVPSFIYLR...
AtpC_Ecol1	46	IRTQFFIVMGLVDA...PMIAGVLGLVFMVFA...

FIG. 5. Alignment of deduced protein sequences of the *C. thermoaceticum* *c* subunit (AtpC\_cthe) with that from *Synechococcus* strain PCC 6716 (AtpC\_Synp1) (accession no. Q05366), *Synechocystis* strain PCC 6803 (AtpC\_Syny3) (accession no. P27182), spinach chloroplasts (AtpC\_Spiol) (accession no. P00843), tobacco (AtpC\_Tobac) (accession no. P06286), *Euglena gracilis* (AtpC\_Eugrr) (accession no. P10603), thermophilic bacterium PS3 (AtpC\_Thp3) (accession no. P00845), and *E. coli* (AtpC\_Ecol1) (accession no. P0084). The consensus DCCD-binding pocket of the *c* subunit is indicated by boxes, and highly conserved residues are in boldface.

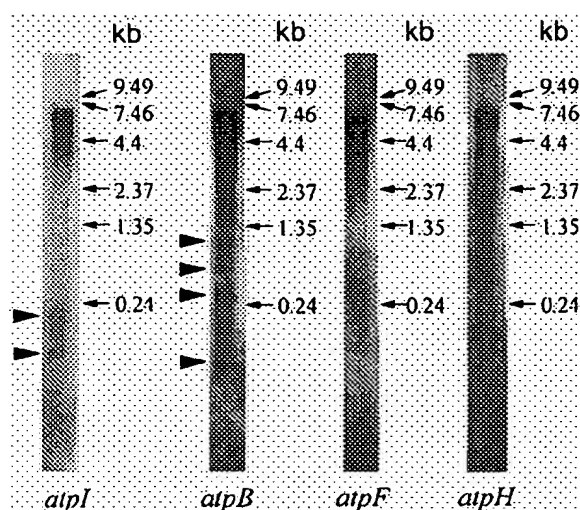


FIG. 6. Northern blots of total RNA from *C. thermoacetatum* after hybridization with different DNA probes. Total RNA extracts were subjected to electrophoresis in the presence of 2.3 M formaldehyde on 1.2% agarose gels. The RNA blots were hybridized to DNA probes specific for the genes *atpI* (lane 1), *atpB* (lane 2), *atpF* (lane 3), and *atpH* (lane 4) as described in Materials and Methods. The relative sizes of the RNA standards are indicated by arrows to the right of each lane. The positions of the smaller RNA fragments that hybridized to *atpI* and *atpB* probes are shown by arrowheads on the left.

ently stable secondary structures (inverted repeats) containing six and seven GC pairs, respectively (Fig. 3), which may reduce or inhibit the translational efficiency of mRNA (34, 40), but we do not have any data to support this possibility. It should be noted that the inverted repeats are also present in other *atp* genes (not shown).

TTG is found to be the start codon for *atpA* and *atpD* (Fig. 3), the two highly expressed genes of the *Ct**atp* operon. TTG has been described as one of the least preferred start codons in both *E. coli* (55) and *C. thermoacetatum* (36). These results indicate that the translational efficiencies of the *atp* genes in *C. thermoacetatum* are not influenced by the use of TTG as a start codon.

It should be noted that the Na-dependent ATP synthase from the obligately anaerobic gram-positive acetogenic bacterium *Acetobacterium woodii* has six different subunits (43) and a subunit structure identical to that of *C. thermoacetatum* (9). The simplest structure of the ATP synthase has been found in the gram-positive anaerobic bacterium *Clostridium pasteurianum*, which contains only four subunits, one in  $F_0$  and three in  $F_1$  (4, 5). These results suggest that in general, the ATP synthases from gram-positive anaerobic bacteria are simpler in subunit composition than those from other bacteria, including the anaerobic gram-negative bacterium *Propionigenium modestum* (27).

#### ACKNOWLEDGMENTS


We gratefully acknowledge Xin-Liang Li for his contribution in the early part of this investigation. We also acknowledge David Gollin for his helpful suggestions regarding sequence analysis.

This research was supported by grants 5 R01 DK 27323 16 from the National Institutes of Health (to L.G.L.). Support for a Georgia Power Distinguished Professorship in Biotechnology (to L.G.L.) is also gratefully acknowledged.

#### REFERENCES

- Abrahams, J. P., A. G. W. Lastie, R. Lutter, and J. E. Walker. 1994. Structure at 2.8 Å resolution of  $F_1$ -ATPase from bovine heart mitochondria. *Nature* 370:621-628.
- Bateson, M. M., J. Wiegel, and D. M. Ward. 1989. Comparative analysis of 16S ribosomal RNA sequences of thermophilic fermentative bacteria isolated from hot spring cyanobacteria mats. *Syst. Appl. Microbiol.* 12:1-7.
- Brusilow, W. S., M. A. Scarpetta, C. A. Hawthorne, and W. P. Clark. 1989. Organization and sequence of the genes coding for the proton-translocating ATPase of *Bacillus megaterium*. *J. Biol. Chem.* 264:1528-1533.
- Clarke, D. J., and J. G. Morris. 1979. The proton-translocating adenosine triphosphatase of the obligately anaerobic bacterium *Clostridium pasteurianum*. 2. ATP synthase activity. *Eur. J. Biochem.* 98:613-620.
- Clarke, D. J., F. M. Fuller, and J. G. Morris. 1979. The proton-translocating ATPase of the obligately anaerobic bacterium *Clostridium pasteurianum*. 1. ATP phosphohydrolase activity. *Eur. J. Biochem.* 98:597-612.
- Cozens, A. L., and J. E. Walker. 1987. The organization and sequence of the genes for ATP synthase subunits in the cyanobacterium *Synechococcus* 6301: support for an endosymbiotic origin of chloroplasts. *J. Mol. Biol.* 194:359-383.
- Curtis, S. E. 1987. Genes encoding the beta and epsilon subunits of the proton translocating ATPase from *Anabaena* sp. strain PCC 7120. *J. Bacteriol.* 169:80-86.
- Das, A., and L. G. Ljungdahl. 1993.  $F_0$  and  $F_1$  parts of ATP synthases from *Clostridium thermoautotrophicum* and *Escherichia coli* are not functionally compatible. *FEBS Lett.* 317:17-21.
- Das, A., D. M. Ivey, and L. G. Ljungdahl. 1997. Purification and reconstitution into proteoliposomes of the  $F_1F_0$  ATP synthase from obligately anaerobic gram-positive bacterium *Clostridium thermoautotrophicum*. *J. Bacteriol.* 179:1714-1720.
- Das, A., X.-L. Li, and L. G. Ljungdahl. 1995. A comparative study on some of the properties of proton-translocating  $F_1F_0$ -ATPases from *Clostridium thermoautotrophicum* and *Escherichia coli*, abstr. K-28. In Abstracts of the 95th General Meeting of the American Society for Microbiology 1995. American Society for Microbiology, Washington, D.C.
- Das, A., J. Hugenholtz, H. Van Halbeek, and L. G. Ljungdahl. 1989. Structure and function of a menaquinone involved in electron transport in membranes of *Clostridium thermoautotrophicum* and *Clostridium thermoacetatum*. *J. Bacteriol.* 171:5823-5829.
- Deckers-Hebestreit, G., and K. Altendorf. 1996. The  $F_1F_0$ -type ATP synthases of bacteria: structure and function of the  $F_0$  complex. *Annu. Rev. Microbiol.* 50:791-824.
- Diekert, G., and G. Wohlfarth. 1994. Metabolism of homoacetogens. *Antonie Leeuwenhoek* 66:209-221.
- Falk, G., A. Hampe, and J. E. Walker. 1985. Nucleotide sequence of the *Rhodospirillum rubrum* *atp* operon. *Biochem. J.* 228:391-407.
- Fillingame, R. H. 1975. Identification of the dicyclohexylcarbodiimide-reactive protein component of the adenosine 5'-triphosphate energy transducing system of *Escherichia coli*. *J. Bacteriol.* 124:870-883.
- Foster, D. L., and R. H. Fillingame. 1979. Energy-transducing  $H^+$ -ATPase of *Escherichia coli*: purification, reconstitution and subunit composition. *J. Biol. Chem.* 254:8230-8236.
- Futai, M., and H. Kanazawa. 1983. Structure and function of proton-translocating adenosine triphosphatase ( $F_1F_0$ ): biochemical and molecular biological approaches. *Microbiol. Rev.* 47:285-312.
- Futai, M., T. N. Noumi, and M. Maeda. 1989. ATP synthase ( $H^+$ -ATPase): results of combined biochemical and molecular biological approaches. *Annu. Rev. Biochem.* 58:111-136.
- Gay, N. J. 1984. Construction and characterization of an *Escherichia coli* strain with *uncI* mutation. *J. Bacteriol.* 158:820-825.
- Hermans, J., C. Rother, J. Biehler, J. Stepphann, and R. G. Herrmann. 1988. Nucleotide sequence of cDNA clones encoding the complete precursor for subunit 8 of thylakoid-located ATP synthase from spinach. *Plant Mol. Biol.* 10:323-330.
- Hugenholtz, J., D. M. Ivey, and L. G. Ljungdahl. 1987. Carbon monoxide driven electron transport in *Clostridium thermoautotrophicum* membranes. *J. Bacteriol.* 169:5845-5847.
- Hugenholtz, J., and L. G. Ljungdahl. 1990. Metabolism and energy generation in homoacetogenic clostridia. *FEMS Microbiol. Rev.* 87:383-390.
- Ivey, D. M. 1987. Generation of energy during  $CO_2$  fixation in acetogenic bacteria. Ph.D. dissertation. Department of Biochemistry, University of Georgia, Athens, Ga.
- Ivey, D. M., and L. G. Ljungdahl. 1986. Purification and characterization of the  $F_1$ -ATPase from *Clostridium thermoacetatum*. *J. Bacteriol.* 165:252-257.
- Ivey, D. M., and T. A. Krulwich. 1991. Organization and nucleotide sequence of the *atp* genes encoding the ATP synthase from alkaliphilic *Bacillus firmus* OF4. *Mol. Gen. Genet.* 229:292-300.
- Laemmli, U. K. 1970. Cleavage of structural proteins during the assembly of the head of bacteriophage T4. *Nature* 227:680-685.
- Laubinger, W., and P. Dimroth. 1988. Characterization of ATP synthase of *Propionigenium modestum* as a primary sodium pump. *Biochemistry* 27: 7531-7537.

28. Lill, H., and N. Nelson. 1991. The *atp1* and *atp2* operons of the cyanobacterium *Synechocystis* sp. PCC 6803. *Plant Mol. Biol.* 17:641-652.
29. Ljungdahl, L. G. 1986. The autotrophic pathway of acetate synthesis in acetogenic bacteria. *Annu. Rev. Microbiol.* 40:415-450.
30. Ljungdahl, L. G. 1994. The acetyl-CoA pathway and the chemiosmotic generation of ATP during acetogenesis, p. 63-87. In H. L. Drake (ed.), *Acetogenesis*. Chapman & Hall, New York, N.Y.
31. Ljungdahl, L. G., and J. R. Andreessen. 1978. Formate dehydrogenase, a selenium-tungsten enzyme from *Clostridium thermoaceticum*. *Methods Enzymol.* 53:360-372.
32. Lu, W.-P., I. Schiau, J. R. Cunningham, and S. W. Ragsdale. 1993. Sequence and expression of the gene encoding the corrinoid/iron-sulfur protein from *Clostridium thermoaceticum* and reconstitution of the recombinant protein to full activity. *J. Biol. Chem.* 268:5605-5614.
33. Mayer, F., D. M. Ivey, and L. G. Ljungdahl. 1986. Macromolecular organization of  $F_1$ -ATPase isolated from *Clostridium thermoaceticum* as revealed by electron microscopy. *J. Bacteriol.* 166:1128-1130.
34. McCarthy, J. E. G., B. Schauder, and P. Ziemke. 1988. Post-transcriptional control in *Escherichia coli*: translation and degradation of the *atp* operon mRNA. *Gene* 72:131-139.
35. McCarthy, J. E. G., G. Gerstel, B. Surin, U. Wiedemanna, and P. Ziemke. 1991. Differential expression from *Escherichia coli atp* operon mediated by segmental differences in mRNA stability. *Mol. Microbiol.* 5:2447-2458.
36. Morton, T. A., C.-F. Chou, and L. G. Ljungdahl. 1992. Cloning, sequencing and expression of genes encoding enzymes of the autotrophic acetyl-CoA pathway in the acetogen *Clostridium thermoaceticum*, p. 389-406. In M. Sebald (ed.), *Genetics and molecular biology of anaerobic bacteria*. Springer-Verlag, New York, N.Y.
37. Morton, T. A., J. A. Runquist, S. W. Ragsdale, T. Shanmugasundaram, H. G. Wood, and L. G. Ljungdahl. 1991. The primary structure of the subunits of carbon monoxide dehydrogenase/acetyl-CoA synthase from *Clostridium thermoaceticum*. *J. Biol. Chem.* 266:23824-23828.
38. Ohta, S., M. Yohda, M. Ishizuka, H. Hirata, T. Hamamoto, Y. Otawara-Hamamoto, K. Matsuda, and Y. Kagawa. 1988. Sequence and over expression of subunits of adenosine triphosphate synthase in thermophilic bacterium PS3. *Biochim. Biophys. Acta* 933:141-155.
39. Pedersen, P. L., and L. M. Amzel. 1993. ATP synthases: structure, reaction center mechanism and regulation of one of nature's unique machines. *J. Biol. Chem.* 268:9937-9940.
40. Platt, T. 1986. Transcription termination of genes expression. *Annu. Rev. Biochem.* 55:339-372.
41. Pribnow, D. 1979. Genetic control signals in DNA, p. 219-277. In R. F. Goldberg (ed.), *Biological regulation and development*, vol. I. Plenum Press, New York, N.Y.
42. Ragsdale, S. W. 1991. Enzymology of acetyl-CoA pathway of  $CO_2$  fixation. *Crit. Rev. Biochem. Mol. Biol.* 26:261-300.
43. Reidlinger, J., and V. Müller. 1994. Purification of ATP synthase from *Acetobacterium woodii* and identification as a  $Na^+$ -translocating  $F_1F_0$  type enzyme. *Eur. J. Biochem.* 223:275-283.
44. Roberts, D. L., S. Zhao, T. Doukov, and S. W. Ragsdale. 1994. The reductive acetyl coenzyme pathway: sequence and heterologous expression of active methyltetrahydrofolate:corrinoid/iron-sulfur protein methyltransferase from *Clostridium thermoaceticum*. *J. Bacteriol.* 176:6127-6130.
45. Sambrook, J., E. F. Fritsch, and T. Maniatis. 1989. *Molecular cloning: a laboratory manual*, 2nd ed. Cold Spring Harbor Laboratory, Cold Spring Harbor, N.Y.
46. Santana, M., M. S. Ionescu, A. Vertes, R. Longin, F. Kunst, A. Danchin, and P. Glaser. 1994. *Bacillus subtilis*  $F_1F_0$  ATPase: DNA sequence of the *atp* operon and characterization of *atp* mutants. *J. Bacteriol.* 176:6802-6811.
47. Schneider, E., and K. Altendorf. 1985. All three subunits are required for the reconstitution of an active proton channel ( $F_0$ ) of *Escherichia coli* ATP synthase ( $F_1F_0$ ). *EMBO J.* 4:515-518.
48. Schneider, E., and K. Altendorf. 1987. Bacterial adenosine 5'-triphosphate synthase ( $F_1F_0$ ): purification and reconstitution of  $F_0$  complexes and biochemical and functional characterization of their subunits. *Microbiol. Rev.* 51:477-497.
49. Senior, A. E. 1988. ATP synthesis by oxidative phosphorylation. *Physiol. Rev.* 68:177-231.
50. Sumi, M., M. H. Sato, K. Denda, T. Date, and M. Yoshida. 1992. A DNA fragment homologous to  $F_1$ -ATPase  $\beta$  subunit was amplified from genomic DNA of *Methanosarcina barkeri*: indication of an archaeobacterial  $F_1$ -type ATPase. *FEBS Lett.* 314:207-210.
51. Swank, R. T., and K. D. Munkers. 1971. Molecular weight analysis of oligopeptides by electrophoresis in polyacrylamide gel with sodium dodecyl sulfate. *Anal. Biochem.* 39:462-467.
52. Tybulewicz, V. L. J., G. Falk, and J. E. Walker. 1984. *Rhodospseudomonas blautia atp* operon. Nucleotide sequence and transcription. *J. Mol. Biol.* 179:185-214.
53. van Walraven, H. S., R. Lutter, and J. E. Walker. 1993. Organization and sequences of genes for the subunits of ATP synthase in the thermophilic cyanobacterium *Synechococcus* strain 6716. *Biochem. J.* 294:239-251.
54. Von Meyenburg, K., B. B. Jørgensen, J. Nielsen, and F. G. Hansen. 1982. Promoters of the *atp* operon coding for the membrane-bound ATP synthase of *Escherichia coli* mapped by *Tn10* insertion mutations. *Mol. Gen. Genet.* 188:240-248.
55. Walker, J. E., M. Saraste, and N. J. Gay. 1984. The *unc* operon: nucleotide sequence, regulation and structure of ATP-synthase. *Biochim. Biophys. Acta* 768:164-200.
56. Walker, J. E., M. Saraste, M. J. Runswick, and N. J. Gay. 1982. Distantly related sequences in the  $\alpha$ - and  $\beta$ -subunits of ATP synthase, myosin, kinases and other ATP requiring enzymes and a common nucleotide binding fold. *EMBO J.* 1:945-951.
57. Wiegel, J., M. Braun, and G. Gottschalk. 1981. *Clostridium thermoautotrophicum* species novum, a thermophile producing acetate from molecular hydrogen and carbon dioxide. *Curr. Microbiol.* 5:255-260.
58. Wood, H. G., and L. G. Ljungdahl. 1991. Autotrophic character of the acetogenic bacteria, p. 210-250. In J. M. Shively and L. L. Barton (ed.), *Variations in autotrophic life*. Academic Press, New York, N.Y.

 **18:** [Aggeler R, Ogilvie I, Capaldi RA.](#)


[Related Articles, Links](#)



Rotation of a gamma-epsilon subunit domain in the Escherichia coli F1F0-ATP synthase complex. The gamma-epsilon subunits are essentially randomly distributed relative to the alpha3beta3delta domain in the intact complex.

J Biol Chem. 1997 Aug 1;272(31):19621-4.

PMID: 9235970 [PubMed - indexed for MEDLINE]

 **19:** [Haughton MA, Capaldi RA.](#)

[Related Articles, Links](#)



Asymmetry of Escherichia coli F1-ATPase as a function of the interaction of alpha-beta subunit pairs with the gamma and epsilon subunits.

J Biol Chem. 1995 Sep 1;270(35):20568-74.

PMID: 7657634 [PubMed - indexed for MEDLINE]

 **20:** [Capaldi RA, Aggeler R, Wilkens S, Gruber G.](#)

[Related Articles, Links](#)



Structural changes in the gamma and epsilon subunits of the Escherichia coli F1F0-type ATPase during energy coupling.

J Bioenerg Biomembr. 1996 Oct;28(5):397-401. Review.

PMID: 8951085 [PubMed - indexed for MEDLINE]

# Deciphering the Message in Protein Sequences: Tolerance to Amino Acid Substitutions

JAMES U. BOWIE,\* JOHN F. REIDHAAR-OLSON, WENDELL A. LIM,  
ROBERT T. SAUER

An amino acid sequence encodes a message that determines the shape and function of a protein. This message is highly degenerate in that many different sequences can code for proteins with essentially the same structure and activity. Comparison of different sequences with similar messages can reveal key features of the code and improve understanding of how a protein folds and how it performs its function.

THE GENOME IS MANIFEST LARGELY IN THE SET OF PROTEINS that it encodes. It is the ability of these proteins to fold into unique three-dimensional structures that allows them to function and carry out the instructions of the genome. Thus, comprehending the rules that relate amino acid sequence to structure is fundamental to an understanding of biological processes. Because an amino acid sequence contains all of the information necessary to determine the structure of a protein (1), it should be possible to predict structure from sequence, and subsequently to infer detailed aspects of function from the structure. However, both problems are extremely complex, and it seems unlikely that either will be solved in an exact manner in the near future. It may be possible to obtain approximate solutions by using experimental data to simplify the problem. In this article, we describe how an analysis of allowed amino acid substitutions in proteins can be used to reduce the complexity of sequences and reveal important aspects of structure and function.

## Methods for Studying Tolerance to Sequence Variation

There are two main approaches to studying the tolerance of an amino acid sequence to change. The first method relies on the process of evolution, in which mutations are either accepted or rejected by natural selection. This method has been extremely powerful for proteins such as the globins or cytochromes, for which sequences from many different species are known (2-7). The second approach uses genetic methods to introduce amino acid changes at

specific positions in a cloned gene and uses selections or screens to identify functional sequences. This approach has been used to great advantage for proteins that can be expressed in bacteria or yeast, where the appropriate genetic manipulations are possible (3, 8-11). The end results of both methods are lists of active sequences that can be compared and analyzed to identify sequence features that are essential for folding or function. If a particular property of a side chain, such as charge or size, is important at a given position, only side chains that have the required property will be allowed. Conversely, if the chemical identity of the side chain is unimportant, then many different substitutions will be permitted.

Studies in which these methods were used have revealed that proteins are surprisingly tolerant of amino acid substitutions (2-4, 11). For example, in studying the effects of approximately 1500 single amino acid substitutions at 142 positions in *lac* repressor, Miller and co-workers found that about one-half of all substitutions were phenotypically silent (11). At some positions, many different, nonconservative substitutions were allowed. Such residue positions play little or no role in structure and function. At other positions, no substitutions or only conservative substitutions were allowed. These residues are the most important for *lac* repressor activity.

What roles do invariant and conserved side chains play in proteins? Residues that are directly involved in protein functions such as binding or catalysis will certainly be among the most conserved. For example, replacing the Asp in the catalytic triad of trypsin with Asn results in a  $10^4$ -fold reduction in activity (12). A similar loss of activity occurs in  $\lambda$  repressor when a DNA binding residue is changed from Asn to Asp (13). To carry out their function, however, these catalytic residues and binding residues must be precisely oriented in three dimensions. Consequently, mutations in residues that are required for structure formation or stability can also have dramatic effects on activity (10, 14-16). Hence, many of the residues that are conserved in sets of related sequences play structural roles.

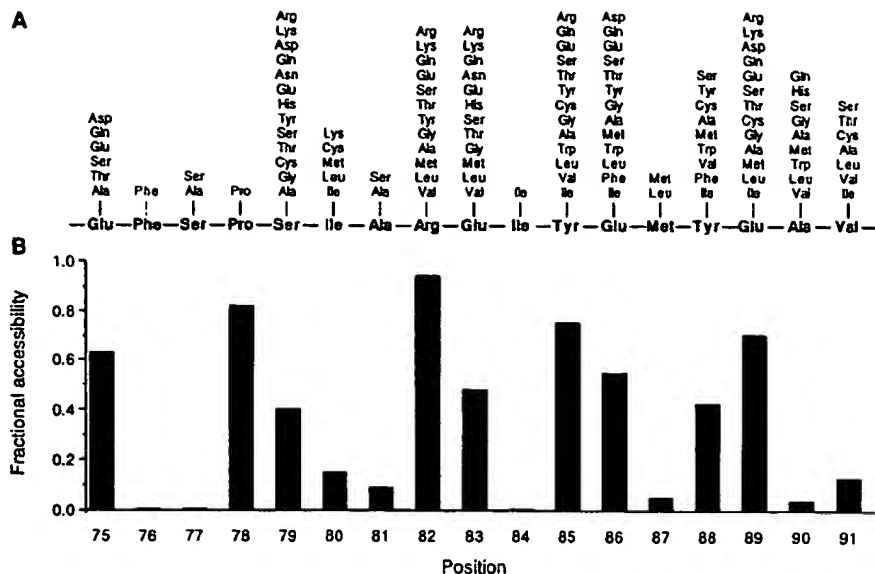
## Substitutions at Surface and Buried Positions

In their initial comparisons of the globin sequences, Perutz and co-workers found that most buried residues require nonpolar side chains, whereas few features of surface side chains are generally conserved (6). Similar results have been seen for a number of protein families (2, 4, 5, 7, 17, 18). An example of the sequence tolerance at surface versus buried sites can be seen in Fig. 1, which shows the allowed substitutions in  $\lambda$  repressor at residue positions that are near the dimer interface but distant from the DNA binding surface of the protein (9). These substitutions were identified by a functional

The authors are in the Department of Biology, Massachusetts Institute of Technology, Cambridge, MA 02139.

\*Present address: Department of Chemistry and Biochemistry and the Molecular Biology Institute, University of California, Los Angeles, Los Angeles, CA 90024.

Fig. 1. (A) Amino acid substitutions allowed in a short region of  $\lambda$  repressor. The wild-type sequence is shown along the center line. The allowed substitutions shown above each position were identified by randomly mutating one to three codons at a time by using a cassette method and applying a functional selection (9). (B) The fractional solvent accessibility (42) of the wild-type side chain in the protein dimer (43) relative to the same atoms in an Ala-X-Ala model tripeptide.



selection after cassette mutagenesis. A histogram of side chain solvent accessibility in the crystal structure of the dimer is also shown in Fig. 1. At six positions, only the wild-type residue or relatively conservative substitutions are allowed. Five of these positions are buried in the protein. In contrast, most of the highly exposed positions tolerate a wide range of chemically different side chains, including hydrophilic and hydrophobic residues. Hence, it seems that most of the structural information in this region of the protein is carried by the residues that are solvent inaccessible.

## Constraints on Core Sequences

Because core residue positions appear to be extremely important for protein folding or stability, we must understand the factors that dictate whether a given core sequence will be acceptable. In general, only hydrophobic or neutral residues are tolerated at buried sites in proteins, undoubtedly because of the large favorable contribution of the hydrophobic effect to protein stability (19). For example, Fig. 2 shows the results of genetic studies used to investigate the substitutions allowed at residue positions that form the hydrophobic core of the  $\text{NH}_2$ -terminal domain of  $\lambda$  repressor (20). The acceptable core sequences are composed almost exclusively of Ala, Cys, Thr, Val, Ile, Leu, Met, and Phe. The acceptability of many different residues at each core position presumably reflects the fact that the hydrophobic effect, unlike hydrogen bonding, does not depend on specific residue pairings. Although it is possible to imagine a hypothetical core structure that is stabilized exclusively by residues forming hydrogen bonds and salt bridges, such a core would probably be difficult to construct because hydrogen bonds require pairing of donors and acceptors in an exact geometry. Thus the repertoire of possible structures that use a polar core would probably be extremely limited (21). Polar and charged residues are occasionally found in the cores of proteins, but only at positions where their hydrogen bonding needs can be satisfied (22).

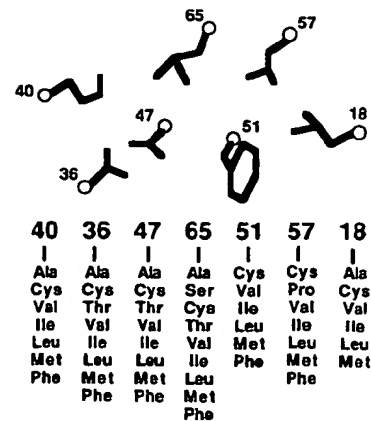
The cores of most proteins are quite closely packed (23), but some volume changes are acceptable. In  $\lambda$  repressor, the overall core volume of acceptable sequences can vary by about 10%. Changes at individual sites, however, can be considerably larger. For example, as shown in Fig. 2, both Phe and Ala are allowed at the same core position in the appropriate sequence contexts. Large volume changes at individual buried sites have also been observed in

phylogenetic studies, where it has been noted that the size decreases and increases at interacting residues are not necessarily related in a simple complementary fashion (5, 7, 17). Rather, local volume changes are accommodated by conformational changes in nearby side chains and by a variety of backbone movements.

## The Informational Importance of the Core

With occasional exceptions, the core must remain hydrophobic and maintain a reasonable packing density. However, since the core is composed of side chains that can assume only a limited number of conformations (24), efficient packing must be maintained without steric clashes. How important are hydrophobicity, volume, and steric complementarity in determining whether a given sequence can form an acceptable core? Each factor is essential in a physical sense, as a stable core is probably unable to tolerate unsatisfied hydrogen bonding groups, large holes, or steric overlaps (25). However, in an informational sense, these factors are not equivalent. For example, in experiments in which three core residues of  $\lambda$  repressor were mutated simultaneously, volume was a relatively unimportant informational constraint because three-quarters of all possible combinations of the 20 naturally occurring amino acids had volumes within the range tolerated in the core, and yet most of these sequences were unacceptable (20). In contrast, of the sequences that contained only

Fig. 2. Amino acid substitutions allowed in the core of  $\lambda$  repressor. The wild-type side chains are shown pictorially in the approximate orientation seen in the crystal structure (43). The lists of allowed substitutions at each position are shown below the wild-type side chains. These substitutions were identified by randomly mutating one to four residues at a time by using a cassette method and applying a functional selection (20). Not all substitutions are allowed in every sequence background.





the appropriate hydrophobic residues, a significant fraction were acceptable. Hence, the hydrophobicity of a sequence contains more information about its potential acceptability in the core than does the total side chain volume. Steric compatibility was intermediate between volume and hydrophobicity in informational importance.

## The Informational Importance of Surface Sites

We have noted that many surface sites can tolerate a wide variety of side chains, including hydrophilic and hydrophobic residues. This result might be taken to indicate that surface positions contain little structural information. However, Bashford *et al.*, in an extensive analysis of globin sequences (4), found a strong bias against large hydrophobic residues at many surface positions. At one level, this may reflect constraints imposed by protein solubility, because large patches of hydrophobic surface residues would presumably lead to aggregation. At a more fundamental level, protein folding requires a partitioning between surface and buried positions. Consequently, to achieve a unique native state without significant competition from other conformations, it may be important that some sites have a decided preference for exterior rather than interior positions. As a result, many surface sites can accept hydrophobic residues individually, but the surface as a whole can probably tolerate only a moderate number of hydrophobic side chains.

## Identification of Residue Roles from Sets of Sequences

Often, a protein of interest is a member of a family of related sequences. What can we infer from the pattern of allowed substitutions at positions in sets of aligned sequences generated by genetic or phylogenetic methods? Residue positions that can accept a number of different side chains, including charged and highly polar residues, are almost certain to be on the protein surface. Residue positions that remain hydrophobic, whether variable or not, are likely to be buried within the structure. In Fig. 3, those residue positions in  $\lambda$  repressor that can accept hydrophilic side chains are shown in orange and those that cannot accept hydrophilic side chains are shown in green. The obligate hydrophobic positions define the core of the structure, whereas positions that can accept hydrophilic side chains define the surface.

Functionally important residues should be conserved in sets of active sequences, but it is not possible to decide whether a side chain is functionally or structurally important just because it is invariant or conserved. To make this distinction requires an independent assay of protein folding. The ability of a mutant protein to maintain a stably folded structure can often be measured by biophysical techniques, by susceptibility to intracellular proteolysis (26), or by binding to antibodies specific for the native structure (27, 28). In the latter cases, it is possible to screen proteins in mutated clones for the ability to fold even if these proteins are inactive. Sets of sequences that allow formation of a stable structure can then be compared to the sets that allow both folding and function, with the active site or binding residues being those that are variable in the set of stable proteins but invariant in the set of functional proteins. The DNA-binding residues of Arc repressor were identified by this method (8). The receptor-binding residues of human growth hormone were also identified by comparing the stabilities and activities of a set of mutant sequences (28). However, in this case, the mutants were generated as hybrid sequences between growth hormone and related hormones with different binding specificities.

## Implications for Structure Prediction

At present, the only reliable method for predicting a low-resolution tertiary structure of a new protein is by identifying sequence similarity to a protein whose structure is already known (29, 30). However, it is often difficult to align sequences as the level of sequence similarity decreases, and it is sometimes impossible to detect statistically significant sequence similarity between distantly related proteins. Because the number of known sequences is far greater than the number of known structures, it would be advantageous to increase the reach of the available structural information by improving methods for detecting distant sequence relations and for subsequently aligning these sequences based on structural principles. In a normal homology search, the sequence database is scanned with a single test sequence, and every residue must be weighted equally. However, some residues are more important than others and should be weighted accordingly. Moreover, certain regions of the protein are more likely to contain gaps than others. Both kinds of information can be obtained from sequence sets, and several techniques have

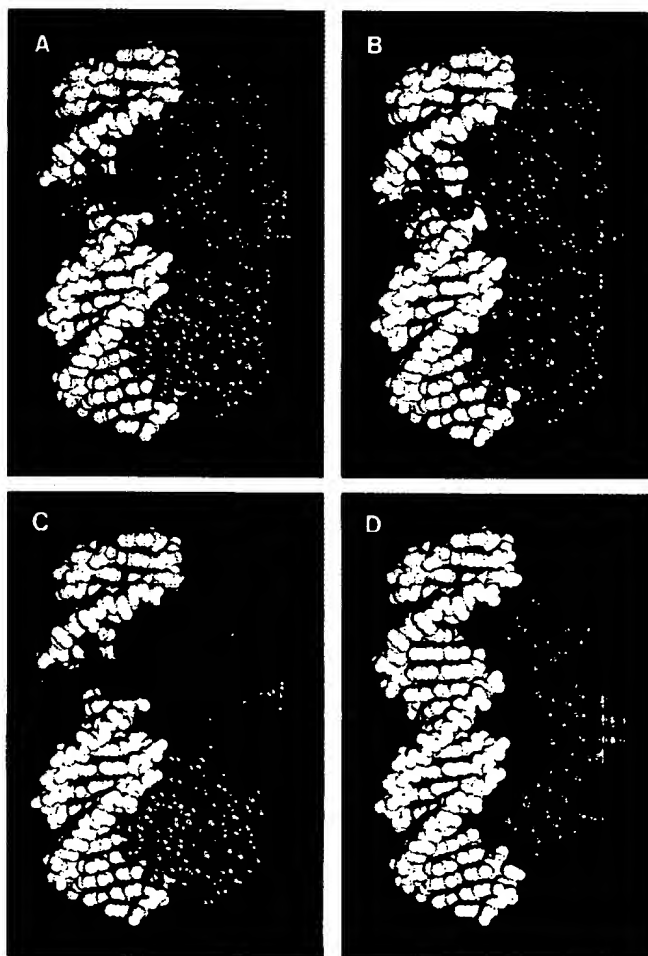


**Fig. 3.** Tolerance of positions in the  $\text{NH}_2$ -terminal domain of  $\lambda$  repressor to hydrophilic side chains. The complex (43) of the repressor dimer (blue) and operator DNA (white) is shown. In (A), positions that can tolerate hydrophilic side chains are shown in orange. The same side chains are shown in (B) without the remaining protein atoms. In (C), positions that require hydrophobic or neutral side chains are shown in green. These side chains are shown in (D) without the remaining protein atoms. About three-fourths of the 92 side chains in the  $\text{NH}_2$ -terminal domain are included in both (B) and (D). The remaining positions have not been tested. Data are from (9, 14, 20, 27, 44).

been used to combine such information into more appropriately weighted sequence searches and alignments (31). These methods were used to align the sequences of retroviral proteases with aspartic proteases, which in turn allowed construction of a three-dimensional model for the protease of human immunodeficiency virus type 1 (29). Comparison with the recently determined crystal structure of this protein revealed reasonable agreement in many areas of the predicted structure (32).

The structural information at most surface sites is highly degenerate. Except for functionally important residues, exterior positions seem to be important chiefly in maintaining a reasonably polar surface. The information contained in buried residues is also degenerate, the main requirement being that these residues remain hydrophobic. Thus, at its most basic level, the key structural message in an amino acid sequence may reside in its specific pattern of hydrophobic and hydrophilic residues. This is meant in an informational sense. Clearly, the precise structure and stability of a protein depends on a large number of detailed interactions. It is possible, however, that structural prediction at a more primitive level can be accomplished by concentrating on the most basic informational aspects of an amino acid sequence. For example, amphipathic patterns can be extracted from aligned sets of sequences and used, in some cases, to identify secondary structures.

If a region of secondary structure is packed against the hydrophobic core, a pattern of hydrophobic residues reflecting the periodicity of the secondary structure is expected (33, 34). These patterns can be obscured in individual sequences by hydrophobic residues on the protein surface. It is rare, however, for a surface position to remain hydrophobic over the course of evolution. Consequently, the amphipathic patterns expected for simple secondary structures can be much clearer in a set of related sequences (6). This principle is illustrated in Fig. 4, which shows helical hydrophobic moment plots for the Antennapedia homeodomain sequence (Fig. 4A) and for a composite sequence derived from a set of homologous homeodomain proteins (Fig. 4B) (35). The hydrophobic moment is a simple measure of the degree of amphipathic character of a sequence in a given secondary structure (34). The amphipathic character of the three  $\alpha$ -helical regions in the Antennapedia protein (36) is clearly revealed only by the analysis of the combined set of homeodomain sequences. The secondary structure of Arc repressor, a small DNA-binding protein, was recently predicted by a similar method (8) and confirmed by nuclear magnetic resonance studies (37).

The specific pattern of hydrophobic and hydrophilic residues in an amino acid sequence must limit the number of different structures a given sequence can adopt and may indeed define its overall fold. If this is true, then the arrangement of hydrophobic and hydrophilic residues should be a characteristic feature of a particular fold. Sweet and Eisenberg have shown that the correlation of the pattern of hydrophobicity between two protein sequences is a good criterion for their structural relatedness (38). In addition, several studies indicate that patterns of obligatory hydrophobic positions identified from aligned sequences are distinctive features of sequences that adopt the same structure (4, 29, 38, 39). Thus, the order of hydrophobic and hydrophilic residues in a sequence may actually be sufficient information to determine the basic folding pattern of a protein sequence.

Although the pattern of sequence hydrophobicity may be a characteristic feature of a particular fold, it is not yet clear how such patterns could be used for prediction of structure *de novo*. It is important to understand how patterns in sequence space can be related to structures in conformation space. Lau and Dill have approached this problem by studying the properties of simple sequences composed only of H (hydrophobic) and P (polar) groups on two-dimensional lattices (40). An example of such a representa-

tion is shown in Fig. 5. Residues adjacent in the sequence must occupy adjacent squares on the lattice, and two residues cannot occupy the same space. Free energies of particular conformations are evaluated with a single term, an attraction of H groups. By considering chains of ten residues, an exhaustive conformational search for all 1024 possible sequences of H and P residues was possible. For longer sequences only a representative fraction of the allowed sequence or conformation space could be explored. The significant results were as follows: (i) not all sequences can fold into a "native" structure and only a few sequences form a unique native structure; (ii) the probability that a sequence will adopt a unique native structure increases with chain length; and (iii) the native states are compact, contain a hydrophobic core surrounded by polar residues, and contain significant secondary structure. Although the gap between these two-dimensional simulations and three-dimensional structures is large, the use of simple rules and sequence representations yields results similar to those expected for real proteins. Three-dimensional lattice methods are also beginning to be developed and evaluated (41).

## Summary

There is more information in a set of related sequences than in a single sequence. A number of practical applications arise from an analysis of the tolerance of residue positions to change. First, such information permits the evaluation of a residue's importance to the function and stability of a protein. This ability to identify the essential elements of a protein sequence may improve our understanding of the determinants of protein folding and stability as well as protein function. Second, patterns of tolerance to amino acid substitutions of varying hydrophilicity can help to identify residues likely to be buried in a protein structure and those likely to occupy

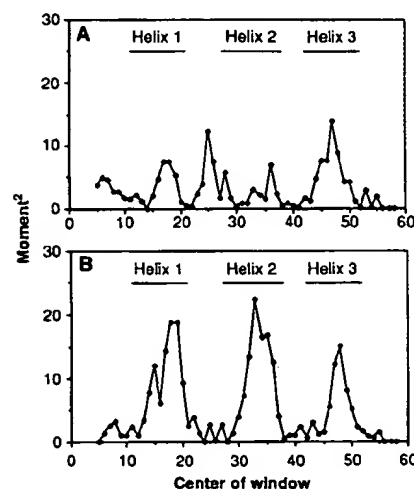


**Fig. 4.** Helical hydrophobic moments calculated by using (A) the Antennapedia homeodomain sequence or (B) a set of 39 aligned homeodomain sequences (35). The bars indicate the extent of the helical regions identified in nuclear magnetic resonance studies of the Antennapedia homeodomain (36). To determine hydrophobic moments, residues were assigned to one of three groups: H1 (high hydrophobicity = Trp, Ile, Phe, Leu, Met, Val, or Cys); H2 (medium hydrophobicity = Tyr, Pro, Ala, Thr, His, Gly, or Ser); and H3 (low hydrophobicity = Gln, Asn, Glu, Asp, Lys, or Arg). For the aligned homeodomain sequences, the residues at each position were sorted by their hydrophobicity by using the scale of Fauchere and Pliska (45). Arg and Lys were not counted unless no other residue was found at the position, because they contain long aliphatic side chains and can thereby substitute for nonpolar residues at some buried sites. To account for possible sequence errors and rare exceptions, the most hydrophilic residue allowed at each position was discarded unless it was observed twice. The second most hydrophilic residue was then chosen to represent the hydrophobicity of each position. An eight-residue window was used and the vectors projected radially every 100°. The vector magnitudes were assigned a value of 1, 0, or -1 for positions where the hydrophobicity group was H1, H2, or H3, respectively.

P H P P H P H P H H H P P H

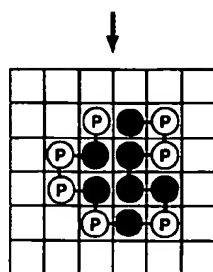


Fig. 5. A representation of one compact conformation for a particular sequence of H and P residues on a two-dimensional square lattice. [Adapted from (40), with permission of the American Chemical Society]

surface positions. The amphipathic patterns that emerge can be used to identify probable regions of secondary structure. Third, incorporating a knowledge of allowed substitutions can improve the ability to detect and align distantly related proteins because the essential residues can be given prominence in the alignment scoring.

As more sequences are determined, it becomes increasingly likely that a protein of interest is a member of a family of related sequences. If this is not the case, it is now possible to use genetic methods to generate lists of allowed amino acid substitutions. Consequently, at least in the short term, it may not be necessary to solve the folding problem for individual protein sequences. Instead, information from sequence sets could be used. Perhaps by simplifying sequence space through the identification of key residues, and by simplifying conformation space as in the lattice methods, it will be possible to develop algorithms to generate a limited number of trial structures. These trial structures could then, in turn, be evaluated by further experiments and more sophisticated energy calculations.

#### REFERENCES AND NOTES

1. C. J. Epstein, R. F. Goldberger, C. B. Anfinsen, *Cold Spring Harbor Symp. Quant. Biol.* **28**, 439 (1963); C. B. Anfinsen, *Science* **181**, 223 (1973).
2. R. E. Dickerson, *Sci. Am.* **242**, 136 (March 1980).
3. M. D. Hampsey, G. Das, F. Sherman, *FEBS Lett.* **231**, 275 (1988).
4. D. Bashford, C. Chothia, A. M. Lesk, *J. Mol. Biol.* **196**, 199 (1987).
5. A. M. Lesk and C. Chothia, *ibid.* **136**, 225 (1980).
6. M. F. Perutz, J. C. Kendrew, H. C. Watson, *ibid.* **13**, 669 (1965).
7. C. Chothia and A. M. Lesk, *Cold Spring Harbor Symp. Quant. Biol.* **52**, 399 (1987).
8. J. U. Bowie and R. T. Sauer, *Proc. Natl. Acad. Sci. U.S.A.* **86**, 2152 (1989).
9. J. F. Reidhaar-Olson and R. T. Sauer, *Science* **241**, 53 (1988); *Proteins Struct. Funct. Genet.*, in press.
10. D. Shortle, *J. Biol. Chem.* **264**, 5315 (1989).
11. J. H. Miller et al., *J. Mol. Biol.* **131**, 191 (1979).

12. S. Sprang et al., *Science* **237**, 905 (1987); C. S. Craik, S. Rocznik, C. Largman, W. J. Rutter, *ibid.*, p. 909.
13. H. C. M. Nelson and R. T. Sauer, *J. Mol. Biol.* **192**, 27 (1986).
14. M. H. Hecht, J. M. Sturtevant, R. T. Sauer, *Proc. Natl. Acad. Sci. U.S.A.* **81**, 5685 (1984).
15. T. Alber, D. Sun, J. A. Nye, D. C. Muchmore, B. W. Matthews, *Biochemistry* **26**, 3754 (1987).
16. D. Shortle and A. K. Meeker, *Proteins Struct. Funct. Genet.* **1**, 81 (1986).
17. A. M. Lesk and C. Chothia, *J. Mol. Biol.* **160**, 325 (1982).
18. W. R. Taylor, *ibid.* **188**, 233 (1986).
19. W. Kauzmann, *Adv. Protein Chem.* **14**, 1 (1959); R. L. Baldwin, *Proc. Natl. Acad. Sci. U.S.A.* **83**, 8069 (1986).
20. W. A. Lim and R. T. Sauer, *Nature* **339**, 31 (1989); in preparation.
21. Lesk and Chothia (5) have argued that a protein core composed solely of hydrogen-bonded residues would also be inviable on evolutionary grounds, as a mutational change in one core residue would require compensating changes in any interacting residue or residues to maintain a stable structure.
22. T. M. Gray and R. W. Matthews, *J. Mol. Biol.* **175**, 75 (1984); E. N. Baker and R. E. Hubbard, *Prog. Biophys. Mol. Biol.* **44**, 97 (1984).
23. F. M. Richards, *J. Mol. Biol.* **82**, 1 (1974).
24. J. W. Ponder and F. M. Richards, *ibid.* **193**, 775 (1987).
25. J. T. Kellis, Jr., K. Nyberg, A. R. Fersht, *Biochemistry* **28**, 4914 (1989); W. S. Sandberg and T. C. Terwilliger, *Science* **245**, 54 (1989).
26. A. A. Pakula and R. T. Sauer, *Proteins Struct. Funct. Genet.* **5**, 202 (1989).
27. B. C. Cunningham and J. A. Wells, *Science* **244**, 1081 (1989); R. M. Breyer and R. T. Sauer, *J. Biol. Chem.* **264**, 13348 (1989).
28. B. C. Cunningham, P. Jhurani, P. Ng, J. A. Wells, *Science* **243**, 1330 (1989).
29. L. H. Pearl and W. R. Taylor, *Nature* **329**, 351 (1987).
30. W. J. Brown et al., *J. Mol. Biol.* **42**, 65 (1969); J. Greer, *ibid.* **153**, 1027 (1981); J. M. Berg, *Proc. Natl. Acad. Sci. U.S.A.* **85**, 99 (1988).
31. W. R. Taylor, *Protein Eng.* **2**, 77 (1988).
32. M. A. Navia et al., *Nature* **337**, 615 (1989).
33. M. Schiffer and A. B. Edmundson, *Biophys. J.* **7**, 121 (1967); V. I. Lim, *J. Mol. Biol.* **88**, 857 (1974); *ibid.*, p. 873.
34. D. Eisenberg, R. M. Weiss, T. C. Terwilliger, *Nature* **299**, 371 (1982); D. Eisenberg, D. Schwarz, M. Komaromy, R. Wall, *J. Mol. Biol.* **179**, 125 (1984); D. Eisenberg, R. M. Weiss, T. C. Terwilliger, *Proc. Natl. Acad. Sci. U.S.A.* **81**, 140 (1984).
35. T. R. Burglin, *Cell* **53**, 339 (1988).
36. G. Otting et al., *EMBO J.* **7**, 4305 (1988).
37. J. N. Breg, R. Boelens, A. V. E. George, R. Kaptein, *Biochemistry* **28**, 9826 (1989); M. G. Zagorski, J. U. Bowie, A. K. Vershon, R. T. Sauer, D. J. Patel, *ibid.*, p. 9813.
38. R. M. Sweet and D. Eisenberg, *J. Mol. Biol.* **171**, 479 (1983).
39. J. U. Bowie, N. D. Clarke, C. O. Pabo, R. T. Sauer, *Proteins Struct. Funct. Genet.*, in preparation.
40. K. F. Lau and K. A. Dill, *Macromolecules* **22**, 3986 (1989).
41. A. Sikorski and J. Skolnick, *Proc. Natl. Acad. Sci. U.S.A.* **86**, 2668 (1989); A. Kolinski, J. Skolnick, R. Yaris, *Biopolymers* **26**, 937 (1987); D. G. Covell and R. L. Jernigan, *Biochemistry*, in press.
42. B. Lee and F. M. Richards, *J. Mol. Biol.* **55**, 379 (1971).
43. S. R. Jordan and C. O. Pabo, *Science* **242**, 893 (1988).
44. R. M. Breyer, thesis, Massachusetts Institute of Technology, Cambridge (1988).
45. J.-L. Fauchere and V. Pliska, *Eur. J. Med. Chem.-Chim. Ther.* **18**, 369 (1983).
46. We thank C. O. Pabo and S. Jordan for coordinates of the NH<sub>2</sub>-terminal domain of  $\lambda$  repressor and its operator complex. We also thank P. Schimmel for the use of his graphics system and J. Burnbaum and C. Francklyn for assistance. Supported in part by NIH grant AI-15706 and predoctoral grants from NSF (J.R.-O.) and Howard Hughes Medical Institute (W.A.L.).

## Defective $\gamma$ Subunit of ATP Synthase ( $F_1F_0$ ) from *Escherichia coli* Leads to Resistance to Aminoglycoside Antibiotics

RICHARD HUMBERT<sup>1</sup>\* AND KARLHEINZ ALTENDORF<sup>2</sup>

Department of Biological Sciences, Stanford University, Stanford, California 94305-5020,<sup>1</sup> and Universität Osnabrück, Fachbereich Biologie/Chemie, D-4500 Osnabrück, Federal Republic of Germany<sup>2</sup>

Received 7 March 1988/Accepted 2 December 1988

A strain of *Escherichia coli* which was derived from a gentamicin-resistant clinical isolate was found to be cross-resistant to neomycin and streptomycin. The molecular nature of the genetic defect was found to be an insertion of two GC base pairs in the *uncG* gene of the mutant. The insertion led to the production of a truncated  $\gamma$  subunit of 247 amino acids in length instead of the 286 amino acids that are present in the normal  $\gamma$  subunit. A plasmid which carried the ATP synthase genes from the mutant produced resistance to aminoglycoside antibiotics when it was introduced into a strain with a chromosomal deletion of the ATP synthase genes. Removal of the genes coding for the  $\beta$  and  $\epsilon$  subunits abolished antibiotic resistance coded by the mutant plasmid. The relationship between antibiotic resistance and the  $\gamma$  subunit was investigated by testing the antibiotic resistance of plasmids carrying various combinations of *unc* genes. The presence of genes for the  $F_0$  portion of the ATP synthase in the presence or absence of genes for the  $\gamma$  subunit was not sufficient to cause antibiotic resistance.  $\alpha$ ,  $\beta$ , and truncated  $\gamma$  subunits were detected on washed membranes of the mutant by immunoblotting. The first 247 amino acid residues of the  $\gamma$  subunit may be sufficient to allow its association with other  $F_1$  subunits in such a way that the proton gate of  $F_0$  is held open by the mutant  $F_1$ .

The proton-translocating ATPase is an enzyme which, in facultative anaerobes such as *Escherichia coli*, functions reversibly to synthesize ATP during aerobic growth or to generate proton motive force during anaerobic growth (10). The enzyme consists of an integral membrane portion,  $F_0$ , and an attached catalytic portion,  $F_1$ , which may be dissociated from the membrane by washing it in a low-ionic-strength medium in the presence of EDTA. The  $F_1$  portion of the enzyme consists of five subunits:  $\alpha$ ,  $\beta$ ,  $\gamma$ ,  $\delta$ , and  $\epsilon$ . The  $F_0$  portion consists of three subunits:  $a$ ,  $b$ , and  $c$ . Biochemical studies involving reconstitution of ATPase activity from isolated  $F_1$  subunits have shown that the  $\alpha$  and  $\beta$  subunits are primarily responsible for nucleotide binding and catalysis but do not associate to perform ATP hydrolysis unless the  $\gamma$  subunit is also present (13). ATP synthesis is only observed when  $F_1$  is bound to  $F_0$ , which is inserted in closed membranes. Studies with plasmids lacking individual  $F_1$  genes have shown that in vivo,  $\alpha$  and  $\beta$  assemble to form a catalytically active partial  $F_1$  only if the  $\gamma$  subunit is also present (25).

The genes for the ATP synthase polypeptides are located in an operon designated *unc*. The gene order is *uncIBEF-HAGDC*, coding for polypeptides  $i$ ,  $a$ ,  $c$ ,  $b$ ,  $\delta$ ,  $\alpha$ ,  $\gamma$ ,  $\beta$ , and  $\epsilon$ , respectively (11, 17). The  $i$  polypeptide is not known to be present in ATP synthase. Studies of a series of amber mutations in the *uncG* gene which result in truncated  $\gamma$  subunits of various lengths support results of biochemical studies which indicate that the  $\gamma$  subunit is required for assembly of catalytically active  $F_1$  (20, 31).

An in-frame internal deletion of 21 nucleotides of the *uncG* gene in strain NR70 results in the absence of 7 amino acid residues near the N terminus of the  $\gamma$  subunit (19). Cells of strain NR70 are deficient in the transport of galactosides and amino acids, and membranes of this strain are leaky to protons (38). Immunological studies indicated that the  $\alpha$ ,  $\beta$ , and  $\gamma$  subunits are absent from membranes and are absent or

much reduced in the cytoplasmic fraction of cell extracts of strain NR70 (27). Strain NR70 was initially selected by resistance to the antibiotic neomycin (38). Strain N<sub>144</sub>, which was also selected by resistance to the antibiotic neomycin, has a defect in the ATP synthase which has not been characterized at the level of the DNA sequence (19). The resistance to neomycin in strains NR70 and N<sub>144</sub> has been hypothesized to be caused by a decreased ability to transport the antibiotic because of proton leak through  $F_0$  (21, 38).

Kauffer et al. (22) have studied strain AT753-26-28, a mutant that is defective in ATP synthase which was derived from a clinically isolated gentamicin-resistant strain of *E. coli*. Strain AT753-26-28 was found to lack ATPase activity. Membranes of strain AT753-26-28 did not exhibit strong succinate-dependent fluorescence quenching, indicating that the membranes were permeable to protons. Strain AT753-26-28 did not grow on nonfermentable carbon sources such as succinate. In the present report we (i) describe the genetic mapping and sequencing of the mutation in strain AT753-26-28, (ii) demonstrate that the cloned ATP synthase genes from strain AT753-26-28 are sufficient to confer antibiotic resistance on a strain lacking ATP synthase genes, and (iii) examine which combinations of individual ATP synthase subunits are required to confer an antibiotic-resistant phenotype.

### MATERIALS AND METHODS

**Bacterial strains.** The *E. coli* K-12 strains AT753 (*unc*<sup>+</sup>) and AT753-26-28 (*uncG270*) were obtained from E. Schwarz and W. Piepersberg. The *uncG270* mutation was initially observed in a gentamicin-resistant clinical isolate of *E. coli* (44). The clinical isolate failed to grow when it was supplied with nonfermentable carbon sources and was presumed to be defective in ATP synthase. The *unc* genes from the antibiotic-resistant strain, including the *uncG270* mutation, were transferred to a K-12 strain by P1 transduction to produce strain AT753-26-28 (22; E. Schwarz and W. Piepersberg, unpublished data). The gentamicin-resistant phenotype

\* Corresponding author.

TABLE 1. Bacterial strains used in this study

Strain	Genotype	Reference or comments
AT753	F <sup>-</sup> <i>thi-1 ilv-1 argH metB1 lacY1</i> or <i>lacZ4 gal-6 strA8 supE44?</i>	22
AT753-26-28	F <sup>-</sup> <i>uncG270 thi-1 argH metB1 lacY1</i> or <i>lacZ4 gal-6 strA8 supE44?</i>	22
CK1703	F <sup>-</sup> $\Delta$ <i>lacU169 araD139 rpsL relA thi-1</i>	26
CK1801	F <sup>-</sup> $\Delta$ <i>uncB-C</i> $\Delta$ <i>lacU169 araD139 rpsL relA thi-1</i>	26
CK1803	F <sup>-</sup> $\Delta$ <i>uncB-C</i> $\Delta$ <i>lacU169 araD139 rpsL relA recA thi-1</i>	26
DK6	F <sup>-</sup> $\Delta$ <i>uncB-C</i> <i>rpsL hsdR minA minB purE pdxC his met</i>	23
DL54	<i>unc lac</i>	41
ML308-225	<i>lac</i>	41
RH270	F <sup>-</sup> <i>uncG270 recA1 srl::Tn10 argH metB1 lacY1</i> or <i>lacZ4 supE44? gal-6 strA8 thi-1</i>	This report; P1 transduction of <i>recA</i> into AT753-26-28
RH401	HfrC <i>uncG270</i>	This report; P1 transduction
RH402	HfrPO1 $\Delta$ <i>uncB-C</i> <i>recA1 srl::Tn10 thi-1 rel-1 thi-1</i>	Carol Kumamoto; derivative of strain 1100
X1488	F <sup>-</sup> <i>rpsL hsdR minA minB purE pdxC his ilv met</i>	23
1100	HfrPO1 <i>thi-1 rel-1 bglR</i>	Laboratory stock

was associated with the failure to grow on nonfermentable carbon sources; both were cotransducible with the *ilv* locus. Other bacterial strains used in this study are given in Table 1.

**Plasmids.** We use a prime symbol (e.g.,  $\alpha'$ ) to indicate a truncated polypeptide produced by a partial gene on a plasmid. We used  $\gamma'$ -*uncG270* to indicate the mutant  $\gamma$  subunit produced by a plasmid carrying the *uncG270* mutation.

A plasmid containing the *uncG270* mutation was constructed by Hfr-mediated chromosome mobilization (4, 26). This technique relies on the fact that the plasmid-borne chloramphenicol resistance can only be transferred in a mating if the plasmid carrying the resistance element has recombined with the chromosome of the Hfr prior to transfer. When transferred into a recombination-proficient recipient, in some cases, recombinational excision gives rise to a plasmid which has received the chromosomal mutation. pDJK37, which is 8.7 kilobases in length, was derived from plasmid pRPG54 (*a, c, b,  $\delta, \alpha, \gamma, \beta, \epsilon$* ; 12.8 kilobases), but contains a deletion extending from *uncH* into *uncC*. Strain RH401 (HfrC *uncG270* streptomycin sensitive) was transformed with plasmid pDJK37 (*a, c, b*). RH401(pDJK37) was mated with strain CK1801 (F<sup>-</sup>  $\Delta$ *uncB-C* streptomycin resistant) with selection for chloramphenicol resistance and streptomycin resistance. A plasmid DNA preparation was made from the pooled exconjugants which were resistant to both chloramphenicol and streptomycin. A recombinant plasmid that received the mutation contained the *uncB* through *uncC* genes and was 12.8 kilobases in length. Uncut plasmid DNA was electrophoresed in a 0.8% agarose gel, with plasmids pRPG54 and pDJK37 used as standards. The region of the gel corresponding in size to pRPG54 was excised, crushed, and soaked in 10 mM Tris hydrochloride (pH 7.8)-1 mM EDTA. The eluate was used to transform strain CK1803 ( $\Delta$ *uncBC recA*). Transformants were purified and plasmid DNA was prepared. Plasmid DNA preparations were digested with *EcoRI* and subjected to agarose gel electrophoresis. Of 12 plasmids tested, 4 had a restriction pattern identical to that of pRPG54 (*a, c, b,  $\delta, \alpha, \gamma, \beta, \epsilon$* ) rather than to that of the starting plasmid pDJK37 (*a, c, b*). These four plasmids were assumed to have received the *uncG270* mutation by recombination. All four isolates had identical properties. Plasmid pRAH4 (*a, c, b,  $\delta, \alpha, \gamma'$ -uncG270,  $\beta, \epsilon$* ) is further characterized in this report. A *BanII* site that was present in the *uncD* gene of pRPG54 was found to be absent in pRAH4. The *uncD* gene does not determine antibiotic resistance, which is the topic of this report (see below).

Plasmid pRAH2 was produced by digesting pDJK2 with *MsrII* and *StuI* to remove a 506-base-pair fragment extending into the *uncG* gene by using the large fragment of DNA polymerase I to fill the ends with nucleotide triphosphates and by ligating the blunt ends. Plasmid pRAH5 was produced by isolating the *MsrII-EcoRI* fragment that makes up the *uncG* gene from plasmid pDJK2 and inserting this fragment into pUC19 that was digested with *EcoRI* and *HindIII*. Plasmid pRAH6 was produced by digesting plasmid pRAH4 with *EagI* to remove DNA extending from 997 base pairs into the *uncD* gene into the plasmid vector, followed by religation of the ends. The resulting plasmid lacked two-thirds of the *uncD* and all of the *uncC* genes.

Other plasmids have been described previously and are given in Table 2.

**Media.** LB plates contained 10 g of tryptone, 5 g of yeast extract, 5 g of NaCl, and 15 g of agar per liter.

**Genetic experiments.** Genetic complementation experiments done with plasmids carrying the genes of the *unc* operon were performed as described previously (18). Growth on minimal succinate medium was scored after the introduction of various plasmids into strain RH270 (*uncG270 recA*), which is a derivative of AT753-26-28.

TABLE 2. Plasmids used in this study

Plasmid	ATP synthase polypeptides <sup>a</sup>	Antibiotic resistance	Source or reference
pDJK1	$\alpha', \gamma$	Ap	24
pDJK2	$\delta, \alpha, \gamma$	Ap	24
pDJK9	<i>a, c, b, <math>\delta, \alpha', \gamma, \beta, \epsilon</math></i>	Cm	25
pDJK19	<i>a, c, b, <math>\alpha'</math></i>	Cm	2
pDJK20	<i>a, c, b</i>	Cm	2
pDJK22	<i>a, c, b, <math>\delta, \alpha, \gamma', \beta, \epsilon</math></i>	Cm	25
pDJK23	<i>a, c, b, <math>\delta, \alpha, \beta, \epsilon</math></i>	Cm	25
pDJK37	<i>a, c, b</i>	Cm	D. Klionsky and R. Simoni
pRAH2	$\delta, \alpha$	Ap	This report
pRAH4	<i>a, c, b, <math>\delta, \alpha, \gamma'</math>-uncG270, <math>\beta, \epsilon</math></i>	Cm	This report
pRAH5	$\gamma'$ - <i>uncG270</i>	Ap	This report
pRAH6	<i>a, c, b, <math>\delta, \alpha, \gamma'</math>-uncG270, <math>\beta'</math></i>	Cm	This report
pRPG23	<i>a, c, b, <math>\delta, \alpha, \gamma'</math></i>	Ap	17
pRPG54	<i>a, c, b, <math>\delta, \alpha, \gamma, \beta, \epsilon</math></i>	Cm	17
pRPG55	$\beta'$	Tc	17
pWSB2	$\beta'$	Cm	17
pWSB7	$\gamma$	Ap	18

<sup>a</sup> The *unc* gene products produced by each plasmid are indicated. Many plasmids carry small portions of *unc* DNA adjacent to the genes coding for the subunits listed as being produced.

Other genetic techniques were done by standard methods (28, 32).

**Antibiotic resistance.** For experiments in which sensitivity to gentamicin and neomycin was tested, colonies were patched onto an LB plate, in some cases with 30  $\mu$ g of chloramphenicol per ml or 100  $\mu$ g of ampicillin per ml to select for retention of plasmids. After 1 day the plate was replicated onto LB plates with the indicated amount of gentamicin sulfate or neomycin sulfate. Growth was scored after 2 to 3 days of incubation at 37°C. For most experiments, the pH of the medium was adjusted to 7.5. The highest concentration of antibiotic at which substantial growth occurred was taken as the level of antibiotic resistance.

**Determination of plasmid-coded gene products in vivo.** The plasmid-coded gene products of plasmids pRPG54 ( $a$ ,  $c$ ,  $b$ ,  $\delta$ ,  $\alpha$ ,  $\gamma$ ,  $\beta$ ,  $\epsilon$ ) and pRAH4 ( $a$ ,  $c$ ,  $b$ ,  $\delta$ ,  $\alpha$ ,  $\gamma'$ -*uncG270*,  $\beta$ ,  $\epsilon$ ) were measured in the minicell strain DK6 (23). Minicells were produced from strain DK6, which carried the plasmid, and synthesis products were measured by labeling the minicells with [<sup>35</sup>S]methionine as described previously (37). The proteins synthesized by minicells were fractionated by electrophoresis on a 13% sodium dodecyl sulfate (SDS)-polyacrylamide gel and detected by autoradiography.

**Immunoblots.** In experiments in which immunoblotting was used to detect the  $\alpha$ ,  $\beta$ , and  $\gamma$  subunits in extracts and membranes, cultures of AT753(pRPG54) and AT753-26-28(pRAH4) were grown to an optical density of 1.0 to 1.2 at 600 nm. Cells were washed and suspended in 5 ml of HM buffer (HM buffer consisted of 50 mM HEPES [*N*-2-hydroxyethylpiperazine-*N'*-2-ethanesulfonic acid; pH 7.5], 10 mM MgSO<sub>4</sub>, 20 mM benzamidine, 20 mM  $\epsilon$ -amino caproic acid, 20 mM dithiothreitol, 100  $\mu$ M phenylmethylsulfonyl fluoride). The cells were broken in a French pressure cell at 14,000 lb/in<sup>2</sup>. The suspension was centrifuged to 5 min at 3,000  $\times$  *g* to remove unbroken cells and debris. The supernatant was removed and centrifuged for 60 min at 100,000  $\times$  *g*. The supernatant from this step was saved and is termed the soluble extract. The membranes were suspended in 5 ml of HM buffer and centrifuged again for 60 min at 100,000  $\times$  *g*. The pelleted membranes were suspended in 2 ml of HM buffer to produce washed membranes. Fractions were frozen at -20°C for later use. Samples were loaded onto a 10% SDS-polyacrylamide gel and run for about 18 h at 25 mA. The blotting procedure was essentially that of Dunn (12), which was found to promote detection of the  $\gamma$  subunit. The gel was soaked in 25 mM Tris hydrochloride (pH 7.4)-20% glycerol for 30 min. The gel was rinsed briefly in 10 mM NaHCO<sub>3</sub>-3 mM Na<sub>2</sub>CO<sub>3</sub>-20% methanol (pH 9.9) and transferred to a nitrocellulose sheet with an electrophoretic transfer apparatus (Novablot; LKB Instruments, Inc., Rockville, Md.) with a current of 0.8 mA/cm<sup>2</sup> for 4 h. The nitrocellulose sheet was washed for 5 h in 10 mM Tris hydrochloride (pH 7.4)-1 mM EDTA-0.2% (vol/vol) Tween 20-0.3% bovine serum albumin (TETB buffer). Antisera directed against the isolated  $\alpha$ ,  $\beta$ , and  $\gamma$  subunits were added at dilutions of 1:10,000, 1:10,000, and 1:1,000, respectively. Antisera directed against  $\alpha$  and  $\beta$  subunits were used at higher dilutions than the anti- $\gamma$  serum in order to make the intensities of the bands comparable. The nitrocellulose was incubated for 12 h at 4°C in the presence of the antisera and washed for 1 h at room temperature with buffer without bovine serum albumin. Goat anti-rabbit antiserum conjugated to horseradish peroxidase was then incubated with the blot for 2 h in TETB buffer. The nitrocellulose was washed for 2 h with buffer without bovine serum albumin. The

presence of bound horseradish peroxidase was visualized with *o*-anisidine (500  $\mu$ g/ml) and hydrogen peroxide (30  $\mu$ g/ml) in 10 mM Tris hydrochloride (pH 7.4).

**Measurement of membrane energization by fluorescence quenching.** Fluorescence quenching experiments were done essentially as described previously (2). Membranes (0.4 mg of protein) were suspended in HM buffer were added to 2 ml of assay buffer, which contained 50 mM MOPS (morpholine-propanesulfonic acid; pH 7.3) and 10 mM MgSO<sub>4</sub>. 9-Amino-6-chloro-2-methoxyacridine was used at 1  $\mu$ M, NADH at 0.5 mM, KCN at 1.5 mM, and ATP at 1 mM. For tests of the effect of *N,N'*-dicyclohexylcarbodiimide (DCCD), 50  $\mu$ M DCCD was incubated with membranes for 10 min at 37°C in 100  $\mu$ l of assay buffer, which were then diluted to 2 ml and assayed for fluorescence quenching.

**Proline transport.** Proline transport in whole cells was measured as described by Simoni and Shallenberger (41). Cells grown in minimal medium were washed twice with minimal salts and suspended in minimal salts. Cells with 0.4 mg of cell protein were added to 5 ml of minimal salts with 0.2% glucose. After a 5-min preincubation, [<sup>14</sup>C]proline was added to 25  $\mu$ M. Portions of 1 ml were removed at the indicated times, rapidly filtered, and washed once with minimal salts. The amount of [<sup>14</sup>C]proline uptake was measured, with correction for the amount of uptake at time zero.

## RESULTS

**Genetic complementation experiments show that the mutation in strain AT753-26-28 is in the *uncG* gene.** Nonsense or missense mutations in each of the genes coding for the subunits that are known to be present in purified ATP synthase have been isolated which lead to the loss of ATP synthase function and the inability to use nonfermentable carbon sources (10, 11, 18). The introduction of normal copies of these genes on F' factors (10), amplifiable plasmids (18), or specialized lambda transducing phage (34) can effect genetic complementation of *unc* point mutations. We examined the growth of strain RH270 (*uncG270 recA*) on minimal succinate medium when plasmids with combinations of *unc* genes were introduced by transformation (18). Complementation of RH270 was observed when plasmids pDJK2 ( $\delta$ ,  $\alpha$ ,  $\gamma$ ) and pDJK9 ( $a$ ,  $c$ ,  $b$ ,  $\delta$ ,  $\alpha'$ ,  $\gamma$ ,  $\beta$ ,  $\epsilon$ ) or other plasmids carrying a normal *uncG* gene but lacking other single *unc* genes were present individually. Weak complementation was observed when pDJK1( $\alpha'$ ,  $\gamma$ ) or pWSB7 ( $\gamma$ ) was present. No complementation of RH270 was observed when it was transformed with plasmid pDJK23 ( $a$ ,  $c$ ,  $b$ ,  $\delta$ ,  $\alpha$ ,  $\beta$ ,  $\epsilon$ ), which carried a defect in the *uncG* gene, or with other plasmids, which did not carry the *uncG* gene. These results indicate that strain RH270 (*uncG270 recA*) contains a mutation in the *uncG* gene.

**Recombination experiments map the mutation to a portion of the *uncG* gene.** To map the *uncG270* mutation within the *uncG* gene, recombination experiments with plasmids containing portions of the *uncG* gene were performed. The portion of the *uncG* gene carried by each of these plasmids is shown in Fig. 1. Strain AT753-26-28 (*uncG270*) was transformed with plasmids pRPG23, pRPG55, pWSB2, and pRAH2. Transformant cultures were examined for the presence of *unc*<sup>+</sup> recombinants by scoring which plasmid-strain combinations produced colonies on minimal succinate plates. Plasmids pWSB2 and pRAH2 produced *unc*<sup>+</sup> recombinants when they were introduced into strain AT753-26-28. No *unc*<sup>+</sup> recombinants were observed when plasmids pRPG23 and pRPG55 were introduced. The only portion of

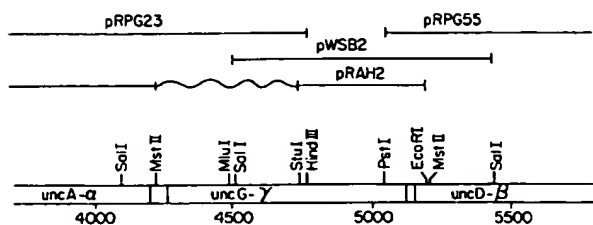


FIG. 1. Plasmids used in recombination mapping of the *uncG270* mutation. The amount of DNA in the region of *uncG* carried by each plasmid is indicated by the solid lines. The wavy line connecting the ends of pRAH2 indicates the region of DNA which was deleted from this plasmid. The restriction sites in the vicinity of *uncG* at which the plasmids terminated are indicated above the double lines, indicating the portion of DNA occupied by the *uncA*, *uncG*, and *uncD* genes. The numbers below indicate the distance from the *unc* promoter.

the *unc* operon present in plasmids pWSB2 and pRAH2, but absent in plasmids pRPG23 and pRPG55, was between the *HindIII* and *PstI* sites in the *uncG* gene. The *uncG270* mutation must therefore lie in this region.

**Construction of a plasmid carrying the ATP synthase genes.** The *uncG270* mutation was moved from the chromosome to a plasmid by Hfr-mediated chromosome mobilization as described above. The plasmid pRAH4 (*a*, *c*, *b*,  $\delta$ ,  $\alpha$ ,  $\gamma'$ -*uncG270*,  $\beta$ ,  $\epsilon$ ) contains the mutant copy of the *uncG* gene and, in addition, normal copies of the other structural genes of the *unc* operon except *uncI*. This plasmid coded for the production of a truncated  $\gamma$  subunit (see below). An analogous plasmid containing normal copies of the eight *unc* structural genes, plasmid pRPG54 (*a*, *c*, *b*,  $\delta$ ,  $\alpha$ ,  $\gamma$ ,  $\beta$ ,  $\epsilon$ ), has been described previously (15) and was used as a control in many experiments. Plasmid pRPG54 has recently been shown to have an alteration in the ribosome-binding site at the start of the *uncE* gene (42). This change reduces expression of the *c* subunit and appears to result in some increase in proton permeability and reduction of the efficiency of coupling of a transmembrane proton gradient to ATP synthesis. When introduced into a strain with point mutations or a deletion of the chromosomal *unc* genes, pRPG54 complemented the mutations to allow growth on nonfermentable carbon sources. The specific activity of the ATPase associated with membranes prepared from strains with chromosomal *unc* deletions harboring pRPG54 was nearly identical to that of ATPase associated with membranes from strains with normal chromosomal *unc* genes. ATP synthase from these membranes effectively energizes them in a fluorescence quenching assay. We do not know whether pRAH4 has the wild-type ribosome-binding site preceding *uncE* or whether it is identical to pRPG54. In contrast to pRPG54, pRAH4 (*a*, *c*, *b*,  $\delta$ ,  $\alpha$ ,  $\gamma'$ -*uncG270*,  $\beta$ ,  $\epsilon$ ) did not complement a strain with a deletion of the *unc* structural genes.

The plasmid carrying the *uncG270* mutation conferred antibiotic resistance on an *unc* deletion strain. The sensitivity to the antibiotic gentamicin of a wild-type strain, 1100, and a strain carrying a chromosomal deletion of the *uncB* through *uncC* genes, RH402, is shown in Table 3. Various plasmids were introduced into strain RH402, and the level of gentamicin resistance was determined. Resistance to gentamicin was found to be strongly pH dependent, as has been shown previously with *Staphylococcus aureus* (29). We focused on the gentamicin concentration, which was limiting for growth at pH 7.5, because this provided a sensitive measure of differences between strains. The strain carrying the chromo-

TABLE 3. Antibiotic resistance of strains and strain-plasmid combinations

Strain and plasmid	Resistance to gentamicin sulfate ( $\mu$ g/ml) at:	
	pH 7.5	pH 6.0
AT753 ( <i>unc</i> <sup>+</sup> )	0.5	10
AT753-26-28 ( <i>uncG270</i> )	14	>18 <sup>a</sup>
1100 ( <i>unc</i> <sup>+</sup> )	0.5	12
RH402 ( $\Delta$ <i>uncBC recA</i> )	0.2	1
RH402 (pRAH4) ( <i>a</i> , <i>c</i> , <i>b</i> , $\delta$ , $\alpha$ , $\gamma'$ - <i>uncG270</i> , $\beta$ , $\epsilon$ )	5	>8 <sup>a</sup>
RH402 (pRPG54) ( <i>a</i> , <i>c</i> , <i>b</i> , $\delta$ , $\alpha$ , $\gamma$ , $\beta$ , $\epsilon$ )	0.2	4
RH402 (pRAH5) ( $\gamma'$ - <i>uncG270</i> )	0.2	1
RH402 (pDJK19) ( <i>a</i> , <i>c</i> , <i>b</i> , $\alpha'$ )	0.2	1
RH402 (pDJK20) ( <i>a</i> , <i>c</i> , <i>b</i> )	0.2	1
RH402 (pDJK22) ( <i>a</i> , <i>c</i> , <i>b</i> , $\delta$ , $\alpha$ , $\gamma'$ , $\beta$ , $\epsilon$ )	0.2	1
RH402 (pRAH6) ( <i>a</i> , <i>c</i> , <i>b</i> , $\delta$ , $\alpha$ , $\gamma'$ - <i>uncG270</i> , $\beta'$ )	<0.5 <sup>b</sup>	ND <sup>c</sup>

<sup>a</sup> Higher levels were not tested for this strain or strain-plasmid combination.

<sup>b</sup> Lower levels were not tested with this plasmid-strain combination.

<sup>c</sup> ND, Not determined.

somal *uncB-C* deletion alone was much more sensitive to gentamicin in the absence of a plasmid than was the corresponding isogenic wild-type strain. When pRAH4 (*a*, *c*, *b*,  $\delta$ ,  $\alpha$ ,  $\gamma'$ -*uncG270*,  $\beta$ ,  $\epsilon$ ) was introduced into an *unc*<sup>+</sup> strain, little change in gentamicin resistance was observed. When pRAH4 (*a*, *c*, *b*,  $\delta$ ,  $\alpha$ ,  $\gamma'$ -*uncG270*,  $\beta$ ,  $\epsilon$ ) was introduced into an *uncB-C* deletion strain, a substantial increase in the level of gentamicin resistance was observed; the resistance was greater than that of the wild-type strain. In all cases the level of gentamicin resistance conferred by plasmid pRAH4 (*a*, *c*, *b*,  $\delta$ ,  $\alpha$ ,  $\gamma'$ -*uncG270*,  $\beta$ ,  $\epsilon$ ) was less than the level of gentamicin resistance exhibited by strain AT753-26-28 (*uncG270*), which carries the *uncG270* mutation in the chromosome.

The hypersensitivity to gentamicin observed with strain RH402 ( $\Delta$ *uncB-C recA*) was not unique to this strain. Two other pairs of otherwise isogenic *unc*<sup>+</sup> and  $\Delta$ *uncB-C* strains (X1488 and DK6, and CK1703 and CK1803) were tested for gentamicin sensitivity in the presence and absence of pRAH4 (*a*, *c*, *b*,  $\delta$ ,  $\alpha$ ,  $\gamma'$ -*uncG270*,  $\beta$ ,  $\epsilon$ ) (data not shown). In each case, the *uncB-C* deletion strain was hypersensitive to antibiotics compared with the wild-type strain. The addition of pRAH4 resulted in an increase in gentamicin resistance to a level well above that observed with the wild-type strain. Introduction of pRPG54 (*a*, *c*, *b*,  $\delta$ ,  $\alpha$ ,  $\gamma$ ,  $\beta$ ,  $\epsilon$ ) into the  $\Delta$ *uncB-C* strain increased the level of gentamicin resistance to a level near that of the wild-type strain, but lower than that observed on introduction of pRAH4 (*a*, *c*, *b*,  $\delta$ ,  $\alpha$ ,  $\gamma'$ -*uncG270*,  $\beta$ ,  $\epsilon$ ).

Other plasmids carrying portions of the *unc* operon did not confer gentamicin resistance. A large number of plasmids derived from pRPG54 (*a*, *c*, *b*,  $\delta$ ,  $\alpha$ ,  $\gamma$ ,  $\beta$ ,  $\epsilon$ ) with mutations in specific *unc* genes, resulting in the absence of individual ATP synthase polypeptides, were tested for their ability to confer antibiotic resistance when they were introduced into chromosomally *unc*<sup>+</sup> or *unc* deletion strains. Some of these results are given in Table 3. These plasmids did not increase antibiotic resistance over the intrinsic level exhibited by RH402 ( $\Delta$ *uncB-C recA*). Aris et al. (2) showed that functional *F*<sub>0</sub> is produced by plasmids DJK19 (*a*, *c*, *b*,  $\alpha'$ ) and DJK20 (*a*, *c*, *b*). If antibiotic resistance was simply caused by the presence of *F*<sub>0</sub> subunits, the level of antibiotic resistance might be expected to increase when these plas-



mids were added. Introduction of pDJK19 and pDJK20 did not lead to increased antibiotic resistance.

We also examined whether the absence of the  $\gamma$  subunit was sufficient to produce resistance to gentamicin. Plasmid pDJK22 (*a*, *c*, *b*,  $\delta$ ,  $\alpha$ ,  $\gamma'$ ,  $\beta$ ,  $\epsilon$ ) is a plasmid that is derived from pRPG54, which codes for a partial gamma subunit with an apparent molecular weight of 18,500, in addition to the other seven genes of the ATP synthase (25). Introduction of this plasmid into RH402 ( $\Delta uncB-C$  *recA*) did not cause resistance to gentamicin. In other experiments (data not shown in Table 3) we examined plasmids that were missing various *unc* genes. In no case was gentamicin resistance conferred by these plasmids. The conferral of gentamicin resistance is thus a specific effect that is caused by only a few mutations rather than a general effect that is caused by the absence of  $F_1$  polypeptides. A derivative of pRAH4 lacking portions of the *uncD* gene and all of the *uncC* gene was created as described in Table 2. This truncated derivative of pRAH4, designated pRAH6 (*a*, *c*, *b*,  $\delta$ ,  $\alpha$ ,  $\gamma'$ -*uncG270*,  $\beta'$ ), did not confer gentamicin resistance when it was introduced into strains containing the *uncB-C* deletion, indicating that the presence of the  $\beta$  subunit, the  $\epsilon$  subunit, or both is required for a gentamicin-resistant phenotype.

A second mutation in the genes coding for the  $\beta$  or  $\epsilon$  subunits is not responsible for the gentamicin-resistant phenotype. The fact that removal of the *uncD* ( $\beta$ ) and *uncC* ( $\epsilon$ ) genes from pRAH4 eliminated the antibiotic-resistant phenotype suggested the possibility that there might be a second mutation that is responsible for gentamicin resistance present in this region. In order to demonstrate that this was not the case, a cloning procedure was performed in which the portion of the *unc* operon coding for the  $\beta$  and  $\epsilon$  subunits was exchanged between plasmids pRPG54 and pRAH4. Plasmids pRPG54 and pRAH4 were digested to completion with *Nsi*I, and then they were partially digested with *Eco*RI. A large fragment of each plasmid encompassing the chloramphenicol acetyltransferase and the genes coding for the *a*, *c*, *b*,  $\delta$ ,  $\alpha$ , and  $\gamma$  subunits and a second smaller fragment of each plasmid making up most of the genes for the  $\beta$  subunit and the entire gene for the  $\epsilon$  subunit were isolated. The large fragment of pRAH4 was ligated to the small fragment of pRPG54 to recreate an entire *unc* operon. When it was transformed into a strain with a chromosomal *uncB-C* deletion, the plasmid conferred gentamicin resistance but did not allow growth on succinate. When the large fragment of pRPG54 was ligated together with the small fragment of pRAH4 and transformed into a chromosomal *uncB-C* deletion strain, the strain did not become gentamicin resistant, but complementation of the deletion to allow growth on succinate was observed. This exchange experiment demonstrates that there are no defective  $\beta$  or  $\epsilon$  subunits coded by pRAH4 which are primary determinants of the antibiotic-resistant phenotype.

In the complementation and recombination experiments described above we mapped the mutation that causes strain AT753-26-28 to fail to grow on minimal succinate medium. In order to provide additional evidence that the mutation causing gentamicin resistance maps close to or is identical with the mutation that causes the failure to utilize succinate, a P1 transduction procedure was performed with P1 *vir* grown on strain AT753-26-28 (Ilv<sup>+</sup> Gm<sup>r</sup> Suc<sup>-</sup>) as the donor and strain AT753 (Ilv<sup>-</sup> Gm<sup>s</sup> Suc<sup>+</sup>) as the recipient. Ilv<sup>+</sup> and Ilv<sup>-</sup> refer to the ability and inability, respectively, to synthesize isoleucine and valine, Gm<sup>r</sup> and Gm<sup>s</sup> refer to resistance and sensitivity to gentamicin, respectively, and Suc<sup>+</sup> and Suc<sup>-</sup> indicate the ability and inability, respectively, to

Amino acid residue #	243	244	245	246	247	248	
DNA sequence	.....CGT	ATG	GTG	GCG	ATG	AAA.....	<i>unc<sup>r</sup></i> sequence
Amino acid sequence	.....Arg	Met	Val	Ala	Met	Lys.....	
DNA sequence	.....CGT	ATG	GGG	TGG	CGA	TGA.....	<i>uncG270</i> sequence
Amino acid sequence	.....Arg	Met	Gly	Trp	Arg	End.....	

FIG. 2. Nucleotide changes detected in the *uncG270* mutant gene. The sequence of a portion of the wild-type *uncG* gene and of strains carrying the *uncG270* mutation together with the predicted amino acid changes in the  $\gamma$  subunit are shown. The two guanosine residues inserted in the *uncG270* mutant gene are shown in boldface type.

use sodium succinate as the sole carbon and energy source. Of 88 Ilv<sup>+</sup> transformants tested, 14 were found to be Gm<sup>s</sup> Suc<sup>+</sup>, while 74 were found to be Gm<sup>r</sup> Suc<sup>-</sup>. No transformants that were Gm<sup>s</sup> Suc<sup>-</sup> or Gm<sup>r</sup> Suc<sup>+</sup> were found. If the phenotype of gentamicin resistance was caused by a mutation that was distant from the mutation, causing a failure to utilize succinate, recombinational separation of Gm<sup>r</sup> from Suc<sup>-</sup> should have been observed.

Strain AT753-26-28 was resistant to neomycin and streptomycin. Other workers previously characterized several *unc* mutations that were selected on the basis of resistance to the antibiotic neomycin (21, 38). When AT753-26-28 (*uncG270*) was tested for resistance to the antibiotic neomycin, it was found to survive on plates containing ~60  $\mu$ g of neomycin per ml. The parental strain AT753 was killed by less than 40  $\mu$ g of neomycin per ml. AT753-26-28 was also somewhat more resistant to streptomycin than AT753.

Strain DL54, known to have proton-permeable membranes, was found to be resistant to gentamicin. Previous studies indicated that antibiotic resistance is usually observed only in *unc* mutants if a strain was initially selected as antibiotic resistant (R. Humbert, unpublished data). Antibiotic resistance also was observed to be associated with proton permeability of membranes of whole cells. It was of interest to determine whether a strain that was not initially selected for antibiotic resistance and whose cells were proton permeable exhibited resistance to antibiotics. Strain DL54 is a strain which was previously shown to lack ATPase activity (41), is defective for active transport in whole cells (41) and membrane vesicles (1, 41), and whose membranes are permeable to protons (1). Tests of gentamicin resistance of DL54 indicated that this strain was resistant to greater than 5  $\mu$ g/ml while the parental strain ML308-225 was resistant to only 2  $\mu$ g/ml.

The molecular nature of the *uncG270* mutation was found to be an insertion of 2 GC base pairs. The sequence of a segment of the *uncG* gene extending from the *Stu*I site of the *Pst*I site of *uncG* from plasmids pRAH4 (*a*, *c*, *b*,  $\delta$ ,  $\alpha$ ,  $\gamma'$ -*uncG270*,  $\beta$ ,  $\epsilon$ ) and pRPG54 (*a*, *c*, *b*,  $\delta$ ,  $\alpha$ ,  $\gamma$ ,  $\beta$ ,  $\epsilon$ ) was determined by the dideoxy method (39). The only difference between the wild-type and *uncG270* sequences was an insertion of 2 GC base pairs following nucleotide 734 of the *uncG* gene. The DNA sequence of the *uncG* gene in the vicinity of the mutation and the predicted changes in the amino acid sequence of the  $\gamma$  subunit are shown in Fig. 2. The insertion of 2 GC base pairs was predicted to cause a nonsense triplet to appear at amino acid position 248.

Synthesis of a truncated  $\gamma$  subunit was observed in minicells. In order to determine which ATP synthase polypeptides were synthesized from the plasmids *in vivo*, minicells of strain DK6 harboring plasmids pRPG54 (*a*, *c*, *b*,  $\delta$ ,  $\alpha$ ,  $\gamma$ ,  $\beta$ ,  $\epsilon$ ) or pRAH4 (*a*, *c*, *b*,  $\delta$ ,  $\alpha$ ,  $\gamma'$ -*uncG270*,  $\beta$ ,  $\epsilon$ ) were incubated in medium containing [<sup>35</sup>S]methionine, and the resulting plasmid-coded synthesis products were detected by SDS-

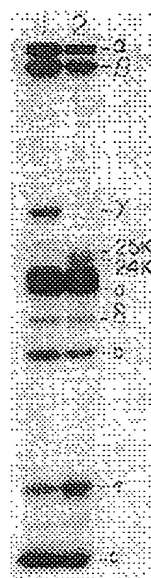


FIG. 3. Autoradiogram of SDS-polyacrylamide gel of [ $^{35}$ S]methionine-labeled minicell synthesis reactions. Lane 1, DK6(pRPG54) (a, c, b,  $\delta$ ,  $\alpha$ ,  $\gamma$ ,  $\beta$ ,  $\epsilon$ ); lane 2, DK6(pRAH4) (a, c, b,  $\delta$ ,  $\alpha$ ,  $\gamma'$ -uncG270,  $\beta$ ,  $\epsilon$ ). The locations of the eight ATP synthase subunits are as indicated on the figure. The 25,000- (25K) and 24,000-molecular-weight (24K) proteins specifically synthesized from plasmid pRAH4 are also indicated.

polyacrylamide gel electrophoresis (Fig. 3). The minicell strain used, DK6, contained a deletion extending from *uncB* into *uncC*, ensuring that only plasmid-coded genes contributed to the ATP synthase products that were observed. Examination of the synthesis products of DK6(pRPG54) (a, c, b,  $\delta$ ,  $\alpha$ ,  $\gamma$ ,  $\beta$ ,  $\epsilon$ ) indicated that the expected eight ATP synthase subunits and chloramphenicol acetyltransferase were synthesized. The  $\alpha$  subunit and chloramphenicol acetyltransferase comigrated in the gel system used for the experiment for which the results are shown in Fig. 3, but they were separated in other experiments (data not shown). The *uncG270* mutation was predicted to result in a truncated  $\gamma$  subunit of 247 amino acids with a molecular weight of 27,400. The normal size  $\gamma$  subunit was missing in minicells of strain DK6(pRAH4) (a, c, b,  $\delta$ ,  $\alpha$ ,  $\gamma'$ -uncG270,  $\beta$ ,  $\epsilon$ ), but there were two bands with apparent molecular weights of approximately 25,000 and 24,000 which were not synthesized by minicells containing pRPG54 (a, c, b,  $\delta$ ,  $\alpha$ ,  $\gamma$ ,  $\beta$ ,  $\epsilon$ ). The relative amounts of the two bands differed depending on the preparation and length of time the sample was stored before electrophoresis; therefore, the band with a lower molecular weight may be a proteolysis product of the larger band of the doublet.

The truncated  $\gamma$  subunit reacted with anti- $\gamma$  antiserum on an immunoblot. Washed membranes and soluble extract from strains AT753(pRPG54), AT753-26-28(pRAH4), and RH402 ( $\Delta$ uncB-C *recA*) were subjected to SDS-polyacrylamide gel electrophoresis, the separated proteins were transferred to a sheet of nitrocellulose, and the sheet was probed with antisera directed against the  $\alpha$ ,  $\beta$ , and  $\gamma$  subunits of wild-type  $F_1$  ATPase. The presence of the  $\alpha$ ,  $\beta$ , and  $\gamma$  subunits could be detected in blots of purified  $F_1$  ATPase (Fig. 4, lanes 1 and 8) and in membranes (Fig. 4, lane 4) and extract (Fig. 4, lane 7) of strain AT753(pRPG54), producing the wild-type  $\gamma$  subunit. A number of nonspecific or cross-

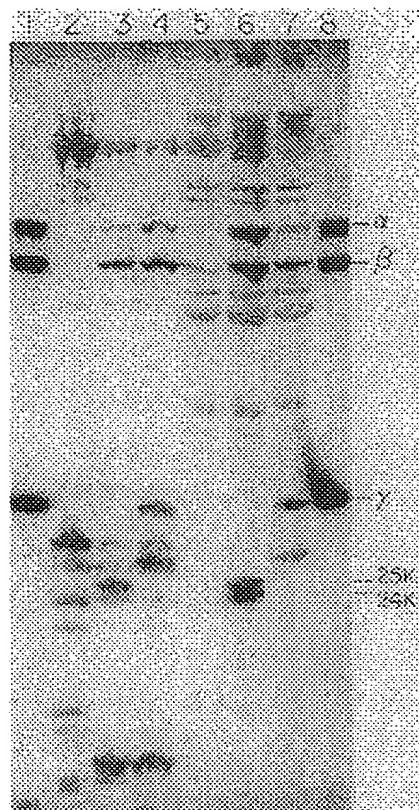


FIG. 4. Immunoblot of fractions from RH402(pRPG54) (a, c, b,  $\delta$ ,  $\alpha$ ,  $\gamma$ ,  $\beta$ ,  $\epsilon$ ), RH402(pRAH4) (a, c, b,  $\delta$ ,  $\alpha$ ,  $\gamma'$ -uncG270,  $\beta$ ,  $\epsilon$ ), and RH402 ( $\Delta$ uncB-C *recA*). Lane 1, Purified  $F_1$ ; lane 2, RH402 membranes; lane 3, RH402(pRAH4) membranes; lane 4, RH402 (pRPG54) membranes; lane 5, RH402 soluble extract; lane 6, RH402 (pRAH4) soluble extract; lane 7, RH402(pRPG54) soluble extract; lane 8, purified  $F_1$ . Blots were reacted with antisera specific for the  $\alpha$ ,  $\beta$ , and  $\gamma$  subunits (25K and 24K indicate the 25,000- and 24,000-molecular-weight proteins, respectively).

reacting bands were detected in extract (Fig. 4, lane 5) and membranes (Fig. 4, lane 2) of the strain deleted for ATP synthase genes. In the strain with *uncG270* on both the plasmid and the chromosome, two bands in the samples of soluble extract (Fig. 4, lane 6) with approximate molecular weights of 25,000 and 24,000 were found to react specifically with the antisera. In membranes of the *uncG270* strain (Fig. 4, lane 3), the band with a molecular weight of 25,000 was detected, but the presence of the band with a molecular weight of 24,000 was difficult to assess because a band was seen in the membranes of the  $\Delta$ uncBC deletion strain at the position at which this band would be expected. The molecular weights of these fragments matched those specifically synthesized by minicells harboring the plasmid carrying the *uncG270* mutation and appeared to be the mutant  $\gamma$  subunit. The  $\alpha$  and  $\beta$  subunits were detected in both membranes and the soluble extract of the strain with the *uncG270* mutation. Relatively more  $\alpha$ ,  $\beta$ , and  $\gamma$  subunits were found in the soluble extract than in the washed membranes of the *uncG270* mutant strain; however, the detection of the  $\alpha$ ,  $\beta$ , and  $\gamma$  subunits after the membranes were washed suggests that these subunits are associated with the membrane *in vivo*. The presence of  $F_1$  subunits in the extract of the

TABLE 4. Fluorescence quenching by unwashed membranes

Strain	% Quenching by:			
	NADH	NADH + DCCD	ATP	F1 + ATP
1100 ( <i>unc</i> <sup>+</sup> )	74	76	31	
RH402 ( $\Delta$ <i>uncB-C recA</i> )	78	77	0	1
RH402(pRPG54) ( <i>a, c, b, \delta, \alpha, \gamma, \beta, \epsilon</i> )	82	81	33	
RH402(pRAH4) ( <i>a, c, b, \delta, \alpha, \gamma'</i> - <i>uncG270, \beta, \epsilon</i> )	69	85	0	22
RH402(pDJK19) ( <i>a, c, b, \alpha'</i> )	80	81	0	7
RH402(pDJK22) ( <i>a, c, b, \delta, \alpha, \gamma', \beta, \epsilon</i> )	66	79	1	14

wild-type strain may be partially due to contamination of the soluble extract by membranes.

Fluorescence quenching experiments indicated that membranes of strains with the gentamicin resistance-conferring plasmid were somewhat permeable to protons. Fluorescence quenching by membrane preparations was measured for several plasmids (Table 4). Unstripped membranes of RH402 ( $\Delta$ *uncB-C recA*)(pRAH4) (*a, c, b, \delta, \alpha, \gamma'*-*uncG270, \beta, \epsilon*) had reduced NADH-driven quenching compared with those of 1100 or RH402 ( $\Delta$ *uncB-C recA*)(pRPG54) (*a, c, b, \delta, \alpha, \gamma, \beta, \epsilon*). The NADH-driven quenching of RH402 ( $\Delta$ *uncB-C recA*)(pDJK22) (*a, c, b, \delta, \alpha, \gamma', \beta, \epsilon*) and RH402( $\Delta$ *uncB-C recA*)(pDJK19) (*a, c, b, \alpha'*) was similar to quenching obtained with RH402( $\Delta$ *uncB-C recA*)(pRAH4).

Strain AT753-26-28 is defective in the transport of proline. The hypothesized mechanism for resistance to antibiotics of mutants defective in ATP synthase is failure to transport the antibiotic because of proton leak through  $F_0$ . Studies by Kauffer et al. (22) previously showed that strain AT753-26-28 (*uncG270*) has membranes that are leaky to protons when tested by the fluorescence quenching assay. In order to provide evidence that the proton leak measured in vitro reflected a proton leak in vivo, the transport of proline into whole cells of strains AT753 (*unc*<sup>+</sup>) and AT753-26-28 (*uncG270*) was measured (Fig. 5). It is apparent that the rate of proline transport was reduced in AT753-26-28 compared with that in the wild-type strain AT753. The experiment for which the results are shown in Fig. 5 was performed at pH 7.5. Transport experiments which are not shown indicated that transport by the mutant was also reduced compared with that by the wild-type strain when the transport was performed at pH 6.0. Results of these experiments are consistent with a proton leak being present in strain AT753-26-28 (*uncG270*) in vivo.

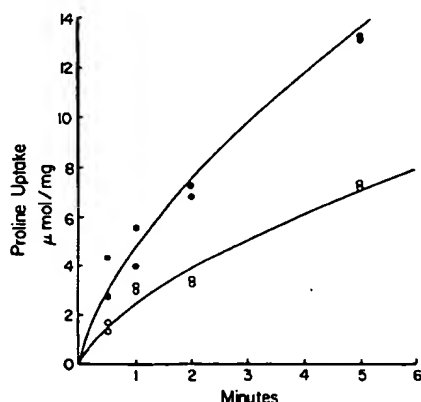


FIG. 5. Proline uptake by whole cells of AT753 (*unc*<sup>+</sup>) (●) and AT753-26-28 (*uncG270*) (○).

## DISCUSSION

The uptake of antibiotics into *E. coli* appears to be a complex process which may involve an initial binding of the antibiotic to the membrane, a second phase that requires protein synthesis, and a third phase of rapid antibiotic accumulation (7, 43). Unlike most known transport systems, aminoglycoside uptake is apparently not a saturable process. In common with other active transport processes, uptake of gentamicin and streptomycin into *E. coli* and *Pseudomonas aeruginosa* has been shown to be inhibited by inhibitors of electron transport and oxidative phosphorylation (7). According to the chemiosmotic hypothesis of Mitchell (33), the proton motive force energizing the membrane,  $\Delta\mu_{H^+}$ , is made up of the pH gradient across the membrane ( $\Delta pH$ ) multiplied by a factor,  $Z$ , plus the membrane potential,  $\Delta\psi$ . These have been measured in *E. coli*, and it has been concluded that some transport systems are driven primarily by  $\Delta\psi$  while others are driven primarily by  $\Delta pH$  (36). Studies of gentamicin uptake in *S. aureus* (29) have indicated that in this species gentamicin uptake is specifically dependent on the  $\Delta\psi$  component of the proton motive force and that there is a threshold value of  $\Delta\psi$  below which little uptake of antibiotic occurs (8, 29). At pH 7.5,  $\Delta\psi$  contributes virtually all of the proton motive force, and  $\Delta pH$  contributes very little. At pH 7.5 cells are quite sensitive to killing by gentamicin. At pH 5.0 the proton motive force has a substantial contribution from  $\Delta pH$ ,  $\Delta\psi$  is much reduced, and cells of *S. aureus* are relatively insensitive to gentamicin. Anaerobic cells of *S. aureus* are resistant to higher concentrations of antibiotic than are aerobic cells at the same pH; this is in accordance with the observation that  $\Delta\psi$  is also reduced in anaerobic cells compared with that in aerobic cells (30).

It has been proposed that the neomycin resistance observed in some *unc* mutants of *E. coli* is due to a failure to concentrate the antibiotic (21). In support of this model, studies of the neomycin-resistant *uncG* mutant strain NR70 have correlated defects in amino acid and sugar transport with proton permeability of isolated membranes and whole cells (38). In contrast to the neomycin-resistant phenotype exhibited by strain NR70, *uncA401* and *uncB402* mutants were found to be hypersensitive to the antibiotic streptomycin (35). It was shown that this hypersensitivity is associated with an increased rate of uptake of the antibiotic by mutant cells. Sensitivity to streptomycin was successfully used to screen for mutants that were defective in the ATP synthase (35).

In our studies we have shown that strain AT753-26-28, which was previously reported to be resistant to the antibiotic gentamicin, is also resistant to neomycin. We found that a strain with a deletion of the *unc* genes was hypersensitive to these antibiotics. There is an apparent paradox that the  $\Delta$ *uncB-C* strain described above and strains carrying the

*uncA401* and *uncB402* alleles are hypersensitive to antibiotics, while the mutants carrying the *uncG270* mutation and strains DL54, NR70, and N<sub>144</sub> are resistant to antibiotics. These results can be plausibly explained by referring to the properties of the ATP synthase, the antibiotic uptake system, and the electron transport system, if antibiotic uptake is primarily dependent on  $\Delta\psi$ . Our observation that the level of antibiotic resistance in *E. coli* increases as the pH of the medium is lowered suggests that *E. coli* behaves similarly to *S. aureus*. This is most consistent with a role for  $\Delta\psi$  since the other component of  $\Delta\mu_{H^+}$ ,  $\Delta pH$ , increases as the uptake decreases. In a wild-type strain, the threshold level of  $\Delta\psi$  required for antibiotic uptake may be only slightly below the steady-state level of  $\Delta\psi$  that is present during normal growth. After  $\Delta\mu_{H^+}$  rises above a minimum level, proton translocation through the ATP synthase begins, driving ATP synthesis and tending to prevent further increases in  $\Delta\mu_{H^+}$  (and  $\Delta\psi$ ). In a mutant strain lacking any portion of the ATP synthase, such as the  $\Delta uncB-C$  strains that we studied, or those strains which contain an inactive  $F_1$  attached to  $F_0$ , such as the *uncA401* mutant,  $\Delta\mu_{H^+}$  might rise to a higher level than that seen with a wild-type strain, because the normal path of protons back through the ATP synthase is absent or blocked. This increase in membrane potential would then be responsible for the increased rate of antibiotic uptake, resulting in hypersensitivity to the antibiotic compared with that in the wild-type strain.

Antibiotic-resistant strain AT753-26-28 might have the  $F_0$  portion of the ATP synthase complex assembled into a functional proton pore, which has an abnormally assembled partial  $F_1$  portion loosely associated with it. The  $F_1$  subunits may be required to produce a leaky membrane *in vivo*. The increased leakage of protons would cause a reduction of  $\Delta\psi$  to a level below the threshold value required for substantial antibiotic uptake, and the cells would be relatively resistant to the antibiotic. In *E. coli* some evidence has been presented favoring a specific role for respiratory quinones in the uptake of aminoglycosides (6). If this is the case, our model might not be applicable.

Reconstitution of  $F_0$  from purified  $F_0$  subunits revealed that all three subunits (*a*, *c*, and *b*) are necessary and sufficient to form a proton channel (40). In strains with a deletion of *unc* genes in which the *a*, *b*, and *c* subunits are produced from a plasmid, the subunits are observed to assemble into proton permeable  $F_0$  which are capable of binding  $F_1$  functionally (2, 16). These experiments demonstrate that  $F_0$  subunits can assemble in the absence of  $F_1$  subunits, but they do not prove that this is the normal assembly pathway. Strains with polar amber point mutations in the *uncA* and *uncD* genes have been observed to have nonfunctional  $F_0$  (8). Derivatives of plasmid pRPG54 in which the gene for the  $\alpha$  subunit was fused in frame to the  $\gamma$  subunit were found to have a deleterious effect on the growth of cells into which they were introduced (5). This deleterious effect was concluded to be due to proton permeability of the membranes because it was specifically reversed by DCCD. Plasmid pRPG54 (*a*, *c*, *b*,  $\delta$ ,  $\alpha$ ,  $\gamma$ ,  $\beta$ ,  $\epsilon$ ) was found to have an alteration in the ribosome-binding site preceding the *uncE* gene (42). This was reported to cause subtle changes in the proton permeability of  $F_0$ . Paradoxically, replacement of the altered ribosome-binding site with the wild-type one present on the chromosome resulted in a plasmid which failed to complement an *unc* deletion strain for growth on nonfermentable carbon sources (42). In our study, plasmids carrying various combinations of *unc* genes were used to examine the requirements for producing the antibiotic-resistant phe-

notype. The gentamicin-resistant phenotype was only conferred by plasmid pRAH4, which contained the *uncG270* mutation together with the other genes for the subunits of  $F_1$  and  $F_0$ . The presence of  $F_0$  genes alone on a plasmid was insufficient to cause antibiotic resistance. This indicates that if gentamicin resistance is solely due to an open proton leak through  $F_0$  subunits, the structure of the proton channel in strains with only  $F_0$  subunits differs from the structure of the proton channel when the mutant  $\gamma'$ -*uncG270* is present together with normal subunits coded by the other  $F_0$  and  $F_1$  genes. In our study we examined the phenomenon of antibiotic resistance of strains which carried the *uncG270* mutation on the chromosome and on a plasmid. Although the level of antibiotic resistance was higher with the chromosomal mutation, the antibiotic-resistant phenotype was observed with the plasmid-borne allele as well.

When the amino acid sequences of the  $\gamma$  subunits of bovine mitochondria, blue-green algae, and photosynthetic nonsulfur bacteria are compared with that of *E. coli* (9), the carboxyl terminus is the most highly conserved element. The *uncG270* mutation results in the loss of much of this highly conserved portion of the  $\gamma$  subunit.

Reconstitution experiments with isolated  $F_1$  and  $F_0$  subunits from a thermophilic pseudomonad led to the initial proposal that a function of the  $\gamma$  subunit is to act as a gate at the proton channel (45). Ehrig et al. (15) found that a portion of residues 205 to 287 of the carboxyl terminus of the  $\gamma$  subunit is accessible to a monoclonal antibody raised against native  $F_1$ . Binding of the antibody to  $\gamma$  disrupted  $F_1$ . It was proposed that the carboxyl terminus of the  $\gamma$  subunit is normally exposed to the cytoplasmic surface of the protein rather than being buried in  $F_1$  during folding of the protein. Disruption of  $F_1$  by anti- $\gamma$  monoclonal antibodies has also been reported by Dunn et al. (14). In studies of other chain-terminating mutations within the *uncG* gene, the truncated  $\gamma$  subunits produced were found to be 13, 156, 225, 260, and 268 amino acids in length (20, 31). Assembly of  $F_1$  subunits with catalytic activity (20, 31) was defective in all of these mutants, although the mutant with a  $\gamma$  subunit of 268 amino acids had  $\alpha$  and  $\beta$  subunits associated with the membranes. None of these *uncG* mutant strains grew on LB plates containing 50  $\mu$ g of neomycin per ml (J. Miki and M. Futai, personal communication). The *uncG270* mutation leads to the production of a  $\gamma$  subunit of 247 amino acids. Immunoblotting experiments indicated that some of the truncated  $\gamma'$ -*uncG270* remains bound to mutant membranes, as do some  $\alpha$  and  $\beta$  subunits. While the  $\beta$  subunit alone has the capacity to associate with membranes in the absence of  $F_0$  subunits (3), the presence of  $\alpha$ ,  $\gamma$ , and  $\beta$  subunits on membranes may indicate a partially assembled  $F_1$ . This association of  $F_1$  that we observed in isolated membranes of a strain with the *uncG270* mutation may reflect the state *in vivo*. Shorter fragments of the  $\gamma$  subunit, such as the 18,500-molecular-weight fragment produced by pDJK22, may be insufficient to allow binding to form even a partial  $F_1$ . Our experiment in which the deletion of the genes coding for the  $\beta$  and  $\epsilon$  subunits abolished antibiotic resistance suggests that the presence of the  $\gamma'$ -*uncG270* and the  $F_0$  subunits are not sufficient to open the proton channel. The  $\gamma'$ -*uncG270* subunit coded by pRAH4 may be sufficient to allow the association of the  $\alpha$  and  $\beta$  subunits to form a partial  $F_1$  subunit which binds to  $F_0$  in such a way that gating is abnormal. This abnormal gating would allow proton leakage and antibiotic resistance. The portion of  $\gamma$  between the terminus of this subunit in pDJK22 (*a*, *c*, *b*,  $\delta$ ,  $\alpha$ ,  $\gamma'$ ,  $\beta$ ,  $\epsilon$ ) and pRAH4 (*a*, *c*, *b*,  $\delta$ ,  $\alpha$ ,  $\gamma'$ -*uncG270*,  $\beta$ ,  $\epsilon$ ) may be required for

stabilization of the open  $F_0$  subunit or, alternatively, for interaction with the  $\alpha$  subunit, the  $\beta$  subunit, or both.

#### ACKNOWLEDGMENTS

We thank C. Kumamoto for suggesting Hfr-mediated chromosome mobilization as a method for the transfer of chromosomal mutations to a plasmid and for bacterial strains. K.A. thanks R. D. Simoni and all the members of his research group for generous hospitality. R.H. thanks the members of the Department of Mikrobiologie of the Universität Osnabrück for advice and assistance during a stay at which a portion of this work was completed. We thank R. D. Simoni, in whose laboratory much of this work was done, for advice, financial support, and the use of bacterial strains and plasmids. We thank E. Schneider and G. Deckers-Hebestreit for critically reading the manuscript.

K.A. thanks the Volkswagenstiftung for financial support (Akademiestipendium), which made his stay at Stanford University possible. This work was supported by Public Health Service grant GM 18539 from the National Institutes of Health (to R. D. Simoni), grant SFB 171 from the Deutsche Forschungsgemeinschaft, the Niedersächsisches Ministerium für Wissenschaft und Kunst, and the Fonds der Chemischen Industrie (to K.A.).

#### LITERATURE CITED

- Altendorf, K., F. M. Harold, and R. D. Simoni. 1974. Impairment and restoration of the energized state in membrane vesicles of a mutant of *Escherichia coli* lacking adenosine triphosphatase. *J. Biol. Chem.* 249:4587-4593.
- Aris, J. P., D. J. Klionsky, and R. D. Simoni. 1985. The  $F_0$  subunits of the *Escherichia coli*  $F_1F_0$ -ATP synthase are sufficient to form a functional proton pore. *J. Biol. Chem.* 260:11207-11215.
- Aris, J. P., and R. D. Simoni. 1985. The  $\beta$  subunit of the *Escherichia coli* ATP synthase exhibits a tight membrane binding property. *Biochem. Biophys. Res. Commun.* 128:155-162.
- Brown, S., and M. J. Fournier. 1984. The 4.5 S RNA gene of *Escherichia coli* is essential for growth. *J. Mol. Biol.* 178:533-550.
- Brusilow, W. S. A. 1987. Proton leakiness caused by cloned genes the  $F_0$  sector of the proton-translocating ATPase of *Escherichia coli*: requirement for  $F_1$  genes. *J. Bacteriol.* 169:4984-4990.
- Bryan, L. E., and S. Kwan. 1983. Roles of ribosomal binding, membrane potential, and electron transport in bacterial uptake of streptomycin and gentamicin. *Antimicrob. Agents Chemother.* 23:835-845.
- Bryan, L. E., and H. M. van den Elzen. 1975. Gentamicin accumulation by sensitive strains of *Escherichia coli* and *Pseudomonas aeruginosa*. *J. Antibiot.* 28:696-703.
- Cox, G. B., J. A. Downie, L. Langman, A. E. Senior, G. Ash, D. R. H. Fayle, and F. Gibson. 1981. Assembly of the adenosine triphosphatase complex in *Escherichia coli*: assembly of  $F_0$  is dependent on the formation of specific  $F_1$  subunits. *J. Bacteriol.* 148:30-42.
- Cozens, A. L., and J. E. Walker. 1987. The organization and sequence of the genes for ATP synthase subunits in the cyanobacterium *Synechococcus* 6301: support for an endosymbiotic origin of chloroplasts. *J. Mol. Biol.* 194:359-383.
- Downie, J. A., F. Gibson, and G. B. Cox. 1979. Membrane adenosine triphosphatases of prokaryotic cells. *Annu. Rev. Biochem.* 48:103-131.
- Downie, J. A., L. Langman, G. B. Cox, C. Yanofsky, and F. Gibson. 1980. Subunits of the adenosine triphosphatase complex translated in vitro from the *Escherichia coli* *unc* operon. *J. Bacteriol.* 143:8-17.
- Dunn, S. D. 1986. Effects of the modification of transfer buffer composition and the renaturation of proteins in gels on the recognition of proteins on Western blots by monoclonal antibodies. *Arch. Biochem. Biophys.* 225:144-153.
- Dunn, S. D., and M. Futai. 1980. Reconstitution of a functional coupling factor from the isolated subunits of *Escherichia coli*  $F_1$  ATPase. *J. Biol. Chem.* 255:113-118.
- Dunn, S. D., R. G. Tozer, D. F. Antczak, and L. A. Heppel. 1985. Monoclonal antibodies to *Escherichia coli*  $F_1$ -ATPase. *J. Biol. Chem.* 260:10418-10425.
- Ehrig, K., J. Hoppe, P. Friedl, and H. U. Schairer. 1986. An antibody-binding site in the native enzyme between amino acid residues 205-287 of the  $\gamma$ -subunit of  $F_1$  from *Escherichia coli*. *Biochem. Biophys. Res. Commun.* 137:468-473.
- Fillingame, R. H., B. Porter, J. Hermolin, and L. K. White. 1986. Synthesis of a functional  $F_0$  sector of the *Escherichia coli*  $H^+$ -ATPase does not require synthesis of the alpha or beta subunits of  $F_1$ . *J. Bacteriol.* 165:244-251.
- Gunsalus, R. P., W. S. A. Brusilow, and R. D. Simoni. 1982. Gene order and gene-polypeptide relationships of the proton-translocating ATPase operon (*unc*) of *Escherichia coli*. *Proc. Natl. Acad. Sci. USA* 79:320-324.
- Humbert, R., W. S. A. Brusilow, R. P. Gunsalus, D. J. Klionsky, and R. D. Simoni. 1983. *Escherichia coli* mutants defective in the *uncH* gene. *J. Bacteriol.* 153:416-422.
- Kanazawa, H., H. Hama, B. P. Rosen, and M. Futai. 1985. Deletion of seven amino acid residues from the  $\gamma$  subunit of *Escherichia coli*  $H^+$ -ATPase causes total loss of  $F_1$  assembly on membranes. *Arch. Biochem. Biophys.* 241:364-370.
- Kanazawa, H., T. Noumi, M. Futai, and T. Nitta. 1983. *Escherichia coli* mutants defective in the  $\gamma$  subunit of proton-translocating ATPase: intracistronic mapping of the defective site and the biochemical properties of the mutants. *Arch. Biochem. Biophys.* 223:521-532.
- Kanner, B. I., and D. L. Gutnick. 1972. Use of neomycin in the isolation of mutants blocked in energy conservation in *Escherichia coli*. *J. Bacteriol.* 111:287-289.
- Kauffer, S., E. Schneider, W. Piepersberg, and K. Altendorf. 1985. Aminoglycoside-resistant strains from *E. coli* with a defect in the ATP synthase, p. 297-301. In S. Papa, K. Altendorf, L. Ernster, and L. Packer (ed.), *H<sup>+</sup>-ATPase (ATP synthase): structure, function, biogenesis. The  $F_0F_1$  complex of coupling membranes*. Adriatica Editrice, Bari, Italy.
- Klionsky, D. J., W. S. A. Brusilow, and R. D. Simoni. 1984. In vivo evidence for the role of the  $\epsilon$  subunit as an inhibitor of the proton-translocating ATPase of *Escherichia coli*. *J. Bacteriol.* 160:1055-1060.
- Klionsky, D. J., and R. D. Simoni. 1983. Assembly of a functional  $F_0$  of the proton-translocating ATPase of *Escherichia coli*. *J. Biol. Chem.* 258:10136-10143.
- Klionsky, D. J., and R. D. Simoni. 1985. Assembly of a functional  $F_1$  of the proton-translocating ATPase of *Escherichia coli*. *J. Biol. Chem.* 260:11200-11206.
- Kumamoto, C. A., and R. D. Simoni. 1986. Genetic evidence for interaction between the *a* and *b* subunits of the  $F_0$  portion of the *Escherichia coli* proton translocating ATPase. *J. Biol. Chem.* 261:10037-10042.
- Maeda, M., M. Futai, and Y. Anraku. 1977. Biochemical characterization of the *uncA* phenotype of *Escherichia coli*. *Biochem. Biophys. Res. Commun.* 76:331-338.
- Maniatis, T., E. F. Fritsch, and J. Sambrook. 1982. Molecular cloning: a laboratory manual. Cold Spring Harbor Laboratory, Cold Spring Harbor, N.Y.
- Mates, S. M., E. S. Eisenberg, L. J. Mandel, L. Patel, H. R. Kaback, and M. H. Miller. 1982. Membrane potential and gentamicin uptake in *Staphylococcus aureus*. *Proc. Natl. Acad. Sci. USA* 79:6693-6697.
- Mates, S. M., L. H. Patel, H. R. Kaback, and M. H. Miller. 1983. Membrane potential in anaerobically growing *Staphylococcus aureus*. *Antimicrob. Agents Chemother.* 23:526-530.
- Miki, J., M. Takeyama, T. Noumi, H. Kanazawa, M. Maeda, and M. Futai. 1986. *Escherichia coli*  $H^+$ -ATPase: loss of the carboxyl terminal region of the  $\gamma$  subunit causes defective assembly of the  $F_1$  portion. *Arch. Biochem. Biophys.* 251:458-464.
- Miller, J. H. 1972. Experiments in molecular genetics. Cold Spring Harbor Laboratory, Cold Spring Harbor, N.Y.
- Mitchell, P. 1966. Chemiosmotic coupling in oxidative and photosynthetic phosphorylation. *Biol. Rev.* 41:455-502.

34. Mosher, M. E., L. K. Peters, and R. H. Fillingame. 1983. Use of lambda *unc* transducing bacteriophages in genetic and biochemical characterization of H<sup>+</sup>-ATPase mutants of *Escherichia coli*. *J. Bacteriol.* 156:1078-1092.
35. Muir, M. E., and B. J. Wallace. 1979. Isolation of mutants of *Escherichia coli* uncoupled in oxidative phosphorylation using hypersensitivity to streptomycin. *Biochim. Biophys. Acta* 547: 218-229.
36. Ramos, S., and H. R. Kaback. 1977. The relationship between the electrochemical proton gradient and active transport in *Escherichia coli* membrane vesicles. *Biochemistry* 16:854-859.
37. Reeve, J. N. 1984. Synthesis of bacteriophage and plasmid-encoded polypeptides in minicells, p. 212-223. In A. Pühler and K. Timmis (ed.), *Advanced molecular genetics*. Springer-Verlag, Berlin.
38. Rosen, B. P. 1973. Restoration of active transport in an Mg<sup>2+</sup>-adenosine triphosphatase-deficient mutant of *Escherichia coli*. *J. Bacteriol.* 116:1124-1129.
39. Sanger, F., S. Nicklen, and A. R. Coulson. 1977. DNA sequencing with chain-terminating inhibitors. *Proc. Natl. Acad. Sci. USA* 74:5463-5467.
40. Schneider, E., and K. Altendorf. 1985. All three subunits are required for the reconstitution of an active proton channel (F<sub>0</sub>) of *Escherichia coli* ATP synthase (F<sub>1</sub>F<sub>0</sub>). *EMBO J.* 4:515-518.
41. Simoni, R. D., and M. Shallenberger. 1972. Coupling of energy to active transport of amino acids in *Escherichia coli*. *Proc. Natl. Acad. Sci. USA* 69:2663-2667.
42. Solomon, K. A., and W. S. A. Bruslow. 1988. Effect of an *uncE* ribosome binding site mutation on the synthesis and assembly of *Escherichia coli* proton-translocating ATPase. *J. Biol. Chem.* 263:5402-5407.
43. Taber, H. W., J. P. Mueller, P. F. Miller, and A. S. Arrow. 1987. Bacterial uptake of aminoglycoside antibiotics. *Microbiol. Rev.* 41:439-457.
44. Walker, S. H. 1976. Aminoglycoside-resistant *Escherichia coli*. *N. Engl. J. Med.* 295:225-226.
45. Yoshida, M., H. Okamoto, N. Sone, H. Hirata, and Y. Kagawa. 1977. Reconstitution of thermostable ATPase capable of energy coupling from its purified subunits. *Proc. Natl. Acad. Sci. USA* 74:936-940.

## Genetics and Complementation of *Haemophilus influenzae* Mutants Deficient in Adenosine 5'-Triphosphate-Dependent Nuclease<sup>1</sup>

JAN KOOISTRA,<sup>2</sup> GARY D. SMALL,<sup>3</sup> JANE K. SETLOW,\* AND ROSLYN SHAPANKA

Biology Department, Brookhaven National Laboratory, Upton, New York 11973

Received for publication 22 December 1975

Eight different mutations in *Haemophilus influenzae* leading to deficiency in adenosine 5'-triphosphate (ATP)-dependent nuclease have been investigated in strains in which the mutations of the originally mutagenized strains have been transferred into the wild type. Sensitivity to mitomycin C and deoxycholate and complementation between extracts and deoxyribonucleic acid (DNA)-dependent ATPase activity have been measured. Genetic crosses have provided information on the relative position of the mutations on the genome. There are three complementation groups, corresponding to three genetic groups. The strains most sensitive to mitomycin and deoxycholate, derived from mutants originally selected on the basis of sensitivity to mitomycin C or methyl methanesulfonate, are in one group. Apparently all these sensitive strains lack DNA-dependent ATPase activity, as does a strain intermediate in sensitivity to deoxycholate, which is the sole representative of another group. There are four strains that are relatively resistant to deoxycholate and mitomycin C, and all of these contain the ATPase activity. Three of these are in the same genetic and complementation group, whereas the other incongruously belongs in the same group as the sensitive strains. It is postulated that there are three cistrons in *H. influenzae* that code for the three known subunits of the ATP-dependent nuclease.

Mutants deficient in adenosine 5'-triphosphate (ATP)-dependent deoxyribonuclease have been isolated from the transformable bacteria *Streptococcus pneumoniae* (20), *Bacillus subtilis* (2, 4), *Escherichia coli* (1, 15), and *Haemophilus influenzae* (9, 21). The role of this enzyme in recombination is not clear, because mutants lacking enzyme activity have not lost a very large fraction of their ability to recombine. The loss of transformability and bacteriophage recombination of some of the *H. influenzae* mutants is hardly perceptible, particularly if the mutation is separated from its heavily mutagenized background (21). In *E. coli*, there is evidence for alternative pathways of recombination (3, 7). Thus, although the ATP-dependent nuclease in *H. influenzae* may normally be of importance in recombination, in the mutants there may be alternative mechanisms that can take over the lost function. It has been postulated that the mutants, unlike the wild

type, are able to insert single-strand pieces of transforming deoxyribonucleic acid (DNA) into only one of the two DNA strands (11).

We have studied eight different mutations leading to enzyme deficiency in *H. influenzae*. All of the mutations have been transformed into the wild-type strain to eliminate additional mutations that could be present in the original mutagenized strain. The mutants were selected in different ways, some by sensitivity to inactivating compounds (9, 17) and some on the basis of enzyme deficiency (21). Our results indicate that indirect selection of mutants produces a more limited type than direct selection, by the criteria of complementation, genetic groups, and DNA-dependent ATPase activity, as well as sensitivity to inactivation by mitomycin C, deoxycholate, and streptomycin.

### MATERIALS AND METHODS

**Microorganisms.** Table 1 gives a list of *H. influenzae* strains used. Mutations were transformed into strain Rd by exposing competent cells to lysates of the mutants. The selective agent used earlier after such transformations was mitomycin C ( $3 \times 10^{-3}$   $\mu$ g/ml in agar plates) for JK30, JK57, and JK43 (17). However, since some of the mutants showed only a small degree of mitomycin C sensitivity, we devel-

<sup>1</sup> The coauthors would like to dedicate this paper to the memory of Roslyn Shapanka, who died October 16, 1975.

<sup>2</sup> Present address: Department of Genetics, University of Groningen, Biological Center, Kerklaan 30-Haren (Gn), The Netherlands.

<sup>3</sup> Present address: Department of Biochemistry, University of South Dakota, Vermillion, S.D. 57069.



TABLE 1. *H. influenzae* strains

Strain	Genotype	Selection method for original mutagenized strain <sup>a</sup>	Mutation transformed into strain <i>Rd</i>	References
<i>Rd</i>	Wild type			
KW31	<i>add-1</i>	Enzyme deficiency	+	21
KW3	<i>add-3</i>	Enzyme deficiency	—	21
JK3	<i>add-3</i>		+	This paper
KW5	<i>add-5</i>	Enzyme deficiency	—	21
JK5	<i>add-5</i>		+	This paper
JK30	<i>add-6</i>	Enzyme deficiency	+	17
JK57	<i>add-7</i>	MC sensitivity	+	17
JK43	<i>add-8</i>	MC sensitivity	+	17
KW14	<i>add-14</i>	Enzyme deficiency	—	21
JK14	<i>add-14</i>		+	This paper
KW60	<i>add-18</i>	MMS sensitivity	—	9, 21
JK60	<i>add-18</i>		+	This paper

<sup>a</sup> MC, mitomycin C; MMS, methyl methanesulfonate.

oped another selective method, based on the greater sensitivity to streptomycin of streptomycin-resistant *Add*<sup>-</sup> strains relative to *Rd* strains carrying the same streptomycin resistance marker (17). The recipient cell was a streptomycin-resistant *Rd*. Transformed cultures after expression were plated on the surface of agar plates containing 2 mg of streptomycin per ml. The mutants appeared as small colonies, which could be picked up and subcultured. JK3, JK5, JK14, and JK60 were obtained with this method. All the experiments reported in this paper were performed with the *Add*<sup>-</sup> mutations transformed into strain *Rd*.

**Viability measurements.** The optical density (at 675 nm) of growing cultures in brain heart infusion medium was read in a Bausch and Lomb Spectronic 20, and samples were removed for plating and microscopic counting. A Petroff-Hausser counter under a Bausch and Lomb phase microscope was used for estimation of total cells. For each determination 150 to 500 cells were counted.

**Mitomycin C treatment.** Mitomycin C treatment was carried out as previously described (17) on stationary cells (optical density at 675 nm, 1.0).

**Deoxycholate treatment.** Exponentially growing cultures (optical density at 675 nm, 0.4) were exposed to 0.2% deoxycholate in brain heart infusion medium for various times at 37°C. Usually three different strains, each resistant to a different antibiotic, were treated in the same test tube, and plating with the antibiotics separately made it possible to distinguish the different strains (17).

**Cell extracts.** Cells grown to stationary phase in brain heart infusion medium were concentrated at 4°C (0.5 g/wet weight) of cells per ml of 0.06 M tris(hydroxymethyl)aminomethane (Tris) - hydrochloride, pH 8.2) and subjected to a French pressure cell at 18,000 lb/in<sup>2</sup>. Cell debris was removed by centrifugation at about 10,000 × *g*. The undiluted extracts contained from 34 to 47 mg of protein per ml, as determined by the method of Lowry et al. (13).

**ATP-dependent nuclease assay.** The enzyme was measured essentially according to Friedman and Smith (6). The reaction mixture (0.3 ml) consisted of

0.1 M Tris-hydrochloride buffer, pH 8.2, 1.3 mM ATP, 10 mM MgCl<sub>2</sub>, about 0.2 µg of *E. coli* DNA labeled with [<sup>3</sup>H]deoxythymidine (2 × 10<sup>5</sup> counts/min per µg) and usually about 50 µg of protein per ml from crude cell extracts. After incubation at 37°C (usually for 15 min), 0.1 ml of bovine serum albumin (1 mg/ml) and 0.1 ml of 25% trichloroacetic acid were added to the mixture on ice, and after 10 min the mixture was centrifuged at low speed and 0.2 ml of the supernatant was counted in a toluene-Perma-blend-Triton X-100 (10:3) scintillator. A similar reaction was carried out without ATP.

**ATPase assay.** The reaction mixture (0.2 ml) consisted of 0.06 M Tris buffer, pH 8.2, 25 µg of calf thymus DNA per ml, 0.03 nmol (about 2 µCi) of γ-[<sup>32</sup>P]ATP (triethyl ammonium salt) purchased from New England Nuclear Corp., and extract (usually about 40 µg of protein per ml). After incubation at 37°C (usually for 10 min), 0.2 ml of 1 N HCl was added, and 0.1 ml of a Norit A slurry (1 g/100 ml of 1 N HCl). The mixture was centrifuged, and 0.3 ml of the supernatant was counted in 3 ml of water in a scintillation counter. A similar reaction was carried out with the DNA omitted.

**Complementation.** Pairs of undiluted cell extracts were mixed, NaCl was added to 0.1 M NaCl, and the mixtures were incubated at room temperature for approximately 18 h. Each mixture was diluted a factor of 750 in the assay for ATP-dependent nuclease.

**Genetic analysis.** In an attempt to find linkage between various *Add*<sup>-</sup> mutations and drug resistance markers, *add-1*, *add-7* and *add-14* were transformed to streptovaricin, streptomycin, erythromycin, nalidixic acid, and viomycin resistance. Transformed colonies were grown individually in 6 ml of growth medium containing the appropriate antibiotic to near stationary phase, and the cultures were washed in 0.05 M Tris buffer, pH 8.3, and resuspended in 1 ml of the same buffer. Triton X-100 was then added (0.1 ml of a 1% solution in water). After 2 min at 37°C the suspension was chilled and used immediately for measurement of ATP-dependent nuclease. The assay conditions were essentially

the same as described above, except that the reaction mix was 0.4 ml and contained 0.1 ml of the treated cell suspension. Incubation was for 30 min at 37 C, and the carrier protein was omitted. For the first screening no reactions were carried out without ATP. All suspected Add<sup>+</sup> transformants were regrown and assayed both with and without ATP.

Various Add<sup>-</sup> mutants were crossed with each other and screened for Add<sup>+</sup> recombinants. Streptomycin-sensitive Add<sup>-</sup> mutants were made competent in MIV medium (16), exposed to lysates of streptomycin-resistant variants of all the Add<sup>-</sup> mutants and the wild type, allowed to express in growth medium, and then selected for streptomycin resistance in liquid growth medium containing 250 µg of streptomycin per ml, as described previously (16). Add<sup>+</sup> transformants were detected as large colonies on agar plates containing 5 mg of streptomycin per ml. The number of total cells was measured by plating suitably diluted samples in agar without streptomycin. Colonies were counted after 2 days of incubation.

## RESULTS

**Viability of Add<sup>-</sup> mutants.** Table 2 shows the results of measurements of total cells by microscopic count and viable cells obtained by plating the cultures. The wild type (strain Rd) is approximately 100% viable, as judged by the ratio of viable cells to total cells. However, the Add<sup>-</sup> mutants show decreased viability. A similar decreased viability was earlier found for the *add-1* strain and some other (unspecified) Add<sup>-</sup> mutants, the latter being the original mutagenized strains (21).

Mitomycin C sensitivity of Add<sup>-</sup> mutants. We showed previously (17) that, when station-

ary-phase cells were treated with mitomycin C in liquid culture for various times, *add-1* and *add-6* were indistinguishable from wild type in sensitivity, whereas *add-7* and *add-8* were slightly sensitive. We have found *add-18* to be similar to *add-7* and *add-8* in sensitivity, whereas *add-3*, *add-5*, and *add-14* are like *add-1* and *add-6* (data not shown).

**Deoxycholate sensitivity of Add<sup>-</sup> mutants.** Figure 1 shows the inactivation of the Add<sup>-</sup> strains and the wild type as a function of time with 0.2% deoxycholate. Although there is considerable scatter to some of the data, it appears that the mutants fall into three groups with respect to sensitivity; *add-1*, *add-3*, *add-5*, and *add-6* are only slightly more sensitive than the wild type, *add-14* is a little more sensitive than these, and *add-7*, *add-8*, and *add-18* are very sensitive. It is clear that the differences in sensitivity to this agent are much greater than the differences in sensitivity to mitomycin C (17).

**Complementation between crude extracts of Add<sup>-</sup> mutants.** All possible pairs of mutant extracts were incubated together and assayed for ATP-dependent nuclease activity, and the extracts were also assayed separately. The results, seen as acid-soluble counts from degraded DNA obtained in the presence and absence of ATP, are presented in Table 3. It is readily seen that the mutants form three complementation groups. The mutant *add-14* complements with all other strains and thus is the sole member of a group. The mutants *add-1*, *add-3*, and *add-5* complement with other strains but not with each other and thus form a group. Similarly

TABLE 2. Viability of exponentially growing *H. influenzae*

Strain or genotype	OD <sub>676</sub> <sup>a</sup>	Viable cells/ml (×10 <sup>-4</sup> ) (A)	Total cells/ml (×10 <sup>-4</sup> ) (B)	Viability (A/B)	Avg
Rd	0.10	2.4	2.7	0.89	0.995
	0.40	6.9	6.4	1.10	
<i>add-1</i>	0.19	1.4	3.5	0.40	0.46
	0.40	4.1	7.9	0.52	
<i>add-3</i>	0.20	0.66	4.2	0.16	0.27
	0.40	2.6	6.8	0.38	
<i>add-5</i>	0.20	1.3	3.7	0.35	0.39
	0.40	3.1	6.9	0.45	
<i>add-6</i>	0.18	1.5	3.2	0.47	0.46
	0.40	3.5	7.8	0.45	
<i>add-7</i>	0.18	1.4	3.6	0.39	0.47
	0.39	4.0	7.3	0.55	
<i>add-8</i>	0.39	4.3	7.5	0.57	0.58
	0.42	5.1	8.5	0.60	
<i>add-14</i>	0.20	1.4	3.5	0.40	0.54
	0.40	4.4	6.5	0.68	
<i>add-18</i>	0.20	1.8	4.2	0.42	0.55
	0.40	5.6	8.2	0.68	

<sup>a</sup> OD<sub>676</sub>. Optical density at 676 nm.

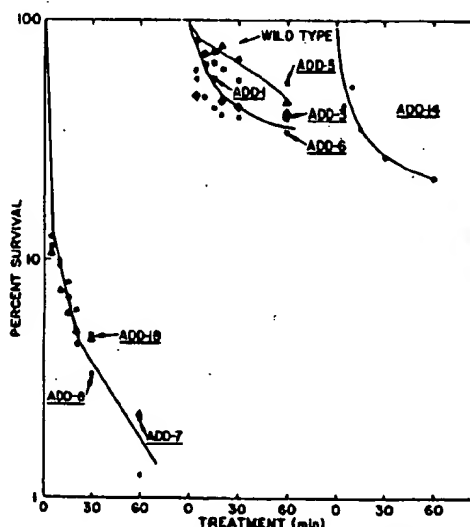


FIG. 1. Inactivation of wild-type and Add<sup>-</sup> mutants by deoxycholate.

TABLE 3. Complementation of *Add*<sup>-</sup> mutants

Extract	Total acid-soluble counts/min		ATP-dependent nuclease activity
	-ATP	+ATP	
<i>add-1</i>	1,102	945	-
<i>add-3</i>	850	705	-
<i>add-5</i>	1,037	1,285	-
<i>add-6</i>	267	342	-
<i>add-7</i>	1,072	1,050	-
<i>add-8</i>	702	755	-
<i>add-14</i>	565	320	-
<i>add-18</i>	880	877	-
<i>add-1</i> + <i>add-3</i>	950	767	-
<i>add-1</i> + <i>add-5</i>	865	1,022	-
<i>add-1</i> + <i>add-6</i>	555	8,312	+
<i>add-1</i> + <i>add-7</i>	1,155	6,372	+
<i>add-1</i> + <i>add-8</i>	602	2,842	+
<i>add-1</i> + <i>add-14</i>	940	6,102	+
<i>add-1</i> + <i>add-18</i>	1,017	9,087	+
<i>add-3</i> + <i>add-5</i>	1,062	1,365	-
<i>add-3</i> + <i>add-6</i>	982	4,945	+
<i>add-3</i> + <i>add-7</i>	837	3,222	+
<i>add-3</i> + <i>add-8</i>	1,070	5,232	+
<i>add-3</i> + <i>add-14</i>	760	2,477	+
<i>add-3</i> + <i>add-18</i>	1,007	6,275	+
<i>add-5</i> + <i>add-6</i>	847	6,465	+
<i>add-5</i> + <i>add-7</i>	720	4,892	+
<i>add-5</i> + <i>add-8</i>	812	6,490	+
<i>add-5</i> + <i>add-14</i>	1,012	7,845	+
<i>add-5</i> + <i>add-18</i>	912	5,782	+
<i>add-6</i> + <i>add-7</i>	795	875	-
<i>add-6</i> + <i>add-8</i>	732	917	-
<i>add-6</i> + <i>add-14</i>	852	7,727	+
<i>add-6</i> + <i>add-18</i>	1,022	922	-
<i>add-7</i> + <i>add-8</i>	670	637	-
<i>add-7</i> + <i>add-14</i>	902	2,497	+
<i>add-7</i> + <i>add-18</i>	922	830	-
<i>add-8</i> + <i>add-14</i>	842	6,225	+
<i>add-8</i> + <i>add-18</i>	1,012	1,070	-
<i>add-14</i> + <i>add-18</i>	797	7,282	+

*add-6*, *add-7*, *add-8*, and *add-18* are a group.

After the complementation experiments with all the mutant extracts were completed, it was found that the reaction goes faster in 0.055 M NaCl than at the higher concentration.

ATPase in *Add*<sup>-</sup> mutants. Figure 2 shows the hydrolysis of ATP by a wild-type extract in the presence and absence of DNA. The difference is taken to represent the associated ATPase activity of the ATP-dependent nuclease. Table 4 shows the results of the assays for this activity in the *Add*<sup>-</sup> mutants. The first five strains in the table appear to contain ATPase activity, whereas the last four contain little or none. The fact that there are differences between the strains gives us confidence that we are indeed measuring the ATPase associated with the nuclease, which is defective in all the *Add*<sup>-</sup> strains. Three of the four *Add*<sup>-</sup> strains

containing ATPase activity comprise a single complementation group.

Genetic analysis of *Add*<sup>-</sup> mutants. Table 5 shows the number of *Add*<sup>+</sup> transformants found among approximately 50 antibiotic-resistant transformants selected for each marker and each recipient cell representing each of the three complementation groups. The distance between the streptovaricin and nalidixic acid resistance markers on the genetic map of *H. influenzae* is approximately  $3 \times 10^6$  daltons, and the streptomycin and erythromycin resistance markers are located between the streptovaricin and nalidixic acid resistance markers (J. W. Bendler, personal communication). The location of the viomycin resistance marker is still unknown. The results show that the *add-1*, *add-7*, and *add-14* mutations are unlinked or only very weakly linked to the antibiotic resistance markers tested. The small number of *Add*<sup>+</sup> transformants scored among the antibiotic-resistant transformants may be ascribed

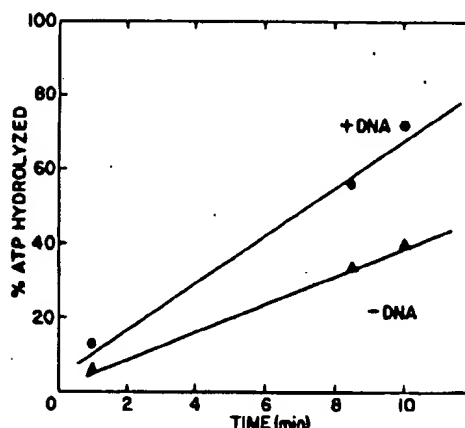


FIG. 2. ATPase activity in a wild-type extract (49  $\mu$ g of protein per ml).

TABLE 4. DNA-dependent ATPase activity

Extract	[ <sup>32</sup> P]ATP hydrolyzed in 10 min at 37 C (counts/min in <sup>32</sup> P not absorbed by norit)		DNA-dependent activity
	-DNA	+DNA	
Wild type	9,627	18,131	+
<i>add-1</i>	6,859	14,327	+
<i>add-3</i>	6,189	12,517	+
<i>add-5</i>	5,676	8,957	+
<i>add-6</i>	6,174	10,551	+
<i>add-7</i>	5,140	5,067	-
<i>add-8</i>	5,743	5,255	-
<i>add-14</i>	4,921	5,149	-
<i>add-18</i>	4,535	5,865	-

TABLE 5. ATP-dependent nuclease activity in transformants of *Add<sup>-</sup>* mutants to drug resistance by *Add<sup>+</sup>* DNA

Recipient cell	Drug resistance	No. of clones assayed for enzyme activity	No. of clones with enzyme activity
<i>add-1</i>	Streptomycin	49	1
	Streptovaricin	50	0
	Erythromycin	50	1
	Nalidixic acid	49	1
	Viomycin	48	5
<i>add-7</i>	Streptomycin	50	3
	Streptovaricin	50	1
	Erythromycin	50	1
	Nalidixic acid	50	2
	Viomycin	60	3
<i>add-14</i>	Streptomycin	50	1
	Streptovaricin	50	0
	Erythromycin	50	0
	Nalidixic acid	50	3
	Viomycin	42	2

to integration of two separate DNA segments into the same recipient genome. Because the *Add<sup>-</sup>* mutants are not linked with any of the antibiotic resistance markers tested, we have not been able to locate the *Add<sup>-</sup>* mutations on the genome.

Linkage between the *Add<sup>-</sup>* mutations was examined by crossing the mutants and screening for *Add<sup>+</sup>* recombinants. Streptomycin-resistant wild-type cells could be distinguished from *Add<sup>-</sup>* cells containing the same resistance marker because of the larger size of colony the wild-type cells form on plates containing 5 mg of streptomycin per ml. The assumption that the larger colonies consist of *Add<sup>+</sup>* cells was supported by the findings that 30 of the large colonies picked at random and tested for ATP-dependent nuclease activity were *Add<sup>+</sup>*, and that in crosses of a pair of *Add<sup>-</sup>* mutants carrying the same *Add<sup>-</sup>* mutation no large colonies were found (Table 6). In none of the crosses was the number of *Add<sup>+</sup>* recombinants among streptomycin-resistant transformants affected by integration of the streptomycin marker into the recipient genome, because in all the mutants the *add* locus is unlinked to the streptomycin marker, or the linkage is negligibly small (Table 5). From the linkage data shown in Table 6 it can be concluded that (i) the mutations of *add-1*, *add-3*, and *add-5* (group A) are rather closely linked, and so are the mutations of *add-6*, *add-7*, *add-8*, and *add-18* (group C); (ii) the mutations of group A are either unlinked or very weakly linked to those of group C; (iii) *add-14* (group B) is linked both to the mutations of group A and to those of group C, so that

*add-14* seems to be located between groups A and C. The result that the *Add<sup>-</sup>* mutants can be classified as three separate linkage groups on the genome is in agreement with the finding that the mutants of groups A, B, and C belong to three different complementation groups (Table 3). The linkage data obtained are in general too poor and too variable to establish a precise genetic map of the *Add<sup>-</sup>* mutations.

## DISCUSSION

We have seen that the *Add<sup>-</sup>* mutants differ among one another in a number of properties, so that they can be classified into groups. However, the relative inviability of the strains seems to be a property of *Add<sup>-</sup>* mutants in general. Table 7 gives a summary of some of the properties of the mutants, grouped according to their sensitivity to deoxycholate, and also the groupings derived from the complementation tests and genetic crosses. There is considerable correspondence between these groupings. However, *add-6*, which belongs in complementation

TABLE 6. Crosses between *Add<sup>-</sup>* mutants

Pairs of strains in cross	Relative distance between mutations*	Avg relative distance (A)	Relative linkage (%) (1-A)
<i>add-1, add-1</i>	0	0	100
<i>add-1, add-3</i>	54, 45	50	50
<i>add-1, add-5</i>	10, 16	13	87
<i>add-1, add-6</i>	70, 100, 100	93	7
<i>add-1, add-7</i>	100, 100	100	0
<i>add-1, add-8</i>	100, 96, 100	99	1
<i>add-1, add-14</i>	43, 46	45	55
<i>add-1, add-18</i>	95, 100	97	3
<i>add-3, add-3</i>	0	0	100
<i>add-3, add-6</i>	100, 100	100	0
<i>add-3, add-7</i>	100	100	0
<i>add-3, add-8</i>	100, 100, 100	100	0
<i>add-3, add-14</i>	62	62	38
<i>add-3, add-18</i>	100	100	0
<i>add-5, add-6</i>	100	100	0
<i>add-5, add-8</i>	81, 100	90	10
<i>add-6, add-6</i>	0	0	100
<i>add-6, add-7</i>	5	5	95
<i>add-6, add-8</i>	20, 0	10	90
<i>add-6, add-18</i>	37	37	63
<i>add-7, add-8</i>	4	4	96
<i>add-8, add-8</i>	0	0	100
<i>add-8, add-14</i>	68, 56, 100, 74	74	26
<i>add-8, add-18</i>	0.3, 0.5	0.4	99.6

\* The relative distance between *Add<sup>-</sup>* mutations is expressed as the ratio of the number of large colonies on 5-mg/ml streptomycin plates to the total number of cells ( $\times 100$ ) relative to this ratio determined in a cross of an *Add<sup>-</sup>* recipient with wild-type donor DNA. The numbers represent the data of various experiments.

TABLE 7. Summary of properties of *Add*<sup>-</sup> mutants

Property	Mutants		
	<i>add-1, add-3, add-5, add-6</i>	<i>add-14</i>	<i>add-7, add-8, add-18</i>
Deoxycholate sensitivity	+	++	++++
Mitomycin C sensitivity			
In liquid (0.5 µg/ml)	-	-	+
In agar (0.03 µg/ml)	+	+	++
Sensitivity of streptomycin-resistant variants to 5 mg of streptomycin per ml	+	+	++
DNA-dependent ATPase activity of extracts	+	-	-
Complementation groups and genetic groups	A (- <i>add-6</i> )	B	C (+ <i>add-6</i> )

and genetic group C, behaves with respect to other properties like a member of group A. It is notable that the strains carrying mutations that were originally selected on the basis of sensitivity to mitomycin C (*add-7* and *add-8*) or methyl methanesulfonate (*add-18*) are in one group, and they are also more sensitive to mitomycin C, streptomycin, and deoxycholate than the other *Add*<sup>-</sup> mutants. We have previously postulated that the sensitivity of the *Add*<sup>-</sup> mutants to mitomycin C and streptomycin results from their permeability to these compounds (17). It is therefore intriguing that the DNA-dependent ATPase activity appears to be missing in the more sensitive mutants, which we might suppose have greater permeability to deoxycholate than the other mutants.

The average length of integrated DNA segments in *H. influenzae* is approximately  $6 \times 10^4$  daltons (14), corresponding to about 17,000 nucleotides. Therefore, the distance between the mutations of group A and group C, which are unlinked or only very weakly linked to each other, may be estimated to be equivalent to of the order of  $10^4$  nucleotides. The molecular weight of the ATP-dependent nuclease is approximately 290,000 (K. W. Wilcox, M. Orlosky, E. A. Friedman, and H. O. Smith, Abstr. 59th Annu. Meet. Am. Soc. Biol. Chem., 1975), corresponding to approximately 7,000 nucleotides. If these 7,000 nucleotides are in one unbroken stretch of DNA, then the relative distances between the mutations measured with the present method is an overestimation of the real distance. Nevertheless, the finding that

there is relatively small linkage between the various groups (A, B, and C) suggests that the mutations of the three linkage groups are located in three different cistrons, possibly separated by base sequences that do not code for the enzyme.

The fact that there are three complementation groups corresponding to three genetic groups, which we consider to be three different cistrons, has caused us to speculate that there are three cistrons that code for different subunits of the enzyme. Indeed, the enzyme, purified to homogeneity, has been shown to have three subunits (Wilcox et al., Abstr. 59th Annu. Meet. Am. Soc. Biol. Chem., 1975). Since ATPase deficiency is caused by mutations in two different complementation groups (B and C), it is likely that at least the gene products of either B and C are required for ATPase activity. The finding that *add-6*, belonging to group C, also shows ATPase activity suggests that in this mutant the gene product of cistron C is not changed in such a way as to prevent formation of the configuration of enzyme required for ATPase activity.

There are a number of similarities between the ATP-dependent nuclease of *H. influenzae* and that of *E. coli*. The molecular weights are reported to be 290,000 (Wilcox et al., Abstr. 59th Annu. Meet. Am. Soc. Biol. Chem., 1975) and 270,000 (8), respectively. Only two subunits have been found for the *E. coli* enzyme (12), and there are mutations at only two loci (3). However, the  $\beta$  subunit purified from wild-type cells complements extracts of both *recB* and *recC* mutants, whereas the  $\alpha$  subunit fails to complement either extract (12). By analogy with the *H. influenzae* results, one interpretation of the *E. coli* data is that the  $\beta$  subunit includes two subunits, each coded for by a different cistron, and that there is a third cistron corresponding to the  $\alpha$  subunit. The *E. coli* mutants have usually been selected on the basis of sensitivity to radiation (5, 10, 19). Thus it is not improbable that a class of mutants of *E. coli* corresponding to group A in *H. influenzae* would be isolated if enzyme deficiency rather than sensitivity to various agents were the criterion. It is noteworthy that, by direct selection for ATP-dependent nuclease deficiency in *H. influenzae*, mutants in three complementation groups have been found.

Our results showing the coincidence of three complementation and genetic groups in *Add*<sup>-</sup> mutants are by no means evidence that there are three cistrons coding for three different subunits of the enzyme in *H. influenzae*. We are at present attempting to provide such evidence.

## ACKNOWLEDGMENTS

This research was carried out at Brookhaven National Laboratory under the auspices of the U.S. Energy Research and Development Administration. G.D.S. was supported by U.S. Public Health Service Fellowship 6-F22 Ca00100-01 from the National Cancer Institute.

We are very grateful to Kent Wilcox for his generous gifts of strains.

## LITERATURE CITED

1. Barbour, S. D., and A. J. Clark. 1970. Biochemical and genetic studies of recombination proficiency in *Escherichia coli*. I. Enzymatic activity associated with *recB*<sup>+</sup> and *recC*<sup>+</sup> genes. *Proc. Natl. Acad. Sci. U.S.A.* 65:955-961.
2. Chestukhin, A. V., M. F. Shemyakin, N. A. Kalinina, and A. A. Prozorov. 1972. Some properties of ATP dependent deoxyribonucleases from normal and *rec*<sup>-</sup> mutant strains of *Bacillus subtilis*. *Fed. Eur. Biochem. Soc. Lett.* 24:121-125.
3. Clark, A. J. 1973. Recombination deficient mutants of *E. coli* and other bacteria. *Annu. Rev. Genet.* 7:57-86.
4. Doly, J., E. Sasarman, and C. Anagnostopoulos. 1974. ATP-dependent deoxyribonuclease in *Bacillus subtilis* and a mutant deficient in this activity. *Mutat. Res.* 22:15-23.
5. Emmerson, P. T. 1968. Recombination deficient mutants of *Escherichia coli* K12 that map between *thyA* and *argA*. *Genetics* 60:19-30.
6. Friedman, E. A., and H. O. Smith. 1972. An adenosine triphosphate-dependent deoxyribonuclease from *Haemophilus influenzae* Rd. I. Purification and properties of the enzyme. *J. Biol. Chem.* 247:2846-2853.
7. Gillen, J. R., and A. J. Clark. 1974. The *RecC* pathway of bacterial recombination, p. 123-126. In R. F. Grell (ed.), *Mechanisms in recombination*. Plenum Press, New York.
8. Goldmark, P. J., and S. Linn. 1972. Purification and properties of the *recBC* DNase of *Escherichia coli* K-12. *J. Biol. Chem.* 247:1849-1860.
9. Greth, M. L., and M. R. Chevallier. 1973. Studies on ATP-dependent deoxyribonuclease of *Haemophilus influenzae*: involvement of the enzyme in the transformation process. *Biochem. Biophys. Res. Commun.* 54:1-8.
10. Howard-Flanders, P., and L. Theriot. 1966. Mutants of *Escherichia coli* K-12 defective in DNA repair and in genetic recombination. *Genetics* 53:1137-1150.
11. LeClerc, J. E., and J. K. Setlow. 1974. Transformation in *Haemophilus influenzae*, p. 187-207. In R. F. Grell (ed.), *Mechanisms in recombination*. Plenum Press, New York.
12. Lieberman, R. P., and M. Olsh. 1974. The *recBC* deoxyribonuclease of *Escherichia coli*: isolation and characterization of the subunit proteins and reconstitution of the enzyme. *Proc. Natl. Acad. Sci. U.S.A.* 71:4818-4820.
13. Lowry, O. H., N. J. Rosebrough, A. L. Farr, and R. J. Randall. 1951. Protein measurement with the Folin phenol reagent. *J. Biol. Chem.* 193:265-275.
14. Notari, N. K., and S. H. Goodgal. 1966. On the nature of recombinants formed during transformation in *Haemophilus influenzae*. *J. Gen. Physiol.* 49(2):197-209.
15. Olsh, M. 1969. An ATP-dependent deoxyribonuclease from *Escherichia coli* with a possible role in genetic recombination. *Proc. Natl. Acad. Sci. U.S.A.* 64:1292-1299.
16. Setlow, J. K., M. E. Boling, K. L. Beattie, and R. F. Kimball. 1972. A complex of recombination and repair genes in *Haemophilus influenzae*. *J. Mol. Biol.* 68:351-378.
17. Small, G. D., J. K. Setlow, J. Koolstra, and R. Shapanka. 1976. Lethal effect of mitomycin C on *Haemophilus influenzae*. *J. Bacteriol.* 125:643-654.
18. Steinhart, W. L., and R. M. Herriott. 1968. Fate of recipient deoxyribonucleic acid during transformation in *Haemophilus influenzae*. *J. Bacteriol.* 96:1718-1724.
19. van de Putte, P., H. Zwenk, and A. Rörsch. 1966. Properties of four mutants of *Escherichia coli* defective in genetic recombination. *Mutat. Res.* 3:381-392.
20. Voris, G. F., and G. Buttin. 1970. An ATP-dependent deoxyribonuclease from *Diplococcus pneumoniae*. II. Evidence for its involvement in bacterial recombination. *Biochim. Biophys. Acta* 224:42-54.
21. Wilcox, K. W., and H. O. Smith. 1975. Isolation and characterization of mutants of *Haemophilus influenzae* deficient in an adenosine 5'-triphosphate-dependent deoxyribonuclease activity. *J. Bacteriol.* 122:443-453.

Biochem J. 1992 Aug 1;285 ( Pt 3):881-8.

[Related Articles, Links](#)**Nucleotide sequence, organization and characterization of the *atp* genes and the encoded subunits of *Mycoplasma gallisepticum* ATPase.****Rasmussen OF, Shirvan MH, Margalit H, Christiansen C, Rottem S.**

Department of Molecular Food Technology, Biotechnological Institute, Lyngby, Denmark.

The nucleotide sequence of a 7.8 kbp DNA fragment from the genome of *Mycoplasma gallisepticum* has been determined. The fragment contains a cluster of nine tightly linked genes coding for the subunits of the *M. gallisepticum* ATPase. The gene order is I (I-subunit), B (a-subunit), E (c-subunit), F (b-subunit), H (delta-subunit), A (alpha-subunit), G (gamma-subunit), D (beta-subunit) and C (epsilon-subunit). Two open reading frames were identified in the flanking regions; one (ORFU), preceding the I gene, encodes at least 110 amino acids and the other (ORFS), following the C gene, encodes at least 90 amino acids. The deduced amino acid sequences of the various subunits are presented and discussed with regard to the structure, function and differing sensitivity of the *M. gallisepticum* enzyme to dicyclohexylcarbodiimide and aurovertin. The alpha- and beta-subunits of the F1 portion are well conserved (51% and 65% identity with those of *Escherichia coli*), whereas the gamma-, delta- and epsilon-subunits, as well as the F0-subunits, show a low percentage identity. Nonetheless, the secondary structure of the F0-subunits show a high degree of similarity to the corresponding subunits of *E. coli*. Two very strong potential amphipathic alpha-helices are predicted in the delta-subunit and the N-terminus of the b-subunit contains two hydrophobic helical stretches. The possible roles of these structural properties in the close association of the F1 and F0 multisubunit complexes among mycoplasmas are discussed.

PMID: 1386735 [PubMed - indexed for MEDLINE]



Extremophiles. 1998 Aug;2(3):217-22.

[Related Articles, Links](#)**pH homeostasis and ATP synthesis: studies of two processes that necessitate inward proton translocation in extremely alkaliphilic *Bacillus* species.****Krulwich TA, Ito M, Hicks DB, Gilmour R, Guffanti AA.**Department of Biochemistry, Mount Sinai School of Medicine, New York, NY 10029, USA.  
[krulwich@msvax.mssm.edu](mailto:krulwich@msvax.mssm.edu)

Alkaliphilic *Bacillus* species that are isolated from nonmarine, moderate salt, and moderate temperature environments offer the opportunity to explore strategies that have developed for solving the energetic challenges of aerobic growth at pH values between 10 and 11. Such bacteria share many structural, metabolic, genomic, and regulatory features with nonextremophilic species such as *Bacillus subtilis*. Comparative studies can therefore illuminate the specific features of gene organization and special features of gene products that are homologs of those found in non-extremophiles, and potentially identify novel gene products of importance in alkaliphily. We have focused our studies on the facultative alkaliphile *Bacillus firmus* OF4, which is routinely grown on malate-containing medium at either pH 7.5 or 10.5. Current work is directed toward clarification of the characteristics and energetics of membrane-associated proteins that must catalyze inward proton movements. One group of such proteins are the Na<sup>+</sup>/H<sup>+</sup> antiporters that enable cells to adapt to a sudden upward shift in pH and to maintain a cytoplasmic pH that is 2-2.3 units below the external pH in the most alkaline range of pH for growth. Another is the proton-translocating ATP synthase that catalyzes robust production of ATP under conditions in which the external proton concentration and the bulk chemiosmotic driving force are low. Three gene loci that are candidates for Na<sup>+</sup>/H<sup>+</sup> antiporter encoding genes with roles in Na(+)-dependent pH homeostasis have been identified. All of them have homologs in *B. subtilis*, in which pH homeostasis can be carried out with either K<sup>+</sup> or Na<sup>+</sup>. The physiological importance of one of the *B. firmus* OF4 loci, *nhaC*, has been studied by targeted gene disruption, and the same approach is being extended to the others. The *atp* genes that encode the alkaliphile's F1F0-ATP synthase are found to have interesting motifs in areas of putative importance for proton translocation. As an initial step in studies that will probe the importance and possible roles of these motifs, the entire *atp* operon from *B. firmus* OF4 has been cloned and functionally expressed in an *Escherichia coli* mutant that has a full deletion of its *atp* genes. The transformant does not exhibit growth on succinate, but shows reproducible, modest increases in the aerobic growth yields on glucose as well as membrane ATPase activity that exhibits characteristics of the alkaliphile enzyme.

1: Biochem J. 1988 Aug 15;254(1):109-22.

[Related Articles](#), [Links](#)

**DNA sequence of a gene cluster coding for subunits of the F<sub>0</sub> membrane sector of ATP synthase in *Rhodospirillum rubrum*. Support for modular evolution of the F<sub>1</sub> and F<sub>0</sub> sectors.**

Falk G, Walker JE.

Department of Biochemistry, Arrhenius Laboratory, University of Stockholm, Sweden.

A region was cloned from the genome of the purple non-sulphur photobacterium *Rhodospirillum rubrum* that contains genes coding for the membrane protein subunits of the F<sub>0</sub> sector of ATP synthase. The clone was identified by hybridization with a synthetic oligonucleotide designed on the basis of the known protein sequence of the dicyclohexylcarbodi-imide-reactive proteolipid, or subunit c. The complete nucleotide sequence of 4240 bp of this region was determined. It is separate from an operon described previously that encodes the five subunits of the extrinsic membrane sector of the enzyme, F<sub>1</sub>-ATPase. It contains a cluster of structural genes encoding homologues of all three membrane subunits a, b and c of the *Escherichia coli* ATP synthase. The order of the genes in *Rsp. rubrum* is a-c-b'-b where b and b' are homologues. A similar gene arrangement for F<sub>0</sub> subunits has been found in two cyanobacteria, *Synechococcus* 6301 and *Synechococcus* 6716. This suggests that the ATP synthase complexes of all these photosynthetic bacteria contain nine different polypeptides rather than eight found in the *E. coli* enzyme; the chloroplast ATP synthase complex is probably similar to the photosynthetic bacterial enzymes in this respect. The *Rsp. rubrum* b subunit is modified after translation. As shown by N-terminal sequencing of the protein, the first seven amino acid residues are removed before or during assembly of the ATP synthase complex. The subunit-a gene is preceded by a gene coding for a small hydrophobic protein, as has been observed previously in the *atp* operons in *E. coli*, bacterium PS3 and cyanobacteria. A number of features suggest that the *Rsp. rubrum* cluster of F<sub>0</sub> genes is an operon. On its 5' side are found sequences resembling the -10 (Pribnow) and -35 boxes of *E. coli* promoters, and the gene cluster is followed by a sequence potentially able to form a stable stem-loop structure, suggesting that it acts as a rho-independent transcription terminator. These features and the small intergenic non-coding sequences suggest that the genes are cotranscribed, and so the name *atp2* is proposed for this second operon coding for ATP synthase subunits in *Rsp. rubrum*. The finding that genes for the F<sub>0</sub> and F<sub>1</sub> sectors of the enzyme are in separate clusters supports the view that these represent evolutionary modules.